Vertebrate Paleobiology and Paleoanthropology Series

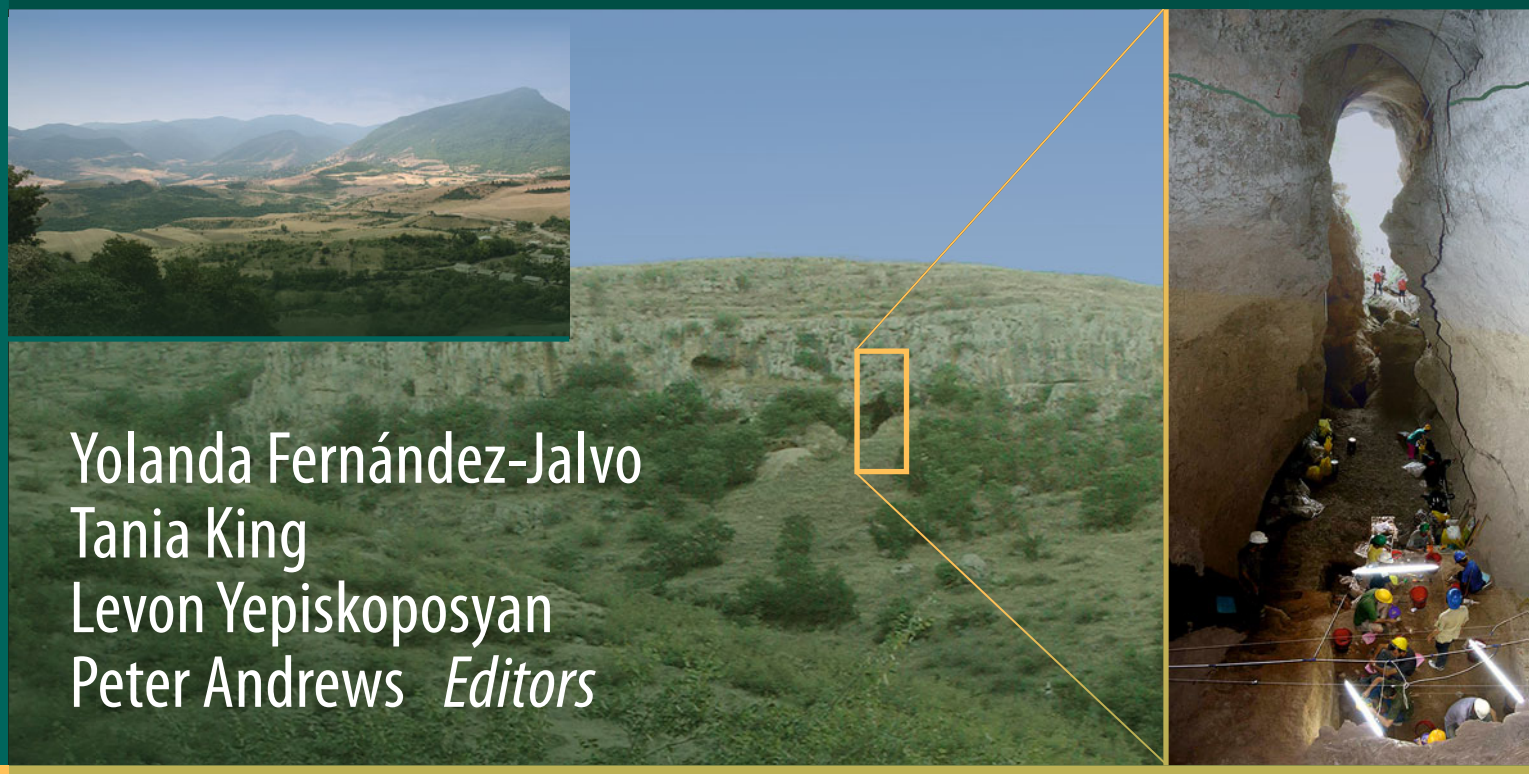

Yolanda Fernández-Jalvo
Tania King
Levon Yepiskoposyan
Peter Andrews *Editors*

Azokh Cave and the Transcaucasian Corridor

Springer

Azokh Cave and the Transcaucasian Corridor

Vertebrate Paleobiology and Paleoanthropology Series

Edited by

Eric Delson
Vertebrate Paleontology, American Museum of Natural History
New York, NY 10024, USA
delson@amnh.org

Eric J. Sargis
Anthropology, Yale University
New Haven, CT 06520, USA
eric.sargis@yale.edu

Focal topics for volumes in the series will include systematic paleontology of all vertebrates (from agnathans to humans), phylogeny reconstruction, functional morphology, Paleolithic archaeology, taphonomy, geochronology, historical biogeography, and biostratigraphy. Other fields (e.g., paleoclimatology, paleoecology, ancient DNA, total organismal community structure) may be considered if the volume theme emphasizes paleobiology (or archaeology). Fields such as modeling of physical processes, genetic methodology, nonvertebrates or neontology are out of our scope.

Volumes in the series may either be monographic treatments (including unpublished but fully revised dissertations) or edited collections, especially those focusing on problem-oriented issues, with multidisciplinary coverage where possible.

More information about this series at http://www.springer.com/series/6978

Azokh Cave and the Transcaucasian Corridor

Edited by

Yolanda Fernández-Jalvo

Museo Nacional de Ciencias Naturales (CSIC), Madrid, Spain

Tania King

Blandford Town Museum, Blandford, Dorset, United Kingdom

Levon Yepiskoposyan

Institute of Molecular Biology, National Academy of Sciences, Yerevan, Armenia

Peter Andrews

Scientific and Editorial Supervisor, Natural History Museum, London, UK

Springer

Editors
Yolanda Fernández-Jalvo
Museo Nacional de Ciencias Naturales (CSIC)
Madrid
Spain

Tania King
Blandford Town Museum
Blandford, Dorset
UK

Levon Yepiskoposyan
Institute of Molecular Biology
National Academy of Sciences
Yerevan
Armenia

Peter Andrews
Scientific and Editorial Supervisor
Natural History Museum
London
UK

ISSN 1877-9077 ISSN 1877-9085 (electronic)
Vertebrate Paleobiology and Paleoanthropology Series
ISBN 978-3-319-24922-3 ISBN 978-3-319-24924-7 (eBook)
DOI 10.1007/978-3-319-24924-7

Library of Congress Control Number: 2015953259

Cover Illustration: Main figure View of the front elevation of the Azokh cave karstic system. The cave entrance to Azokh 1 is marked in a square. *Right figure* View of the interior of Azokh 1 looking towards the entrance, and excavations at Unit Vm in 2005.

Printed on acid-free paper

This Springer imprint is published by Springer Nature
The registered company is Springer Science+Business Media B.V. Dordrecht

Dedicated to Patricio Domínguez-Alonso

Preface

Our investigations in the Lesser Caucasus arose from a visit to the site made by Tania King in 1998 while on a six month academic visit to the Institute of Geology, National Academy of Sciences. The Republic of Armenia. At that time there was increasing interest in discoveries being made at the site of Dmanisi, Georgia, which is located approximately 30 km from the border of Armenia. Armenian scientists were keen to collaborate on survey projects in the region with scientists from overseas.

One of the sites that Tania was shown during that first visit was the cave at Azokh. She noted that a large amount of sediment had been excavated from the front of the chamber, but she also saw that sediments still remained *in situ* at the rear of the cave, and hence, there was a potential for further excavation and discoveries. On returning to the UK, a collaboration was formed with Yolanda Fernández-Jalvo (who was then an EU Post-doctoral Research Fellow at The Natural History Museum), Peter Andrews (then head of the Human Origins Program of The Natural History Museum – NHM), and Levon Yepiskoposyan (who was a visiting researcher at University College London). We first carried out a survey of regions in northern, western and southern Armenia in collaboration with Yuri Sayadyan and other members of the Institute of Geology, the Armenian National Academy of Sciences, in 1999. This was followed in the same year by a short visit to Azokh Cave and nearby Tughlar Cave in Nagorno-Karabakh.

After a second survey in 2001 (King et al. 2003; Fernández-Jalvo et al. 2004), we agreed to undertake excavations at Azokh Cave to investigate archaeological, geological and paleontological context of this site. The Azokh sites are located in the region of Nagorno-Karabakh, a territory at the southeastern end of the Lesser Caucasus range. This volume describes the results from the eight excavations from 2002 to 2009 and the scientific research conducted on the excavated material. This work is still ongoing.

At the time when we started this project, there were no specialists in Paleolithic Archaeology, Anthropology, Geology or Palaeontology at the State University of Arstakh (Nagorno-Karabakh), and few in The Republic of Armenia, and so we brought together a group of specialists that would continue the work at the site of Azokh and other localities, with the long term intention of setting up relevant departments in the local university, and ultimately increasing science capacity in Nagorno-Karabakh. We placed particular emphasis on the training of local students. In this respect, two local students are receiving postgraduate training in Archaeology and Palaeontology at European institutions (IPHES/University of Tarragona – under the direction of Isabel Caceres and Ethel Allué) supported by the Erasmus Mundus (Master's degrees in Quaternary and Prehistory) and Wenner-Gren (Wadsworth International Fellowship for Ph.D. research) Foundations. Additional students from both local and overseas participate in the excavations, we have a number of field assistants from Azokh village who joined the excavation team each year. Several have received training in excavation techniques and also in the field laboratory, and some of the assistants are now well qualified in excavation techniques and are included in the excavation team.

The project has received support from a great number of individuals, academics, and officials, institutions and organizations, particularly from the Government of Nagorno-Karabakh (NK). We are especially grateful to the Ministers for Culture, Educations and Sport, NK, from 2002 to 2009, who have provided permissions to work at the site, supported the work in numerous ways, and have generously provided access to materials and loaned parts of the collection for conservation and study at institutions outside Nagorno-Karabakh. Since 2009 the Department of Tourism and Protection of Natural Monuments has been responsible for the site, and the project has benefitted from the support and interest of Mr. Sergei Shahverdyan, Head of the Department of Tourism, NK. We are extremely grateful for the interest and support of Mr. Ashot Ghulyan, Head of the National Assembly, and Ms. Narine Aghalbalyan, Minister for Culture, NK. Since the start of the project Dr. Melanya Balayan, Director, Artsakh State Museum for Country and History, has provided support and assistance in numerous ways, and has been extremely generous with providing access to the material. We also thank the staff of the museum for their help in many ways over the years. We are very grateful to Mr. Artur Mkrtumyan, Director, Base Metals Ltd., for his support and for the donation, loan and transport of scaffolding, the loan of a total station in 2007/8, and for providing the assistance of his specialists as advisors for the project. We thank Mr. Seyran Hayrbedyan, Base Metals Ltd. for specialist technical assistance over the course of many years. We are grateful to Museo Regional de Madrid for the loan of a total station in 2009, and to Ms. M.C. Arriaza who carried out the work. We also thank Análisis y Gestión del Subsuelo S.L., Spain, and most especially to E. Aracil for geophysical works carried out at the site in 2007 and 2009. We are very grateful for the institutional support of the Armenian Institute, London, and especially Dr. Susan Pattie, whose interest and support have benefitted the project since its start. We thank Dr. Yuri Sayadyan and Dr. Razmik Panossian for the invitation to collaborate with Tania King and the suggestion to visit the site. Most especially we thank the enormous help given in many ways over the years by Mr. Samvel Gabrielyan, the renowned artist who lived and worked in Stepanakert, Nagorno-Karabakh. We have been greatly saddened by his recent death (22 July 2015). Samvel was a bastion of support for this project and an inspiration to us all.

Most importantly, we thank the people of Azokh village whose generous support has made possible the fieldwork that is now in its 14th year. We thank the mayors of the village (2002–present) – Mr. Levon Asryan, Mr. Gevork Gevorkyan and Mr. Georgy Avanesyan, for their assistance and interest over the years. We are especially grateful to Mr. Ilias Poghosyan, Headmaster of Azokh Village School, who was instrumental from our very first visit to the site in 1998 and who generously accommodated us and facilitated our visit in 1999 during which we visited several caves in addition to Azokh caves. We thank Mr. Poghosyan for his interest and help in numerous ways, and especially for the use of the school premises as a field laboratory in recent years. We thank all our field assistants past and present. We are very grateful to a large number of local staff who has provided essential support for the project during the field season each year.

We are grateful to the The Harold Hyam Wingate Trust, for providing the fellowship to TK that funded her initial six month research visit to Armenia in 1998. In 1999, PA received an exchange grant from the Royal Society to collaborate with the Armenian Academy of Science. We are hugely indebted to an anonymous donor who has provided funding each year from 2002 to the present day, enabling us to carry out fieldwork each year, and providing continuity for the work. We are also grateful to three other donors who have provided financial assistance to the project. The other major source of funding during the early years was the Museo Nacional de Ciencias Naturales (CSIC) and The Spanish Ministry of Science (research projects BTE2000-1309, BTE2003-01552; BTE 2007-66231). Since 2009 the project has received substantial funding for fieldwork from the NK government, which has also provided further continuity for the work. We are also very grateful to AGBU (UK) which provided funding for the fieldwork for several seasons. Individual team members have also received funding for their participation in the fieldwork for several years and we are grateful for funding

from the NUIG Triennial Travel Grant, the Graduate School, University College London, and The State Committee of Science, Ministry of Education and Science of Armenia and the National Academy of Sciences of Armenia. Finally, the project has been very fortunate to receive funding from the Wenner-Gren Foundation in 2010, and this institution has supported the Ph.D. research of one of the local Ph.D. students.

Thanks are also extended to nearly 40 experts, most of them anonymous reviewers of the chapters in this volume, whose critical comments have greatly improved the final work. Special thanks are also given to Eric Delson and Eric Sargis, the editors of the Springer series "Vertebrate Paleobiology and Paleoanthropology" for their constant support and advice, as well as to Sherestha Saini, Publishing Editor of Springer.

Lastly, we thank all the Azokh Cave team members, past and present, for their invaluable and individual contributions to the project over the last years. Each team member has brought unique skills to the project that have helped advance the work in important ways. In addition, each member has also created a strong atmosphere of teamwork, which has facilitated the progress of the fieldwork and scientific aspects of the project.

This book is *in memoriam* of Patricio Domínguez-Alonso, a good friend, an important scientific member of the Azokh team, and an invaluable field manager and researcher. He has recently left us (15 November 2013).

Yolanda Fernández-Jalvo
Tania King
Levon Yepiskoposyan
Peter Andrews

References

Fernández-Jalvo, Y., King, T., Andrews, P., Moloney, N., Ditchfield, P., Yepiskoposyan, L. et al. (2004). Azokh Cave and Northern Armenia. In E. Baquedano & S. Rubio Jara (Eds.), *Miscelánea en homenaje a Emiliano Aguirre, Vol. IV: Arqueología* (pp. 158–168). Alcalá de Henares: Museo Arqueológico Regional.

King, T., Fernández-Jalvo, Y., Moloney, N., Andrews, P., Melkonyan, A., Ditchfield, P. et al. (2003). Exploration and survey of Pleistocene Hominid Sites in Armenia and Karabakh. *Antiquity, 77s*. http://antiquity.ac.uk/projgall/king/king.html.

Contents

About the Editors

Dr. Yolanda Fernández-Jalvo is a researcher and Head of the Department of Paleobiology at the Museo Nacional de Ciencias Naturales (CSIC), Spain. Dr. Tania King is a Research Associate at Blandford Museum, UK and is current director of the Azokh Project. Dr. Levon Yepiskoposyan is Head of the Ethnogenomics Laboratory at the Institute of Molecular Biology in the National Academy of Sciences, Armenia. Dr. Peter Andrews is Emeritus Research Scientist at the Natural History Museum, London and Curator of the Blandford Museum, UK.

Contributors

Note * indicates preferred address for correspondence

Ethel Allué
*IPHES, Institut Català de Paleoecologia Humana i Evolució Social, Tarragona, Spain;
Àrea de Prehistòria, Universitat Rovira i Virgili (URV), Tarragona, Spain

Peter Andrews
Scientific and Editorial Supervisor, Natural History Museum, London, UK

Sylvia Hixson Andrews
Blandford Museum, Blandford, Dorset, UK

Enrique Aracil
*Análisis y Gestión del Subsuelo, S.L. (AGS), Madrid, Spain;
Departamento de Geodinámica. Facultad Ciencias Geológicas., Universidad Complutense de Madrid (UCM), Madrid, Spain

Lena Asryan
Àrea de Prehistòria, Universitat Rovira i Virgili (URV), Tarragona, Spain;
*IPHES, Institut Català de Paleoecologia Humana i Evolució Social, Tarragona, Spain;
Artsakh State University, Stepanakert, Nagorno-Karabakh

Milo Barham
Earth & Ocean Sciences, School of Natural Sciences, National University of Ireland, Galway, Galway, Ireland

E. Andrew Bennett
Institut Jacques Monod. Laboratoire “Epigénome et Paléogénome”, Paris, France

Hugues-Alexandre Blain
*IPHES, Institut Català de Paleoecologia Humana i Evolució Social, Tarragona, Spain;
Àrea de Prehistòria, Universitat Rovira i Virgili (URV), Tarragona, Spain

Isabel Cáceres
Àrea de Prehistòria, Universitat Rovira I Virgili (URV), Tarragona, Spain;
*IPHES, Institut Català de Paleoecologia Humana I Evolució Social, Tarragona, Spain

Tim Compton
Institute of Molecular Biology, National Academy of Sciences, Yerevan, Armenia

Carlos Cordova
Department of Geography, Oklahoma State University, Stillwater, OK, USA

Arantxa Díaz-Bautista
Biomolecular Stratigraphy Laboratory (BSL), E.T.S.I. Minas, Polytechnical University of Madrid, Madrid, Spain

Peter Ditchfield
Research Laboratory for Archaeology and the History of Art, University of Oxford, Oxford, UK

Patricio Domínguez-Alonso
Departamento de Paleontología, Facultad de Ciencias Geologicas & Instituto de Geociencias (IGEO-CSIC), Universidad Complutense de Madrid (UCM), Madrid, Spain

Marisol Faraldos
Instituto de Catálisis Y Petroleoquímica (CSIC), Madrid, Spain

Yolanda Fernández-Jalvo
Museo Nacional de Ciencias Naturales (CSIC), Madrid, Spain

Eva-Maria Geigl
Institut Jacques Monod. Laboratoire "Epigénome et Paléogénome", Paris, France

Olivier Gorgé
Institut Jacques Monod. Laboratoire "Epigénome et Paléogénome", Paris, France

Thierry Grange
Institut Jacques Monod. Laboratoire "Epigénome et Paléogénome", Paris, France

Rainer Grün
Research School of Earth Sciences, The Australian National University, Canberra, ACT, Australia

Tania King
Blandford Town Museum, Blandford, Dorset, UK

Wendy Lees
Research School of Earth Sciences, The Australian National University, Canberra, ACT, Australia

Edward P. Lynch
Earth & Ocean Sciences, School of Natural Sciences, National University of Ireland, Galway, Galway, Ireland

M. Dolores Marin-Monfort
Museo Nacional de Ciencias Naturales (CSIC), Madrid, Spain

Norah Moloney
Museo Nacional de Ciencias Naturales (CSIC), Madrid, Spain

Laura Moreno-Pérez
Biomolecular Stratigraphy Laboratory (BSL), E.T.S.I. Minas, Polytechnical University of Madrid, Madrid, Spain

John Murray
Earth & Ocean Sciences, School of Natural Sciences, National University of Ireland, Galway, Galway, Ireland

Manuel Nieto-Díaz
Molecular Neuroprotection Laboratory, Hospital Nacional de Parapléjicos (SESCAM), Toledo, Spain

Andreu Ollé
Àrea de Prehistòria, Universitat Rovira i Virgili (URV), Tarragona, Spain;
*IPHES, Institut Català de Paleoecologia Humana i Evolució Social, Tarragona, Spain

Jose Eugenio Ortiz
Biomolecular Stratigraphy Laboratory (BSL), E.T.S.I. Minas, Polytechnical University of Madrid, Madrid, Spain

Simon A. Parfitt
Institute of Archaeology, University College London, London, UK

Ana C. Pinto-Llona
Instituto de Historia (CCHS-CSIC), Madrid, Spain

Jose Angel Porres
Departamento de Geodinámica. Facultad Ciencias Geológicas., Universidad Complutense de Madrid (UCM), Madrid, Spain

Jan Risberg
Department of Physical Geography, Stockholm University, Stockholm, Sweden

Antonio Rosas
Paleoanthropology Group, Museo Nacional de Ciencias Naturales (CSIC), Madrid, Spain

Lloyd Rossouw
Department of Archaeology, National Museum, Bloemfontein, South Africa

Louis Scott
Department of Plant Sciences, University of the Free State, Bloemfontein, South Africa

Paloma Sevilla
Facultad de Geología, Departamento de Paleontología, Universidad Complutense de Madrid (UCM), Madrid, Spain

Colin I. Smith
Department of Archaeology and History, La Trobe University, Melbourne, VIC, Australia

Trinidad Torres
Biomolecular Stratigraphy Laboratory (BSL), E.T.S.I. Minas, Polytechnical University of Madrid, Madrid, Spain

Jan Van der Made
Museo Nacional de Ciencias Naturales (CSIC), Madrid, Spain

Levon Yepiskoposyan
Institute of Molecular Biology, National Academy of Sciences, Yerevan, Armenia

Chapter 1
Introduction: Azokh Cave and the Transcaucasian Corridor

Yolanda Fernández-Jalvo, Tania King, Levon Yepiskoposyan, and Peter Andrews

Abstract Azokh Cave (also known as Azikh or Azykh) contains Pleistocene and Holocene stratified sediment infill. The site was discovered by M. Huseinov (also named Guseinov by other authors) who led the previous phase of excavations. The geographic location of the site is at an important migratory route between Africa and Eurasia. The site has yielded Middle Pleistocene hominin remains (a mandible fragment) recovered in the 1960s during a previous phase of excavation work, together with Acheulean (Mode 2) stone tools and contemporaneous fauna. An important characteristic of the Azokh 1 cave site is a continuous sedimentary record along a 7 m section, ranging in age from Middle Pleistocene (MIS 9-8) to Late Pleistocene (Mousterian industry/Mode 3, MIS 5), and to Holocene periods at the top of the series. This detailed record documents three species of *Homo*: ancestors of Neanderthals, *Homo neanderthalensis* and *Homo sapiens*. In addition, two new fossiliferous sites, Azokh 2 and Azokh 5 (which are currently being explored), constitute a potential new source of information, especially about the Middle to Late Paleolithic transition and Holocene periods in the area. Plans for preservation and protection of the whole site are currently in progress.

Y. Fernández-Jalvo (✉)
Museo Nacional de Ciencias Naturales (CSIC), José Gutiérrez Abascal 2, 28006 Madrid, Spain
e-mail: yfj@mncn.csic.es

T. King
Blandford Town Museum, Bere's Yard, Blandford, Dorset, DT11 7AZ, UK
e-mail: taniacking@gmail.com

L. Yepiskoposyan
Institute of Molecular Biology, National Academy of Sciences, Yerevan, Armenia
e-mail: lepiskop@yahoo.com

P. Andrews
Natural History Museum, Cromwell Road, London, SW7 5BD, UK
e-mail: pjandrews@uwclub.net

Резюме Пещера получила свое название от деревни Азох, расположенной в двухстах метрах от нее в долине. Это карстовый комплекс Южного Кавказа с узкими коридорами и входами, заканчивающимися более широкими камерами, в которых в настоящее время обитает большая популяция летучих мышей.

Карст имеет сложное происхождение, и седиментные наполнения содержат информацию о различных стадиях развития пещеры и ее экологии. Некоторые входы пещеры богаты ископаемыми организмами, указывая тем самым, что эти пространства в прошлом – от среднего плейстоцена до голоцена – были заселены людьми и различными формами животных. Главный и самый большой вход, известный в литературе как Азых, был обнаружен в 1960 г. М.Гусейновым, который до 1980 г. возглавлял раскопки стоянки. Ископаемые организмы в двух новых входах и соединениях последних с внутренними камерами, как и остатки отложений в задней части главного входа, в настоящее время исследуются международной экспедицией, с 2002 г. проводящей здесь раскопки.

Стоянка расположена на естественной магистрали через Кавказ, по которой ранние гоминиды и животные могли мигрировать из Африки в Европу и Азию. Азохская пещера была поочередно заселена тремя видами гоминид – *Homo heidelbergensis*, *Homo neanderthalensis* и *Homo sapiens*, ископаемые останки которых, хотя и разрозненные, найдены здесь.

Среди видов животных наиболее богато представлен гигантский пещерный медведь, здесь обнаружены и другие травоядные и плотоядные формы. Каменные орудия, встречающиеся вместе с ископаемыми костями животных, со следами разрезов указывают на активную деятельность людей на данной стоянке. Непрерывный слой плейстоценовых отложений содержит сведения о переходе от среднего к позднему плейстоцену, которые могут быть ключевыми для понимания происхождения неандертальцев и их предков. Ископаемая фауна и культурные свидетельства предоставляют информацию

Yolanda Fernández-Jalvo et al. (eds.), *Azokh Cave and the Transcaucasian Corridor*, Vertebrate Paleobiology and Paleoanthropology, DOI 10.1007/978-3-319-24924-7_1

о поведении человека и животных и их социальных стратегиях. Обнаруженные остатки флоры и фауны в этих отложениях характеризуют экосистемы и климат в эпоху плейстоцена.

К сожалению, поверхностный слой подразделения II подвержен сильной эрозии, и находки эпохи голоцена появляются в прямом контакте с плейстоценовыми отложениями. Таким образом, если в действительности и существовали материальные свидетельства о переходном периоде средний–поздний палеолит (т.е. *H. neanderthalensis – H. sapiens*), то во входе *Азох 1* они были размыты. К счастью, недавно открытые и все еще находящиеся в стадии предварительного исследования входы *Азох 2* и *Азох 5* имеют достаточно толстый слой седиментов для возможной регистрации временно́го пробела последних 100 тыс. лет.

В книге представлены результаты исследования, которые главным образом основаны на коллекции фаунальных, ботанических и культурных образцов, собранных за 2002–2009 гг. Данная глава описывает историю раскопок и иных форм исследований в пещере в течение начальных восьми полевых сезонов.

Keywords Azykh, Azikh • Human evolution • Pleistocene • Paleofaunas and paleobotany • Stone tools

Introduction

Azokh Cave is located in Nagorno-Karabakh, within the Lesser Caucasus (39º 37.15′ N; 46º 59.32′ E Fig. 1.1). It is an important site for the understanding of human evolution in its archeological, paleontological, environmental and ecological context. The site takes its name from the nearby village, situated in a valley 200 m from the cave (Fig. 1.1b), but it is also known in the literature as Azykh or Azikh. This area was a natural corridor and refuge between Africa and Eurasia during the Pleistocene (Fig. 1.2), indicated by the number of Pleistocene sites in the region (Grün et al. 1999; Gabunia et al. 2000; Lioubine 2002; Fernández-Jalvo et al. 2004, 2010; Tushabramishvili et al. 2007; Doronichev 2008; Mosar et al. 2010).

This chapter includes an introduction to the sites, their location, and the relevance of Azokh Caves to studies of the Middle to Late Pleistocene of the Caucasus. The history of the archaeological expeditions and excavations at Azokh from first discovery to the present are briefly described, and the renewed investigations (2002–2009) at Azokh Cave are described in detail. Two new sites (Azokh 2 and Azokh 5, Fig. 1.3a) have been discovered and provide an additional interest to the previously known site (hereinafter referred to as Azokh 1). Finally, the content of each chapter in the volume is briefly described together with the main findings.

Azokh Cave is significant for several reasons. The site is situated on the migration route through the Caucasus that early hominins and fauna may have followed during passage from Africa into Europe and Asia. Secondly, the caves of Azokh were occupied by three species of hominin for which fossil remains are known. Early research delineated ten stratigraphic “units”, numbered X–I from oldest to youngest. Our analysis has identified these units, except for the bed-rock, Unit X, that we have not recognized (see below). In 1968 the first hominin fossil was discovered in Unit V during the Huseinov excavations. This specimen is a small fragment of mandible assessed by Kasimova (2001) as a Middle Pleistocene hominin with affinities closest to the Ehringsdorf sample. We consider this specimen to be *Homo heidelbergensis* (Fernández-Jalvo et al. 2010; King et al. 2016). The current

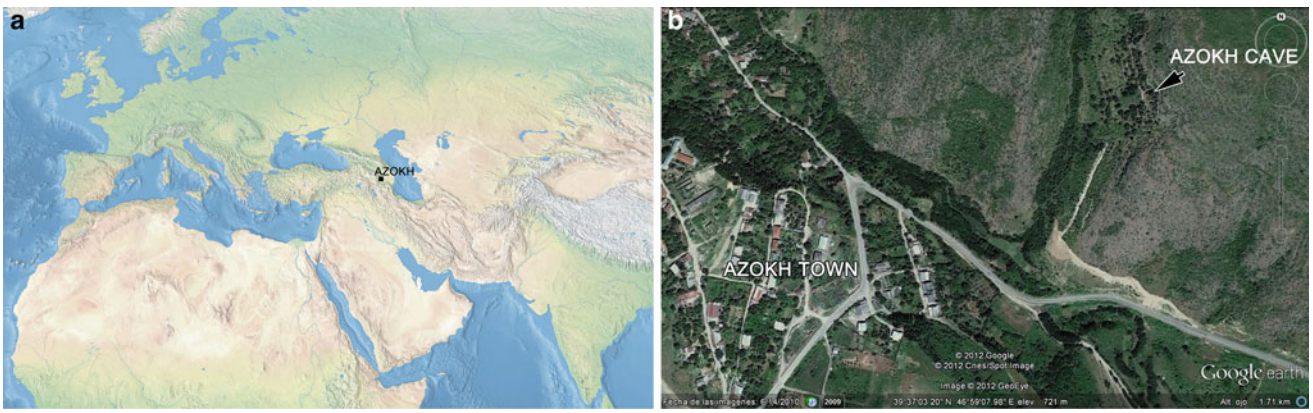

Fig. 1.1 **a** Location of Azokh in Eurasia. **b** Satellite view of the Azokh Cave site (from Google Earth), named from the closest town nearby. The site is located 200 m up on the hill

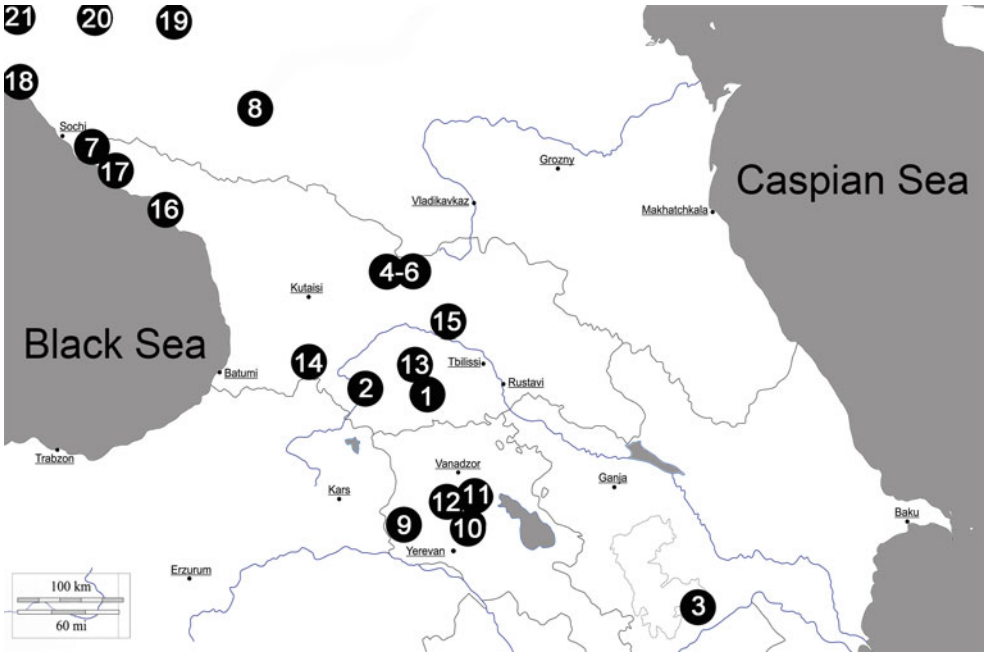

Fig. 1.2 Location of Azokh Cave (3), and pre-Acheulean and Acheulean sites described by Lioubine (2002). 1: Dmanisi; 2: Mont Amniranis; 3: Azokh; 4: Koudaro I; 5: Koudaro II; 6: Tsona; 7: Akhchtyr Cave; 8: Treugolnaya Cave; 9: Satani-Dar, Erkar-Blour, Aregouni-Blour, etc.; 10: Arzni; 11: Djraber; 12: Atiss; 13: Tchikiani; 14: Perssati; 15: Lache-Balta, Kaleti, Tigva, Gorisstavi, etc.; 16: Yachtoukh, Gvard, Otap, etc.; 17: Bogoss; 18: Cap de Kadoch; 19: Abadzekhaya, Chakhanskaja, etc.; 20: Ignatenkov koutok; 21: Abin (from Fernández-Jalvo et al. 2010)

research team has recovered a *Homo neanderthalensis* tooth from Unit II of Azokh 1, and teeth and postcrania of *Homo sapiens* from Azokh 2 and Azokh 5 (King et al. 2016). The main chamber of Azokh 1 Cave has a continuous sedimentary sequence that documents the time span of the first two of these Pleistocene human species.

Recent paleontological and genetic results (Krause et al. 2010; Reich et al. 2010) at Denisova, Siberia, raise questions about the diagnosis of *Homo heidelbergensis* and whether it was the potential ancestor of *Homo neanderthalensis* or *H. sapiens* (Stringer 2012). In this respect, Azokh cave sediments contain a detailed and nearly continuous record that includes the cultural remains of different technologies (from Acheulean to Mousterian-Levallois), in association with hominin fossils. Contemporaneous sites located in the Northern Caucasus (e.g., Mezmaiskaya, Tsona, Djruchula, Kudaro I, Kudaro III, and the slightly older Treugol'naya) have limited records of this transition affected by time averaging events (Liubin et al. 1985; Lioubine 2002; Tushabramishvili et al. 2007; Doronichev 2008; Zeinalov 2010). However, all these sites together provide a complete context of the Middle–Late Pleistocene interval along the Trans-Caucasian corridor.

Another important period in human evolution is the transition between Middle and Late Paleolithic, the cultural transition from *Homo neanderthalensis* to *Homo sapiens*. Unfortunately, the sedimentary sequence at Azokh 1 has an erosional disconformity at the top of Unit II, so that Holocene periods (Unit I) are in direct contact with Middle Paleolithic sediments. No record of the Middle–Late Paleolithic transition is, therefore, recorded in Azokh 1, although it was present in the past, as shown by scattered finds of typical Late Paleolithic stone tools at the bottom of Unit I sediments. The transition may be present at two adjacent cave entrances, named Azokh 2 and Azokh 5, which open into the same underground cave sequence, and which contain enough sediment thickness to potentially record such a transition in place and undisturbed (Domínguez-Alonso et al. 2016; Murray et al. 2016).

The top of the sedimentary sequences of Azokh caves (Azokh 1, Azokh 2 and Azokh 5) provides evidence that the cave was inhabited by humans during Holocene times. A collection of ceramics from Azokh 2 dated to the 8th century AD (1265 ± 23 years BP, see Appendix radiocarbon) has been recovered during the recent excavations. All *in situ* fragments are associated with hearths and domestic

Fig. 1.3 **a** Panoramic view of the localities of Azokh cave sites, Azokh 1 (The main cave passageway dug by Huseinov's team), Azokh 2 (formerly named 'Azokh North') and Azokh 5. **b** View of the trench dug by Huseinov's team near the mouth of the cave, leaving exposed Units IX to VII. The white arrow points to the 'pedestal' a landmark of the cave. The black arrow points to the Unit VI at the base of the pedestal. **c** View of Azokh 1 cave taken from the Uppermost Platform. The green line on the cave wall indicates the original sediment height removed between 1960 and 1980 (the white arrow indicates the 'pedestal' as landmark)

animal remains. The ceramics were made on pottery wheels belonging to a tradition that can be linked to the Iberian Peninsula, where this style persisted to the 12th century. In both this area and Iberian regions we find similar techniques and decorative motifs, such as green-manganese decoration. This tradition originated in Baghdad with a clear Byzantine influence, and it is based on the applications of copper oxide to achieve the green color and manganese oxide for purple, both set against a white luster-glazed background. It is certainly of great interest to recognize how this modern human civilization spread its culture, behaviors and art across different geographic areas becoming successfully adapted to the necessities of different populations. An international team of specialists (J. Gómez, B. Márquez, H. Simonyan, T. Sanz) is currently investigating these ceramics, and they provided these preliminary results.

The current excavations have concentrated on the deep parts of the cave entrance in Azokh 1. They have revealed evidence of seasonal occupations of the site, as well as social living and survival strategies of both hominins and fauna, particularly cave bears. The faunal and botanical remains recovered from Azokh provide information on the past ecosystems and environments, i.e. the context in which these hominins (both extinct and modern species) evolved, as well as the cultural techniques they developed.

History of Excavations at Azokh Caves

Excavations 1960–1988

Excavations were initiated by Mammadali Huseinov (National Academy of Sciences of the Azerbaijan SSR), who discovered the site in 1960 (see Mustafayev 1996; Lioubine 2002; Doronichev and Golovanova 2010). Early excavations at the site (1962 to 1974) led by Huseinov focused on the main entrance of the Azokh 1 passageway, when the cave sediments reached to within 3 m of the roof (Lioubine 2002). In 1968, Huseinov discovered a human mandibular fragment from Unit V that he named as 'Azikh anthropos' or 'Palaeoanthropus azykhensis'.

Huseinov (1965, 1974) differentiated 10 stratigraphic layers, but paleogeographers Velichko and colleagues distinguished 17 horizons (see references and descriptions in Lioubine 2002). Units distinguished by Huseinov (Velichko's horizons in brackets) are as follows:

- Layer I (Horizon 1) Humus Medieval-Chalcolithic/Copper Age.
- Layer II light yellow silts with angular clasts of almost no thickness at the central part of the entrance gallery (~Horizon 1) with some Mousterian flint/chert.
- Layer III originally described as grey silts with angular clasts (horizons 2–3) and limestone blocks covering a large surface (Mousterian). The description of this layer was further distinguished by Huseinov and divided into three horizons: (1) crumbly dark grey silt, having manganese-staining at the bottom and containing Mousterian tools. (2) grey silt with mixed clasts at the anterior part of the circular hall containing limestone plaques 1.5 × 0.6 × 0.12 cm and Mousterian tools. (3) light grey silt and yellow silts at the bottom, without clasts, containing late Acheulean or early Mousterian tools.
- Layer IV (Horizon 4) dark brown silts with angular limestone plaques, sterile in archaeology and large mammals.
- Layer V yellow silty unit containing different horizons of diverse colors (Horizons 6–11) Acheulean (Horizon 10 yielded the human mandible).
- Layer VI yellow-grey sandy silt containing rounded clasts (Horizon 12).
- Layers VII–X, 4–4.5 m of grey-bluish clayey silt (Horizons 13–17), with 'Kuruchai pebble culture'.

Layers VII to X sediments are exposed today in a trench at the entrance to the Azokh 1 passageway (Fig. 1.3b). Pebbles found in Layers X, IX and VII were considered to document an ancient Paleolithic industry, named by Huseinov the *Kuruchai pebble culture*, "… as the Azikh Cave is located in the Kuruchai River basin. The only other known civilization equivalent to Kuruchai Culture dates back 1.5 million years to the Olduvai Gorge in Tanzania. Huseinov believed the Kuruchai Culture dated from between 1.5 million years to 730,000 years ago" (Mustafayev 1996, p. 26). The pebble culture described by Huseinov, however, has been challenged by several authors (e.g., Lioubine 2002; Doronichev 2008; Doronichev and Golovanova 2010 and references therein) who dispute the likelihood of human manufacture of the stones from the lowermost layers, and this issue is still under debate. Huseinov (1985) also mentions that the Matuyama-Brunhes paleomagnetic reversal is located in Layer VIII, suggesting an Early Pleistocene age for the very basal part of the stratigraphy. Huseinov (1974) also described several hearths from Layers VI, V, and III and

a series of pits that were encircled with cave wall blocks that the author stated were made by prehistoric humans.

After 1975, a multi-disciplinary Russian-Azerbaijani collaboration took place. This collaboration among different specialists resulted in a more complete description of the lithology and sedimentology of the site. These workers measured sections from the edge of the cave to deeper in the cave entrance. They also described the faunal and lithic remains that had been found. The volume of sediment excavated was extensive, with about 70% of the intact sediments extending as far back as 35–40 m from the cave entrance opening, being removed (Fig. 1.3c). Excavations focused on the trench at the edge of the cave entrance (Layers VII–X), as most of the upper units (Layers I to VI) had already been excavated. Unfortunately, the information and descriptions of excavation procedures and finds before 1975 have either been lost or were too schematic, causing difficulties in interpreting these investigations as described by Lioubine (2002), and Kasimova (2001) expressed uncertainty about where the hominin mandible had been found within the sequence of Layer V (now known as Unit V). Originally it was stated that it had been recovered from the third horizon of Layer V, suggesting an age of about 250 ka (Lioubine 2002), but in 1985 the mandible was referred to the fifth horizon of layer V. Kasimova (2001, p. 44) concluded: "We may change archaeological age if we have some reason to do it, but it is inadmissible to change a horizon where osseous remains of fossil man were found". Lioubine (2002) describes the partial damage of the mandible and the uncertainty about its exact location as a result of the absence of early records. Despite this, however, Huseinov's extensive work has provided a large collection of both fossils and stone tools, as well as the direct evidence of Middle Pleistocene hominins.

Excavations 2002–2009

An initial survey of the site was carried out in 1999 and 2001 by a team of researchers (P. Andrews, P. Ditchfield, Y. Fernández-Jalvo, R. Jrbashyan, S. Karapetyan, T. King, N. Moloney, Y. Sayadyan, and L. Yepiskoposyan, as well as local students) who also briefly investigated other localities in Armenia and Nagorno-Karabakh (see King et al. 2003 and Fernández-Jalvo et al. 2004, as well as the Preface to this volume).

Following the initial survey work, we started excavations at Azokh Cave in 2002. Eight field seasons were conducted during 2002 and 2009 by an international research team. When the Azokh cave project was resumed in 2002, about 970 m^3 (approximately) of intact sediment situated at the rear of the Azokh 1 entrance chamber remained from the previous excavations (Fig. 1.3c). Almost no sediments remained along the sides of the cave walls, but fortunately the top limits of Huseinov's levels I, II, III and IV were visible on the limestone cave walls, allowing confirmation of the contacts between units and correlation of the sediments at the back of the cave with those described by Huseinov.

Excavations conducted between 2002 and 2009 have yielded around 9000 specimens, including 1879 large mammal fossils and 387 lithic artifacts, plus several hundreds each of amphibians, squamate reptiles, bats, rodents, insectivores and lagomorphs. Detailed sampling was undertaken every 20 cm for starch, phytolith and pollen from sections of Azokh 1 and Azokh 5, and samples were also taken during excavation. Several samples were also taken for DNA testing, collagen analyses, dating and for histological and diagenetic studies as part of pre- and post-doctoral research projects. All these studies have furnished material for the multidisciplinary investigation that is described in this volume. The researchers involved in this work include 35 authors representing eight countries (Armenia, UK, Spain, Ireland, France, Germany, Australia and South Africa). The progress of these investigations has been presented at several congresses (INQUA, 2003 and 2007; Quaternary Research Association meeting, 2005; Spanish Society of Paleontology, 2008; Hominins-Carnivores co-evolution 2008 and 2011; Workshop on Site Formation and Post-depositional Processes in Archaeology, 2010; 8th International Meeting of the French Association of Quaternary Studies (AFEQ), 2012; Irish Geological Research Meeting & Lithosphere Workshop, 2012).

Previous publications by the team (King et al. 2003; Fernández-Jalvo et al. 2004, 2009, 2010) named the sedimentological strata as Beds, but the latest publication by Murray et al. (2010) named them as Units, and this nomenclature has been followed here. Fernández-Jalvo et al. (2010) and Murray et al. (2010) mentioned preliminary dating results provided as personal communications by the different laboratories, and these have been refined here (see the Appendix).

Field Seasons

2002 (23rd August–19th September)

When we resumed excavations after a nearly 15-year hiatus, it was necessary to clear the vegetation and large limestone blocks that had collapsed from the cliff overhanging the entrance (Fig. 1.4a, b). These blocks were broken up by our field assistants and used to make steps to facilitate access to the trench dug by Huseinov's team (Fig. 1.4c). A rope was also attached to the cave wall to provide safe passage into the cave. For practical reasons, and for future reference, we described the sediments as platforms of various heights produced by tourist visitors and previous excavations before we started our work at the site, and before the stratigraphy could be definitively set. These platforms were named the Lower, Middle, Upper and Uppermost Platforms (Fig. 1.4d). This nomenclature has been used and referred to in the excavation and fossil labels (e.g., Van der Made et al. 2016).

The Lower Platform is the level at which the cave could be accessed from the outside and corresponds to the bottom of Unit V and Unit VI. The Middle Platform is the level of *in situ* sediment covered by collapsed sediments from the section (Unit Vm[1]). The Upper Platform forms the top part of Unit V and the base of Unit IV near the wall (Vu[1]), and the Uppermost Platform is located at the first ledge of the section situated at mid Unit II, both of them formed as a result of visitors passing through the cave entrance in order to see the bat colonies in the cave interior.

Fig. 1.4 **a** View of the site in 1999. **b** View of the site in 2002 after removal of the vegetation and limestone blocks that prevented access to the cave. **c** View of the steps made with broken limestone blocks fallen from the vertical cliff. **d** View of the site before site preparation (Dr. Yepiskoposyan on the left and Dr. Safaryan on the right) and three visitors that came with us to the cave. The Lower and Middle Platforms are excavation surfaces left by previous excavators. The Middle Platform was covered by a cone of collapsed sediments (note the broken white line contours the side of the cone, the asterisk points to the reference mark on the section, see Fig. 1.5d). The Upper and Uppermost Platforms were made by visitors

Platforms	Digging units	Stratigraphic units
Uppermost	I, II & III	I, II & III
Upper Platform	Vu	IV/Va
Middle Platform	Vm	Vb
Lower Platform		VI

An aerial grid was installed by anchoring bolts to the walls of the cave, forming a permanent reference for the terrestrial grid. It is oriented along the long axis of the cave (Fig. 1.5a, b), and the origin of the Y axis was fixed outside the cave (Fig. 1.5c), on the edge of the limestone bedrock. The excavations on the Middle Platform (Unit Vm) could not be extended laterally to the other side of the cave (lines H and I) in 2002, as we needed to have access to the platforms above. Thus, 2 m were left for access to the top of the sequence and to evacuate sediments using a ladder (Fig. 1.5d).

A laser pointer was fixed to the Middle platform at a fixed point (7.20 m) below the permanent datum (point 0 above the top of the sedimentary sequence). The aerial grid and heights measured using the laser pointer provide three dimensional reference spatial coordinates for each find. Secondary height datum points were fixed for the different platforms. Overburden was removed and dry sieved outside the cave (Fig. 1.6a) and finds (stone tools and fossils) from these disturbed sediments were collected, identified and labeled. A lighting system was installed, powered from a generator placed outside the cave entrance.

[1]The contact between Units IV and V did not become apparent for several years because it was obscured by debris, and the upper part of Unit V was initially identified as Unit IV. What was formerly called Unit V is now labelled Vm, the middle part of Unit V, and what was formerly part of Unit IV is now labelled Unit Vu, the upper part of Unit V An ESR date of 205 ± 16 ka has been calculated for the general area of the contact between the top of Unit V and the base of Unit IV.

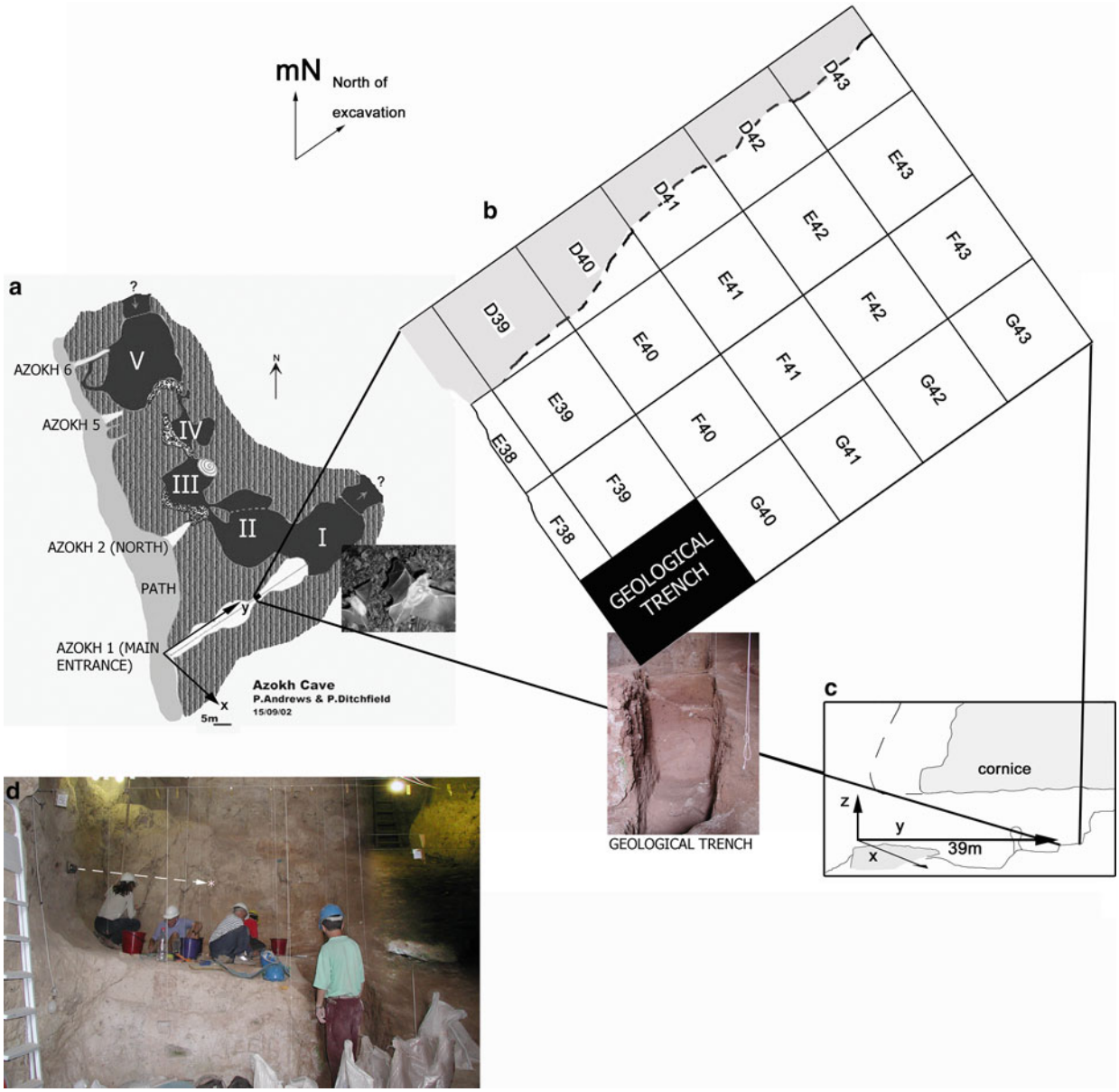

Fig. 1.5 **a** Former topography by P. Andrews and P. Ditchfield in 2002. The dark grey cavities are inner chambers inhabited by bats named as chambers I to V, the white cavities are entrance passageways to the cave system named as Azokh 1 to 6. **b** Initial aerial grid in the Middle Platform. The shaded squares (line D) are the edges of the cave walls. The small inset shows the geological trench already made in 2002 on the front of the Middle Platform. **c** The aerial grid was fixed 39 m from the cave entrance, above the present day cornice, so as to coordinate potential finds below the cornice as it was in the past (broken line). **d** View of the excavations during 2002 in the Middle Platform (Unit Vm). Note the broken white arrow goes from the laser pointer to the reference mark (asterisk) on the sediment section shown in Fig. 1.4d for vertical measurements (height). Note the right side maintains the cone of collapsed sediments to give access to the platforms above and to evacuate sediments using a ladder

Excavations of the Middle Platform (Unit Vm) started on the 1st of September, 2002. A geological trench was made on the front of the Middle Platform (Fig. 1.5b in black) as a stratigraphic reference column for the disturbed and *in-situ* sediments. Huseinov's layers were identified, described and measured. After ten days, the excavation was moved to the Upper Platform, a narrow passageway, and the laser pointer was fixed 4.90 m below the datum (Fig. 1.6d). Good deposits of sediment were found that were softer and richer in fossil content and the rest of the season was focused on this part of the excavation.

The topography of the entire cave system was measured and mapped (Fig. 1.5a). The trench aimed to locate the top of Unit VI, but no clear evidence of this unit was found, probably because it thins out towards this area of excavation. Sediment in the Middle Platform was cemented and finds

Fig. 1.6 2002 season. **a** Dry sieving outside the cave. **b** Wet sieving at the riverside, in the valley. **c** Azokh 2 clearing the collapsed modern cone and view of the test trench dug at the entrance. **d** Fixing the laser pointer and preparation of the excavation in Upper Platform (pathway made by visitors)

were limited, although remarkable (e.g., bear canines, chert, and flint scrapers, and quartz and obsidian stone tools). Obsidian is an exotic raw material, so finding it from this early period might indicate trading with other groups in the vicinity, or collection during seasonal movements. Sediment recovered from the trench excavation as well as from excavations was labeled and wet sieved at the riverside, down in the valley (Fig. 1.6b). Field surveys of areas near Azokh were also carried out in order to search for comparative sites.

Just a few meters to the north from Azokh 1 Cave, Azokh 2 (originally named Azokh North) was discovered at a similar height as the main entrance and with a great thickness of sediments (Figs. 1.3a and 1.6c). The cave floor was covered by a thick layer of disturbed and mixed sediments. These sediments were dry sieved, and remains from Holocene ages appear mixed. All this mixed sediment was thought to be the result of collapse from a potential upper gallery. A trench was dug in the entrance to try to correlate the sediments with those of the interior of the cave system and Azokh 1 (Fig. 1.6c).

On the 16th of September, 2002, the team was invited to visit Azokh school by the headmaster, Ilias Poghosyan, and we gave a presentation to pupils and teachers about our work at the cave, focusing on the significance of Azokh Cave in the context of human evolution, with reference to recent discoveries of hominin fossils, cultural remains and fossil animals found in Georgia, Europe (Spain and UK) and in Africa (Fig. 1.7).

The participants in the 2002 season were P. Andrews, P. Ditchfield, Y. Fernández-Jalvo, T. King, A. Melkonyan,

Fig. 1.7 Picture taken by Y. Fernández-Jalvo at the Azokh school with part of the excavation team and the school pupils and teachers (on the right hand first row, the Head Master (dark blue shirt), Tania King (with a bouquet of flowers) and Peter Andrews (behind T. King), on the left hand, Levon Yepiskoposyan). M. Nieto at the very back of the group in the middle-left part of the picture

N. Moloney, M. Nieto, V. Safarian and L. Yepiskoposyan. Our local Field Assistants from the Azokh village were: A. Balasanyan, G. Balasanyan, H. Boghosian, A. Gervorkian, and A. Ohanyan.

2003 (4th–31st August)

Excavations resumed on the Middle Platform (Fig. 1.8a). In order to establish the limits between stratigraphic units, as well as to confirm lithic and fossil content richness, a test trench of roughly 2 × 2 m was made on the Uppermost Platform at the side of the sediment section next to the wall (square D46 and annexes). The aerial grid was extended to the top part of the sequence and the laser pointer fixed 2.15 m below the datum (Fig. 1.8b). The top of the Upper Platform (Unit I) was not yet prepared for excavation as this unit contained a manure hearth, and the excavation's methodology had to be slightly different. A stratigraphic test trench was started from mid Unit II. Simultaneous excavations of the test trench and the Middle Platform (Unit Vm) were carried out. During excavations in the test trench, we observed that the vertical section had deep cracks running through it, and blocks of sediment were at risk of collapsing. A two-day rescue excavation was carried out to recover all fossils from the front section that was in danger of collapsing, and especially to make safe the excavation of the Middle Platform (Unit Vm). Fossils and lithics found during the rescue excavation were spatially coordinated and sediments were sieved in the river.

By the end of the season, the test trench reached the bottom of Unit III. Abundant fossils (mainly cave bear, *Ursus spelaeus*) and stone tools (of obsidian and chert) were recovered indicating a rich archeo-paleontological content. The sediment of Unit Vm was harder and less rich than that of the test trench (Units II and III). Nonetheless, Unit Vm also yielded important fossils (more ungulates than cave bears) and stone tools (also of obsidian).

Work in Azokh 2 continued, led by the team geologist and two other team members, together with most of our field assistants. Clearing of the overburden covering the sediment of Azokh 2 was extended deeper in the cave, and a second trench (Fig. 1.8c) was made to confirm the tilts of these units. An aerial grid was installed in this small chamber in preparation for its excavation. When clearing the sediment at the back of Azokh 2, a massive accumulation of large blocks was found (Fig. 1.8d). The instability of these blocks posed a safety problem for excavation at the site, forcing us to stop work in Azokh 2 and look for means of stabilizing the blocks. The survey of the inner galleries at the other end of the Azokh 2 chamber (done in 2002) showed there to be even bigger boulders, part of a gravitational cone extending down into Azokh 2 and blocking the connection between the

Fig. 1.8 2003 season. **a** View of the excavations on the Middle Platform and the Uppermost test trench. **b** Excavations in the Uppermost test trench, Dr. Safaryan taking coordinates. **c** View of the test trenches in Azokh 2: the one outside (1) was made in 2002, the one further into the interior (2) was made during the 2003 season (the white arrow points to the cone of stones that was blocked with sacks). **d** View of the cone of blocks at the back of Azokh 2. **e** View of the boulders from the interior of the galleries (with Dr. Safaryan). **f** Sampling fossils and sediment for DNA by Colin Smith

cave entrance and the inner galleries (Fig. 1.8e). These large blocks derive from a vertical shaft about 18 m above Azokh 2, seven meters of which are occupied by the boulder choke.

The test trenches dug in Azokh 1 and Azokh 2 revealed that the beds sloped down from the interior of the cave outwards towards the entrance, indicating the inner karstic system as the sediment source. This inclination was also confirmed for Unit Vm, as well as at Units II and III in Azokh 1.

A further test pit was dug deeper into the floor of the trench in Azokh 1 to find Layer X (bedrock). The floor of the trench is a very hard irregular crust of cemented silty clay and a conglomerate with chert, flint, and possibly jasper, all well rounded. Thickness of this conglomeratic unit could not be estimated as the unit is too hard and cannot be dug with normal tools (the tips of two pick axes were completely bent when trying to break the crust). We were not able to confirm the presence of the bedrock at the floor of the trench at that point. During the 2003 season, we took several samples for collagen and DNA analyses (Fig. 1.8f), as well as for dating.

The participants of the 2003 season were L. Asryan, R. Campos, Y. Fernández-Jalvo, T. King, A. Melkonyan, N. Moloney, J. Murray, M. Nieto, C. Smith, V. Safarian, and L. Yeposkoposyan. Our local field assistants from the Azokh village were:

K. Arakelian, A. Azatkhanian, E. Balasanyan, G. Balasanyan, H. Balasanyan, M. Balasanyan, and A. Gevorkian.

2004 (28th July–6th August)

Early in 2004 one of our field assistants drew our attention to fossils in the sediments outside another entrance to the cave. This entrance was mapped in 2002 and identified as a possible connection with the inner galleries of the cave, but access was too narrow (Fig. 1.9a), and it could not be investigated. In 2004 we explored this entrance further and about 3 m in from the opening we discovered an untouched 4-m section, with fossils visible in the section (Fig. 1.9b). We could not estimate the extent of the sediments beneath the 4-m section, but we established that there is a direct connection with one of the biggest chambers of the inner cave (see Fig. 1.5a) and we subsequently named the cave entrance Azokh 5.

To investigate Azokh 2, we invited Mr. Seyran Hayrabetyan, a mining engineer from Drambon Mine Company near Stepanakert, to visit Azokh in order to discuss with us and advise how we might make the site safe for long term excavations. Mr Hayrabetyan suggested a structure of treated wood to contain the boulders, a proposal that supported other advice we had received from engineers based in Spain. He further proposed that preparation for engineering work for this structure should take place in 2005. In the meantime, he advised us to remove 2 m of sediment and unstable boulders from the rear of the cave. Mr. Hayrabetyan also installed an interim wooden safety structure. As part of the

Fig. 1.9 2004 season. **a** Access to Azokh 5 when it was first discovered. **b** View of the section facing the new entrance of Azokh 5 (with Dr. John Murray). At the back of the section (asterisk) there is direct access to the interior of the cave. See Figs. 1.11d, f and 1.14c. **c** Return of the 2002 fossils and 2003 stone tools. Dr. Fernández Jalvo (left), Dr. Balayan, Director, Artsakh State Museum of Country and History (middle) and Dr. Yepiskoposyan (right) on the return of the fossils

survey work a 1 × 2 m trench was excavated outside Azokh 2 in order to determine the degree of extension of the fossiliferous sediments and their association with the cave walls.

Fossils from the 2002 season were prepared for return to the Artskakh State Museum of Country and History (Fig. 1.9c). These fossils had been conserved and prepared for exhibitions and analyzed by specialists. Albums of photographs of these fossils were also given to the director of the museum, Dr. Melanya Balayan. After the 2004 excavation season in Azokh, the team conducted a survey with Armenian archaeologists in the Aragats region of Armenia for a week.

The participants of the 2004 season were L. Asryan, V. Bessa-Correia, P. Domínguez-Alonso Y. Fernández--Jalvo, T. King, A. Melkonyan, N. Moloney, J. Murray, V. Safarian, and L. Yepiskoposyan. Our local field assistants from the Azokh village were: K. Arakelian, S. Arakian, A. Arzumian, M. Balasanyan, A.Boghosian, Z. Boghosian, A. Gevorkian, A. Minassian, and A. Ohanyan.

2005 (26th July–12th August)

The Middle Platform (Unit Vm) of Azokh 1 was excavated for the whole of the 2005 season. In addition, excavation of Unit II started on the 2nd of August. Stone tools recovered from Unit II showed traits of Levallois technique. Several of our most experienced and skilled field assistants were given training in excavation techniques and were included in the excavation team under the supervision of one of the team members (Fig. 1.10a). This training was focused on excavations in Unit Vm, and the results were very satisfactory.

Fig. 1.10 2005 season. **a** Supervision by Dr. T. King of a field assistant on excavation procedures. **b** View of the excavation area at the Uppermost Platform (Unit II) by senior and experienced team members. **c** and **d** Three dimensional topographic mapping in the interior of the cave system and at the exterior, respectively

Excavations in Unit II, with a more complicated process of fossil recovery, were only carried out by expert team members (Fig. 1.10b). Other field assistants were assigned to help in the geological survey and with the wet sieving team at the river.

We investigated the back of Azokh 2 to determine how the cone of boulders blocking the connection between Azokh 2 and the interior of the cave might be removed manually from the vertical shaft above Azokh 2. We found that this would involve a great deal of manpower and more equipment than we had available, and we therefore postponed activity in the site except for replacing the wooden safety structure that was placed as a safety measure at the end of 2004 by a structure of iron bars weighted down with stones.

In Azokh 5, the main aim for this year was to continue stratigraphic exploration of this exposed section and to assess requirements for excavation in 2006.

Three-dimensional mapping of the cave system was completed this season. Geologists Drs Alonso Dominguez and Murray with two local field assistants from Azokh Village, M. Ohanyan and Z. Assyrian, undertook this work, both inside (Fig. 1.10c) and outside the cave (Fig. 1.10d), in order to determine cave formation processes. Masks and gloves were worn to protect against pathogens carried by the large colony of bats that inhabit the cave. Topographic investigations were made in the interior chambers of Azokh cave as well as outside it, in order to understand the source of sediments.

The participants of the 2005 season were: L. Asryan, P. Domínguez-Alonso, Y. Fernández-Jalvo, T. King, A. Melkonyan, N. Moloney, E. Mkrtichyan, J. Murray, and L. Yepiskoposyan. Our local field assistants from the Azokh village were: R. Abrahamian, A. Arzumian, Z. Assyrian, A. Gevorkian, M. Hayrabetian, A. Minassian, M. Ohanyan, G. Petrossian, and M. Zacharian.

2006 (30th July–23rd August)

The primary aim in 2006 was to excavate the "*fumier*" – a manure hearth from Unit I of Azokh 1. Azokh village elders told us that their ancestors had taken refuge in the cave, together with livestock, during periods of Russian, Turkish, and Persian conflicts since the XVIII century. Unfortunately, animals burrowing into the sediments had disturbed much of the unit, and some of these burrows also affected the top of Unit II (bw in Fig. 1.11a). The thickness of this hearth was about 40 cm and extended over 12 m^2. Ceramics, bones and remains of vegetation and excrement were recovered from this hearth and mapped. Human chewing marks were observed on bones recovered from this Unit (Fernández-Jalvo and Andrews 2011). The location of the hearth, in the entrance of the interior part of the cave system, might have had the purpose of deterring the incursion of animals and bats into the human occupation area.

The aerial grid system was extended to the very rear of the cave passageway, reaching 52 m from the cave entrance, and a laser pointer was fixed at 60 cm below the permanent datum as a reference for the depth (Z) coordinates. An aerial rope and pulley system was installed for the removal of excavated sediment from the Uppermost Platform of the sedimentary sequence (Fig. 1.11b).

Once the *fumier* was excavated, the excavation continued into Unit II. Its contact with Unit I is erosive (Fig. 1.11c, black arrow). The top of Unit II sediment has a crumbly appearance, and fossils are extremely damaged (Fig. 1.11c). Studies of temperature, humidity and pH were also carried out by the geologists, and detailed sampling every 20 cm for starch and pollen was carried out in sections in Azokh 1 and Azokh 5 (K. Hardy).

Excavation of the Azokh 5 passageway started that year in order to obtain a detailed stratigraphic log (Fig. 1.11d). Safety and feasibility for excavation were evaluated. The contact between soil and sediments containing fossils was found, photographed and mapped (Fig. 1.11e). Excavations of the fossiliferous sediments were carried on at the front of the sediment cone, and trenches were dug at the entrance and in the interior of Azokh 5, which showed that the sediments at the entrance of the cave passageway were formed as a wide gravitational cone. The sedimentary cone was formed by a mixture of sediment from several units at the top of the series, which had collapsed, probably several thousand years ago, blocking the present entrance from the passageway.

Inside the cave the vertical section of sediment was exposed (Fig. 1.11d), and we excavated a test pit to evaluate the fossil and artifact content of these deposits and to determine the characteristics of the units exposed in the section. Isolated teeth of *Homo sapiens* were found in the mixed cone at the entrance, and we located further isolated human teeth *in situ* in Unit A. Samples for radiocarbon dating were taken from Unit A (top of the series), and from Unit B for ESR dating. The thickness of fossiliferous sediments below unit E

Fig. 1.11 2006 season. **a** General view of Unit I and top of Unit II at the beginning of the 2006 season showing the uneven surface of Unit I and the extensive animal burrowing. The white arrow points to the manure hearth (fumier) before excavation in Unit I and the black arrow shows the erosional contact with Unit II (bw = modern burrows). **b** Sediment evacuation system using a pulley to reach the outside of the cave where sediment is processed. **c** View of Unit I at the end of the 2006 season; remains of the fumier reach the connection to the inner galleries (white arrow). Note the circle marking a large block of partially buried limestone that was taken as a reference mark (also shown in Fig. 1.11a). **d** Azokh 5 section and the stratigraphic layers (A to E) distinguished in the 4 m long section. Note the asterisk indicating the top of the section and connection with chamber V (see Fig. 1.11d). **e** Entrance to Azokh 5, clearance of the modern soil at the most distal trench (buckets) and small test pit (broken line) on the cone of collapsed and mixed sediments. **f** View of chamber V, in the inner cave system inhabited by bats. Note the asterisk indicating the connection with the 4 m long section in Azokh 5 (see Figs. 1.11d and 1.14c) covered by a large plastic sheet to prevent air currents that may disturb the bats

and their extent into the internal chamber V (Fig. 1.11f) were unknown at this time. Geophysical analyses of the cave were planned for the following season.

The participants of the 2006 season were: E. Allué, L. Asryan, I. Cáceres, P. Domínguez-Alonso, Y. Fernández-Jalvo, K. Hardy, H. Hayrabetyan, S. Hayrabetyan (our local engineer collaborator), T. King, D. Marin-Monfort, E. Mkrtichyan, N. Moloney, J. Murray, T. Sanz Martín, and L. Yepiskoposyan. Local Field Assistants from Azokh village were: A. Arzumanian, T. Assyrian, S. Avanessyan,

K. Azatkhanyan, A. Balasanyan, A. Bagdasaryan, Z. Boghosian, V. Dalakyan, A. Gevorkian, M. Hayrabetian, H. Martirossyan, and M. Zacharian.

2007 (9th July–4th August)

Geophysical analysis of the cave system of Azokh was carried out during the 2007 field season (Fig. 1.12a). This method is based on the different electrical conductivity/resistivity properties provided by empty cavities, sediments and rock. Unfortunately, the boulder collapse at the rear of Azokh 2 hampered any geophysical investigation there. The results of this geotechnical study provided further information on sediment thickness in Azokh 1 and 5, as well as the exact location of the bedrock, inner and upper galleries and connections that are blocked today (Domínguez-Alonso et al. 2016). Furthermore, total station equipment supplied this year by the Drambon Mine Company provided fixed coordinates for the topographic data measured the previous year and enabled us to reconstruct the three-dimensional

Fig. 1.12 2007 season. **a** Geophysical work outside the cave by Dr. Aracil (left) and Dr. Porres (right). **b** Total station operated by a Drambon Mine Company operator. **c** View of excavations in Azokh 1 taken at the end of 2007 season. Note the burrows made by modern animals (filled with sand sacs to prevent their collapse) affect the Holocene sediments of Unit I and the very top of Unit II (Middle Paleolithic). The small inset (bottom left) shows cleared sections of the fumier and sediments below for sedimentological study. The asterisk indicates the location of an end-scraping at the immediate limit between Unit I and Unit II (broken line). **d** Section of Azokh 5, the vertical white lines demarcate the 2 m^2 dug in the section during the 2007 season. **e** Excavations at Azokh 2. **f** Wet screening by the river

topography of the cave system (Fig. 1.12b). In addition, further work concentrating on Units I and II of the Azokh 1 stratigraphic series was carried out. The section was cleaned, and samples taken to analyze the geochemical and sedimentological traits of each unit.

Several expeditions to nearby valleys, aided by GPS and satellite pictures, were carried out in order to map outcrops of different rock types (limestone, volcanic rocks and sediments and tuffs). This was the first phase of work in preparing a regional geological map since there was currently no such map of the area. This was a long-term project that required further expeditions in order to map the entire area. Several samples were taken to date volcanic outcrops interbedded in the limestone that form the Azokh karstic system.

The excavations of Azokh 1 continued the systematic excavation of the top of the series in Unit I (Fig. 1.12c). Excavations focused on removing the remains of this unit beneath the large hearth (*fumier*) that was excavated the previous season. Our initial aim at that time was to preserve the lateral side of Unit I (Fig. 1.12c, section on right hand) and remains of the hearth (Fig. 1.12c, small inset) as reference sections for future studies.

Below the hearth, Unit I appeared poor in bone content and artifacts, probably because this was a distal part of the human occupation. Furthermore, as mentioned above, this unit was intensively burrowed by modern animals, and several erosive layers were also distinguished. These burrows, which were still in use and increased in size and number each year, facilitated the introduction of modern objects into underlying sediments, such as wire, paper and even labels and masks used by the excavation team during the previous season. Furthermore, remains from Unit II (such as Levallois stone tools and cave bear [*Ursus spelaeus*] fossils) were also introduced into Unit I by these burrowers. The sediments of Unit I compared with Unit II were found to have different directions and inclinations. Unit II sediments in the central squares contained poorly preserved large mammal fossils and a sparse microvertebrate fossil content. Fossils contained within the squares close to the cave walls were better preserved (see Marin-Monfort et al. 2016). A laser pointer was fixed at 1.60 m below the datum on the 29th of July 2007 to take coordinates from the middle part of Unit II.

In order to test the archaeological and paleontological richness of the Azokh 5 passageway, excavation work was concentrated on a 2 × 1 m test trench at the exposed section. The test trench produced limited remains, some charcoal and a few fossils (Fig. 1.12d), which is possibly due to the fact that these sediments are at the distal part originally attached to the walls of the cave infilling. The complexity of the site needed careful work and excavations were carried out from the top of the sequence in the large inner gallery (chamber V), rather than continuing work on the section.

Work in Azokh 2 continued in 2007. During preparation of the excavation area, a trench was extended between the two test pits made in 2002 and 2003 respectively. The 2 m^2 excavation was extended laterally to the southern side to obtain further information (Fig. 1.12e). These sediments yielded remains of butchered animals (mainly cow) and artefacts of different ages. In spite of the bad preservation of bone that lead to the low abundance of small vertebrates from the central squares of the excavation of Unit II in Azokh 1, the processing of the excavated sediments was difficult this season due to the large volume of material produced by the simultaneous excavation of Azokh 1 Unit I, Azokh 2 Units 1 and 2, and Azokh 5 Units A to E. An efficient but careful procedure was developed in order to effectively process these excavated sediments (Fig. 1.12f).

The participants of the 2007 season were: E. Allué, P. Andrews, L. Asryan, I. Cáceres, R. Campos, P. Domínguez-Alonso, Y. Fernández-Jalvo., H. Hayrabetyan, S. Hixson Andrews, N. Moloney, J. Murray, D. Marin-Monfort, M. Nieto, A. Pinto, and T. Sanz Martín. Specialists collaborators were: S. Hayrabetyan, E. Aracil, and J. Porres. Local field assistants from Azokh village were: T. Assyrian, K. Azatkhanyan, A. Arzumanian, S. Avanessyan, A. Bagdasaryan, A. Balasanyan, G. Balasanyan, M. Balasanyan, Z. Boghosian, V. Dalakyan, A. Gevorkian, M. Hayrabetian, H. Martirossyan, M. Ohanyan, and M. Zacharian.

2008 (8th July–14th August)

Geological work during the 2008 season was focused on the Azokh 1 sedimentary sequence, providing information on the formation of the cave and the nature of the different deposits recorded in the cave of Azokh 1. A trench was dug from the Lower platform of the cave to make a connection between the geological trench opened by the present excavation team in 2002 and the trench at the entrance opened by Huseinov's team. These trenches exposed the bedrock below the Lower Platform and confirmed the distinct topography of the bedrock (Fig. 1.13a) indicated the previous year by the geophysical work (Fig. 1.13b). Geological results also indicated that the Azokh 5 sequence contained up to 10 m of continuous sedimentation, 4 m of which were exposed in the entrance section. This finding greatly increased the potential of this new site, and excavation was started in the top units. There were, however, difficulties in installing an aerial grid (see Fig. 1.5a) above the section discovered from the Azokh 5 entrance (the connection between these two areas is marked by an asterisk in Fig. 1.11d, f) because of the high chert content of the limestone.

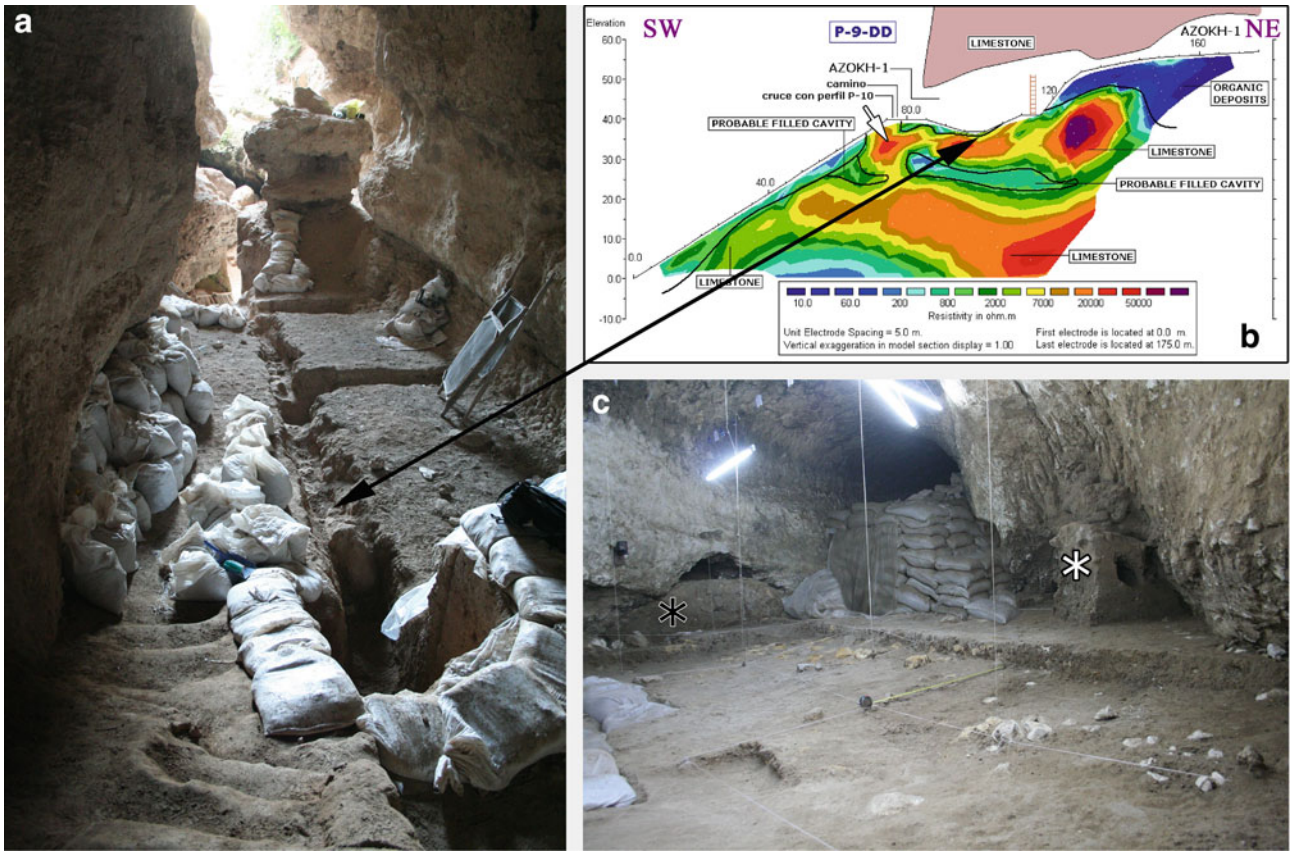

Fig. 1.13 2008 season. **a** View of the trench dug during the 2008 season in Azokh 1 Lower Platform connecting the trench dug by Huseinov's excavation team in the 1970s (on the left of the 'pedestal') and the geological trench dug by us in 2002 (see Fig. 1.5b) uncovering the limestone bedrock. **b** Electrical tomography of Azokh 1 showing the irregular topography of the bedrock underneath the Lower Platform (double head arrow relates the tomography and the uncovered bedrock). **c** View of the extended excavation surface of Unit I and top of Unit II (see text). In addition to the reference section of the 'fumier' (here covered by sacks) two more areas were left as reference sections, a small one encased in an irregularity of the cave wall (black asterisk) and a section next to the fumier (white asterisk) burrowed by modern animals; note the latest section was not exposed in Fig. 1.12c

Excavations in Azokh 1 completed the work in Unit I (Fig. 1.13c). The lateral section, which was left as a reference section, was intensively burrowed and there was a high risk of collapse. Extending the excavation area also allowed us to better interpret sedimentation processes in the cave. The broadening of the excavation area also provided further information about the behavior and social strategies of humans during the occupations of the cave in the past.

The large hearth–*fumier* uncovered in 2006 and sediments below will be left as a reference section for future studies and for guided visits to the cave. This reference section is situated at the connection between the entrance chamber and the interior gallery, inhabited today by bats (Fig. 1.13c) and considered to be the best for archaeological purposes. At the end of each excavation season, the section is covered and protected and has so far survived intact. However, the location of the section on the pathway used by visitors accessing the cave interior puts it at risk of damage and endangers its preservation. Therefore, it was apparent that restricting access through this passage was necessary to ensure the section preserved in the long-term. This would also be of benefit for the large bat colonies inhabiting the interior galleries, since they have been subject to disturbances by large number of unsupervised visitors using fire torches. This suggestion was reinforced by a report written on the protection of bat communities by one of our research team, which discussed the negative impact of such visits on the bat colonies (Sevilla 2008).

We continued excavating the test pit on the Uppermost Platform (Units II and III) that was started in 2003. Further excavation of this test pit from Unit IV to the contact with Unit V was aimed at coming to a better understanding of the stratigraphy and sediments, as well as the fossil and lithic content of these units. Unfortunately, the unstable nature of the remaining sections of sediment exposed made work unsafe, and Unit IV has yet to be excavated. Only a small portion of this unit (smaller than 1 m^2) could be dug in 2008. We can confirm the presence of large mammal fossils and

artifacts in Unit IV, but further studies and especially broader extension of the excavation are needed.

Excavation in Azokh 2 continued during the 2008 season.

The participants of the 2008 season were: E. Allué, L. Asryan,, I. Cáceres Y. Fernández-Jalvo, H. Hayrabetyan, L. Hovsepyan, T. King, N. Moloney, D. Marin-Monfort, J. Murray, T. Sanz Martín, S. Turner, and L.Yepiskoposyan. Local field assistants were: Z. Asryan, K. Avagyan, M. Avagyan, A. Azumanyan, A. Balasanyan, M. Balasanyan, A. Gevorkyan, A. Hairbetyan, A. Ohanjanyan, M. Ohanyan, and E. Zakharyan.

2009 (17th July–12th August)

Before starting the excavations, part of the team gave a presentation at the National Assembly in Stepanakert on the research at Azokh caves carried out by our team. The Head of the National Assembly, the Minister of Culture, the Head and other members of the Department of Tourism, as well as the Director of the Artsakh State Museum of History and Country Study, relevant academic members of the State University of Artsakh and colleagues from the archeological project at Tigranakert, all attended this meeting. Local

Fig. 1.14 2009 season. **a** Scaffolding installation in Azokh 1 and view of the excavation area in Unit Vm excavating the lateral side that could not be reached before. **b** View of the extended excavation in Azokh 1 Unit II on the edge of the section. **c** View of the extended excavation area in chamber V above Azokh 5 (the asterisk marks the connection with Azokh 5 section, see Fig. 1.11d, f). **d** View of the small chamber discovered at the basal (entrance trench) of Azokh 1 (underneath the steps built in 2002, compare with Fig. 1.4c) white arrow in Fig. 1.13b. **e** View of the interior of the small chamber with stalactites, stalagmites and 'dog tooth' formation

authorities also attended the presentation from Azokh, including the past and present mayors of the village, and the headmaster of the school. Several specialists from our team made the presentation in English, with simultaneous translation into Armenian by two members of the team. After the talk, several questions from the audience gave rise to interesting exchanges of information and support for the continuation of our project at Azokh. Several of the academics and authorities that attended the presentation also visited the site, some for the first time.

Excavations in Azokh 1 were focused on extending the excavations of Unit Vm and Unit II (Fig. 1.14a, b). In previous years we had left the areas lateral to the Unit V excavation surface covered by overburden to facilitate access to the excavation area at the top of the sequence using a ladder. In 2009 the ladder was removed and replaced by scaffolding, donated by Base Metals Ltd, a local mining company. The scaffolding allowed us to extend the excavation of Unit Vm to squares H and I (Fig. 1.14a). The augmented collections from Units II and Vm are to provide material for two doctoral theses and a master thesis by three students in our team. A second aim was to start systematic excavation of the deposits of Azokh 5. The excavation proceeded from the top of the series, which dates from the Iron Age and yielded a collection of ceramics. Given the difficulties of this cave chamber for installing an aerial grid, we used a total station (Fig. 1.14c). The total station was also used in Azokh 1 to coordinate some geological samples, as well as finds that appeared during the clearing of sections at different points near the cave entrance.

Geological and geomorphological investigations of the cave deposits continued. The studies required detailed sampling to accomplish investigations on the sedimentology and geochemical traits of the sediments. A second study of electrical tomography (made by Análisis y Gestión del Subsuelo S.L. specialists) was also carried out that season (Fig. 1.14d), with the aim of increasing information about the extent and depth of the sediments in the interior of the cave (especially chamber V which connects to Azokh 5 see Fig. 1.5a). Further investigations of the trench adjacent to the cave entrance made by the previous excavation team (lead by Huseinov) led to the discovery of a small chamber at the entrance to Azokh 1 (Fig. 1.14e). There are no sediments present, but samples for dating were taken from a speleothem in the interior of the chamber. This chamber has delicate 'dog tooth' calcite crystals and copious development of speleothems, both stalactites and stalagmites (Fig. 1.14f). 'Dog tooth' formation indicates that the chamber was partially immersed in calcareous water, allowing crystals to grow. The previous excavation team did not refer to this small cave, and there was no evidence of anthropic activity there. However, the cave was originally sealed by a stalagmite flow crust and isolated from the trench, but only a small piece of this crust remained *in situ*, most having been broken. A sample taken from this part of the cave yielded an age of 1.19 ± 0.08 Ma (see Appendix, uranium–lead).

During this season gates were installed in all the cave entrances to protect the excavation areas from visitors to the site during the year. The Government of Nagorno-Karabakh facilitated this, and at the same time, the Government employed a guardian and official guide at the site, who conducts visits to the cave. In addition, from this time onwards visitors wishing to visit the interior of the cave inhabited by the bat colonies must obtain written permission from the relevant government department. The gates were designed according to the guidelines of the International Group of Chiroptera specialists in order to prevent disturbance to the bats that inhabit the interior of the cave during their daily transit in and out of the cave. These gates do not completely prevent all unauthorized or unsupervised visits to the cave, but rather convey to visitors that this site is important and must be protected.

The participants in the 2009 season were: E. Allué, M.C. Arriaza, L. Asryan, S. Bañuls, I. Cáceres, P. Domínguez-Alonso, V. Faundez, Y. Fernández-Jalvo, N. Ghambaryan, H. Hayrabetyan, L. Hovanisyan, L. Hovsepyan, A. Mardiyan, D. Marin-Monfort, N. Moloney, J. Murray, T. Sanz Martín, and L.Yepiskoposyan, Specialist Collaborators: J. Porres and M. Miranda. Local field assistants were: T. Asryan, A. Arzumanian, S. Avanesyan, K. Azatkhanyan, A. Bagdasaryan, A. Balasanyan, G. Balasanyan, M. Balasanyan, Z. Boghosian, V. Dalakyan, A. Gevorkian, M. Hayrabetian, H. Martirosyan and M. Zacharian.

Correlating Huseinov's Layers to Our Units

Units distinguished in the current excavations may not correspond in detail with layers distinguished by Huseinov, but it can be assumed that the original stratigraphy has been identified in general terms. There are some descriptions that are imprecise or that are at odds with our observations. Layer X, for instance, has been described to be either the bedrock or a unit that we have not identified. Lioubine (2002, p. 25) refers to this unit as follows: "Nous remarquerons que la couche archéologique X est considérée par les géologues comme située plus bas dans le profil et comme étant la roche-mère altérée (Gadziev et al. 1973, p. 13), à l'intérieur de laquelle 'des découvertes n'ont pas été réalisées' (Suleimanov 1979, p. 45). Cependant, Guseinov y voit 'le stade initial de l'occupation de la grotte' et décrit 16 outils lithiques apparemment trouvés là (Guseinov 1985: 14)." If Layer X is the bedrock, it would be unusual to recover stone tools from it. If it was a layer at the base of the

series, it would have been very thin and heterogeneous. We have not yet resolved this issue.

Sediments in the trench (Units IX to VI) have been distinguished by Murray et al. (2010, 2016) as a separate sequence (Sequence 1) that is distinct from fossiliferous Units V to I containing lithics and evidence of human presence (Sequence 2). Original descriptions by Huseinov and colleagues stated that this trench produced 186 tools assigned to the Oldowan technique (Mode 1) (Mustafayev 1996), although the human manufacture of these stones is still under debate. We have not found fossils or lithics in the sediments of Sequence 1 so far except for Unit VI, that yielded some fossils. Murray et al. (2016) suggest that either the limited sediments left in the trench by previous excavations may explain the lack of fossils, or this may reflect that the cave was not open to the outside when it was deposited (Murray et al. 2010). However, only traces of sediments from Unit IX to VII remain, and the only trace of Unit VI is in irregularities of the cave walls and at the base of the 'pedestal' (see Fig. 1.3b black arrow, and Murray et al. 2016)..

In the course of digging the connecting trench from the middle platform to the cave entrance trench, we found that bedrock outcropped at the level of what we called the Lower Platform (Fig. 1.13a). This discovery definitively indicates two episodes during deposition of the cave sediment, with Sequence 1 (Units IX to VII) restricted to the trench at the entrance. The outcropping bedrock indicates correlation between the base of Unit VI and the base of Unit V (Murray et al. 2010). Unit VIc was laid down by water, probably a small river, and the fact that it wedges out towards the interior of the cave means that it cannot be readily identified at the base of the Middle Platform. This may suggest that it was produced by water flowing into the cave from the exterior (Murray et al. 2010). Before the Unit VI event, the cave was probably below the water table (Fig. 1.15).

There is a variation in the sedimentation pattern within the cave in Unit VI and after deposition of sediments in the trench, and it may represent the opening of the cave that allowed animals and humans to enter and occupy it (Murray et al. 2010). The small valley in front of the cave formed when the cave was opening. The flooding indicated by Unit VIc may then represent the moment at which the small river valley was at the same height as the cave. As the base level of the valley lowered through erosion (Fig. 1.15), the cave would become free of flooding, and animals and humans would be able to enter and occupy the cave.

Unit V extends towards the back of the cave from the bedrock to what we named the Upper Platform. The contact between Unit V and Unit IV is diffuse and irregular, and it is difficult to distinguish the contact precisely (Fig. 1.16). Geological studies in this part of the section have shown that Unit V extends above the surface of the Upper Platform, and fossils found here were labeled as belonging to Vu (V upper,

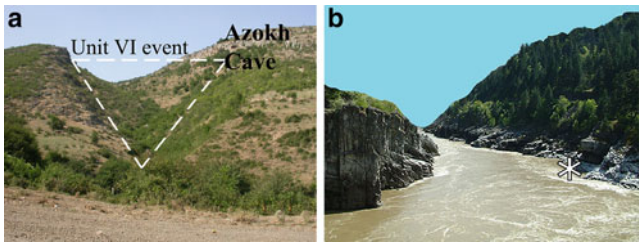

Fig. 1.15 **a** View of the small valley in front of the Azokh caves. The "Unit VI event" indicates the height of the paleo-river when Unit VI was accumulating in Azokh Cave. **b** Possible reconstruction of the landscape before the "Unit VI event" (the asterisk points to the hypothetical emplacement of Azokh Cave)

which corresponds to the top of the stratigraphic Unit Va described by Murray et al. (2010, 2016). Recently we have confirmed that Unit Vu may contain fossils from the base of Unit IV, especially from squares near the wall where the

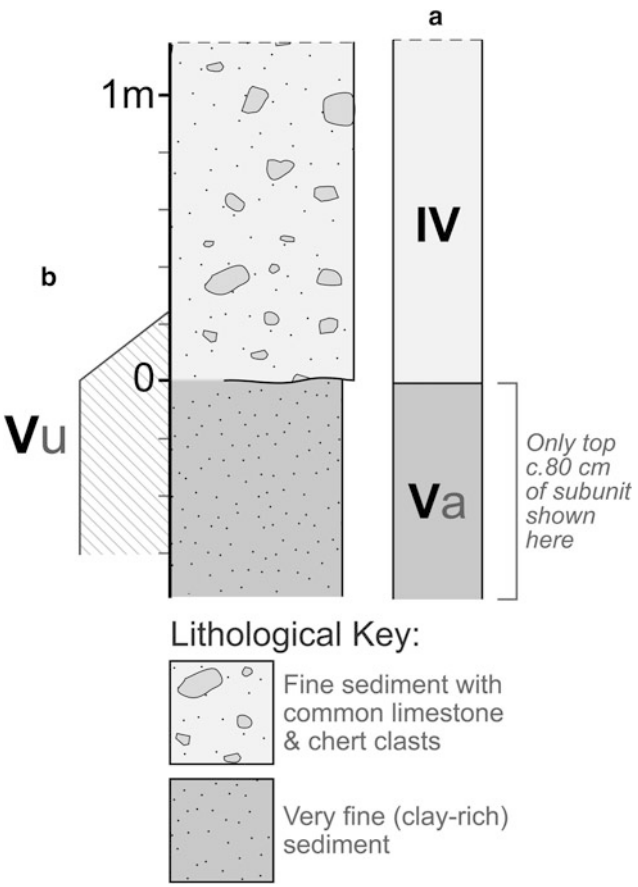

Fig. 1.16 Detailed view of the stratigraphic contact between Units V and IV in Azokh 1. **a** Lithostratigraphic unit terminology employed by Murray et al. (2010, 2016) for this part of the succession; **b** Terminology for richly fossiliferous interval recovered from Upper Platform (mentioned in Chaps. 4 and 6–15 in this volume). Note that Unit Vu may include the base of Unit IV in the transitional zone close to the cave wall where the limit between IV and V was difficult to distinguish precisely

contact between Units IV and V is at a different level. Excavations of Unit IV in the future will solve the current problem, and we have still to distinguish the Unit IV–V contact near the wall. We have assigned Unit Vm (V middle) to fossils and lithics recovered from the Middle Platform (surface left by previous excavations), which corresponds to the middle part of the stratigraphic Unit Vb described by Murray et al. (2010, 2016).

According to Huseinov, only microfauna was recovered from Layer IV (Lioubine 2002), and the lack of large mammals and stone tools from Huseinov's excavations suggested that humans abandoned the cave during this period (Mustafayev 1996). We can, however, confirm the presence of large mammal fossils and artifacts in Unit IV, although further studies and especially proper excavation are needed.

Currently, excavations in Unit I and Unit II have been almost completed over a wide area, although the remaining part of Unit I did not extend over more than 18 m^2. Unit II extends at present to roughly 40 m^2. The contact of Units I and II is a disconformity indicating that sediments deposited during the Late Pleistocene were removed by erosion. The contact shows laminar sediments in some parts of Unit I (Fig. 1.11a black arrow), and this may suggest that the erosion was produced by floodwater.

Chapters of This Book

The following fourteen chapters have been devoted to different aspects of research on the Azokh caves, plus an Appendix documenting the dating of the sediments and fossils using different methods. They are briefly summarized below.

Chapter 2: *Stratigraphy and Sedimentology of Azokh Caves, South Caucasus* Murray et al. (2016).

The stratigraphic sequences of Azokh 2 and Azokh 5 are described fully here for the first time, together with a detailed description of Azokh 1. The sedimentary sequence of Azokh 1 is broadly divisible into nine units that are divided between two geographically isolated sequences. The lowermost sequence or Sequence 1 (Unit IX to Unit VI) is predominantly non-fossiliferous but becomes both fossiliferous and calcareous at the very top, which displays evidence of fluvial deposition Unit VI. The upper sequence or Sequence 2 (Units V to I) is richly fossiliferous and has yielded many different species of mammals (macro and micro) and evidence for human occupation. The Azokh 2 sedimentary sequence is at least 1.65 m in depth, although the base has not been reached, and a boulder collapse in the rear of the chamber has hampered comprehensive investigation efforts. The connection of Azokh 5 with the largest cave hall of the Azokh karstic system has revealed at least 4.5 m of cave-filling sediment, which is divisible into five stratigraphic units (A–E), but the sequence continues about six more meters in depth.

Chapter 3: *Geology and Geomorphology of Azokh Caves* Domínguez-Alonso et al. (2016).

The geomorphology of the currently accessible portions of the karstic cave network at Azokh, and data relating to the surface topography of the internal cave fill, document the pattern of karst formation and speleological processes. Analytical methods include electrical tomography, total station coordinates and topographic measurements of the interior and exterior of the caves. The most interesting result from electrical resistivity (tomography) is the thickness of sedimentary sequences in Azokh 1 and Azokh 5 (up to 10 m). These geophysical studies indicate the presence of a small blind chamber at the cave entrance of Azokh 1, as well as the irregular bedrock topography at the passage (lower platform) to the rear of the cave chamber of Azokh 1.

Chapter 4: *Lithic Assemblages Recovered from Azokh 1* Asryan et al. (2016).

Descriptions of the lithics recovered in the stratigraphic units and their significance in the Middle–Late Pleistocene of the Caucasus concentrate particularly on those from Middle Paleolithic contexts. Artifacts are predominantly made from local raw materials. Levallois technology is well represented in core preparation and a range of blank types (flakes, points and blades). Retouch of Levallois and non-Levallois pieces is generally non-invasive but also includes some examples of basal thinning. The Middle Paleolithic assemblage presented here is consistent with the lithic traditions evident in other areas of the Lesser Caucasus. In contrast to previous excavations, the lithic assemblage of Azokh 1 is not abundant from these excavations, probably as result of the location of the excavation at the rear of the cave. Evidence of knapping in this part of the cave has not been observed. Further microwear investigations of these lithics, field work to localize obsidian, hornfels and siliceous raw material sources, as well as experimental work (e.g., trampling, corrosion) to explain post-depositional modifications of these tools, are in progress.

Chapter 5: *Azokh Cave Hominin Remains* King et al. (2016).

The hominin remains discovered from the three different passageways connecting the outside with the internal chambers are described in this chapter. A fragment of Middle Pleistocene hominin mandible was found in Azokh 1 by the previous excavation team in the 1960s and named as "Palaeoanthropus"; this specimen is described based on a replica. It is tentatively assigned to *Homo heidelbergensis*. In 2010 a complete permanent first upper left molar tooth was found at the top of the series in Azokh 1 in deposits dating to 100 ka. A preliminary description and metric analysis of the

tooth assigns the specimen to *Homo neanderthalensis*. In 2007 an incomplete partial skeleton and two teeth, thought to belong to the same individual, were found in Azokh 2. Human teeth and a phalanx have been found in Azokh 5. Dental description is detailed in this chapter.

Chapter 6: *The New Material of Large Mammals from Azokh and Comments on the Older Collections.* Van der Made et al. (2016).

All fossiliferous units have large mammal taxa that in mid-latitude Europe are considered to be "interglacial" elements, while there are no clear "glacial" elements, which suggests warm temperate conditions despite the altitude of the cave. Situated just south of the Lesser Caucasus mountains, the area is by definition Asian, though it might be more useful to consider this area part of western Eurasia. Many "typically European" species range far into Asia, as did Neanderthals. The most abundant large mammal species in the Azokh I sequence are the cave bear *Ursus spelaeus*, several species of cervids and bovids (*Cervus elaphus*, *Dama¸ Capra aegagrus*), together with tortoise, lagomorphs, rodents, reptiles and amphibians, all of which are ubiquitous at all levels. Large felids (*Panthera pardus*), canids (*Canis lupus, Vulpes vulpes*) and bison are present in Unit II; rhino (*Stephanorhinus*) and badger are known from Unit Vu, wolf, jackal and hyaena (*Crocuta crocuta*), *Megaloceros* and roe deer are present in Unit V, and wild pigs (*Sus scrofa*) have been identified at most units so far. An interesting aspect of the study area is its geographical and biogeographical position as they relate to inter-continental faunal movements. Most species present are common in western Eurasia.

Chapter 7: *Rodents, Lagomorphs and Insectivores from Azokh Cave* Parfitt (2016).

Small mammals are abundant in Azokh 1. The rodent assemblages are dominated throughout by arvicoline rodents indicative of dry steppes and semi-deserts. Several regionally extinct arid-adapted or montane taxa are also well represented throughout the sequence. Unit Vu has yielded the earliest Caucasian record of rat (*Rattus* sp.), a genus previously thought to have been a relatively recent (late Holocene) introduction. The small mammal fauna shows broad similarities to those from semi-desert and steppe regions to the south, implying dispersals from southwestern Asia; there appear to be only tenuous links with the Pleistocene small mammals north of the Caucasus. The striking difference in environmental reconstruction between the small and large mammals is interpreted as due to taphonomic bias.

Chapter 8: *Bats from Azokh Caves* Sevilla (2016).

Azokh Cave is one of the most important shelters for living colonies of bats in the Caucasus. Over 70,000 bats have been recorded in the cave during the winter, consisting mainly of colonies of the Lesser Mouse-eared bat (*Myotis blythii*) and Mehely's Horseshoe bat (*Rhinolophus mehelyi*). These numbers increase during the summer, as Schreiber's Long-Fingered bats (*Miniopterus schreibersii*) breed in the cave, forming large nursery colonies. Four other species occur either as smaller colonies or roosting singly, mainly occupying rock crevices. The abundant bat fossils preserved in the sediments of the cave show that the three main species found today in Azokh Cave have been using this same shelter for the past 300 kyr. However, their relative abundances vary from one layer to another, with variations in the rarer species also being observed. Since the sediments excavated at Azokh Cave were formed during a time interval with major climatic changes, an excellent example of how environmental changes in the past may have caused changes in the bat populations of a cave is provided by the long stratigraphic sequence in Azokh 1.

Chapter 9: *Amphibians and Squamate Reptiles from Azokh 1* Blain (2016).

Lower vertebrate fossils from Azokh cave include three anuran species, at least five lizards and seven species of snakes. Some of them are characteristic of high altitudes in the Caucasus today, while other taxa have greater similarities with the fossil and extant herpetofauna of the Irano-Turanian or Mediterranean biogeographical provinces. No mid Asian desert taxa have been found. Through the Azokh 1 chronological sequence, the evolution of the paleoherpetofaunal assemblages suggest a progressive increase in aridity between Unit Vu (late Middle Pleistocene) and Units II and I (Late Pleistocene to Holocene periods), with replacement of meadow-steppe environments by an arid mountain steppe environment.

Chapter 10: *Taphonomy and Site Formation of Azokh 1* Marin-Monfort et al. (2016).

The taphonomic study reported here is based on the large mammal assemblage recovered from Azokh 1. We have been able to distinguish the sources of the large mammal fauna recovered from Azokh 1, the interactions between cave bears and humans, the extent to which bat guano influenced fossil preservation, and the role of humans and bears in the accumulation/dispersal of the fossils. The extensive guano deposits in the cave have heavily damaged these fossils and produced geochemical changes. The taphonomic sequence of events that gave rise to the site formation of Azokh 1 is described here. Small mammal taphonomy is described in Chap. 15.

Chapter 11: *Bone Diagenesis at Azokh Caves* Smith et al. (2016).

Bone diagenesis processes transform the organic and mineral phases of bone during decay and fossilization. In order to understand how these processes have affected the skeletal material recovered from Azokh caves (and in particular to assess the organic preservation of the bones), "diagenetic parameters" of skeletal material from Holocene, Late Pleistocene and Middle Pleistocene deposits from Azokh caves have been measured. These indicate that the bone organic content from the Pleistocene layers of Azokh is

poorly preserved, and many bones show evidence of extensive infilling of the pores with secondary minerals. This type of preservation has not previously been described in archaeological material.

Chapter 12: *Coprolites, Paleogenomics and Bone Content Analysis* Bennett et al. (2016).

Coprolites from fossil sites and present day scats/excrements are signs of the activity of carnivores and herbivores present at the site or nearby environment. Unit II from Azokh 1 yielded two complete undamaged coprolites. Taphonomic, geochemical and biometric indications were not conclusive about the identity or source of the coprolites. Targeted mitochondrial DNA analyses performed on one of the coprolites yielded mitochondrial sequences identical to those of modern brown hyena (*Hyaena brunnea*). However, this finding was not supported by further investigation using next-generation high throughput sequencing. The most parsimonious interpretation of the results of the genetic analyses is that the highly sensitive PCR assay reveals contamination of the coprolite with minute amounts of modern brown hyena DNA presumably originating from brown hyena scats sampled recently in the same laboratory.

Chapter 13: *Paleoenvironmental Context of Coprolites and Plant Microfossils from Unit II, Azokh 1* Scott et al. (2016).

No pollen was found in the sediments of Azokh 1, probably due both to oxidation from persistent humidity changes in the cave and to increasing scarcity of pollen with distance from the cave opening. One possible source, however, is from the complete and undamaged coprolites recovered from Unit II. These coprolites contained rare diatoms and pollen, which indicate proximity to water; and numerous phytoliths were found. The phytoliths in the coprolites were compared with those in associated deposits in the cave and modern soils, both in order to interpret the past environment in the area and to build up a complete spectrum of the vegetation in the area.

Chapter 14: *Charcoal Remains from Azokh 1: Preliminary Results* Allué (2016).

Charcoal from fires in the caves is well preserved in the upper sedimentary units of Azokh 1. The taxonomic study of the charcoal has identified some of the wood used as firewood by the human groups occupying the caves. Changes in taxonomic composition can be related both to human activities in the caves and to availability of plants in the surrounding region. The plants identified indicate that deciduous woodland was the predominant vegetation type in the vicinity of the caves. There is no indication of vegetation or climatic change up through the sedimentary sequence.

Chapter 15: *Paleoecology of Azokh 1* Andrews et al. (2016).

Paleoecological interpretations obtained from data on the fauna and flora provide evidence on past environments. Plant data from charcoal and phytoliths indicate the presence of local and regional woodland vegetation; small mammal, amphibian and reptile species richness patterns indicate the presence of arid environments; large mammals and bats indicate warm temperate conditions and woodland again. The contrast between these different lines of evidence are attributed to taphonomic processes, for the small vertebrates are shown to be the result of predator accumulations, and the identity of the predators suggest that they preferentially hunted in open environments some distance from the cave. Large mammals and plants are more proximal to the cave and indicate local conditions. The conclusion is that woodland was present on the mountain slope adjacent to the cave, with arid areas on the lower slopes away from the cave, which is exactly what is present in the area today in the Azokh region.

Chapter 16: *Appendix: Dating Methods Applied to Azokh Cave Sites.* Introduction: Fernández-Jalvo; Radiocarbon: Ditchfield; Electron Spin Resonance: Grün, Lees & Aubert; Amino acid racemization: Torres, Ortiz & Díaz Bautista; Uranium Lead: Pickering (2016).

Racemization combined with ESR and U/Th series dating shows an age of around 300 ka for Unit V from which a human mandible fragment was found in the 1980s. An ESR date of 205 ± 16 ka has been calculated for the area of the contact between the top of Unit V and the base of Unit IV. U–Pb dating has been applied to a speleothem sample brought from the small cave at the entrance to Azokh 1 'Lowermost Level' giving an age of 1.19 ± 0.08 Ma. This is currently the oldest age for any material from the Azokh Cave Complex and gives a minimum age for the formation of the cave itself. Other methods of dating have been tried, but some such as thermoluminiscence (TL), cosmogenic or optically stimulated luminescence (OSL) could not be carried out because sediments currently under excavation are too deep inside the cave and derived from within the cave. Bat guano has caused diagenetic alteration of fossil bones that affected radiocarbon dating of the actual fossils, and the influence of diagenesis on samples is discussed in the chapters on bone diagenesis and taphonomy. Radiometric methods for the top of the sequence have provided dates of ~2300 years BP (384 calBC) for middle Unit A of Azokh 5, and 1265 ± 23 years BP (8th century) for the Unit 2 of the Azokh 2 sequence. Dates from the top of Azokh 1 are too young and results are not isotopically reliable.

Acknowledgments The publication of this volume has been made possible thanks to the research team members and invited colleagues who contributed to these chapters. To all of them our deep recognition of their professional work. These excavations and, therefore, this book could not have been possible without the strong commitment and good work of the field team members: those who participated in the excavations, whose names are given in the yearly seasons described above, those who recovered, recorded and prepared the different items, and the authors of each of these chapters.

References

Allué, E. (2016). Charcoal remains from Azokh 1: Preliminary results. In Y. Fernández-Jalvo, T. King, L. Yepiskoposyan & P. Andrews (Eds.), *Azokh Cave and the Transcaucasian Corridor* (pp. 297–304). Dordrecht: Springer.

Andrews, P., Hixson Andrews, S., King, T., Fernández-Jalvo, Y., & Nieto-Díaz, M. (2016). Palaeoecology of Azokh 1. In Y. Fernández-Jalvo, T. King, L. Yepiskoposyan & P. Andrews (Eds.), *Azokh Cave and the Transcaucasian Corridor* (pp. 305–320). Dordrecht: Springer.

Appendix: Fernández-Jalvo, Y., Ditchfield, P., Grün, R., Lees, W., Aubert, M., Torres, T., et al. (2016). Dating methods applied to Azokh cave sites. In Y. Fernández-Jalvo, T. King, L. Yepiskoposyan & P. Andrews (Eds.), *Azokh Cave and the Transcaucasian Corridor* (pp. 321–339). Dordrecht: Springer.

Asryan, L., Moloney, N., & Ollé, A. (2016). Lithic assemblages recovered from Azokh Cave 1. In Y. Fernández-Jalvo, T. King, L. Yepiskoposyan & P. Andrews (Eds.), *Azokh Cave and the Transcaucasian Corridor* (pp. 85–101). Dordrecht: Springer.

Bennett, E. A., Gorgé, O., Grange, T, Fernández-Jalvo, Y., & Geigl, E. M. (2016). Coprolites, paleogenomics and bone content analysis. In Y. Fernández-Jalvo, T. King, L. Yepiskoposyan & P. Andrews (Eds.), *Azokh Cave and the Transcaucasian Corridor* (pp. 271–286). Dordrecht: Springer.

Blain, H.-A. (2016). Amphibians and squamate reptiles from Azokh 1. In Y. Fernández-Jalvo, T. King, L. Yepiskoposyan & P. Andrews (Eds.), *Azokh Cave and the Transcaucasian Corridor* (pp. 191–210). Dordrecht: Springer.

Domínguez-Alonso, P., Aracil, E., Porres, J. A., Andrews, P., Lynch E. P., & Murray, J. (2016). Geology and geomorphology of Azokh Caves. In Y. Fernández-Jalvo, T. King, L. Yepiskoposyan & P. Andrews (Eds.), *Azokh Cave and the Transcaucasian Corridor* (pp. 55–84). Dordrecht: Springer.

Doronichev, V. B. (2008). The Lower Paleolithic in Eastern Europe and the Caucasus: A reappraisal of the data and new approaches. *Paleoanthropology*, 107–157.

Doronichev, V., & Golovanova, L. (2010). Beyond the Acheulean: A view on the lower Paleolithic occupation of Western Eurasia. *Quaternary International, 223–224*, 327–344.

Fernández-Jalvo, Y., & Andrews, P. (2011). When humans chew bones. *Journal of Human Evolution, 60*, 117–123.

Fernández-Jalvo Y., King, T., Andrews, P., Moloney, N., Ditchfield, P., Yepiskoposyan, L., et al. (2004). Azokh Cave and Northern Armenia. In E. Baquedano & S. Rubio Jara (Eds.), *Miscelánea en homenaje a Emiliano Aguirre, Vol. IV: Arqueología*. Alcalá de Henares, Museo Arqueológico Regional, 158–168.

Fernández-Jalvo, Y., Hovsepian-King, T., Moloney, N., Yepiskoposyan, L., Andrews, P., Murray, J., et al. (2009). *Azokh Cave project excavations 2002–2006: Middle-Upper Palaeolithic transition in Nagorno-Karabagh*. Coloquios de Paleontología, Special Issue: Homage to Dr. D. Soria Madrid, Universidad Complutense de Madrid Press.

Fernández-Jalvo, Y., King, T., Andrews, P., Yepiskoposyan, L., Moloney, N., Murray, J., et al. (2010). The Azokh Cave complex: Middle Pleistocene to Holocene human occupation in the Caucasus. *Journal of Human Evolution, 58*, 103–109.

Gabunia, L., Vekua, A., Lordkipanidze, D., Swisher III, C. C., Ferring, R., Justus, A., et al. (2000). Earliest Pleistocene hominid cranial remains from Dmanisi, Republic of Georgia: Taxonomy, geological setting, and age. *Science, 288*, 1019–1025.

Grün, R., Tani, A., Gurbanov, A., Koshchug, D., Williams, I., & Braun, J. (1999). A new method for the estimation of cooling and denudation rates using paramagnetic centres in quartz: A case study on the Eldzhurtinskiy Granite, Caucasus. *Journal of Geophysical Research, 104*(B8), 17531–17549.

Huseinov, M. M. (1965). O resul'tatah archaeologicheskich raskopok y Azykskoy pesheri. *Archaeologicheskie Otkrytia, 1971*, 477.

Huseinov, M. M. (1974). Ochagi azikantropov baku-chazarskogo (mindel-riss) vozrasta. *Azerbaijan University, N1*, 54–63.

Huseinov, M. M. (1985). *Drevniy paleolit Azerbaidjana (cul'tura Kuruchay i etapy ee razvitia) (The Early Palaeolithic of Azerbaijan (Kuruchai culture and stages of its development).* Baku: Elm (Russian).

Kasimova, R. M. (2001). Anthropological research of Azykh Man osseous remains. *Human Evolution, 16*, 37–44.

King, T., Fernández-Jalvo, Y., Moloney, N., Andrews, P., Melkonyan, A., Ditchfield, P., et al. (2003). Exploration and survey of Pleistocene Hominid Sites in Armenia and Karabagh. *Antiquity, 77s*. http://antiquity.ac.uk/projgall/king/king.html.

King, T., Compton, T., Rosas, A., Andrews, P. Yepiskoyan, L., & Asryan, L. (2016). Azokh Caves Hominin Remains. In Y. Fernández-Jalvo, T. King, L. Yepiskoposyan & P. Andrews (Eds.), *Azokh Cave and the Transcaucasian Corridor* (pp. 103–106). Dordrecht: Springer.

Krause, J., Fu, Q., Good, J. M., Viola, B., Shunkov, M. V., Derevianko, A. P., & Pääbo, S. (2010). The complete mitochondrial DNA genome of an unknown hominin from southern Siberia. *Nature, 464*, 894–897.

Liubin [Lioubine], V. P. (2002). *L'Acheuléen du Caucase*. Liège: Études et Recherches Archéologiques de l'Université de Liège, ERAUL *93*.

Liubin [Lioubine], V. P., Tcher Niacho Vski, A. G., Bar Ych Niko, V. G. F., Levko Vskaia, G. M., & Se Livanova N. B. (1985). La grotte de Koudaro I (Résultats de recherches pluridisciplinaires). *L'Anthropologie, 89*, 159–180.

Marin-Monfort, M. D., Cáceres, I., Andrews, P., Pinto, A. C. & Fernández-Jalvo, Y. (2016). Taphonomy and Site Formation of Azokh 1. In Y. Fernández-Jalvo, T. King, L. Yepiskoposyan & P. Andrews (Eds.), *Azokh Cave and the Transcaucasian Corridor* (pp. 211–249). Dordrecht: Springer.

Mosar, J., Kangarli, T., Bochud, M., Glasmacher, U. A., Rast, A., Brunet, M. F., & Sosson, M. (2010). Cenozoic-Recent tectonics and uplift in the Greater Caucasus: A perspective from Azerbaijan. In M. Sosson, N. Kaymakci, R. A. Stephenson, F. Bergerat & V. Starostenko (Eds.), *Sedimentary basin tectonics from the Black Sea and Caucasus to the Arabian Platform* (pp. 261–280). Bath: The Geological Society of London.

Murray, J., Domínguez-Alonso, P., Fernández-Jalvo, Y., King, T., Lynch, E. P., Andrews, P., et al. (2010). Pleistocene to Holocene stratigraphy of Azokh 1 Cave, Lesser Caucasus. *Irish Journal of Earth Sciences, 28*, 75–91.

Murray, J., Lynch, E. P., Domínguez-Alonso, P., & Barham, M. (2016). Stratigraphy and Sedimentology of Azokh Caves, South Caucasus. In Y. Fernández-Jalvo, T. King, L. Yepiskoposyan & P. Andrews (Eds.), *Azokh Cave and the Transcaucasian Corridor* (pp. 27–54). Dordrecht Springer.

Mustafayev, A. (1996). Jawbones and dragon legends, Azerbaijan's prehistoric Azikh Cave. *Azerbaijan International, 4*, 24–32.

Parfitt, S. (2016). Rodents, lagomorphs and insectivores from Azokh Cave. In Y. Fernández-Jalvo, T. King, L. Yepiskoposyan & P. Andrews (Eds.), *Azokh Cave and the Transcaucasian Corridor* (pp. 161–175). Dordrecht: Springer.

Reich, D., Green, R. E., Kircher, M., Krause, J., Patterson, N., Durand, E. Y., et al. (2010). Genetic history of an archaic hominin group from Desinova Cave in Siberia. *Nature, 468*, 1053–1060.

Scott, L., Rossouw, L., Cordova, C., & Risberg, J. (2016). Palaeoenvironmental context of coprolites and plant microfossils from Unit II. Azokh 1. In Y. Fernández-Jalvo, T. King, L.

Yepiskoposyan & P. Andrews (Eds.), *Azokh Cave and the Transcaucasian Corridor* (pp. 287–295). Dordrecht: Springer.

Sevilla P. (2008). *Identifying and preserving the bats of Azokh Cave.* Unpublished report.

Sevilla, P. (2016). Bats from Azokh Caves. In Y. Fernández-Jalvo, T. King, L. Yepiskoposyan & P. Andrews (Eds.), *Azokh Cave and the Transcaucasian Corridor* (pp. 177–189). Dordrecht: Springer.

Smith, C. I., Faraldos, M., & Fernández-Jalvo Y. (2016). Bone Diagenesis at Azokh Caves. In Y. Fernández-Jalvo, T. King, L. Yepiskoposyan & P. Andrews (Eds.), *Azokh Cave and the Transcaucasian Corridor* (pp. 251–269). Dordrecht: Springer.

Stringer, C. (2012). The status of *Homo heidelbergensis* (Schoetansack 1908). *Evolutionary Anthropology, 21*, 101–107.

Tushabramishvili, N., Pleurdeau, D., Moncel, M.-H., & Mgeladze, A. (2007). Le Complexe Djruchula-Koudaro au Sud Caucase (Géorgie). Remarques Sur Les Assemblages Lithiques Pléistocènes de Koudaro I, Tsona et Djruchula. *Anthropologie, XLV*, 1–18.

Van der Made, J., Torres, T., Ortiz, J. E., Moreno-Pérez, L., & Fernández-Jalvo, Y. (2016). The new Material of Large Mammals from Azokh and Comments on the Older Collections. In Y. Fernández-Jalvo, T. King, L. Yepiskoposyan & P. Andrews (Eds.), *Azokh Cave and the Transcaucasian Corridor* (pp. 117–159). Dordrecht: Springer.

Zeinalov, A. A. (2010). *Karabakh in the stone age*, dedicated to the fiftieth anniversary of the opening of a multilayer Palaeolithic Cave of Azykh in Azerbaijan.

Chapter 2
Stratigraphy and Sedimentology of Azokh Caves, South Caucasus

John Murray, Edward P. Lynch, Patricio Domínguez-Alonso, and Milo Barham

Abstract The Pleistocene to Holocene stratigraphy of sediments from three entrance passages to Azokh Cave, Lesser Caucasus, is presented. The larger Azokh 1 passage preserves approximately 11–12 m of *in situ* cave-fill, divisible into nine stratigraphic units based on their sedimentary characteristics. The base of the succession (Units IX to VI) is predominantly non-fossiliferous, but becomes both fossiliferous and calcareous upwards and displays evidence of fluvial and cave spall deposition. The upper part of the succession (Units V to I) is a (largely) continuous sequence of generally fossiliferous fine-grained sediments dating from the Middle Pleistocene to the present. The Pleistocene-Holocene transition is not represented in the succession due to a marked erosional disconformity between Units II and I (at the top of the sequence). The entrance passage to Azokh 2 contains a fill of at least 1.65 m depth that is divisible into two distinct units, whilst the interior of Azokh 5 has revealed at least 4.5 m of cave-filling sediment, which is divisible into five stratigraphic units (A–E). Unit A, at the top of the Azokh 5 sequence, has produced charcoal which provided an age of 2.3 ka and sits with marked discontinuity on the irregular upper surface of Unit B below. The ages of the units beneath this level are unknown at present.

Резюме Пещерная сеть Азоха образовалась в мезозойском известняке. Значительные объемы отложений были выявлены в трех из ее входных коридоров. Стратиграфия коридора *Азох 1* наиболее полно изучена среди трех обнаруженных входов; он раскапывается с 1960-х гг. и охватывает примерно 11–12-метровый слой седимента, датирующегося от по меньшей мере среднего плейстоцена (и, возможно, еще древнее) до настоящего времени. Переход между плейстоценом и голоценом визуально не обнаруживается по причине выраженного эрозионного несоответствия в седиментной последовательности по направлению к вершине.

Нижерасположенная в *Азох 1* и находящаяся близко с выходу субкамера вмещает в себя то, что получило название *седиментная последовательность 1*. Ее почти 4,5-метровой толщины срез включает подразделения *IX–VI* (в восходящем стратиграфическом порядке) и, за исключением самого верхнего слоя, вероятнее всего, преимущественно не содержит окаменелостей. Предшествующее палеомагнетическое исследование подсказало, что основание последовательности фактически может быть раннеплейстоценовым (калабрийским) по возрасту. *Седиментная последовательность 2* расположена далее вовнутрь от выхода в *Азох 1* и в значительной степени залегает над *седиментной последовательностью 1*. Эта около 8,5-метровой толщины последовательность разделяется на пять подразделений (*V–I*). Подразделения *V–II* содержат богатую и разнообразную средне- и верхнеплейстоценовую фауну. Свидетельства человеческой активности (в форме каменных орудий и следов разреза на костях) также были найдены в этих слоях. Среднеплейстоценовый (пренеандертальский) фрагмент нижней челюсти человека был обнаружен примерно на уровне подразделения *V*, хотя

Patricio Domínguez-Alonso – Deceased

J. Murray (✉) · E.P. Lynch · M. Barham
Earth & Ocean Sciences, School of Natural Sciences,
National University of Ireland, Galway,
University Road, Galway, Ireland
e-mail: john.murray@nuigalway.ie

E.P. Lynch
e-mail: edward.lynch@nuigalway.ie

Present Address:
M. Barham
Department of Applied Geology, Curtin University,
GPO Box U1987, Perth, WA 6845, Australia
e-mail: milobarham@yahoo.co.uk

P. Domínguez-Alonso
Departamento de Paleontología, Facultad de Ciencias Geologicas
& Instituto de Geociencias (IGEO-CSIC), Universidad
Complutense de Madrid (UCM), Madrid, Spain

Yolanda Fernández-Jalvo et al. (eds.), *Azokh Cave and the Transcaucasian Corridor*,
Vertebrate Paleobiology and Paleoanthropology, DOI 10.1007/978-3-319-24924-7_2

его точная датировка неизвестна. Седиментное наполнение коридора *Азох 1* преимущественно мелкозернистое, свидетельствуя или о низкоэнергетическом водном потоке (возможно, вследствие запруживания как результата затопления внутреннего сегмента пещерной системы), или, вероятно, из-за изменения его направления по причине сильных ветров. Обнаружены также горизонты, содержащие скопления осколков крупнозернистого известняка. Их значение непонятно, однако они могут указывать на изменения в палеоэкологических условиях, такие как рост просачивания воды через пещеру или заметное похолодание климата. Влияние геоморфологических и тектонических факторов, как, например, увеличение сейсмической активности, также нельзя не принимать в расчет.

Меньший по размерам коридор *Азох 2* расположен примерно в 42 м на северо-восток от коридора *Азох 1*. К настоящему времени полностью идентифицируемыми в отношении наполнителей являются два стратиграфически подразделения. Самое верхнее из них (подразделение *1*) содержит различные слои очагов, в одном из которых был найден скелет человека, датированный периодом голоцена. Лежащее ниже подразделение *2* заметно светлее по окраске и более кальцифицировано. Его общая толщина пока не выяснена и, поскольку в нем не обнаружено никаких окаменелостей или артефактов, возраст данного подразделения остается неизвестным.

На расстоянии около 100 м от *Азох 1* находится коридор *Азох 5*. Это маленькая фреатическая труба, которя ведет к внутренней камере, с седиментным покрытием толщиной, по меньшей мере, 4,5 м. Данная величина, вероятнее всего, значительно занижена, поскольку вершина и основание последовательности слоев не были визуально идентифицированы, а геофизики оценили общую толщину седиментного наполнения около 10 м. К настоящему времени идентифицированы пять подразделений (помеченных как *A–E* в стратиграфически нисходящем порядке). Седиментные слои обычно мелкозернистые, хотя подразделения *D* и *B* характеризуются повышенным содержанием крупнозернистого известняка и обломков кремня, большинство из которых имеет местное происхождение. Обратное соотношение было обнаружено между подразделениями *B* и *A* на самой вершине седиментного покрытия. В подразделении *A* найден древесный уголь, датируемый 2300 г. до н.э., однако возраст подразделения под находками до сих пор остается неизвестным.

Keywords Azokh Cave • Lesser Caucasus • Stratigraphy • Middle Pleistocene • Sediment

Introduction

Cave systems are a typical feature of karst landscapes where they develop through the dissolution of soluble bedrock, leading to the formation of a variety of open-space cavities and passageways. They represent a geomorphologic link between the surface and sub-surface environments, provide a conduit for the flow of groundwater and act as a natural repository for the accumulation of sediment (e.g., Bogli 1980; White 1988; Sasowsky and Mylroie 2004). Caves also act as natural shelters for animals and have been similarly exploited for thousands of years by humans. Consequently, caves and rock shelters represent a habitat that may have assisted in the intellectual development of human kind (e.g., Chauvet et al. 1996).

In recent years, investigations into the geological, hydrogeological and biogeochemical properties of cave systems have transformed our understanding of cave genesis (Moore and Sullivan 1997; Engel et al. 2004; Ford and Williams 2007). In particular, studies of cave-fill sediments have provided new insights into the timing of cave formation, subterranean environmental processes, karst landscape evolution, groundwater dynamics and paleoclimatology (e.g., Bretz 1942; Polyak et al. 1998; Musgrave and Webb 2004; Pickering et al. 2007; White 2007). Thus, the study of cave sediments can increase our understanding of the sedimentological and environmental conditions that existed during the formation and evolution of a cave system. In addition, cave sediment deposits are frequently associated with fossil preservation and have proven to be important sites for the discovery of archaeological artifacts and hominin remains (Jelinek 1982; Torres et al. 2003; Pinhasi et al. 2008; Dirks et al. 2010; Moldovan et al. 2011; Pickering et al. 2011).

This chapter reviews the stratigraphic and sedimentary characteristics of Azokh Cave, with particular emphasis on its three main entrance passages: Azokh 1, Azokh 2 and Azokh 5. We summarize the nature of cave-fill sediments within Azokh 1 passage, as previously reported by Murray et al. (2010), and provide additional data (sedimentological, textural, mineralogical) that further constrain the stratigraphy. Azokh 1 has been the principal site of archaeological excavation at the cave since 2002 (Fernández-Jalvo et al. 2009, 2016). In addition, an assessment of the stratigraphy and sedimentology of Azokh 2 and Azokh 5 entrance passages is also made. Knowledge of the sedimentary infill within these smaller passageways is presently at a reconnaissance level and the data presented herein should thus be viewed as preliminary.

Fig. 2.1 Geographic location of Azokh Cave in the South Caucasus. **a** General view of region relative to the Eastern Mediterranean, Black and Caspian seas. **b** More detailed view of location, with an indication of topographic elevation shown. Position of (**b**) is indicated by inset box in (**a**)

Geological Setting and Overview of the Azokh Cave System

Azokh Cave (located at 39º 37.15′ north; 46º 59.32′ east; Fig. 2.1) is hosted in a thickly-bedded sequence of Mesozoic (possibly Jurassic) limestone that has experienced variable levels of uplift and karstification since the Pleistocene (Lioubine 2002). The carbonate bedrock forms part of a limestone massif that is developed on a regional-scale across the Southern Caucasus (Khain 1997). In the vicinity of the cave, the host limestone is a fossiliferous grainstone which has undergone partial silicification, possibly due to the combined input of volcanogenic siliciclastics and siliceous fossil material. The cave system comprises a series of dissolution cavities that may have developed partly in response to vadose zone fluviokarst processes (e.g., White 1988; Domínguez-Alonso et al. 2016). The cave consists of a NNW- to SSE-aligned internal zone that is composed of several interconnected, sub-rounded chambers extending over approximately 130 m (Fig. 2.2). This main body of the cave is transected on its western flank by several WSW- to ENE-trending entrance passageways that connect the internal zone to the exterior (Figs. 2.2 and 2.3). The orientation of the main chamber and entrance passages broadly corresponds with the alignment of conjugate joint sets and fractures that are pervasively developed in the limestone bedrock (Domínguez-Alonso et al. 2016).

The initial investigations of Azokh Cave by the Huseinov team in the 1960s did not establish a clear and detailed record of the Pleistocene and Holocene sedimentary infill of the cave system (Mustafayev 1996; Lioubine 2002). In particular, early excavations lacked any rigorous stratigraphic control. Sedimentary units were more commonly distinguished based on their archaeological content, rather than their sedimentological properties (Lioubine 2002). Definitive thickness estimates for the sedimentary units identified at that time appear not to have been unequivocally

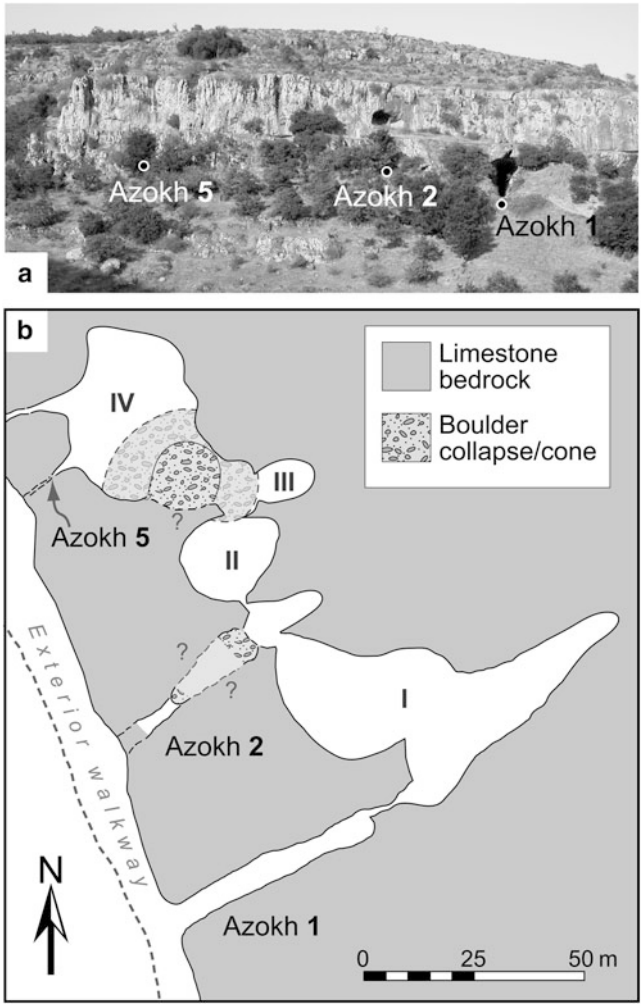

Fig. 2.2 **a** Field photograph of the west-facing hillside containing the Azokh Cave system. Locations of Azokh 1, 2 and 5 entrance passages are indicated. **b** Simplified plan-view sketch map of the cave system showing the location of the main entrance passages. Internal cave chambers are labeled with roman numerals (I–IV). Reproduced from Murray et al. (2010)

established and any lateral shifts in sedimentary facies were not made apparent. In addition, systematic archaeological excavation methods, utilizing aerial grids and three-dimensional spatial recording of finds, were not employed. These factors have combined to make the understanding of the context and significance of the large volume of fossil and lithic artifacts recovered prior to 2002 a challenging prospect.

Azokh 1

The Azokh 1 passageway is a broadly linear chamber measuring 40 m long by 11.5 m high with a WSW-ENE alignment (Fig. 2.4). This orientation results in the entranceway being well illuminated, particularly by the afternoon sun. Towards the interior of the passage, in an ENE direction ("Uppermost Platform" in Fig. 2.4), the light is not as good and artificial illumination has been employed there during excavation work. The floor of the chamber drops (slopes) down at approximately the midway point in the passage, which increases the height of the chamber to approximately 14 m towards the entrance. The sedimentary infill of Azokh 1 passage yielded a human jaw fragment in 1968 that was later assessed as Middle Pleistocene in age (Kasimova 2001). The nature of this discovery in the southern Caucasus (Fig. 2.1), coupled with additional archaeological and paleontological finds, has established Azokh 1 as a site of significant archaeological and paleoanthropological interest (e.g., Ljubin and Bosinski 1995; Bridgland et al. 2006; Fernández-Jalvo et al. 2010; Pinhasi et al. 2011).

During these early phases of excavation, a considerable amount of sediment was removed from the passageway (Fig. 2.3a), and Lioubine (2002) noted that before the first excavations in the 1960s, the chamber was filled to within 2–3 m of the roof. A graphical estimate of the original sediment thickness is provided in Figs. 2.3a and 2.4 and it is apparent that a considerable amount of the stratigraphic section is now gone. Huseinov initially identified 10 stratigraphic horizons infilling the chamber during the 1960s. This was increased to 17 by Veilicko in 1979 and then to 25 by the Gadzhiev team in 1980 (Huseinov 1985; Lioubine 2002). Detailed records of the extent of these excavations and the amount of sediment removed are no longer readily available. Therefore, an appraisal of the sedimentology incorporating the full pre-2002 stratigraphic sequence is extremely difficult to ascertain. In this regard, what is presented below is a description based on the stratigraphic remnants that we found remaining in the passage.

When excavation work restarted in 2002, the Azokh 1 passageway was an obvious priority for renewed investigation and was initially termed *Azokh Main*. Subsequently, the passage was renamed *Azokh 1* following reconnaissance geophysics and geological work that identified appreciable thicknesses of sediment fill in two other entrance

Fig. 2.3 Field photographs of entrance passages to Azokh Cave. **a** Azokh 1. The distinctive sediment pedestal marking the entranceway is visible towards the bottom of the image. The white asterisk indicates the approximate position of the original sediment infill of the passage, prior to excavation in the 1960s and 70s. **b** Azokh 2 and **c** Azokh 5. Both (**b**) and (**c**) were photographed in 2004. The hammer for scale (highlighted with a white arrow in both images) is 35 cm long

passageways – Azokh 2 and Azokh 5 (Fig. 2.3b, c; see also Fig. 2.2 for general location). Post-2002, systematic and detailed archaeological investigations have been conducted in the upper half of the sedimentary sequence remaining in Azokh 1 (Asryan et al. 2016; Fernández-Jalvo et al. 2016; King et al. 2016).

The most recent assessment of the stratigraphy of Azokh 1 was provided by Murray et al. (2010) and their proposed lithostratigraphic framework is retained here. Nine sedimentary units, occurring within two physically separated stratigraphic remnants (termed Sediment Sequences – see Fig. 2.4), are recognized based on their sedimentological properties. Sediment Sequence 1 is located at the ENE end of a basal trench at the cave entrance and accounts for 4.5 m of stratigraphy (Fig. 2.5). Sediment Sequence 2 is located towards the rear of Azokh 1 passage and is estimated to be at least 8.5 m thick (Fig. 2.6). This latter sequence is interpreted to have overlain the former, although since no physical connection remains between the two sequences, and practically no sediments remain along the sides of the cave walls, this inference is equivocal.

Table 2.1 summarizes the main stratigraphic subdivisions of the infill of Azokh 1. It provides average estimates of the color, texture and sedimentary characteristics of the various lithostratigraphic units and is built upon the descriptions presented in Murray et al. (2010). Detailed excavation work, particularly towards the top of the stratigraphic succession, has revealed much intra-unit variation. This has become particularly evident as horizons have been tracked laterally from the center of the passageway, where most of the lithostratigraphic units were originally diagnosed, and out towards the cave walls.

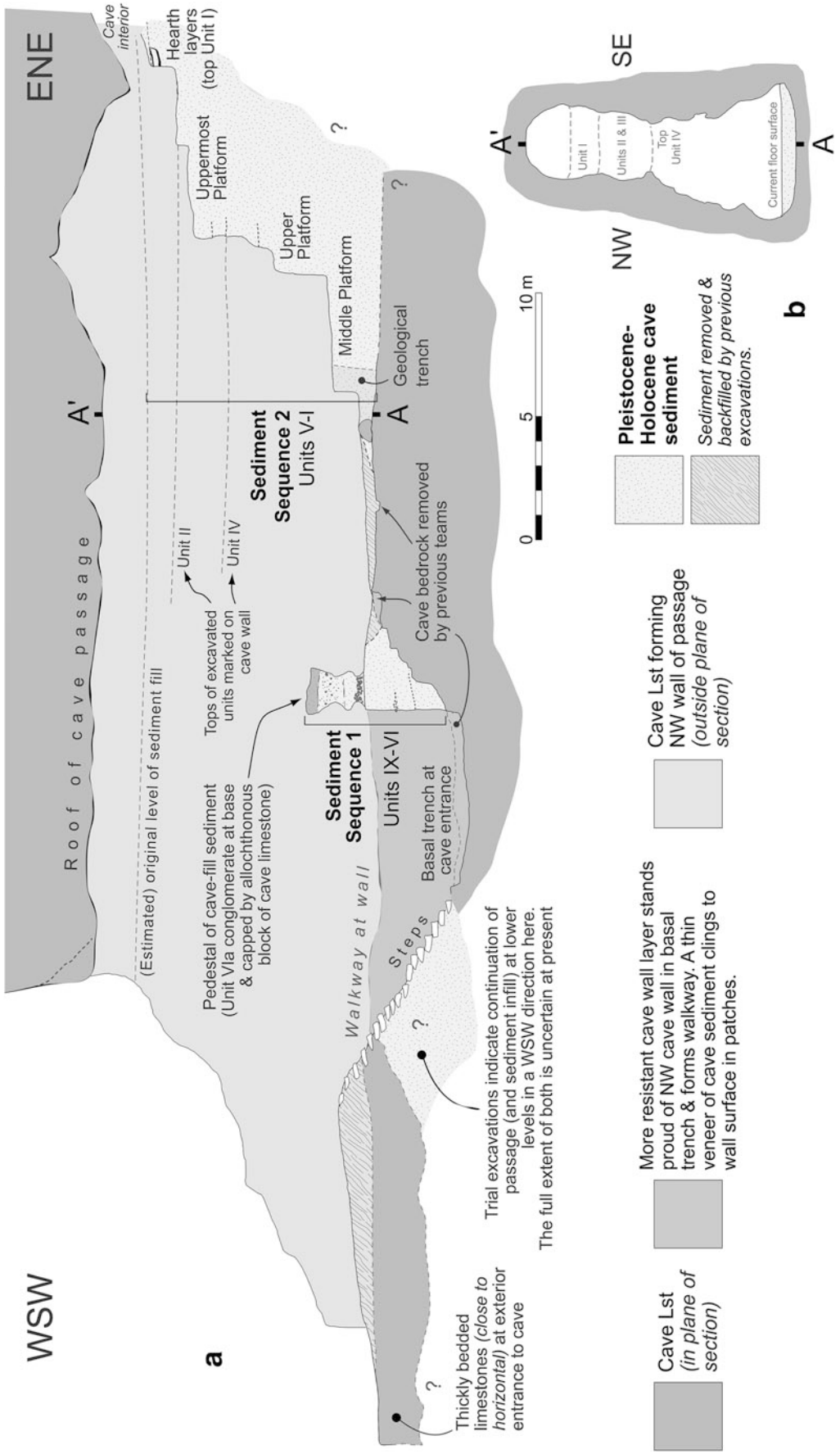

Fig. 2.4 **a** Sketch cross-section through Azokh 1 cave passage (drawn facing NW). The estimated amount of cave-fill sediment removed by previous excavation teams is indicated by the upper dashed line. The floor of the passage is illustrated insofar as its extent is currently known and the height of the roof was measured at various points along the section using a telemeter with an accuracy of 1 cm. **b** Cross-section (A–A') across the axis of the passage [orthogonal to (**a**) and drawn to the same scale] indicates levels of sediment infill. Reproduced from Murray et al. (2010)

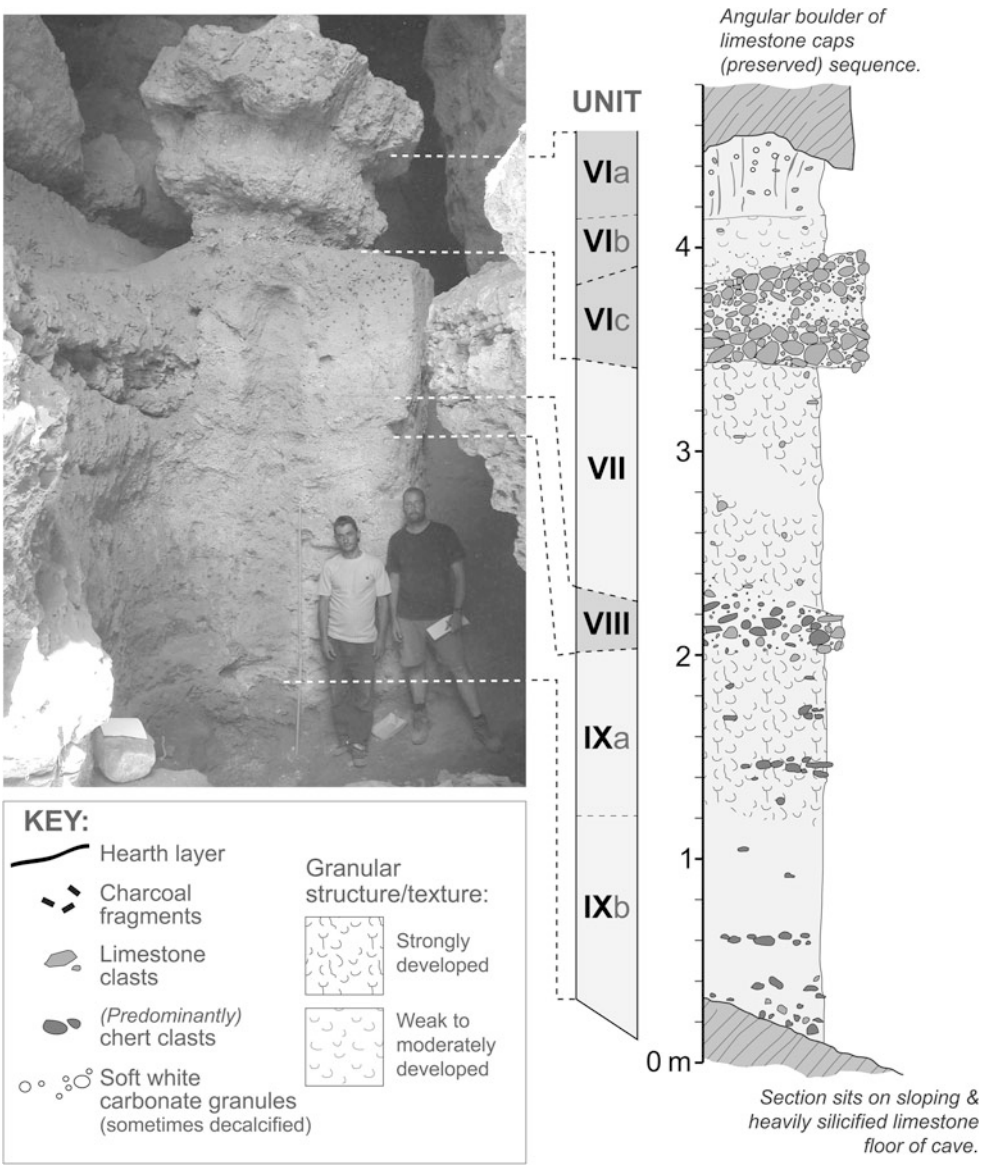

Fig. 2.5 Stratigraphic column for Sediment Sequence 1 in Azokh 1 passage. Unit numbers are indicated in the central column with roman numerals. The photograph of the actual section to the left of the column is for reference and indicates precisely where the boundaries of the units have been set. Much of this section is exposed in the basal trench in the entrance to the cave (see Fig. 2.4). The key to the various sedimentological features is also applicable to Fig. 2.6. Reproduced from Murray et al. (2010)

Sediment Sequence 1

This sequence occupies a lower sub-level within Azokh 1 passage (Fig. 2.4) and it contains Units IX to VI (Fig. 2.5). Given that it rests on a down-sloping cave floor surface (Fig. 2.7; see also Fig. 2.4), the section effectively wedges out, so the amount of remaining stratigraphy becomes progressively more limited moving downwards. The base of the sequence (Units IX and VIII) is largely composed of non-calcareous sandy loam/loamy sand (Table 2.1). A gradual and pronounced development of a granular structure midway through Unit IX (Fig. 2.8) marks the contact between its two constituent subunits. The overlying Unit VIII is characterized by a higher concentration of limestone and chert clasts. The contacts of Unit VIII with its bounding (enclosing) units are not sharply defined and it is possible that it may represent a localized accumulation of larger clast types within a loamy sand matrix.

Units VII and VI above see a shift to clay-loam textures, with the exception of subunit VIc which is a conspicuous clast-supported pebble to cobble conglomerate (Fig. 2.9). The two subunits (VIb and VIa) overlying the conglomerate are calcareous, and this contrasts with the non-calcareous units beneath. Sediment Sequence 1 is capped by a large

Table 2.1 Stratigraphic divisions and character of the remaining sediments in Azokh 1

	Unit/ Sub-unit	Thickness	Consistence & Texture	Structure	Color (Munsell)	Rocks/clasts/comments	Carbonates	Age	
Sediment Sequence 2 (Units V–I)	I	80–150 cm	Generally friable to loose clay loam	Moderate granular	7.5YR 4.5/3 (Brown)	Limestone clasts are rare and are often strongly altered. This unit contains the very distinctive fumier near the top	Non-calcareous	157 ± 26 years BP	Holocene
	II	c. 101–140 cm (Minimum – unit appears to thicken towards cave interior)	Quite variable (vertically & laterally), but generally [sandy] clay loam. Base is firm becoming friable-firm upwards	Moderate granular at base, granular at top	10YR 5/3 (Brown)	Pebble-grade limestone clasts (0.5–5 cm) are present and commonly decalcified and/or altered. Small white carbonate granules dispersed throughout. Disseminated charcoal fragments noted in the top 30 cm. Bone fragments are common and are often poorly preserved. The top of this unit is quite irregular and accounts for much of the thickness variation	Base is calcareous; however, top is non-calcareous, particularly in center of cave passage	*Top:* 100 ± 7 ka *Base:* 184 ± 13 ka	Late Pleistocene
	III	60–70 cm	Friable clay to silty clay	Top half is weak to moderate granular. Bottom half is very weak granular (almost massive)	10YR 4.5/4.5 (Dark yellowish brown)	Limestone clasts are reduced in size and concentration; however, fragments up to 18 cm noted. Bone and charcoal are also present. The contact with Unit IV below is indistinct in places, particularly when traced out laterally towards the cave walls	Very strongly calcareous	–	Middle Pleistocene (Units V–III)
	IV	100–122 cm	Friable silty clay	Weak fine granular at base, becoming moderate medium granular upwards	10YR 5/4 (Yellowish-brown)	Limestone clasts are dispersed and uncommon in the base. Flattened sub-angular to rounded limestone pebble and cobble clasts become more common towards the top of the unit. Bone and charcoal are present	Weakly calcareous	Units V–IV (contact): 205 ± 16 ka	
	V Va	220–230 cm	Predominantly friable silty clay	Variable, but generally massive with a granular base	Variable between 10YR 5/5 (Yellowish brown) at base and 7.5YR 4.5/5 (Brown) above	2–10 mm flattened angular limestone clasts are common in basal c. 55 cm. The overlying c. 105 cm has dispersed sand-grade material in lower 2/3^{rds} followed by horizontal flattened limestone clasts. The contact between Va and Vb is marked in places by a thin, yet conspicuous cream-white to white non-calcareous crust	Calcareous		
	Vb	220–230 cm	Variable between friable-firm loamy sand (particularly near base) and friable clay loam	Variable, but generally massive	10YR 6/3 (Pale brown) at base, 7.5YR 4/4 (Brown) above	This unit is best exposed in a geological trench (see Figs. 2.4 and 2.10). Contains rare limestone clasts, but lensoidal "channel" structures contain elevated concentrations of clasts	Largely non-calcareous	293 ± 23 ka	

(continued)

Table 2.1 (continued)

	Unit/ Sub-unit		Thickness	Consistence & Texture	Structure	Color (Munsell)	Rocks/clasts/comments	Carbonates	Age
Sediment Sequence 1 (Units VI–IX)	VI	VIa	10–40 cm	Soft friable clay/clay loam	Moderate granular with an additional prismatic component	7.5YR 5/4 (Brown)	The variation in the thickness of this subunit reflects the irregularity of the base of a large angular limestone boulder which caps the preserved sequence. Abundant mm-scale white carbonate clasts are present along with bone and charcoal	Strongly calcareous	**Sequence 1 is undated** Previous paleomagnetic work reported by Huseinov (1985) and also Ljubin and Bosinski (1995) suggest lower part of this sequence is Early Pleistocene in age (Units IX–VI)
		VIb	30–33 cm	Very firm to firm sandy clay loam	Weakly developed fine to medium granular	7.5YR 4/4 (Brown)	Rounded and angular pebble and granule-grade clasts occur throughout. Flattened and degraded white carbonate clasts are common in parts of the base. Bone fragments present, but uncommon	Calcareous	
		VIc	30–60 cm	*Friable to loose clast-supported conglomeratic marker horizon*			Fossil bone fragments noted in the base of this conspicuous subunit	Conglomerate clasts react with HCl	
	VII		110–115 cm	Friable to firm clay loam	Granular top (30–50 cm) and base (48–60 cm) Midsection is massive	10YR 5.5/3.5 (Brown to yellowish brown)	Gravel to small pebble-grade chert and decalcified limestone clasts are dispersed throughout; however, they are rare in the midsection of the unit. The contact with underlying Unit VIII is gradational and is marked by a conspicuous drop in clast content	Non-calcareous	
	VIII		20–30 cm	Firm loamy sand	Medium granular	10YR 6/4 (Light yellowish brown)	Poorly-sorted (largely) matrix-supported conglomerate. Clasts are generally sub- to well-rounded cherts and decalcified limestones and range in size from gravel to cobble grade. This appears to be quite a localised feature	Non-calcareous	
	IX	IXa	70–85 cm	Firm loamy sand to sandy loam	Strongly medium to coarse granular	10YR 6.5/3 (Pale to light yellowish brown)	Contains a matrix-supported population of sub-rounded to angular limestone and chert clasts ranging 2–6 cm. Granular texture is main distinguishing feature from subunit IXb below and it develops over a c. 15 cm stratigraphic interval	Non-calcareous	
		IXb	110–125 cm	Firm to very firm sandy loam	Massive	10YR 6/4 (Light yellowish brown)	This subunit drapes the irregular topography of the cave floor. Dispersed granules of cave rock, some concentrated in poorly defined bedding-parallel seams/pockets, are present in the basal c. 60 cm. Rare clasts noted in the top 60 cm, which is more uniform in character	Non-calcareous	

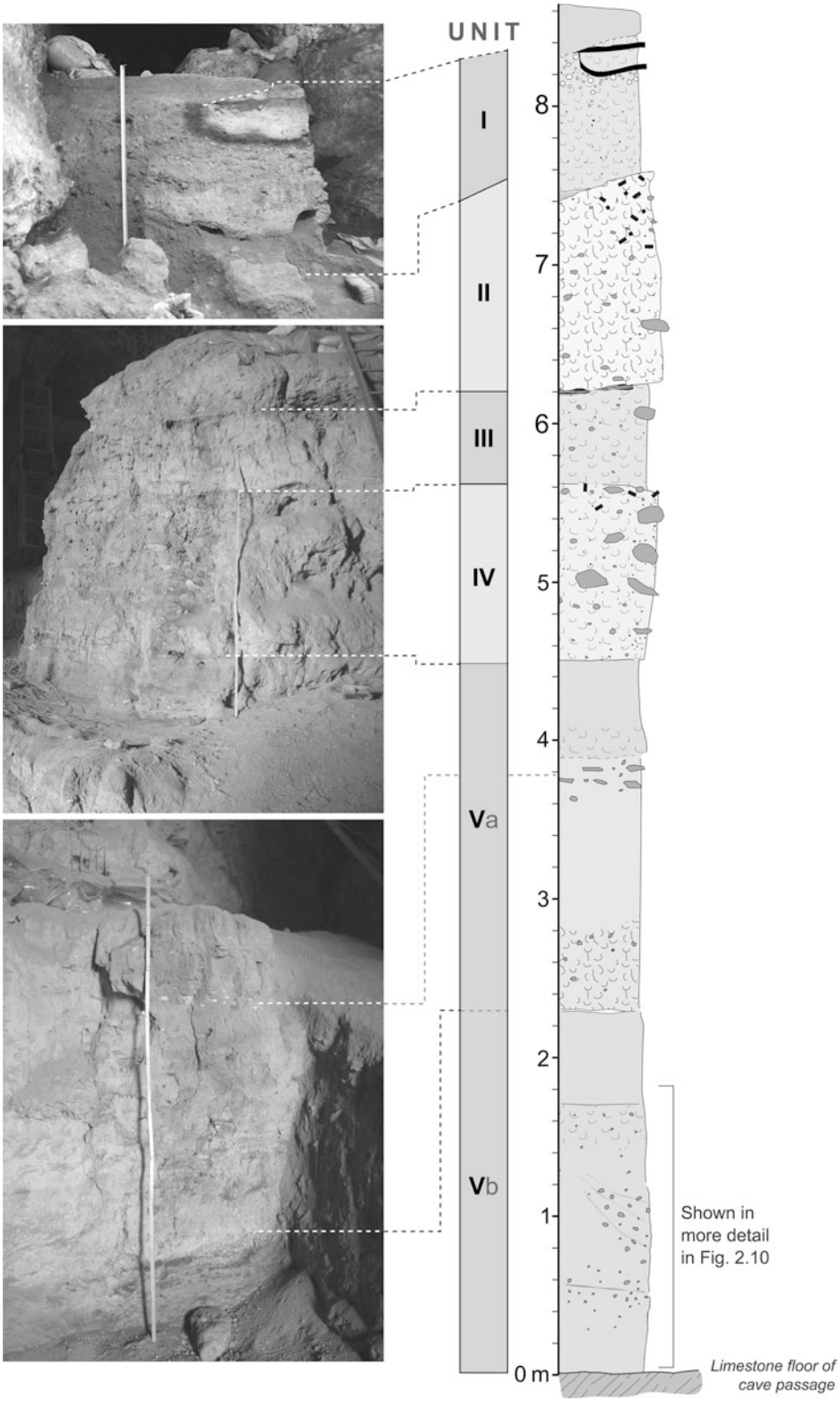

Fig. 2.6 Composite stratigraphic column for Sediment Sequence 2 in Azokh 1 passage. The height of the wooden ruler in the lower and middle photograph is 2 m whilst in the upper photograph the length of the tape is 88 cm. See Fig. 2.5 for a general sedimentological key. Modified from Murray et al. (2010)

Fig. 2.7 Thinning of the base of what remains of Sediment Sequence 1 (Unit IX) which rests on the sloping cave floor. The tape measure (for scale) is showing 1 m

Fig. 2.8 Detail of the transition seen in the middle of Unit IX. The base of the unit (IXb) is more massive in character whilst the upper half (IXa) becomes progressively more granular in appearance towards the top of the photograph. The visible length of the scalebar is 86 cm

limestone boulder, which has presumably fallen into position from the cave roof. Excavation by previous teams around this collapse feature has resulted in the characteristic "mushroom" shaped pedestal close to the entrance to the passage (Figs. 2.4 and 2.5).

Fossils and lithic artifacts have not been observed or recorded so far in Units VII, VIII and IX. Given the limited extent of the remaining stratigraphy this is perhaps unsurprising and it partly explains why this portion of the succession remains largely undated (Table 2.1). Huseinov (1985) reported the recovery of very fragmentary fossils from this lower part of the stratigraphy, along with pollen. Clearly identifiable fossil fragments and charcoal are present in Unit VI towards the very top of Sediment Sequence 1. Murray et al. (2010) speculated that this divide between (largely) unfossiliferous and fossiliferous strata might be a reflection of a shift between the cave being closed during accumulation of most of Sediment Sequence 1 to a more open system towards the top. In particular, conglomeratic subunit VIc (Fig. 2.9) is unequivocally the product of energetic water flow through the passage (probably a small river) and the coincidence of this horizon with the first appearance of fossils supports this contention.

According to M.M. Huseinov (reported in Lioubine 2002), Sediment Sequence 1 equates to *"cultural"* layers V–VI (at the top) and VII down to X (below) [compare Fig. 2.5 herein to Fig. 8 of Lioubine (2002)]. Huseinov (1985) recorded over 200 lithic artifacts from layers VII–X (as he had interpreted the strata); however, the validity and stratigraphic integrity of these finds has subsequently been questioned and claims that they are "Lower Paleolithic" in character have been largely dismissed (Doronichev 2008; Doronichev and Golovanova 2010).

Fig. 2.9 Clast-supported subunit VIc conglomerate. Clasts are sub- to well-rounded. Scale bar is 21.5 cm in length

Sediment Sequence 2

This is a composite sequence that has been reconstructed from a series of vertical sections or "steps" (largely a by-product of the pre-2002 excavations) in the cave filling strata (Fig. 2.4). Sediment Sequence 2 can be subdivided into five constituent units (I–V; Fig. 2.6) totaling about 8.5 m in thickness. Over half of this thickness is accounted for by Unit V (approximately 4.5 m), which is located at the base. All five units of Sediment Sequence 2 have proven to be fossiliferous and much of the excavation work by the current team has been focused in this part of the succession.

Unit V is predominantly fine-grained in character and is divisible into two subunits: Vb (located at the base and largely non-calcareous) and Va (located directly above and calcareous in nature; see Table 2.1). It is likely that Unit V can be further subdivided beyond this two-part scheme; however, subunit Va presents a steep vertical face (just over 2 m; Fig. 2.6) in the section and, for safety reasons, it has not been possible to thoroughly examine the stratigraphy in detail.

Subunit Vb is best exposed in a small trench that was initially excavated through the Middle Platform in 2002 (Fig. 2.10; see also Fig. 2.4a for general location in Azokh 1 passage). Murray et al. (2010) described five horizons within this trench section and a refinement of some of their sedimentological details is outlined in Table 2.2.

The uppermost horizon (e) of subunit Vb can be traced laterally across the excavation surface of the Middle Platform and is seen to continue stratigraphically upwards for a further 35–40 cm. It is capped in places by a distinctive 1 cm-thick cream-white to white, non-calcareous phosphatic crust (see lowest photo correlation line at top of subunit Vb in Fig. 2.6), which forms a useful marker horizon.

Subunit Va is 220–230 cm thick and is predominantly composed of friable calcareous silty clay. The basal 55 cm is granular with common angular limestone clasts (2–10 mm), which are typically flattened parallel with bedding. The overlying 105 cm is more massive in structure and contains a distinctive horizon of flattened (cm-scale) clasts in the top third (see photo correlation line in Fig. 2.6). Charcoal was noted in this zone also. The uppermost 70–80 cm of subunit Va comprises friable calcareous silty clay. Its base is finely granular, however, its top is predominantly massive, lacks limestone clasts, and has a more reddish hue (resulting in 7.5YR rather than 10YR color designation; see Table 2.1). This subtle color transition is generally gradual in nature.

The contact between the top of Unit V and overlying Unit IV is diffuse; and is irregular and undulose when tracked laterally from the centre of the passage towards the cave walls. Where it is more clearly displayed it presents a subtle shift in

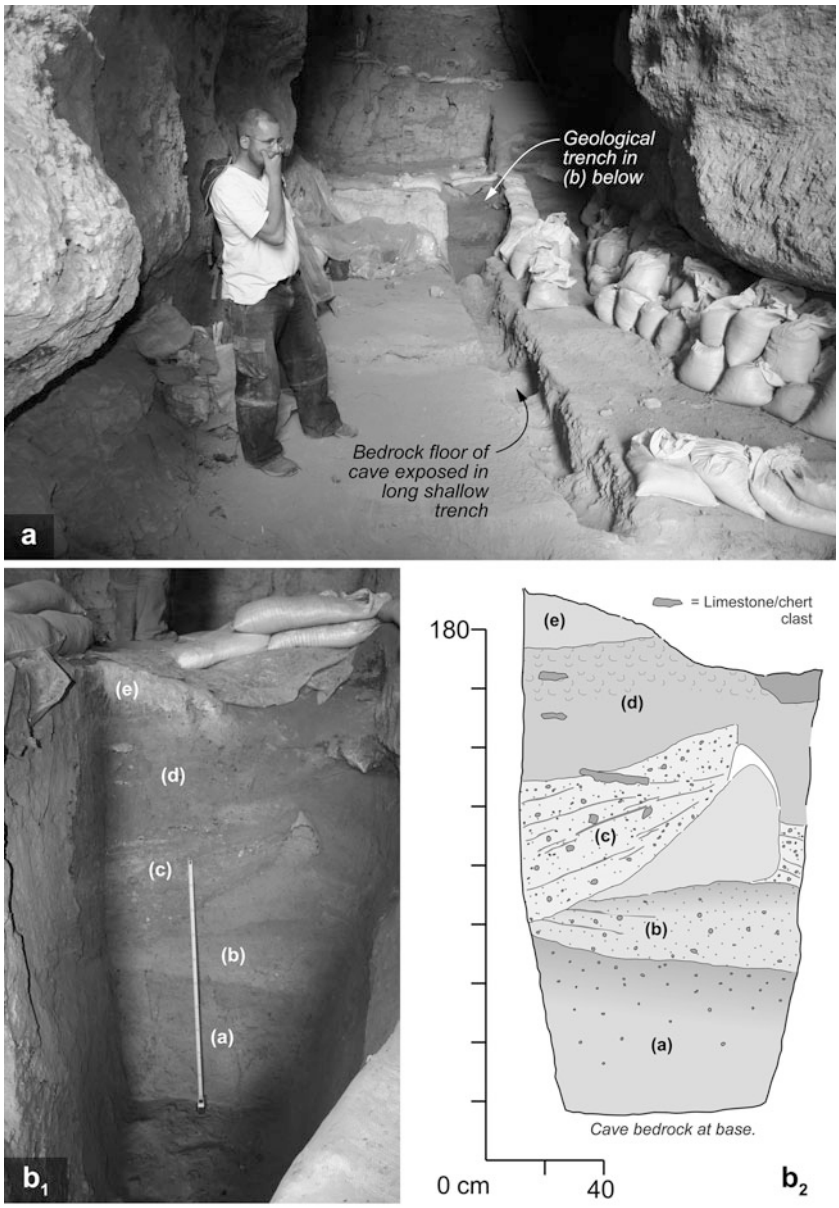

Fig. 2.10 The base of Sediment Sequence 2. **a** General location of the geological trench in the base of Unit V within Azokh 1 passage. This photo faces ENE and was taken in 2008, when the bedrock floor to the cave was found only a short distance below the (present) sediment level on the *"Lower Platform"*; $\mathbf{b_1}$ Photo and $\mathbf{b_2}$ corresponding scaled panel diagram of the sedimentary succession in the geological trench. A description of horizons (a) to (e) is provided in Table 2.2. Tape measure in $\mathbf{b_1}$ is showing 1 m. $\mathbf{b_2}$ is modified from Murray et al. (2010)

texture (moving upward from predominantly massive to fine granular) and color (the "reddish" 7.5YR top of Va is overlain by 10YR Unit IV; see Table 2.1). A characteristic feature of Unit IV is a progressive increase in flattened sub-angular to rounded (cave-wall) pebbles and cobbles towards the top of the unit, along with fragments of bone and charcoal.

When examined in the centre of the passage, the contact between Unit IV and (overlying) Unit III is quite obvious and sharp (see relevant photo correlation line in Fig. 2.6) and is marked by a shift in structure and a noticeable decrease (in Unit III) in the limestone clast content of the sediments. However, the contact has proven difficult to trace laterally when moving away from the centrally positioned reference section. At the time of writing, detailed excavation has begun to reveal more (from a lateral perspective) of this transition and it is likely that a reassessment of this particular contact may have to be made with new exposure. A possible two-part subdivision of Unit III into a lower (largely) massive subunit and an upper weak to moderate granular subunit is also becoming apparent.

Table 2.2 Subunit Vb succession evident in geological trench, Middle Platform, Azokh 1

Subunit	Horizon	Thickness	Consistence & Texture	Color	Rocks/clasts/comments	Carbonates
Vb	(e)	c. 20 cm (*In trench*)	Very firm clay loam	7YR 4/4 (Brown)	Contains common small soft (decalcified) white carbonate granules	Very weakly calcareous
	(d)	40–47 cm	Friable-loose clay loam	7YR 4.5/4 (Brown)	Angular limestone clasts are common, but dispersed. The base is massive, becoming weak granular towards the top	Non-calcareous
	(c)	50–0 cm (*Tapers out*)	Firm loamy sand	10YR 5/3.5 (Brown)	Forms a conspicuous "channel" structure in the section. Granule and pebble-scale clasts common, including angular dark chert clasts in matrix	Non-calcareous
	(b)	c. 20–30 cm	Friable loamy sand at base passing upwards into clay loam	Top:10YR 5/3 (Brown) Base:10YR 6/3 (Pale brown)	Noticeable gravel content. Internal stratification evident with a color gradation from the base to top (where it is darker)	Non-calcareous
	(a)	50–56 cm	Friable-firm sandy loam to loamy sand	10YR 6/3 (Pale brown)	Horizon rests directly upon the floor of the cave	Non-calcareous

Fig. 2.11 Lateral view of contact between Units III and II, Azokh 1. Hammer (arrowed) for scale

The contact between Unit III and (overlying) Unit II is conspicuous and is defined by a marked increase in the granularity of the sediments (Fig. 2.11). Murray et al. (2010) noted reddish-brown staining along this contact close to the northwestern wall of the chamber. Analysis of red- and orange-stained sediment from several units in Azokh 1 using Raman spectroscopy indicates the presence of fine-grained hematite and magnetite within the sediment (see below for further discussion). Subsequent excavation of the Unit III/II boundary has shown the hematitic staining to be more laterally widespread and the irregular nature of the contact to be more pronounced than initially thought.

Unit II rapidly (and somewhat irregularly) becomes non-calcareous upwards and also contains an elevated amount of limestone clasts (0.5–5 cm). These clasts, along with fossil bone fragments, are often strongly degraded, particularly in the non-calcareous zones. The deterioration of bone material within Unit II has been linked to accumulations of bat guano during its deposition, resulting in a non-calcareous, more acidic sediment (Murray et al. 2010). These authors reported the detection of tinsleyite (K and Al-rich hydrated phosphate) in the sediment. This particular mineral phase likely reflects syn-diagenetic processes where phosphatic mineralisation can precipitate due to the presence of bat guano (Magela da Costa and Rúbia Ribeiro 2001; Marincea et al. 2002; Shahack-Gross et al. 2004). It is evident that there is considerable lateral heterogeneity within Unit II in terms of its consistency, texture, geochemistry and the quality of taphonomic preservation (personal observations; see also Smith et al. 2016 and Marin-Monfort et al.

2016). Unit II was initially examined in a small cut section, near the Upper Platform and adjacent to the northern wall of the cave passage, where it measured c. 120–140 cm in thickness. More recent investigations of newly exposed surfaces of the Unit III/II contact in a more central position within the chamber, and also the overlying Unit II/I contact located approximately five meters deeper within the cave passage, have suggested potential thickness variation for Unit II of 150–200 cm. However, since these contacts are exposed in different positions within the passage, and neither section reveals Unit II in its entirety, it is unclear whether the thickness disparities inferred (from the differences in the elevations of the contacts) reflect real lateral thickness variation, or simply a slope in either/both of the unit boundaries towards the cave entrance.

The contact between Units II and I is sharp and irregular when traced out in detail, and the latter appears to infill the uneven topographic surface of the former. Unit I, which caps the entire cave-fill succession, is non-calcareous and predominantly a friable to loose clay loam. Excavation work on the Uppermost Platform (Fig. 2.4a) has shown this unit thins from more than 135 cm to between 80 and 90 cm towards the interior of the cave. A reference section for Unit I has been preserved in the rear of Azokh 1 passage (Fig. 2.12). Murray et al. (2010) noted that this particular section demonstrated two key features:

- Considerable disturbance and reworking of the sediment by recent mammal burrowing activity. Fossils of *Ursus spelaeus* and coprolites, as well as Paleolithic stone tools have been recovered from these burrows (Marin-Monfort et al. 2016). This large-scale bioturbation has served to greatly complicate the internal stratigraphic details of Unit I.
- Close to the top of the unit a conspicuous c. 30–40 cm thick fumier (manure hearth) occurs (Fig. 2.12; see also Fig. 2.6). This feature consists of a series of black, carbon-rich bands with greyish-white ash-rich interlayers. Dispersed, but common, soft white carbonate granules (occasionally these are decalcified) in the top 35 cm of Unit I may possibly be related to the heating effect of this large hearth structure on the surrounding sediment.

A conspicuous component of several of the stratigraphic units within Azokh 1 is the presence of disseminated clay-like pedofeatures within the sediment groundmass (Fig. 2.13). These features typically occur as millimeter- to centimeter-scale, sub-circular to lensoidal nodules and disseminated specks, as well as thin (c. 1–3 mm) discontinuous sub-horizontal seams (typically 1–5 cm long). They are composed of fine-grained (<0.05 mm), white to buff, powdery, clay-like material and generally do not display any internal banding or lamination. Similar clay-like material also forms partially developed concentric laminae within and around decomposing bone fragments in the sediment (Fig. 2.13d). The occurrence of these nodules appears to begin within Unit VI at the top of Sedimentary Sequence 1 and remains variably developed, moving up the stratigraphy, throughout Sedimentary Sequence 2 (Units V–I). This distribution appears to broadly correlate with marked increases in numbers of fossils and the calcareousness of the sediment (see Table 2.1).

The analysis of nodule material was performed using Raman spectroscopy in an attempt to characterize its mineralogy/composition and help identify a likely formational mechanism. Representative material was sampled from several stratigraphic horizons (e.g., Units VIa, VIb, Va, Vb and IV; Fig. 2.13) and analyzed following the procedure outlined in the Spectroscopy Methodology section (preceding the references). Preliminary results indicate that the nodules are predominantly composed of fine-grained phosphatic material including apatite and/or hydroxylapatite (Fig. 2.14). Representative Raman spectra display strong peaks shifts in the range 967–1020 cm^{-1}, diagnostic of phosphatic minerals (e.g., Sinyayev et al. 2005; Kizewski et al. 2011). The variation in the width of these Raman peaks for phosphates likely reflects a spectroscopic response between crystalline phases (narrow peak) and more amorphous mineral forms giving broader peaks (cf. Fig. 2.14).

The likely provenance of the phosphatic nodules includes the weathering of bone material, as evident by its association with partially decomposed bone fragments (Fig. 2.13a, d), and/or diagenetic formation following the syn-sedimentary accumulation of bat guano and a subsequent increase in the concentration of dissolved phosphate within infiltrating aqueous fluids (e.g., Karkanas et al. 2000, 2002; Shahack-Gross et al. 2004). Thus, the nodules appear to be autochthonous and formed as a result of post-sedimentation weathering/alteration and diagenetic processes resulting in the formation of authigenic phosphate. This hypothesis is supported by the general disseminated, undeformed and granular appearance of the nodules that display little evidence of mobilization or re-working.

Additional diagenetic features of the sedimentary sequence within Azokh 1 include the occurrence of rust-red to orange-brown colored staining, coatings, nodules and grains throughout the succession (Fig. 2.13e, f). Raman analysis of representative orange-stained sediment and sub-rounded nodules and specks from Units IXa, IXb and Vb indicates that this material is primarily of iron oxide composition and is dominantly hematite with lesser magnetite (Fig. 2.14).

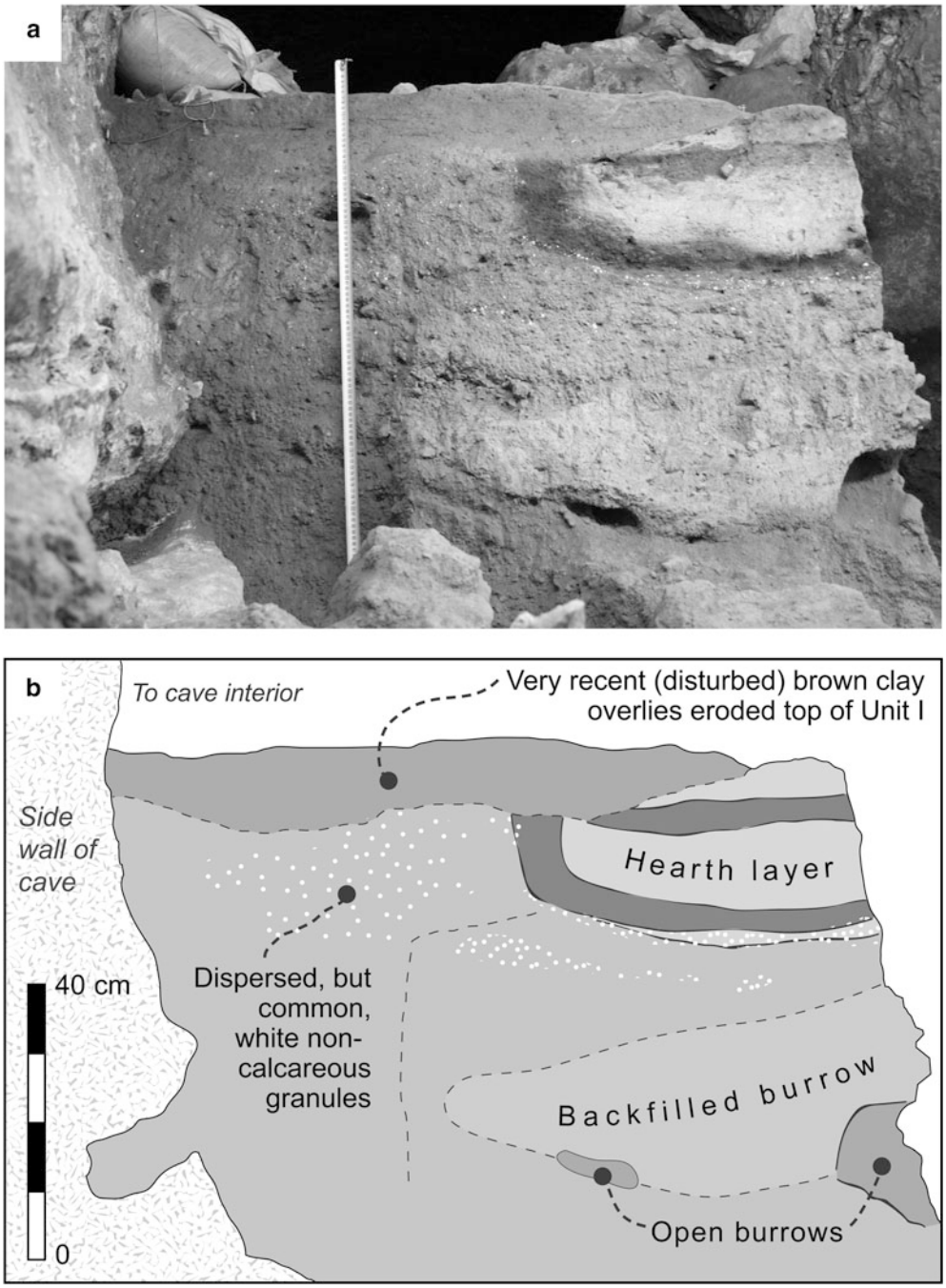

Fig. 2.12 **a** Photograph of the top of Unit I after it was exposed and cleaned during the 2007 field season. The visible length of the tape measure is 88 cm. **b** Sketch interpretation of the photograph in (**a**) showing hearth layer (fumier), disturbance by burrows and eroded top of Unit I. Reproduced from Murray et al. (2010)

Dating and Correlating the Sediment Sequences

A range of radiometric dates for Sediment Sequence 2 is reported in the Appendix of this volume. Age determinations are included here and also summarized in Table 2.1. Moving from the base to the top of the sequence:

Units V and IV: Uranium series dating suggested an age of c. 200 ka for Unit V, whilst racemization (D/LAsp) indicated an age closer to 300 ka. However, the most up to date ESR estimate indicates an age of 293 ± 23 ka. An ESR date of 205 ± 16 ka has been calculated for the base of Unit IV, very close to the contact with underlying Unit V.

Unit III: No dates are available for this unit.

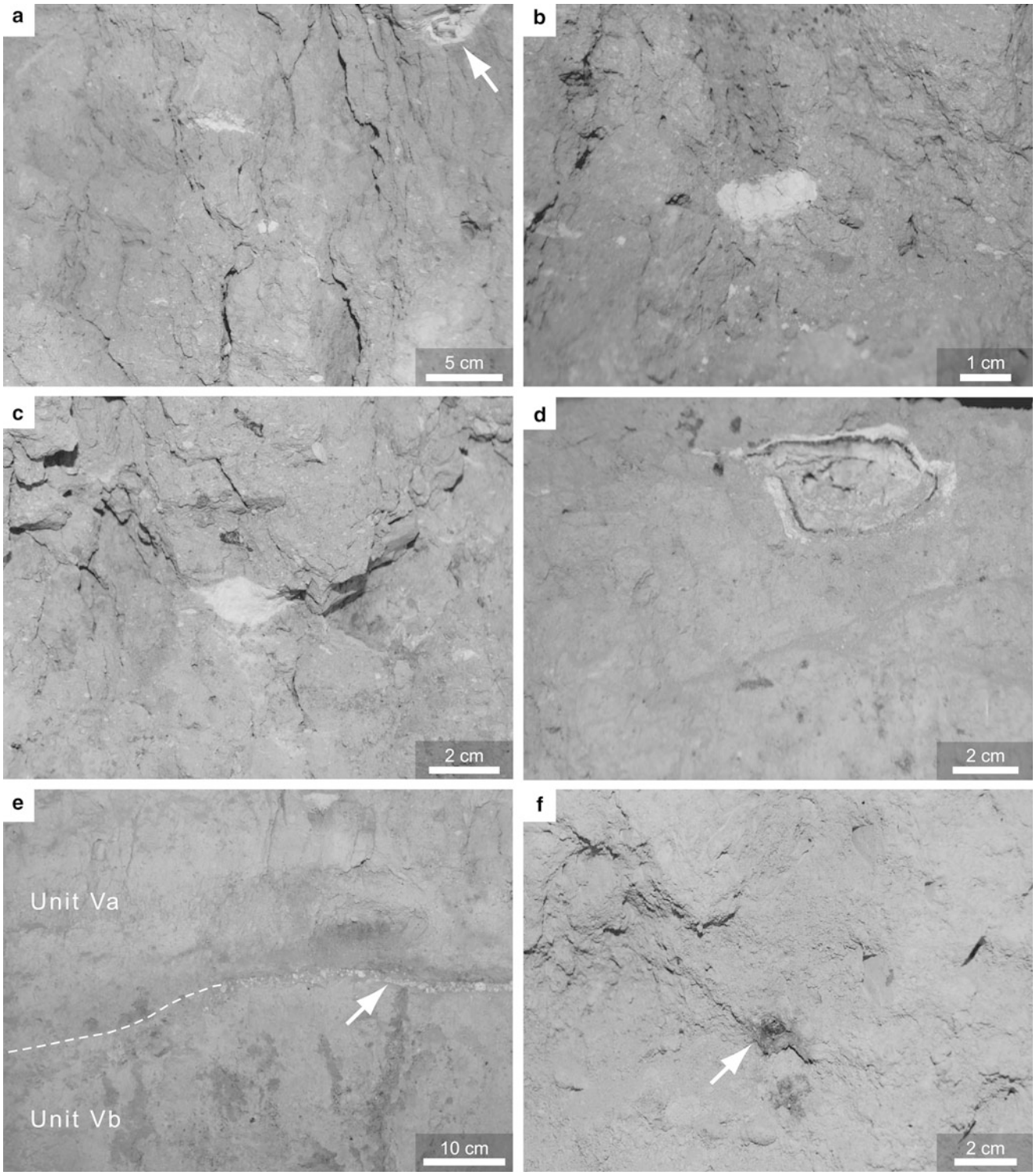

Fig. 2.13 **a** Phosphate nodules in Unit VIa. Nodules occur as cream to white, clay-like lenticular concretions and disseminated specks, or as partially developed concentric laminae within decomposing bone material (arrowed). **b**, **c** Detailed views of phosphate nodules disseminated in Unit VIa. In (**c**) the lenticular form of the nodule in the center of the image is similar to the shape of the bone material shown in (**a**) and (**d**). **d** Partially decomposed bone fragment in Unit Vb displaying concentric phosphate (white) and hematite (dark grey) banding. **e** Contact between Unit Vb and Va partially defined by a 1 cm nodular seam of phosphatic material (arrowed). The dark grey, sub-vertical patches seen in Unit Vb represent hematitic-stained sediment. View looking approximately east. **f** Rounded hematite nodule in Unit IXa (arrowed)

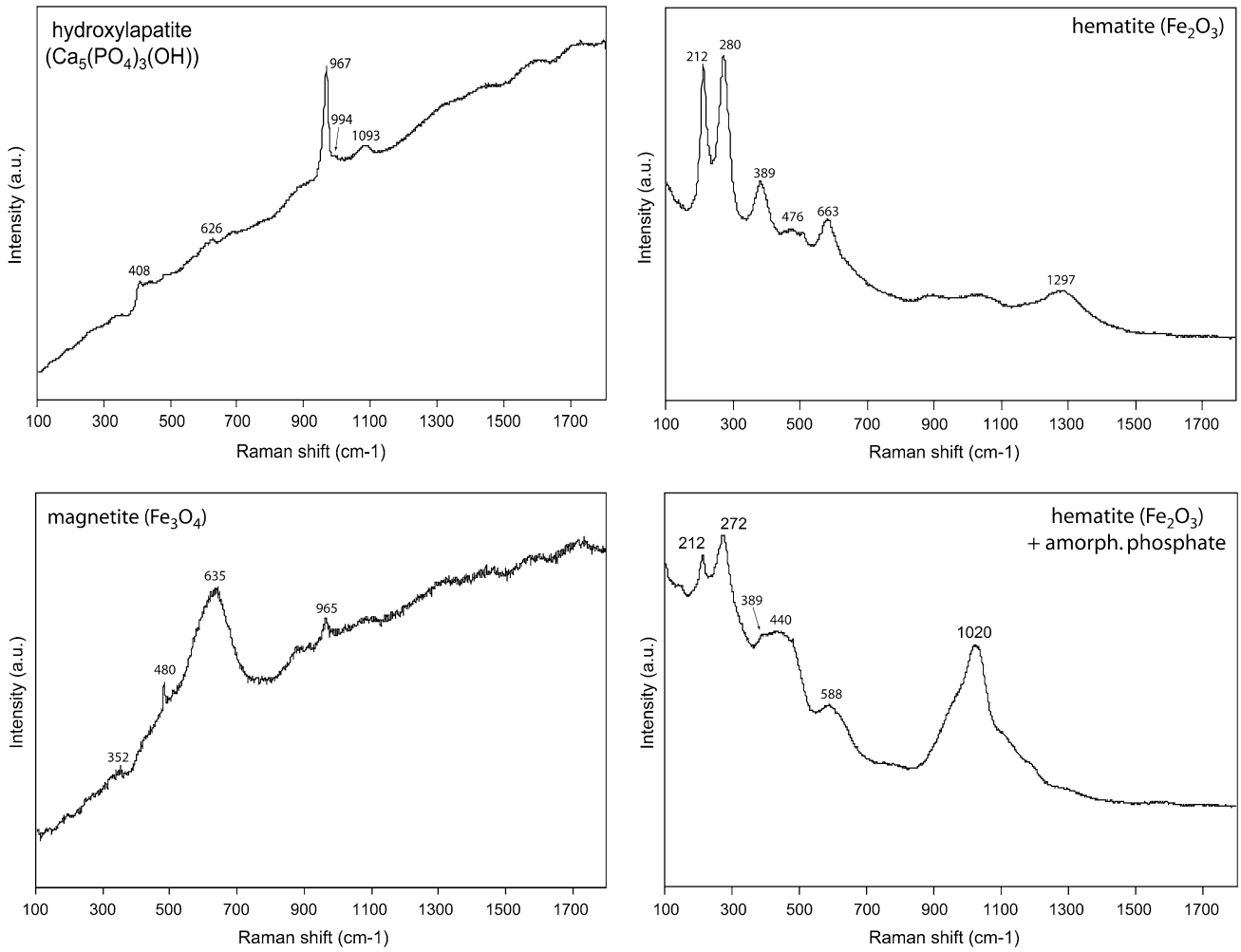

Fig. 2.14 Representative Raman spectra of mineral phases present within several Azokh 1 sedimentary units. Diagnostic peak positions are labeled using Raman shift values (cm^{-1}). Raman intensity is in arbitrary units (a.u.)

Unit II: Murray et al. (2010) noted an unsuccessful attempt to radiocarbon date this unit and suggested its age likely exceeded the lower radiocarbon range of 60 ka. Subsequent ESR dating has provided an age of 184 ± 13 ka for the base and 100 ± 7 ka for the top of Unit II (see Appendix, ESR).

Charcoal from the fumier in Unit I provided a radiocarbon age of 157 ± 26 ^{14}C BP (see Appendix, radiocarbon). Murray et al. (2010) noted that a Russian coin, from around the mid-1960s, was discovered in 2006 (although it had been moved by subsequent bioturbation). Below the hearth in Unit I, the sediments are highly disturbed (Fig. 2.12), so confident dating this unit remains problematic.

It is clear that Sediment Sequence 2 ranges in age from Middle to Late Pleistocene (Units V to II; Table 2.1). The Middle Pleistocene age for Unit V is significant as it is from this level in the succession that the hominin mandible was recovered in the 1960s (Kasimova 2001; see also King et al. 2016). The sharp, irregular contact between Units II and I at the top of Sequence 2 is disconformable and may represent a hiatus in sedimentation, with possible subsequent erosion, between Late Pleistocene and Holocene times (Table 2.1). This relationship suggests that the Pleistocene-Holocene boundary transition is not fully represented in the succession (Murray et al. 2010).

The details of the age of Sediment Sequence 1 remain unclear. Attempts to resolve the matter are hampered by two principal factors:

1. *The limited extent of the remaining stratigraphy*. This has already been discussed, but the lack of fossil remains and bona-fide lithic artifacts in Units IX to VII is also problematic.

2. *Uncertainty in how the two sediment sequences precisely correlate.* This is a function of the fact that no *in-situ* sediment connection now remains between the two sediment sequences in Azokh 1. The simplest view of the situation (Occam's razor) would be to assume that Sediment Sequence 1 is positioned at a lower level in the passage (Fig. 2.4) and therefore must stratigraphically (directly) underlie Sediment Sequence 2. However, with the lack of information about the lateral connection of strata, it is impossible to establish with any degree of certainty if the cave-fill sequence is progradational. The presence of conglomeratic subunit VIc (Fig. 2.9) signifies a period of increased water flow through the passage. This may have eroded parts of any pre-existing strata, introducing a time gap of unknown duration into the sequence, casting an element of doubt into the assumption that Sediment Sequence 1 records a smooth, unbroken succession from Middle Pleistocene (near the top) to older times (moving stratigraphically downwards).

Correlation between the two sediment sequences in Azokh 1 is discussed in detail by Murray et al. (2010), who propose several possibilities:

- Using the bedrock floor of the cave as a datum, the base of subunit Vb in Sequence 2 is equivalent to the base of subunit VIc or possibly even the upper portion of Unit VII in Sequence 1.
- The highly conspicuous conglomeratic subunit VIc in Sediment Sequence 1 (Fig. 2.9) may correlate with the lenticular unit (horizon (c) in Fig. 2.10b) in the base of Vb. The latter displays an erosive, channel style geometry and exhibits an elevated gravel content. Although the sedimentological details of the two units are not identical, both *could* have been produced by fluvial processes and the differences between the two may be a reflection of lateral facies variation.
- The increase in calcareousness in the units overlying conglomeratic VIc and horizon (c) in subunit Vb may provide grounds for a chemostratigraphic correlation. In Sequence 1, subunit VIb is mildly calcareous, whilst VIa at the very top of the preserved section is strongly calcareous (Table 2.1). A similar transition is seen towards the very top of subunit Vb in Sequence 2.

According to Huseinov (1985) paleomagnetic work on the sediments infilling Azokh 1 indicated that the bulk of the middle and upper part of the stratigraphy lies within the Brunhes Polarity Chron (i.e. dating back to 0.781 Ma). Huseinov (1985) noted though, that *his* "Layer VIII" (*very broadly* equivalent to the middle of Sediment Sequence 1, as defined herein) was reversely magnetized, suggesting possible placement within the Matuyama Polarity Chron. Ljubin and Bosinski (1995) also noted this possible magnetic reversal in the lower part of the succession. If this is indeed correct, it would imply that the very basal part of the stratigraphy of Azokh 1 is Early Pleistocene in age.

Discussion on the Stratigraphy of Azokh 1

Depending on the method of lateral correlation employed between the two sediment sequences, a total of between 11.2 and 12 m of stratigraphic infill can be accounted for in Azokh 1 passage. Much of this sediment has been removed by previous excavations (Fig. 2.4) and the lack of rigorous recording of this material compromises the information potential of the stratigraphic remnant described here. A graphic illustration of this is the confusion over the precise level within Unit V of the find of the partial Middle Pleistocene human mandible (see discussion in Murray et al. 2010 and references therein).

Lioubine (2002) noted that the "stepped back" appearance of the excavation in the passage (Fig. 2.4) severely hinders any potential study of paleoclimatic proxies, which are generally best preserved in the sediments close to the cave entrance. A similar argument can be made for evidence for human occupation and activity, which is usually best preserved near entranceways in cave settings. Uncertainty over the lateral connection of strata through the cave passage has already been discussed here. Lioubine (2002, p. 23) noted, for example, that Unit V apparently thinned dramatically from 5 to 2 m. This was based on a review of previous reports on the stratigraphy and, admittedly, more precise details were not available to him.

The distinction between the largely unfossiliferous Sediment Sequence 1 and fossiliferous Sediment Sequence 2 above is not easy to explain. It may be a taphonomic artifact; a result of the limited amount of stratigraphy remaining in Sediment Sequence 1 or it may simply be a function of accessibility, with the lower level of the passage (see "basal trench at cave entrance" in Fig. 2.4) not as easy to enter at the time it was originally infilling with sediment. Murray et al. (2010) also highlighted this fossiliferous distinction between the two sequences and tentatively suggested that this may reflect the degree to which the cave passage was open to the outside world. Conglomeratic subunit VIc (Fig. 2.9) is located at the top of this apparently unfossiliferous sequence. It is a particularly distinctive horizon that

contrasts with the largely fine-grained units below and directly above. Sedimentologically, it represents a marked increase in the strength of water flow through the passage at this point and it may *possibly* be related to improved accessibility of the passage (discussed previously herein; see also commentary in Murray et al. 2010).

Sediment Sequence 2 dates from the Middle Pleistocene to the present (Table 2.1; see also Appendix of this volume); although the disconformable relationship between the top of Unit II and base of Unit I means the actual Pleistocene-Holocene transition is not represented. A rich and diverse Pleistocene fauna has been recovered from Units II–V and preliminary findings are listed in Fernández-Jalvo et al. (2010). Cave bears dominate the macro-mammal fraction (Van der Made et al. 2016), whilst bats are a common constituent of the micro-mammal component of the fauna (Sevilla 2016).

The sedimentological differences between the various units infilling Azokh 1 may reflect individual episodes of deposition and sedimentation in response to karst development and paleoenvironmental change, as opposed to a gradual evolution of the entire sedimentary sequence. Much of the sediment in Sequence 2 is quite fine-grained (see Table 2.1) suggesting generally low levels of depositional energy. However, two levels within this portion of the cave-fill (Units IV and II) contain elevated amounts of relatively coarse, angular, limestone debris (Fig. 2.6). Murray et al. (2010 [p. 87] and references therein) suggested that this could represent frost action during cooler climatic intervals but cautioned that other geomorphological processes, such as seismic activity, dissolution and hydration shattering, may produce similar results. These authors also noted that the slope of the various chambers and passages comprising the Azokh Cave system (Fig. 2.2) suggested water and fine-sediment flow from the interior towards the exterior. However; it is entirely possible that the patterns of sedimentation varied throughout the cave's history, with alternation between the two flow directions occurring. As noted in the opening paragraphs of this section, due to the fact that lateral facies changes were undocumented during the original excavation phase and the fact that the sediment is now removed, this will have to remain a point of conjecture.

Azokh 2

The entrance to the passage we have named Azokh 2 (Fig. 2.3b) is located approximately 42 m NNW from the Azokh 1 entrance (Fig. 2.2). The present level of archaeological excavation has resulted in a chamber that is accessible for about 7.5 m (length) by 3.5 m wide (Fig. 2.15), while the unexcavated level of sediment within the chamber begins approximately 2 m below the roof of the passage. A large boulder collapse has choked the rear, or northeastern end, of the passage where it leads into the interior of the cave (Fig. 2.15; see also Fig. 2.2). This blockage has been a hindrance to further exploration and excavation work within this passage. Azokh 2 is sunlit during daylight hours.

Two geological test trenches (see Fig. 2.15) were dug in 2002 [Pit 1] and 2003 [Pit 2] to begin investigating the stratigraphy of the sedimentary infill of Azokh 2. This preliminary work sub-divided the sediments into two stratigraphic units which are readily distinguishable on the basis of color. The lower Unit 2 is light yellow-brown in color, which contrasts sharply with the dark greyish-brown appearance of Unit 1 above. Details of the findings of that work are summarized in Table 2.3. Measurement of the elevation of the contact between the two units (below the level of the cave datum) exposed in the two test pits suggested a possible slope of c. 10° towards the southwest (i.e. towards the cave exit; Fig. 2.15). This slope is less apparent when examined in detail near the entrance to the passage.

Unit 2 is at least 90 cm thick (the base was not seen) and can be divided into a lower subunit with rare limestone clasts (2b) and an upper subunit with an increased proportion of limestone clasts (2a). Unit 1 is considerably more complex and heterogeneous in character. A subtle shift in granular structure of the sediment effectively marks the distinction between its two constituent subunits (Table 2.3), although this is not always apparent when traced laterally. Unit 1 contains numerous hearth layers, particularly in subunit 1b. These are commonly white to light grey and ashy in appearance, with an associated reddening of the surrounding sediment.

In 2007 the two test excavation pits in Azokh 2 were reopened in order to excavate the intervening sediment section (see details on Fig. 2.16) and during this work, modern human postcranial skeletal remains were discovered. This particular find was reported by Fernández-Jalvo et al. (2010), who noted an age estimate of 1265 ± 23 ^{14}C BP.

Discussion on the Stratigraphy of Azokh 2

Knowledge of the stratigraphy of Azokh 2 is still very much at a preliminary stage. This is largely a function of the boulder choke at the rear of the passage (Fig. 2.15) that has imposed a physical restriction on the direction and degree of

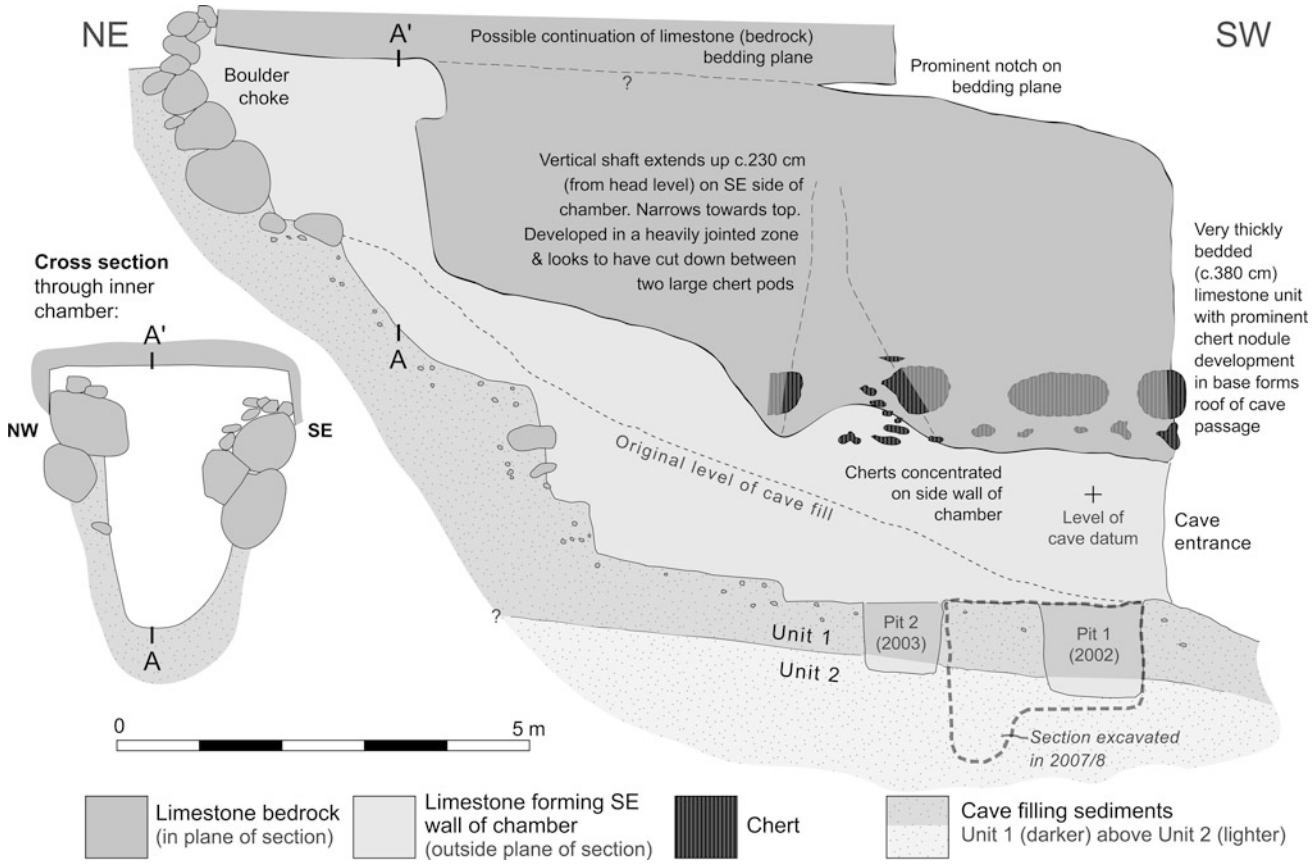

Fig. 2.15 Sketch cross-section through the Azokh 2 chamber (drawn facing SE). The locations of various trenches developed over several field-seasons (2002, 2003 and 2007) are indicated. Note that the SE walls of these trenches are out of the plane of section and are thus unornamented. Note also the original level of cave fill prior to the current phase of excavation and the boulder filled inner chamber in the rear of the cave passage

excavation work possible. The possible distinction between the two sedimentary units may possibly reflect the passage shifting from a closed (Unit 2) to a more open (Unit 1) system. The increase in the abundance of limestone clasts between subunits 2b and 2a (above) may represent a gradual shift towards wetter and/or cooler climatic conditions, but this remains debatable (see discussion on coarse limestone debris in sediments in Azokh 1 above).

The overlying sediments of Unit 1 are conspicuously more humic and organic rich. They are noticeably heterogeneous when tracked laterally and the presence of numerous hearth layers attest to a sustained period of past human activity in the passage. The first hearth layer appears directly on the contact between Units 1 and 2, which may possibly support the contention that humans only entered the passage when it became open to the outside world. The age of the underlying Unit 2 is uncertain since no artifacts or fossil remains have been recovered from this unit.

Azokh 5

The entrance to the Azokh 5 passage is located about 100 m NNW from Azokh 1 and it connects to one of the largest inner chambers of the Azokh Cave system (Chamber IV; see Fig. 2.2 and also Domínguez-Alonso et al. 2016). The roof of the entrance passageway bears morphological characteristics suggestive of formation as a phreatic tube (Fig. 2.3c). This passage continues northeastwards from the entrance for 5 m before rapidly opening upwards and outwards, creating an inner sub-chamber (Fig. 2.16) which has a significant sediment infill. Chert development is quite prominent in the limestone forming the roof to this connecting passage.

Excavation and investigation of the stratigraphy in Azokh 5 has been conducted intermittently since 2006. The *in situ* sediments were covered by a ramp of mixed sediments containing, amongst other things, human teeth and tools, as well as additional fauna (see Fig. 2.16 for an indication of the

Table 2.3 Stratigraphy of Azokh 2 Passage

Unit/ Sub-unit		Thickness	Consistence & Texture	Structure	Color (Munsell)	Rocks/clasts/comments	Carbonates
1	1a	20 cm (*Present in trench, but thickens considerably in direction of cave interior – the top of this unit was not seen*)	Friable-firm clay to silty clay	Fine granular to massive	10YR 4/2 (Dark greyish brown)	(In logged section): Matrix-supported greyish angular limestone clasts (up to 21 cm across) and abundant recent plant rootlets. Charcoal fragments noted near base. Boundary with underlying subunit is topographically irregular. Above this level, this subunit currently includes the thick (mixed and disturbed) deposits of the boulder collapse at the rear of the passage	Calcareous
	1b	c. 55–60 cm	Friable silty clay	Medium granular	10YR 3.5/2 (Dark greyish brown)	Angular grey limestone clasts dispersed throughout, but they are particularly concentrated in the basal 25 cm on the WNW wall of the trench (i.e. closest to the cave wall). Recent plant roots penetrate this layer. This horizon is quite heterogeneous laterally and vertically. A prominent 3 cm thick pale grey ash layer (hearth) was located 7 cm from the top of this subunit. It dipped gently in a southerly direction (i.e. the direction of the cave entrance) and passed laterally into a unit with abundant flecks of charcoal. Charcoal was concentrated (broadly) in the top 20 cm of the subunit as a whole. Pottery fragments were recorded in this upper zone also	Calcareous
2	2a	c. 40 cm	Friable sandy/silty clay	Largely massive, granular in places	10YR 6/4–6.5/4 (Light yellowish brown)	Sub-rounded to angular limestone clasts common. Limestone clast content increases gradationally across contact with subunit 2b below	Strongly calcareous
	2b	50 cm+ (*Base not seen*)	Firm clay (*With minor sand/granule component*)	Massive	10YR 6/4 (Light yellowish brown)	Limestone clasts generally rare	Strongly calcareous

original level of cave fill). A 145 cm deep trench [Pit 3] in the entranceway to the chamber (Fig. 2.17; see also Fig. 2.16 for general location) revealed the following stratigraphy:

1. [Top]: 45 cm (minimum) very weakly calcareous medium-brown clay-rich soil (humus). A very strong granular structure was developed and many modern plant rootlets were present throughout. Angular limestone clasts (on all scales) were dispersed throughout, and gastropod shells and bat bones were also present.
2. [Middle]: 62–70 cm light beige-yellow firm calcareous clay, with a noticeable carbonate sand and granule component. Scattered limestone and (angular) chert clasts (generally 2–7 cm) were present; however, they were less abundant in comparison to unit 1 above. A moderate to strong granular texture was developed.
3. [Base]: 30 cm (minimum – base not seen) medium reddish-brown calcareous silty clay. It was reasonably well sorted with a moderate to fine granular texture.

Currently, five sedimentary units (labeled A–E) have been identified in the inner chamber (see Table 2.4 and also Figs. 2.16 and 2.18), comprising a predominantly fine-grained succession that is punctuated by two horizons containing elevated amounts of coarser clasts (Units B and D, see Table 2.4, Fig. 2.18). The larger clasts in these layers comprise limestone and chert debris, some of which appears to have simply dropped from the roof above. The significance of these two horizons with elevated amounts of coarse angular cave-wall debris may be that they indicate a shift towards wetter or cooler conditions, but (as discussed above for both Azokh 1 and 2) this line of reasoning is somewhat speculative. The stratigraphic horizons which directly follow Units B and D (Units A and C respectively) both drape and infill their irregular top surfaces.

The contact between Units A and B (at the top of the inner chamber sequence in Azokh 5) is both conspicuous and significant. The top surface of Unit B is quite irregular and rough and is progressively infilled by the laminated fine clays and silts of Unit A. Thin seams of fine to medium sand-grade material also occasionally occur in the latter. Unit A represents a switch to calcareous sediment deposition within Azokh 5 (Table 2.4).

The sedimentary laminations of Unit A are inclined and appear to have banked up in this corner of the chamber,

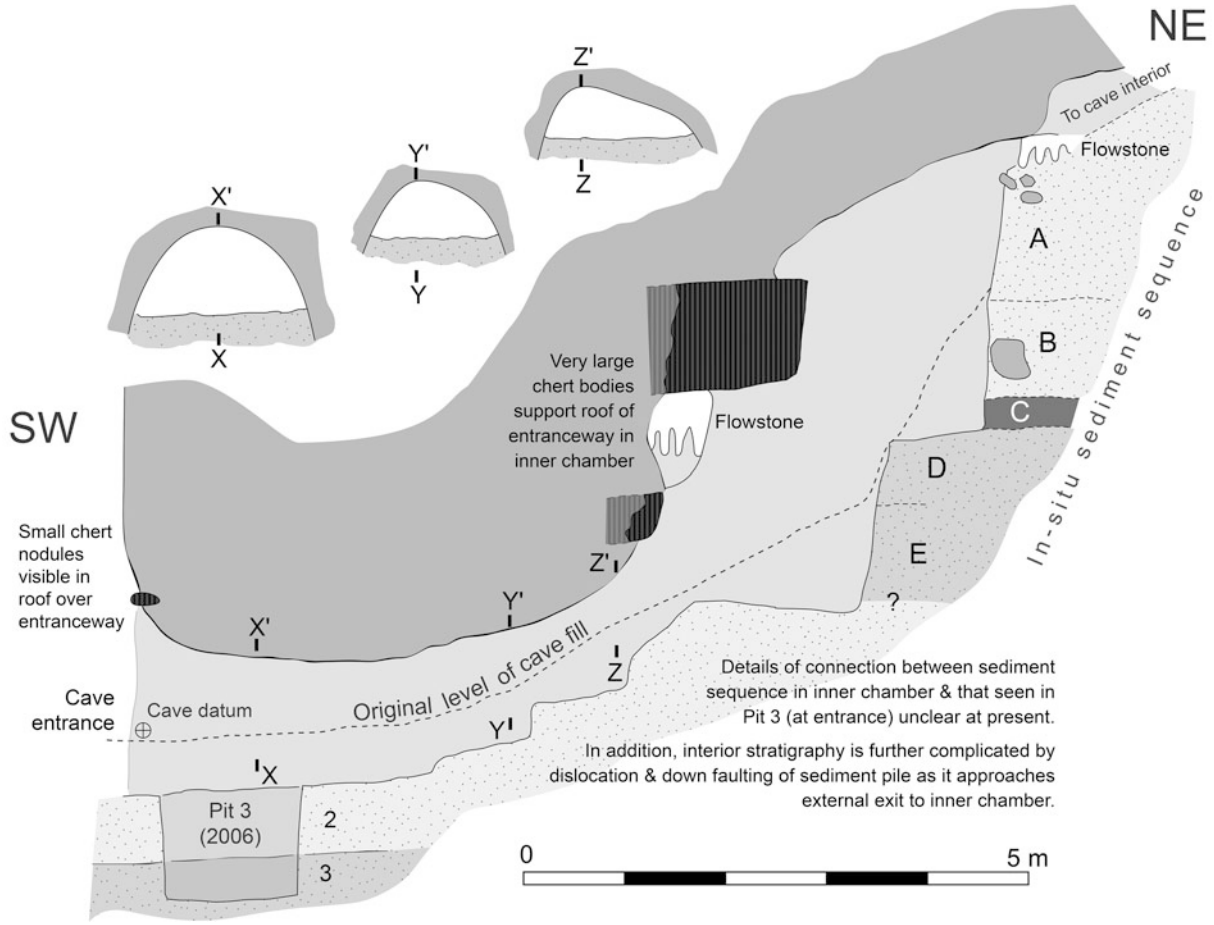

Fig. 2.16 Sketch cross-section through the Azokh 5 chamber (drawn facing NW). The locations of Pit 3 and the *in-situ* sediments exposed in the inner chamber are indicated. The NW wall of Pit 3 is out of the plane of section and is thus unornamented. Note the original level of cave fill prior to the current phase of excavation. Three consecutive cross-sections (*X*, *Y* and *Z*) illustrating the profile and shape of the entrance tunnel are presented. These are drawn to the same scale as the main section. These sections were drawn before any systematic excavation took place in Azokh 5, and consequently the level of sediment fill corresponds with the dashed "original level of cave fill" line. For key to ornaments see Fig. 2.15

effectively onlapping the top of Unit B. This may have introduced a time gap of unknown duration into the sequence. Fernández-Jalvo et al. (2010) reported modern human remains (teeth and cranial fragments) with associated charcoal from Unit A. The latter provided a radiocarbon age of c. 2.3 ^{14}C kBP. These authors suggest a possible relationship between this material and finds from near the base of Unit I in Azokh 1. It is interesting therefore that both Unit A (Azokh 5) and Unit I (Azokh 1) have discordant relationships with the units they succeed and both infill irregular topographic surfaces of their respective underlying strata. However, despite these general similarities, and in the absence of criteria allowing direct and precise correlation, any broad correlation in terms of the infilling history of the two passageways remains entirely hypothetical.

Unit B thins to 34 cm in the northwestern corner of the chamber and is covered and cemented on the upper surface by flowstone. A mineralised cylindrical structure, possibly a calcified mammal burrow (Fig. 2.19), occurs just below this level. Flowstone has also been observed in association with Units A and D, suggesting that this portion of the cave has remained wet for some time.

The sediments of Unit C are clay-rich and display weak internal stratification. Extrapolation across the cave-chamber,

Fig. 2.17 Photograph of the geological trench (Pit 3; see Fig. 2.16) excavated in the entranceway to Azokh 5. Two units (1 and 2) are clearly visible. The northeastern edge of the trench is indicated with a dashed black line. Hammer (circled) for scale

southwest towards the exit, indicates that when this horizon was being deposited the passage connecting to the outside may have been sealed. Unit C most likely was produced by very quiet conditions (still-water deposition), and, given its thickness of 26–34 cm, it may have taken an appreciable amount of time to form. Therefore, although Unit A may be (perhaps late) Holocene in age, with the discordant relationship with underlying Unit B and the potential amount of time required to deposit Unit C, it is possible that Units D and E below may be significantly older.

Discussion on the Stratigraphy of Azokh 5

At present, it is unclear precisely how the two sedimentary sections (external and internal) in Azokh 5 physically and temporally relate to one another. A simple topographic assessment suggests that Units A–E in the inner chamber may overlie Units 2–3 located closer to the cave entrance (see Fig. 2.16); however, this requires more excavation work to unequivocally confirm or disprove this relationship. A further complication is that natural fracturing and

Fig. 2.18 Photomontage of the sediment section present inside Azokh 5 inner chamber. The five units (A–E) are marked in the photo and the tape measure scale is extended to 318 cm ►

Table 2.4 Stratigraphy of Azokh 5 inner chamber

Unit	Thickness	Consistence & Texture	Structure	Color (Munsell)	Rocks/clasts/comments	Carbonates
A	200 cm+ (*Minimum value – unit thickens considerably in direction of cave interior; top not seen*)	Friable-firm clay	Fine granular to massive	10YR 6/4 (Light yellowish brown)	Limestone clasts are very rare. This unit is well sorted and stratified (laminated) and drapes the irregular surface topography of Unit B below	Strongly Calcareous
B	c. 55–85 cm+ (*Thins to c. 34 cm in NW corner of chamber, appears to be thickest in SE corner*)	Friable silty clay	Medium granular	7.5YR 5/4 (Brown)	Highly mixed and unsorted unit. Varies between essentially a matrix- and clast-supported breccia. Contains abundant limestone clasts (on all scales). Chert clasts noted also	Non-calcareous
C	26–34 cm	Friable clay (*Very firm when dry*)	Largely massive	7.5YR 4/2.5 (Brown)	Clasts generally rare: granule and pebble-scale clasts of limestone and angular chert present but not conspicuous. Unit has some weak internal stratification. Drapes irregular topography of Unit D below; basal contact is sharp	Non-calcareous
D	64–66 cm	Friable sandy clay	Medium granular	7.5YR 4.5/3 (Brown)	Matrix-supported breccia. Clasts of all sizes, although 2–7 mm whitish granules and pebbles are most conspicuous. Larger clasts (up to 13 cm across) are generally located in the upper half of the unit. Clasts consist of limestone (displaying varying degrees of decalcification) and angular dark clasts of chert (up to 7.5 cm)	Non-calcareous
E	90 cm (*Minimum – base not seen*)	Friable (to loose) sandy clay	Medium granular	7.5YR 5/3 (Brown)	Moderately well sorted unit, although rare 1–3 mm granules are present. Basal 50–60 cm has a vague horizontal internal stratification developed. Thin white non-calcareous crust (3–5 mm) caps unit in northern corner of cave chamber	Non-calcareous

Fig. 2.19 Flattened cylindrical structure, possibly a calcified mammal burrow, from the inner chamber of Azokh 5

displacement of Units A–E has been observed in the inner chamber. It appears that these units have begun to slip progressively downwards in the direction of the cave exit (Fig. 2.16). In addition, Domínguez-Alonso et al. (2016) note that geophysical investigations have indicated over 10 m (stratigraphic thickness) of sediments infilling Azokh 5. Thus, further investigation of the passage is likely required to improve our understanding of the sediments within Azokh 5.

Conclusions

1. Of the three passages connecting to the interior of the Azokh Cave system, the stratigraphy of Azokh 1, previously documented in detail by Murray et al. (2010), is the most completely known. This particular passage has been excavated since the 1960s and contains an 11–12 m thick sedimentary record dating from at least the Middle Pleistocene (and possibly even older; see Table 2.1) to the present. The Pleistocene-Holocene transition is not seen due to a marked erosional disconformity in the sequence towards the very top.
2. A lower-lying sub-chamber in the Azokh 1 Passage (see Fig. 2.4), close to the entrance, accommodates Sediment Sequence 1. This 4.5 m thick section includes Units IX to VI (in ascending stratigraphic order), and, with the

exception of the very top, it is apparently largely unfossiliferous. For this reason, the precise age of these sediments remains unknown. Previous paleomagnetic work suggested that the base of the succession, in this part of the cave, might in fact be Early Pleistocene in age.

3. Sediment Sequence 2 is located further in from the cave entrance in Azokh 1 and is interpreted to have largely overlain Sediment Sequence 1, although this is not possible to verify as they are no longer physically connected due to past excavation work. This sequence is about 8.5 m thick and is divisible into five units (V–I). The lowermost Unit V accounts for almost half this thickness estimate. Units V–II have produced a rich and diverse Middle to Upper Pleistocene fauna. Associated and isolated cave bear skeletal and dental elements are particularly conspicuous throughout this part of the succession. Evidence of human activity (in the form of stone tools and cut marks on bones) has also been found in these levels. In the past, a Middle Pleistocene human mandible fragment was recovered from about the level of Unit V, although the precise datum of this find is unclear.
4. The sedimentary infill of the Azokh 1 passage is generally fine-grained, suggesting either very low energy water-flow, perhaps due to ponding as a result of flooding further inside the cave system, or due to possible wind-blown deposition, although this is unlikely for sediments located further inside from the cave entrance. Horizons containing concentrations of coarser limestone debris also occur. Their significance is unclear; however, they may indicate a change in paleoenvironmental conditions, such as an increase in water percolation through the cave or a marked climatic cooling. Geomorphological and tectonic factors, such as an increase in earthquake activity, cannot be discounted either.
5. Azokh 2 is a smaller cave located 42 m NNW from the entrance to Azokh 1. At present two stratigraphic units are clearly identifiable infilling the passage. The uppermost of these (Unit 1) appears to be Holocene in age and below this, Unit 2 is conspicuously lighter in color and more calcareous. Its total thickness is unproven and, as it did not produce any fossils or artifacts, its age is unknown. A significant boulder collapse in the rear of Azokh 2 continues to pose serious logistical problems for further excavation of the cave passage.
6. Azokh 5 is located 100 m NNW from Azokh 1. It is a small phreatic tube that leads to an inner chamber containing at least 4.5 m of infill, although that value is likely to be a gross underestimate as the base and top of the sequence were not seen and geophysical results reported by Domínguez-Alonso et al. (2016) suggests a total sediment infill of at least 10 m. At present five units (labeled A–E in descending stratigraphic order) have been identified. The sediments are generally fine-grained, although Units D and B both contain elevated amounts of coarse limestone and chert debris, much of which has been locally sourced. A disconformable relationship has been identified between Units B and A at the very top of the succession. Unit A has produced charcoal dating to c. 2,300 years BP (Fernández-Jalvo et al. 2010); however, the age of the units beneath remains unknown at present.

Spectroscopy Methodology

Raman Spectroscopy of Azokh 1 Sediment Samples: Analytical Methodology

Raman spectroscopy of sediment samples was conducted at the School of Natural Sciences, NUI Galway, using a Horiba LabRam HR laser Raman spectrometer. The instrument is equipped with a 600 groove.mm^{-1} diffraction grating, confocal optics and a Peltier-cooled CCD detector (255 × 1024 pixel array at −67 °C) coupled to an Olympus BX51 microscope. Dry, friable samples were placed on a glass slide and analysed in 180° backscatter mode using either 532 nm or 784 nm laser excitation channeled through a 50× microscope objective. Individual analyses were performed for between 60–90 s over the spectral range 100–1800 cm^{-1} (Fig. 2.14). The number of spectral accumulations per analysis typically ranged between 50 and 100 in order to maximize the signal-to-noise efficiency of the spectrometer. Calibration of the instrument was routinely performed between analyses using the Raman peak of a crystalline silicon wafer (520.2 ± 0.5 cm^{-1}; Parker et al. 1967). Spectral uncertainty associated with the generation of Raman peak positions is estimated to be ±1.5 cm^{-1} (2σ) under 532 nm laser excitation and ±1.0 cm^{-1} (2σ) using the 783 nm laser.

Acknowledgments Many colleagues have helped and offered much valuable advice to us on numerous aspects of the stratigraphy and sedimentology over the years. In particular, we wish to sincerely thank Yolanda Fernández-Jalvo, Peter Andrews and Peter Ditchfield for very generously sharing their expertise, knowledge and opinions. Teresa Sanz Martín supplied some of the photographs used in the figures. The Royal Irish Academy is thanked for kindly granting permission to reproduce several figures from Murray et al. (2010). The help and assistance of the local people at the excavation at Azokh, year after year, is much appreciated. Without their input, the Azokh Project simply could not run.

References

Appendix: Fernández-Jalvo, Y., Ditchfield, P., Grün, R., Lees, W., Aubert, M., Torres, T., et al. (2016). Dating methods applied to Azokh cave sites. In Y. Fernández-Jalvo, T. King, L. Yepiskoposyan & P. Andrews (Eds.), *Azokh Cave and the Transcaucasian Corridor* (pp. 321–339). Dordrecht: Springer.

Asryan, L., Moloney, N., & Ollé, M. (2016). Lithic assemblages recovered from Azokh 1. In Y. Fernández-Jalvo, T. King, L. Yepiskoposyan & P. Andrews (Eds.), *Azokh Cave and the Transcaucasian Corridor* (pp. 85–101). Dordrecht: Springer.

Bogli, A. (1980). *Karst hydrology and physical speleology*. Berlin: Springer.

Bretz, J. H. (1942). Vadose and phreatic features of limestone caverns. *Journal of Geology, 50*, 675–811.

Bridgland, D. R., Antoine, P., Limondin-Lozouet, N., Santisteban, J. I., Westaway, R., & White, M. J. (2006). The Palaeolithic occupation of Europe as revealed by evidence from the rivers: Data from IGCP 449. *Journal of Quaternary Science*, *21*, 437–455.

Chauvet, J.-M., Deschamps, E. B., & Hillaire, C. (1996). *Dawn of art: The Chauvet Cave*. New York: Harry N. Abrams.

Dirks, P. H. G. M., Kibii, J. M., Kuhn, B. F., Steininger, C., Churchill, S. E., Kramers, J. D., et al. (2010). Geological Setting and Age of *Australopithecus sediba* from Southern Africa. *Science, 328*, 205–208.

Domínguez-Alonso, P., Aracil, E., Porres, J. A., Andrews, P., Lynch E. P. & Murray, J. (2016). Geology and geomorphology of Azokh Caves. In Y. Fernández-Jalvo, T. King, L. Yepiskoposyan & P. Andrews (Eds.), *Azokh Cave and the Transcaucasian Corridor* (pp. 55–84). Dordrecht: Springer.

Doronichev, V. B. (2008). The Lower Paleolithic in Eastern Europe and the Caucasus: A reappraisal of the data and new approaches. *PaleoAnthropology*, 107–157.

Doronichev, V., & Golonova, L. (2010). Beyond the Acheulean: A view on the Lower Palaeolithic occupation of Western Eurasia. *Quaternary International, 223–224*, 327–344.

Engel, A. S., Stern, L. A., & Bennett, P. C. (2004). Microbial contributions to cave formation: New insights into sulfuric acid speleogenesis. *Geology, 32*, 369–372.

Fernández-Jalvo, Y., Hovsepian-King, T., Moloney, N., Yepisko posyan, L., Andrews, P., Murray, J., et al. (2009). *Azokh Cave project excavations 2002–2006: Middle-Upper Palaeolithic transition in Nagorno-Karabagh*. Coloquios de Paleontología, Special Issue: Homage to Dr. D. Soria Madrid, Universidad Complutense de Madrid Press.

Fernández-Jalvo, Y., King, T., Andrews, P., Yepiskoposyan, L., Moloney, N., Murray, J., et al. (2010). The Azokh Caves complex: Middle Pleistocene to Holocene human occupation in the Caucasus. *Journal of Human Evolution, 58*, 103–109.

Fernández-Jalvo, Y., King, T., Andrews, P., & Yepiskoposyan, L. (2016). Introduction: Azokh Cave and the Transcaucasian Corridor. In Y. Fernández-Jalvo, T. King, L. Yepiskoposyan & P. Andrews (Eds.), *Azokh Cave and the Transcaucasian Corridor* (pp. 1–26). Dordrecht: Springer.

Ford, D. C., & Williams, P. (2007). *Karst Hydrogeology and Geomorphology*. Chichester: Wiley.

Huseinov, M. M. (1985). *The Early Palaeolithic of Azerbaijan (Kuruchai culture and stages of its development).* Baku (in Russian).

Jelinek, A. J. (1982). The Tabun Cave and Paleolithic Man in the Levant. *Science, 216*, 1369–1375.

Karkanas, P., Bar-Yosef, O., Goldberg, P., & Weiner, S. (2000). Diagenesis in Prehistoric Caves: The Use of Minerals that Form *In Situ* to Assess the Completeness of the Archaeological Record. *Journal of Archaeological Science, 27*, 915–929.

Karkanas, P., Rigaud, J.-P., Simek, J., Albert, R., & Weiner, S. (2002). Ash, bones and guano: A study of the minerals and phytoliths in the sediments of Grotte XVI, Dordogne, France. *Journal of Archaeological Science, 29*, 721–732.

Kasimova, R. M. (2001). Anthropological research of Azykh Man osseous remains. *Human Evolution, 16*, 37–44.

Khain, V. E. (1997). Azerbaijan. In E. M. Moores & R. W. Fairbridge (Eds.), *Encylcopedia of European and Asian regional geology*. London: Chapman & Hall.

King, T., Compton, T., Rosas, A., Andrews, P. Yepiskoyan, L., & Asryan, L. (2016). Azokh Cave Hominin Remains. In Y. Fernández-Jalvo, T. King, L. Yepiskoposyan & P. Andrews (Eds.), *Azokh Cave and the Transcaucasian Corridor* (pp. 103–106). Dordrecht: Springer.

Kizewski, F., Liu, Y. T., Morris, A., & Hesterberg, D. (2011). Spectroscopic approaches for phosphorus speciation in soils and other environmental systems. *Journal of Environmental Quality, 40*, 751–766.

Lioubine, V. P. (2002). *L'Acheuléen du Caucuase*. ERAUL 93 Études et Recherches Archéologiques de l'Université de Liège. Liège.

Ljubin, V. P., & Bosinski, G. (1995). The earliest occupation of the Caucasus region. In W. Roebroeks & T. van Kolfschoten (Eds.), *The Earliest Occupation of Europe* (pp. 207–253). Leiden: University of Leiden.

Magela da Costa, G., & Rúbia Ribeiro, V. (2001). The occurrence of tinsleyite in the archaeological site of Santana do Riacho, Brazil. *American Mineralogist, 86*, 1053–1056.

Marin-Monfort, M. D., Caceres, I., Andrews, P., Pinto A. C. & Fernández-Jalvo, Y. (2016). Taphonomy and Site Formation of Azokh 1. In Y. Fernández-Jalvo, T. King, L. Yepiskoposyan & P. Andrews (Eds.), *Azokh Cave and the Transcaucasian Corridor* (pp. 211–249). Dordrecht: Springer.

Marincea, S., Dumitras, D., & Gibert, R. (2002). Tinsleyite in the "dry" Cioclovina Cave (Sureanu Mountains, Romania): The second occurrence. *European Journal of Mineralogy, 14*, 157–164.

Moldovan, O. T., Mihevc, A., Mikó, L., Constantin, S., Meleg, I., Petculescu, A., et al. (2011). Invertebrate fossils from cave sediments: A new proxy for pre-Quaternary paleoenvironments. *Biogeosciences, 8*, 1825–1837.

Moore, G. W., & Sullivan, N. (1997). *Speleology: Caves and the cave environment*. St. Louis: Cave Books.

Murray, J., Domínguez-Alonso, P., Fernández-Jalvo, Y., King, T., Lynch, E. P., Andrews, P., et al. (2010). Pleistocene to Holocene stratigraphy of Azokh 1 Cave, Lesser Caucasus. *Irish Journal of Earth Sciences, 28*, 75–91.

Musgrave, R. J. & Webb, J. A. (2004). Palaeomagnetic analysis of Sediments on the Buchan Caves, Southeastern Australia, Provides a Pre-Late Pleistocene Date for Landscape and Climate Evolution. In I. D. Sasowsky & J. E. Mylroie (Eds.), *Studies of Cave Sediments. Physical and Chemical Records of Paleoclimate*. Dordrecht: Springer/Kluwer Academic Publisher.

Mustafayev, A. (1996). Jawbones and Dragon Legends. *Azerbaijan's Prehistoric Azikh Cave. Azerbaijan International, 4*(2), 24–32.

Parker, J. H., Feldman, D. W., & Ashkin, M. (1967). Raman Scattering by silicon and germanium. *Physical Review, 155*(3), 712–714.

Pickering, R., Hancox, P. J., Lee-Thorp, J. A., Grün, R., Mortimer, G. E., McCulloch, M., et al. (2007). Stratigraphy, U-Th chronology, and paleoenvironments at Gladysvale Cave: Insights into the climatic control of South African hominin-bearing cave deposits. *Journal of Human Evolution, 53*, 602–619.

Pickering, R., Kramers, J. D., de Hancox, P. J., Ruitere, D. J., & Woodhead, J. D. (2011). Contemporary flowstone development links early hominin bearing cave deposits in South Africa. *Earth and Planetary Science Letters, 306*, 23–32.

Pinhasi, R., Gasparian, B., Wilkinson, K., Bailey, R., Bar-Oz, G., Bruch, A., et al. (2008). Hovk 1 and the Middle and Upper Paleolithic of Armenia: A preliminary framework. *Journal of Human Evolution, 55*, 803–816.

Pinhasi, R., Gasparian, B., Nahapetyan, S., Bar-Oz, G., Weissbrod, L., Bruch, A. A., et al. (2011). Middle Palaeolithic human occupation of the high altitude region of Hovk-1, Armenia. *Quaternary Science Reviews, 30*, 3846–3857.

Polyak, V. J., McIntosh, W. C., Güven, N., & Provencio, P. (1998). Age and origin of Carlsbad Cavern and related caves from $^{40}Ar/^{39}Ar$ of alunite. *Science, 279*, 1919–1922.

Sasowsky, I. D., & Mylroie, J. E. (2004). *Studies of Cave Sediments. Physical and Chemical Records of Paleoclimate*. Dordrecht: Springer/Kluwer Academic Publisher.

Sevilla, P. (2016). Bats from Azokh Caves. In Y. Fernández-Jalvo, T. King, L. Yepiskoposyan & P. Andrews (Eds.), *Azokh Cave*

and the Transcaucasian Corridor (pp. 177–189). Dordrecht: Springer.

Shahack-Gross, R., Berna, F., Karkanas, P., & Weiner, S. (2004). Bat guano and preservation of archaeological remains in cave sites. *Journal of Archaeological Science, 31*, 1259–1272.

Sinyayev, V. A., Shustikova, E. S., Griggs, D., & Dorofeev, D. V. (2005). The nature of P–O bonds in the precipitated amorphous calcium phosphates and calcium magnesium phosphates. *Glass Physics and Chemistry, 31*, 671–675.

Smith, C. I., Faraldos, M., & Fernández-Jalvo Y. (2016). Bone Diagenesis at Azokh Caves. In Y. Fernández-Jalvo, T. King, L. Yepiskoposyan & P. Andrews (Eds.), *Azokh Cave and the Transcaucasian Corridor* (pp. 251–269). Dordrecht: Springer.

Torres, T., Ortiz, J. E., & Cobo, R. (2003). Features of Deep Cave Sediments: Their Influence on Fossil Preservation. *Estudios Geológicos, 59*, 195–204.

Van der Made, J., Torres, T., Ortiz, J. E., Moreno-Pérez, L., & Fernández-Jalvo, Y. (2016). The new material of large mammals from Azokh and comments on the older collections. In Y. Fernández-Jalvo, T. King, L. Yepiskoposyan & P. Andrews (Eds.), *Azokh Cave and the Transcaucasian Corridor* (pp. 117–159). Dordrecht: Springer.

White, W. B. (1988). *Geomorphology and hydrology of karst terrains*. New York: Oxford University Press.

White, W. B. (2007). Cave sediments and paleoclimate. *Journal of Cave and Karst Studies, 69*, 76–93.

Chapter 3
Geology and Geomorphology of Azokh Caves

Patricio Domínguez-Alonso, Enrique Aracil, Jose Angel Porres, Peter Andrews, Edward P. Lynch, and John Murray

Abstract Azokh Cave is located in the Lesser Caucasus and is hosted in Mesozoic limestone. It comprises a series of karstic cavities, chambers and passageways that interconnect to form a larger cave network, the trend of which appears to have been influenced by fracture patterns in the bedrock. The geomorphology of the currently accessible areas of the cave is presented, with many of its speleological features described in detail for the first time. Electrical resistivity tomography is used to examine variation in thickness of sediments infilling the inner chambers of the cave. This information, coupled with data relating to the surface topography of the cave infill, sheds light on patterns of sediment deposition within the cave system. It remains unclear whether the cave formed from epigenic or hypogenic speleological processes (or a combination of the two). This question is further hampered by the presence of a large bat population in the interior of the cave, the guano deposits of which have modified the inner galleries.

Резюме Полное и детальное описание геоморфологии пещерной системы Азоха представлено здесь впервые. Пещера сформировалась в богатой карстовой сети мезозойского известняка и состоит из четырех больших внутренних камер (помеченных как галереи Азоха *I–IV*), которые латерально связаны между собой и расположены в направлении от северо-запада на юго-восток. С внешним миром камеры связаны посредством ряда перпендикулярно выходящих проходов (*Азох 1, 5* и *6*). Эти пещерные каналы имеют одинаковую ориентацию с региональной особенностью соединения на уровне бедрока. В геоморфологии пещеры явно заметны признаки карстового провала. В одном из "слепых" внешних проходов (*Азох 2*) доступ к внутренним галереям заблокирован. Образование черта (сланца) в известняке имело обратный эффект: на местах он укреплял и поддерживал структуры потолка, помогая сохранить различные камеры пещеры. На перекрестной топографии пещеры заметна высокая центральная зона (между внутренними камерами *Азох 2* и *Азох 3*) с уклоном в сторону двух концов пещерной системы, хотя это снижение несколько более выражено по направлению к проходу *Азох 1*.

Толщина седиментного слоя в различных камерах пещеры определена геофизическим методом – вычислением удельного электрического сопротивления. Этот подход позволяет картировать заполненную толщину внутри пещеры, и эта величина варьирует в пределах от <1 м до 3 м+. Максимальная толщина седимента отмечена в камере *Азох 1*, хотя участки с большой толщиной встречаются и у входа в *Азох 2*, а также в более центральных местах камер *Азох 2, 3* и *4*. С помощью компьютерной программы *Surfer* была вычислена площадь поверхности (примерно 1,390 м^2) большого объема седимента (около 1,367 м^3), лежащего на известняковом бедроке во внутренних галереях Азохской пещеры.

Patricio Domínguez-Alonso – Deceased

P. Domínguez-Alonso
Departamento de Paleontología, Facultad de Ciencias Geologicas & Instituto de Geociencias (IGEO-CSIC), Universidad Complutense de Madrid (UCM), Madrid, Spain

E. Aracil
Análisis y Gestión del Subsuelo, S.L. (AGS), c/Luxemburgo, 4; Oficina 3; E-28224-Pozuelo de Alarcón, Madrid, Spain
e-mail: e.aracil@ags-geofisica.com

E. Aracil · J.A. Porres
Departamento de Geodinámica. Facultad Ciencias Geológicas., Universidad Complutense de Madrid (UCM), c/ José Antonio Novais n. 12, 28040 Madrid, Spain
e-mail: japorres@ubu.es

P. Andrews
Natural History Museum, Cromwell Road, London, SW7 5BD, UK
e-mail: pjandrews@uwclub.net

E.P. Lynch · J. Murray (✉)
Earth & Ocean Sciences, School of Natural Sciences, National University of Ireland, Galway, University Road, Galway, Ireland
e-mail: john.murray@nuigalway.ie

E.P. Lynch
e-mail: Edward.lynch@nuigalway.ie

Yolanda Fernández-Jalvo et al. (eds.), *Azokh Cave and the Transcaucasian Corridor*, Vertebrate Paleobiology and Paleoanthropology, DOI 10.1007/978-3-319-24924-7_3

Геофизические профили выявляют также различные аномалии внутри известняка, которые, судя по их морфологии и величинам удельного сопротивления, возможно, представляют собой полости в бедроке, заполненные, как правило, мелкозернистым материалом. Все обнаруженные полости обычно ассоциированы с аномалиями проводимости в профилях, причинами которых являются разломы. Это подтверждает взаимосвязь между развитием разлома, образованием карстового рельефа и формированием полостей.

Остается неясным, сформировалась ли Азохская пещера под воздействием поверхностных вод, уходящих в почву и растворяющих нижележащий известковый бедрок (эпигенетический спелеогенез), или альтернативно, т.е. поднимающейся снизу водой, растворяющей горную породу (гипогенетичесский спелеогенез). Возможно также сочетанное влияние этих двух процессов. Рассматриваемая проблема усложняется из-за наличия большой колонии летучих мышей в пещерной системе. Толстые отложения гуано, выработанные этими существами, в некоторых направлениях изменили (и продолжают изменять) поверхность внутренних галерей.

Keywords Lesser Caucasus • Limestone • Karstic • Electrical resistivity • Epigenic • Hypogenic

Introduction

Azokh Cave is located at the southern end of the Lesser Caucasus at 39° 37.15′ north and 46° 59.32′ east (Fig. 3.1). The wider region surrounding the site effectively marks the boundary between Europe and Asia. Both the Lesser and Greater Caucasus (positioned further north; see Fig. 3.1c) run broadly parallel to each other and formed during the Himalayan-Alpine orogeny in Late Mesozoic to Cenozoic times. These two mountain ranges cross the Caucasian isthmus between the Black and Caspian seas and they are separated by the intermontane Kura Basin, which contains Paleogene to Quaternary molasse sediments.

The cave is part of a much larger karst network developed in Mesozoic limestone, which is now abandoned. It contains an appreciable amount of sediment infill and, as it is presently home to one of the largest bat populations in the Southern Caucasus, thick deposits of guano are present in the interior.

Murray et al. (2010) recently described between 11 and 12 m of sediments infilling the largest of the entrance passages to the cave [Azokh 1]. This particular passage had been extensively excavated in the past by a Soviet-Azeri team (Huseinov 1985; Ljubin and Bosinski 1995; Lioubine 2002) and the stratigraphy remaining is split between two sedimentary sequences, which are no longer physically connected. The lower (and presumably oldest) of the two sequences is very limited in extent and has produced very few fossils; however, the upper sequence, preserved at the rear of the passage, has produced abundant fossil specimens, including numerous types of macro- and micro-mammals (Fernández-Jalvo et al. 2010). The base of the upper sequence is dated between 200 and 300 ka (i.e. Middle Pleistocene), whilst the uppermost horizon is Holocene. The actual Pleistocene-Holocene transition is apparently not preserved and is marked by an erosional disconformity (Murray et al. 2010, 2016).

Azokh Cave is significant from a paleoanthropological perspective for three reasons. Firstly, it is geographically located at an important migratory route-way between the African subcontinent and Eurasia (Fernández-Jalvo et al. 2010); secondly, middle-Pleistocene hominin remains were recovered from Azokh 1 passage during the previous phase of excavation work (Kasimova 2001); and thirdly, the presently available evidence shows that the cave contains a long sedimentary sequence recording different phases of occupation by three different hominin groups (King et al. 2016).

The purpose of this contribution is to provide a review of the geology and geomorphology of Azokh Cave. Understanding the intricacies of the cave system is crucial in helping us interpret how humans and animals may have utilized it as a shelter in the past. Both topographic and geophysical surveying techniques have been employed for this purpose. The former approach examines the shape and form of cave development between the surface of the sediment infill and the cave ceiling. This represents the space one can presently walk through and will be described first. Geophysics allows visualization of the cave system beneath ground-level and, in particular, it is quite effective at resolving the space between the surface of the infill and the rocky floor of the cave beneath, in addition to highlighting any buried (open) cavities.

Geological Background

The Caucasus Mountains were produced during tectonic collision between the Arabian and Eurasian plates, which resulted in the closure of the Tethyan Ocean during Mesozoic and Cenozoic times (Saintoti et al. 2006). As a result, the regional geology is dominated by sedimentary (typically carbonates) and volcanic rocks (Fig. 3.2; see also Fig. 3.1b, c), which have subsequently been subjected to varying degrees of folding and thrusting.

Subduction of the ocean floor of, what has been termed, the *Neo*tethys is believed to have possibly initiated during the Jurassic. Volcanic arcs and back-arc basins formed during the Late Jurassic and Cretaceous, while in the Late Cretaceous and (particularly) early Cenozoic, compressional deformation,

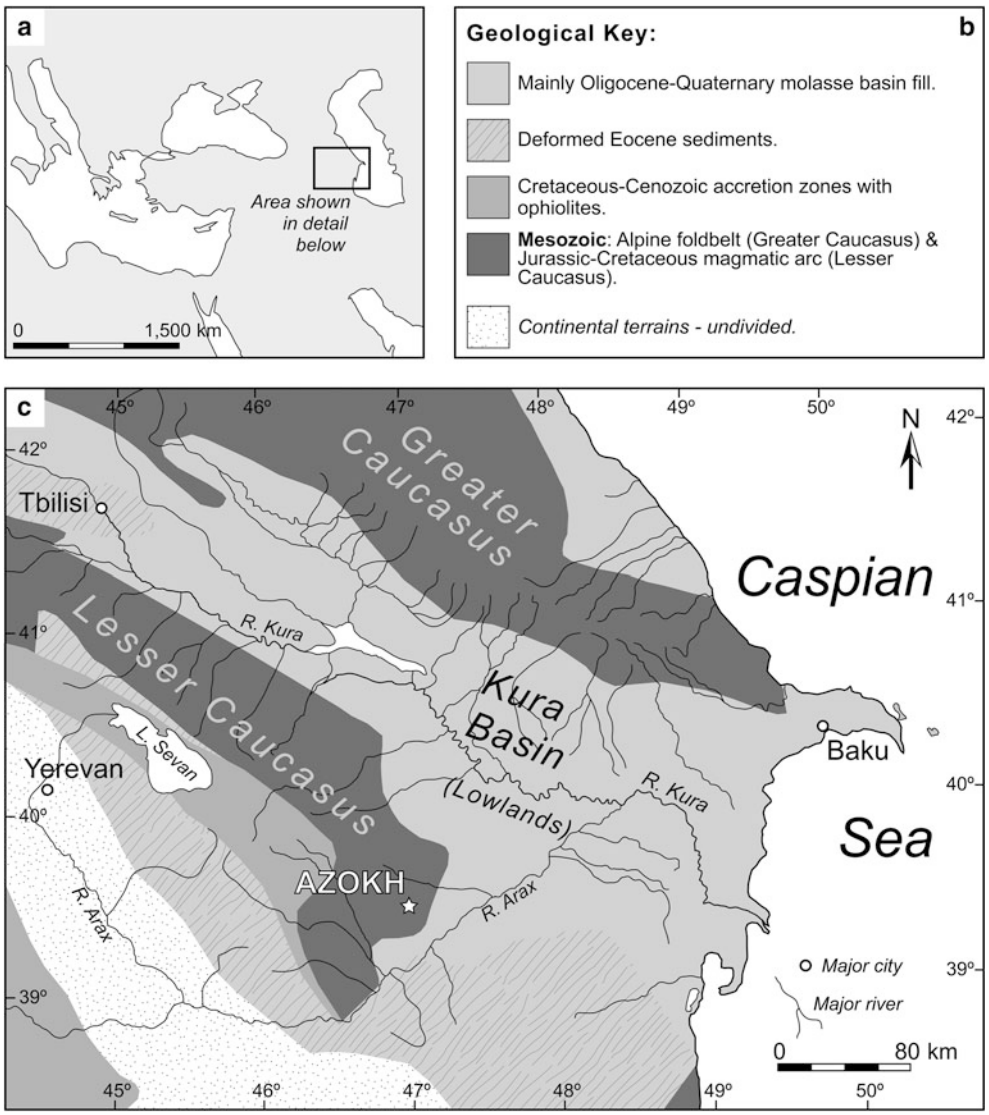

Fig. 3.1 Regional geological setting of Azokh Cave. **a** General geography of the wider region showing location (inset) of geological map in (**c**); **b** Key to geological map in (**c**); **c** Simplified geological map of the Southern Caucasus, with the location of Azokh Cave shown with a white star. Reproduced from Murray et al. (2010). Geographic and hydrographic information has been sourced from UN Map no. 3761, Revision 6, 2007. Geological information has been adopted and modified from that of Brunet et al. (2003)

basin inversion and subduction- to collision-related magmatism were characteristic of the region (Sosson et al. 2010; Dilek et al. 2009). The compressional tectonic regime generated by this collision resulted in uplift of the Caucasian mountain ranges and these have continued to rise since Miocene times (Egan et al. 2009). Mosar et al. (2010) note that the average (annual) convergence of the Arabian and Eurasian plates is on the order of 18–23 mm, resulting in tectonic activity (earthquakes) continuing to affect the wider region (see for example Karakhanian et al. 2004; Mellors et al. 2012).

Karst development, leading to the formation of the Azokh Cave system, took place in this geomorphologically and tectonically dynamic environment, presumably in mid to late Cenozoic times. The landscape surrounding the cave-site is mountainous (particularly towards the west) and deeply carved valleys and abandoned river terraces testify to rapid lowering of the base level in the past, which forced fluvial incision and deactivated endokarst systems.

Azokh Cave is developed in thickly bedded Mesozoic limestones, which are pale gray and commonly display a variety of textures, ranging from wackestone to grainstone. A significant level of partial or complete silicification, including development of conspicuous chert horizons, is often observed. Throughout the limestone sequence hosting the cave, these siliceous masses (which may be metric to decimetric in scale) have played an important role in controlling the formation of cavities and in the stabilization of roofs and vaults.

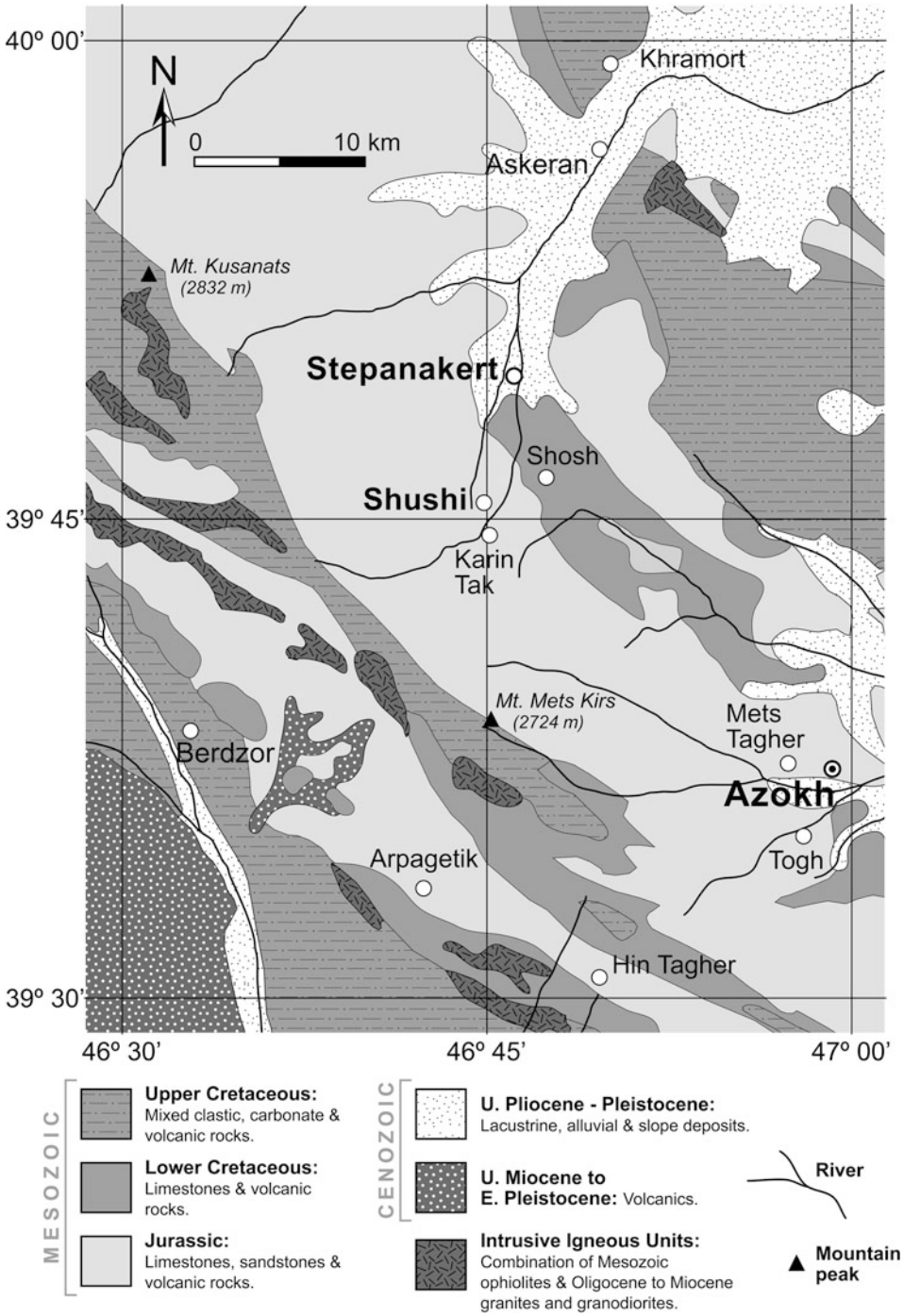

Fig. 3.2 Mesozoic to Cenozoic geology of the area surrounding Stepanakert and Azokh. Simplified from Vardanyan et al. (2010)

Marine fossils have been recovered from the limestone (Fig. 3.3a–c). Samples of silicified sponge and both open branching (dendroid) and massive scleractinian corals have been collected from outcrops in the vicinity of the cave. Very conspicuous *Thalassinoides*-type fossil burrows are evident in the bedrock at the main entranceway to Azokh Cave (Fig. 3.3d). This ichnofossil is characterized by a series of fairly large diameter tubes (20–40 mm at Azokh), which branch in a complex manner, leading to development of a 3-dimensional network. These burrows typically form in reasonably shallow, open shelf settings. Crucially, the burrow network has been pervasively silicified (presumably due to the infilling sediment having a more favorable porosity for percolating silica-rich fluids), resulting in a strong interconnected barrier to karstic solution. In places along the cave wall where the host limestone has been dissolved away, sandy/silty cave-filling sediments are observed infilling the

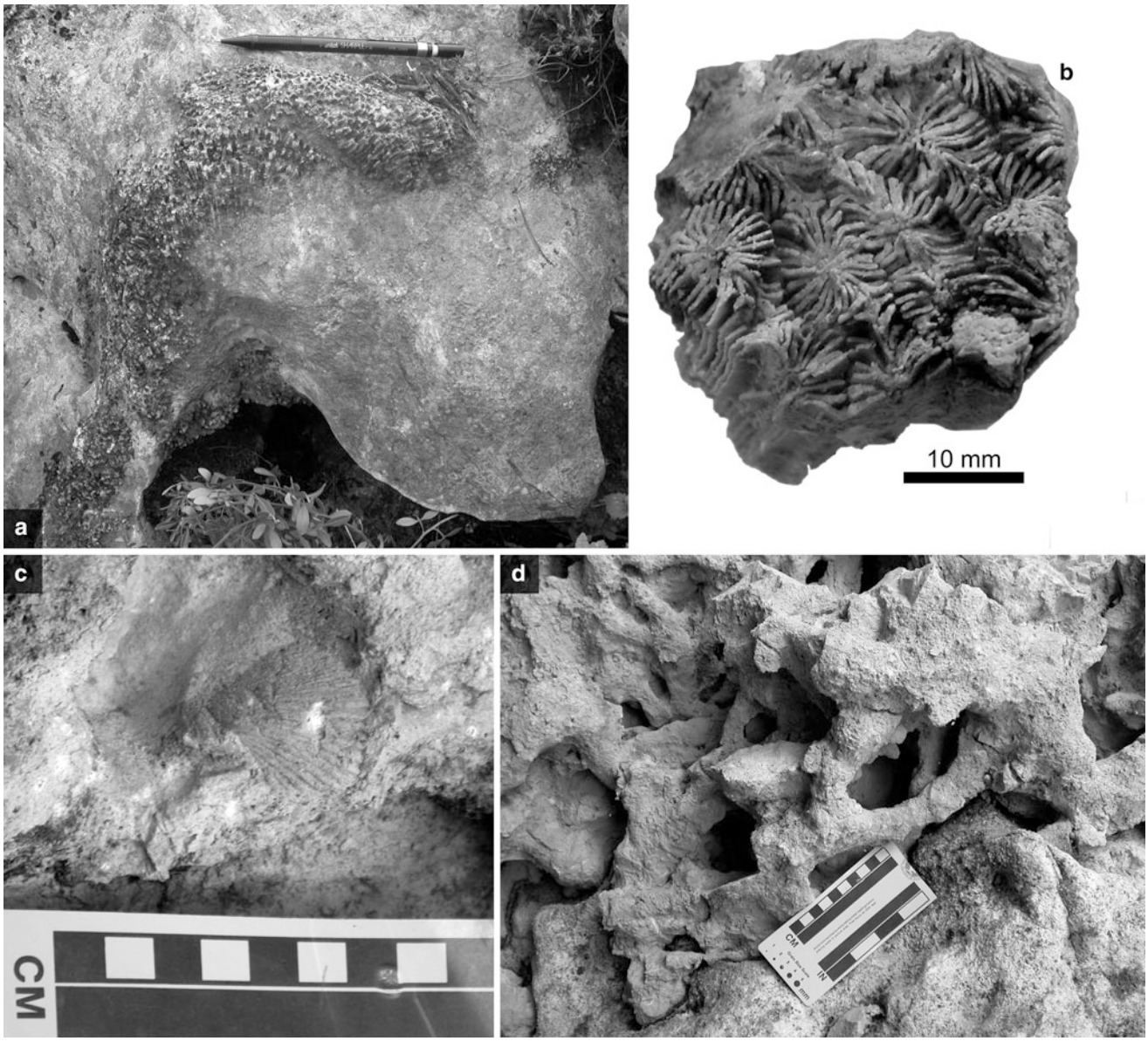

Fig. 3.3 Mesozoic fossils from the limestone at Azokh. **a** Silicified colonial coral weathering proud of the limestone matrix (pencil for scale); **b** Detail of a silicified colonial coral (found loose). Note in some instances the septa are confluent; **c** Valve of a marine shell *in-situ* in the wall of Azokh 1 passage; **d** Silicified *Thalassinoides*-type burrow network (basal trench, Azokh 1 passage)

interstitial areas between the silicified burrows; however, in some instances buff-yellow clays drape these spaces.

The precise age of the cave bedrock is still uncertain. Lioubine (2002) states that the cave is located on the calcareous massif of the Jurassic. This certainly seems to fit, in a broad sense, with descriptions of the wider regional geology (Fig. 3.2). The best hope of fixing an absolute age for the cave's host bedrock will perhaps come from a thick volcaniclastic interval found interbedded with the limestone 2 km to the west of the cave site. Murray et al. (2010) reported reworked (detrital) fine-grained igneous material interspersed in some of the sedimentary infill at Azokh Cave.

Geomorphology of Azokh Cave

Azokh Cave is located about 1 km to the east of a nearby village with the same name. The cave system is developed in a hillside on the eastern side of a small (broadly north-south trending) valley (Fig. 3.4). The bedrock at the site forms a prominent NNW-SSE trending escarpment (Fig. 3.5), which is west facing and divisible into two very thick carbonate units (termed *Lower* and *Upper Limestone [Lst.] Units* on Fig. 3.5a). Several different cave entrances are present in the *Lower Limestone Unit*. Locally the bedding in the limestone appears to be orientated horizontally; however, it is in fact

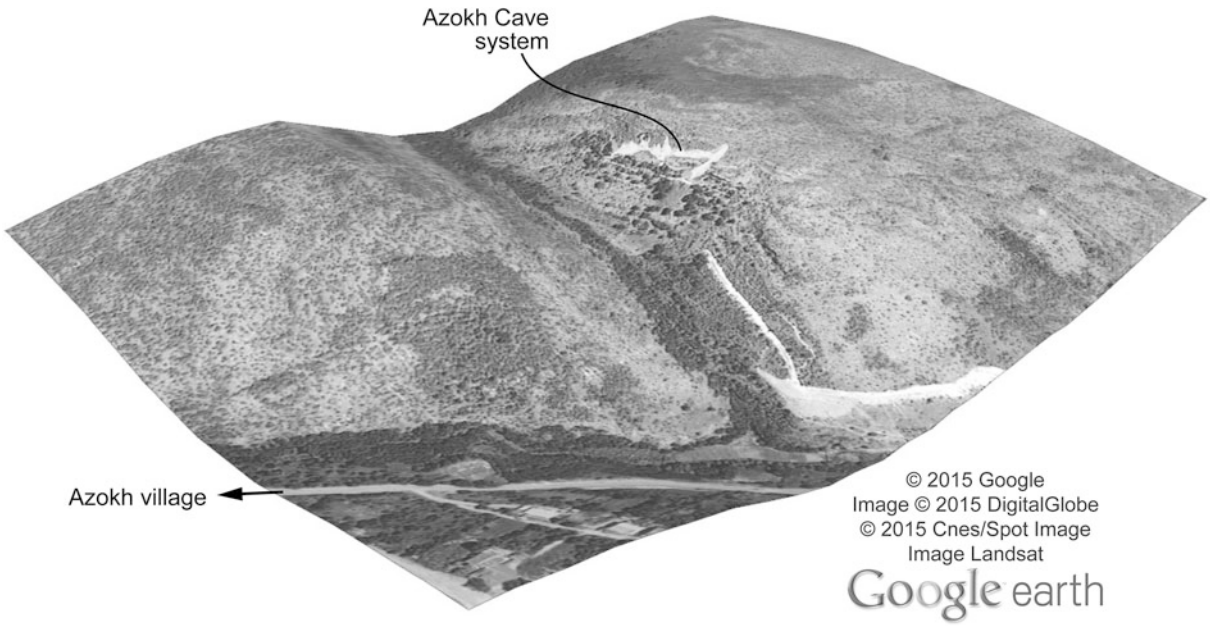

Fig. 3.4 Oblique 3-d view (looking towards the northeast) of the hillside hosting the Azokh Cave system (shown in white). The road in the foreground runs into the center of Azokh Village. Sourced from Google Earth

very gently folded on a larger scale, with the axis of the resultant anticline orientated broadly perpendicular to the escarpment.

When traversing through the interior of the cave, most of the chambers are carved through the lowermost part of the *Upper Limestone Unit*. However, detailed survey work, presented below, has shown cave galleries to be developed also in at least the uppermost part of the *Lower Limestone Unit*. A series of vertical shafts (cupolas) penetrate the uppermost part of the *Upper Limestone Unit*, breaking out at the surface in one open pit and also a collapse doline (see Fig. 3.5a, c). The cave-hosting limestone escarpment is actually truncated at either end by two large collapse features (Fig. 3.5a).

The bedrock hosting the cave system at Azokh displays pervasive fracturing and jointing (Fig. 3.6). Strongly developed vertical and horizontal joint sets occur throughout the limestone and appear to have played an influential role in the development of the karst system. Joints represent discrete brittle extensional fractures within bedrock where there has been little or no displacement along the plane of fracture (e.g., Fossen 2010). They develop during uplift, cooling, shrinkage and decompression of the rock unit, and joint orientations are principally controlled by the direction of regional and tectonic deformational stresses, combined with the mineralogical and mechanical properties of the host rock (e.g., Narr and Suppe 1991; Gross et al. 1995). Sub-aerial weathering and erosion (enhanced by percolating groundwater) can accentuate the development of joint sets and fracture systems.

Limestone joint mapping was carried out in the vicinity of Azokh Cave in order to identify the types of jointing present, to find the number of joint sets, to quantify the 3-dimensional orientation of the fractures (with respect to geographic north) and to establish spatial and genetic relationships between the jointing and the main cave system. Joint azimuths (0°–360°) and dips (0°–90°) were recorded along a linear traverse that ran along the upper ledge of the NNW-SSE limestone escarpment. In total, nine measurement stations were established, at 30 m spacing, and their positions recorded using GPS. Joint exposure varied along the traverse; however, individual measurements on both vertical and horizontal joint planes were made during the exercise. The results of part of this dataset (n = 171) are presented in Fig. 3.7, which shows the orientation of sub-vertical joint sets for each mapping station in the form of directional rose diagrams created using Stereonet 9.5 (Cardozo and Allmendinger 2013).

The directional data for the sub-vertical joints indicates that two principal joint orientations, approximately toward the NE and NW, are developed in the limestone. Field observations suggest that both joint sets are contemporaneous and comprised of systematic, regular extensional fractures. The most common joint set is a NE to ENE coaxial set, although this observation may be due to its preferential exposure along the traversed NNW-aligned escarpment (Fig. 3.7). Overall, the measured orientations define a conjugate joint system of sub-parallel fracture sets that remains broadly consistent between the measurement stations, particularly in the immediate vicinity of Azokh Cave. Joint sets

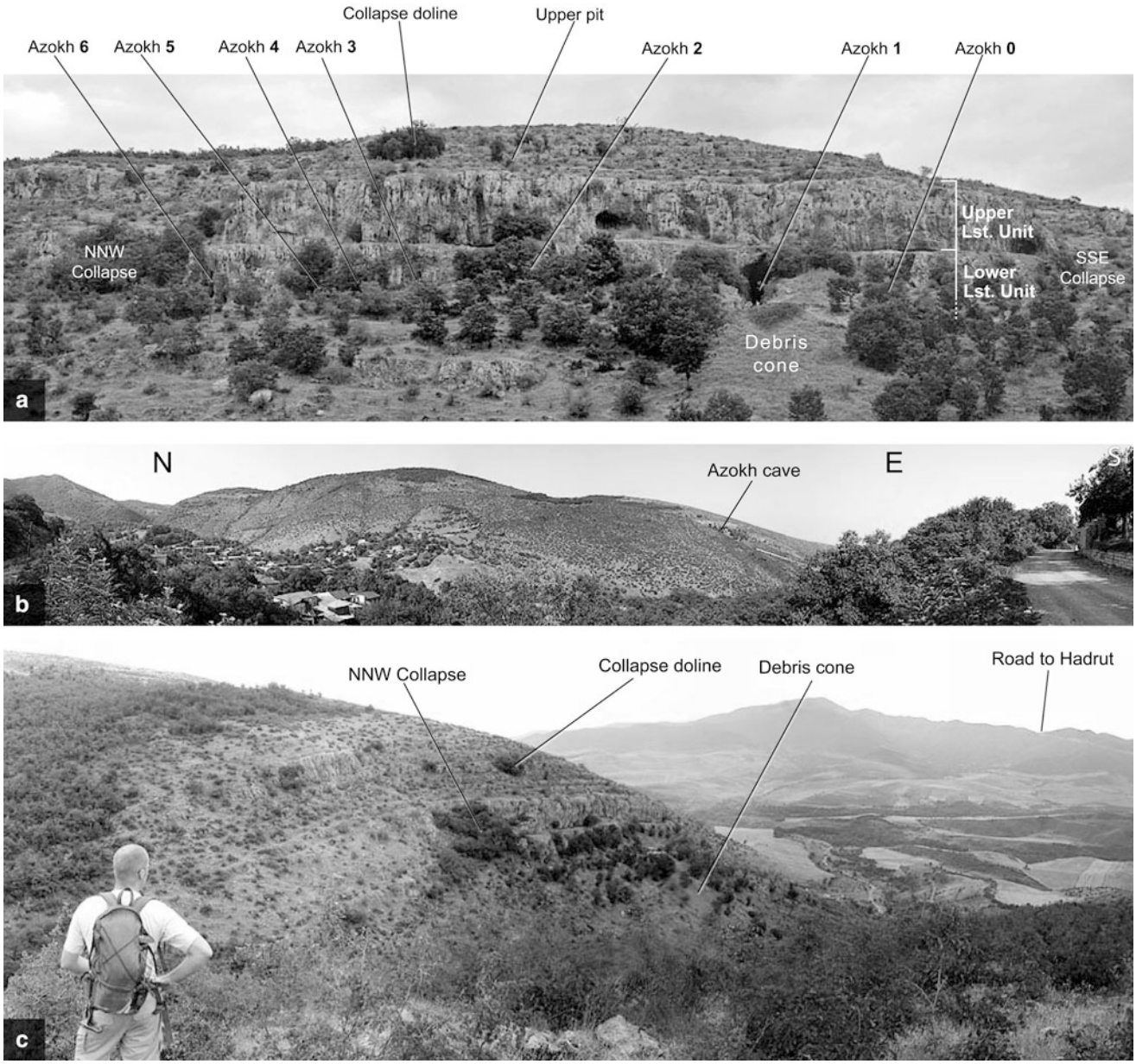

Fig. 3.5 External views of the Azokh Cave system. **a** Field photograph of the west-facing hillside containing the various entrances to the cave. Local visitors to the site would normally enter through Azokh 1 and exit through Azokh 6. Azokh 5 is a recently discovered entrance passage and Azokh 2 is a small gallery blocked by a choke. This blockage can be seen from the upper pit (labeled) and a collapse doline is marked by a small dense thicket of trees. Azokh 0 is a 3 m long narrow (and low) pass. The *Upper* and *Lower Limestone (Lst.) Units*, in which the cave system is developed, are clearly indicated in the cliff section. The intersection between these two units is stepped back and marked by a walkway. The continuous limestone cliff section is truncated at either end by two (NNW and SSE) collapsed dolines; **b** General landscape panorama from the top of Azokh village (taken around the area of the school); **c** General view southwards from the valley in which Azokh Cave opens

that deviate from the general NE and NW alignment are generally located furthest from the cave system. These 'distal' sets have a more NNE and WNW orientation and maintain a conjugate nature, albeit with a larger dihedral angle (Fig. 3.7).

The joint orientation data broadly corresponds with the alignment of various linear features seen across the cave system, such as passageways and elongate chambers. This association is particularly developed along a NE-SW direction. Likewise, the four inner chambers of the cave (Azokh I

Fig. 3.6 Example of sub-vertical and sub-horizontal joints in the limestone bedrock close to Azokh Cave. Hammer (circled) for scale

to IV; Fig. 3.8), if considered as a single broad lineament, also appear to be aligned sub-parallel to the broadly NW-orientated joint sets mapped in Fig. 3.7. This concordance suggests that joint formation, in response to local and/or regional stress fields, had an influence on subsequent karst development and cave morphology.

Materials and Methods of the Topographic Survey

This survey was completed over several field-seasons, to an accuracy of grade 5D according to the standards of the British Cave Research Association (Day 2002), although most of the internal survey within the cave was conducted at grade 6. Grade 5 is accomplished if compass and clinometer readings are accurate to ±1° (with ±0.5° used in practice) and the error in spatial positioning of the base-stations is ±10 cm. The compass and clinometer used for the survey work both need to be calibrated locally and immediately before and after the surveying. Measurements were always taken to the next base-station and then in reverse from the previous. Class D implies that additional measurements of cave passage profile were taken at survey stations and also wherever else needed.

Bearing and elevation were measured with precision compasses and clinometers [*Silva Sight Master Compass SM 360* and *Silva Clino Master Clinometer CM 360*, both PA (surveys 2004–2005) and LA series (2006 and later surveys)]. Distances were measured with a 50 m low-stretch tape. Additional measurements were taken using a 10 m retractable tape and distance to inaccessible areas (such as points along the ceiling or deepness of pits) was recorded using laser rangefinders. Magnetic north was consistently used during survey work.

In 2002 a general rough plan of the cave system was made at grade 3. In 2004, a preliminary survey to grade 4B was conducted to record the general profile of the ground surface within the cave. In 2005, this ground survey was completed, which incorporated the external pathway connecting the various cave entrances and the cliff edges. During the period 2006–2010, further measurements and profiles were taken at base-stations and along the ceiling. A total of 207 different measurements have been recorded between the various topographic base-stations (including azimuth, elevation and distance). These topographic stations form a polygonal traverse of fixed primary stations, representing the centerline of the main cave galleries.

During the survey work, measurements were always recorded twice. If a significant difference was encountered, the measurement would be retaken a third time. A network of secondary base-stations was also established, usually radiating from most of the primary stations and reaching the contact of the ground surface with the cave walls. These were created to control the 'closing loop' errors in the survey polygons and to get an accurate areal plan of the galleries. The primary topographic stations were marked with 12 cm

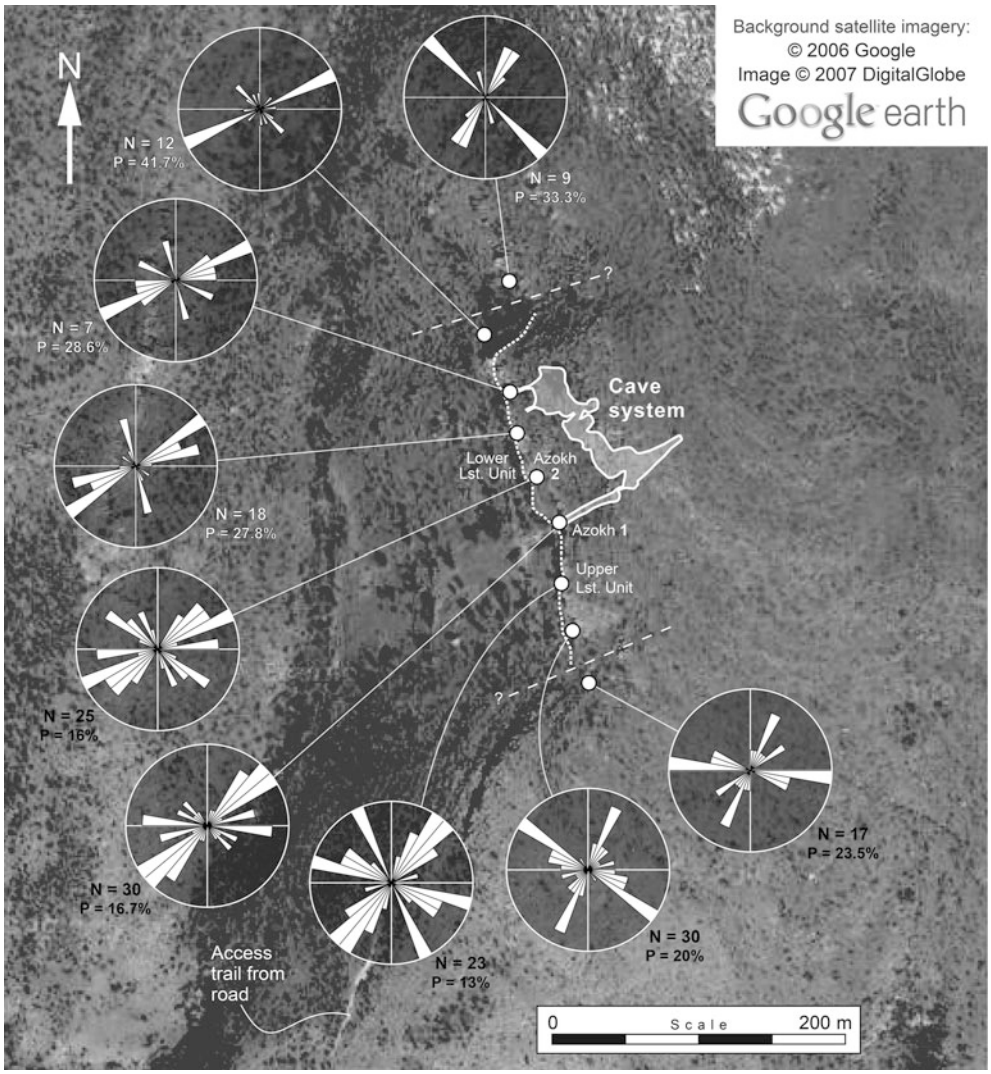

Fig. 3.7 Aerial view of the Azokh Cave area (sourced from Google Earth) with directional rose diagrams for sub-vertical joint sets developed in the limestone bedrock. Mapping was conducted along the central terrace of the escarpment (top of Lower Limestone Unit, base of Upper Limestone Unit) above the main entrance passages. Small filled white circles represent mapping locations on the terrace. Axes in rose diagrams represent geographic N–S and E–W, while each rose petal represents 10 degrees. N is the number of measurements per location, while P refers to the maximum perimeter value of each rose diagram, as a percentage of the total dataset. WSW to ENE trending dashed lines (with question marks) towards either end of the traverse intersect collapse features in the limestone bedrock and may be possible faults

nails and polyethylene labels on the ground and, where appropriate, discrete marker points on the limestone walls. In 2010, several transverse profiles were drawn using a minimum of 20 measurements per profile.

Computer analysis of the topographic data facilitated the creation of a 3-dimensional plot of the various base-stations (and survey lines connecting them) throughout the entire cave system. Speleological software used included *Therion* (Mudrák and Budaj 2010), *COMPASS Cave Survey Software* and *Visual Topo* (David 2008). The main 'centerline' of the cave system (running from Azokh 1 entrance around to Azokh 6) and the centerline of the external pathway (connecting these two particular entrances) produced a 305.57 m long polygon, with a 3-dimensional loop-closure error of 1.57% (>14 cm/station). However, the secondary base-station network created a mesh of triangles and loops (35 loops in total), which further corrected and controlled this closing error. As a result, the total 3-dimensional closing loop-error for the cave survey (with respect to the entrances) is only c. 0.61%. It is slightly lower again for the 2-dimensional plan (0.59%; in most cases >2 cm/station, and with a maximum of 14 cm over more than 2 km of total measurements). For the final assembly of the cave topography the closing loop-error was averaged to fit over the total length of measurements.

Results of the Topographic Survey

An accurate 2-dimensional plan of the presently accessible portion of the cave network at Azokh is presented in Fig. 3.8, based on the corrected plots of the various topographic stations described above. The accessible part of the cave is estimated to be about 1,840 m^2 in areal extent, although this is complicated by 3-dimensional considerations. An attempt has been made, for example, in Fig. 3.8 to provide an indication of the slope of the floor in the interior of the cave (see gray topographic contours in 1-m divisions). The sediment infill (floor level) is seen to rise towards the

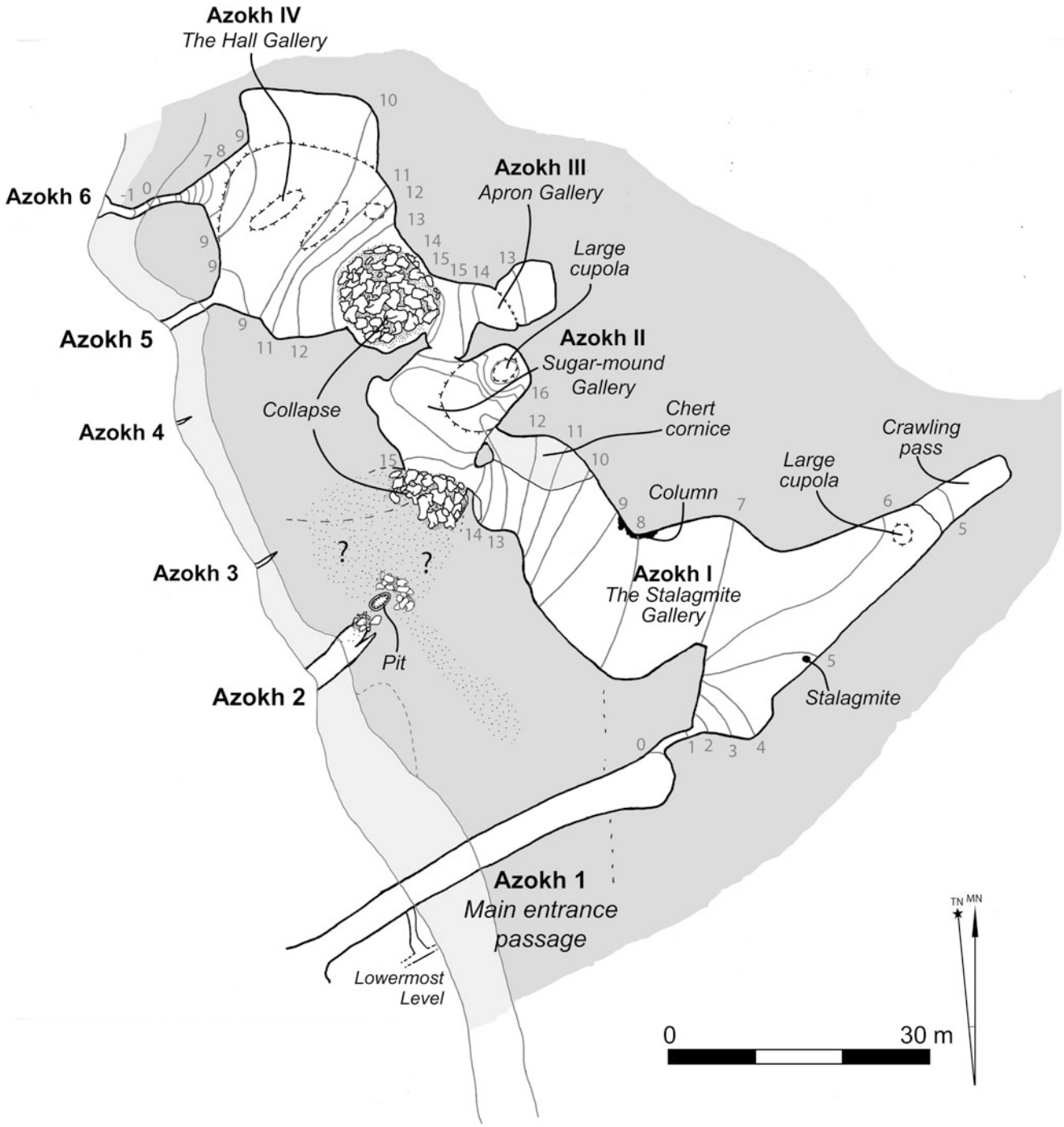

Fig. 3.8 Detailed plan map of Azokh Cave system. Entrance passages are denoted with Arabic numerals and internal chambers, or galleries, are differentiated with Roman numerals. Gray topographic contours (in meters) provide an approximate indication of the slope of the floor surface in the cave interior. The zero for these contours is the cave datum located in the rear of Azokh 1 passage

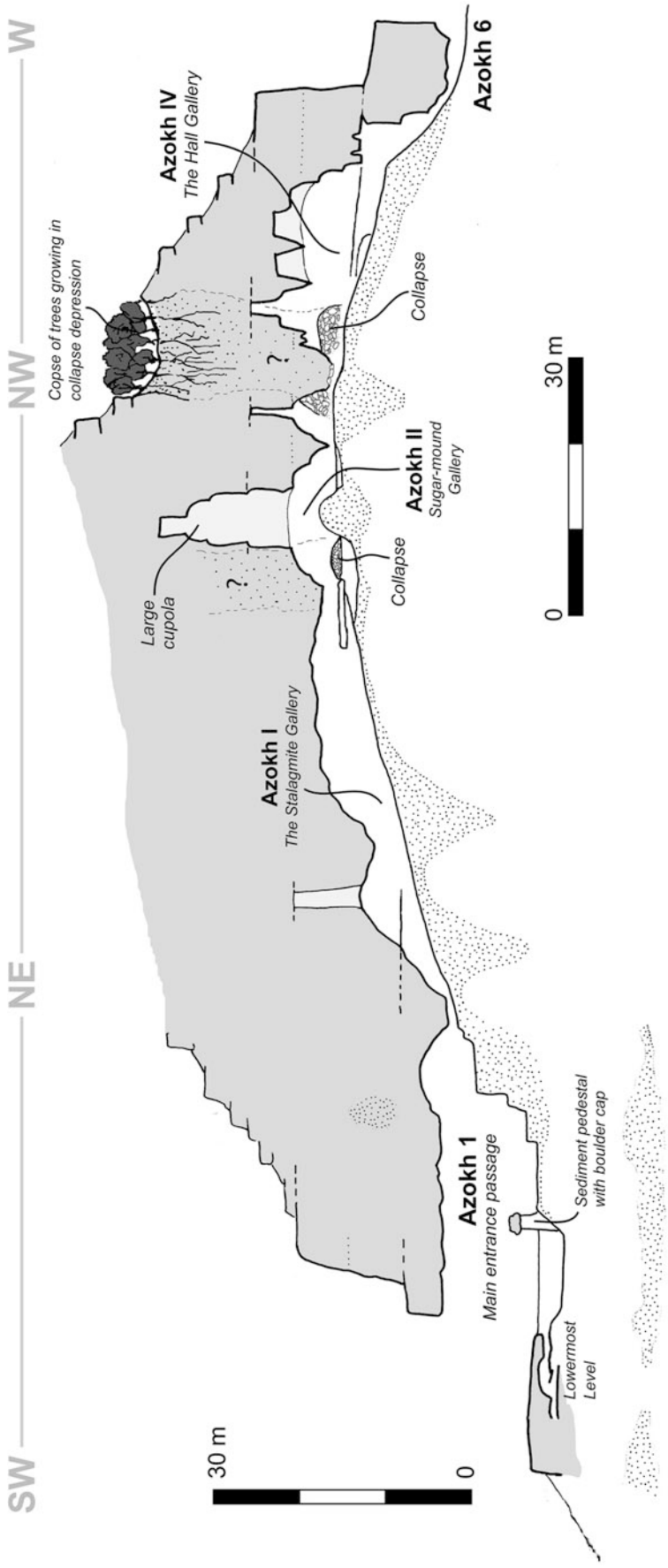

Fig. 3.9 Cross-section profile through the entire cave system at Azokh (entering through Azokh 1 passage and exiting through Azokh 6). The trajectory of the line of section is indicated across the top (note how it deflects around (bends) through approximately 180°). Horizontal and vertical scales are approximately equal

middle of the cave network. This elevation in the ground surface level is also quite apparent in the cross-sectional profile produced for the entire cave system (Fig. 3.9).

The cave system at Azokh is seen to comprise a series of broadly NW to SE trending chambers (Fig. 3.8). These are connected (to varying degrees) to the exterior by a series of orthogonally directed (i.e. NE to SW) entrance passages. The entrance passages are denoted with Arabic numerals (Azokh 1, 2 etc.) whilst the internal chambers are labeled with Roman numerals (Azokh I, II etc.). Six passageways have been identified to date, although only three of these (Azokh 1, 5 and 6) are sufficiently developed to permit access right the way through to the interior of the cave. Four separate internal chambers are identified (each with their own informal name, e.g., Azokh I – *The Stalagmite Gallery*). Murray et al. (2010) provided a simplified version of this map (their Fig. 3.2b) in which they identified five (I–V) internal chambers. This is rationalized to four here – specifically their chambers I and II have been amalgamated.

General Description of the Cave Galleries

Azokh 1: Main Entrance Passageway

The passageway labeled Azokh 1 is the main entranceway to the interior of the cave (Figs. 3.8 and 3.9) and it had been extensively excavated prior to the arrival of the current team (Huseinov 1985; Ljubin and Bosinski 1995; Lioubine 2002). Much of the present excavation effort has been concentrated in this passage since 2002 (Murray et al. 2010; Fernández-Jalvo et al. 2009, 2010). Azokh 1 runs for 35 m in a broadly straight NE/ENE direction from the entrance cornice. It is about 12–15 m high and 5–8 m wide and has a characteristic keyhole shape (Fig. 3.10). This represents what was once a rounded phreatic tube, which then followed a vadose regime forming a meander. The total floor area of this passage, from beneath the entrance cornice to the narrow passage at the rear, is 175–280 m^2. This narrow passage at the rear of Azokh 1 (Fig. 3.8; see also Fig. 3.10d) is less than 3 m long and it connects to Azokh I inner chamber.

Azokh 2, 3 and 4: Blind Passages

Azokh 2 is a short passage (it is only about 7.5 m long by 3.5 m wide) located NNW from Azokh 1 (Fig. 3.11; see also Fig. 3.8 for general location). A prominent NE-SW trending fracture (joint) in the bedrock runs the length of the roof and appears to have mediated the formation of the chamber. A large boulder collapse has blocked the rear of this passage and, on the exterior, a vertical pit occurs over this passage on the top surface of the *Upper Limestone Unit* (see relative positions of these features in Fig. 3.8). The boulder collapse prevents access to the inner galleries of the cave system and it has also limited the amount of archaeological excavation possible in the passage. Fernández-Jalvo et al. (2010) reported a partial skeleton dated to 1265 ± 23 years $C^{14}BP$ which was recovered near the top of the sedimentary sequence infilling in Azokh 2.

The locations of Azokh 3 and 4 are shown in Fig. 3.8 and the hillside panorama in Fig. 3.5a. Both are narrow and high, essentially widened joints with similar orientation trends to Azokh 1 and 2, and access to these is only possible for less than 1 m.

Azokh 5: A Recently Discovered Connection to the Inner Chambers

Access to the cave's interior through Azokh 5 was first discovered in 2004. This is a fairly short passage (only 10 m long) with a rounded roof, which continues inwards for 5 m before expanding upwards and outward and connecting to the Azokh IV chamber inside (Fig. 3.8). Large chert developments in the limestone feature prominently in the roof, and they are particularly conspicuous on the interior of the chamber. At the time of its initial discovery the gap between the sediment fill and the cave roof in Azokh 5 passage was only about 20 cm (Fig. 3.12). The ground surface was composed of unaltered, very dry loose sediment and the entrance to the chamber was hidden by vegetation.

Azokh 5 has proven to contain a relatively undisturbed sedimentary section replete with numerous fossils and archaeological artifacts. Fernández-Jalvo et al. (2010) reported modern human remains with associated charcoal [dated to ~2,300 years $C^{14}BP$] from near the top of the infill in the rear of this passage. The excavation work conducted in Azokh 5 since its initial discovery has improved access through this passage and, rather than crawling inside in a prone position, it is possible now to enter by walking and stooping.

Azokh 6: Vacas Passageway

This passageway is located at the northwestern extremity of the cave system (Fig. 3.8; see also Fig. 3.9) and it is the traditional exit route for local visitors to the cave. It takes its

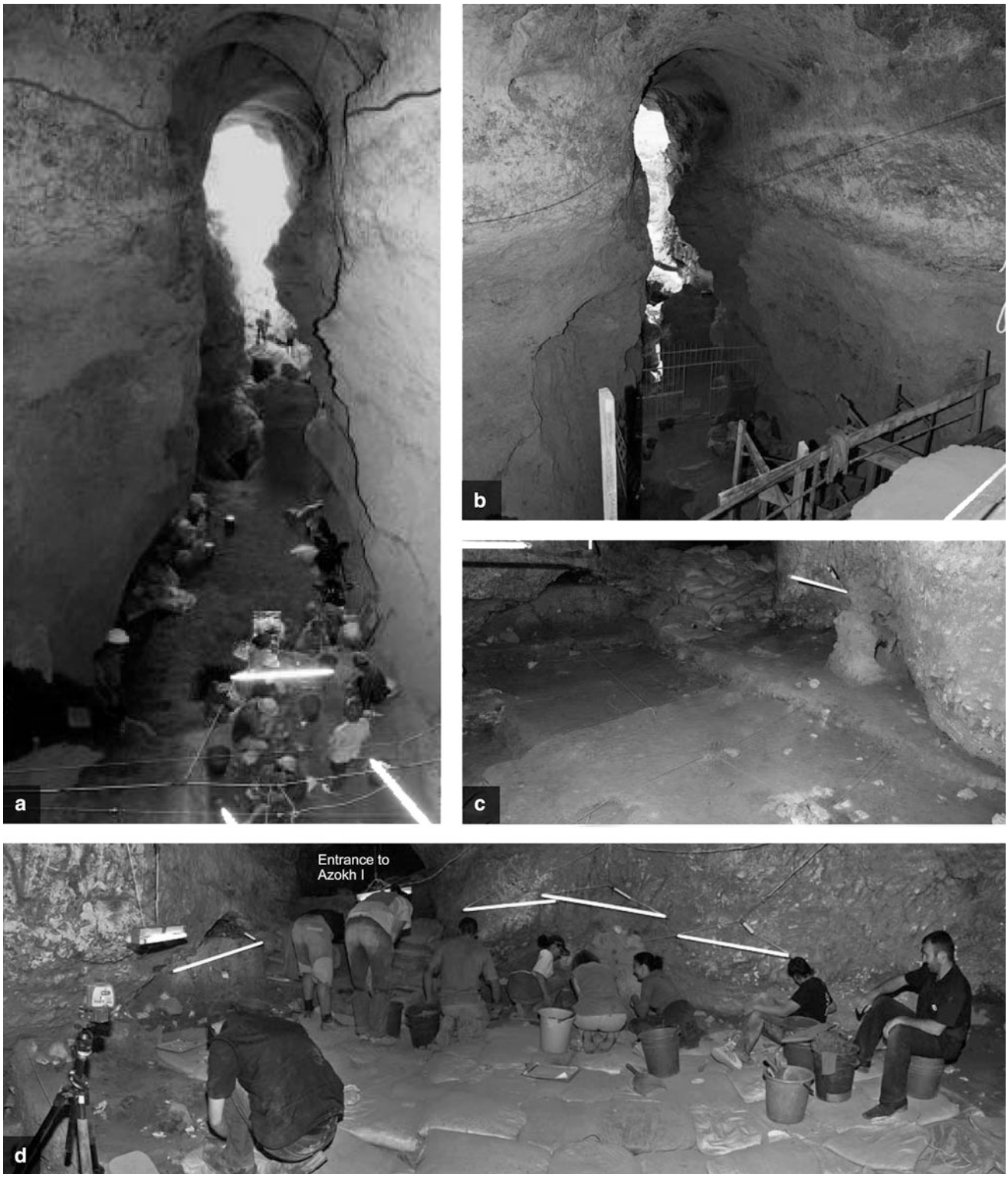

Fig. 3.10 Azokh 1, the main entrance gallery. **a**, **b** Photographs of the entrance passage taken from the top of the uppermost platform looking southwestwards towards the cave opening. The image in (**a**) is reproduced and slightly modified from Fernández-Jalvo et al. (2009). Note in (**b**) the scaffolding erected to support the section and the zip-line installed to assist in the evacuation of sacks of excavated sediment; **c**, **d** General views of the uppermost platform

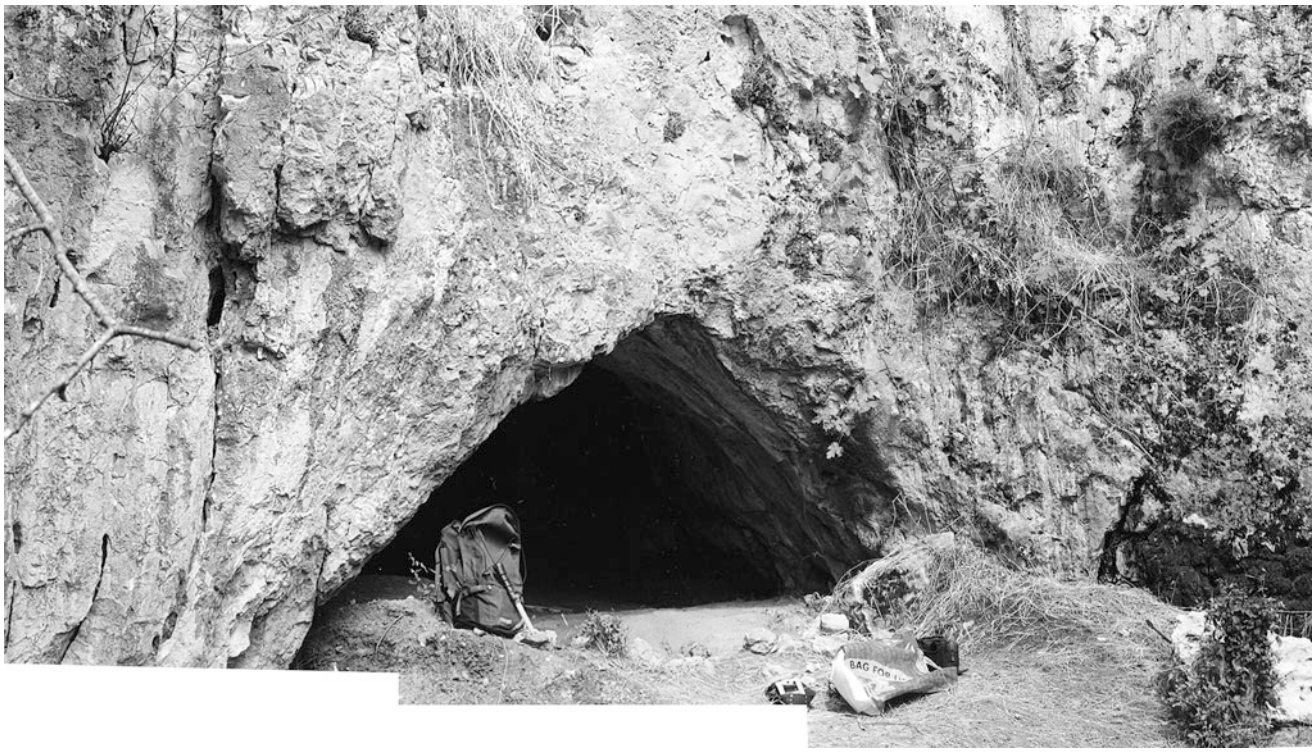

Fig. 3.11 Entrance to Azokh 2, photographed in 2004. Geology hammer and rucksack for scale

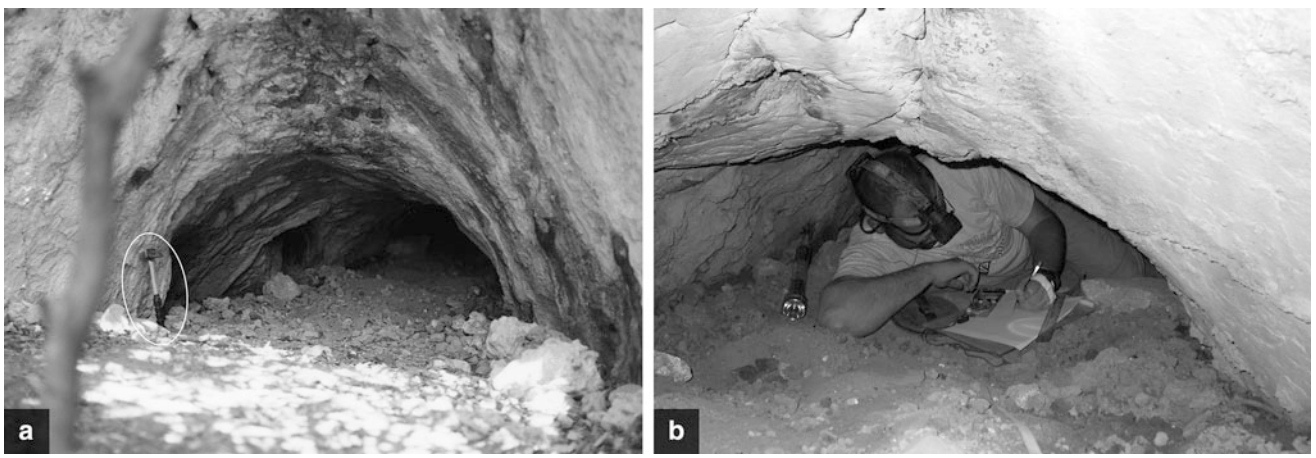

Fig. 3.12 Azokh 5 entrance. **a** Original (undisturbed) level of sediment fill in the passage just after the first survey was completed of the interior. Hammer (circled) for scale; **b** Early survey work being conducted through Azokh 5 passage, viewed from the interior

name from the Spanish word for cows – local livestock commonly frequent the entranceway and their dung may be thickly deposited underfoot. This narrow passage is about 12 m long (with a surface area of 7 m^2) and it rises upwards on entering the cave interior, before connecting with Azokh IV chamber inside.

Azokh I: The Stalagmite Gallery

With a total surface area of 843.5 m^2 the *Stalagmite Gallery* is the largest inner chamber of the cave system at Azokh (Figs. 3.13 and 3.14; see also Fig. 3.8 for general location). The name was originally coined by the previous excavation

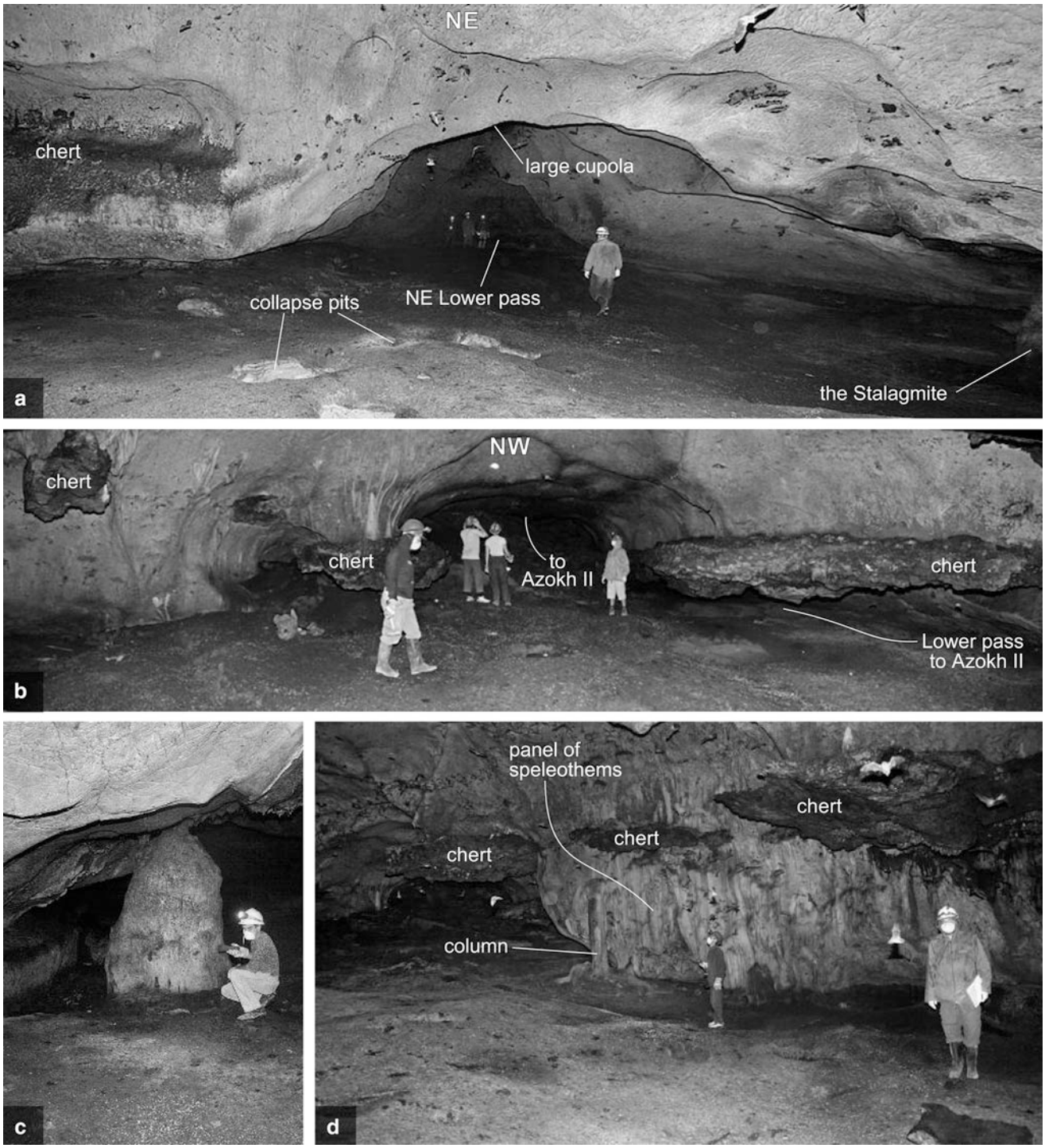

Fig. 3.13 Azokh I [*The Stalagmite Gallery*: Part 1]. **a** View of the NE branch of this gallery, as seen from the entrance passage. At the far end of the field of view are a lower pass and a high cupola. A large conspicuous stalagmite, which gives the gallery its name, is located at the extreme right of this image (along the SE wall of the chamber); **b** The termination of the NW branch of this gallery, leading into the second gallery (Azokh II). Note the thick bands of chert, which are laterally persistent for several meters, forming cornices; **c** The stalagmite; **d** The largest known panel of speleothems in the cave system, protected from corrosion by overlying chert cornices. This panel includes flags and a c. 2 m high column

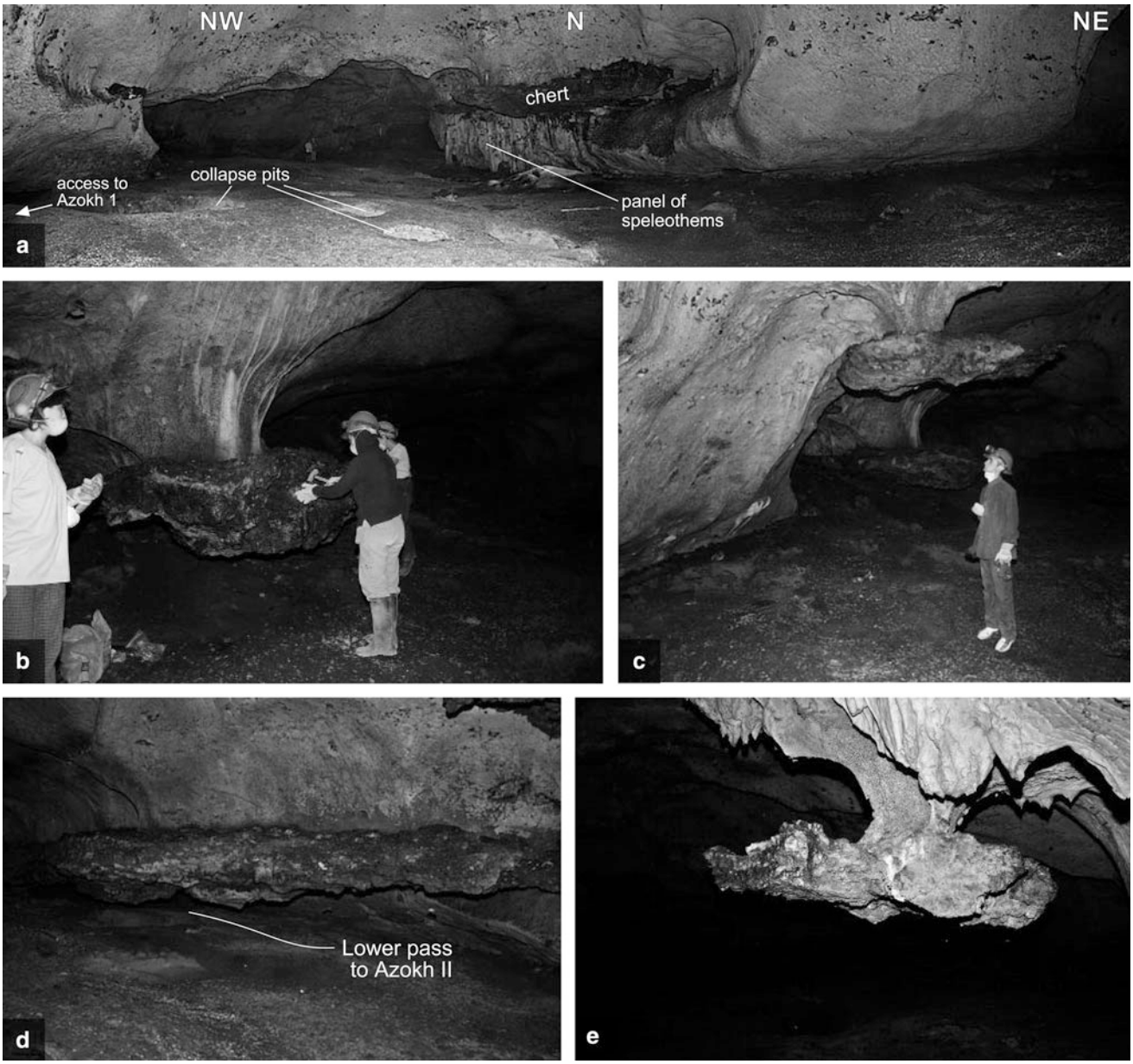

Fig. 3.14 Azokh I [*The Stalagmite Gallery*: Part 2]. **a** General panorama of the gallery from entrance passage from Azokh 1; **b–e** Detailed views of some hanging chert blocks, pendants and cornices. **b** Pedicled hanging block of chert; **c** View showing the spatial relationship of the hanging blocks in (**b**) and (**e**); **d** Large chert cornice with the lower pass to Azokh II: note the gentle slope of the ground surface; **e** Pedicled hanging block of chert. This structure is very narrow and the pendants in front of it (which are not stalactites) provide evidence of appreciable corrosion of the cave walls (probably by condensation-corrosion processes)

team (Huseinov 1985) in reference to the large conspicuous stalagmite found along the SE wall of the chamber (Fig. 3.13c), a short distance from the narrow connecting passage to Azokh 1.

The Azokh I chamber divides into two branches (Fig. 3.8), as follows:

- *Branch 1* continues internally from the rear of Azokh 1 passage in a NE direction, before terminating in a low cul-de-sac (Fig. 3.13a), at which point there is a distinctive inflection in the cave ceiling and the ground slopes slightly distally. This lower part of the gallery (overlain by the low ceiling) has a surface area of 38 m^2. The ground surface of the crawling pass is composed of loose sediment, most of which is completely undisturbed.
- *Branch 2* opens towards the left hand side (NW) as one enters from Azokh 1 passage and continues for some 47 m in a northwesterly direction (i.e. orthogonal to the first branch), before connecting with the next inner

chamber (Azokh II). There is a steady slope on the floor of this gallery, ascending 8 m elevation in less than 23 m. The NW end of this chamber ends with a large chert cornice on the northern wall (Fig. 3.13b). A second (lower-level) access route to Azokh II is present below this feature (Figs. 3.13b and 3.14d).

The limestone walls of the *Stalagmite Gallery* are mostly light in color, with broad and shallow concave surface depressions. In the northern wall of *Branch 2* a large band of overhanging chert is located at about 2.5 m above ground level. This is a common place for bats to congregate and, as a result, a half meter thick mound of guano has developed beneath it. This block of chert also protects parts of several speleothems covering the wall from corrosion. This panel of speleothems is about 3 m long and 2.5 m high, and stalactites, flags and a 2 m high column are present (Figs. 3.13d and 3.14a).

Very close to the walking passage connecting through to Azokh II, a large block of chert hangs from the ceiling via a narrow pedicle of limestone (Fig. 3.14e). This feature provides evidence for the intense corrosion of the cave walls during the late evolution of the karst system. A short distance beyond this (Fig. 3.14c), is another large block of chert hanging from the ceiling at waist level (Fig. 3.14b). It is less obvious, due in part to its close proximity to a large underlying debris cone of sediment (from a collapsed gallery).

The ground sediment in the Azokh I chamber is a sandy-clay, with a thin veneer of more clay-rich material. During the summer months, when excavation and survey work is in progress, this sediment is usually found to be slightly damp. The access route to Azokh II was dry during a visit made by PDA in November 2007. The ceiling in this part of the cave used to have a few thin straw stalactites, which were fairly recent in age and active during the summer. The debris of a large collapsed chamber is located nearby (Fig. 3.8) and possibly acts as a water reservoir for this feature. Several meter-scale depressions occur on the

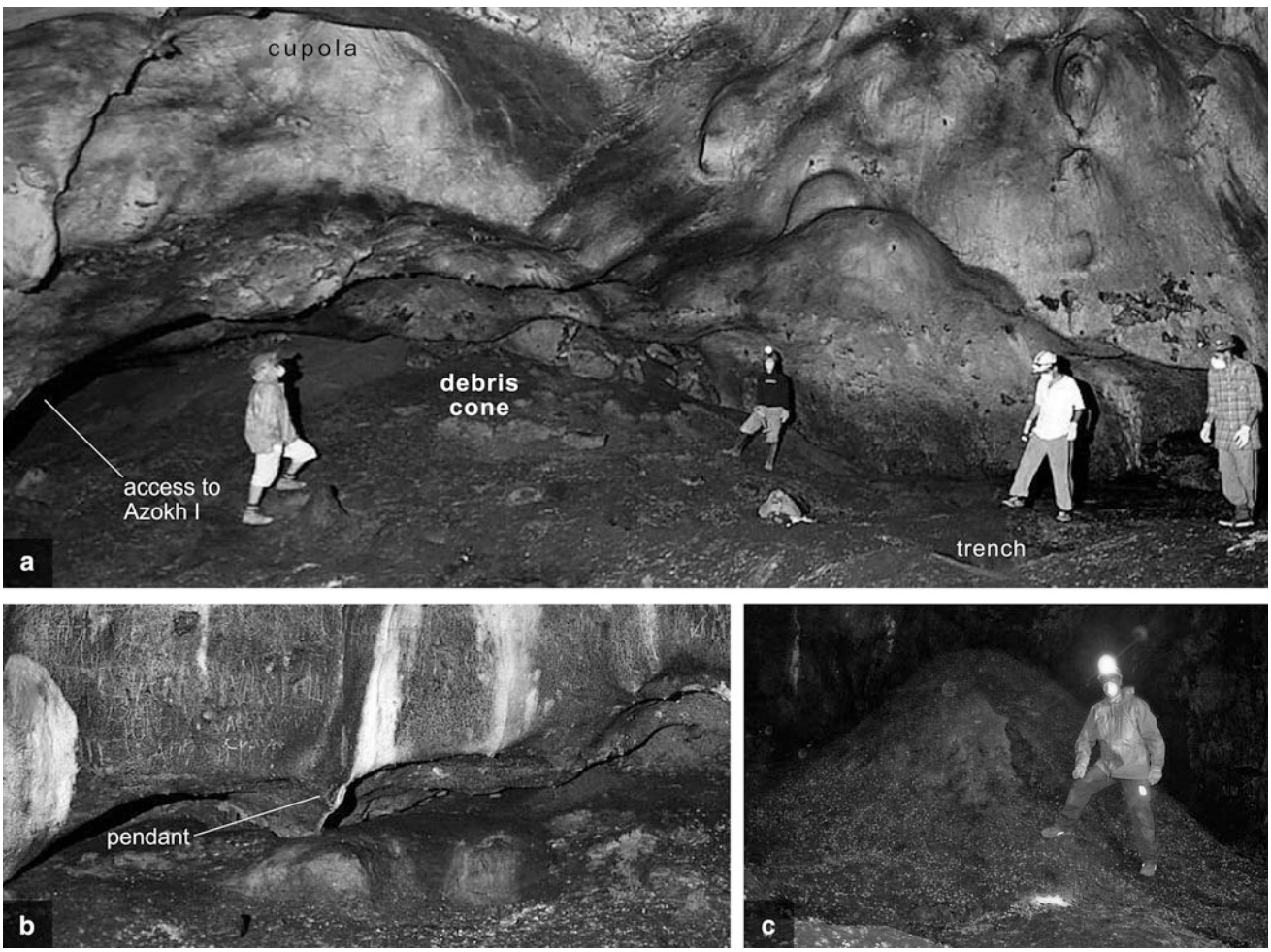

Fig. 3.15 Azokh II [*The Sugar-mound Gallery*]. **a** General panorama of the southwestern part of this cave gallery. A boulder choke and resultant debris cone blocks access to it from the upper pit over Azokh 2 on the exterior (see Fig. 3.8). **b** The NW wall of the gallery, composed largely of pendants; **c** Very large pile of bat guano present inside the chamber. The gallery is named after this feature

ground in this chamber and are labeled as 'collapse pits' in Figs. 3.13a and 3.14a; however, it is equally quite plausible that they were excavated by local visitors to the cave.

Azokh II: The Sugar-Mound Gallery

The *Sugar-Mound Gallery* is broadly oval-shaped with a surface area of 178 m^2 (Fig. 3.15). A conspicuous characteristic of this chamber is a very large pile of sediment with a rounded profile, which is covered by a very substantial amount of guano (Fig. 3.15c) and which gives the name to this chamber. It is located close to the northeastern wall, beneath a large cupola indicated on the cross section in Fig. 3.9. The walls of the chamber are noticeably darker compared with Azokh I and are covered with a brownish cinnamon-like color coating.

Upon entering the *Sugar-Mound Gallery* (Azokh II) from Azokh I, just to the left by the western wall is a significant collapse feature with decimeter-scale boulders of limestone (labeled "debris cone" in Fig. 3.15a). The deposit is largely clast-supported and finer reddish-brown sediment makes up the matrix in the interstitial areas between the boulders. This feature forms a sediment cone which extends NW across the Azokh II chamber and also SE into the (NW) terminal portion of Azokh I (*Branch 2*). Despite the scale of this collapse, no clear sign of it is evident on the exterior of the cave. We suggest that this allochthonous sediment cone possibly corresponds to a collapse dome which remained largely internal, within the *Upper Limestone Unit*, and which probably has kept an air cavity above it.

Azokh III: The Apron Gallery

This inner chamber is developed on two topographic levels and has a total surface area of 93 m^2 (Fig. 3.16). Entrance to this gallery is made from Azokh II through a low crawl-way (Fig. 3.16a), which leads directly onto the upper of the two levels. A fairly steep incline on the ground surface leads down in an easterly direction towards the lower level of the chamber (Fig. 3.16d). This slope is principally due to the presence of an apron of debris radiating from a very large collapse feature (Fig. 3.8).

The walls of the *Apron Gallery* have experienced intense weathering, possibly due to the concentrated presence of bats there. Signs of micro-corrosion are clearly evident on many surfaces:

- Shallow concave (millimeter-scale) cavities, probably formed by chemical corrosion of the limestone *and*
- Striations (cuttings) most probably formed by continuous erosion from the claws of bats.

The exit from this particular chamber through to Azokh IV is positioned on the same topographic level as the entrance (it is a horizontal narrow path made by the footsteps of frequent visitors), and the connection is a short, narrow passage, which skirts around the periphery of the large debris cone.

Azokh IV: The Hall Gallery

This large gallery has a broadly rounded or ovoid shape in plan and occupies a total surface area of 442 m^2 (Fig. 3.17; see also Fig. 3.8). At the northern end of this large and spacious chamber, a large chert cornice protects and supports the roof of a small, but quite distinct, underlying side-chamber or "hall" (Fig. 3.17a).

A large collapse feature, filled with large limestone boulders, with finer sediment infilling the interstitial gaps, is located at the SE end of the *Hall Gallery* (labeled "debris cone" on Fig. 3.17d). This allochthonous deposit is a continuation of the boulder cone forming the NW wall of the *Apron Gallery* (Azokh III), discussed previously. On the hillside outside the cave, positioned broadly above this feature, there is a dense copse of trees growing in the depression (doline) created by this collapse (Fig. 3.5a, c; see also the cross section in Fig. 3.9). These trees sink their roots some 20 m vertically through the soil and the roots themselves are visible in the cave chamber beneath.

The exit from the *Hall Gallery* (Azokh IV) to the exterior may be made through either Azokh 5 or Azokh 6 passages on the western side of the chamber (Fig. 3.17c). The latter involves a moderately steep descent down a sloping surface and through a narrow pathway corridor, which then leads to the outside of the cave (see Fig. 3.9).

Geophysical Investigation of the Cave System

The topographic mapping of the cave system at Azokh, discussed above, and illustrated in Figs. 3.8 and 3.9, can only ever provide an indication of the open spaces that are possible to physically explore and document. The full extent of the various karstic conduits is obscured by the level of sediment infilling them and, in some cases (such as Azokh 2), blocking of the galleries by collapse features. Geophysics provides a tool to investigate the nature of the subsurface within the cave. DC electrical resistivity has proven a useful method for constraining the boundary between buried limestone bedrock and overlying unconsolidated sediments

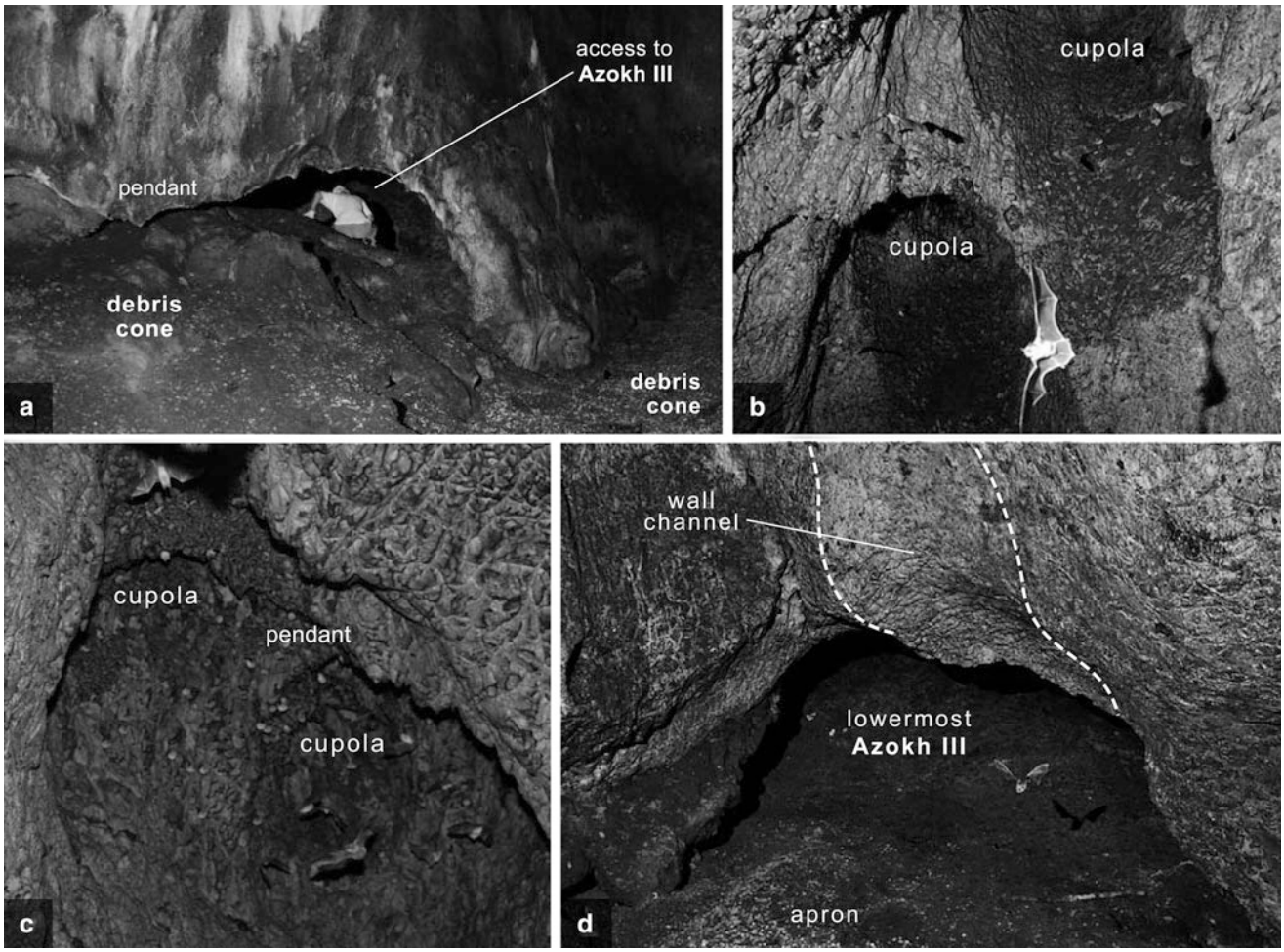

Fig. 3.16 Azokh III [*The Apron Gallery*]. **a** Access route to this gallery (from Azokh II); **b**, **c** Complex cupolas in the ceiling of Azokh III. Note the coarse texture of the walls and the darkening because of the activity of bats; **d** View of the topographically lowermost part of this gallery from the general cave pathway. Note the possible carved 'channel' feature in wall

(e.g., Aracil et al. 2003; Porres 2003). The application of this particular technique makes it possible to estimate infill thicknesses and the volume of sedimentary material sitting on the rocky floor of the cave; to determine the sectors of the cave system with the greatest accumulation of infill; to characterize the different types of infill; and, as far as possible, identify possible cavities in the limestone bedrock beneath the sediments (e.g., Gautam et al. 2000; Griffiths and Barker 1993; Zhou et al. 2000).

Materials and Methods of the Geophysical Survey

As a complementary study to the physical description of the Azokh Cave system, a geophysical survey was conducted both internally and externally (Fig. 3.18). The survey lines were concentrated near the various entrances and across the top surface of the limestone escarpment (*Upper Limestone Unit*; see Fig. 3.5a), with the dual purpose of identifying new subsoil cavities and determining the extent of fracture development and its relationship to cave formation.

Electrical resistivity tomography is a geo-electrical surveying method that analyzes subsoil materials according to their electrical impedance, which, in other words, allows them to be differentiated according to their resistivity (Aracil et al. 2002, 2003). The level of concentration of ions which carry the electrical signal depends on the nature and composition of the rocks and sediment and also the degree to which they are compacted or porous, which in turn influences their fluid content. Greater mobility of ions results in greater electrical conductivity or conversely less resistivity. This parameter produces 2-dimensional or 3-dimensional profiles which allow the materials at different depths to be investigated at different degrees of resolution (e.g., Martínez-Pagán et al. 2005).

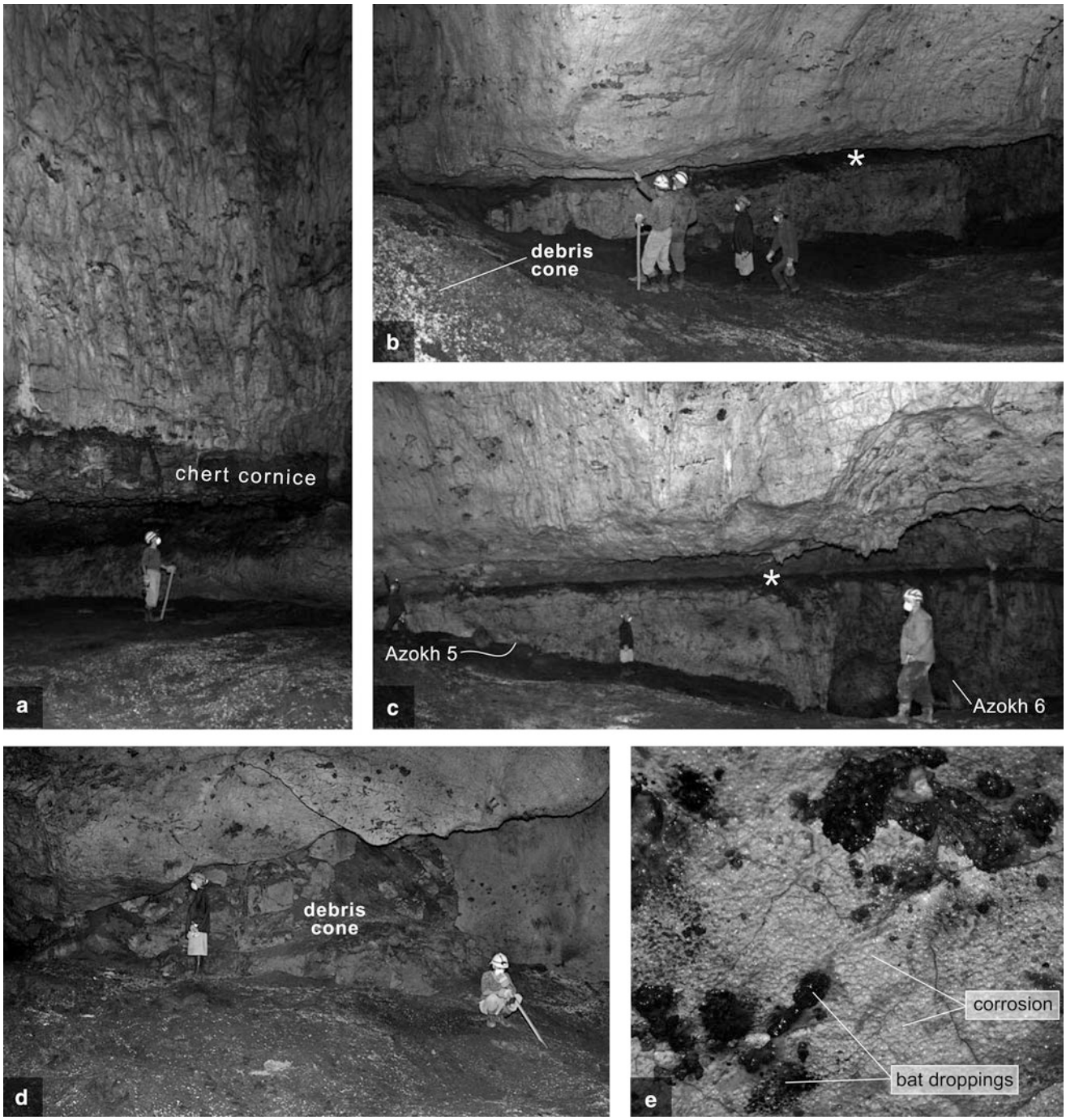

Fig. 3.17 Azokh IV [*The Hall Gallery*]. **a** Small side-chamber in this gallery, protected by an overlying layer of chert. Note the corrosion evident on the walls; **b**, **c** General views of the western side of the *Hall Gallery* showing the inclined surface of the sediment apron from the collapsed doline. A major bedding plane interface between the *Upper* and *Lower Limestone* units is indicated with a white asterisk in both photographs. The exits to the exterior through Azokh 5 and 6 passages are also indicated in (**c**); **d** View of the boulder choke (debris cone) feature (looking east across this gallery); **e** Detailed view of corrosion on the limestone walls of the gallery. This picture is about 6 cm wide

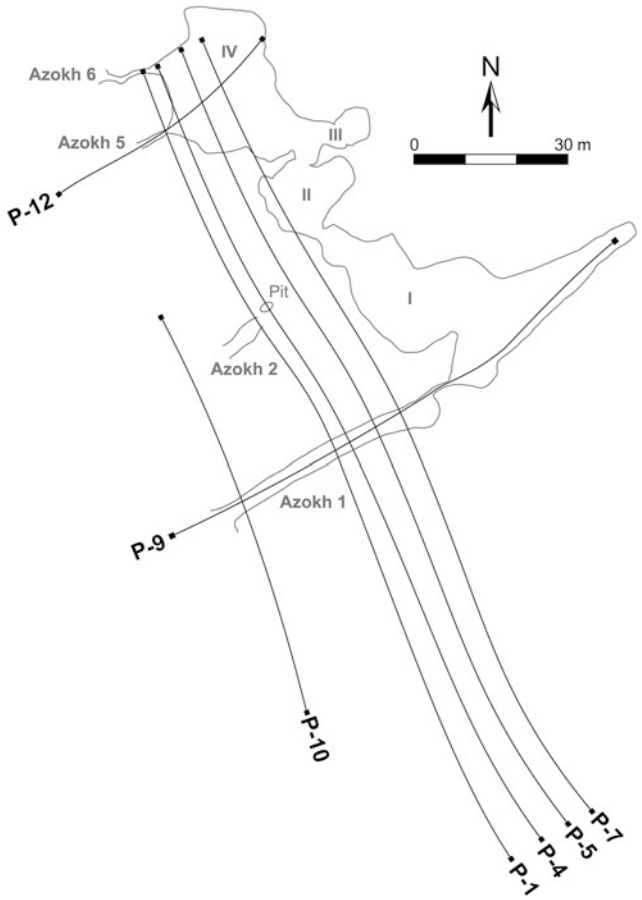

Fig. 3.18 Location (plan) map for geophysical electrical resistivity survey lines presented in Figs. 3.19, 3.20 and 3.22 and discussed in the main text. An outline of the cave system at Azokh is shown for ease of reference (internal chambers are denoted with Roman numerals). Lines P-9 and P-12 were taken from the interior of the cave, out through entrance passages (Azokh 1 and 5 respectively) and down the exterior hillside. Line P-10 was taken on the exterior of the cave, at the level of the entrance walkway to Azokh 1. Lines P-1, P-4, P-5 and P-7 were also taken externally, but at a higher topographic level, on the top surface of the limestone escarpment (*Upper Limestone Unit*) on the hillside

The resistivity in the rock or sediment will depend fundamentally on four factors:

1. The proportion of pore volume within the context of the total volume of the rock. Lower resistivity may be expected where there is a greater volume of pores (high porosity), provided these are filled with water, clay, etc.
2. The geometric layout of the pores (known as the formation factor). Limited pore morphology or a disconnected pore layout will lead to greater resistivity.
3. The nature of the material infilling the pores. If empty (vadose) cavity spaces are present, resistivity should be abnormally high, given the dielectric properties of air. Conversely, the greater the proportion of water-filled pores, the lower the resistivity, as the electric current circulates more freely through water than it does through air.
4. The resistivity or conductivity of the pore water concerned. Saline water, for example, has higher conductivity than fresh water. This will have the effect of altering the resistivity of the rock or sediment in which it is found (e.g., Sumanovac and Weisser 2001).

The electrical resistivity readings were recorded at Azokh Cave using a multi-electrode array set out along a set linear distance (see Fig. 3.18). The electrodes were pushed into the sediment by hand; however, where the ground surface was particularly rocky, a hammer was utilized. The degree to which the electrical current penetrates the subsurface is dependent on the electrode spacing – the wider the spacing, the deeper the penetration. In order to generate useful plots of the acquired geophysical data, it is necessary to link and correct the various survey lines to the cave topography (discussed above), to compensate for differences in slope.

Results of the Geophysical Survey

The results from the geophysical survey are presented in Figs. 3.19, 3.20, 3.21 and 3.22. Figures 3.19, 3.20 and 3.22 show vertical sections through the substratum which are color-coded according to their differing electrical resistivity properties (see legend at the bottom of each profile). In all of these profiles, it is possible to differentiate the subsoil from the limestone bedrock with a fair degree of clarity, due to the highly pronounced geo-electric contrast between both units. The unit comprising the sediment infill is more conductive or, conversely, is not very resistive; whereas the unit that forms the rocky substrate is very resistive, which is to say that it transmits the electric current with great difficulty, giving high resistivity values as a consequence.

Two electrical resistivity profiles from Azokh 1 passage (P-9), and the surrounding area outside (P-10), are shown in Fig. 3.19. Section P-9 is 175 m in length and runs from the interior of the cave (Azokh I: *The Stalagmite Gallery*), out in a broadly SW direction through Azokh 1 and down the hillside outside. This section shows the extent of the limestone bedrock as areas of relatively high resistivity directly beneath the floor of Azokh 1. This is the main area of excavation at present and the presence of bedrock in this part of the cave had been confirmed during previous geological and sedimentological survey work (see the cross section of this passage provided by Murray et al. 2010, their Fig. 3). Electrical resistivity profile P-9 (Fig. 3.19a) provides a more complete impression of the full extent of the limestone bedrock and, more significantly, suggests that there may be several infilled cavities beneath the present floor level; that is

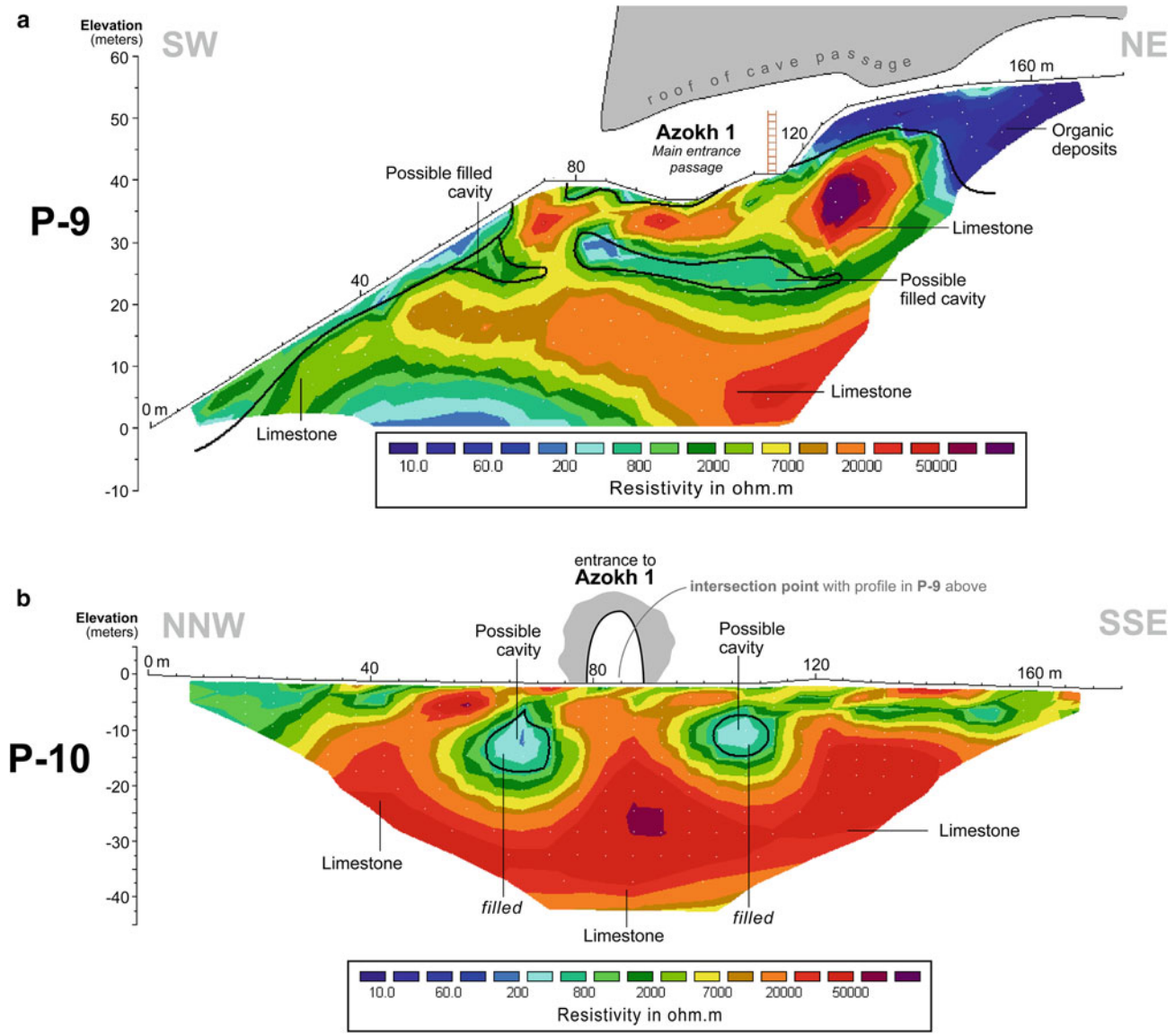

Fig. 3.19 2-D electrical resistivity profiles from Azokh 1. The two profiles intersect outside the cave at the mouth of the passage (see Fig. 3.18 for general location). **a** Profile P-9 was measured along the long axis of Azokh 1, in a SW (external) to NE (internal) direction, and shows the presence of a possible infilled chamber at about 8–10 m depth beneath the cave floor; **b** Transverse profile P-10 [broadly perpendicular to P-9] showing two possible infilled cavities at around 5–8 m depth beneath the surface. The cavity on the left may possibly correspond to the SW side of the cavity identified in P-9

lower levels not yet reached or investigated within the cave system. Resistivity profile P-10 (Fig. 3.19b) was measured across the entranceway to Azokh 1 passage in a NNW to SSE direction, broadly orthogonal to profile P-9. The intersection between these two profiles was at the cave mouth and is indicated on Fig. 3.19b (see also Fig. 3.18). This transverse section also suggests the possible presence of two discrete filled cavities at a lower level in the cave system.

Electrical resistivity profile P-12 was taken from Azokh IV (*The Hall Gallery*) and out through Azokh 5 passage (Fig. 3.20; see also Fig. 3.18 for general location). Importantly, this section indicates at least 10 m vertical thickness of sediment infilling the inner chamber. Excavation work is at a very early stage in this relatively undisturbed part of the cave and these geophysical results suggest considerable potential for future archaeological investigation there.

A number of additional 2-dimensional electrical resistivity profiles were recorded through the interior of the cave system and, in all, a clear differentiation between solid limestone bedrock and overlying unconsolidated sediment was observed. This facilitated the measurement of infill thickness from all the resultant sections, which then provided data for a points file with all the thicknesses recorded.

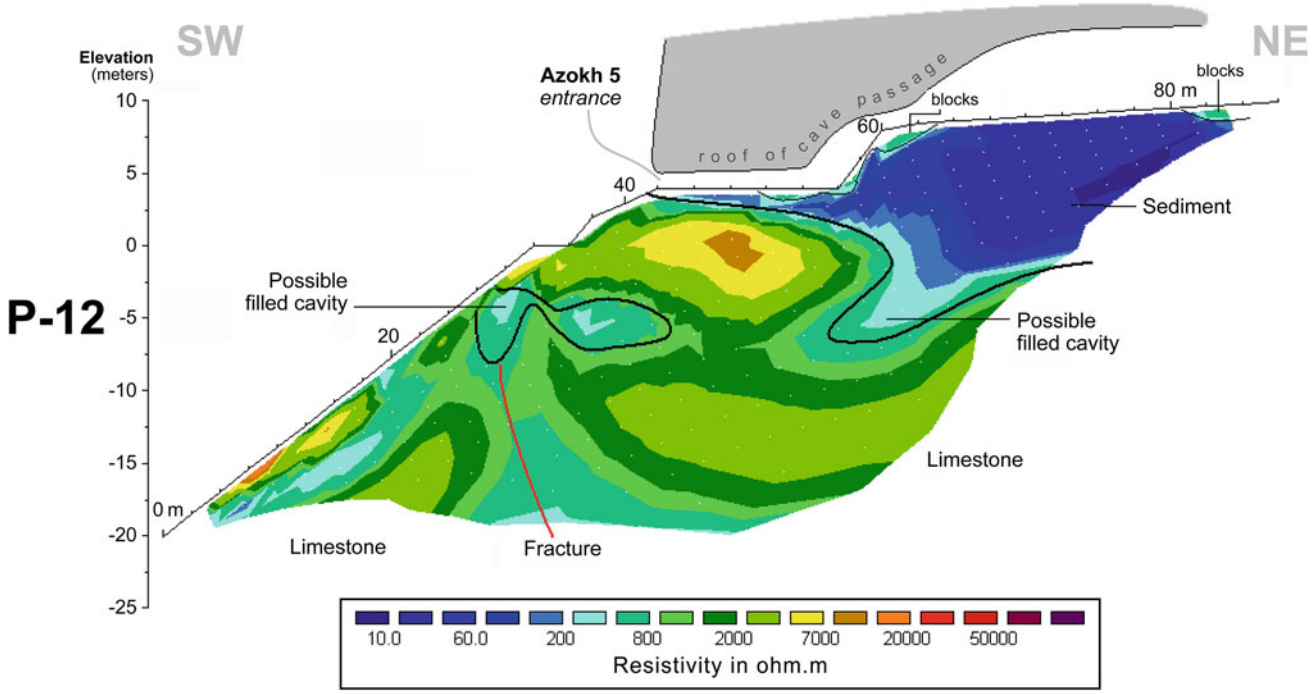

Fig. 3.20 2-D electrical resistivity profile P-12 through Azokh 5 passage. The large area of low resistivity (upper right on the profile) suggests appreciable sediment thickness in the inner chamber at that location. See Fig. 3.18 for general location of profile

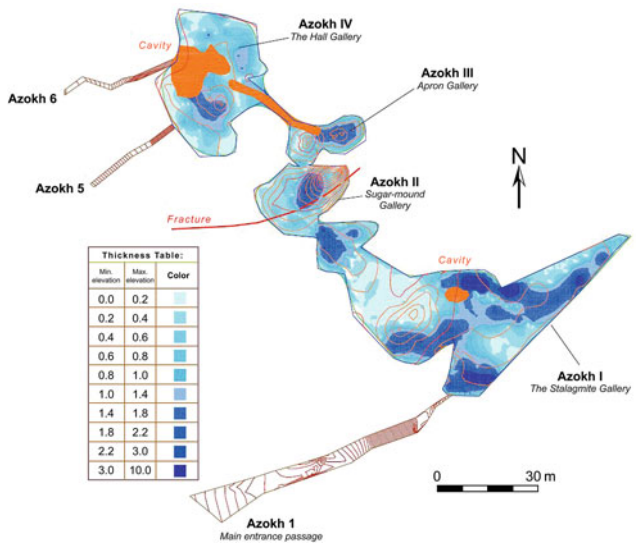

Fig. 3.21 Isopach plan map of entire sedimentary infill of the inner cave system at Azokh, calculated from electrical resistivity profiles

Using these values an isopach map of sediment infill thickness was generated (Fig. 3.21). According to this map, a concentration of thicker amounts of infill are observed in Azokh I (*The Stalagmite Gallery*), principally at the SE end, where it reaches thicknesses of between 2 and 3 m at various points and where areas with infill thicknesses of between 1 and 2 m are also frequently encountered.

Other areas of the interior of the cave also have elevated thicknesses of cave fill (Fig. 3.21) such as:

1. The area close to the entrance to Azokh II (*The Sugar-mound Gallery*) – probably related to the large cone of collapsed sediment;
2. The central area of Azokh II (*The Sugar-mound Gallery*) – probably related to the large pile of sediment and guano located there (see Fig. 3.9);
3. The lower level within Azokh III (*The Apron Gallery*); and
4. The south central portions of Azokh IV (*The Hall Gallery*).

Although the isopach map in Fig. 3.21 was drawn with all the infill considered as a homogenous entity, it is quite likely that the sediments do not all share a common origin. Beneath the organic surface layer of bat guano, which is in itself highly variable in thickness, part of the infill could be the product of the accumulation of coarse, medium and fine sediment detritus, including from the dissolution and fragmentation of limestone that forms the bedrock of the hillside.

The morphology and layout of the various cave galleries was probably strongly influenced by the presence of fractures in the limestone (Figs. 3.6 and 3.7), which would have logically been the conduits through which water flow was focused. An effort was made to analyze these fractures using electrical resistivity. Several parallel profiles (P-1, P-4, P-5 and P-7) were measured on the external surface of the

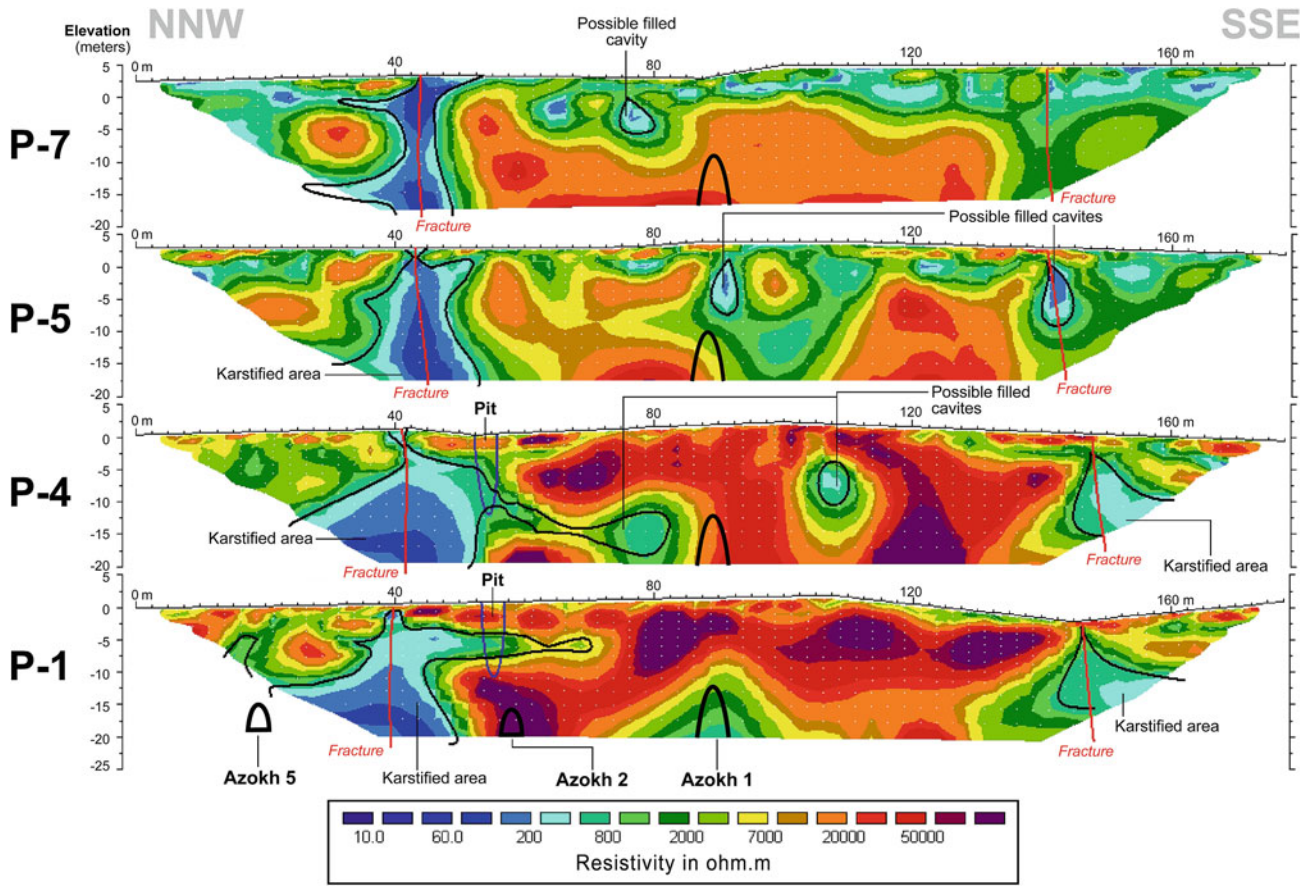

Fig. 3.22 Parallel 2-D electrical resistivity profiles (P-1, P-4, P-5 and P-7) taken sequentially across the top of the *Upper Limestone Unit* hosting the Azokh Cave system. See Fig. 3.18 for location details and also Fig. 3.5a for a general panoramic view of the hillside

limestone escarpment (Fig. 3.22; see Fig. 3.18 for general location), specifically on the top of the *Upper Limestone Unit* (see Fig. 3.5a). These profiles identify certain anomalies, which, due to their morphology, must represent fractures in the limestone, in which the circulation of water, and deposition of finer sediment, results in them displaying low resistivity values.

The anomalies interpreted as fractures and possible cavities are indicated in Fig. 3.22. A large conductive anomaly is evident towards the start (towards NNW) of each of the profiles, at about the 40–45 m point, and this may relate to a large fracture that runs through Azokh II gallery. The importance of this anomaly is that it corresponds to the inner chamber with the highest ceiling (cupola) within the cave system (see section in Fig. 3.9).

The profiles taken from the external surface of the hill in Fig. 3.22 also showed several fractures and possible cavities, apparently unconnected with the presently accessible part of the cave system. Some of these appear have an exit on the upper part of the *Upper Limestone Unit* through a shaft visible on the surface on the hillside (see Figs. 3.8 and 3.18 for location of this "pit" feature; it is also labeled on profiles P-1 and P-4 in Fig. 3.22).

Discussion

The plan of the cave system at Azokh presented in Fig. 3.8 is the most detailed and accurate version produced to date. The structural geological data in Fig. 3.7 shows that strongly

developed conjugate NE to SW and NW to SE joint sets are present in the limestone bedrock across the cave system, and these have influenced the orientation of the Azokh cave chambers beneath in the subsurface beneath (compare to Fig. 3.8). Sub-vertical joints appear to deflect away from this preferential cave system orientation at the northern and southern ends of the joint traverse. These data, combined with an interpretation of the aerial photograph presented in Fig. 3.7, along with the landscape panoramic in Fig. 3.5a, suggest the possibility that the thick limestone escarpment hosting the cave system may be bounded to the north and south by two large collapse features (*perhaps* influenced by the possible presence of two ENE-trending, sub-parallel faults; see Fig. 3.7).

The geophysical (electrical resistivity) survey work has shown a system of hidden galleries beneath Azokh 1 (Fig. 3.19). Recent clearing and excavation work in the basal entrance trench of this particular cave passage has revealed a small gallery, which is not infilled by sediment (Fig. 3.23; its position is also indicated as "*Lowermost Level*" in Figs. 3.8 and 3.9). This lowermost known level within the cave system was completely undisturbed when first discovered and contains several speleothems, including a spectacular "Christmas tree" shaped dogtooth calcite deposit (Fig. 3.23a–d). The latter grew subaqueously and indicates that the chamber was at least partially submerged, at least to the top level of the "tree". A speleothem development covered the entrance to this lower chamber (Fig. 3.23e, g).

At present, Azokh Cave does not follow a path for major conduits receiving groundwater recharge from higher levels in the limestone above, or indeed from the surface. On the contrary, it presents a 3-dimensional structure of large oblong-contour galleries directly connected laterally (Fig. 3.8). The keyhole profile of Azokh 1 passage (see Fig. 3.10a, b) suggests transition from phreatic to vadose conditions and is an indication of an epigenic cave system. According to Klimchouk (2007, 2009) in epigenic speleogenesis the process is dominated by shallow groundwater systems receiving recharge directly from above or areas immediately adjacent. The development of different levels or "storeys" at different elevations within the cave system thus reflects a progressive lowering of the water-table due to the evolution and incision of river valleys in the surrounding region. Thus upper storeys are older than lower ones. However, the presence of numerous cupolas (see discussion below; Fig. 3.24); pendants of isolated rock structures suspended from the cave ceiling (essentially the remains of rock pillars separating karstic channels cut through closely spaced paragenetic ceiling channels; for example see Fig. 3.14b, c, e); and abundant signs of dissolution or corrosion on the walls of the cave seems to suggest a hypogenic mode of speleogenesis. If *both* epigenic *and* hypogenic interpretations are valid, it may possibly suggest a polygenic origin for the formation of the cave.

Cupolas are dome-shaped solution cavities or wide vertical chimneys, which terminate abruptly and develop in certain cave ceilings. They are thought to form by condensation corrosion by convecting/circulating air (Osborne 2004; Piccini et al. 2007). According to Osborne (2004), cupolas are common in caves with thermal, hydrothermal, artesian, hypogene or mixed water origins, and they occur in caves which form through polygenetic processes; but are uncommon in stream caves.

In a hypogenic system, in contrast to an epigenic one, the various levels form almost contemporaneously: the lower storeys recharge and feed into the main system above through rising conduits. Laterally connected fractures in the bedrock may facilitate development of larger "master storeys" in the mid-levels of the system, whilst the upper levels are largely responsible for outflow. High cupola structures, sometimes with lateral extensions, may develop in the highest parts of the cave system (Klimchouk 2007, 2009). This description of a cave system underlain by a series of tubes and passages, with larger chambers developed in the (overlying) midsection and cupola developments present towards the very top, is reminiscent to that observed at Azokh Cave (Fig. 3.25).

After karst development ended, due to a lowering of the water table, the cave system was subsequently exposed and became accessible to animals and humans. As mentioned in the introduction, the cave is occupied by extremely large colonies of bats in the interior chambers of the cave system, and the evidence from excavation work in Azokh 1 passage suggests that they have resided there in large numbers for some time (Fernández-Jalvo et al. 2010; Sevilla 2016). At present, the most active speleogenic processes within the cave system appear to be those associated with the activities of bats, including their waste-products (guano and urine). Given the long amount of time they have been occupying the galleries, a considerable amount of guano has accumulated in the interior and these deposits have further modified the

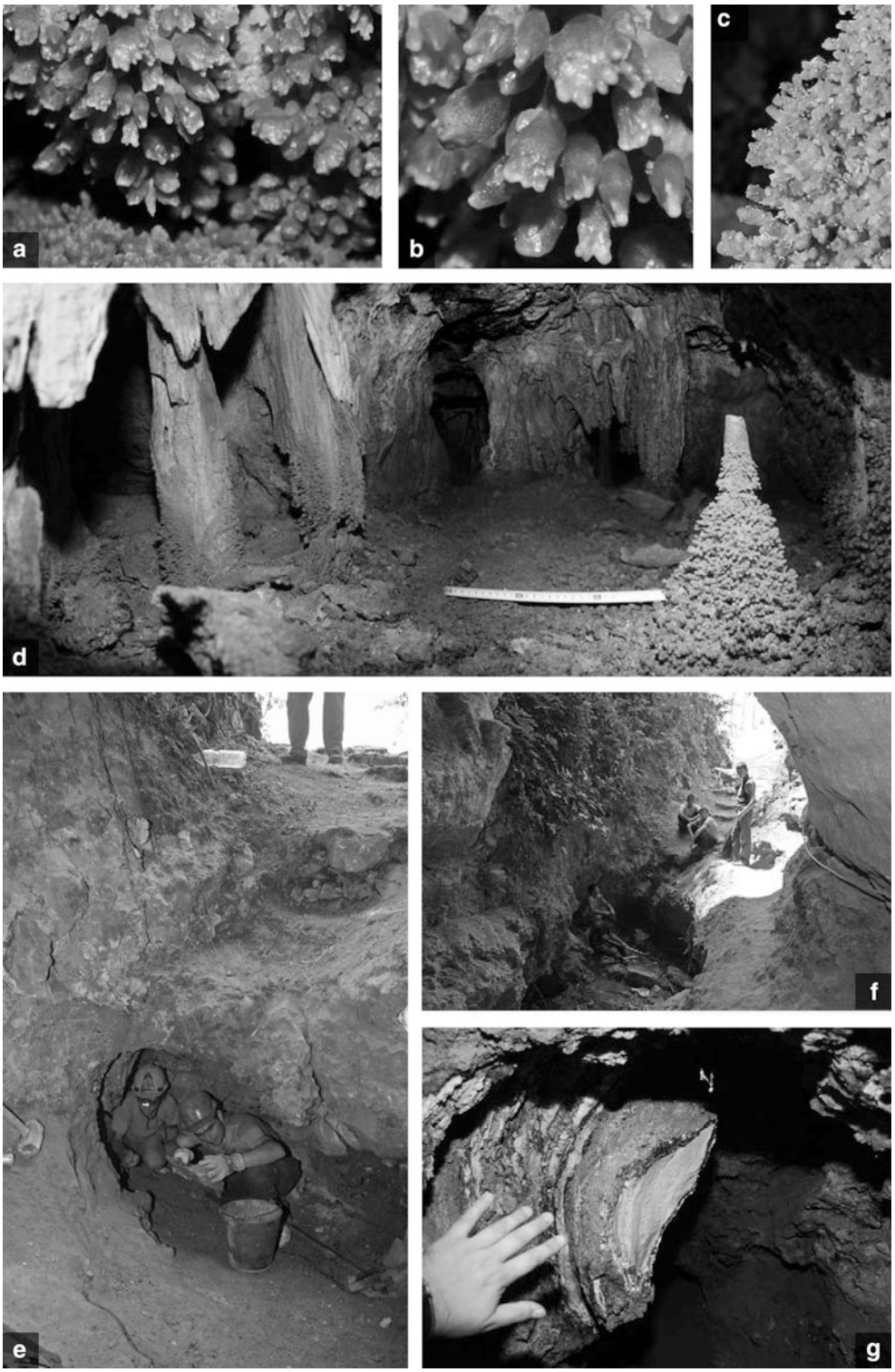

Fig. 3.23 The lowermost accessible gallery of the cave system at Azokh. **a**–**c** Detailed photographs of dogtooth calcite deposits which grew subaqueously; **d** General view of this lowermost gallery, as photographed the day it was discovered. Note the level of the watershed, as indicated by the upper limit of the dogtooth calcite development. The horizontal measuring tape is showing approximately 29 cm; **e**, **f** General views of the entrance to Azokh 1 passage showing the position of the lowermost gallery in the basal trench; **g** Speleothem found beneath the entrance to Azokh 1 passage. It is also visible immediately left of the helmet on person to left in (**e**). Access to the lowermost gallery was possible after excavating sandy sediments beneath this speleothem

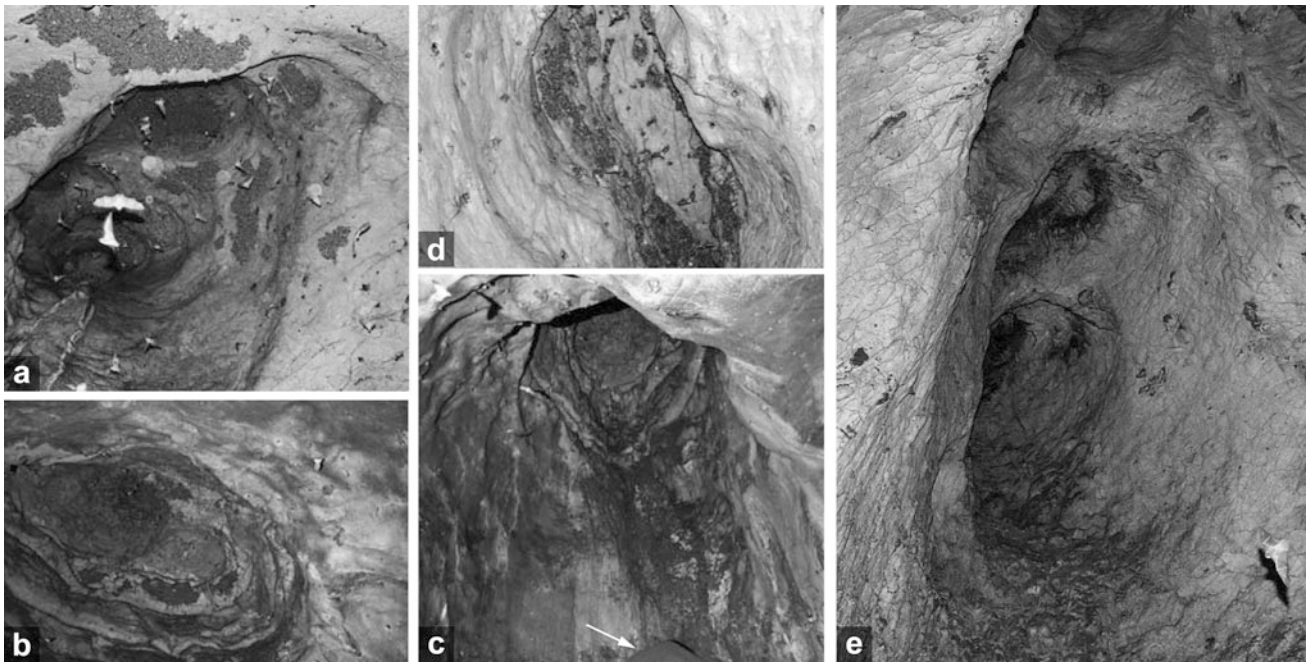

Fig. 3.24 Cupolas within the cave system at Azokh. **a** Cupola in the ceiling of the NE branch of Azokh I [*The Stalagmite Gallery*]; **b**, **c** Complex cupola in Azokh II [*The Sugar-mound Gallery*]. This is the largest cupola within the entire cave system and was formed by coalescence of a number of minor cupolas. In the very bottom of (**c**), the peak of a large mound of debris and bat guano is just visible (arrowed). This feature gives the gallery its name; **d**, **e** Elongated and complex (respectively) cupolas in the ceiling of Azokh IV [*The Hall Gallery*]

cave in a number of ways. Firstly, the heat from the guano pile helps to stimulate convective air flows in the cave atmosphere, and secondly, decomposition and alteration of this material produces a large amount of CO_2 and water vapor along with a number of strong, corrosive acids. These may then lead to biogenic corrosion, evident elsewhere, for example in the polygenetic Cuatro Ciénegas caves of Mexico (Piccini et al. 2007). At this particular site, large concave structures are developed in side walls; ceiling domes were generated due to condensation corrosion; and gullies and corrosion holes were produced in the floor of the cave due to the lowered pH of percolating fluids. In addition, condensation waters, enriched in salts, produced concretions and speleothems. Several of these features are also evident in the interior of Azokh Cave, and more importantly, where the modifying effect of bat guano is particularly strongly developed, it serves to obscure some of the original speleological features of the cave system, making interpretation problematic.

In summary, the multi-level, complex 3-dimensional morphology of the Azokh Cave system could be interpreted as epigenic, but also as hypogenic. A spongework cave pattern is not evident; instead cave formation is developed as a series of large, rounded galleries with interconnecting linear passages (Fig. 3.8). The change in cave pattern moving upwards through the limestone bedrock sequence (Fig. 3.25) makes interpretation complex. It is possible that most of the lower levels of the cave system formed in an epigenic regime; however, the upper levels may have had more of a hypogenic influence, leading to cupola and pendant formation. An additional issue is the general absence of speleothems inside of the cave, with the exception of the speleothem panel (Figs. 3.13d and 3.14a) and the large stalagmite (Fig. 3.13c) in Azokh I chamber and also the lowermost level beneath the entrance to Azokh 1 passage (Fig. 3.23). Clearly more investigation needs to be conducted to completely understand the origin of the cave; however, our preliminary interpretations indicate a complex, multifaceted history of formation and evolution.

◀ **Fig. 3.25** Plan views of cave development in the different layers (or levels) of the limestone bedrock at Azokh. **a** Passage development in the *Lower Limestone Unit*. Many of these are influenced by the trends of major joints and in some instances they meander; **b** The large main internal chambers or galleries are developed in the lower part of the *Upper Limestone Unit*; **c** Cupolas, collapse dolines, chokes and pits are developed in the upper part of the *Upper Limestone Unit*. The inset box in each image shows, in profile, the relative elevation of each type of cave development within the limestone sequence. The scale and north arrow on map (**a**) are also applicable to plan views (**b**) and (**c**)

Conclusions

1. A clear and detailed account of the geomorphology of the cave system at Azokh has been provided here for the first time. The cave formed from an abandoned karstic network developed in Mesozoic limestones and is composed of four large inner chambers (Azokh Galleries I–IV), which are laterally connected and arranged in a NW-SE trend. These are connected to the exterior via a series of NE-SW passages (Azokh 1, 5 and 6). These conduits all share a similar orientation with the regional pattern of jointing in the bedrock.
2. Doline collapse features figure prominently in the geomorphology of the cave. In the case of one of the entrance passages (Azokh 2), it has blocked access through to the inner galleries. Chert development within the limestone has had the opposite effect; in places it has served to stabilize and support ceiling structures, helping to reinforce and preserve various cave chambers.
3. The cross-sectional topography of the cave shows a higher central region (between inner chambers Azokh II and Azokh III), with a slope towards the two extremities of the cave system, although this descent is somewhat more pronounced towards Azokh 1 passage.
4. The thickness of the sediment infilling the various chambers may be determined from the electrical resistivity profiles, which have allowed the infill thicknesses to be mapped throughout the interior of the cave system. A variation in thickness is observed of <1 m to over 3 m. The greatest thicknesses of sediment occur in Azokh I, although there are also areas with elevated thicknesses at the entrance to Azokh II, along with more centralized areas in Azokh II, III and IV. A first order volume estimate of 1,367 m^3, based on a calculated surface area of approximately 1,390 m^2, was made for all the loose materials (sediment) lying on the surface of the limestone bedrock in the inner galleries at Azokh.
5. The geophysical profiles have identified several anomalies within the limestone bedrock, which, due to their morphology and resistivity values, probably represent cavities that are filled with fine materials. All the cavities that have been identified are associated in a general way with

conductive anomalies in the profiles that are interpreted as fractures. This confirms a relationship between fracture development, karstification and the formation of cavities.

6. It remains unclear whether the cave formed through epigenic or hypogenic speleological processes. This issue is further complicated by the presence of very large bat colonies in the interior of the cave system. The thick guano deposits generated by these creatures modify the inner galleries in a number of ways.

Acknowledgments We wish to thank the local people from Azokh Village for wholeheartedly supporting this endeavor, over a number of years and always making us feel welcome when we visit. In particular, Masis Ohanyan and Zorig Asryan very ably assisted us with the survey of the cave interior. The Royal Irish Academy is thanked for kindly granting permission to reproduce Fig. 3.1 (herein) from Murray et al. (2010). PDA, EA and JP acknowledge support from the Spanish Ministry of Science and Education (Projects BTE2000-1309, BTE2003-01552 and BTE 2007-66231).

References

Aracil, E., Maruri, U., Porres, J. A., & Espinosa, A. B. (2002). La tomografía eléctrica: una herramienta al servicio de la obra pública. *Rock Máquina, 76*, 30–34.

Aracil, E., Maruri, U., Vallés, J., Martínez Pagán, P., & Porres, J. A. (2003). Evaluación de problemas medioambientales mediante tomografía eléctrica. *Ingeopress, 122*, 34–39.

Brunet, M. F., Korotaev, M. V., Ershov, A. V., & Nikishin, A. M. (2003). The South Caspian Basin: A review of its evolution from subsidence modelling. *Sedimentary Geology, 156*, 119–148.

Cardozo, N., & Allmendinger, R. W. (2013). Spherical projections with OSXStereonet. *Computers & Geosciences*, *51*, 193–205.

David, E. (2008). *Visual Topo*. Available online at: http://vtopo.Free.fr.

Day, A. (2002). *Cave Surveying. Cave Studies Series 11*. Buxton: British Cave Research Association, 40 pp.

Dilek, Y., Imamverdiyev, N., & Altunkaynakc, Ş. (2009). Geochemistry and tectonics of Cenozoic volcanism in the Lesser Caucasus (Azerbaijan) and the peri-Arabian region: Collision-induced mantle dynamics and its magmatic fingerprint. *International Geology Review, 52*(4–6), 536–578.

Egan, S. A., Mosar, J., Brunet, M.-F., & Kangarli, T. (2009). Subsidence and uplift mechanisms within the South Caspian Basin: insights from the onshore and offshore Azerbaijan region. In M.-F. Brunet, M. Wilmsen & J. W Granath (Eds.), *South Caspian to Central Iran Basins* (Vol. 312, pp. 219–240). London: Geological Society (Special Publication).

Fernández-Jalvo, Y., Hovsepian-King, T., Moloney, N., Yepisko posyan, L., Andrews, P., Murray, J., et al. (2009). Azokh Cave project excavations 2002–2006: Middle-Upper Palaeolithic transition in Nagorno-Karabakh. Coloquios de Paleontología, Special Issue: Homage to Dr. D. Soria Madrid, Universidad Complutense de Madrid Press.

Fernández-Jalvo Y., King T., Andrews P., Yepiskoposyan L., Moloney N., Murray, J., et al. (2010). The Azokh Caves complex: Middle Pleistocene to Holocene human occupation in the Caucasus. *Journal of Human Evolution, 58*, 103–109.

Fossen, H. (2010). *Structural geology* (463 pp.). Cambridge: Cambridge University Press.

Gautam, P., Paj Pant, S., & Ando, H. (2000). Mapping of subsurface karst structure with gamma ray and electrical resistivity profiles: A case study from Pokhara valley, central Nepal. *Journal of Applied Geophysics, 45*, 97–110.

Griffiths, D. H., & Barker, R. D. (1993). Two-dimensional resistivity imaging and modelling in areas of complex geology. *Journal of Applied Geophysics, 29*, 211–226.

Gross, M. R., Fischer, M. P., Engelder, T., & Greenfield, R. J. (1995). Factors controlling joint spacing in interbedded sedimentary rocks: Integrating numerical models with field observations from the Monterey Formation, USA. In M. S. Ameen (Ed.), *Fractography: Fracture Topography as a Tool in Fracture Mechanics and Stress Analysis* (Vol. 92, pp. 215–233). Geological Society of London, Special Publication.

Huseinov, M. M. (1985). *The Early Palaeolithic of Azerbaijan (Kuruchai culture and stages of its development).* Baku (in Russian).

Kasimova, R. M. (2001). Anthropological research of Azykh Man osseous remains. *Human Evolution, 16*, 37–44.

Karakhanian, A. S., Trifonov, V. G., Philip, H., Avagyan, A., Hessami, K., Jamali, F., et al. (2004). Active faulting and natural hazards in Armenia, eastern Turkey and northwestern Iran. *Tectonophysics*, *380,* 189–219.

King, T., Compton, T., Rosas, A., Andrews, P. Yepiskoyan, L., & Asryan, L. (2016). Azokh Cave Hominin Remains. In Y. Fernández-Jalvo, T. King, L. Yepiskoposyan & P. Andrews (Eds.), *Azokh Cave and the Transcaucasian Corridor* (pp. 103–106). Dordrecht: Springer.

Klimchouk, A. B. (2007). *Hypogene Speleogenesis: Hydrogeological and Morphogenetic Perspective*. Special Paper no. 1, National Cave and Karst Research Institute, Carlsbad, NM, 106 pp.

Klimchouk, A. B. (2009). Morphogenesis of hypogenic caves. *Geomorphology, 106*(1–2), 100–117.

Lioubine, V. P. (2002). *L'Acheuléen du Caucuase*. ERAUL 93 Études et Recherches Archéologiques de l'Université de Liège. Liège.

Ljubin, V. P., & Bosinski, G. (1995). The earliest occupation of the Caucasus region. In Roebroeks, W. & van Kolfschoten, T. (Eds.), *The Earliest Occupation of Europe* (pp. 207–253). Leiden: University of Leiden.

Martínez-Pagán, P., Aracil, E., Maruri, U., & Faz, Á. (2005). Tomografía eléctrica 2D/3D sobre depósitos de estériles mineros. *Ingeopress, 138*, 34–36.

Mellors, R.J., Jackson, J., Myers, S., Gok, R., Priestley, K., Yetirmishli, G., et al. (2012). Deep Earthquakes beneath the Northern Caucasus: Evidence of Active or Recent Subduction in Western Asia. *Bulletin of the Seismological Society of America, 102,* 862–866.

Mosar, J., Kangarli, T., Bochudi, M., Glasmacher, U. A., Rast, A., Brunet, M-F., et al. (2010). Cenozoic–Recent tectonics and uplift in the Greater Caucasus: A perspective from Azerbaijan. In M. Sosson, N. Kaymakci, R. A. Stephenson, F. Bergerat & V. Starostenko (Eds.), *Sedimentary Basin Tectonics from the Black Sea and Caucasus to the Arabian Platform* (Vol. 340, pp. 261–279). London: Geological Society (Special Publications).

Mudrák, S., & Budaj, M. (2010). *The Therion Book*. Distributed under the GNU General Public License. 105 pp. Available online at: http://therion.speleo.sk.

Murray, J., Domínguez-Alonso, P., Fernández-Jalvo, Y., King, T., Lynch, E. P., Andrews, P., et al. (2010). Pleistocene to Holocene stratigraphy of Azokh 1 Cave, Lesser Caucasus. *Irish Journal of Earth Sciences, 28,* 75–91.

Murray, J., Lynch, E. P., Domínguez-Alonso, P., & Barham, M. (2016). Stratigraphy and Sedimentology of Azokh Caves, South Caucasus. In Y. Fernández-Jalvo, T. King, L. Yepiskoposyan & P. Andrews (Eds.), *Azokh Cave and the Transcaucasian Corridor* (pp. 27–54). Dordrecht: Springer.

Narr, W., & Suppe, J. (1991). Joint spacing in sedimentary rocks. *Journal of Structural Geology*, *13*, 1037–1048.

Osborne, R. A. L. (2004). The troubles with cupolas. *Acta Carsologica, 33*(2), 9–36.

Piccini, L., Forti, P., Giulivo, I., & Mecchia, M. (2007). The polygenetic caves of Cuatro Ciénegas (Coahuila, Mexico): Morphology and speleogenesis. *International Journal of Speleology, 36*(2), 83–92.

Porres, J. A. (2003). *Caracterización de cavidades en el subsuelo mediante la interpretación de perfiles de Tomografía Eléctrica: Aplicación al yacimiento arqueológico de Clunia.* Unpublished PhD Dissertation, University of Burgos, Spain. ISBN 978-84-96394-55-1.

Saintoti, A., Brunet, M.-F., Yakolev, F., Sébrier, M., Stephenson, R., Ershov, A., et al. (2006). The Mesozoic–Cenozoic tectonic evolution of the Greater Caucasus. In D. G. Gee & R. A. Stephenson (Eds.), *European Lithosphere Dynamics* (Vol. 32, pp. 277–289). London: Geological Society (Memoirs).

Sevilla, P. (2016). Bats from Azokh Caves. In Y. Fernández-Jalvo, T. King, L. Yepiskoposyan & P. Andrews (Eds.), *Azokh Cave and the Transcaucasian Corridor* (pp. 177–189). Dordrecht: Springer.

Sosson, M., Kaymakci, N., Stephenson, R., Bergerat, F., & Starostenko, V. (2010). Sedimentary basin tectonics from the Black Sea and Caucasus to the Arabian Platform: Introduction. In M. Sosson, N. Kaymakci, R. Stephenson, F. Bergerat & V. Starostenko (Eds.), *Sedimentary Basin Tectonics from the Black Sea and Caucasus to the Arabian Platform* (Vol. 340, pp. 1–10). London: Geological Society (Special Publication).

Sumanovac, F., & Weisser, M. (2001). Evaluation of resistivity and seismic methods for hydrogeological mapping in karst terrains. *Journal of Applied Geophysics, 47*, 13–28.

Vardanyan, M. (editor in chief) and others. (2010). *Atlas of the Nagorno-Karabakh Republic*. State Committee of the Real Estate Cadastre of the Nagorno-Karabakh Republic, Stepanakert, 96 pp.

Zhou, W., Beck, B. F., & Stephenson, J. B. (2000). Reliability of dipole-dipole electrical resistivity tomography for defining depth to bedrock in covered karst terrains. *Environmental Geology, 39*(7), 760–766.

Chapter 4
Lithic Assemblages Recovered from Azokh 1

Lena Asryan, Norah Moloney, and Andreu Ollé

Abstract Between 2002 and 2009, renewed investigations of Units II, III, IV and V at Azokh 1 cave were undertaken following rigorous systematic methods of excavation and recording. New dates suggest an age of 184–100 ka for Unit II and ~300 ka for Unit Vm. The excavations produced a range of fossil faunas dominated by cave bears, and 387 lithic artifacts: 68 from Unit Vm, 4 from Unit III, and 315 from Unit II. Although a range of rock types was exploited for tool production, most artifacts are on siliceous rocks, with a few made from non-local obsidian. There is little evidence for the early stages of production on-site. It is possible that initial working may have occurred elsewhere, and cores, blanks and tools transported to the cave. However, given the restricted area of excavations at the rear of the cave, we cannot discount the possibility of knapping activities having occurred in other areas of the cave, the sediments of which were removed in earlier excavations. The stone artifacts from Unit II, with their Levallois component, are clearly Middle Paleolithic, and may be among the earliest evidence for Middle Paleolithic presence in the Southern Caucasus. The material from Unit Vm could be late Acheulean on the basis of dating, lack of Levallois technology, the general larger sizes of the pieces (although no bifaces have been found), and its stratigraphic position below Units II, III, and IV.

Резюме При предыдущих раскопках под руководством М.Гусейнова в период с 1960-х по 1980-е гг. было обнаружено около 6000 каменных орудий, относящихся к среднему и нижнему палеолиту, хотя сегодня аутентичность большей части “галечных орудий” из самых нижних уровней вызывает сомнение. К сожалению, сами раскопки и метод регистрации были не систематизированы, что мешает достоверно идентифицировать каменные артефакты в их пространственном и – чаще – правильном стратиграфическом контексте.

Текущие мультидисциплинарные раскопки проводятся на ограниченной по площади, но ненарушенной осадочной секвенции на верхних слоях (подразделения *I–V*), которые сохранились в задней части пещеры. Методы раскопок и система регистрации соответствуют самым строгим современным требованиям. Обнаружено относительно небольшое количество каменных орудий, но они расположены в правильной пространственной, стратиграфической и хронологической последовательности.

К настоящему времени найдено 387 каменных орудий: 68 из *V* подразделения, 4 из *III* и 315 из *II*. Их малое количество, несомненно, обусловлено ограниченной площадью отложений *in situ*, остающихся в *Азох 1*. Тем не менее, разница в количестве находок между подразделениями *V* и *II* отмечена и в раскопках М.Гусейнова, во время которых больше артефактов было найдено в горизонтах над и под подразделением *V*, чем внутри нее.

Каменные орудия *V* подразделения изготовлены из нескольких видов исходного материала. На данный момент в регионе отсутствуют геологические карты местности, которые могли бы помочь определить источники многих видов сырья, хотя большинство из них, кроме обсидиана, возможно, имеет местное

L. Asryan (✉) · A. Ollé
Àrea de Prehistòria, Universitat Rovira i Virgili (URV),
Avinguda de Catalunya 35, 43002 Tarragona, Spain
e-mail: lenaprehistoria@gmail.com

A. Ollé
e-mail: aolle@iphes.cat

L. Asryan · A. Ollé
IPHES, Institut Català de Paleoecologia Humana i Evolució
Social, Zona Educacional 4, Campus Sescelades URV
(Edifici W3), 43007 Tarragona, Spain

L. Asryan
Artsakh State University, M. Gosh 5, Stepanakert,
Nagorno-Karabakh

N. Moloney
Museo Nacional de Ciencias Naturales (CSIC),
28006 Madrid, Spain
e-mail: moloneynorah@gmail.com

Yolanda Fernández-Jalvo et al. (eds.), *Azokh Cave and the Transcaucasian Corridor*,
Vertebrate Paleobiology and Paleoanthropology, DOI 10.1007/978-3-319-24924-7_4

происхождение. Детальное исследование фрагментов обсидиана поможет установлению мест залегания данной породы.

Коллекция каменных орудий из подразделения *V* включает отщепы, их фрагменты, ядрища, ретушированные пластины и манупорты. Очевидно использование техники одно- и двухсторонней редукции ядрища, но отсутствие кортекса и осколков позволяет предположить, что начальные стадии изготовления каменного орудия были за пределами пещеры. Ретушь, если она присутствует, является непрерывной и маргинальной вдоль одной или двух кромок и влияет на дорзальную поверхность. Интенсивная ретушь присутствует лишь на обсидиановых орудиях. Типологически многие артефакты являются скребками. Никаких двусторонних, галечных или с техникой леваллуа орудий не обнаружено.

Каменные орудия из подразделения *II* изготовлены из местного сырья, с включением нескольких орудий и обломков обсидиана. Коллекция включает отщепы и фрагменты, несколько лезвий, наконечников и ядрищ, являющихся результатом использования прямого удара твердым молотком преимущественно некортикального происхождения. Использование стратегии одно-, двусторонней и радиальной редукции ядра также очевидно, и изготовление искусно ограненных оснований было обычной практикой. Ранние стадии последовательности операций при изготовлении каменного орудия незаметны. Ретушь обычно представлена короткими участками на кромках, но на обсидиановых орудиях данная техника использована на значительно большей поверхности. Типологически наиболее широко представлены боковые скребки, хотя обнаруживаются и некоторые типично среднепалеолитические варианты.

Хорошо представлены орудия типа леваллуа. Для производства широких отщепов, лезвий и наконечников использованы линейная (наиболее часто встречающаяся), одно- и двунаправленная рекуррентные техники. Орудия леваллуа крупнее по размерам и тяжелее, чем другие, что указывает на отбор более крупных ядрищ для производства с использованием данной технологии. Многие заготовки с техникой леваллуа в последующем подверглись ретуши.

С учетом описанных ранее особенностей находок из подразделений *II* и *III* (Lioubine, 2002), обнаруженные в Азохской пещере среднепалеолитические каменные орудия характеризуются в рамках традиций, свойственных наиболее южным областям Кавказа и, возможно, связанных с неандертальцами. Относительно небольшое количество артефактов, обнаруженных в подразделении *II*, наряду с немногочисленными свидетельствами их изготовления на месте, свидетельствует об определенной стратегии производства орудий и кратковременном пребывании гоминид в данном регионе в эпоху среднего палеолита.

Keywords Caucasus • Middle Paleolithic • Lithic technology • Operational chain • Raw material procurement • Post-depositional surface modifications

Introduction

Azokh 1 Cave in the Lesser Caucasus has provided evidence of repeated occupation by hominin groups during the Middle to early Late Pleistocene. Following its discovery by M. Huseinov in 1960, extensive excavations conducted for more than 20 years removed most of the cultural deposits, leaving a volume of about 970 m^3 of *in situ* sediment at the back of the cave out of an estimated original 3400 m^3 (Ljubin and Bosinski 1995; Lioubine 2002; Fernández-Jalvo et al. 2010). Early excavations revealed episodes of human presence spanning Pleistocene to recent times, including Acheulean and Middle Paleolithic lithics, faunal remains, and a mandible fragment described as pre-Neanderthal (Kasimova 2001; Lioubine 2002). According to Lioubine (2002), the first 15 years of excavation lacked an interdisciplinary approach, with excavation results poorly recorded and documented. As most of the deposits were removed during that period, much information on hominin occupation episodes has been lost. The first multidisciplinary program undertaken was conducted by Azerbaijani and Russian researchers between 1975 and 1980 focusing on stratigraphy and paleoclimate (Lioubine 2002).

In 2002 renewed exploration of archaeological and fossil materials was undertaken by a multidisciplinary team of international researchers (Fernández-Jalvo et al. 2004, 2010). Current excavations have focused primarily on the undisturbed sequence of deposits in the upper levels (Units I–V) at the back of Azokh 1 (Fig. 4.1). As we have not had personal access to materials recovered from previous excavations, we have had to rely on published sources for comparative analyses. Nevertheless, the systematic recovery and detailed recording of material and application of new methodologies of the current excavations provide invaluable information on site formation, and human behavior and evolution.

While the sediments of Unit I had been extensively disturbed by recent and ancient animal burrows, various indicators suggest that the underlying Units II to V are

undisturbed (Murray et al. 2016). The association of large bear bones with small sized animals (e.g., *Capra, Dama*), together with fragmented bones, coprolites and stone tools, all suggest absence of any preferential orientation or hydrodynamic sorting or size selection due to water or sediment flow processes. There is no visible alteration of sediment type or diagenetic alteration such as that affecting the top of Unit II, and the association of stone tools and cut-marked bones suggest the context of the deposits has not been disturbed (Marin-Monfort et al. 2016). The available dates through the sequence are also consistent (Appendix). Nevertheless, artifacts in the units may have suffered from some post-depositional alterations as will be discussed later.

Large faunal remains include cervids, bovids, horses, small canids, felids, suids, rhinos, hyaenas, wolves, and hippos (Van der Made et al. 2016). Bears (*Ursus spelaeus*) are present in all levels. Among the small fauna are rodents, lagomorphs, tortoises, birds (Parfitt 2016; Blain 2016) and bats (the cave system hosts numerous colonies of bats (Sevilla 2016).

Methods of Analysis

The materials recovered between 2002 and 2009 originate from the unexcavated sediments of Units Vm, IV, III and II (Fernández-Jalvo et al. 2016) at the rear of the chamber through a combination of open-area excavation, test trenches and a rescue excavation. Excavation methods include three-dimensional recording; dry and wet sieving of all sediments to recover microfauna, lithic debitage and botanical remains; and sampling of soil, pollen, phytoliths, starch and charcoal for analyses.

Open area excavation was undertaken in Unit V between 2002 and 2009. Initial test trench exploration of Units III and II in 2003 revealed deep ash lenses interspersed with charcoal, faunal and lithic remains. Between 2006 and 2011, open area excavation of Unit II uncovered an area of about 40 m^2 remaining from previous excavations.

The morphotechnical and typological study of the lithics was undertaken using a combination of the *Logical Analytical System* (Carbonell et al. 1992; Carbonell and Rodríguez 1994; Rodríguez 2004), Anglo-Saxon, and French approaches (Bordes 1961; Laplace 1972; Clark 2001).

To gain an understanding of site formation processes affecting Azokh 1, a database of characteristics of post-depositional alterations was developed based on the work of a number of researchers (McBrearty et al. 1998; Karkanes et al. 2000; Burroni et al. 2002; Bordes 2002; Shahack-Gross et al. 2004; Thiébaut 2007). Attributes considered included: presence/absence of patina, concretion, manganese, edge rounding, edge damage, surface polish, striations, pits, mechanical cracks, fractures and chemical weathering (the latter due primarily to bat guano) (Asryan 2010). This chapter is based on results from the Master's Thesis of one of us (LA). Updated data from lithic assemblages of Azokh 1 recovered after 2009 excavation season are described in Asryan (2015).

Results

The lithic assemblages include 387 artifacts recovered from the 2002–2009 excavation seasons: 68 from Unit Vm, 4 from Unit III, and 315 from Unit II. Safety problems have hampered a proper excavation of Unit IV, but some indications of the presence of large mammals and lithic artifacts have been observed that require further study and extended excavation (see Fernández-Jalvo et al. 2016). No lithic artifacts were found in Unit Vu. The relatively low numbers of artifacts recovered from the three units is no doubt due to the restricted area of *in situ* deposits remaining in Azokh 1, and its location at the back of the cave (Fig. 4.1). Following a discussion of raw material procurement and exploitation, the lithic assemblages from each unit are discussed separately.

Raw Material Procurement and Exploitation

The type of stone on which tools are made can provide revealing insights into hominin behavior. It is strongly linked with aspects of procurement, manufacture, use, curation and discard of material. Choice may depend on a range of variables, among them: availability of stone sources, fracture mechanics of particular types of stone, quality of the edge produced, or the suitability of the resulting tool for particular functions. Determination of such choices is one of the first steps in attempting to understand initial stages of the sequence of stone procurement, production, use and discard events that form the operational chains evident in assemblages.

The lihics recovered from all units in Azokh 1 are primarily on chert. Basalts and obsidian are also present in Units Vm and II, as are, to a much lesser degree, quartzite, agate, and limestone. There are a few examples of hornfels in Unit Vm, an obsidian piece in Unit III, and sandstone and jasper in Unit II (Table 4.1). There are no regional geological maps that we can access to help determine original

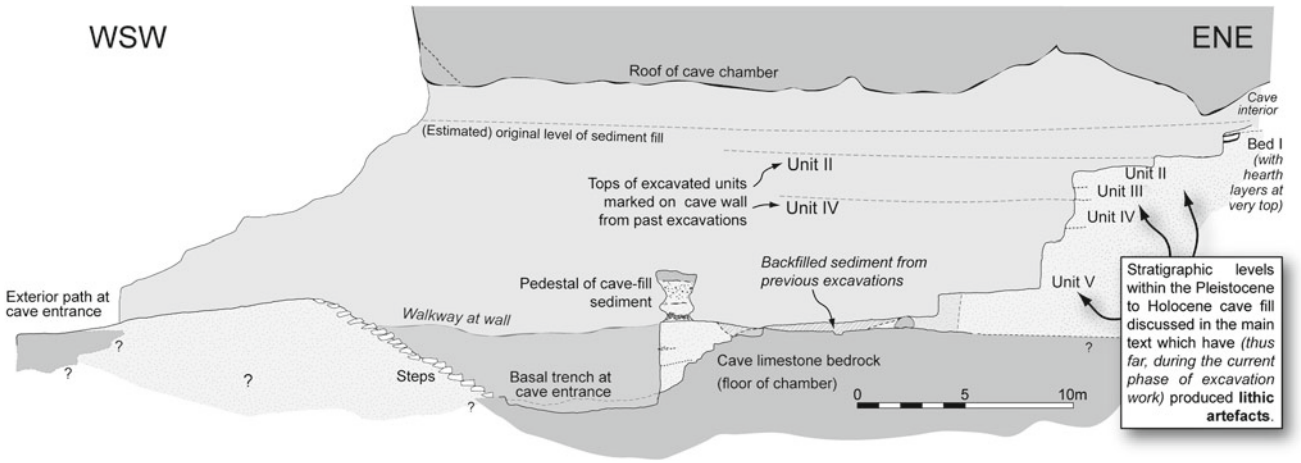

Fig. 4.1 Cross section through Azokh 1 chamber (facing NW). Adapted from Murray et al. 2010 (used and modified with permission of J. Murray and the *Irish Journal of Earth Sciences*)

Table 4.1 Raw materials present in Units Vm, III and II (percentages not given for Unit III due to the small number of pieces recovered)

Raw material	Unit V No. present	Unit V % of total	Unit III No. present	Unit II No. present	Unit II % of total
Chert	40	58.8	3	190	60.3
Flint	6	8.8	–	65	20.6
Basalt	15	22.1	–	36	11.4
Obsidian	3	4.4	1	9	2.9
Limestone	1	1.5	–	5	1.6
Jasper	–	–	–	3	1
Sandstone	–	–	–	2	0.6
Tuff	–	–	–	2	0.6
Quartzite	1	1.5	–	2	0.6
Agate	1	1.5	–	1	0.3
Hornfels	1	1.5	–	–	–
Total	68	100	4	315	100

Fig. 4.2 Sites mentioned in the text and obsidian sources in Armenia

sources of most raw materials found at Azokh 1. However, it is possible that much of the stone comes from reasonably local sources within a 5 km radius of the cave. The host bedrock of the region is Mesozoic limestone with chert deposits present at several levels within the limestone and within the cave system (Murray et al. 2010). Basalt outcrops occur in Azokh village and within 10 km of the village and thus, are of local as well as regional (within a 5–20 km radius of the site) occurrence. Our observations in Ishkhanaget River (5 km from the cave) revealed fragments and also some pebbles of siliceous rocks, quartzite, basalts, sandstones and limestones in the river valley.

At present, the only known obsidian sources in Nagorno Karabakh are Mt. Kelbadjar and Ketchaldag/Merkasar in the Shahumyan region (Blackman et al. 1998) about 150–180 km from Azokh (Fig. 4.2). Numerous obsidian sources are known in Armenia, many of which were exploited during the Pleistocene, but characterization studies of the Azokh 1 obsidian remain to be undertaken. The closest, and possibly most likely source of obsidian is on the high plateau of the Zangezur mountain range in southeast Armenia which is more than 80 km from Azokh (Liagre et al. 2006; Cherry et al. 2008).

Unit Vm: Lithic Assemblage

The Unit Vm lithic assemblage is small, consisting of 68 pieces, made on a range of raw materials but primarily on chert and basalt. The assemblage consists predominantly of flake fragments, that is flakes without a striking platform but on which it is possible to distinguish dorsal and ventral surfaces (n = 27). There are some broken flakes that have a striking platform or butt but have lost part of their distal or lateral edges (n = 8). There are also unretouched flakes

Table 4.2 Units Vm and II: composition of the lithic assemblages

Category	Unit V assemblage		Unit II assemblage	
	No. present	%	No. present	%
Manuport	–	–	3	0.9
Core	3	4.4	8	2.5
Unretouched flake	11	16.2	51	16.2
Retouched flake	7	10.3	11	3.5
Broken flake (with platform and bulb)	8	11.8	57	18.1
Flake fragment (having distal or lateral segments but no platform or bulb)	27	39.7	126	40
Fragment	12	17.6	59	18.7
Total	68	100	315	100

(complete flakes, n = 11), and retouched flakes (flakes that have been modified, n = 7), three cores (nodules exploited to obtain products, whether for direct use i.e. flakes, or for subsequent configuration or exploitation, i.e. retouched flakes and flake-cores). Finally, there are non-diagnostic fragments consisting of angular waste, chunks and pieces without clear ventral and dorsal surfaces or that cannot be clearly identified technologically or typologically (n = 12). No knapping debitage less than 2 cm in size or with clear signs of percussion has been recovered from Unit Vm (Table 4.2).

Cores form 4.4% of the total assemblage from Unit Vm. They show no systematic approach in their exploitation for the production of flakes, nor any evidence for the use of centripetal or prepared core/Levallois technology. The simple technology of core production is also evident in the flake industry (including retouched and unretouched pieces which form 26.5% of the assemblage), as there is no evidence of striking platform preparation, no facial hierarchy, and often, but not always, no patterning of removals. Flakes are predominantly non-cortical (71.2%), and comprise a range of morphologies and dimensions (Table 4.3 and Fig. 4.3). Dorsal surfaces generally indicate at least two previous

Table 4.3 Units Vm and II: maximum, minimum and average dimensions of cores and whole flakes

Dimensions	Unit V		Unit II	
	Cores	Whole flakes	Cores	Whole flakes
Length (mm)				
Max	75	102	65	90
Min	48	31	44	18
Average	62	52.87	50.25	49.71
Width (mm)				
Max	65	85	56	63
Min	30	12	33	9
Average	50	39.5	45.5	32.08
Thickness (mm)				
Max	45	28	30	24
Min	21	4	13	1
Average	31	13	22.37	7.81

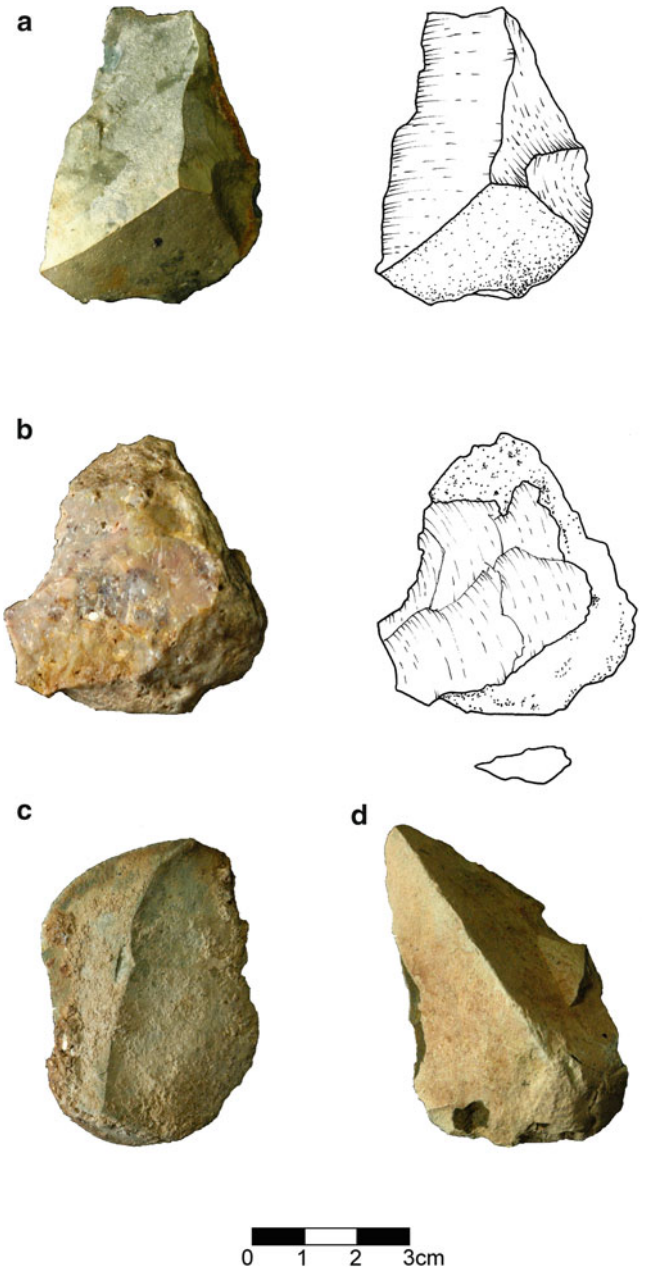

Fig. 4.3 Unit Vm unretouched flakes: **a** (Az1'03 un V, D42 – 14), **c** (Az1'03 un V, G42 – 2) and **d** (Az1'09 un V, H41 – 27) on basalt, and **b** (Az1'03 un V, F41 – 11) on chert (illustrations by J. Vilalta)

removals which tend to be unidirectional, although bi-directional and multi-directional removals are evident on some pieces. Seven pieces (10.3% – 4 chert, one each of obsidian, hornfels and basalt) have been modified by retouch that is primarily partial and marginal along one edge, affecting the dorsal surface at a simple or semi-abrupt angle (Table 4.2 and Fig. 4.4). One notable exception is an intensively retouched obsidian piece. Retouched artifacts are generally on medium-sized blanks (46–75 mm long) and typologically most are side scrapers. The general lack of

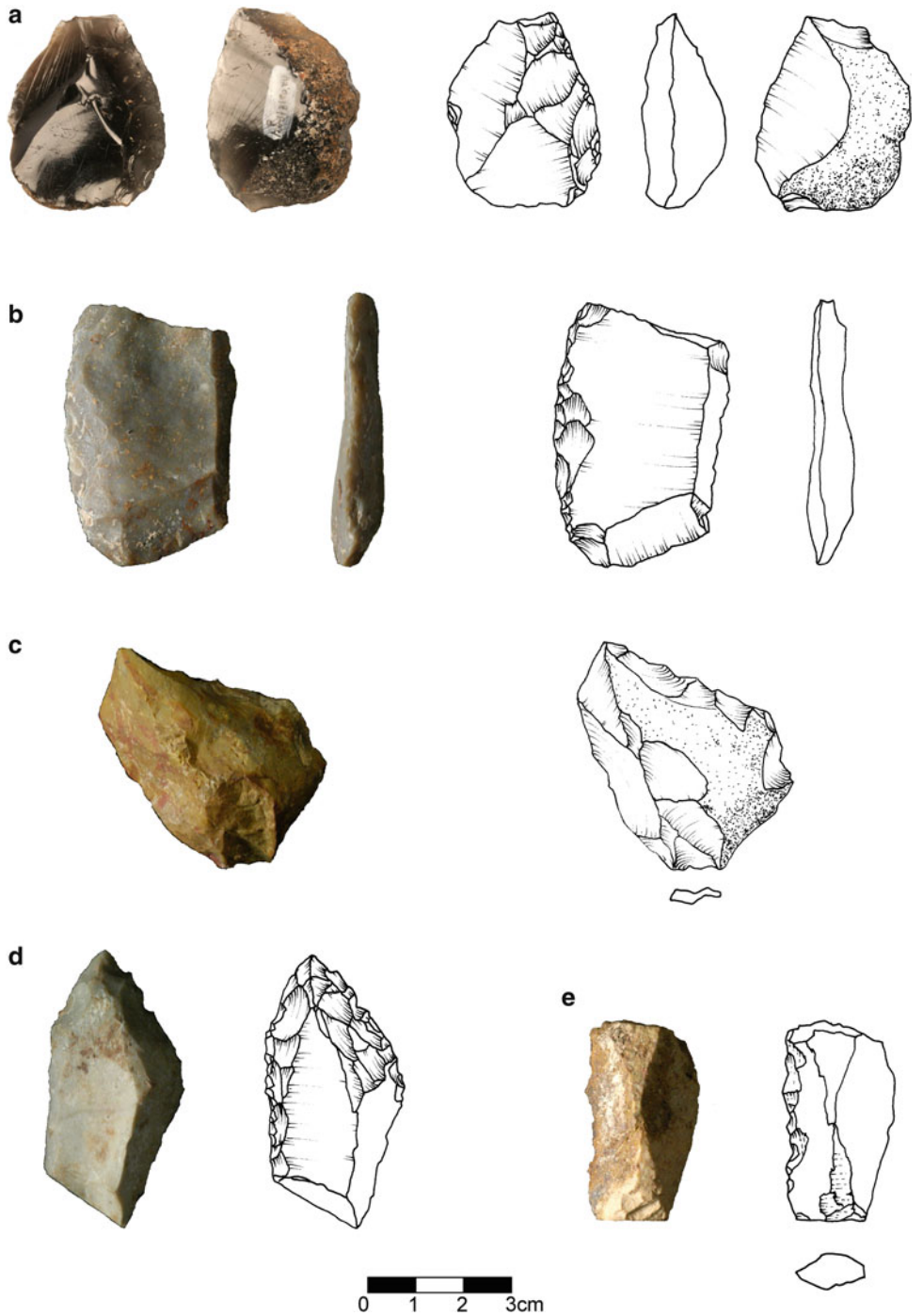

Fig. 4.4 Unit Vm retouched flakes: **a** (Az1'03 un V, F42 – 3) side-scraper on obsidian, **b** (Az1'09 un V, E40 – 2), **c** (Az1'09 un V, H41 – 10) side-scraper on flint, **d** (Az1'09 un V, I42 – 42) point on chert and **e** (Az1'09 un V, I42 – 43) side-scraper on chert (illustrations by J. Vilalta)

cortex on retouched and unretouched flakes combined with a lack of debris suggests that initial stages of the operational chain did not occur at this location. The refitting of three flakes forming a single blank could be interpreted as a result *in situ* knapping, but it could also be the result of post − depositional processes. At the moment these hypothesis can neither be confirmed nor refuted.

Unit III: Lithic Assemblage

Three flake fragments (two chert and one obsidian) with dorsal scars indicating prior working of the stone) were recovered from Unit III. Retouch, present only on the ventral surface of one chert piece, is continuous and profound. Likewise, there is one example of a striking platform (on the

obsidian flake) which is unifaceted (having a single knapping plane). Two pieces show post-depositional alteration.

Unit II: Lithic Assemblage

The Unit II industry consists of 315 pieces recovered from an area of 40 m^2. Siliceous materials (chert and flint) dominate the range of raw materials present (Table 4.1). The assemblage is characterized by a high number of flake fragments (n = 126), and it also includes broken flakes (n = 57), unretouched (n = 51) and retouched flakes (n = 11), cores (n = 8), some knapping debris (n = 4), and non-diagnostic fragments (n = 55) (Table 4.2). Levallois technology is well represented, forming 27.6% of the assemblage (Table 4.4). The percentage of retouched pieces and cores is low (3.5% and 2.5% respectively).

The eight cores listed above include five on siliceous materials and three on basalt. Most are fully exploited (i.e. exhausted) with mean dimensions of 51 × 50 × 19 mm. (Table 4.3). They are primarily bifacial and show clear facial hierarchy. Five cores are Levallois (two of which are on basalt), with evidence for opposed bipolar and centripetal working; two have preferential removals. The three non-Levallois cores have unipolar removals (i.e. struck from one direction) (Fig. 4.5).

Flakes are mainly small (26–45 mm) to medium (46–75 mm) in size (Table 4.3) and dominated by trapezoidal and triangular forms. A range of morphologies is represented (Fig. 4.6), with many (75.4%) having multifaceted (i.e. with two or more knapping planes) and bifaceted platforms, with two convergent knapping planes. Levallois and retouched flakes, which form 32.9% and 3.4% of the flakes respectively, were made on good quality raw material, primarily siliceous including obsidian, but some are on basalt (Fig. 4.7). Levallois flake techniques include radial, bidirectional and at times unidirectional removals. Retouch tends to be direct, marginal and continuous along one edge at an angle of between 35º and 75º. However, two obsidian pieces show intensive, stepped retouch on the dorsal face. Typologically, retouched pieces are simple side scrapers, but also include two end scrapers on flakes. A substantial number of flakes (69.3%) show pseudo retouch and edge damage caused, we believe, by post-depositional processes discussed below. Given the small extent of cortex on flake surfaces combined with the limited presence of knapping debris, we suggest that initial stages of the operational chain did not occur at this location of the cave.

Table 4.4 Unit II: Levallois component

Category	No. present	% whole assemblage	% Levallois component
Levallois core	5	1.6	5.7
Levallois flake (whole and broken flakes and flake frags.)	75	23.8	86.2
Retouched Levallois flakes	7	2.2	8.1
Total Levallois	87	27.6	

Post-Depositional Evidence

Post-depositional processes have affected a substantial number of pieces in Units II and Vm. While edge rounding, edge damage, fractures and high levels of patina (especially on basalt) are the most characteristic features, pits, mechanical cracks and thermal alteration are indicated too (Fig. 4.8).

Some post-depositional alterations may be related to trampling, especially in Unit II, and as some erosive processes were evident at the contact surface between Unit I (Holocene) and Unit II, we cannot reject the potential effects of erosive or sediment movement processes (Fernández Jalvo et al. 2004, 2010). However, we believe that erosion is not the primary cause of post-depositional damage; chemical weathering by bat guano is well attested, especially in Unit II, where most often it tends to affect limestone and some volcanic materials such as basalt and tuff, as well as fossils (Marin-Monfort et al. 2016; Smith et al. 2016).

Discussion of the Lithic Assemblages

As indicated at the beginning of this paper, most of the sediments from Azokh 1 Cave were removed during excavations of the 1960s–1980s. As a result, the remaining *in situ* deposits lie at the rear of the cave, some 40 m from its entrance (Fig. 4.1). It is reasonable to suppose that as the front of the cave would have been much better lit than the back, it would have been a more desirable area for hominin occupation, a factor that may account for the limited lithic evidence of occupation revealed by recent excavations.

By 2009, Unit III had only been subjected to test trench excavation as the extended areas below Unit II had not been reached. Excavations conducted in 2010 and 2011 reached the top of Unit IV. Analysis of lithic artifacts recovered from both units in 2010 and 2011 is currently ongoing. Units II and V underwent open area excavations, so that the higher number of lithics from the former is probably a valid result.

It is important to emphasize the substantial chronological time period that separates these three units and the different

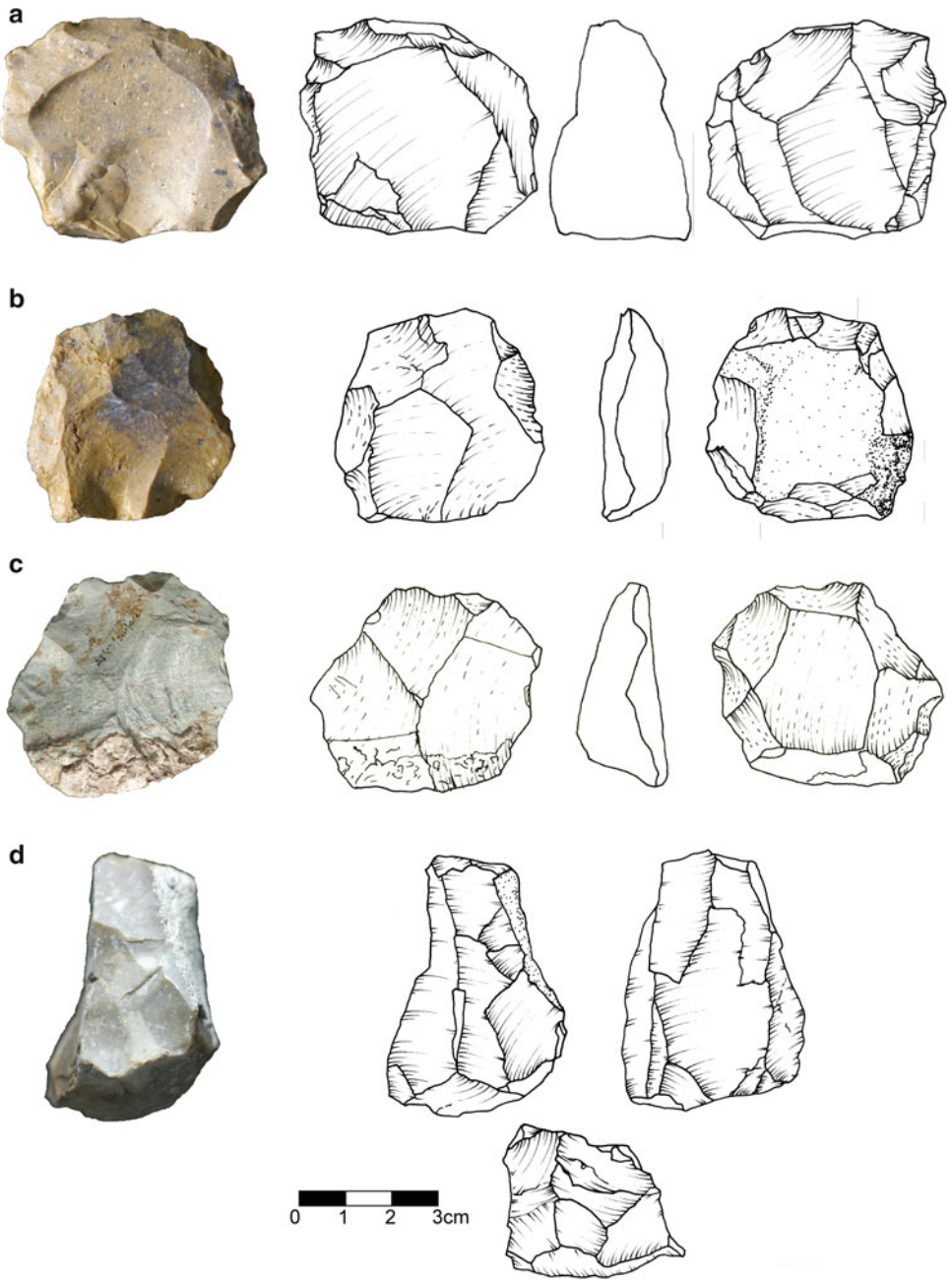

Fig. 4.5 Unit II cores: **a** (Az1'05 un II, G47 – 3) and **b** (Az1'06 un II, F48 – 139) Levallois cores on flint, **c** (Az1'03 un II, D46 – 15) Levallois core on basalt, and **d** (Az1'05 un II, E48 – 4) non-Levallois core on chert (illustrations by J. Vilalta)

Middle Pleistocene hominin species involved. The hominin species is *Homo heidelbergensis* in Unit Vm and *Homo neanderthalensis* in Unit II (King et al. 2016), having different technological and cultural traditions. Given the greater numbers of artifacts in Unit II, we are better able to consider behavioral patterns for the hominins of this unit, although there are some aspects of behavior that the evidence in Unit Vm, and arguably in Unit III, may suggest.

In all units we see a similar range of raw materials (although limited in Unit III) exploited for tool production. These are chert originating from the immediate cave vicinity, siliceous materials most likely from river gravels that today are about 2 km from the site, and basalt that may originate from the river and nearby outcrops. Raw material retrieval strategies, therefore, are predominantly local, that is less than 5 km from the site. The presence of obsidian is the only evidence of material originating from distant sources more than 80 km away from the cave, perhaps at Mt. Kelbadjar and Kechaldagh/Merkasar in Nagorno-Karabakh and near Syunik in the Zangezur mountain range (Fig. 4.2). Although the

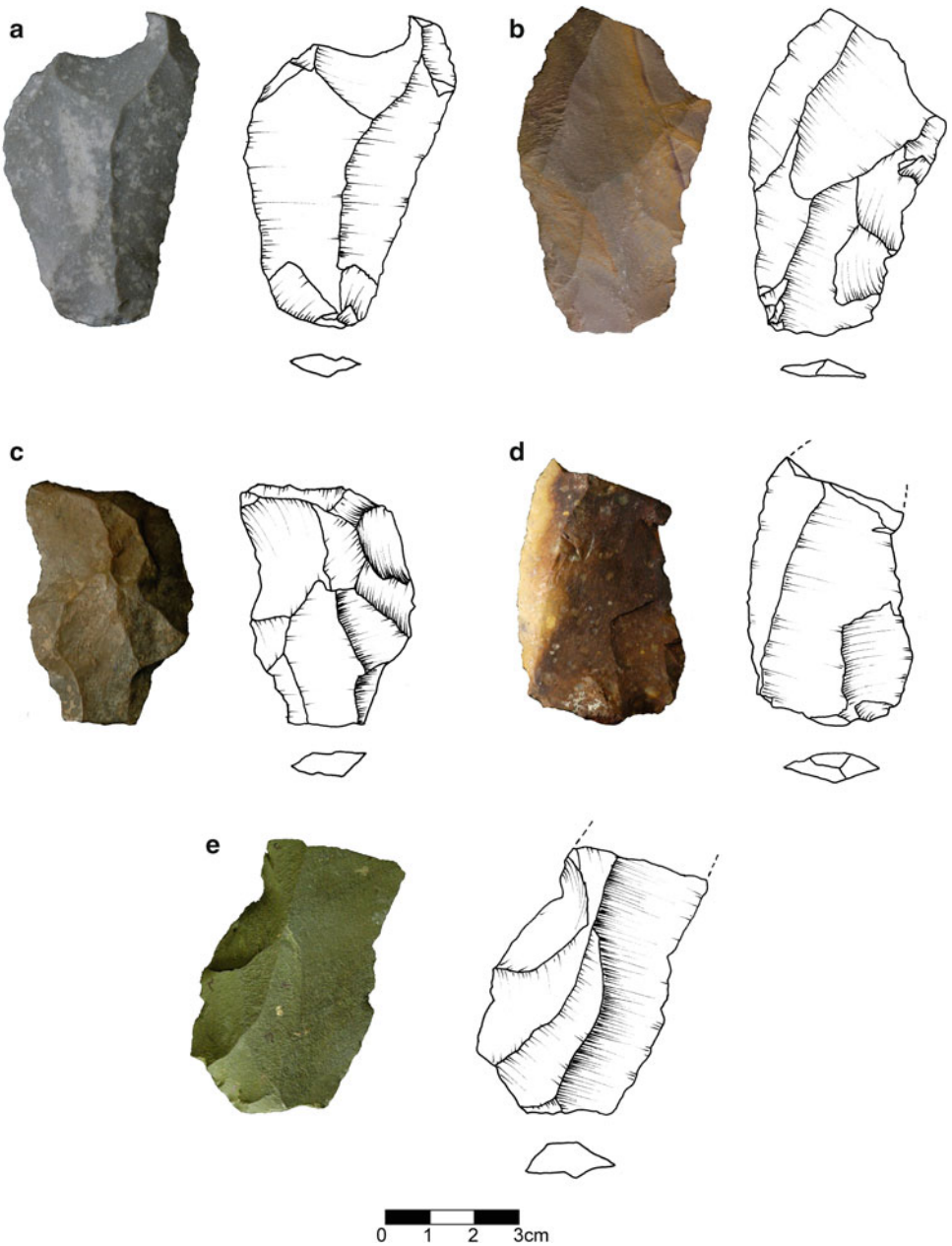

Fig. 4.6 Unit II unretouched flakes: **a** (Az1'08 un II, C50 – 9), **c** (Az1'08 un II, H50 – 2) and **d** (Az1'06 un II, G47 – 15) Levallois flakes on flint, **b** (Az1'05 un II, E48 – 17) Levallois flake on jasper, and **d** (Az1'08 un II, C46 – 41) Levallois flake on basalt (illustrations by J. Vilalta)

Zangezur mountains may be the closest source of the Azokh obsidian, their altitude at 2500 m would have restricted access to the time of year when the region was free of snow (Barge and Chataigner 2003). However, it is possible that fluvial action could have transported some obsidian to lower altitudes where it could have been available year round. While obsidian might have come from more distant sources, the distance between Syunik and Azokh is compatible with raw material procurement and network territories suggested for Neanderthals (Geneste 1991; Gamble 1999).

The proposal for small Neanderthal territories finds support in the Middle Paleolithic levels of Ortvale Klde in western Georgia (Adler et al. 2008). Here, hominins exploited local raw materials for most of their tools, while the few obsidian pieces from a source 100 km away formed less than 1% of the lithic assemblage. Similarly, a recent review of the Djruchula lithic assemblages (Meignen and Tushabramishvili 2006) indicated predominant exploitation of local raw material and minimal use of obsidian, the source of which is found at a distance of 100 km. We hope that

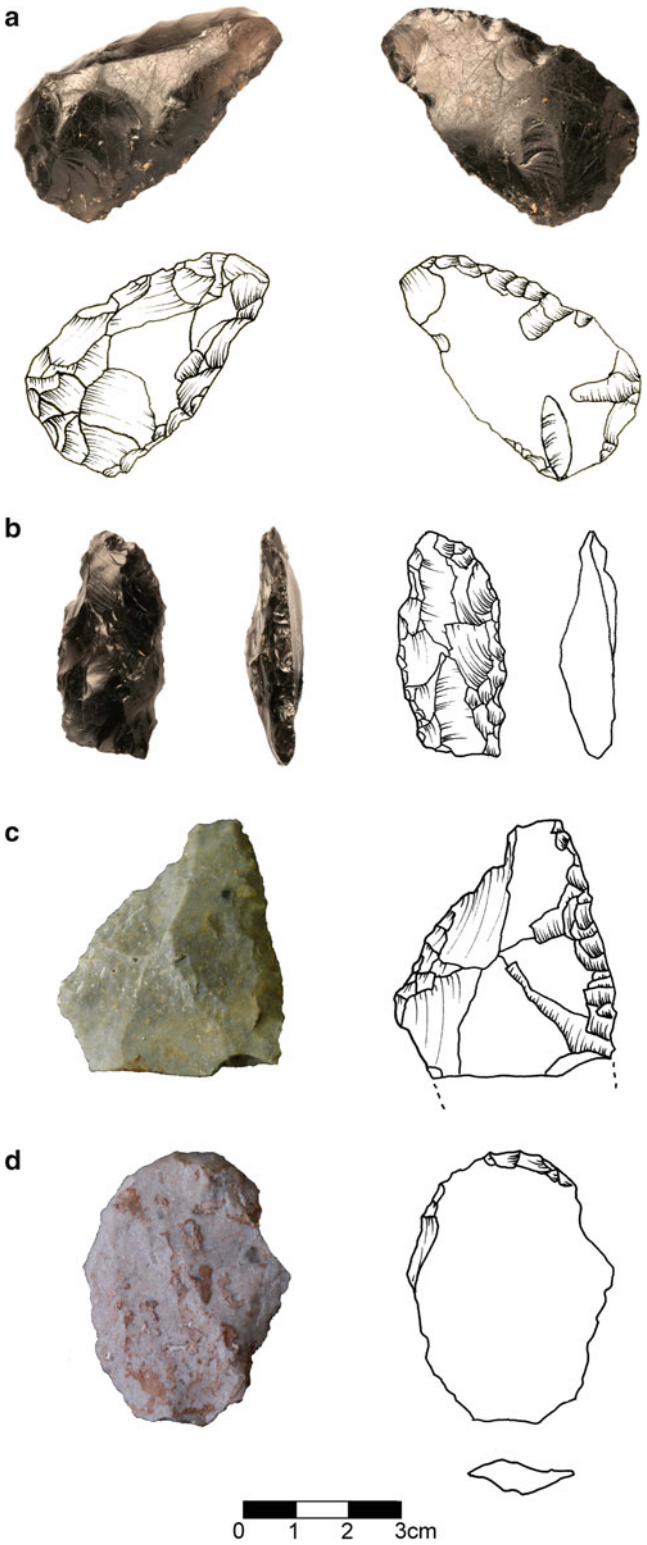

Fig. 4.7 Unit II retouched flakes: **a** (Az1'08 un II, D46 – 27) and **b** (Az1'03 un II, D46 – 141) obsidian side-scrapers, **c** (Az1'09 un II, E47 – 14) flint side-scraper, and **d** (Az1'07 un II, D51 – 49) chert end-scraper (illustrations by J. Vilalta)

future characterization analysis of the Azokh obsidian will identify its sources.

There is no evidence for the complete operational chain in any unit, and only limited indications of potential *in situ* knapping as suggested in Unit Vm where, despite the absence of knapping debris, a refit of three pieces, the largest of which is cortical, may suggest some knapping activity in the area. The presence of some debris in Unit II may indicate possible *in situ* activity. Nevertheless, the general non-cortical nature of the assemblages, the relatively high number of scars on flake surfaces in the Unit II assemblage (6% of the flake component have more than 3 prior scar removals), the predominance of small- to medium-sized flakes, and highly reduced nature of cores, all suggest that, for the most part, initial stages of reduction occurred elsewhere, and cores, blanks and tools were taken into the cave, particularly in the case of Unit II. However, given the restricted area of current excavations, we cannot discard the possibility of knapping activities having occurred in other areas inside the cave that can no longer be identified.

Retouched tools are not common in any unit. However, it is interesting to note that a few obsidian pieces from Unit II have been intensively retouched, which tentatively suggests curation of stone originating from distant sources. We have noted a difference between Unit II and Unit Vm in the presence of pseudo retouch, i.e. edge damage through use or post-depositional processes, which is much more common in Unit II. We are uncertain of why this should be so, but it may relate to greater cave bear activity in Unit II where the number of bear bones indicates denning episodes. Indeed, as with Azokh, most cave sites in the Caucasus, which have cave bear remains and which also have evidence of hominin occupation during both the Middle and Upper Pleistocene, were bear dens e.g., Matuzka Cave (Golovanova 1990), Treugol'naya Cave (Doronichev 2000), Kudaro Caves (Lioubine 2002), Tsona Cave (Tushabramishvili et al. 2007), Hovk 1 Cave (see Pinhasi et al. 2008, 2011; Bar-Oz et al. 2012), Bronze Cave (Díez Martín et al. 2009), Sakažhia (Rivals and Arellano 2010).

The presence of Levallois in Unit II clearly indicates Mode 3 technology. At present, however, it is not possible to describe a specific technological mode for Units III and Vm. The small assemblage studied in Vm is flake-based with no indication of Levallois technology, but there is also no indication of large bifacial working that might suggest Mode 2/Acheulean technology. Given the chronological difference between Units Vm and II (see Appendix ESR), it might be tempting to assign the material from Unit Vm to the late Acheulean, based on the older date of the Unit of ~300 ka, or alternatively to the early Middle Paleolithic, based on the

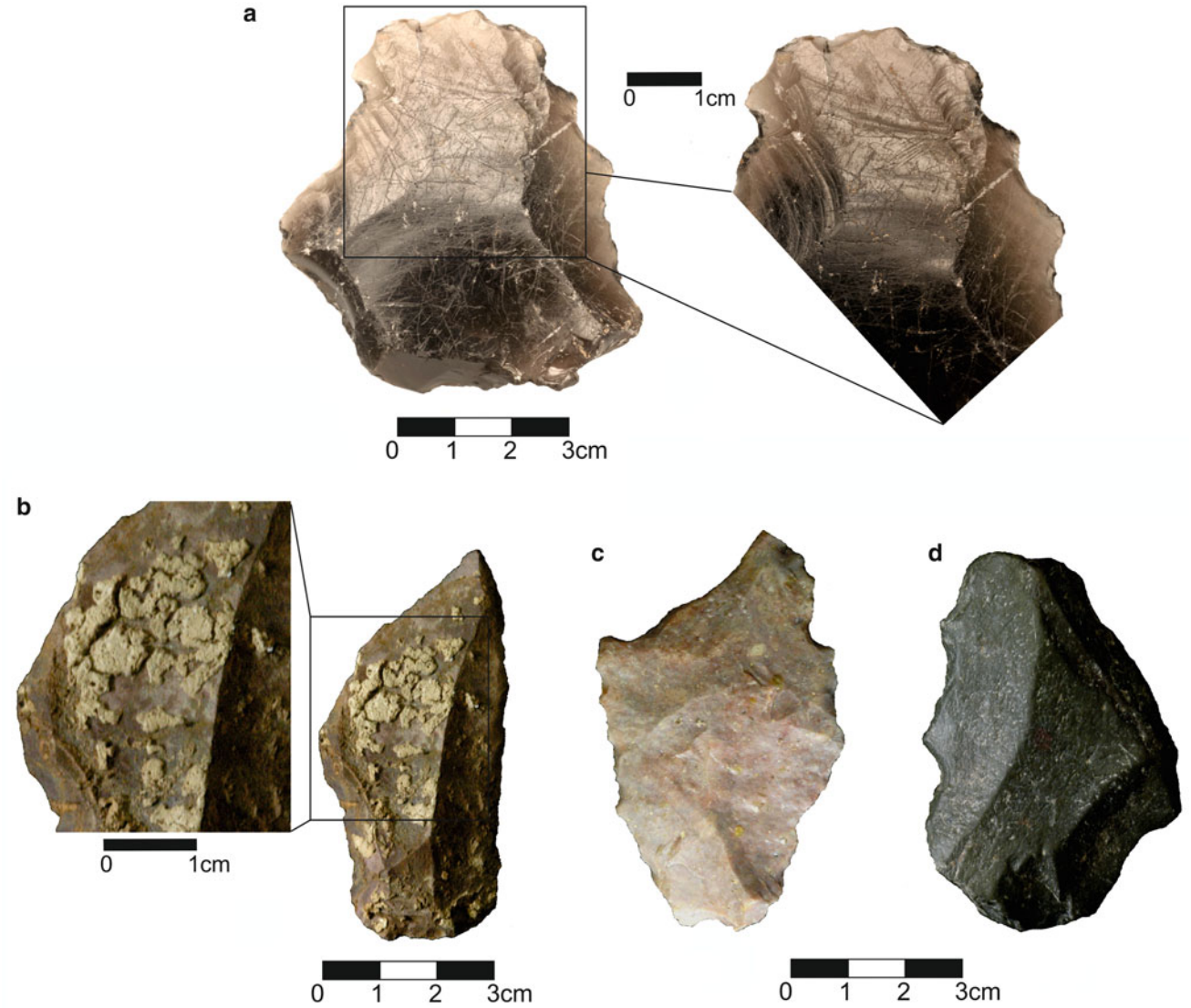

Fig. 4.8 Units Vm and II post-depositional alterations: **a** (Az1'08 un II, I49 – 3) striations and edge damage on an obsidian piece, **b** (Az1'05 un II, E48 – 2) evidence of chemical weathering, and **c** (Az1'08 un II, C50 – 7) & **d** (Az1'03 un II, D46 – 12) ridge and edge rounding and edge damage on flint and basalt flakes

younger date of ~260 ka, but at present we have no secure basis to support either hypothesis. However, chronology alone does not indicate technological mode.

Use of stone tools for butchery purposes is indicated by animal bones bearing stone tool cut marks that have been found in all units of the Upper Sequence (Units V–I). In Units II, III and Vm they form 6.38%, 11.9% and 3.78% of the faunal assemblage respectively (Marin-Monfort et al. 2016), and cut marks are associated generally with activities relating to meat and marrow removal, primarily from large- and small-sized large mammals, including the cave bear *Ursus spelaeus*. Further food-related activities might be suggested by the spatial association of lithics and bones. However, given the quantity of bear bones recovered from Unit II, we must take into consideration the effect of probable post-depositional movement of materials, including lithics, caused by bear behavior in preparation for hibernation (Stiner et al. 1996). None of the tools show signs of hafting to use as spears similar to that seen in other Middle Paleolithic sites, for example at Starosele in the Ukraine (Hardy et al. 2001) or Umm el Tlel in Syria (Boëda et al. 2008). Therefore we cannot, as yet, propose methods of meat acquisition. However, the number of bear bones with cut marks indicating hominin activity suggests exploitation of hibernating bears, or bear carcasses encountered in the cave. Use wear studies of Unit II lithics are currently in progress,

and they may indicate other materials on which tools were used, how they were used e.g., cutting, slicing, pounding actions, and direction of use, thus increasing our understanding of hominin activities in the cave.

At present, the small number of stone tools, the predominant exploitation of local raw material sources, lack of evidence for extensive knapping episodes, and limited evidence of intensive retouching of pieces, suggest expedient strategies of tool production relating to short term, sporadic occupations of the cave. The potential exploitation of meat from hibernating bear carcasses may also support such an interpretation. Notwithstanding, we must keep in mind the location and small area of our excavations which may bias interpretation. A number of sites with small lithic assemblages in the Caucasus have been interpreted as short stay occupations in which lithics were introduced into the site in their final form. It is evident at these sites that earlier stages of the operational chain are missing and must have occurred elsewhere as is indicated at Matuzka (Baryshnikov et al. 1996), Hovk 1 (Pinhasi et al. 2008) and Double Cave (Díez Martín et al. 2009). In such a context, the most recent assemblages from Azokh Units Vm and II are not unusual in their limited evidence for *in situ* knapping activities.

Comparison of Assemblages from the Earlier and Current Excavations

As we have not been able to study the lithic materials recovered from M. Huseinov's excavations, we have had to rely on information provided primarily by Huseinov (1985), Lioubine (2002), Golovanova and Doronichev (2003) and Doronichev (2008). These sources indicate an assemblage of 289 pieces recovered from the designated Layer V of the earlier excavations, considered by them to be Acheulean, and also a larger assemblage of 3039 pieces from Layer III, considered to be Middle Paleolithic. Although units Vm, III and II of the current excavations may not correspond entirely with layers determined in earlier excavations, the relative numbers of recently recovered lithics also indicate a Middle Paleolithic assemblage of 315 pieces from Unit II positioned stratigraphically above the 68 pieces from Unit Vm. While we are more confident in comparing the Middle Paleolithic assemblages, a comparison of the assemblages from the earlier level is rather more difficult, but it is useful, nevertheless, to attempt such an exercise.

Apart from numerical differences (far fewer pieces were recovered from Huseinov's Layer V and our Unit Vm than from the Middle Paleolithic layers), assemblage composition from both excavations is similar. The most notable difference lies in the presence of macro/heavy duty tools in Layer V of the earlier excavations, which include choppers, chopping tools, and a few Acheulean bifaces (Huseinov 1985; Lioubine 2002; Doronichev 2008), and their absence from the recently excavated Unit Vm. While debitage is well represented in the Middle Paleolithic layer of the earlier excavations, it is markedly limited in the current assemblage. The higher frequency of debitage waste and cores recovered from the earlier excavations may support the hypothesis that knapping occurred in other, possibly better lit areas of the cave. However, there is no spatial mapping of the previous excavations to confirm such an hypothesis. Three macro/heavy duty tools were recovered during the earlier investigations of the Middle Paleolithic layers but no similar pieces have been recovered in recent excavations. An interesting point to note is the important presence of denticulates and notches documented in the earlier excavations. As discussed above, current post-depositional studies have highlighted the problem of pieces which display pseudo retouch which potentially could have been considered typologically as denticulates or notches.

Azokh Lithic Assemblages in the Context of the Caucasus Region

While the geographic location of the Caucasus might be perceived as a barrier to hominin movement, the number of Paleolithic sites in the region contradicts such an assumption. Hominin presence in the Caucasus at 1.77 Ma is evidenced by the rich assemblage of physical and cultural remains found at Dmanisi, Georgia (Gabunia et al. 2000, 2001; Rightmire et al. 2006). Other Lower, Middle and Upper Paleolithic sites attest to hominin activity throughout the Middle Pleistocene. Nevertheless, differences in Middle Paleolithic assemblages between the northern and southern regions suggest that the Caucasus mountain chain hindered hominin movement between these two regions during the Middle Paleolithic (Meignen and Tushabramishvili 2006). Differences in Acheulean assemblages with and without bifaces may indicate different origins of the Acheulean complex (Doronichev 2008).

The size of lithic assemblages recovered from cave sites in the Caucasus is variable: large (>1000+ pieces) for example at Mesmaiskaya Cave (Golovanova et al. 1999), Ortvale Klde (Adler et al. 2006), Djruchula (Meignen and Tushabramishvili 2006); and small (<1000 pieces) such as seen at Matuzka (Golovanova 1990; Baryshnikov et al. 1996; Hoffecker and Cleghorn 2000), and Kudaro (Lioubine 2002), and Double Cave (Díez Martín et al. 2009). The small size of the recently excavated Azokh Unit Vm and Unit II lithic assemblages is not, then, unusual in the context of the Caucasus.

While we cannot confidently place Unit Vm in a particular cultural, techno-complex, we can consider the Unit Vm assemblage in light of others in the region which potentially are comparable chronologically. Doronichev (2008) suggests that the Acheulean in the southern Caucasus occurs only after 350 ka. Given the older date of ~300 ka for Azokh Unit Vm, we might review the assemblage to determine whether it includes elements comparable with Acheulean assemblages in the region. Doronichev (2008) proposes two variants of the Acheulan complex in the southern Caucasus on the basis of raw materials, technology and assemblage composition. One variant, which he terms "Kudarian", relates to those lithic assemblages that are generally on siliceous materials, are flake-based, include a good proportion of side scrapers among retouched tools, have few Acheulean bifaces, and lack Levallois technology. He suggests that examples of this "Kudarian" variant are found in Kudaro I, III (Doronichev 2008, Figs. 14–17) and Azykh (sic) Layer VI and V (lithics from the early excavations). The second Acheulean variant is characterized by the use of volcanic rocks, with numerous bifaces, a laminar element and Levallois technique.

Some elements of the Azokh Unit Vm assemblage discussed here, small though it is, may support its inclusion in Doronichev's Kudarian complex. This is based primarily on the use of siliceous rocks, on flake production, the predominance of side scrapers among the limited number of retouched tools, the lack of bifaces, the absence of Levallois technology, and its dating to ~300 ka.

In terms of Middle Paleolithic assemblages in the region (Fig. 4.2), the geographic tripartite division of the Caucasus, presented in the introduction is also reflected in techno-typological characteristics of lithic industries (Beliaeva and Lioubine 1998; Golovanova and Doronichev 2003). European Micoquian affinities are indicated in the bifacial technology and tool types evident in many assemblages in the northwest Caucasus in both open air and cave sites such as Mezmaiskaya and Il'skaya I and II (see also Golovanova et al. 1999, Fig. 3; Golovanova and Doronichev 2003, Figs. 8 and 9). The Kudaro-Djruchula tradition, in which some Middle Paleolithic assemblages of southern central Caucasus have been placed, is characterized by the presence of scrapers, denticulates, notches and Levallois products, while variation is evident in the extent of facetting and Levallois techniques. The medium and large Levallois flakes, blades and points that are present in many sites, for example Djruchula, Tsona and Kudaro caves, and possibly also Hovk 1, show affinities with those Levantine industries which have long triangular or sub-quadrangular blanks produced by Levallois technology (Meignen 1994, Figs. 2, 6, 7; Golovanova and Doronichev 2003, Figs. 23–25; Meignen and Tushabramishvili 2006, Figs. 3–6; Tushabramishvili et al. 2007, Figs. 5, 6; Pinhasi et al. 2008, Figs. 4, 5; Mercier et al. 2010; Pinhasi et al. 2011). Characteristics such as uni- and bi-directional Levallois technology, use of the truncated-faceted technique (ventral surface preparation prior to dorsal thinning, mainly of the proximal but also the lateral areas) and a high percentage of retouched pieces present in industries in the southernmost part of the Lesser Caucasus, link them to the Zagros Middle Paleolithic (Beliaeva and Lioubine 1998; Golovanova and Doronichev 2003). Similar characteristics are present in western Iranian sites such as Warwasi rockshelter (Dibble and Holdaway 1993, Figs. 2.3–2.6) and Bisitun (Dibble 1984, Figs. 3–5).

Evidence for raw material strategies indicates a general pattern in the Middle Paleolithic of the Caucasus for the predominant use of local sources, with rare exploitation of stone from distant sources. Many later (i.e. younger than 50 ka) Middle Paleolithic assemblages of the Lesser Caucasus share some or all of the following characteristics: presence of Levallois flakes, points and blades, use of facetting in platform preparation, use of the truncated-faceted technique as a thinning mechanism, and a high percentage of Levallois and Mousterian points. The obsidian assemblages of Yerevan 1 in Armenia are characterized by frequent use of the truncated-faceted technique, particularly on a range of points, and some use of Levallois. At the nearby site of Lusakert 1, Levallois production is prevalent in the obsidian assemblages from most levels, which also include some truncated-faceted pieces (Fourloubey et al. 2003, Figs. 3, 5–7; Golovanova and Doronichev 2003, Fig. 29). The industry from Taglar Cave in Nagorno-Karabakh has been likened to Yerevan 1 with the presence of truncated-faceted pieces and points, although the Taglar assemblage differs in its greater number of Levallois products (Golovanova and Doronichev 2003, Fig. 9). Liagre et al. (2006) note similarities between the small surface assemblage of Angeghakot 1, Armenia, and the later levels of Yerevan 1, particularly in the presence of points and use of the truncated-faceted technique (Liagre et al. 2006, Fig. 9). However, while there are similarities between many assemblages, variability is seen in the relative degree of presence of particular characteristics or tools, and in the presence of distinct technologies; for example a microlithic element that is evident at Lusakert 1 and Angeghkot 1.

The Unit II Middle Paleolithic assemblage from Azokh 1 shares similarities with many other sites of the region that have been included within the lithic traditions of the Zagros Middle Paleolithic. These include raw material strategies based on local sources, use of Levallois technology to produce large and small flakes, regular use of faceting in platform preparation, and a range of scrapers. It is evident that such characteristics are insufficient to confidently place the Azokh Unit II assemblage within the Zagros Middle Paleolithic tradition; in particular the truncated-faceted technique which is often an element of other assemblages is absent.

Furthermore, it should be stressed that the dates for Azokh Unit II indicate it to be between 50 and 100 ka older than sites attributed to the Zagros Middle Paleolithic, so that such comparisons are not particularly compelling.

Comparison with assemblages from the earlier Middle Paleolithic, such as the Djruchula assemblage, are worth considering. This is characterized by the production of long Levallois blanks, often retouched into points, and regular use of facetting. Typologically, apart from a few side scrapers, there are limited numbers of cores, debitage and other Middle Paleolithic tool types (Meignen and Tushabramishvili 2006; Mercier et al. 2010). It has been suggested that the small assemblage from the older (c. 104 ka) levels of Hovk 1 shares techno-typological similarities with the Kudaro-Djruchula group (Pinhasi et al. 2011).

While Levallois and facetting are well represented in the Unit II assemblage described here, there are few of the elongated products that are important in the Djruchula assemblage, and as such, the characteristics of the Azokh Unit II assemblage do not provide much support for affiliation with the Kudaro-Djruchula tradition. However, a preliminary review of materials from our later 2010 and 2011 excavations indicates a greater presence of elongated pieces that may give cause for a re-evaluation of the situation. If we take into consideration the Middle Paleolithic assemblage from Azokh 1 described briefly by Lioubine (2002, 38), we note that it includes a range of scrapers, elongated pieces, facetting and a few scrapers with thinning of their ventral surface (*amincis*). Such characteristics could support its inclusion in the Zagros tradition, or conversely in the Kudaro-Djruchula tradition. At present, we cannot confidently place the Unit II assemblage discussed here in a particular regional, cultural tradition.

Chronology

Formerly, much of the chronological framework for the Lower and Middle Paleolithic of the Caucasus relied heavily on techno-typological associations, a combination of OIS correlations and some chronometric dates. Recent work in the region has provided additional dating information, particularly with regard to the Middle Paleolithic (Adler et al. 2006; Liagre et al. 2006; Pinhasi et al. 2008; Fernández-Jalvo et al. 2010; Mercier et al. 2010; Le Bourdonnec et al. 2012). The published dates indicate three Middle Paleolithic phases for the region:

- sites that are dated between 250 and 128 kyr and corresponding to OIS 7-6 (Early Middle Paleolithic), e.g., Djruchula Cave (Layers 1 and 2), Kudaro (Layer 5), Tsona (Layers 1 and 2); Azokh 1 (Unit V);
- sites that are dated between 128 and 71 kyr and correspond to OIS 5 (Middle Middle Paleolithic) such as Hovq 1 (Unit 8), Azokh 1 (Unit II on the basis of the younger date of 100 ka), Il'skaya 1;
- and sites that are between 70 and 35 kyr corresponding to OIS 4 and partly also to OIS 3, among them Lusakert 1, Yerevan 1, Mezmaiskaya, Ortvale Klde.

The dates of 184–100 ka for Azokh 1 Unit II (Appendix ESR) potentially place hominin occupation in the Early Middle Paleolithic and as such it may be among the earliest evidence of a Middle Paleolithic presence in the area. Unit Vm with dates around 300 ka may indicate Late Acheulean occupation, or as with Unit II, Early Middle Paleolithic.

Conclusions

1. Between 2002 and 2009 renewed investigations of Units II, III and Vm at Azokh 1 cave were undertaken following rigorous systematic methods of excavation and recording that are the norm in present-day excavations. New dates suggest an age of 184–100 ka for Unit II and ~300 ka for Unit Vm. The excavations have produced fossil faunas with an important cave bear component, and three different lithic assemblages of 315 pieces from Unit II, four from Unit III, and 68 from Unit Vm.
2. Hominin raw material procurement strategies in Units Vm, III and II indicate exploitation of a range of local materials but with an emphasis on chert of local origin. Evidence for the use of non-local rock can be seen in the few obsidian pieces found in all levels. The closest known obsidian sources are 80–150 km away. This distance falls within the range of Neanderthal network territories suggested by Geneste (1991) and Gamble (1999).
3. Technological differences are noted between the lithic assemblages of Units Vm and II. The lithics in Unit V were manufactured using a simple flake technology in which there is no evidence for core preparation. The assemblage consists of retouched and unretouched flakes, flake fragments, a few cores and some undiagnostic elements. The stone artifacts from Unit II, with their Levallois component, indicate the use of prepared core technology and are unquestionably Middle Paleolithic. Both units have been affected by post-depositional processes and show an elevated presence of pseudo retouch, especially in Unit II. Of the few clearly retouched pieces in both units, most can be classed typologically as side scrapers.
4. The limited presence of cortex and the paucity of knapping debris suggests that the early stages of

knapping did not take place at our excavation area towards the back of the cave. Initial knapping activities may have occurred in other parts of the cave or in locations (unknown) outside the cave, with the products transported to the back of the cave. Given the greater area excavated between the 1960s and 1980s, it is possible that some knapping activities took place within the cave proper in areas that are now impossible to determine.

5. The current assemblages recovered from Units V and II, although fewer in number, are technologically similar to those from earlier excavations, but typologically the earlier assemblages are more diverse. However, current post-depositional studies indicate substantial presence of pseudo retouch, a factor that may also relate to the earlier assemblages.
6. The Unit II lithic assemblage may indicate Early Middle Paleolithic presence in the Southern Caucasus, and may form part of the earliest chronological group of the Middle Paleolithic of the Southern Caucasus. The material from Unit Vm may be late Acheulean on the basis of dating, lack of Levallois, the general larger size of the pieces (although no bifaces have been found), and its stratigraphic position below Units II, III, and IV. Alternatively, it could also represent an Early Middle Paleolithic occupation.
7. Azokh 1 is one of numerous cave sites in the Caucasus, often in karstic areas, that have evidence of hominin occupation during both the Middle and Upper Pleistocene. Many of these sites contain a range of fauna, among which cave bear is often common. Indeed, as with Azokh, most sites with bear remains were bear dens.
8. The small sizes of the recently excavated Azokh Unit Vm and Unit II lithic assemblages are not unusual in the context of the Caucasus. Nevertheless, the Middle Paleolithic assemblage from the earlier excavations indicates a larger assemblage, so that the present small assemblage may reflect the limited size and location of the recent excavations. However, the difference in artifact numbers between Units II and V is also seen in the materials from the earlier excavation and therefore may reflect real disparity in assemblage size or length of human occupation.
9. A number of sites in the Caucasus that have yielded small lithic assemblages, missing earlier stages of the operational chain, have been interpreted by other authors as short stay occupations. The limited evidence for *in situ* knapping activities in the most recent assemblages from Azokh Units Vm and II could also fit with short human occupations, at least at the rear of the cave.
10. The future of Paleolithic research in the Caucasus is encouraging. The rigorous methodology that is standard today, coupled with increasingly sophisticated techniques of excavation and analysis, serve to further knowledge of Early and Middle Paleolithic occupation of the region and contribute towards a greater understanding of hominin behavior during the Middle Pleistocene, both within and beyond the geographic boundaries of the Caucasus and adjacent areas.

Acknowledgements We thank our field assistants and the people of Azokh village who facilitated our excavation work and who welcomed us so warmly. We thank the institutions and people who have provided funding for the project: Museo Nacional de Ciencias Naturales (CSIC); Spanish Ministry of Science (BTE2000-1309, BTE2003-01552; BTE2007-66213); the Spanish MICINN project CGL2012-38434-C03-03 and the Catalan AGAUR project 2009SGR-188; AGBU (London Trust); and anonymous donors. L. Asryan is grateful to the grants received from Erasmus Mundus programme of European Commission and Wenner-Gren Foundation (WIF-212). Thanks to I. de la Torre, M. Wollstonecroft, three anonymous reviewers and editors for their comments. We are also grateful to S. Laidlaw and J. Vilalta for their unstinting assistance with illustrations.

References

Adler, D. S., Bar-Yosef, O., Belfer-Cohen, A., Tushabramishvili, N., Boaretto, E., Mercier, N., et al. (2008). Dating the demise: Neandertal extinction and the establishment of modern humans in the Southern Caucasus. *Journal of Human Evolution, 55*, 817–833.

Adler, D. S., Belfer-Cohen, A., & Bar-Yosef, O. (2006). Between a rock and a hard place: Neanderthal-modern human interactions in the Southern Caucasus. In N. J. Conard (Ed.), *When Neanderthals and modern humans met* (pp. 165–187). Tübingen: Kerns Verlag.

Appendix: Fernández-Jalvo, Y., Ditchfield, P., Grün, R., Lees, W., Aubert, M., Torres, T., et al. (2016). Dating methods applied to Azokh cave sites. In Y. Fernández-Jalvo, T. King, L. Yepiskoposyan & P. Andrews (Eds.), *Azokh Cave and the Transcaucasian Corridor* (pp. 321–339). Dordrecht: Springer.

Asryan, L. (2010). *A study of the stone tool assemblages of Azokh Cave site, Nagorno Karabakh (Lesser Caucasus).* MA thesis. Universitat Rovira i Virgili, Tarragona.

Asryan, L. (2015). *Azokh Cave lithic assemblages and their contextualization in the Middle and Upper Pleistocene of Southwest Asia*. PhD thesis. University Rovira i Virgili, Tarragona, 707 p.

Barge, O., & Chataigner, C. (2003). The procurement of obsidian: Factors influencing the choice of deposits. *Journal of Non-Crystalline Solids, 323*, 172–179.

Bar-Oz, G., Weissbrod, L., Gasparian, B. Nahapetyan, S., Wilkinson, K., & Pinhasi, R. (2012). Taphonomy and zooarchaeology of a high-altitude upper Pleistocene faunal sequence from Hovk-1 Cave, Armenia. *Journal of Archaeological Science, 39,* 2452–2463.

Baryshnikov, G., Hoffecker, J. F., & Burgess, R. L. (1996). Palaeontology and zooarchaeology of Mezmaiskaya Cave (Northwestern Caucasus, Russia). *Journal of Archaeological Science, 23*, 313–335.

Beliaeva, E. V., & Lioubine, V. P. (1998). The Caucasus-Levant-Zagros: Possible relations in the Middle Paleolithic. In M. Otte (Ed.), *Préhistoire d'Anatolie: Genèse de Deux Mondes* (pp. 39–55). Liège: ERAUL *85*.

Blackman, J., Badaljan, R., Kikodze, Z., & Kohl, Ph. (1998). Chemical characterization of Caucasian obsidian geological sources. In M.-C. Cauvin, A. Gourgaud, B. Gratuze, N. Arnaud, G. Poupeau, J.-L. Poidevin & C. Chataigner (Eds.), *L'obsidienne au Proche et Moyen Orient. Duvolcan à l'outil* (pp. 206–231). Oxford: BAR International Series *738*.

Blain, H-A. (2016). Amphibians and Squamate Reptiles from Azokh 1. In Y. Fernández-Jalvo, T. King, L. Yepiskoposyan & P. Andrews (Eds.), *Azokh Cave and the Transcaucasian Corridor* (pp. 191–210). Dordrecht: Springer.

Boëda, E., Bonilauri, S., Connan, J., Jarvie, D., Mercier, N., Tobey, M., et al. (2008). Middle Paleolithic bitumen use at Umm el Tlel around 70,000 BP. *Antiquity, 82*, 853–861.

Bordes, F. (1961). *Typologie de paléolithique ancien et moyen*. Bordeaux: Publications de l'Institut de Préhistoire de l'Université de Bordeaux. Mémoire No. 1

Bordes, J. G. (2002). *Les interstratifications Châtelperronien/Aurignacien du Roc-de-Combe et du Piage (Lot, France)*. Analyse taphonomique des industries lithiques; implications archéologiques. PhD disertation: Université de Bordeaux.

Burroni, D., Donahue, R. E., & Pollard, A. M. (2002). The surface alteration of flint artifacts as a record of environmental processes. *Journal of Archaeological Science, 29*, 1277–1287.

Carbonell, E., Mosquera, M., Ollé, A., Rodríguez, X. P., Sala, R., Vaquero, M., et al. (1992). New elements of the logical analytic system. *Cahier Noir, 6*, 5–61.

Carbonell, E., & Rodríguez, X. P. (1994). Early Middle Pleistocene deposits and artifacts in the Gran Dolina site (TD-4) of the Sierra de Atapuerca (Burgos, Spain). *Journal of Human Evolution, 26*, 291–311.

Cherry, J., Faro, E., & Minc, L. (2008). Field exploration and instrumental neutron activation analysis of the obsidian sources in Southern Armenia. *International Association for Obsidian Studies (IAOS) Bulletin, 39*, 3–6.

Clark D. J. (2001). The stone age cultural sequence: Terminology, typology and raw material. In J. Cormark, S. Chin, J.D. & Clark (Eds.), *Kalambo Falls Prehistoric site, 3. The middle and earlier Stone Age* (pp. 35–65). Cambridge: Cambridge University Press.

Dibble, H. L. (1984). The Mousterian industry from Bisitun Cave, (Iran). *Paléorient, 10*(2), 23–34.

Dibble, H. L., & Holdaway, S. J. (1993). The Middle Paleolithic industries of Warwasi. In D. I. Olszewski & H. L. Dibble (Eds.), *The Paleolithic Prehistory of the Zagros-Taurus* (pp. 75–99). Pennsylvania: University Museum, University of Pennsylvania.

Díez Martín, F., Martínez Molina, K., García Garriga, J., Gómez González, J. A., Cáceres, I., et al. (2009). El Paleolítico medio en el Cáucaso meridional: La Cueva Doble (Valle de Tsutskhvati, República de Georgia). *Zephyrus LXIII* enero-junio, 15–44.

Doronichev, V. B. (2008). The Lower Paleolithic in Eastern Europe and the Caucasus: A reappraisal of the data and new approaches. *PaleoAnthropology, 2008*, 107–157.

Doronichev, V. B. (2000). Lower Paleolithic occupation in the Northern Caucasus. In D. Lordkipanidze, O. Bar-Yosef & M. Otte (Eds.), *Early humans at the gates of Europe* (pp. 67–77). Liége: ERAUL *92*.

Fernández-Jalvo, Y., King, T., Andrews, P., Moloney, N., Ditchfield, P., Yepiskoposyan, L. et al. (2004). Azokh Cave and Northern Armenia. In E. Baquedano & S. Rubio Jara (Eds.), *Miscelanea en Homenaje a Emiliano Aguirre, Volumen IV: Arqueología* (pp. 158–168). Alcalá de Henares: Museo Arqueológico Regional Series.

Fernández-Jalvo, Y., King, T., Andrews, P., Yepiskoposyan, L., Moloney, N., Murray, J., et al. (2010). The Azokh Cave complex: Middle Pleistocene to Holocene human occupation in the Caucasus. *Journal of Human Evolution, 58*, 103–109.

Fernández-Jalvo, Y., King, T. Andrews, P. & Yepiskoposyan, L. (2016). Introduction: Azokh Cave and the Transcaucasian Corridor. In Y. Fernández-Jalvo, T. King, L. Yepiskoposyan & P. Andrews (Eds.), *Azokh Cave and the Transcaucasian Corridor* (pp. 1–26). Dordrecht: Springer.

Fourloubey, C., Beauval, C., Cologne, D., Liagre, J., Olliver, V., & Chataigner, C. (2003). Le Paléolithique en Arménie: État des connaisances acquises et données récentes. *Paléorient, 29*(1), 5–18.

Gabunia, L., Antón, S., Lordkipanidze, D., Vekua, Justus, A., & Swisher III, C. C. (2001). Dmanisi and dispersal. *Evolutionary Anthropology*, *10*, 158–170.

Gabunia, L., Vekua, A., Lordkipanidze, D., Swisher, C. C., Ferring, R., Justus, A., et al. (2000). Earliest Pleistocene hominid remains from Dmanisi, Republic of Georgia: Taxonomy, geological setting and age. *Science, 288*, 1019–1025.

Gamble, C. (1999). *The Paleolithic societies of Europe*. Cambridge: Cambridge University Press.

Geneste, J.-M. (1991). L' approvisionnement en matières premières dans les systemes de production lithique: La dimension spatiale de la technologie. In R. Mora, X. Terradas, A. Parpal, & C. Plana (Eds.), *Tecnología y Cadenas Operativas Líticas* (pp. 1–36). Barcelona: Servei de Publicacions de la Universitat Autónoma de Barcelona.

Golovanova, L. V., & Doronichev, V. R. (2003). The Middle Paleolithic of the Caucasus. *Journal of World Prehistory, 17*, 71–140.

Golovanova, L. V. (1990). Novie peshernie stoyanki rannego paleolita na Severo-zapadnom KavKaze (New Early Paleolithic Cave Sites on the Northwestern Caucasus). In D. Tushabramishvili (Ed.), *Paleolit KavKaza i sopredel'nikh territoriy* (pp. 35–36). Tbilisi: CA (in Russian).

Golovanova, L. V., Hoffecker, J. F., Kharitonov, V. M., & Romanova, G. P. (1999). MezmaisKaya Cave: A Neanderthal occupation in the Northern Caucasus. *Current Anthropology, 40*, 77–86.

Hardy, B. L., Kay, M., Marks, A. E., & Monigal, K. (2001). Stone tool function at the paleolithic sites of Starosele and Buran Kaya III, Crimea: Behavioral implications. *Proceedings of the National Academy of Sciences of the United States of America, 98*, 10972–10977.

Hoffecker, J. F., & Cleghorn, N. (2000). Mousterian hunting patterns in the Northwestern Caucasus and the ecology of the Neanderthals. *International Journal of Osteoarchaeology, 10*, 368–378.

Huseinov, M. M. (1985). *Drevniy paleolit Azerbaidjana (cul'tura Kuruchay i etapy ee razvitia)* (Early Paleolithic of Azerbaijan (Kuruchay culture and the periods of its development)) (p. 96). Baku: Elm.

Karkanas, P., Bar-Yosef, O., Goldberg, P., & Weiner, S. (2000). Diagenesis in Prehistoric Caves: The use of minerals that form *in situ* to assess the completeness of the archaeological record. *Journal of Archaeological Science, 27*, 915–929.

Kasimova, R. M. (2001). Anthropological research of Azykh Man osseous remains. *Human Evolution, 16*, 37–44.

King, T., Compton, T., Rosas, A., Andrews, P. Yepiskoyan, L., & Asryan, L. (2016). Azokh Cave Hominin remains. In Y. Fernández-Jalvo, T. King, L. Yepiskoposyan & P. Andrews (Eds.), *Azokh Cave and the Transcaucasian Corridor* (pp. 103–106). Dordrecht: Springer.

Laplace, G. (1972). La Typologie Analytique et Structurale: Base Rationnelle d'Étude des Industries Lithiques et Osseuses. *Banques des données archéologiques*. *Colloques nationaux du CNRS, 932*, 91–143.

Le Bourdonnec, F.-X., Nomade, S., Poupeau, G., Guillou, H., Tushabramishvili, N., Moncel, et al. (2012). Multiple origins of Bondi Cave and Ortvale Klde (NW Georgia) obsidians and human mobility in Transcaucasia during the Middle and Upper Paleolithic. *Journal of Archaeological Science, 39*, 1317–1330.

Liagre, J., Gasparyan, B., Ollivier, V., & Nahapetyan, S. (2006). Angeghakot 1 (Armenia) and the identification of the Mousterian cultural facies of 'Yerevan Points' type in the Southern Caucasus. *Paléorient, 32*(1), 5–18.

Lioubine, V. P. (2002). *L'Acheuléen du Caucase*. Liège: Études et Recherches Archéologiques de l'Université de Liège, ERAUL *93*.

Ljubin, V. P., & Bosinski, G. (1995). The earliest occupation of the Caucasus region. In W. Roebroeks & T. Van Kilfschoten (Eds.), *The Earliest Occupation of Europe* (pp. 207–253). Leiden: University of Leiden.

Marin-Monfort, M. D., Cáceres, I., Andrews, P., Pinto, A. C., & Fernández-Jalvo, Y. (2016). Taphonomy and site formation of Azokh 1. In Y. Fernández-Jalvo, T. King, L. Yepiskoposyan & P. Andrews (Eds.), *Azokh Cave and the Transcaucasian Corridor* (pp. 211–249). Dordrecht: Springer.

McBrearty, S., Bishop, L., Plummer, T., Dewar, R., & Conard, N. (1998). Tools underfoot: Human trampling as an agent of lithic artifact edge modification. *American Antiquity, 63*, 108–129.

Meignen, L. (1994). Paléolithique moyen au Proche Orient: Le phénomène laminaire. In S. Révillion & A. Truffreau (Eds.), *Les Industries Laminaires au Paléolithique Moyen* (pp. 125–159). Paris: CNRS.

Meignen, L., & Tushabramishvili, N. (2006). Paléolithique moyen laminaire sure les flancs sud du Caucase: Production lithiques et fonctionnement du site de Djruchula (Georgie). *Paléorient, 32*(2), 81–104.

Mercier, M., Valladas, H., Meignen, L., Joron, J.-L., Tushabramishvili, N., Adler, D. S., et al. (2010). Dating the early Middle Paleolithic laminar industry from Djruchula Cave. *Republic of Georgia. Paléorient, 36*(2), 163–173.

Murray, J., Domínguez-Alonso, P., Fernández-Jalvo, Y., King, T., Lynch, E. P., Andrews, P., et al. (2010). Pleistocene to Holocene stratigraphy of Azokh 1 Cave, Lesser Caucasus. *Irish Journal of Earth Science, 28*, 75–91.

Murray, J., Lynch, E. P., Domínguez-Alonso, P., & Barham, M. (2016). Stratigraphy and sedimentology of Azokh Caves, South Caucasus. In Y. Fernández-Jalvo, T. King, L. Yepiskoposyan & P. Andrews (Eds.), *Azokh Cave and the Transcaucasian Corridor* (pp. 27–54). Dordrecht: Springer.

Parfitt, S. (2016). Rodents, Lagomorphs and Insectivores from Azokh Cave. In Y. Fernández-Jalvo, T. King, L. Yepiskoposyan & P. Andrews (Eds.), *Azokh Cave and the Transcaucasian Corridor* (pp. 161–175). Dordrecht: Springer.

Pinhasi, R., Gasparian, B., Wilkinson, K., Bailey, R., Bar-Oz, G., Bruch, A., et al. (2008). Hovk 1 and the Middle and Upper Paleolithic of Armenia: A preliminary framework. *Journal of Human Evolution, 55*, 803–816.

Pinhasi, R., Gasparian, B., Nahapetyan, S., Bar-Oz, G., Weissbrod, L., Bruch, A., et al. (2011). Middle Paleolithic human occupation of the high altitude region of Hovk-1, Armenia. *Quaternary Science Reviews, 30*, 3846–3857.

Rightmire, G. P., Lordkipanidze, N. D., & Vekua, A. (2006). Anatomical descriptions, comparative studies and evolutionary significance of the hominin skulls from Dmanisi, Republic of Georgia. *Journal of Human Evolution, 50*, 115–141.

Rivals, F., & Arrellano, A. (2010). Les faunes des sites du Pléistocène supérieur du Caucase méridional: Grotte de Sakažhia, Grotte d'Ortvala et Grotte du Bronze (République de Géorgie). *L'Anthropologie, 114*, 305–323.

Rodríguez, X. P. (2004). *Technical systems of lithic production in the Lower and Middle Pleistocene of the Iberian Peninsula. Technological variability between North-Eastern sites and Sierra de Atapuerca sites*. B.A.R. International Series, 1323. Oxford: Archaeopress.

Sevilla, P. (2016). Bats from Azokh Caves. In Y. Fernández-Jalvo, T. King, L. Yepiskoposyan & P. Andrews (Eds.), *Azokh Cave and the Transcaucasian Corridor* (pp. 177–189). Dordrecht: Springer.

Shahack-Gross, R., Berna, F., KarKanas, P., & Weiner, S. (2004). Bat guano and preservation of archaeological remains in cave sites. *Journal of Archaeological Science, 31*, 1259–1272.

Smith, C. I., Faraldos, M., & Fernández-Jalvo Y. (2016). Bone diagenesis at Azokh Caves. In Y. Fernández-Jalvo, T. King, L. Yepiskoposyan & P. Andrews (Eds.), *Azokh Cave and the Transcaucasian Corridor* (pp. 251–269). Dordrecht: Springer.

Stiner, M. C., Arsebük, G., & Clark Howell, F. (1996). Cave bears and Paleolithic artifacts in Yarimburgaz Cave, Turkey: Dissecting a palimpsest. *Geoarchaeology, 11*, 279–327.

Thiébaut, C. (2007). Les pièces encochées au Paléolithique moyen et les pseudo-outils: Peut-on les distinguer? In J. Evin (Ed.), *Un siècle de construction du discours scientifique en Préhistoire. Volume III ¨…Aux conceptions d'aujourd'hui¨,* Actes du Congrès Préhistorique de France, XXVIe session, Congrès du Centenaire, 21–25 septembre 2004, Avignon; pp. 201–216.

Tushabramishvili, N., Pleurdeau, D., Moncel, M.-H., Mgeladze, A. (2007). Le Complexe Djruchula-Koudaro au Sud Caucase (Géorgie). Remarques Sur Les Assemblages Litiques Pléistocènes de Koudaro I, Tsona et Djruchula. *Anthropologie, XLV*, 1–18.

Van der Made, J., Torres, T., Ortiz, J. E., Moreno-Pérez, L., & Fernández-Jalvo, Y. (2016). The new material of large mammals from Azokh and comments on the older collections. In Y. Fernández-Jalvo, T. King, L. Yepiskoposyan & P. Andrews (Eds.), *Azokh Cave and the Transcaucasian Corridor* (pp. 117–159). Dordrecht: Springer.

Chapter 5
Azokh Cave Hominin Remains

Tania King, Tim Compton, Antonio Rosas, Peter Andrews, Levon Yepiskoposyan, and Lena Asryan

Abstract Hominin remains have been discovered at Azokh Cave from three different entrance passageways during the early and present phases of excavation. Evidence for three different species of hominin – *Homo heidelbergensis*, *Homo neanderthalensis*, and *Homo sapiens* – has been found at Azokh Cave. A fragment of hominin mandible was found in Azokh 1 in 1968. Previous studies, published in Russian and summarized here, suggest this specimen is most similar to the Ehringsdorf (adult) specimen which may now be considered as an early Neanderthal. An original assessment of a replica of the mandible carried out here indicates the specimen is similar to European Middle Pleistocene hominins, and we assign it tentatively to *Homo heidelbergenis*. A complete permanent first upper left molar tooth was found higher in the Azokh 1 sequence by the present excavation team. Preliminary description and metric analyses of the tooth indicate the specimen is typical of Neanderthal first upper molars and is most similar to Neanderthal specimens from Krapina, Croatia. A partial skeleton and two teeth of modern *Homo sapiens* have been found in Azokh 2 by the current excavation team, and evidence suggests death was accidental. Eight modern *Homo sapiens* teeth, discovered in Azokh 5 and thought to represent a minimum of three individuals (a child, a juvenile and an adolescent), are described here.

Резюме В данной главе рассматриваются останки гоминид, обнаруженные в трех различных входных камерах Азохской пещеры в течение предшествующего и современного этапов раскопок. К настоящему времени на стоянке выявлены свидетельства присутствия трех различных видов гоминид – *Homo heidelbergensis, Homo neanderthalensis* и *Homo sapiens*. В *Азох 1* фрагмент нижней челюсти гоминида был найден предшествующей группой исследователей в период раскопок, проводимых в 1960-х гг. Есть неопределенность относительно возраста находки, которая была обнаружена в отложениях 250–400-тысячелетней давности. Образец представляет собой фрагмент правой половины нижней челюсти и содержит полностью сохранившийся третий моляр. Результаты предыдущих исследований, опубликованные на русском языке, обобщены в данном разделе. Находка имеет наибольшее сходство с образцом (взрослая особь) из Эрингсдорфа и может представлять собой локальный вариант того же вида. Мы провели тщательную экспертизу реплики данного фрагмента, которая показала, что находка хорошо вписывается в морфологические

T. King (✉)
Blandford Town Museum, Bere's Yard, Blandford, Dorset, DT11 7AZ, UK
e-mail: taniacking@gmail.com

T. Compton · L. Yepiskoposyan
Institute of Molecular Biology, National Academy of Sciences, Yerevan, Armenia
e-mail: tim.compton10@btinternet.com

L. Yepiskoposyan
e-mail: lepiskop@yahoo.com

A. Rosas
Paleoanthropology Group, Museo Nacional de Ciencias Naturales (CSIC), C/José Gutiérrez Abascal, 28006 Madrid, Spain
e-mail: arosas@mncn.csic.es

P. Andrews
Natural History Museum, Cromwell Road, London, SW7 5BD, UK
e-mail: pjandrews@uwclub.net

L. Asryan
Àrea de Prehistòria, Universitat Rovira i Virgili (URV), Avinguda de Catalunya 35, 43002 Tarragona, Spain
e-mail: lenaprehistoria@gmail.com

IPHES, Institut Català de Paleoecologia Humana i Evolució Social, Zona Educacional 4, Campus Sescelades URV (Edifici W3), 43007 Tarragona, Spain

and

Artsakh State University, M. Gosh 5, Stepanakert, Nagorno-Karabakh

Yolanda Fernández-Jalvo et al. (eds.), *Azokh Cave and the Transcaucasian Corridor*, Vertebrate Paleobiology and Paleoanthropology, DOI 10.1007/978-3-319-24924-7_5

границы европейских среднеплейстоценовых гоминид. Использование различных моделей для объяснения эволюции данной группы гоминид показывает, что рассматриваемый образец может быть классифицирован как *H. heidelbergensis* или ранний неандерталец. Основываясь на примитивных признаках находки и некоторых специфических деталях, мы отдаем предпочтение предшествующему предположению и относим ее к виду *Homo heidelbergensis*.

Во время раскопок, проводимых нашей группой в 2010 г., в верхних слоях *Азох 1*, в отложениях возрастом около 100 тыс. лет, был найден полностью сохранившйхся коренной первый верхний левый моляр гоминида. В данной главе представлены предварительное описание и метрический анализ находки. Полученные результаты указывают, что обнаруженный зуб является типичным первым верхним моляром неандертальца и наиболее близок по форме к неандертальским образцам из Карпины (Хорватия). Третья серия находок датируется голоценом: останки расчлененных нижних конечностей современного *Homo sapiens* были обнаружены в *Азох 2* в течение полевого сезона 2007 г. Найдены также два зуба – верхний правый премоляр и нижний правый боковой резец, которые могли принадлежать той же особи, возраст которой был оценен в 12–13 лет на момент смерти. В текущей фазе раскопок в *Азох 5* были обнаружены зубы и фаланга, принадлежащие анатомически современному человеку.

Keywords *Homo heidelbergensis* • Neanderthals • *Homo sapiens* • Teeth • Mandible

Introduction

Azokh 1 was intensively excavated over many years. In 1968 a fragment of a hominin mandible was found by a team of Azerbaijani and Russian scientists (Huseinov 1985; Lioubine 2002). It was thought to represent the transition between *Homo erectus* and *Homo neanderthalensis* (Gadziev and Huseinov 1970), and the species was subsequently regarded as a local variant of early "*Palaeoanthropus*" (Kasimova 1986, 2001). Ten stratigraphic layers were described: Layer III was associated with Mousterian stone tool technology, Layer V was associated with Acheulian lithics together with the hominin mandible, while pebble tools discovered in the lower layers (VII to X) were described as having affinities with those found at Olduvai (Huseinov 1985). In addition, a rich fauna of large and small vertebrates was described, with 45 species from Layer V (Huseinov et al. 1985). The faunal remains and stone tools recovered from these extensive initial excavations are currently housed at the Natural-Historical Museum and Medical University of Baku in Azerbaijan.

Excavations were resumed by the present international and multidisciplinary research group in 2002 and continue to the present day (see Fernández-Jalvo et al. 2016). This new phase of excavation has revealed a long and almost continuous stratigraphic sequence at Azokh 1 from the Middle Pleistocene to the Holocene. A number of new cave entrances have been discovered during the course of this work, including Azokh 2 and 5, both of which are intact chambers with undisturbed fossiliferous and archaeological remains (Murray et al. 2010, 2016; Fernández-Jalvo et al. 2010, 2016). There is now evidence of three species of hominin: from Azokh 1 the partial mandible now referred to *Homo heidelbergensis* and an isolated molar of *H. neanderthalensis*; and several specimens of *H. sapiens* recovered from Azokh 2 and 5. We follow Rosas and Bermúdez de Castro (1998) for the definition of *H. heidelbergensis*, considered as the European Middle Pleistocene species directly ancestral to Neanderthals.

Here we focus on the hominin remains found at Azokh Cave, which span the period from the Middle Pleistocene to the Holocene. The partial mandible found in 1968 from Layer V is associated with a Middle Pleistocene fauna, and its description forms the first part of this chapter based on the publications in Russian describing the specimen. This section also includes an original assessment of the Azokh mandible using direct observations made on a cast of the specimen. This is followed by a preliminary description, presented for the first time here, of a recently discovered Neanderthal tooth from Unit II in Azokh 1. The last part of the chapter focuses on the modern human Holocene remains that have been discovered during recent excavations in Azokh 2 and Azokh 5 Caves.

Hominin Mandibular Fragment from Azokh 1

In 1968 a fragment of hominin mandible was discovered during excavations of Azokh 1 (Fig. 5.1). It was recovered from Unit V, which was assigned to the end of the "Mindel-Riss" period (Gadziev and Aliev 1969; Kasimova

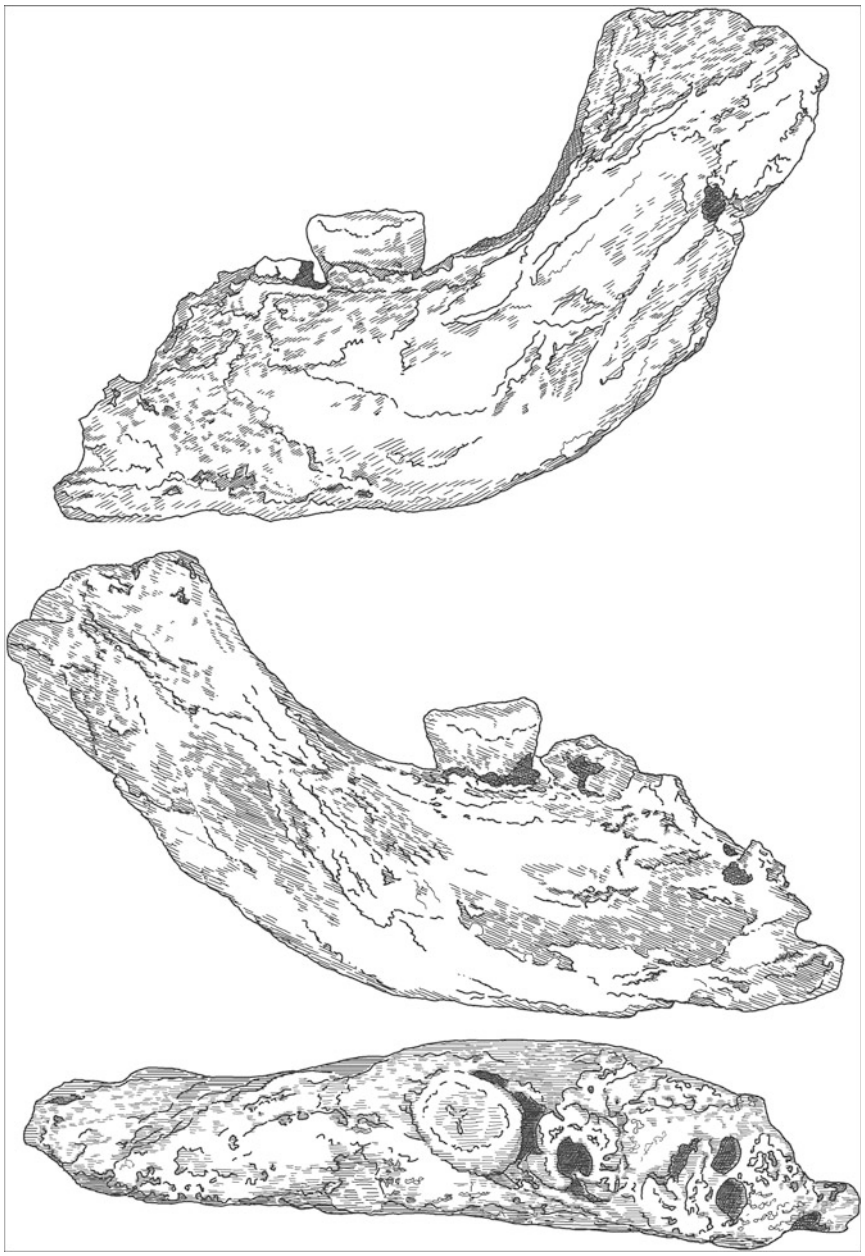

Fig. 5.1 Illustration of the Azokh 1 mandible. Lateral (top), medial (middle) and occlusal (bottom) views are shown

2001). Stone tools recovered from this level have been identified as Acheulian (Djafarov 1983; Doronichev 2008), and an extensive fossil fauna was analyzed (Huseinov 1985).

There is uncertainty about the exact location of the mandible within Layer V, which was subdivided into six horizons, thereby making it difficult to provide a precise age for the specimen. No radiometric dating was carried out during this phase of excavations. Gadziev and Huseinov (1970, p. 15) state that the fragment was recovered from the third horizon of Layer V, which was said to have an age of 250,000 years (Huseinov 1973, p. 20). However, in another publication, the specimen is reported as coming from the fifth horizon of Layer V with an age of 350,000–400,000 years (Huseinov et al. 1985). These dates were apparently based on correlations with the old concept of glacial-interglacial cycles.

One study of the mandible has been carried out to date and published in Russian (Kasimova 1986), with a more recent, shorter version published in English (Kasimova 2001). Kasimova describes it as a fragment of right mandible consisting of the posterior portion of the body and inferior part of the ramus, which is incomplete (Fig. 5.1). The mandibular body is broken at the level of the second premolar, and the inferior border is broken at the level of the mental foramen (Kasimova 1986, 2001). The ramus lacks the coronal and condylar processes. The third molar is present and complete with roots, the second molar is broken off at the base of the crown with the roots remaining, and the first molar is absent except for its distal root (Kasimova 1986, 2001). The third molar is worn and polished but does not have any dentine exposures (Kasimova 1986).

Morphology and Metrics of the Azokh Mandible

According to Kasimova (2001) the mandibular body is broad, with its greatest thickness at the level between M_2 and M_3, and it has a relatively low height in comparison with breadth. The alveolar margin is thicker than the basal edge, and widens towards the ramus (Kasimova 2001). The molar tooth crypts are positioned in the middle of the alveolar edge (towards the center), such that they are positioned far from the lingual margin; the distance from the alveolar margin lingually to the molar tooth crypts is 3 mm, rising to 5 mm at the level of M_3 posteriorly. On the lateral surface the oblique line is weakly developed. On the medial surface the mylohyoid line is barely visible. The mandible has a single large mental foramen 15 mm from the alveolar edge, at the level of the fourth premolar. A retromolar space is present, which Kasimova in (1986, 2001) states is 38 mm in length. However, in her 1986 publication she also states the length of the retromolar space is 8.0 mm, and from the views of the mandible presented in Fig. 5.1 it is apparent that the length of the retromolar space is more consistent with the latter measurement than the former, and appears to be similar in length to the M_3.

The ramus is oriented posteriorly, and the medial surface is smoother than the lateral surface. A foramen mandibula is present on the medial surface and has a diameter of 2 mm. Also present on the medial surface is a weakly developed lingula mandibula and posterior to this is the mylohyoid groove. On the lateral surface there is a weakly developed attachment for the masseter muscle, and a more strongly developed and longer attachment for the pterygoid muscle. The medial pterygoid is strongly developed and has a greater extension than the lateral pterygoid (Kasimova 2001).

Kasimova (1986) provides a metric comparison between the Azokh mandible, modern humans, and a series of different hominin groups. In some instances, these measurements have been taken at points that are non-standard in the literature, which may in part reflect absence of key landmarks/anatomy due to the fragmentary nature of the Azokh specimen. In order to characterize the thickness of the Azokh mandible Kasimova devised a "massiveness index": the percentage ratio of mandibular body thickness to mandibular height measured between M_2 and M_3, the point at which thickness of the mandibular body is greatest (Kasimova 1986, 2001). This index is equivalent to the mandibular corpus robusticity index normally measured at M_1. In addition, Kasimova (1986) has provided three sets of data describing and comparing the Azokh specimen: (i) the Azokh mandible only; (ii) the Azokh mandible and modern humans; and (iii) the Azokh mandible and a number of other hominins. However, these data sets do not compare the same suite of measurements.

Comparison with Modern Humans According to Kasimova (2001), the Azokh mandible differs markedly from modern humans due to its "massiveness". The Azokh mandible is larger than modern humans for each variable measured apart from robustness at the basal edge and mandibular body height (both measured between M_2 and M_3 where thickness is greatest). According to Kasimova (1986) the Azokh mandible differs from modern humans in the morphology of the alveolar edge, and in the distance from the alveolar margin lingually to the molar tooth crypts (3 mm, rising to 5 mm at the level of M_3 distally in the Azokh specimen, whereas modern humans usually have a smaller distance between the alveolar margin and molar tooth crypts). The Azokh mandible is similar to modern humans in having a single mental foramen.

Comparisons with Other Hominins The thickness of the Azokh mandible at M_2–M_3 is 19.0 mm. This is most similar to values for the Le Moustier Neanderthal (19.0 mm), *Homo erectus* (Zhoukoudian G/I) (19.6 mm), *Homo heidelbergensis* from Arago (Arago II) (18.0 mm) and early modern *Homo sapiens* from Skhul V (18 mm). Body height at the level of M_2–M_3 in the Azokh mandible is 23 mm, and is most similar to values for *Homo erectus* (25.0 mm), and *Homo neanderthalensis* from Ehringsdorf (26.0 mm). The

robustness of the Azokh mandible stands out from most other hominins in having a high index (that is, high robusticity), the index being 82.6%. In this regard it groups closely with *Homo heidelbergensis* from Arago (Arago XIII) (85.7%). Other similarities with *Homo heidelbergensis* include the well-developed alveolar edge and the large distance between the alveolar margin on the lingual side and the molar teeth (3–5 mm in the Azokh mandible). Kasimova (1986) notes that there is strong, broad development of the alveolar edge present in the Azokh M_3 as well as *Homo heidelbergensis* from Arago (Arago XIII) and the (adult) specimen from Ehringsdorf, which might be considered now as early Neanderthal (Stringer 2012). In addition these latter two specimens also have a wide space between the alveolar margin lingually and the molar teeth (approximately 4 mm), as does the Azokh specimen (Kasimova 1986).

Morphology and Metrics of the Dental Remains

Kasimova (1986) describes the single preserved tooth according to the odontoglyphic system developed by Russian anthropologist A.A. Zubov. There are five cusps present on the M_3 described as "smooth" or rounded. The largest is the protoconid, the metoconid smaller, as in modern humans, and the smallest cusp is the hypoconulid, which is located centrally, again as in modern humans. The Azokh M_3 trigonid is larger than its talonid, in contrast with modern humans. The most prominent of the furrows separating the cusps are the mesial and distal furrows. The distal furrow is positioned slightly lingually. The lingual furrow is weakly developed. In addition to the intertubercular furrows, Kasimova (1986) notes the presence of disto-vestibular grooves, and she states that all these features give the occlusal surface a "+5A" form (Zubov 1968). The frontal fossa (anterior fovea) is clearly pronounced. The crest joining the protoconid with the metaconid (mid-trigonid crest) is well developed, and separates the frontal fossa from the mesial sulcus. Occurrence of mid-trigonid crest in M_3 increases through the Middle Pleistocene and is unusual in *Homo heidelbergensis*. It is also unusual in early (archaic) *Homo sapiens* (Kasimova 1986, 2001). The mesio-distal diameter (length) is 11.0 mm, and the bucco-lingual diameter (breadth) is 8.9 mm. Crown area (length × breadth) is 97.9 and crown index (ratio of breadth:length expressed as a percentage (breadth/length × 100)) is 80.9%.

The roots of the second and third molars are convergent on the Azokh specimen (Kasimova 1986). X-ray imaging showed that the pulp cavity of the Azokh M_3 is large and extends into the roots, indicating that the tooth is taurodont (Kasimova 2001).

Comparison with Modern Humans In comparison with modern humans Kasimova (1986) shows that the length and breadth of the Azokh M_3 is smaller than the mean M_3 length and breadth for a sample of modern humans (11.5 mm and 9.8 mm, respectively) (Kasimova 1986). Crown area (length × breadth) is slightly less for the Azokh M_3 as compared with the sample of modern humans, but the Crown Index (breadth/length × 100) is much less in the Azokh M_3.

Comparison with Other Hominins The Azokh M_3 preserved in the mandible is most similar in size to hominin specimens from the Middle and Late Pleistocene (Kasimova 1986) such as the early Neanderthal specimen from Ehringsdorf (adult) (length 11.0 mm, breadth 9.0 mm) and the *Homo heidelbergensis* specimen Arago II (length 10.8 mm, breadth 9.6 mm), and the early modern human Skhul IV (length 11.0 mm, breadth 9.0 mm). Similarly, the values for crown area and crown index in the Azokh M_3 are most similar to those of the early Neanderthal specimen from Ehringsdorf (99.0 and 81.8% respectively) and the early modern human Skhul IV (99.0 and 81.8% respectively).

Discussion of Early Work on the Azokh Mandible

Kasimova (1986, 2001) states that the Azokh mandible is larger and more robust in comparison to modern humans. She observes that usually robustness is related to the development of the dental system, but she points out that this is weakly developed in the Azokh mandible, as evidenced by the small size of the M_3 and the weakly developed attachment areas for the muscles of mastication. On the basis of size of the mandible, muscle markings and occlusal surface of the M_3, Kasimova (2001) suggests that the mandible belonged to a female aged 20–25 years.

Other traits present in the Azokh mandible and M_3 that differ from modern humans include the broad alveolar edge in comparison to the basal edge of the Azokh mandible, the elongation of the M_3 mesio-distally, the large trigonid, the well-developed frontal fossa of the trigonid, and taurodontism. Taurodontism is found in *Homo erectus*, *Homo floresiensis*, and *Homo antessesor* from Atapuerca, and the teeth in the mandibular fragment from Atapuerca TD-6 display this trait (Carbonell et al. 2005), with the third molar being mesotaurodont and the second molar appearing to be hypotaurodont. Taurodontism is also found in Middle Pleistocene hominin specimens such as those from Mauer, Arago, and Ehringsdorf. Weidenreich (1937) noted the presence of taurodontism in the chimpanzee and orang-utan, and so thought it was a primitive trait, but this seems unlikely given the much greater extent of the hominin fossil record now.

Similarities with modern humans include the rounded, flattened, low cusps of the Azokh M_3. In addition, Kasimova (1986) states the Azokh M_3 is similar to those of modern humans in the greater size of the protoconid relative to the metaconid, the centrally placed hypoconulid, the "+5A" pattern of the cusps, convergent roots, reduction in the size of M_3, and absence of a cingulum. Kasimova (1986) observes that the Azokh specimen displays a suite of primitive and derived traits making it difficult to assign it to a hominin species. She lists the primitive and derived traits as follows:

- Derived characters shared between the Azokh hominin and *Homo erectus* referred to as "Archanthropus" by Kasimova (1986): transformation of "dryopithecus-pattern" to plus-pattern ("+5A"). Kasimova (2001) notes that she has also observed this trait in *Homo heidelbergensis* and *Homo erectus*. However, this character is more strongly developed in the Azokh specimen than the latter two groups.
- Specific characters differentiating the Azokh hominin from *Homo erectus* (again, referred to as by Kasimova 1986): a small mandibular body height in the region of M_2 and M_3, and a large retromolar space.

Kasimova (2001) observes that there are more differences between *Homo erectus* and the Azokh specimen than similarities. She notes that the comparatively small sizes of third molar and the large mandibular body size are similarities that link the Azokh mandible with *Homo heidelbergensis*, but states that there are other differences between these two taxa. Based on the dental and mandibular morphology and metric evidence, Kasimova (2001) observes that there are derived characters linking the Azokh hominin, on the one hand to the chronologically closer group of early *Homo neanderthalensis*, specifically to the Ehringsdorf hominin, and on the other hand to the chronologically later hominin Skhul IV. Kasimova (2001) also suggests that the combinations of very archaic and derived characters present in the Azokh mandible give support to assigning this specimen to an early form of what she called "*Palaeoanthropus*", which later evolved into modern humans (*Homo sapiens*).

New Assessment of the Azokh Mandibular Remains Based on a Replica of the Specimen

One of us (AR) has been able to examine a replica of the Azokh mandible (Fig. 5.2), which is housed in the collection of Profs. Henri and Marie Antoinette de Lumley. This has provided further information about its morphology and taxonomic assignment. The alveolar plane is thick giving a robust appearance to the bone. The alveolar border follows a straight trajectory, even at the level of M_3. This disposition, together with the fact that the anterior border of the ramus lies just behind the M_3, indicates that the Azokh mandible has a well-developed retromolar space. This is confirmed when the mandible is observed in superior view, as two anatomical features that further define the presence of a retromolar space, the external crest of the buccinator and the secondary crest of the retromolar triangle, are evident. A narrow extramolar sulcus can be seen, defined by a smooth external oblique line that runs on the body for a short stretch. Behind this line, part of a relatively deep masseteric fossa is preserved.

On the ramus, the triangular torus is thick, denoting a robust architecture of the mandible. In addition, the alveolar wall is thick at the level of M_3. The mylohyoid groove is open, and, even though the region is eroded, it is evident that the mental foramen opening differs from the O-D type present in Neanderthals.

The Azokh mandible presents a combination of features that allow a tentative taxonomic attribution. The great thickness of the mandibular body, the relatively small size of the molar in relation to the mandible, and the large retromolar space are all features that are typical of the *Homo heidelbergensis – Homo neanderthalensis* evolutionary line (*sensu* Rosas and Bermúdez de Castro 1998). However, the presence of a deep masseteric fossa excludes the specimen from being a classic Neanderthal. Thus, the Azokh mandible falls well within the morphological pattern of the European Middle Pleistocene hominins.

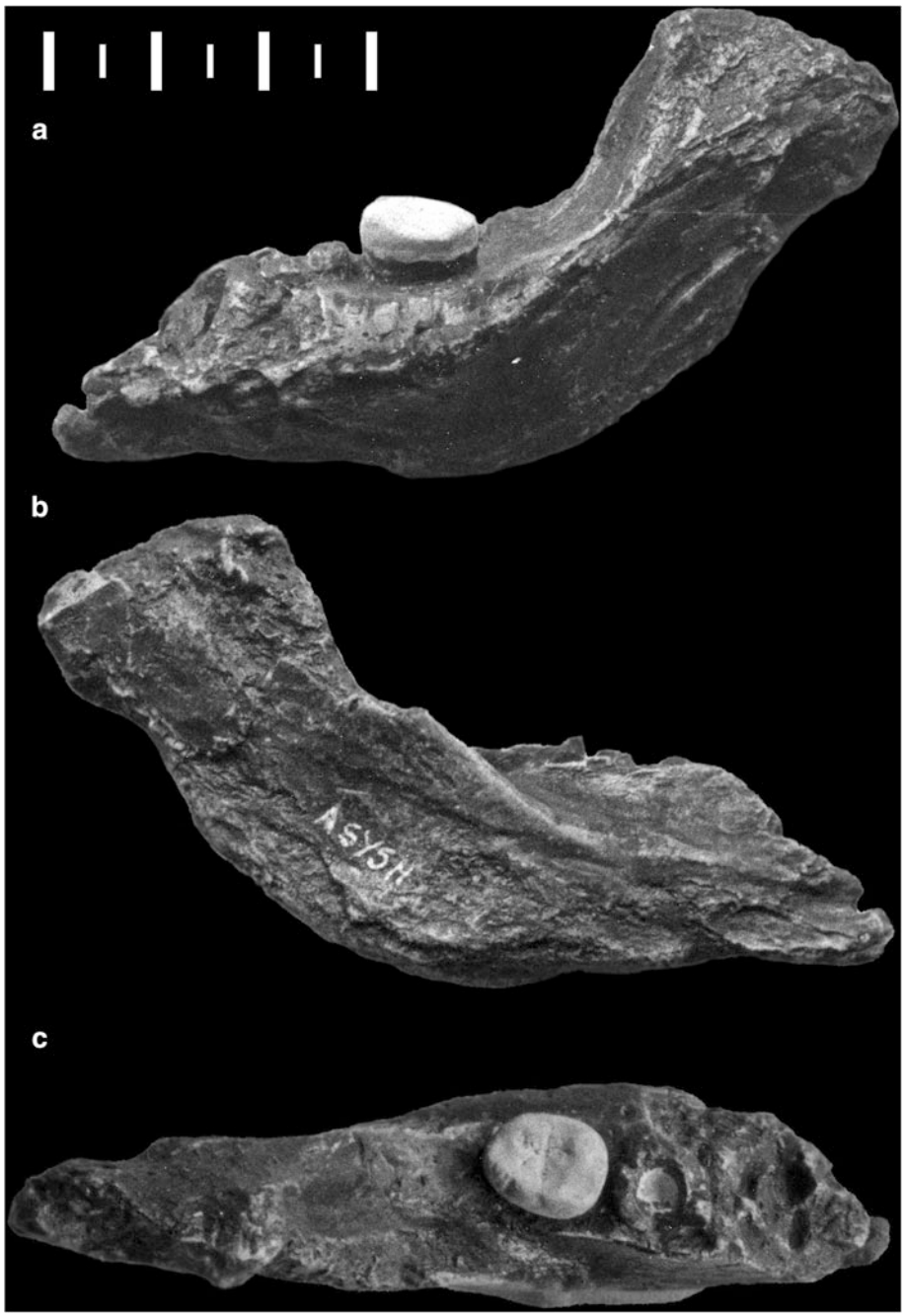

Fig. 5.2 Images of a replica of the Azokh 1 mandible: medial (top), lateral (middle) and occlusal (bottom) views of the specimen are shown

Discussion, Azokh Mandible

Kasimova (2001) states that the Azokh mandible has the closest affinity with the Ehringsdorf specimen, thus, to what may be considered as *Homo neanderthalensis* (Stringer 2012). She states further that the particular combination of characters evident in the Azokh mandible, as well as the geological age (>300 kyr) and material culture (Middle Acheulian) present in Unit V, indicate it may have been a local variant or primitive form of this species.

We note that the specimen combines a primitive robust architecture of the bone (elevated robusticity and thickness of the mandibular walls, and a smooth mylohyoid line) with a derived aligned disposition of the mandibular body and ramus (as denoted by a weak and short external oblique line and a retromolar space). This mosaic of features is reminiscent of older European Pleistocene specimens, such as those from

Mauer (Germany), Arago (France) and Atapuerca-SH (Spain). In this way, depending on the evolutionary model used for western Eurasian Middle Pleistocene hominin evolution, the Azokh mandible can be considered either as an archaic Neanderthal or as a member of the ancestral species to the Neanderthals, *H. heidelbergensis* (Stringer 2012, *sensu* Rosas and Bermúdez de Castro 1998). Even though the number of preserved features is rather small, we favor the last view on the basis of the primitive features present in the specimen and some specific details (e.g., relief of the mylohyoid line). In any case, the morphology of this mandible fits well with its supposed associated Acheulian cultural context (Asryan et al. 2016) and mid-Pleistocene faunal remains (Van der Made et al. 2016). Thus, this specimen is tentatively assigned to *Homo heidelbergensis*.

Neanderthal Remains from Azokh 1

In August 2010, during excavations of Azokh 1 Cave by the current excavation team, an isolated hominin tooth was discovered by I. Caceres. The tooth was found in sediments located towards the top of the stratigraphic sequence in Unit II in a part of the excavation adjacent to the cave wall, where a high concentration of cave bear remains (*Ursus spelaeus*) has also been found. ESR (electron spin resonance) dating of a cave bear molar from this level in Unit II has indicated an age of 100 ka (±7 ka) (Appendix, ESR). A preliminary morphological and metric analysis of the tooth is provided here, which identifies the tooth as belonging to a Neanderthal.

Description of the Isolated Tooth from Azokh Cave (E52-no. 69)

The specimen is a maxillary left first permanent molar. The crown is complete and in a good state of preservation. It had three roots that have been cleanly broken off above the root trunk. There is a moderate degree of wear on the occlusal surface, the greatest mesially, with small exposures of dentine on the protocone (approximately 0.5 mm wide) and the paracone (approximately 0.3 mm wide). There is a small amount of calculus (dental plaque) on the buccal surface of the tooth. A mild hypoplastic furrow occurs on the lingual surface approximately one mm from the cervix.

The grading system of the Arizona State University Dental Anthropology System (ASUDAS) (Turner et al. 1991) is used to describe the morphology of the Azokh tooth. The method of Moorrees (1957) is used for the measurement of the mesio-distal (M-D) and bucco-lingual (B-L) diameters of the tooth crown.

Images of the specimen are shown in Fig. 5.3. The crown has the swollen hypocone and the skewed shape that are typical of Neanderthal upper first molars (Bailey 2004). The metacone is well developed in the Azokh specimen, exceeding the size of the highest grade on the ASUDAS plaque (see Fig. 5.3). The hypocone is also well developed and, likewise, exceeds the size of the highest grade on the ASUDAS plaque. A small cusp 5 (grade 1) is present on the distal margin and two small metaconule cusps, with associated mesial and distal ridges, can be seen on the oblique ridge. Two small accessory tubercles occur on the mesial marginal ridge just lingual to its interruption by the mesial occlusal groove. Carabelli's Trait is present on the Azokh specimen as a large Y-shaped depression, scored as grade 4. There is also a grade 2 parastyle in the form of an attached cusp, with an additional weakly developed mesial vertical groove on the buccal surface of the metacone. An anterior transverse ridge is present connecting to the mesial marginal ridge and running distolingually to the mesial occlusal groove, but it does not connect to the triangular ridge of the mesiobuccal cusp (paracone). An offshoot running lingually from the anterior transverse ridge forms a crest across the mesial occlusal groove that delineates a deep anterior fovea. Amongst morphological traits not found are wrinkling of the enamel, buccal cingulum, anomalies of the buccal groove, enamel extension, and pearls.

The three roots of the tooth are well separated and with single canals. X-ray imaging of the tooth shows an expanded pulp chamber, indicating that it is taurodont (see Fig. 5.4). Most methods of quantifying the degree of taurodontism depend on the roots being complete. However, Shifman and Chananel (1978) used the distance between the bicervical line and the highest point on the floor of the pulp cavity of the tooth to distinguish between taurodont and non-taurodont molars, and proposed the following categories: non-taurodont molars (<2.5 mm); taurodont molars: hypotaurodont (2.5–3.7 mm); mesotaurodont (3.7–5.0 mm) and hypertaurodont (5.0–10.0 mm). The measurement for the Azokh tooth is 4.5 mm making it mesotaurodont.

Measurements of the Azokh molar are presented in Table 5.1. The mesio-distal diameter (length) is 12.5 mm, and the bucco-lingual diameter (breadth) is 12.6 mm. This is close to the mean figures for the Krapina Neanderthals: crown length 12.4 mm and crown breadth 12.6 mm (Compton and Stringer 2012, calculated from data in Wolpoff 1979). Measurements at the cervix of the crown were also taken, using the method described by Hillson et al. (2005). The M-D cervical diameter is 9.8 mm and the B-L cervical

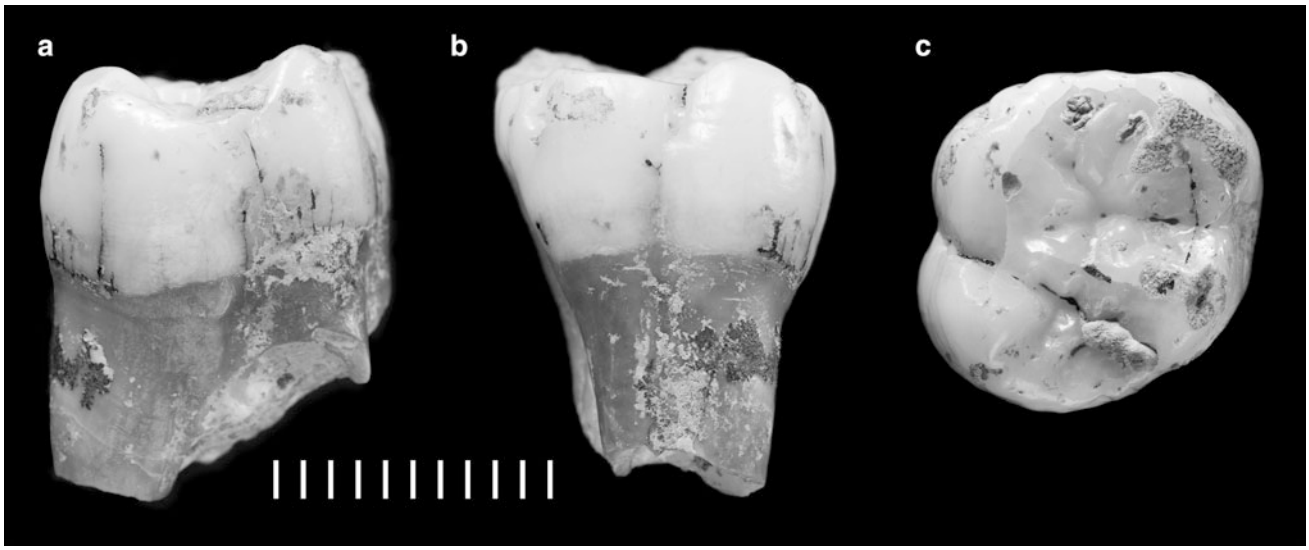

Fig. 5.3 Azokh 1 Neanderthal tooth. **a** distal, **b** lingual, and **c** occlusal views

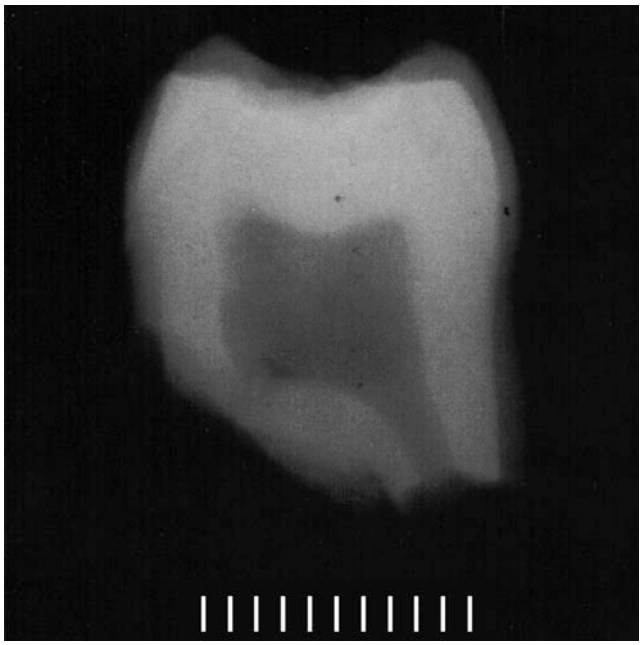

Fig. 5.4 X-ray image of the Azokh 1 Neanderthal molar. Examination and measurement of the pulp chamber indicates that it is mesotaurodont

diameter is 12.2 mm. Crown height (the disto-buccal measurement taken on the metacone) is 7.2 mm (Moorrees 1957). Finally, root robusticity at the cervix (defined as M-D diameter × B-L diameter at the cervix) was determined (Weidenreich 1937; Compton and Stringer 2012). The M-D diameter of the root is 9.0 mm and the B-L diameter is 12.1 mm, giving a root robusticity value of 109, also close to the mean value of 110 for Krapina (Higham et al. 2011).

Table 5.1 Dental measurements of the Azokh 1 Neanderthal tooth

	Measurement (mm)
Crown	
M-D* Length	12.5
B-L** Breadth	12.6
Crown height***	7.2
Cervical	
M-D	9.8
B-L	12.2
Root Robusticity	
M-D	9.0
B-L	12.1
M-D × B-L	109

Key
*M-D mesio-distal
**B-L bucco-lingual
***Disto-buccal measurement taken on the metacone

Hominin Remains from Azokh 2

Modern human remains have been found in two other cave passageways at Azokh, named Azokh 2 and Azokh 5. Both have been trenched and preliminary excavations made, but both still remain to be further explored by the present excavation team. The sites and stratigraphy are described by Murray et al. (2016) and by Domínguez-Alonso et al. (2016).

Azokh 2 is located approximately 42 m NNW from the main chamber Azokh 1 (Murray et al. 2016). The lithology of the sediments is similar to that of Azokh 1, but there is no way of correlating the sediments in the two caves. In 2002 and 2003 two test pits were dug in order to better understand the stratigraphy of the infill (see Murray et al. 2016 for full

details). Excavation was started in 2007 when the two pits were re-opened, and articulated remains of a modern *Homo sapiens* were discovered. AMS radiocarbon dating has provided an estimated age of Holocene age for the skeleton (Appendix, radiocarbon).

Two human teeth were also found in the test pits, a permanent lower right lateral incisor and a permanent maxillary right third premolar. The incisor has completed its development, having a closed root apex. Based on the work of Al Qatani et al. (2010) this might indicate an age at death of at least 9 years if maturation was fast or 13 years if maturation slow. However, the tooth is worn with an extensive dentine exposure, correlating with wear stage 5 (Murphey 1959), and suggesting this individual was older than 13 years at death. The premolar is complete with one root. It has also completed its development. Based on the work of Al Qatani et al. (2010) this might suggest an age at death of at least 13 years if maturation was fast or 15 years if maturation slow. The tooth has wear facets but no dentine exposures, correlating with wear stage 2 (Murphey 1959). The appearance, developmental stage and degree of wear of both teeth suggest that they could belong to the same individual, which was older than 15 years at death.

Human Remains from Azokh 5

Azokh 5 Cave is located approximately 100 m NNW from Azokh 1 (Murray et al. 2016). Four stratigraphic units – A (top) to D (bottom) (Murray et al. 2016) – have been described, and again the lithology of the sediments is similar to that of Azokh 1, but there is no way of correlating the sediments in the two caves. There is also a cone of collapsed sediments that contains fossil remains of a number of macro- and micro-fossil species from these four stratigraphic units. Several human teeth were discovered in place in unit A in 2006 and are described here (Table 5.2). They were associated with charcoal that has been radiocarbon dated to ~2300 years BP (384calBC_OxA 17589; see Appendix, radiocarbon). A single middle phalanx was also found (Specimen 6). Seven of the specimens are displayed in Fig. 5.5, and details of the dimensions are given in Table 5.3.

Table 5.2 List of human specimens and specimen numbers from Azokh 5

Specimen number	Specimen
1	Permanent maxillary right second molar
2	Permanent maxillary left canine
5	Permanent mandibular right first molar
6	Second phalanx
7	Deciduous maxillary right third premolar
8	Permanent mandibular left second molar
9	Permanent maxillary left third premolar
10	Permanent mandibular right canine
11	Permanent maxillary left first molar

Table 5.3 Azokh 5 human tooth crown dimensions

Specimen	Bucco-lingual length (mm)	Mesio-distal length (mm)
1	11.37	9.32
2	8.17	6.98
5	10.38	11.12
7	8.87	6.82
8	9.95	11.40
9	8.15	6.98
10	6.76	7.10
11	11.59	9.26

1. Specimen 1, permanent maxillary right second molar. The crown is quadrilateral in shape. There is destruction of the enamel particularly on the distal surfaces and mesial lingual cusp. The largest cusp is the mesio-lingual cusp. Three roots are present and two are complete in their development, with the apical canal of the lingual root still open. Based on the work of Al Qatani et al. (2010) this might suggest an age of 14 years if maturation was fast in this individual or 17 years if maturation was slow. This tooth is little worn, with wear facets visible but no dentine exposures present, which correlates with attrition category 2 (Murphey 1959), and on the basis of this and the developmental stage, the age at death of this individual may have been 15 years (see Table 5.4). This specimen may be associated with specimens 2, 5, 8, and 10 (see Table 5.4).
2. Specimen 2, permanent maxillary left canine. The crown is intact with a large dentine exposure distally on the labial surface. Four linear enamel hypoplasias are evident around the circumference of the crown. The root is intact and has completed its development. The root apex is fully closed. Using the work of Al Qatani et al. (2010) this might suggest an age of 12 years in this individual if maturation was slow or an age of 15+ years if maturation was accelerated. However, wear displayed by this specimen correlates with wear category 3 (Murphey 1959), indicating that this individual was most likely aged 15+ years at death (see Table 5.4). This specimen may belong to the same individual as specimens 1, 5, 8, and 10 (see Table 5.4).
3. Specimen 5, permanent mandibular right first molar. There is very little wear on the crown surface, indicating it may be associated with wear stage 3 (Murphey 1959). There are two roots. The distal root is broken. The light

wear present indicates a younger adult individual, and it could represent an adolescent who was about 15 years old at death (see Table 5.4). It may belong to the same individual as Specimens 1, 2, 8, and 10 (see Table 5.4).

4. Specimen 6, middle phalanx.
5. Specimen 7, deciduous maxillary right third premolar. The crown is intact and is quadrilateral in shape. It has four cusps – the largest is the mesio-buccal cusp. There is a small dentine exposure on the occlusal surface of the mesio-buccal cusp, with a larger dentine exposure on the mesio-lingual cusp. The degree of wear present correlates with wear stage 3 (Murphey 1959). There is a prominent tubercle on the buccal surface (Brown 1985). This tooth had three roots, the bucco-distal and lingual roots broken almost at the mid point of their lengths and the mesio-buccal root broken just below the crown. The dimensions of the tooth crowns are given in Table 5.3. The degree of wear present and the fact that there has been no root resorption suggest that the age of this individual at death was about 5 years (see Table 5.4).
6. Specimen 8, permanent mandibular left second molar. The tooth crown has moderate wear, with greater wear on the buccal cusps, but no dentine exposure. There is a small caries mesially on the occlusal surface in the groove between the mesio-lingual and mesio-buccal cusps. The roots have broken off. There are wear facets apparent on the tooth crown surface but no dentine exposures, and the category of wear may be stage 2 (Murphey 1959). This specimen may represent an individual aged about 15 years at death based on the wear and may belong to the same individual as Specimens 1, 2, 5 and 10 (see Table 5.4).
7. Specimen 9, permanent maxillary left third premolar. This specimen is a tooth crown with little wear present. Perikymata are visible to the naked eye. Horizontal bands spanning the circumference of the tooth crown may represent linear enamel hypoplasias. The root has broken off at the margin with the tooth crown. There are no wear facets present on the occlusal surface nor any visible dentine patches, indicating the tooth either had not yet erupted or was newly erupted but not in occlusion. Thus the category of wear corresponds to stage 1 (Murphey 1959).
8. Specimen 10, permanent right mandibular canine. The root has broken, off at the margin of the crown. This specimen has very little wear, with small wear facets of minimal size, which may correspond to wear category 2 (Murphey 1959). Perikymata can be seen by the naked eye. Linear enamel hypoplasias are evident around the circumference of the tooth crown. Given the stage of wear it is likely that this was an adolescent individual, and although the roots are broken by wear stage comparison it may belong to the same individual as Specimen 2 (upper left canine), which is likely to be aged about 15 years, and hence also associated with specimens 1, 2, 5, and 8 (see Table 5.4).
9. Specimen 11, permanent maxillary left first molar. The specimen is square in shape with four cusps. It is heavily worn with dentine coalescence between the mesio-lingual and disto-lingual cusps. The enamel is polished and no perikymata are visible by naked eye or microscopically. The tooth has three roots that are intact – two buccal roots and one lingual root that have not quite completed their development, with the apical canals being still open. Thus, if this individual matured at a fast rate it would have been about 8 years at death and if maturation was slow age at death would have been about 13 years (Al Qatani et al. 2010). The level of wear apparent in this specimen corresponds to category 5 (Murphey 1959). Taking both the developmental and wear stages into consideration indicates this individual may have been about 11 years at death, and may belong to the same individual as Specimen 9 (see Table 5.4).

Table 5.4 Wear stages, age estimations and associations of human tooth specimens from Azokh 5

Specimen No.	Identification	Wear category	Age estimation (years)	Associated with other specimens
1	Permanent maxillary right second molar	2	15	2, 5, 8, 10
2	Permanent maxillary left canine	3	15	1, 5, 8, 10
5	Permanent mandibular right first molar	3	15	1, 2, 8, 10
7	Deciduous maxillary right third premolar	3	5	
8	Permanent mandibular left second molar	2	15	1, 2, 5, 10
9	Permanent maxillary left third premolar	1	11	11
10	Permanent mandibular right canine	2	15	1, 2, 5, 8
11	Permanent maxillary left first molar	5	11	9

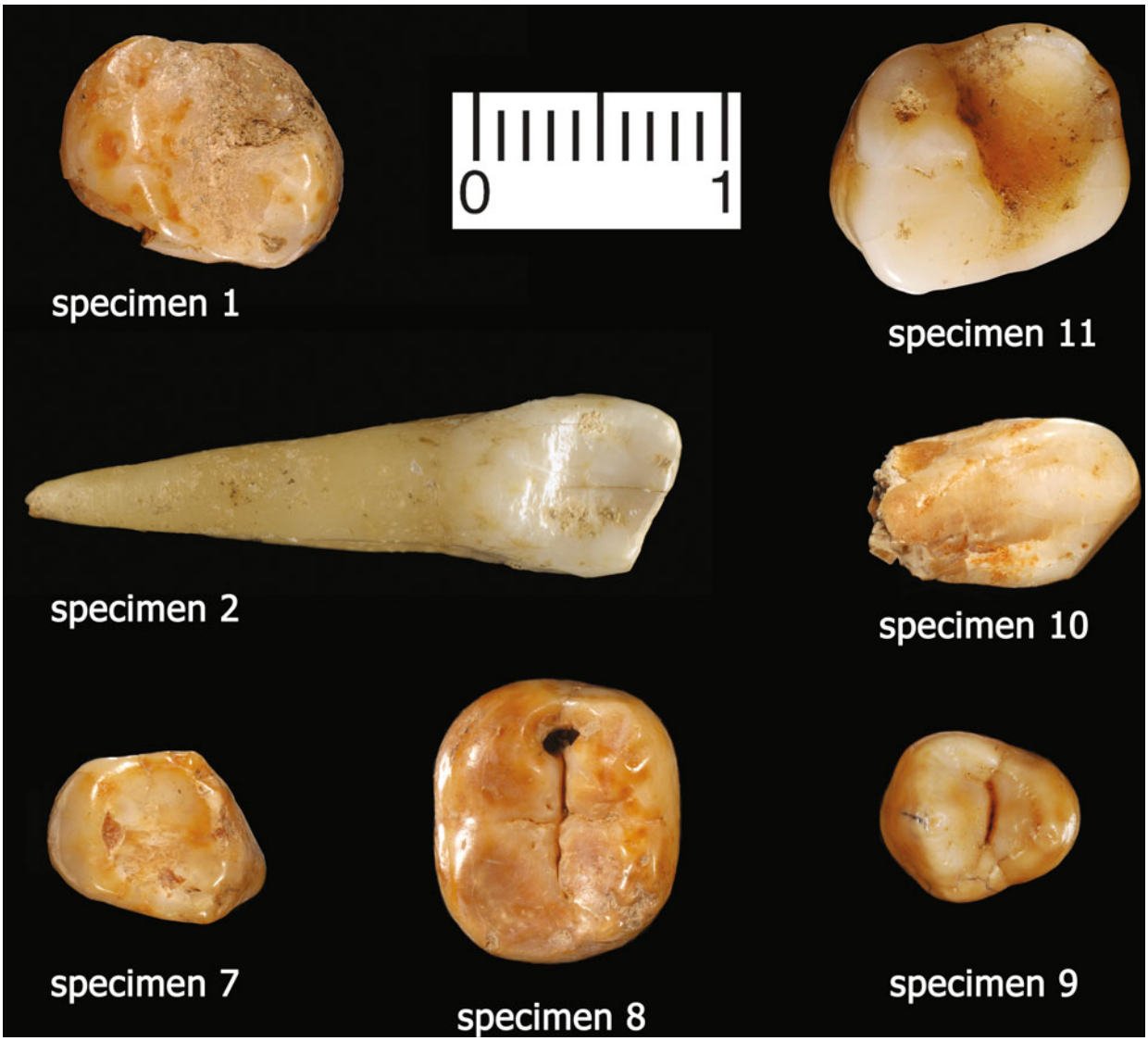

Fig. 5.5 Azokh 5 human teeth. Anti-clockwise from top left: Specimen1 (right M^2, occlusal view), Specimen 2 (left upper canine, lingual view), Specimen 7 (deciduous right P^3, occlusal view), Specimen 8 (left M_2, occlusal view), Specimen 9 (left P^3, occlusal view), specimen 10 (right lower canine, lingual view), Specimen 11 (left M^1, occlusal view)

Conclusions

1. The mandible from Azokh 1, dated ca. 250,000–400,000 ka is tentatively assigned to *Homo heidelbergensis* after analysis of previously published data and a replica.
2. The maxillary left first permanent molar from Azokh 1 from Unit II has an age of 100 ka (±7 kyr). It is identified as Neanderthal on the basis of morphology (swollen hypocone and skewed shape) and taurodontism, and the crown dimensions and root robusticity are similar to the mean figures for Neanderthal upper first molars from the similarly dated site of Krapina in Croatia, dated at ~130,000 ka (Rink et al. 1995).
3. DNA analysis, and a full description and morphometric analysis of the Azokh 1 Neanderthal molar are currently underway.
4. The two modern teeth from Azokh 2, associated with skeletal remains dated to 1265 ± 23 y BP, may be from the same individual, an adolescent who was aged about 12–13 years at death.
5. The eight modern human teeth from Azokh 5, dated to ~2300 years BP, comprise a minimum of three individuals: a child aged about 5 years at death, a juvenile aged about 11 years at death, and an adolescent aged about 15 years at death.
6. Enamel growth disruptions (linear enamel hypoplasias) are evident on some of the teeth.

Acknowledgements We are grateful to a number of individuals at several different institutions for the help they have provided in the preparation of this chapter. We thank Dr. Melanya Balayan, Director, and staff of Artsakh State Museum for Country and History Study for facilitating access to the Azokh 2 modern human remains. We are particularly grateful to Prof. Chris Dean and Dr. Helen Liversidge for helpful discussions, advice, and interest in the course of preparation of this manuscript. We also thank Dr. Liversidge for her help in preparation of the X-ray image of the Neanderthal specimen. We thank Dr. Yolanda Fernandez-Jalvo for her help and advice in the preparation of this chapter, and also for her careful review of the manuscript. We are very grateful to Felicity Baker for preparing the illustrations of the Azokh mandible shown in Fig. 5.1. We thank the Photography Department of MNCN for the preparation of the images of specimens from Azokh 5. We thank Drs. Patricio Dominguez Alonso, Yolanda Fernandez-Jalvo and John Murray for their help in preparing images of the Azokh mandible, Neanderthal tooth and the Azokh 5 specimens. We are grateful to three anonymous reviewers for their thorough review of this chapter.

References

Al Qahtani, S. J., Hector, M. P., & Liversidge, H. M. (2010). Brief communication: The London atlas of human tooth development and eruption. *American Journal of Physical Anthropology, 142*(3), 481–490.

Appendix: Fernández-Jalvo, Y., Ditchfield, P., Grün, R., Lees, W., Aubert, M., Torres, T., et al. (2016). Dating methods applied to Azokh Cave sites. In Y. Fernández-Jalvo, T. King, P. Andrews & L. Yepiskoposyan (Eds.), *Azokh Cave and the Transcaucasian Corridor* (pp. 321–339). Dordrecht: Springer.

Asryan, L., Moloney, N., & Ollé, M. (2016). Lithic assemblages recovered from Azokh 1. In Y. Fernández-Jalvo, T. King, L. Yepiskoposyan & P. Andrews (Eds.), *Azokh Cave and the Transcaucasian Corridor* (pp. 85–101). Dordrecht: Springer.

Bailey, S. E. (2004). A morphometric analysis of maxillary molar crowns of Middle–Late Pleistocene hominins. *Journal of Human Evolution, 47*, 183–198.

Brown, W. A. B. (1985). *Identification of Human Teeth*. Institute of Archaeology, 1985, Bulletin No. 21/22.

Carbonell, E., Bermudez de Castro, J. M., Arsuaga, J. L., Allué, E., Bastir, M., Benito, A., et al. (2005). An early Pleistocene hominin mandible from Atapuerca-TD6, Spain. *Proceedings of the National Academy of Sciences USA, 102*(16), 5674–5678.

Compton, T., & Stringer, C. B. (2012). The Human Remains. In S. Aldhouse-Green, R. Peterson E. A. Walker (Eds.), *Neanderthal s in Wales: Pontnewydd and the Elwy Valley Caves* (pp. 118–230). Oxbow Books: Oxford.

Djafarov, A. (1983). Mustierskaya kultura Azerbajana (po materialam Taglarskoi pesheri) (The Mousterian Culture of Azerbaijan). Baku.

Domínguez-Alonso, P., Aracil, E., Porres, J. A., Andrews, P., Lynch, E. P. & Murray, J. (2016). Geology and Geomorphology of Azokh Caves. In Y. Fernández-Jalvo, T. King, L. Yepiskoposyan & P. Andrews (Eds.), *Azokh Cave and the Transcaucasian Corridor* (pp. 55–84). Dordrecht: Springer.

Doronichev, V. B. (2008). The Lower Palaeolithic in Eastern Europe and the Caucasus: A reappraisal of the data and new approaches. *PaleoAnthropology*, pp. 107–157.

Fernández-Jalvo, Y., King, T., Andrews, P., Yepiskoposyan, L., Moloney, N., Murray, J., et al. (2010). The Azokh Cave complex: Middle Pleistocene to Holocene human occupation in the Caucasus. *Journal of Human Evolution, 58*, 103–109.

Fernández-Jalvo, Y., King, T., Andrews, P., & Yepiskoposyan, L. (2016). Introduction: Azokh Cave and the Transcaucasian Corridor. In Y. Fernández-Jalvo, T. King, L. Yepiskoposyan & P. Andrews (Eds.), *Azokh Cave and the Transcaucasian Corridor* (pp. 1–26). Dordrecht: Springer.

Gadziev, D. V., & Aliev, S. D. (1969). Plaeontological reasoning of the stratigraphy of the Palaeolithic site of Azokh (Paleontologicheskoe obosnovanie stratigrafii Azychskoi paleoliticheskoi stoyanki). UZ Azgosmedinstitut, T. XXX (in Russian).

Gadziev, D. V., & Huseinov, M. M. (1970). Pervaya dlyz SSSR nakhodka ashel'skogo cheloveka (Azerbaijan, Azykh Cave) (The first find of Acheulean man in the USSR). Compendium of Azerbaijan State Medical Institute, vol. XXXI.

Hillson, S., FitzGerald, C., & Flinn, H. (2005). Alternative dental measurements: Proposals and relationships with other measurements. *American Journal of Physical Anthropology, 126*, 413–426.

Huseinov, M. M. (1973). *Tainy Azykhskoi peschery (The mysteries of Azykh cave)*. Gyanjlik: Baku. (in Azerbaijani).

Huseinov, M. M. (1985). Drevniy paleolit Azerbaidjana (cul'tura Kuruchay i etapy ee razvitia) (Lower Palaeolithic of Azerbaijan (*Kuruchai* culture and its development periods)). Baku.

Huseinov, M. M., Aliev, S. D., Velichko, A. A., Gadziev, D. V., Djafarov, A. K., Mamedov, A. V., et al. (1985). Main results of the complex research works of the Early Palaeolithic cave site of Azykh (Glavnie itogi komleksnikh issledovanii drevnepaleoliticheskoi peshernoi stoianki Azykh). In Achievements of Soviet anthropologists. Baku.

Higham, T., Compton, T., Stringer, C., Jacobi, R., Shapiro, B., Trinkaus, E., et al. (2011). The earliest evidence for anatomically modern humans in northwestern Europe. *Nature, 479*, 7374, 521–524 & SI 1–76.

Kasimova R. M. (1986). Pervaya nakhodka samogo drevnego peschernogo cheloveka na territorii SSSR (Azerbaidzhanskaia SSR. Azykh). – Baku: Elm, 1986. – 68 s. [The first find of the most ancient cave human on the territory of the USSR (Azerbaijan SSR. Azykh). – Baku: Elm, 1986. – 68 p.].

Kasimova, R. M. (2001). Anthropological research of Azykh Man osseous remains. *Human Evolution, 16*, 37–44.

Lioubine, V. P. (2002). *L'Acheuléen du Caucuase*. ERAUL 93 Études et Recherches Archéologiques de l'Université de Liège. Liège.

Moorrees, C. F. A. (1957). *The Aleut Dentition*. Cambridge: Harvard University Press.

Murphey, T. (1959). The changing pattern of dentine exposure in human tooth attrition. *American Journal of Physical Anthropology, 17*, 167–178.

Murray, J., Domínguez-Alonso, P., Fernández-Jalvo, Y., King, T., Lynch, E. P., Andrews, P., et al. (2010). Pleistocene to Holocene stratigraphy of Azokh 1 Cave, Lesser Caucasus. *Irish Journal of Earth Sciences, 28*, 75–91.

Murray, J., Lynch, E. P., Domínguez-Alonso, P., & Barham, M. (2016). Stratigraphy and Sedimentology of Azokh Caves, South Caucasus. In Y. Fernández-Jalvo, T. King, L. Yepiskoposyan & P. Andrews (Eds.), *Azokh Cave and the Transcaucasian Corridor* (pp. 27–54). Dordrecht: Springer.

Rink, W. J., Schwarcz, H. P., Smith, F. H., & Radovčić, J. (1995). ESR ages for Krapina hominids. *Nature, 378*, 24.

Rosas, A., & Bermúdez de Castro, J. M. (1998). The Mauer mandible and the evolutionary significance of *Homo heidelbergensis*. *Geobios, 31*, 687–697.

Shifman, A., & Chananel, I. (1978). Prevalence of taurodontism found in radiographic dental examination of 1,200 young adult Israeli patients. *Community Dental. Oral Epidemiology, 6*, 200–203.

Stringer, C. (2012). The Status of *Homo heidelbergensis* (Schoetensack 1908). *Evolutionary Anthropology, 21*, 101–107.

Turner II, C. G., Nichol, C. R., & Scott, G. R. (1991). Scoring procedures for key morphological traits of the permanent dentition: The Arizona State University Dental Anthropology System. In M. Kelley & C. Larsen (Eds.), *Advances in Dental Anthropology* (pp. 13–31). New York: Wiley Liss.

Van der Made, J., Torres, T., Ortiz, J. E., Moreno-Pérez, L., & Fernández-Jalvo, Y. (2016). The new material of large mammals from Azokh and comments on the older collections. In Y. Fernández-Jalvo, T. King, L. Yepiskoposyan & P. Andrews (Eds.), *Azokh Cave and the Transcaucasian Corridor* (pp. 117–159). Dordrecht: Springer.

Weidenreich, F. (1936). The mandibles of *Sinanthropus pekinensis*: A comparative study. *Palaeontologia Sinica*, series D, *7*, 1–162.

Weidenreich, F. (1937). The dentition of Sinanthropus pekinensis: A comparative odontography of the Hominids. *Palaeontologia Sinica. Whole series 101, New series D1*, 1–180.

Weidenreich, F. (1943). The skull of Sinanthropus pekinensis: A comparative study on a primitive hominin skull. *Palaeontologia Sinica*, Series *127*, 1–298.

Wolpoff, M. H. (1979). The Krapina dental remains. *American Journal of Physical Anthropology, 50*, 67–114.

Zubov A. A. (1968). Odontology. Methods of anthropological research/Odontologia. Metodika antropologicheskikh isledovanii. The Science Publishers, Moscow.

Chapter 6
The New Material of Large Mammals from Azokh and Comments on the Older Collections

Jan Van der Made, Trinidad Torres, Jose Eugenio Ortiz, Laura Moreno-Pérez, and Yolanda Fernández-Jalvo

Abstract During the 1960s to 1980s a human mandible, together with fossils of other animals and a lithic industry, were recovered from Units I to VI of Azokh Cave. After the year 2002, new excavations in Units I to V were undertaken. The new large mammal fossils are described and the fauna is revised, using part of the older collections. The only clear break in the sequence is the appearance of domestic mammals in Unit I. The following taxa recovered from Pleistocenic sediments were identified: *Ursus spelaeus* (the most abundant), *Ursus* sp. (*U.* aff. *arctos/thibetanus*), *Vulpes vulpes*, *Canis aureus*, *Canis lupus*, *Meles meles*, *Martes* cf. *foina*, *Crocuta crocuta*, *Felis chaus*, *Panthera pardus*, *Equus hydruntinus*, *Equus ferus*, *Stephanorhinus hemitoechus, Stephanorhinus kirchbergensis*, *Sus scrofa*, *Capreolus pygargus*, *Dama* aff. *peleponesiaca*, *Dama* sp., *Megaloceros solilhacus*, *Cervus elaphus*, *Bison schoetensacki*, *Ovis ammon*, *Capra aegagrus* and *Saiga*. Most species present are common in western Eurasia. All fossiliferous Units have taxa that in mid-latitude Europe are considered to be "interglacial" elements, while there are no clear "glacial" elements, which suggests temperate conditions despite the altitude of the cave. The evolutionary levels of various species suggest ages of about 300 ka for Units VI–IV, while Units III–II are slightly younger. Domestic mammals indicate a Holocene age for Unit I. Most sediments represent a normal transition between units. Processes of erosion, however, affected the top of the Pleistocene sediments recorded in the cave. Therefore, Unit I (Holocene sediments containing domestic animals) lies disconformably over Unit II (Late Pleistocene).

Резюме За период с 1960-х по 1980-е гг. в *уровнях I–VI* азохской пещеры были обнаружены фрагмент нижней челюсти человека, окаменелости других животных и каменные орудия. После 2000 г. раскопки были возобновлены на уровнях *I–V*. В данной главе описаны находки новых крупных млекопитающих, полностью пересмотрена коллекция фауны с включением в нее части более ранних собраний.

Единственный отчетливый перерыв в последовательности находок связан с появлением домашних животных в подразделении *1*. В ходе исследования удалось идентифицировать следующие виды, обнаруженные в плейстоценовых отложениях: *Ursus spelaeus* (наиболее богато представленный), *Ursus* sp. *(U.* aff. *arctos/thibetanus), Vulpes vulpes, Canis aureus, Canis lupus, Meles meles, Martes* cf. *foina, Crocuta crocuta, Felis chaus, Panthera pardus, Equus hydruntinus, Equus ferus, Stephanorhinus hemitoechus, Stephanorhinus kirchbergensis, Sus scrofa, Capreolus pygargus, Dama* aff. *peleponesiaca, Dama* sp., *Megaloceros solilhacus, Cervus elaphus, Bison schoetensacki, Ovis ammon, Capra aegagrus и Saiga*. Останки плотоядных животных были раскопаны главным образом из подразделения 1.

Dama aff. *Peleponesiaca* интересна тем, что сочетает в себе примитивное качество сильного разветвления лобного отростка и ствола рога с прогрессивной характеристикой хорошо развитой лапчатости. Эта особенность приписана боковой ветви таксона *Dama* в том же регионе, существовавшей до появления вида *D. mesopotamica. Megaloceros solilhacus* примечателен тем, что его находка в Азохе является самой молодой из всех известных нам. Этот вид широко представлен в Европе и юго-западной Азии (Убейдия, Латамна), он

J. Van der Made (✉) · Y. Fernández-Jalvo
Museo Nacional de Ciencias Naturales CSIC, José Gutiérrez Abascal 2, 28006 Madrid, Spain
e-mail: jvdm@mncn.csic.es

Y. Fernández-Jalvo
e-mail: yfj@mncn.csic.es

T. Torres · J.E. Ortiz · L. Moreno-Pérez
Biomolecular Stratigraphy Laboratory (BSL). E.T.S.I. Minas, Polytechnical University of Madrid, Rios Rosas 21, 28003 Madrid, Spain
e-mail: trinidad.torres@upm.es

J.E. Ortiz
e-mail: joseeugenio.ortiz@upm.es

L. Moreno-Pérez
e-mail: laura_mope@hotmail.com

Yolanda Fernández-Jalvo et al. (eds.), *Azokh Cave and the Transcaucasian Corridor*, Vertebrate Paleobiology and Paleoanthropology, DOI 10.1007/978-3-319-24924-7_6

является наиболее вероятным предком *M. algericus*, который намного позднее появился в Северной Африке. Находки свидетельствуют о том, что данный род выжил в пределах юго-западной Азии после полного вымирания в Европе и до его распространения в Северную Африку.

Большинство видов, представленных в Азохе, являются или были обычными формами в западной Евразии, но некоторые из них имеют или в прошлом имели область распространения вплоть до Дальнего Востока. Основной ареал других видов был представлен юго-восточной, южной или центральной Азией, или Северной Африкой. Все горизонты с ископаемыми организмами включают в себя таксоны, которые в средних широтах Европы квалифицируются как "межледниковые", в то время как в этих же слоях отсутствуют явные "ледниковые" артефакты, что указывает на умеренные климатические условия несмотря на высоту расположения пещеры.

Многие из обнаруженных видов живут и сегодня, однако *Ursus spelaeus, Equus hydruntinus*, два вида *Stephanorhinus* и *Bison schoetensacki* вымерли в эпоху позднего плейстоцена, в то время как *M. solilhacus* и *Dama* aff. *pelopenesiaca*, должно быть, вымерли или эволюционировали в другие виды значительно ранее.

Поскольку большинство видов дожило до наших дней, многие из них характеризуют предельные возраста для стратиграфических подразделений: *Stephanorhinus hemitoechus, Ursus spelaeus* и *Canis lupus* свидетельствуют в пользу более молодого возраста некоторых слоев, чем это предполагалось ранее. Эволюционное положение *Cervus elaphus* и различных видов рода *Dama* предоставляет дополнительную информацию о возрасте подразделений. Биохронологические данные указывают на возраст около 300 тыс. лет для подразделений *VI–IV*, в то время как подразделения *III–II* немного моложе. Наличие останков домашних животных свидетельствует о голоценовом возрасте подразделения *I*. Отложения указывают на нормальный переход между большинством из подразделений. Процессы эрозии, однако, повлияли на поверхность плейстоценовых отложений в пещере. По этой причине подразделение *I* (голоценовые отложения, содержащие домашних животных) находится в явном несоответствии с подразделением *II* (поздний плейстоцен).

Keywords Middle Pleistocene • Palaeontology • Caucasus • Azikh • Nagorno-Karabakh

Introduction

The site of Azokh (also known as Azykh or Azikh), in the Lesser Caucasus (Fig. 6.1), has provided an extensive large mammal assemblage recovered from excavations from 1963 to 1988 and from 2002 to present. The largest mammal fossil collection was recovered during the 25 years of the former excavations lead by M. Huseinov (see Fernández-Jalvo et al. 2016) from Units VI to II. This collection is currently hosted at the Medical University of Baku in Azerbaijan. Excavations from 2002 to the present have been carried out at the back of the cave. Fossils have been referred to units following the same nomenclature and stratigraphy established by Huseinov from Units V to I. The top of the sequence (I) Holocene (Appendix, radiocarbon) was not palaeontologically studied by previous authors. The bottom of the sequence (Unit Vm) comes from an excavation surface left by Huseinov's team that is located at about a metre above the bottom of this unit. Sediments from Unit VI are recorded at the cave entrance (at present on the sides of the cave walls), but it loses thickness towards the back of the cave and has no identifiable record in the area where excavations were performed from 2002 to present (Murray et al. 2016).

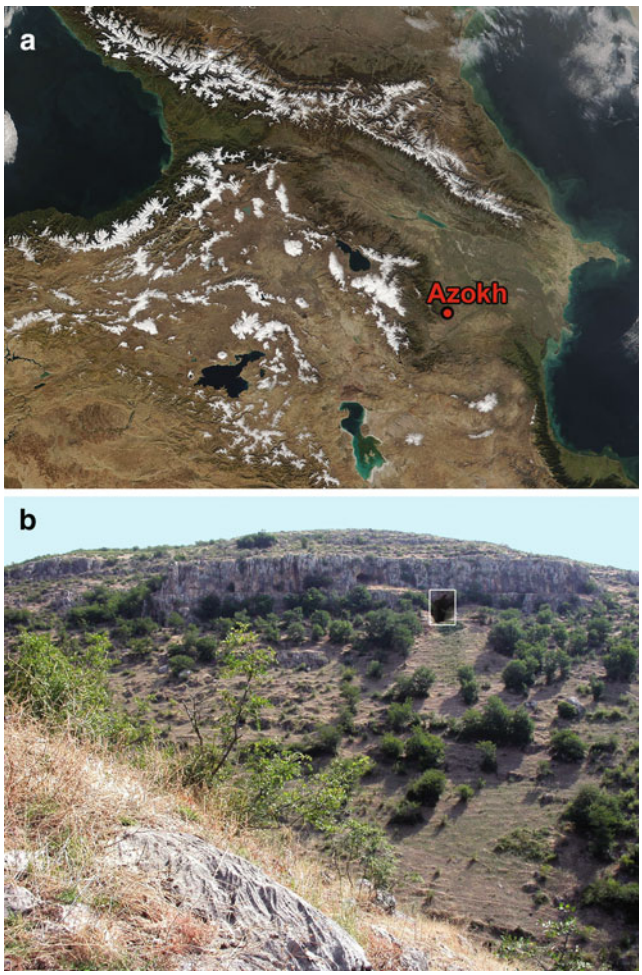

Fig. 6.1 **a** Location of Azokh Cave in the Caucasus. **b** The cave entrance of Azokh site is located uphill, around 200 m above the village of the same name in the Nagorno-Karabakh region of the southeastern part of the Lesser Caucasus

Fossils from this unit were excavated during the previous seasons lead by Huseinov, and taxonomic identifications refer to the fossil collection currently hosted in Baku.

Excavations performed from 2002, located at the back of the cave, yielded fossils that show differences in the mammalian faunal composition compared to excavations performed by Huseinov (1960–1980) closer to the open-air connection. The new material has a larger and better representation of bears, probably as result of relatively prolonged hibernation and occupation periods of cave bears. Humans have entered the cave and transported in some animals inhabiting the area in the vicinity of the cave (Marin-Monfort et al. 2016). We are here describing the large mammal taxonomy, comparing results with previous identifications, and discussing the meaning of these groups and their geographic distribution across the area that gave access from and to Eurasia from and to Africa.

An interesting aspect of the study area is its geographical and biogeographical position. Situated on the southern flanks of the Lesser Caucasus, the area is west Eurasian in its biogeographic affinities. Many "typically European" species range far into Asia, as did Neanderthals. With increasing distance, such species may show morphological change or be replaced by other species eastward, but also southward. Towards the south, species adapted to more dry or open environments replace the species with European affinities. To the east, there may be gradual or abrupt morphological or metrical changes within a species. Such changes are probably related to periods of isolation during the cold phases and thus these phenomena contain information on past environmental conditions, conditions in which the Neanderthals also lived. Ideally, long detailed records of faunal composition and of morphological and metrical evolution of the different species should be compared with the European records. At present this is not possible, but it is possible to compare the fauna of a single or few localities with the European record.

The fauna from Azokh was formerly studied by Aliev (1969). Lioubine (2002) gave faunal lists per unit based on Aliev (1969, 1989, 1990), Gadziev et al. (1979), Velichko et al. (1980), Markova (1982) and Burchak-Abramovitch and Aliev (1989, 1990) and mentioned later additions or modifications by Guérin and Barychnikov (1987) and Barychnikov (1991), who identified the presence of *Dicerorhinus etruscus brachycephalus* (presently mostly *Stephanorhinus hundsheimensis*) and *Ursus mediterraneus*. Rivals (2004) gave the composite list of large mammals according to Aliev (1969). There are small differences between the two lists, which probably reflect the work done between 1969 and 2002, such as the elimination of several "cf." citations, the assignment to *Equus suessenbornensis* instead of to *Equus caballus*, the omision of *Gazella* aff. *subgutturosa*, etc. Table 6.1 shows the large mammal taxonomic identification cited by previous authors.

Table 6.1 Faunal list provided by Rivals (2004) based on Aliev's (1969) and Lioubine's (2002) identifications (material hosted in the Medical University of Baku (Azerbaijan) from 1960 to 1989 seasons lead by Huseinov)

	Unit VI	Unit V	Unit III
Vulpes vulpes	X		
Canis cf. *Lupus*		X	
Canis aureus		X	
Meles meles		X	
Martes cf. *Foina*		X	
Crocuta spelaea		X	
Felis chaus		X	
Felis lynx		X	
Panthera pardus		X	
Ursus mediterraneus		X	
Spelarctos spelaeus	X	X	X
Ursus aff. *arctos*	X		X
Equus hydruntinus	X	X	X
Equus suessenbornensis/E. caballus	X		
Dicerorhinus etruscus brachycephalus	X		
Dicerorhinus mercki	X	X	X
Sus scrofa		X	X
Capreolus capreolus	X	X	**X**
Dama cf. *mesopotámica*	X		X
Megaloceros giganteus	X		X
Cervus elaphus	X		X
Bison schoetensacki	X		
Capra aegagrus		X	X
Gazella aff. *subgutturosa*		X	

The faunal material from the previous excavations is kept in the Medical University of Baku (Azerbaijan). One of us (JvdM) had the opportunity to study the Artiodactyla and Rhinocerotidae of this collection. It is the aim of this chapter to describe the new material, to discuss the older collections, present an updated faunal list and make comparisons with the European faunal record.

Materials and Methods

Conventional methods were used in the morphological studies, based on visual comparisons and simple morphometrics. The measurements of the Equidae are taken as indicated by Eisenmann et al. (1988), those of the Rhinocerotidae as indicated by Van der Made (2010a), those of the Artiodactyla as indicated by Van der Made (1996) and Van der Made and Tong (2008), and those of the carnivores are taken in a comparable way. All measurements are given in mm, unless indicated otherwise. The measurements are indicated by same abbreviations as used by Van der Made (1996) and Van der Made and Tong (2008). DAP, DT, DMD, DLL mean respectively antero-posterior, transverse,

medio-distal and labio-lingual diametre respectively. L and H mean length and height. Additions of letters as in DTa mean DT of the anterior lobe of a tooth or of the anterior side of a bone. Similarly: a = anterior, b = basal, dors = dorsal, f = of the facet, h = of the head (as in a calcaneum), l = lower, la = labial, li = lingual, max = maximum, mini = minimum, n = neck, o = occlusal, p = posterior, root = of the root, sf = at the height of the sustenacular facet, trigonid = of the trigonid, u = upper. Ta is the enamel thickness measured at the metaconid, h and l are alternative height and length of a bone. R1–5 are five dimensions of the distal condyle of the humerus, numbered from medial to lateral. Lint, Lm and Lext are the medial, middle and lateral lengths of the astragalus.

The terminology of the tooth morphology follows Van der Made (1996). If ungulate, phalanges, sesamoids and distal metapodials are indicated to be right or left, this means the position relative to the axis of the foot, not of the complete animal. Example a "right first phalanx" of an artiodactyl means thus a proximal phalanx III of the right foot or a phalanx IV of the left foot.

The fossils of the recent excavations at Azokh are housed in the Artsakh State Museum of History and Country Study in Stepanakert (ASMHCS). These fossils were compared with fossils from many other localities or bones of recent mammals. When such comparisons are made, either the relevant literature is cited, or the institute is indicated where the material was studied or where it is kept at present (which need not be the same institute). The institutes are indicated with the following acronyms: AUT = Aristotle University of Thessaloniki; BGR = Bundesanstalt für Geowisenschaften und Rohstoffe, Hannover; CENIEH = Centro Nacional de Investigación sobre la Evolución Humana, Burgos; CIAG = Centre d'Investigacions Arquelògics de Girona; EBD = Estación Biológica de la Doñana, Sevilla; FASMN = Römisch-Germanisisches Zentralmuseum, Forschungsinstitut für Vor- und Frühgeschichte, Forschungsbereich Altsteinzeit Schloss Monrepos, Neuwied; FBFSUJB = Forschungstelle Bilzingsleben, Friedrich Schiller-Universität Jena, Bilzingsleben; GIN = Geological Institute, Moscow; GSM = Georgian State Museum, Tbilisi; HGSB = Hungarian Geological Survey, Budapest; HMV = Historisches Museum, Verden; MNHUB – Museum für Naturkunde der Humboldt-Universität, Berlin; HUJ = Hebrew University, Jerusalem; IGF = Istituto di Geologia, Firenze; IPGAS = Institute of Palaeobiology, Georgian Academy of Sciences, Tbilisi; IPH = Institut de Paléontologie Humaine, Paris; IPS = Instituto de Paleontología, Sabadell; IQW = Institut für Quartärpaläontologie, Weimar; IVAU = Instituut Voor Aardwetenschappen, Utrecht; IVPP = Institute for Vertebrate Paleontology and Paleoanthopology, Academia Sinica, Beijing; LAUT = Laboratori de Arqeologia de la Universitat Rovira i Virgili, Tarragona; LPT = Laboratoire de Prehistoire de Tautavel, Université de Perpignan; LVH = Landesmuseum für Vorgeschichte, Halle; MCP = Musée Crozatier, Le Puy-en-Velay; MMB = Moravian Museum, Brno; MNCN = Museo Nacional de Ciencias Naturales, Madrid; MPRM = Musée de Préhistoire Régionale, Menton; MPT = Musée de la Préhistoire Tautavel; MRA = Museum Requien, Avignon; MUB = Medical University, Baku; NCUA = National and Capodistrian University of Athens; NHM = Natural History Museum, London; NHMB = Natural-Historical Museum, Baku; NMM = Naturhistorisches Museum, Mainz; NMMa = Natuurhistorisch Museum, Maastricht; NMP = National Museum, Prague; NNML = Nationaal Natuurhistorisch Museum, Leiden; PIN = Palaeontological Institute, Moscow; SIAP = Servei d'Investigacions Arqueològiques i Prehistòriques, Castellón; SMNK = Staatliches Museum für Naturkunde, Karlsruhe; SMNS = Staatliches Museum für Naturkunde, Stuttgart; SMS = Spengler Museum, Sangerhausen; TMH = Teylers Museum, Haarlem; TUC = Technische Universität Clausthal, Insitut für Geologie und Paläontologie; UCM = Universidad Complutense, Madrid; ZSM = Zhoukoudian Site Museum.

Systematic descriptions

Order Carnivora Bowdich, 1821
Family Ursidae Fischer de Waldheim, 1817
Ursus sp.

New material

Unit II
E45-46B – third cuneiform.

Description of the new material and taxonomic classification

A third cuneiform bone shows size and articular facet morphology that clearly differ from *Ursus spelaeus* and *Ursus deningeri*, which indicates a small sized bear with narrow paws. If the measurements are plotted in the corresponding bivariate plot of the third cuneiform bones of Iberian *U. deningeri*, *U. spelaeus* and recent *U. arctos* (Torres 1989), it shows it to be smaller and more slender than *U. spelaeus,* clustering well with the other two species. Taking into account the general size of the Azokh bear skeletal elements, it seems very possible that there is a subtle presence of an ancient brown bear, but in some cave records of the Great Caucasus the presence of *Ursus* (*Ursus*) *thibetanus* G. Cuvier has been attested by Doronichev (2000). Therefore, we cannot ascertain to which of the two species this bone belongs.

Ursus spelaeus Rosenmüller and Heinroth, 1794

New material

The specimens are listed and their measurements given in Tables 6.2, 6.3, 6.4, 6.5 and 6.6. Cave bear fossils studied here have been selected from the fossil collection recovered from Azokh, but some measurements could not be taken because most of these fossils are broken or damaged (see Marin-Monfort et al. 2016). The numbers of elements are indicated in brackets after each element type.

Unit Vm

Cuboid (1), first phalanx (2), second phalanx (1), I^3 (1), P^4 (1), M^1 (1), M^2 (3), I_2 (1), M_3 (1).

Unit Vu

Scapula fragment (1), radius (1), scapholunate (1), first metacarpal (1), fifth metacarpal (1), femur (1), fibula (1), cuboid (1), fourth metatarsal (2), sesamoid (2), first phalanx (4), third phalanx (3), M^2 (1), I_3 (2), lower canine (1), M_1 (1), M2 (1), M_3 (1).

Unit III

Humerus (1), radius (1), ulna (1), scapholunate bone (2), pisiform (1), magnum (1), second metacarpal (3), fibula (3), calcaneus (1), first metatarsal bone (1), fifth metatarsal (1), cervical vertebra (2), dorsal vertebra (1), lumbar vertebra (1), hyoid (cerato) bone (1), rib (1), sternum (xiphoid proc.) (1), pelvis (1), baculum (1), first phalanx (1), third phalanx (2), I^3 (1), M^2 (1), M_3 (1), canine indet. (1).

Unit II

Skull fragment (1), maxilla fragment (10), mandible (1), scapula (6), humerus (9), radius (5), ulna (9), scapholunate (3), hamatum (2), magnum (3), pisiform (3), trapezoid (1), first metacarpal (2), second metacarpal (2), third metacarpal (3), fourth metacarpal (2), fifth metacarpal (5), femur (10), patella (3), tibia (3), fibula (9), calcaneus (5), astragalus (2), scaphoid (2), second cuneiform (1), third cuneiform (1), first metatarsal (1), second metatarsal (1), third metatarsal (2), fourth metatarsal (3), fifth metatarsal (1), hyoid-cerato bone (1), vertebra fragment (3), axis (1), dorsal vertebra (4), rib (1), pelvis (2), baculum (2), first phalanx (17), second phalanx (8), third phalanx (7), I^1 (1), I^2 (1), I^3 (3), upper canine (4), P^4 (1), M^2 (2), I_1 (1), I_2 (1), I_3 (2), lower canine (2), P_4 (2), M_1 (3), M_2 (3), M^3 (1) canine indet. (2).

Unit I

Femur fragment (1), I^3 (1), M^2 (1), I_1 (2), I_3 (2), C_L (1), P_4 (1)

Unit I is of Holocene age and mainly contains domestic animals. It has been heavily altered by recent animal burrowing. The result is the presence of fossils and stone tools reworked from Unit II and currently mixed with sediments from Unit I (Murray et al. 2016).

Most of the bear remains are from Unit II. The minimum number of individuals is: 1 in Unit I, 3 in Unit II, 1 in Unit III, 1 in Unit Vu, and 2 in Unit Vm, making a total number of eight individuals. This is not enough to ascertain any morphological change in skeleton and dentition in the recorded time-span.

Description of the new material and taxonomic classification

The most impressive specimen, at least according to its size (Table 6.3), is a complete and big right ulna (II C46 320 Z = 124). It is larger than those from the cave bear localities in the Iberian Peninsula that we used for comparison (cf. Torres 1989) (Fig. 6.2) and many other European localities (cf. Koby 1951). In order to discern whether this ulna falls into the *spelaeus* or the *deningeri* group, we used a bivariate analysis of the maximum anteroposterior diameter of the distal diaphysis against the total length of the bone (Fig. 6.2). In these diagrams the ulna from Azokh aligned with the *U. spelaeus* trend. The Azokh ulna, though bigger than all the ones comprised in the composite Iberian sample, matches well with the robustness of *U. spelaeus* individuals, diverging markedly from the small sample of *U. deningeri* and, in a more marked way, from the *U. arctos* group. Size differences (size trends) were explained by Kurten (1955). Though there is a low number of articular bones, their metrics are compared in bivariate plots (Fig. 6.3) with data of *Ursus deningeri* and *Ursus spelaeus*. In some cases, the plots of Torres (1989) were also used although they are not included in this chapter. Scapholunates II E 48 117B, II 132, II 256 and II D45 30 = 144–159 match with the *U. spelaeus*

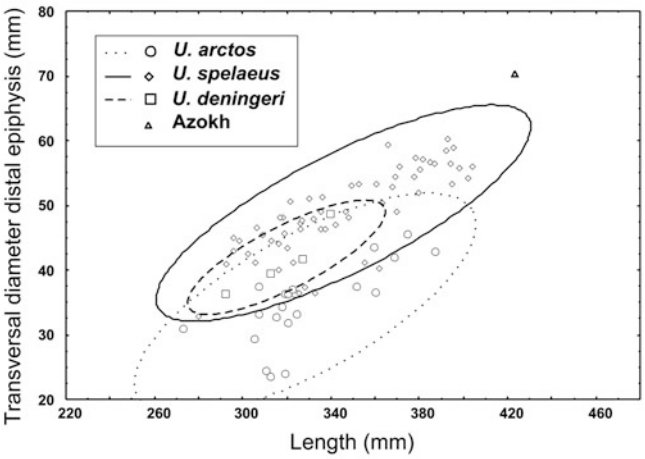

Fig. 6.2 Metrical comparison of the ulna of *Ursus* from Azokh 1 and those from the Iberian populations of *U. spelaeus* (El Reguerillo cave and Arrikrutz cave) composite sample), *U. deningeri* (La Lucia, Quintanilla Cantabria cave) and *U. arctos* (composite sample). Equiprobability (95%) ellipses were added. Anteroposterior diameter of the distal epiphysis is plotted against bone length. Data after Torres (1989) and Torres et al. (2006)

Table 6.2 Tooth measurements of *Ursus spelaeus* from Azokh 1: incisor; M: molar; P: premolar; C: canine. For incisors and canines: M1-transverse diameter of the crown; M2-anteroposterior diameter of the crown. For P^4: M1-crown length; M2-crown width; M3-paraconid height. For M^1: M1-crown length; M2-trigon width; M3-talus width; M4-trigon/talus striction width. All measurements are in mm

Number	Element	Side	M1	M2	M3	M4	M5
I F52 11 Z = 140	I^3	D	14.8	16.0			
I 54	M^2	D	46.5	11.9	22.2		
I D45 Gen. Finds	I_3	D	12.7	11.9			
I D4	I_1	D	5.6	9.4			
I–III D45 resc. 26?	I_1	D	6.0	9.4			
I 94	I_3	D	10.9	11.3			
I 4	C_1	D	19.7				
IB	P_4	D	17.8	11.8			
II I49 17 Z = 86	I^1	D	9.5	12.0			
II C46 380 Z = 126	I^2	S	10.0				
II C46 380 Z = 126	I^2	D	10.4				
II D46 70 Z = 138	I^3	D	13.1	15.6			
II Rescue C45 7 (sec 17)	I^3	S	11.9	13.9			
II C46 380 Z = 126	I^3	S	14.5				
II H49 3 Z = 191	C^u	D	23.0				
II C46 376 Z = 120	C^u	S	23.6				
II C46 380 Z = 126	C^u	S	20.9				
II D46 84 Z = 128	C^+	D	19.2				
II C46 380 Z = 126	P^4	S	20.5	14.9			
II C46 375 Z = 120	M^2	D	48.0		19.9		
II C46 378 Z = 119	M^2	D	47.4	15.5	23.0		
II D45 17 Z = 179	I_2	S	7.6	9.9			
II C46 316 Z = 144	$I_{1/2}$	S	7.8	10.4			
II C26 326 Z = 112	I_3	S	11.3	10.8			
II C26 340 Z = 121	I_3	S	11.6	11.6			
II C46 88 Z = 77	C_1	S	20.7				
II 33	C_1	D	25.0				
II C46 166 Z = 93	P_4	D	15.3	10.4	10.8		
II C46 294 Z = 104	P_4	D	14.2	9.0	8.8	3.7	
II C46 294 Z = 104	M_1	D	24.8	10.0	11.8	9.4	7.2
II 86	M_1	D	27.4	11.3	14.3	11.1	7.9
II C46 360 Z = 130	M_1	S			13.6	10.8	
II C46 294 Z = 104	M_2	D	25.5	15.5	16.1	17.2	15.0
II 54	M_2	S	26.2	15	14.2	15.2	12.2
II Rescue C45 15 Z = 110	M_2	D	27.6	16.9	16.8	18.2	16.3
II C46 294 Z = 104	M_3	D	24.2	18.7			
III D46 154 Z = 220	I^3	S	11.7	14.4			
III C46 8 Z = 173	M_3	D	27.4	19.2			
III C46 7 Z = 173	M^2	D	46.2	11.8	23.4		
Vu E45 Gen finds	M_1	S			13.0		
Vu D45 4 Z = 36	I_3	S	10.6				
Vu D45 45 Z = 58	M_2	S	29.9	15.6	19.4	19.9	17.8
Vu D45 27 Z = 54	M_3	D	29.0	18.8			
Vm F42 1b Z = 102	I^3	S	14.7	15.7			
Vm E42 13 Z = 122	P^4	S	20.5	15.0	12.0		
Vm D42 8 Z = 96	M^1	S	26.3	19.9	19.7	18.7	
Vm D42 8 Z = 96	M^2	S	44.0		22.5		
Vm F43 3 Z = 92	M^2	S	50.0	13.5	24.5		
Vm D42 27 Z = 105	M^2	D		15.6	23.3		
Vu D44 11 Z = 65	M^2	D	43.1	12.2	21.8		
D Vm E42 2	I_2	S	8.9	10.6			
Vm F42 Z = 102	C_1	D	23.1				
Vm E41 1 Z = 113	M_3	D	28.3	19.8			

Table 6.3 Measurements of the long bones of *Ursus spelaeus* from Azokh Cave. All measurements are in mm

Number	Bone	Side	Measurements
II C46 294 Z = 104	Mandible	D	Diastema Length 46.9; Horizontal branch elevation (P4) 54.0; Horizontal branch elevation (M3) 60.3; Mandible thickness (M2–M3) 24.3; Molar series length 76.0; Canine transversal diameter 15.1
II–III D45 10 Z = 108	Scapula		Glenoid cavity vertical diameter 54.4
II C49 7 Z = 90	Humerus	S	Diaphysis transversal diameter 41.5
II 380	Humerus	D	Diaphysis transversal diameter 13.8 (cub)
II H49 9 Z = 106	Radius	S	Femur head transversal diameter 42.5; Diaphysis transversal diameter 28.5
II C46 301 Z = 111	Radius	S	Prox epiphysis transv. Diam. 34.0; Prox epiphysis ant-post diam. 28.7; Diaphysis transversal diameter 32.8
II C46 320 Z = 124	Ulna	S	Length 423.2; Sygmoidean notch transversal diameter 93.1; Diaphysis antero-posterior diameter 48.6; Diaphysis antero-posterior diameter 70.4; Styloid apophysis anteroposterior diameter 62.5
II C46 367 Z = 124	Ulna	D	Diaphysis antero-posterior diameter 53.0; Distal epiphysis anteroposterior diameter 61.0
III D46 78 Z = 162	Ulna	S	Diaphysis antero-posterior diameter 40.5; Sygmoidean notch transversal diameter 51.4
II D46 89 Z = 107	Ulna		Distal epiphysis transversal diameter 55.6
II 118	Femur		Proximal epiphysis transversal diameter 101.3; Head transversal diameter ca. 45
II D47 1 Z = 96	Femur	S	Diaphysys transversal diameter 35.9
II Rescue D45 13 Z = 129	Femur	D?	Diaphysys transversal diameter 45.9
II C46 335 Z = 120	Femur	S	Transversal diameter of the diaphysis 48.6
II C46 154 Z = 93	Femur	D	Length 400.7; Proximal epiphysys transversal diameter 100.0; Diaphysys antero-posterior diameter 49.5; Distal epiphysys transversal diameter 83.0. Distal epiphysis antero-posterior diameter 68.3
II I49 9 Z = 179	Femur		Diaphysis transversal diameter 32.6
II C46 305 Z = 119	Femur	D	Diaphysis transversal diameter 42.4
II D47 2 Z = 44	Tibia	S	Proximal epiphysis transversal diameter 119.8
II C46 364 Z = 123	Tibia	D	Distal epiphysis transversal diameter 80.0; Distal epiphysis antero-posterior diameter 51.0
II G51 20 Z = 180	Tibia	S	Distal epiphysis transversal diameter 60.7; Distal epiphysis antero-posterior diameter 36.3
II D46 62 Z = 128	Fibula	D?	Diaphysis antero-posterior diameter 16.0
II D45 14 Z = 121	Fibula	S	Distal epiphysis transversal diameter 33.5
II D46 63 Z = 132	Fibula	D	Distal epiphysis transversal diameter epiphysis 33.6
II Rescue D45 3 Z = 82	Fibula	D?	Diaphysis anteroposterior diameter 17.3
II Rescue D45 24	Fibula	D	Diaphysis anteroposterior diameter 15.8
II 6	Fibula	D	Distal epiphysis antero-posterior epiphysis 35.4
II D 45 section	Fibula	D	Diaphysis transversal diameter 17.6 Distal epiphysis transversal diameter epiphysis 36.3
Vu G44 1 Z = 145	Fibula	S	Length 321.4; Proximal epiphysis transversal diameter 36.4; Distal epiphysis transversal diameter 43.1; Diaphysis transversal diameter 15.8

trend, but they are bigger. Vu D45 26 matches with the *Ursus spelaeus* trend (female sized). Magnums II D46 7 Z = 96, III D46 160 Z = 226 and II I49 22 match with the *Ursus spelaeus* trend and size, while II 25 matches with the *Ursus spelaeus* trend, although it is bigger. Hamates (or hook bones) II C46 303 and II C46 318 match with *Ursus spelaeus* in height. Pisiforms II C46 108 and II F51 1 match the *Ursus spelaeus* trend and are big sized. Trapezium II C46 204 matches the *Ursus spelaeus* trend. Calcanei II I50 9, II-69 and III D46 105 Z = 166 match the *Ursus spelaeus* trend. Astragali II 45 and II C46 150 match with the *Ursus spelaeus* trend. Cuboids Vu B, I, Vu B and Vm D42 12 Z = 90 match the *Ursus spelaeus* trend, while II F52 167 is slightly more robust. Scaphoid II C46 281 matches with the *Ursus spelaeus* trend and is big sized.

The metrical relationships between the length and the transverse or anteroposterior diameter of epiphysis and diaphysis of the metapodials discriminate well between samples of *U. deningeri* and *U. spelaeus* (Torres 1989; Torres and Guerrero 1993; Torres et al. 2001). There are not enough

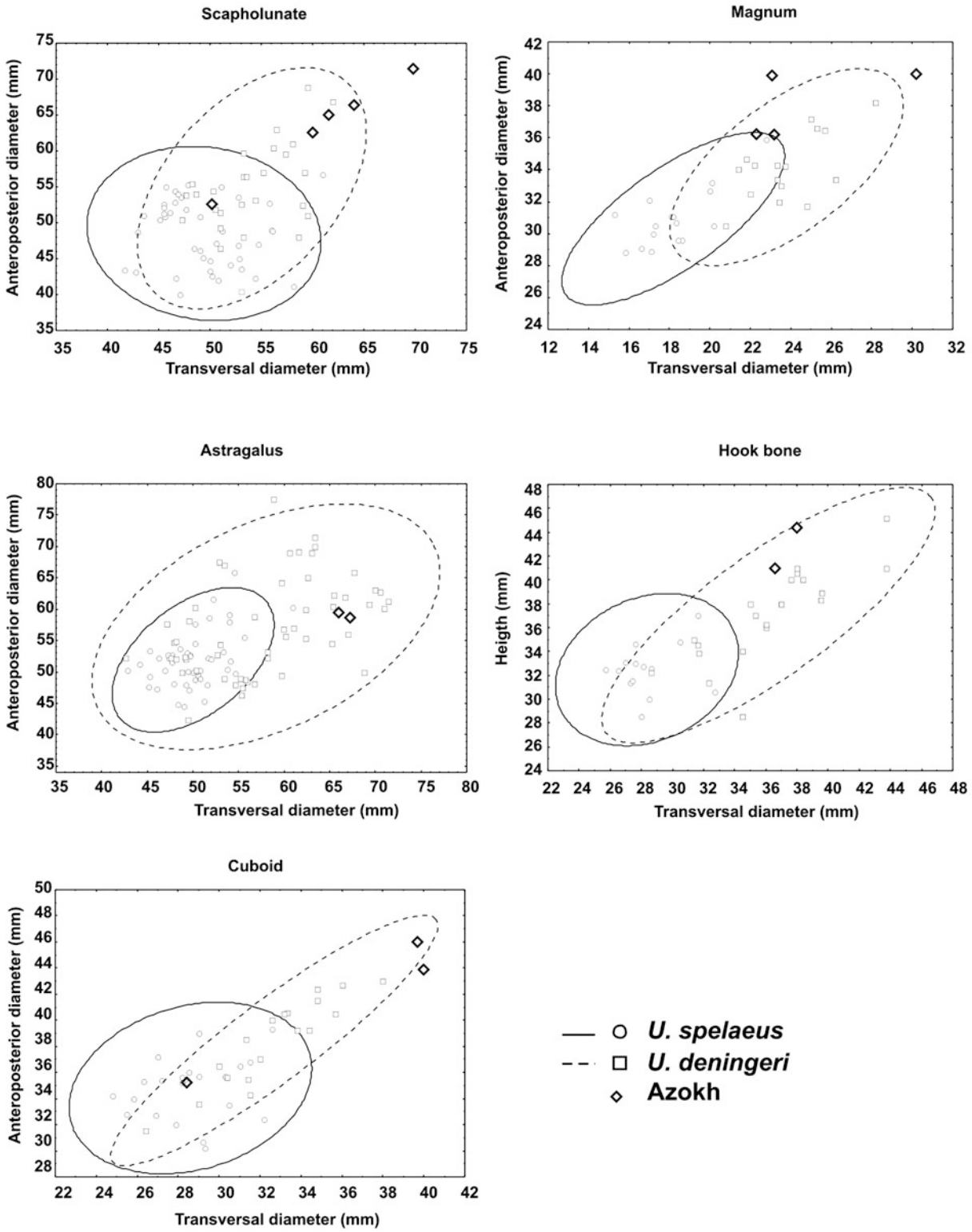

Fig. 6.3 Metrical comparison of some carpals and tarsals of *Ursus* from Azokh 1 and those from the Iberian populations of *U. spelaeus* (El Reguerillo cave, Patones-Madrid and Arrikrutz cave, Oñati, Guipuzcoa) and *U. deningeri* (Sima de los Huesos, Atapuerca-Burgos). Equiprobability (95%) and regression lines have been added. For all cases (hamatum or hook bone excepted) antero-posterior diameter is plotted against transverse diameter. Data after Torres (1989)

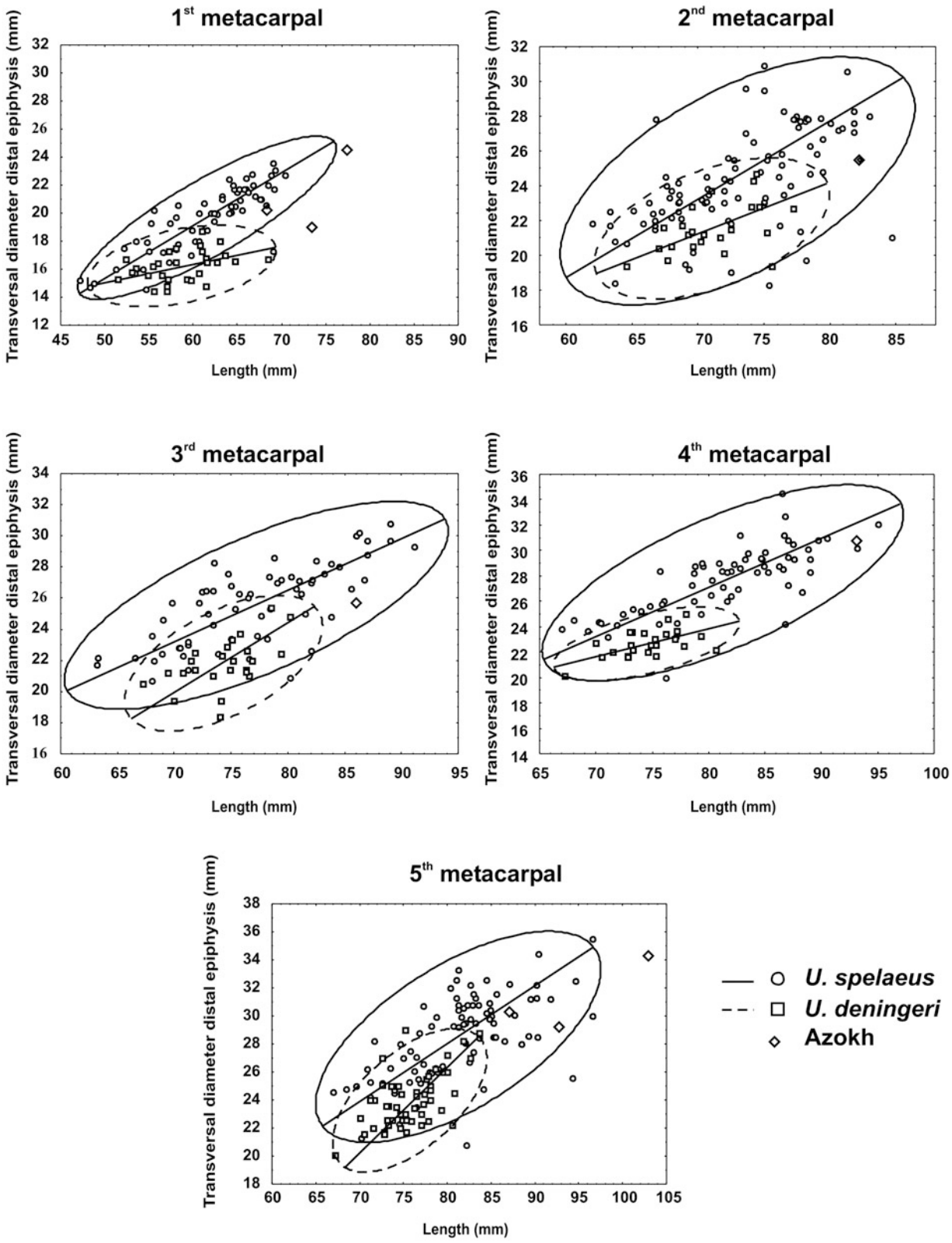

Fig. 6.4 Metrical comparison of the metacarpals of *Ursus* from Azokh 1 with those from the Iberian populations of *U. spelaeus* (El Reguerillo cave, Patones-Madrid and Arrikrutz cave, Oñati-Guipuzcoa) and *U. deningeri* (Sima de los Huesos, Atapuerca-Burgos). Equiprobability (95%) and regression lines have been added. Transversal diameter of the distal epiphysis is plotted against bone length. Data after Torres (1989)

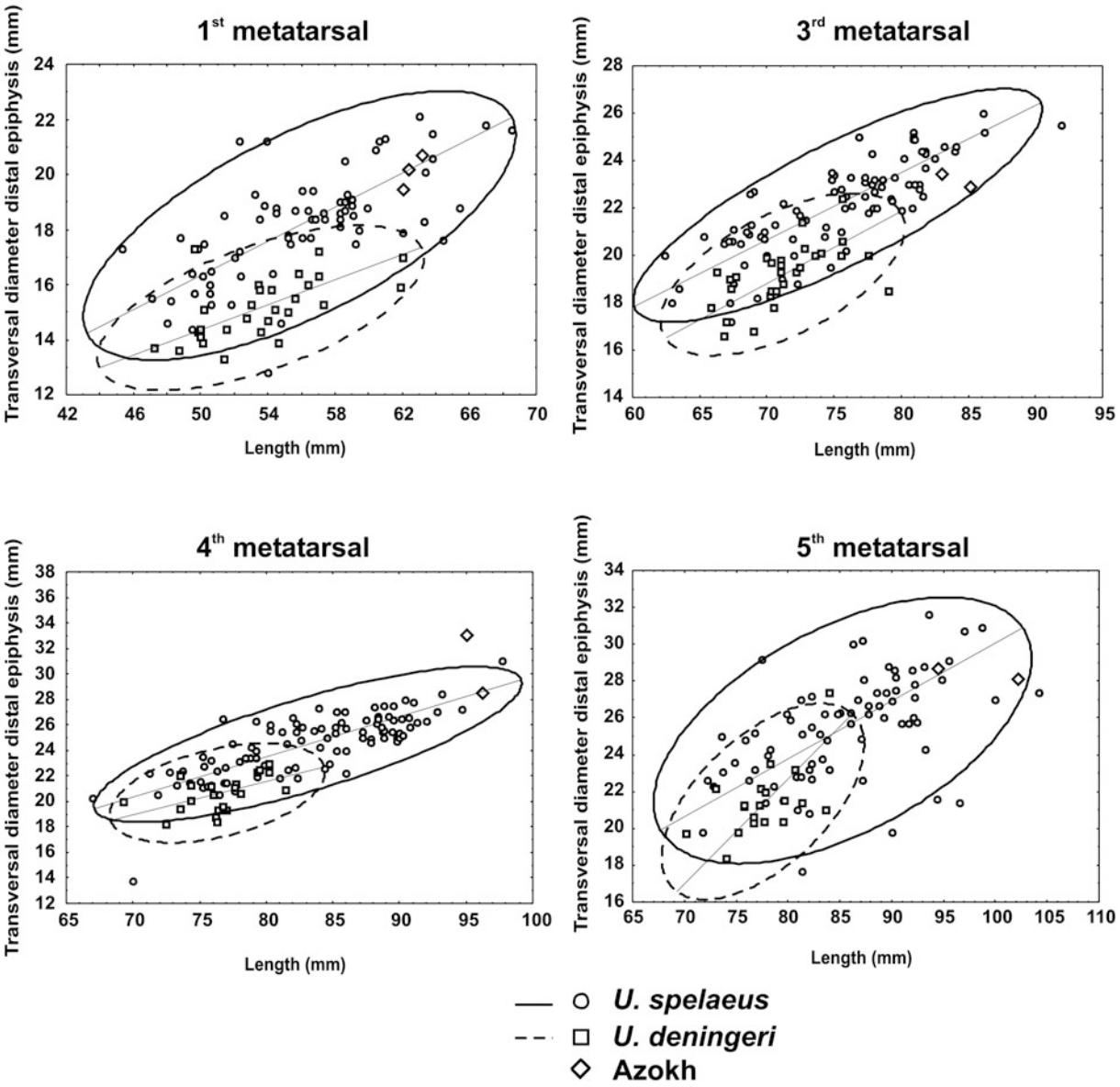

Fig. 6.5 Metrical comparison of the metatarsals of *Ursus* from Azokh 1 and those from the Iberian populations of *U. spelaeus* (El Reguerillo cave, Patones-Madrid and Arrikrutz cave, Oñati-Guipuzcoa) and *U. deningeri* (Sima de los Huesos, Atapuerca-Burgos). Equiprobability (95%) and regression lines added. The transverse diameter of the distal epiphysis is plotted against bone length. Data after Torres (1989)

complete metapodials from Azokh for a multivariate analysis, but Figs. 6.4 and 6.5 show bivariate diagrams of the transverse diameter of the distal epiphysis plotted against the total length of the bone. In all cases the size and robustness of the metapodials from Azokh match well the maximum values reached in the Iberian *U. spelaeus* samples and they are much larger and more robust than the metapodials of *U. deningeri*.

Dentition

The teeth form a mixed sample with elements from different Units and with different wear stages, which from a metrical point of view do not differ from *Ursus spelaeus*. In two second upper molars (III C46 7 Z = 173; I 54) the paracone is simply built, the protocone has a metaconule; the hypocone and metacone are duplicated and the talus is rounded.

The first (fourth) premolars (II C46 166 C = 193; II C46 294 Z = 104; IB) show a sharp protoconid with cutting anterior and posterior edges, an absent or poorly developed paraconid and a very small cusp (hypoconid) in the talonid region. In two first lower molars (II C46 294 Z = 104; II 86) the paraconid is simply built and with its oclusal face having a *U. spelaeus*-like arrangement: protoconid simple, metaconid duplicated, entoconid made of three cusplets of growing elevation towards the distal tip of the molar, hypoconid simple or more complex.

Table 6.4 Measurements of articular bones of *Ursus spelaeus* and *Ursus* sp. (II E45-46 B) from Azokh Cave. For patella: M1-vertical diameter; M2 transversal diameter; for calcaneus: M1-height; M2-maximum transversal diameter; M3-maximum anteroposterior diameter. For the remaining articular bones: M1-transversal diameter; M2-anteroposterior diameter; M3-height. Measurements are in mm

Number	Bone	Side	M1	M2	M3
II F52 167	Cuboid	D	40.0	48.7	31.0
II E 48 117B	Scapholunate	D	69.8	71.5	40.0
III D46 Z = 117	Scapholunate	D	60.0	62.6	
II C46 132 Z = 81	Scapholunate	D	64.0	66.4	
II C46 256 Z = 103	Scapholunate	S	61.6	65.0	
II C46 108 Z = 90	Pisiform	D	41.1	56.2	
II F51 1 Z = 173	Pisiform	S	41.6	59.3	33.3
II C46 89 Z = 80	Pisiform	S	36.6	56.2	36.3
II G51 25 Z = 187	Magnum	D	30.2	40.0	35.2
II RESCUE C45 10 Z = 117	Magnum	D	23.1	39.9	30.7
II I49 22 Z = 93	Magnum	D	22.3	36.2	29.5
II C46 303 Z = 118	Hamatum	D	38.0	39.0	44.4
II C46 318 Z = 112	Hamatum	D	36.6	35.2	41.0
II C46 204 Z = 92	Trapezius	D	18.7	32.9	23.8
II Rescue D45 4 Z = 89	Patella	D	63.1	33.4	67.2
II D45 3 RESC Z = 82	Patella	D	67.2	63.1	33.4
II D46 53 Z = 109	Patella	D	65.7	49.2	
II C46 348 Z = 123	Calcaneus	D			
II C46 169 Z = 92	Calcaneus	D	110.6	68	54.3
II 46	Calcaneus	D		66.4	
II I50 9 Z = 73	Calcaneus	D	105	75.1	67.3
II C46 339 Z = 121	Astragalus	D	67.2	58.7	
II C46 150 Z = 89	Astragalus	S	66.0	59.4	
II 45	Astragalus	D	67.2	58.7	
II 29	Cuboid	D	39.7	46.0	30.4
II I49 4 Z = 174	Scaphoid	D	43.6	45.7	16
II C46 281 Z = 106	Scaphoid	S	42.6	45.1	
II I49 12 Z = 181	Second cuneiform	D	18.2	27.8	15.8
II E45-46 B	Third cuneiform		19.6	27.0	13.4
III 114 Z = 165	Scapholunate	D	55.9		
III D46 160 Z = 226	Magnum	D	23.2	36.2	30.0
III D46 105 Z = 166	Calcaneus	D	101.9	65	55.4
Vu D45 26 Z = 55	Scapholunate	D	50.2	52.5	
Vu B clearing	Cuboid	S	28.4	35.2	24.7
Vm D42 12 Z = 90	Cuboid	D	39.6	43.9	29.4

In the second lower molars (Vu D45 45 Z = 46, II C46 294 Z = 104, II 54), the protoconid consists of a single cusp, the metaconid duplicated (one case) or more complex, the entoconid highly variable, and the hypoconid simple. The two third lower molars (Vu D47 27 Z = 54; II C46 294 Z = 104) show a squared crown perimeter and lingual sinus well developed. Since the sample size is small, no conclusions can be drawn from these observations. The only remarkable aspect is the lower morphology of the fourth lower premolars that looks "archaic". These morphologies were figured in the *Spelaearctos deningeri* subspecies of Baryshnikov (1998) but they also appear in low frequencies in large *Ursus spelaeus* samples.

Discussion

The bear remains from Azokh have been identified as *U. spelaeus,* matching well with those from Iberian localities that have been dated through amino acid racemization (AAR) to the upper part of the Middle Pleistocene (Torres et al. 2002). Similarly, Aliev (1969) identified the cave bear remains from Azokh as *Ursus spelaeus*, although other remains from the Caucasus have been identified as *Spelaearctos deningeri kudarensis* (Baryshnikov 1998, 2006; Doronichev 2000). However, today there is an almost general consensus to include the cave bear in the genus *Ursus*. Rohland et al. (2008) placed *Spelaearctos deningeri kudarensis* at the beginning of the MIS5 (120 ka) based on molecular chronology. This is confusing, since this date is much younger than the widely accepted last appearance of *U. deningeri* in west European localities, which are all of Early-Middle Pleistocene age): Petralona (Kurten and Poulianos 1977), Westbury (Andrews and Turner 1992), Sima de los Huesos (Torres and Cervera 1992; García et al. 1997), Santa Isabel cave (Torres et al. 2001), Cueto de la Lucia cave (Torres et al.

Table 6.5 Measurements of metapodial bones of *Ursus spelaeus* from the Azokh 1 (MC: metacarpal; MT: metatarsal) from Azokh Cave: M1-length; M2-transversal diameter epiphysis proximal; M4-transversal diameter diaphysis; M5-transversal diameter epiphysis distal. All measurements are in mm

Number	Bone	Side	M1	M2	M4	M5
II D45 5 Z = 88 RESC	MC/T1		49.8	27.7	18.1	20.6
II D46 19 Z = 98	MC1	S	73.4	29.6	13.4	19.0
II D46. 8 Z = 100	MC1	S	68.3	27.7	13.6	20.3
II B (stone) Z = 164	MC2	S		14.4		
II C46 279 Z = 107	MC2	D	82.2	22.3	17.6	25.5
II F51 23 Z = 169	MC3	D		23.2	19.3	
II C46 328 Z = 114	MC3	S	86.0	21.7	15.3	15.7
II C45 gen finds	MC3	D		22.5	20.5	
II F52 18 Z = 169	MC4	S	93.2	34.9	21.4	30.7
II D46 97 Z = 152	MC4	D		26.6	19.2	
II D45 Rsc. 26 Z = 121	MC5	D	87.6	35.6	20.2	30.2
II F52 3 Z = 160	MC5	D	93.4	35.0	17.4	
IIa F52 161	MC5	S	92.8	38.6	19.0	29.2
II C46 313 Z = 107	MC5	D		32.1	29.6	
II C46 280 Z = 100	MT1	D	62.0	26.4	13.6	19.4
II 16	MT2	D	74.2	18.5	15.6	22.2
II I50 8 Z = 77	MT3	D	82.9	19.3	17.6	23.5
II D46 87 Z = 138	MT3	D	85.3	22.9	15.7	22.8
II C46 276 Z = 101	MT4	S		19.4	14.6	
II 17	MT4	S		26.7	14.6	
II G51 24 Z = 178	MT4	D	96.2	27.5	19.3	28.6
II I50 4 Z = 74	MT5	S	94.4	36.3	16.6	28.6
III D46 155 Z = 221	MC2	D		22.7	16.3	
III D45 21 Z = 198	MT1	D	63.2	28.5	13.0	20.7
III D46 152 Z = 219	MT5	S	102.3	36.3	15.6	28.0
Vu E45 Gen finds	MC1	S	77.4	33.8	17.6	24.5
Vu E45 4 Z = 61	MC5	S	103.0	36.6	22.9	34.3
Vu E44 11 Z = 131	MT4	S		22.0	16.7	
Vu D45 18 Z = 35	MT4	D	95.0	30.0	21.0	33.0

2006), L'Escale (Bonifay 1971, 1975a), Mosbach and Süssenborn (Soergel 1926), Hundsheim (Zapfe 1946), Cal Guardiola (Madurell-Malapeira et al. 2009).

Ursus deningeri has specific characters (Kurten and Poulianos 1977; Torres 1978; Rabeder et al. 2010), among others:

- The *ramus ascendensis* of the mandible is tilted backwards in a characteristic way.
- Bones and teeth are smaller than in *Ursus spelaeus*.
- Limb and paw bones are more slender than in *U. spelaeus*.
- Frequent, though erratic, presence of some of the first, second and third upper and lower premolars or their alveoli.
- Frequently, but not in all the cases, the heel of the second upper molar shows an acute end.
- The third lower molar is small and, in many cases, the crown perimeter is elliptical or almost circular.
- In some cases the fourth lower premolar shows a simple architecture, the protoconid being the only cusp.

With the sole exception of the last one, these characters are absent in the Azokh Cave bear, but these more "carnivorous-like" premolars are present in 1% of the sample from the Iberian Peninsula (Torres 1989) compared with 14% of the Iberian sample of *Ursus deningeri*. We can conclude therefore that the Azokh bear can be placed in *Ursus spelaeus*.

Recent work based on fossil DNA (Rabeder et al. 2004) revealed a scenario that is more complex than expected, with three subspecies (*U. spelaeus*, *U. s. ladinicus*, *U. s. eremus*), while the new *speleus*-like species *Ursus ingressus* was also defined. Further DNA studies on Asian cave bears (Knapp et al. 2009) confirm differences between European cave bears (*U. spelaeus* and *U. ingressus*) and Asian cave bears (*U. deningeri kudarensis*) adding more confussion to the well known chronostratigraphical range of *U. deningeri.* Thus, the small morphological and metrical differences between the Azokh bears and typical *U. spelaeus* cannot be interpreted in the way of a "recent" *U. deningeri* representative, but we do not discard the possibility that they represent a local subspecies.

Table 6.6 Measurements of phalanx (F) *Ursus spelaeus* from Azokh 1. For F1 and F2: M1-length; M2-transversal diameter epiphysis proximal; M3-transversal diameter diaphysis; M4-transversal diameter epiphysis distal. For F3: M1-maximum proximal epiphysis transversal diameter; M2-length. All measurements are in mm

Number		M1	M2	M3	M4
D45 5 Z = 82	F1	49.8	27.7	18.1	20.6
E45 46C	F1			17.6	19.6
II Rescue D45 32 Z = 133	F1	53.6		21.4	24.7
II D46 61 Z = 125	F1	40.0	22.5	15.4	17.2
II Rescue C45 Gen finds	F1	43.0	23.7	16.0	18.2
II D45 7 Z = 142	F1	41.0	24.5	17.1	18.7
Rescue D45 29 Z = 123	F1	50.0	25.1	17.5	19.6
Rescue C44/C45. Gen finds	F1	45.8		15.5	18.4
II Rescue D45 Gen finds	F1	44.4			
II D46 13 Z = 104	F1	44.2	22.1	14.4	16.8
II F48 64 Z = 69	F1	49.4	28	16.9	20.0
II C46 325 Z = 111	F1	45.3	25.0	17.3	11.4
II C46 332 Z = 119	F1	44.0	23.1	17.2	11.8
II C45 5 Z = 63	F1	46.2	21.7	16.2	11.2
II C46 222 Z = 94	F1		28.0	19.4	
II C46 246 Z = 99	F1	50.2	28.0		
II G51 27 Z = 191	F1	51.3	28.9	24.3	14.6
III D46 161 Z = 227	F1	47.7	18.5	19.8	
III Trench clearing B	F1	43.7	23.5	20.4	16.2
Vu E43 voyager	F1	50.1	38.1	17.0	20.6
Vu E43 3 Z = 109	F1	39.9	24.1	15.6	17.8
Vu D44 3 Z = 59	F1	44.0	24.1	15.9	19.5
Vu F44 11 Z = 142 (CUTS)	F1	50.9	25.3	11.6	18.9
Vm E41 10 Z = 123	F1	47.2		14.8	20.0
Vm E40 2 Z = 113	F1				18.3
F52 153	F2	34.8	26.8	19.7	19.8
II D46 40 Z = 106	F2	29.0		16.8	9.7
II Rescue C45/D45 mixed	F2	34.0	22.2	15.5	16.8
II D46 39 Z = 111	F2	33.9	22.3	17.2	18.7
II F51 24 Z = 169	F2	35.4			19.3
II H49 16 Z = 116	F2	30.6	20.4	18	9.3
II C46 74 Z = 73	F2	25.2	24.2	19.8	9.2
II C46 199 Z = 99	F2	26.3	19.5		9.9
II F49 4 Z = 99	F2	28.8	18.1	16.1	8.6
Vm F41 gen finds	F2	29.0	21.1	16.1	19.0
II 4	F3	34.5	14.4		
II Rescue D45 gen finds	F3	35.0	13.3		
II C45 gen finds	F3	39.7	18.4		
II D46 17 Z = 95	F3	38.3	18.4		
II F52 14 Z = 162	F3	49.0	21.2		
II C46 46 Z = 65	F3	15.8	35.5		
II C46 170 Z = 93	F3	20.2	37.9		
III Rescue D45 gen finds	F3		16.2		
III D46 120 Z = 188	F3	42.3	17.3		
Vu E44 31 Z = 111	F3	46.8	17.7		

The presence of a Middle Pleistocene *Ursus spelaeus* matches very well with the interpretations of the first appearance of the species around 300 ka (Rabeder et al. 2004; Croitor and Brugal 2010), and with the numerical ages obtained through ESR and AAR dating of Azokh tooth samples (Murray et al. 2016). This also coincides with the ages obtained after systematic ESR and AAR dating of a large number of *U. spelaeus* localities that reveals that while most of them clustered in the Upper Pleistocene, two localities, El Reguerillo cave and Arrikrutz cave were much older: ca. 150–160 ka (upper part of the Middle Pleistocene; Torres et al. 2002). Cave bears remains from these two localities show a predominance of big sized bones and teeth.

Family Mustelidae Fischer de Waldheim, 1817

Meles meles (Linnaeus, 1758)

New material

Unit Vu

Azokh 1, Unit Vu, D-45, 53 (z = 63, 7-8-08) – left mandible with P_{3-4} and M_1, alveoles of P_2 and C_x; P_3: DAP = 5.8, DTa = 2.8, DTp = 3.4; P_4: DAP = 7.0, DTa = 3.4, DTp = 4.0; M_1: DAP = 17.1, DAPtrigonid = 9.1, DTa = 5.4, DTp = 7.9.

Description of the new material and taxonomic classification

The P_3 and P_4 (Fig. 6.6) are simple teeth with a main cusp from which anterior and posterior smooth crests descend. There are no cusps on the talonids. The crowns are short and high. Each tooth has two roots. The M_1 is a carnassial with a trigonid with low cusps, the metaconid being well developed; the talonid is enlarged with four well developed cusps. From the protoconid backwards all cusps are heavily worn. The low trigonid on the carnassial and a very extended talonid points to *Meles*.

Discussion

Various species and subspecies of *Meles* have been named on the basis of fossils (e.g., Crégut-Bonnoure 1996). Wolsan (2001) noted that these species and subspecies fit within the ranges of variation of the living species, but refrained from formally synonymizing them until the problem is resolved about whether or not the living Asiatic badgers belong to a different species, called *Meles anakuma*. At present that species is not recognized as different from *Meles meles* (Wilson and Reeder 1993; Duff and Lawson 2004).

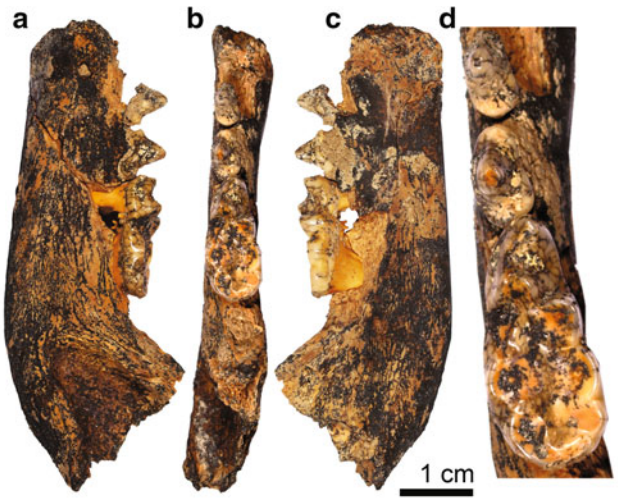

Fig. 6.6 *Meles meles*: Azokh 1, Unit IV, D-45, 53 – left mandible with P_{3-4} and M_1 (**a**–**c** buccal, occlusal and lingual views; **d** close up of occlusal view)

Material from Unit V was assigned to *Meles meles*, the living species of badger (Aliev 1969; Lioubine 2002; Rivals 2004). Likewise we assign the new material from Unit Vu to *Meles meles*. The badger appeared in Europe during the Late Pliocene with the species *Meles thorali* (Crégut-Bonnoure 1996), which is inseparable from the living species *Meles meles* (Wolsan 2001). A variety of species of the genus *Meles* are cited from the Early to the Late Pleistocene of north China, while *Meles meles* is cited from the Middle and Late Pleistocene (Xue and Zhang 1991). The species lives in wooded areas from western Europe to the Middle East and to Japan.

Martes cf. *foina* (Erxleben, 1777)

Material from Unit V was attributed to *Martes* cf. *foina* or *Martes foina* (Aliev 1969; Lioubine 2002; Rivals 2004), but the new collections do not include fossils that are attributable to this species. At present it lives in an area that extends from Europe to China. Excepting the larger species, the fossil record of the mustelids is not well known.

Family Canidae Fischer de Waldheim, 1817

Vulpes vulpes Linnaeus, 1758

New material

Unit V

Azokh'03, uppermost platform, D-44, 10-8-03, 3 – left mandible with canine and P_{2-3}: canine DAP = 4.9, DT ≥ 3.6; P_2 DAP = 8.5, DTa = 2.5, DTp = 2.8; P_3 DAP = 9.0, DTa = 2.6, DTp = 2.9.

Azokh'03, uppermost, D-45, rescue general finds – right mandible fragments with P_4 and alveoles P_3 and M_{1-3}: P_4 DAP = 9.5, DTa = 3.2, DTp = 3.7.

Description of the new material and taxonomic classification

Both specimens seem to belong to the same individual. The mandible is gracile and shallow (Fig. 6.7). The canine is slender and relatively high, and the premolars are high and narrow. The P_2 has a main cusp with anterior and posterior crests that are concave in side view. The P_3 and P_4 both have a cusp on the talonid. There are two alveoles for the P_1 and one alveole for the M_3. Size and morphology are similar to the recent and fossil *Vulpes vulpes* from l'Escale (Bonifay 1971).

Discussion

Material from Unit VI was assigned to *Vulpes vulpes* (Aliev 1969; Lioubine 2002; Rivals 2004). The new material shows this species to be present also in Unit II. *Vulpes* foxes were present already in the Pliocene. The red fox *Vulpes vulpes* is known in Europe from localities as old as Arago (Crégut-Bonnoure 1996). *Vulpes vulpes* is cited from the Late Pleistocene of northern

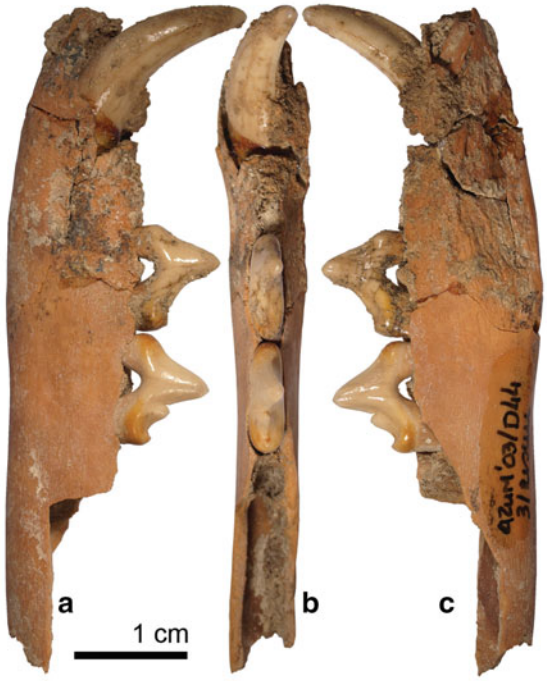

Fig. 6.7 *Vulpes* from Azokh II: Azokh'03, uppermost platform, D-44, 10-8-03, 3 – left mandible with canine and P_{2-3} (**a–c** buccal, occlusal, and lingual views)

China and *Vulpes* cf. *vulgaris* and *Vulpes vulgaris* from the Middle and Late Pleistocene, respectively (Xue and Zhang 1991). The latter species is considered to be synonymous with *Vulpes vulpes* (Wilson and Reeder 1993). At present the species occurs in an area extending from Europe to north Africa, northern Asia, the north of India and north America.

Canis aureus Linnaeus, 1758

New material

Unit Vm

G-40, 6/9/02, G940 – right calacaneum: L = 39.6, Lu = 27.6, Ll = 14.5, DAPh = 12.4, DTh = 11.3, DAPn = 10.3, DTn = 7.2, DAPsf = 15.9, DTsf = 13.5.

Description of the new material

The calcaneum has the general morphology of a carnivore (Fig. 6.8). It is a little smaller and more gracile than that of *Lynx spelaea*, similar to that of *Canis lupus*, but much smaller. It is similar to those of *Vulpes vulpes* and *Vulpes praeglacialis*, but it is larger than several specimens attributed to these species (Bonifay 1971; Schmid and Garraux 1972; Dufour 1989).

Discussion

Material from Unit V was described as belonging to the jackal *Canis aureus* (Aliev 1969; Lioubine 2002; Rivals 2004). *Canis aureus* is of a size intermediate between

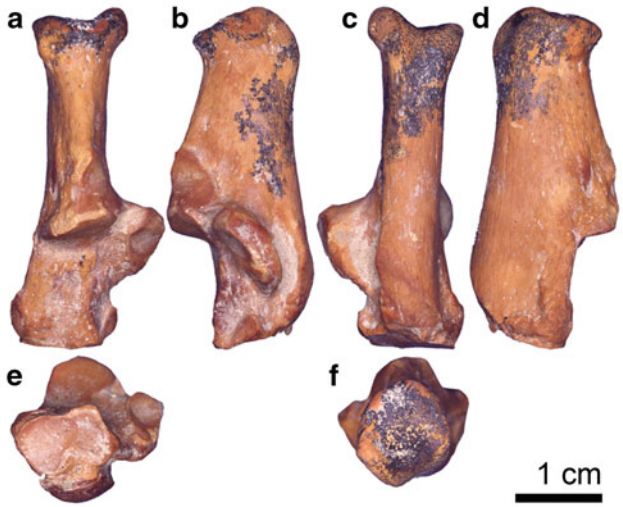

Fig. 6.8 *Canis aureus* from Unit V: G-40, 6/9/02, G940 – right calacaneum (**a–f** anterior, medial, posterior, lateral, lower and upper views)

C. lupus and *Vulpes*. It seems likely that the specimen described above belongs to this species. Morphological resemblances suggest a link between *Canis aureus* and the Late Pliocene *Canis arnensis* (Torre 1967; Crégut-Bonnoure 1996). The jackal is a living species in SE Europe, North Africa, the Middle East and south and central Asia.

Canis lupus Linnaeus, 1758

New material

Unit II

AZUM'03, D46, 14 – left M_1, talonid: DTp = 10.3. Figure 6.9.

Unit Vu

AZM Middle plat, cleaning, 26-07-05, right D_4: DTp = 3.8. Figure 6.9.

Unit Vm

AZM'05/F38/1 – third phalanx: L = 15.8, DAPp = 10.1, DTp = 6.8. Figure 6.9.

Description of the new material and taxonomic classification

The talonid of the lower carnassial from Unit II has two major cusps (Fig. 6.9/1), as in *Canis* and unlike in *Cuon* and *Lycaon*. Size increase in European *Canis* is well illustrated by large numbers of measurements of the length of the lower carnassial (Van der Made 2010b, Fig. 4). Usually the maximum width of this tooth is given in the literature, but not the slightly smaller talonid width. As a consequence, the size trend in the talonid is illustrated here by fewer measurements (Fig. 6.9/2). The large size of the talonid of the M_1 suggests that the material belongs to *Canis lupus*. A third phalanx (Fig. 6.9/4) and deciduous carnassial (Fig. 6.9/3) seem to belong to the same or a similar species.

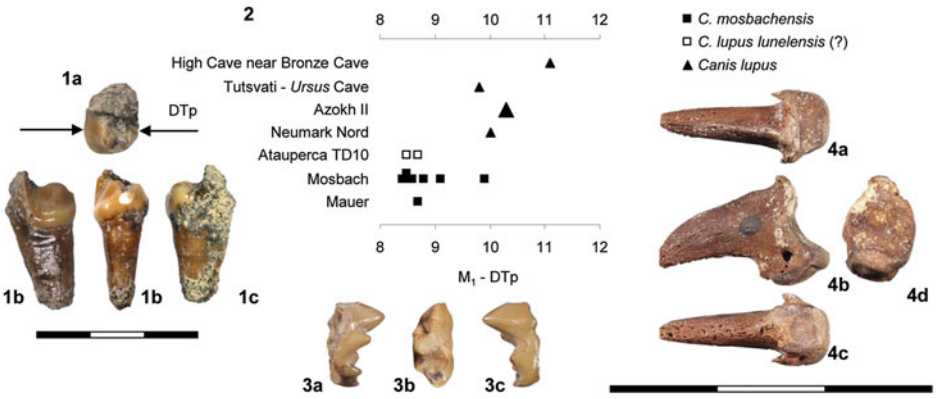

Fig. 6.9 **1** *Canis lupus* from Azokh: AZUM'03, D46, 14 – talonid of left M_1 (**a**–**d** occlusal, bucal, posterior, and lingual views). **2** Size increase of the width of the talonid (DTp) of the M_1 in *Canis.* Localities in approximate stratigraphic order from old (bottom) to young (top): Mauer (SMNK), Mosbach (NMM), Atapuerca (LAUT, CENIEH), Neumark Nord (LVH), Azokh, Tutsvati (GSM), High Cave (GSM). **3** *Canis* cf. *lupus* from Azokh IV: AZM, middle plat, 26-7-05 -right D_4 – lingual, occlusal and buccal views). **4** *Canis* cf. *lupus* from Azokh V: AZM'05, F38, 1 – third phalanx (**a**–**d** dorsal, side, plantar, and proximal views). Scale bars indicate 3 cm: left scale bar for M1 and right scale bar for the remaining photographs

Discussion

Material from Azokh V was assigned to *Canis* cf. *lupus* (Aliev 1969; Lioubine 2002; Rivals 2004). If the presence of that species in Unit V could be confirmed, this would be important for the biochronology of that unit, but the new material from Units IV and V is too poor; the new material that can be assigned to this species is from the younger unit Unit II.

At the end of the Pliocene, *Canis* dispersed from the New to the Old World. The first European species of the wolf lineage, *Canis etruscus* and *Canis mosbachensis*, were small, but they were replaced by *Canis lupus*, which may have evolved from the latter species or from a form close to it (Kahlke 1994). The wolf appeared initially with the somewhat larger subspecies *Canis lupus lunellensis* (in Lunel Viel, Heppenloch and TD10a; Bonifay 1971; Adam 1975; approximatly OIS 9-11) and later by the still larger *Canis lupus lupus* (Neumark Nord, Ehringsdorf, Chatillon St. Jean; OIS7). *Canis lupus* is cited from the middle and late Middle Pleistocene of China (Xue and Zhang 1991). The actual geographic distribution of the wolf extends from Europe and Asia to North America.

Family Hyaenidae Gray, 1821

Crocuta crocuta (Erxleben, 1777)

New material

Unit Vu

Middle plat., cleaning, 26-07-05 – left I_3: DMD = 11.1, DLL = 11.1, Hli = 15.7, Hla = 17.0.

Unit Vm

Azokh, 28-7-05, plat middle, Unit V, z = 138-147, F-39, river sieving coarse – right mandible with canine and P_2: Canine: DAP ≥ 15.4, DT ≥ 12.4; P_2: DAP = 16.1, DTa = 9.5, DTp = 11.1, Hli = 9.8, Hla = 11.2.

Description of the new material and taxonomic classification

The mandible is massive (Fig. 6.10/1). The canine is stout and short; its tip is about level with the tip of the premolar and was probably not fully erupted. The diastema between canine and P_2 is about 3.8 mm. The premolar is massive, as in the Hyaenidae, while in the Felidae it would be more elongate. It has a relatively low main cusp as in *Crocuta* and unlike in *Hyaena*, where the tip tends to be higher. No wear can be seen on this tooth, suggesting again that the individual was relatively young when it died. The I_3 is very large and has a well developed lateral cusp (Fig. 6.10/2).

Discussion

Material from Unit V was assigned to *Crocuta spelea* (Aliev 1969; Lioubine 2002; Rivals 2004). Many authors consider this to be a subspecies of the living spotted hyena *Crocuta crocuta* (e.g., Crégut-Bonnoure 1996; García and Arsuaga 1999). During the earliest Pleistocene, the genus *Crocuta* was present in Africa and the Indian Subcontinent (De Vos et al. 1987; Turner 1990), The genus was present in Europe at about 1.4 Ma in Ubeidiyah and dispersed not later than at 0.8 Ma into western Europe (García and Arsuaga 1999), and the species *Crocuta crocuta* was present in the area long before the formation of Unit V at Azokh. There were different subspecies of *C. spelaea*, which may have stratigraphic significance (Crégut-Bonnoure 1996). The new material confirms the presence of *Crocuta* in Azokh, but it is insufficient for a subspecific assignment and a discussion of the biochoronological implications.

Fig. 6.10 *Crocuta crocuta* from Unit IV and V: Azokh, 28-7-05, plat middle, Unit V, z = 138-147, F-39, river sieving coarse – right mandible with canine and P_2 (**1/a–c** lingual, occlusal and buccal views); Middle plat., cleaning, 26-07-05 – left I_3 (**2/a–e** apical, lingual, mesial, labial, and distal views)

Family Felidae Fischer de Waldheim, 1817

Felis chaus Schreber, 1777

Felis chaus was cited from Unit V (Aliev 1969; Lioubine 2002; Rivals 2004). This species is not represented in the new collections. *Felis chaus* lives at present in an extensive area stretching from Egypt to the Middle East and to southern China and SE Asia. Though its vernacular name is jungle cat, it occurs in a variety of habitats, including dry environments.

Lynx sp.

Felis lynx was cited from Unit V (Aliev 1969; Lioubine 2002; Rivals 2004). The new collections do not include any lynx material. At present several species are recognised in the genus *Lynx*: the living *Lynx pardina* in the Iberian Peninsula and *Lynx lynx* in nothern Eurasia and the fossil *Lynx pardina spelea* of the late Middle and Late Pleistocene of large parts of Europe and a still older form called *Lynx issiodorensis* (Argant 1996). On the one hand, it has been suggested that material from Mauer and Soleilhac, that is usually assigned to the latter species, might in fact belong to *L. pardina spelaea* (Argant 1996), while on the other hand, it has been argued that the species *Lynx issiodorensis* should better be placed in the genus *Caracal* (Morales et al. 2003). The material from Azokh might be expected to belong to *Lynx pardina spelaea*, but we cannot confirm this.

Panthera pardus Linnaeus, 1758

New material

Unit III

Azokh uppermost, 21-8-03, D-46, in sample for palynology, z = 162 – left I^3: DLL = 8.1, DT = 5.4.

Unit II

Azokh 1, Unit II, 3-8-08, C45, 21 (z = 123) – left humerus: DAPd = 37.2, DTd = 61.9, DTdf = 41.1, R1-4 = 28.4-18.3-23.9-21.7.

Azokh uppermost, 12-8-03, C-45, rescue, 19 (z = 134) – right calcaneum: L = 72.8, Lu = 51.7, Ll = 24.4, DAPh ≥ 23.7, DTh > 17.2, DAPn = 23.5, DTn ≥ 14.7, DAPsf = 29.1, DTsf = 29.3.

?Azokh uppermost, 14-8-03, D-46, 11 (z = 100) – first phalanx, distal part: DAPd = 9.6, DTd = 12.2, L ≫ 38.

Description of the new material and taxonomic classification

The distal humerus has a supracondylar foramen (Fig. 6.11), which is common in Felidae, but lacking in Hyaenidae, Canidae and Ursidae. The distal articulation is wide and with a relatively small radius of curvature. This is unlike in Hyaenidae and Canidae. The specimen is much smaller than

Fig. 6.11 *Panthera pardus* Unit II, 3-8-08, C45, 21 (z = 123) – left humerus (**a–c** anterior, distal, and posterior views)

its homologue of a recent or fossil *Panthera leo* (LAUT; Dufour 1989), smaller also than in *Panthera onca gombaszoegensis* (Hemmer 2001), but larger than those of recent and fossil *Lynx* (Hemmer 2001). The calcaneum is intermediate in size between those of a wolf and a lion.

Discussion

Panthera pardus was described or cited from Azokh Unit V (Aliev 1969; Lioubine 2002; Rivals 2004). The new finds show this species to be present in Units II and III as well. The leopard may have originated in Africa and it dispersed into Europe around 0.5–0.6 Ma ago (e.g., its presence in Mauer), where it survived until close to the end of the Pleistocene (Crégut-Bonnoure 1996). In China it is cited from the Early to Late Pleistocene (Xue and Zhang 1991).

Order Perissodactyla Owen, 1848

Family Equidae Gray, 1821

Equus cf. *ferus* Boddaert, 1784

New material

Unit V

?Azokh 1, Unit V, 21-8-09, H-41, 42 (z = 854) – fragment of a cheek tooth.

Description of the new material and taxonomic classification

The tooth fragment belonged to a tooth with a crown height of well over 45 mm. It is a small fragment consisting of enamel, dentine and cementum. The enamel is folded in a complex way as is common in the cheek teeth of *Equus*, but it is not possile to see which part it represents, and it is not possible to be sure of its species designation: for example it may belong to *E. hydruntinus*.

Discussion

Material from Unit VI was assigned to *Equus caballus* (Aliev 1969; Rivals 2004) but later the assignment seems to have been changed into *Equus suessenbornensis* (Lioubine 2002).

During the Middle and Late Pleistocene, there were two groups of equids in western Europe. One group included the relatively small and gracile "stenonid" species, with *Equus altidens* in the early Middle and *Equus hydruntinus* in the late Middle and Late Pleistocene. (Stenonid/caballoid refers to the shape of the lingua flexid, separating the genus in two groups, following Forsten 1992). The other group was made up of predominantly large forms with "caballoid" morphology. Some authors, like Eisenmann (1991) recognized many caballoid species, while others like Forsten (1988) recognized fewer species (*E. mosbachensis*, *E. germanicus*, *E. caballus*); still others, like Azzaroli (1990), recognized just the single species *E. caballus*. The very large stenonid *Equus suessenbornensis* may have given rise to the caballoid horses, which further declined in size. The transition must have occurred around 600 ka. At present the name *Equus caballus* is restricted to the domestic horse, while the wild form, including przewalski's horse, is referred to as *Equus ferus*.

A second phalanx from Unit V in the collections in Baku is larger than a specimen from Unit 1 that is here assigned to *Equus caballus* (see below). It is also larger than the second phalanges from the Würmian of Villa Seckendorf, which were assigned to *E. germanicus* (Forsten and Ziegler 1995), larger than the phalanges from Taubach (Musil 1977) and Atapuerca TD10 (LAUT), but it is close in size and robusticity to two phalanges of *E. suessenbornensis* from Süssenborn (Musil 1969). The large size of this equid probably gave rise to the determination as *E. suessenbornensis*, but the material might well belong to a caballoid horse of the size of the Mosbach horse. In view of the likely age of Unit V, we favor Aliev's (1969) earlier assignment, but with updated nomenclature: *Equus* cf. *ferus*.

Equus cf. *caballus* Linnaeus, 1758

New material

Unit I

Azokh 1, Unit I, subunit I, 14-7-2007, C-50, 4 (z = 116) – left second phalanx: L = 49.0, Ldors = 37.1, DTmini = 40.3, DTp = 47.5, DAPp = 30.7, DTd > 40.4, DAPd ≥ 25.2.

Description of the new material and taxonomic classification

The second phalanx from Unit I is of the common equid morphology (Fig. 6.12/1). It is relatively large and robust and it is larger than its homologue in *E. hydruntinus*, but similar in size to those of the wild *E. ferus* and its domestic descendant *E. caballus*. We are not able to distinguish between the wild and domestic species, but since Unit 1 is very recent, the phalanx probably represents *Equus caballus*.

Equus hydruntinus Regalia

Aliev (1969) assigned material from Units VI, V and III to *Equus hydruntinus*. This was a small and gracile species, probably closely related (or ancestral) to the living *Equus hemionus*, which was widespread during the late Middle and Late Pleistocene.

Equus cf. *asinus* Linnaeus, 1758

New material

Unit I

Azokh 1, Unit I, E-51, 49 (z = 46, 4-8-06) – right navicular: DT = 36.8.

Description of the new material and taxonomic classification

The navicular of equid morphology is very small (Fig. 6.12/2). The surface of the bone is smooth. The posterior part is

Fig. 6.12 *Equus* cf. *caballus* Unit I, subunit I, 14-7-2007, C-50, 4 (z = 116) – left second phalanx (**1/a**, **b** dorsal and distal views); and *Equus* cf. *asinus* from Azokh I: Azokh I, unit I, E-51, 49 (z = 46, 4-8-06) – right navicular (**2/a**, **b** approximal and distal views)

broken, showing that the compact bone is very thin at this place. This might indicate that the individual was not fully adult, although the smooth surface of the bone suggests that the individual was nearly adult and may have attained more or less its adult size.

Discussion

The fossil bone may have belonged to an individual that was not fully adult, but neither was it very young, and its small size thus suggests a small species rather than a small individual of a large species. *Equus hydruntinus* is a small and gracile species, probably closely related (or ancestral) to the living *Equus hemionus*. Alternatively (and depending on its geological age), the bone may have belonged to the domestic donkey *Equus asinus*, which is a descendant of the african wild ass *Equus africanus,* and which was introduced in Eurasia during the Holocene. Since the material from Unit I is Holocene, it probably is a domestic donkey.

Family Rhinocerotidae Gray, 1821
Stephanorhinus kirchbergensis (Jäger, 1839)

New material

Unit Vm

Azokh 1, Unit V, 27/7/09, D-15, 1 – left mandible fragment with $M_{2\text{-}3}$; M_2: DTp = 37.4; M_3: DAP = 58.3, DAPb = 53.7, DTa > 28.9, DTp = 31.6, H = 29.6.

Description of the new material and taxonomic classification

In lingual view, the posterior valley of the third lower molar (Fig. 6.13/3) is U-shaped or slightly parabolus shaped. This is typical for *Stephanorhinus kirchbergensis*, while it is clearly V-shaped in *Stephanorhinus hemitoechus* (Van der Made 2000) and more variable and intermediate in *Stephanorhinus hundsheimensis*. The teeth have finely crenelated enamel, unlike in *Coelodonta* or *S. hemitoechus*, where the crenelation is much more coarse. The transverse diameter and crown height are in the range of *S. kirchbergensis*, while the latter variable is larger than in *S. hundsheimensis* (Fig. 6.13/1).

Discussion

Aliev (1969) and Rivals (2004) assigned all rhinoceros material from Azokh to *Dicerorhinus mercki*, while Lioubine (2002), following Guérin and Barychnikov (1987), cited "*Dicerorhinus etruscus brachycephalus* (défenition C. Guérin)" from Unit VI. Most specialists now apply the names *Stephanorhinus kirchbergensis* and *Stephanorhinus hundsheimensis*, respectively, for these taxa (Fortelius et al. 1993).

A third molar (MUB 4/227) from Unit VI has a similar morphology, size and degree of hypsodonty as the specimen described above, but most other specimens in the old collections seem to belong to *S. hemitoechus* (see below).

Stephanorhinus kirchbergensis appears first in localities like Mosbach, with an age of 500–600 ka (Van der Made 2000, 2010a; Van der Made and Grube 2010). It is an "interglacial species", dispersing during the interglacials from an unkown area into Europe. Though material from many localities in Spain was formerly assigned to *S. mercki*, in a revision by Cerdeño (1990) all this material was assigned to to *S. hemitoechus*. *Dicerorhinus mercki* (*S. kirchbergensis*) is cited from Zhoukoudian (Choukoutien) and other localities in China, suggesting a possible source area for the interglacial dispersals of that species to Europe (e.g., Xue and Zhang 1991). However, the material (IVPP; ZSM) is not completely identical and others assign it to *Stephanorhinus choukoutienensis* (or *Dicerorhinus choukoutienensis*). *Stephanorhinus kirchbergensis* was still abundant during the Eemian, but went extinct during a later part of the Late Pleistocene.

Stephanorhinus hemitoechus (Falconer, 1859)

New material

Unit Vu

? – Azokh upper, 15/09/02, D-43, 10 (z = 72) – nasalia.

Unit Vm

Azokh 1, unit V, 2-8-2009, I-4, 15 (z = 251) – left M_3: DAP = 52.9, DAPb = 51.0, DTa ≥ 31.3, DTp = 28.2, H > 27.4.

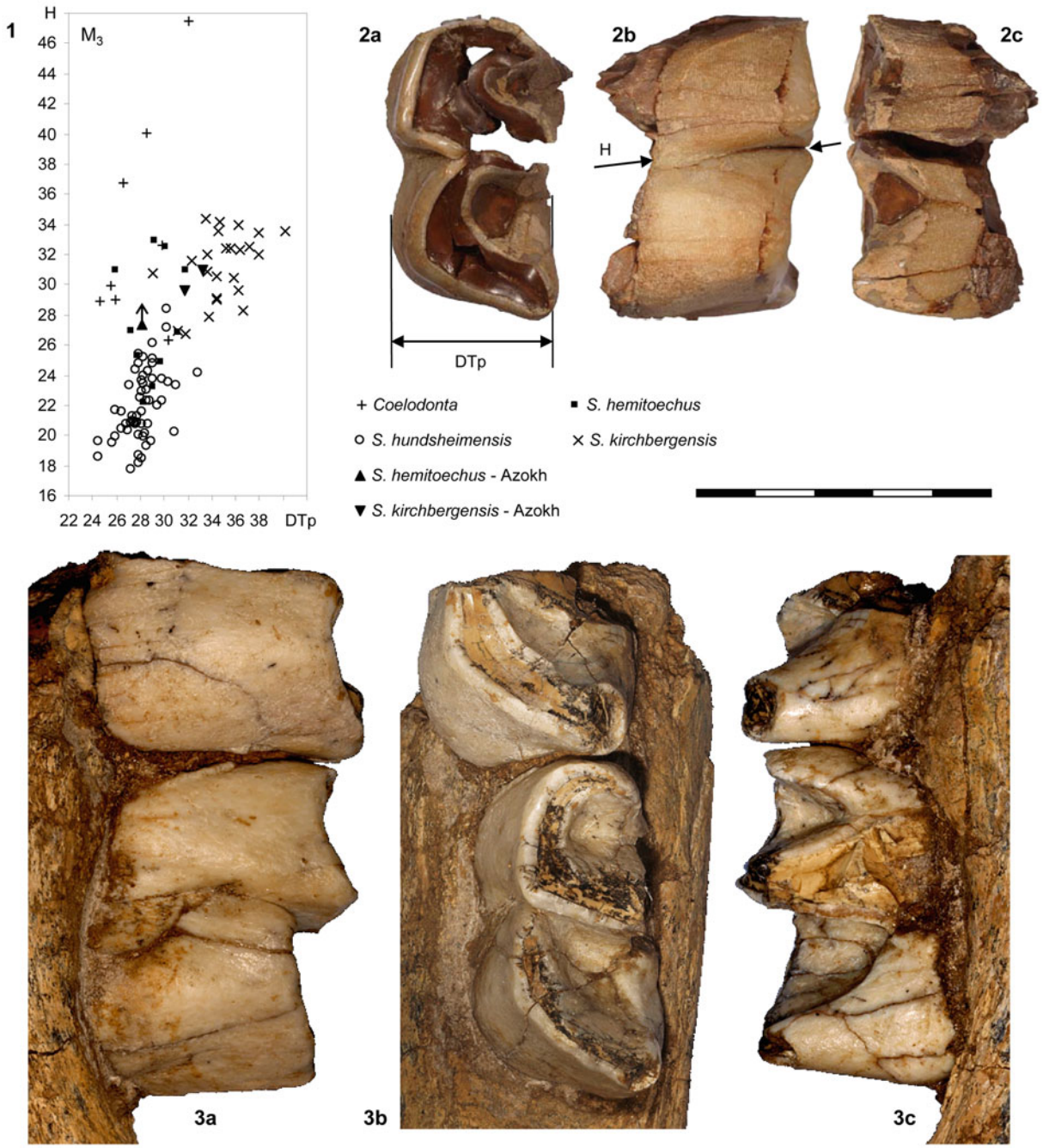

Fig. 6.13 **1** The third lower molar (M_3) in Rhinocerotidae. Bivariate diagram of the width of the posterior lobe (DTp) versus the height (H) at the trigonid-talonid junction: *Coelodonta* from Steinheim (SMNS), Maastricht-Belvedère (NMMa), Backleben (IQW), Heldrungen (IQW), Eich (NMM); *Stephanorhinus hundsheimensis* from Voigtstedt (IQW), Süssenborn (IQW), Soleilhac (MCP), Mauer (SMNK); *Stephanorhinus hemitoechus* from Steiheim (SMNS), Taubach (IQW), Eich/Gimbsheim (NMM), Gimbsheim (NMM); *Stephanorhinus kirchbergensis* from Bilzingsleben (FBFSUJ), Mosbach (NMM, SMNS), Ehringsdorf (IQW), Taubach (IQW), Eich (NMM), Gimbsheim (NMM). **2** Material from Azokh 1, Unit V, 2-8-2009, I-4, 15 – left M_3 of *S. hemitoechus* (occlusal, buccal and lingual views). **3** Azokh 1, Unit V, 27/7/09, D-15, 1 – left $M_{2\text{-}3}$ of *S. kirchbergensis* from Unit V (buccal, occlusal and lingual views). The scale bar represents 5 cm. As can be seen the M_3 of *S. hemitoechus* from Unit Vm is worn at the place where the height is measured; the value for H of this specimen is too low, which is indicated by an arrow in the bivariate diagram

Akokh 1, Unit V, 4-8-2009, I-42, 41 (z = 847) – fragment of a left upper first or second molar, buccal wall: DAP = 46.5.

Azokh 1, Unit V, 26-7-2009, E-40, 7 (z = 861) – left Mc V: DAPp = 33.2, DTp = 24.0, L > 29.1.

Description of the new material and taxonomic classification

The M_3 (Fig. 6.13/2) is moderately worn and has a well developed anterior contact facet, but no posterior facet. In lingual view, it has clear v-shaped lingual valleys, which is typical for *Stephanorhinus hemitoechus*. The enamel is crenelated as in that species, but not as strongly as in *Coelodonta*, and there is deposition of cementum in the valleys. The place where the crown height is measured is slightly worn out, so the value for H in Fig. 6.13/1 is a minimum value (indicated by the arrow in this figure). Despite dental wear, the crown is still high and must have been higher than in *S. hundsheimensis*. The tooth is smaller than in *S. kirchbergensis* and the same is the case for the foot bones (Fig. 6.14).

A symetrical bone fragment with a more or less T-shaped transverse section from Unit Vu seems to represent the nasals of a rhino, the vertical bone being the ossified nasal septum, and the upper surface, which curves down at the

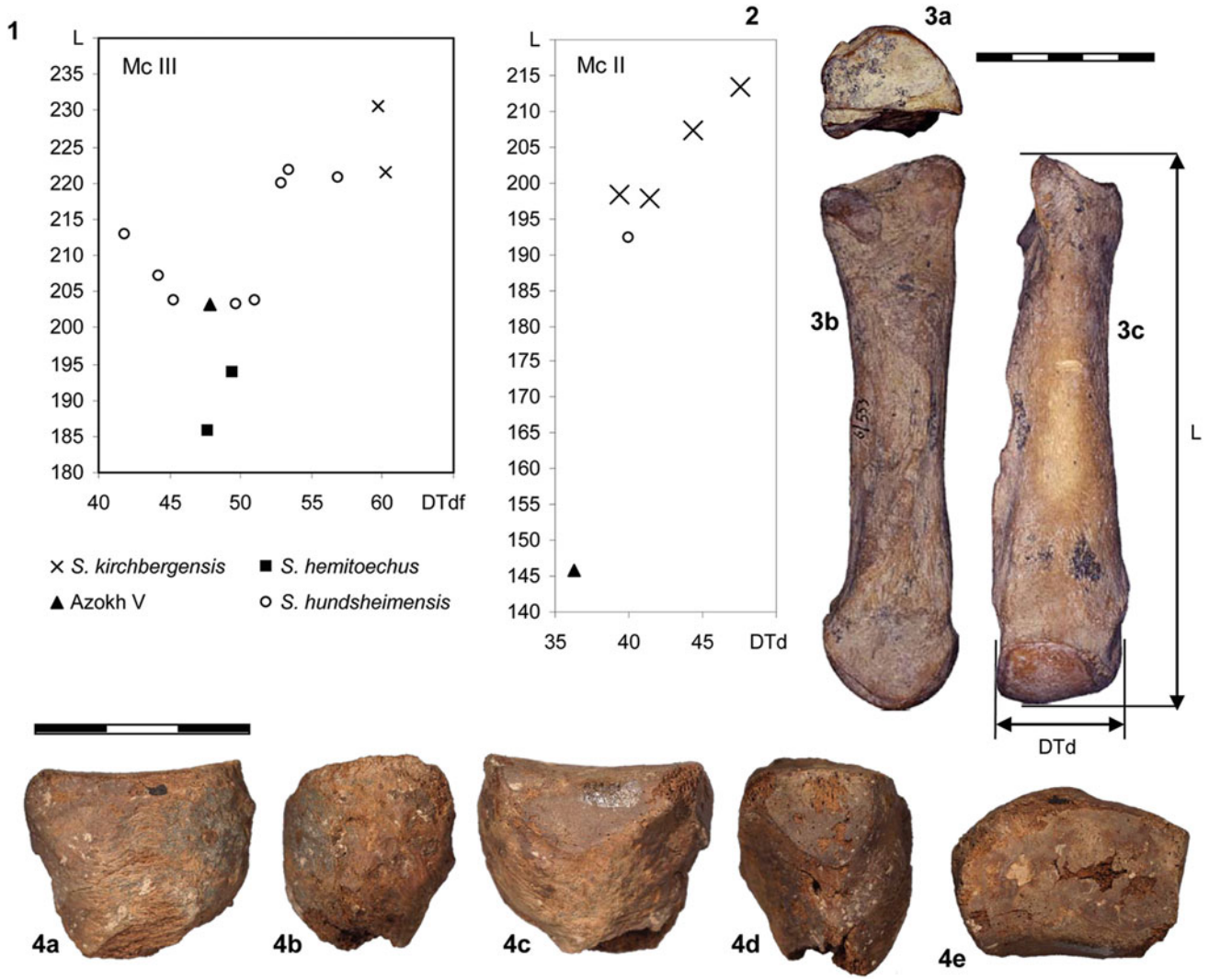

Fig. 6.14 *Stephanorhinus* post cranial elements. **1** Bivariate diagram of the length (L) versus the distal width (at the articulation DTdf) of the third metacarpal (Mc III) of *Stephanorhinus hundsheimensis* from Untermassfeld (IQW), Soleilhac (MCP), Hundsheim (IPUW), Mauer (SMNK); *S. hemitoechus* from Bilzingsleben (FBFSUJ), Cova del Gegant (MNCN, cast), and Unit V (MUB); *Stephanorhinus kirchbergensis* from Bilzingsleben (FBFSUJ). **2** Bivariate diagram of the length (L) versus the distal width (DTd) of the second metacarpal (Mc II) of *Stephanorhinus hundsheimensis* from Soleilhac (MCP); *S. kirchbergensis* from Bilzingsleben (FBFSUJ) and *S. hemitoechus* from Unit V (MUB). **3** Material from Unit V: MUB 6/553 – right Mc II of *S. hemitoechus* (**a**–**c** proximal, axial and anterior views). **4** Azokh 1, Unit V, 26/7/09, E-40, 7 – left fifth metacarpal of *Stephanorhinus hemitoechus* (**a**–**e** lateral, posterior, medial, anterior, and proximal views). The scale bars represent 5 cm for the Mc II and 3 cm for the Mc V, respectively

sides, being the nasals. The preserved part is about 11 cm long and 6 cm wide. There is no suture visible between the nasals or between nasals and septum. All sides of the bone are broken before reaching a natural border. The upper surface is smooth. The minimum preserved thickness of the septum is 5.8 mm, while the minium thickness of the nasals near their presumed edge is about 1 mm.

Discussion

Nasals supported by an ossified septum occur in *Stephanorhinus* and *Coelodonta*. The living genera of Rhinocerotidae do not have ossified nasal septa. *Stephanorhinus* and *Coelodonta* tend to have thick nasals with a well developed "cauliflower structure" marking the spot where the horns originate. However, such a structure is not always well developed (e.g., Loose 1975, Pl. 4, Fig. 3). Azzaroli (1962) interpreted skulls with narrower nasals and a smoother surface as females, and it is also likely that the cauliflower structure is less developed in juveniles. The nasals described here are insufficient for a determination at the species level. The material of the old collections include a fragment of nasals, similar to the one described here, but with a moderate "cauliflower structure".

Most specimens in the old collections have *Stephanorhinus hemitoechus* morphology and size. Most of the postcranial and dental specimens that can be measured are small, in particular the premolars which are too small for attribution to *S. kirchbergensis*. *Stephanorhinus hundsheimensis* is a species with large premolars, and the very small premolars from Azokh point to a species with reduced premolars like *Stephanorhinus hemitoechus*.

Stephanorhinus hemitoechus is assumed to have evolved from *S. etruscus* in an area outside western Europe and to have dispersed into the latter area around 450 ka ago, where it may have survived until the end of the Pleistocene (Guérin 1980; Fortelius et al. 1993; Van der Made 2000, 2010a; Van der Made and Grube 2010).

Order Artiodactyla Owen, 1848
Family Suidae Gray, 1821
Sus scrofa Linnaeus, 1758

New material

Unit Vm

AZM'03, small finds (27-08-2003, Plat middle, Unit V, small finds) – left second phalanx: DAPp ≥ 16.2, DTp ≥ 16.6, L ~ 31.6, DAPd ~ 20.3, DTd–.

Unit II

Azokh uppermost, 11-8-03, D45, 19 (z = 133) – left C_m: Li = 23.8, La = 18.1, Po = 17.0.

Azokh 1, Unit II, 2-8-08, C-46, 269 (z = 99) – left C_f: DAP = 20.5, DT = 14.1.

Unit I

Azokh 1, Unit I, F-50, 3-8-06, 17 (z = 19) – juvenile right scapula: L = 41.6, DAPmax = 26.5, DAPn = 6.9, DTn = 3.9.

Azokh, 29-7-05, Unit II, square "passage into cave", no surface find – fragment of the right side of the skull with occiput, and part of zygomatic arc.

Description of the new material and taxonomic classification

The C_m has a triangular section. Suid male lower canines are assigned to two types: the "scrofic section" with a posterior side that is wide, generally wider than the labial side, and the "verrucosic section" with a narrower posterior side. In the specimen from Azokh the posterior side is wide, but not wider than the labial side. The section is "scrofic" and such a section occurs in the genus *Sus* only in *Sus scrofa* and the rare and very small *Sus salvanius*, which is restricted to some area in Asia. The C_f (Fig. 6.15) is large.

Two fragments belong to a second phalanx. The morphology cannot be well seen because of the poor preservation of the specimen. If this is a lateral phalanx (digit II or V) it would be extremely large, but the size is acceptable for a central phalanx (III or IV) of a smaller representative of the species.

The skull fragment from Unit I has a very obtuse angle between the axis of the posterior side and dorsal side. This angle tends to be sharp in wild boars, resulting in an overhanging occiput, while in domestic pigs and juveniles, the angle tends to be obtuse and the occipital condyles are situated more posteriorly than the occiput. Between the brain

Fig. 6.15 *Sus scrofa* from Unit II, 2-8-08, C-46, 269 (z = 99) – left C_f (**a**, **b** buccal and posterior views)

and occiputal crest there is spongious bone instead of sinuses, another feature that is common in domestic pigs.

A small scapula of a very young individual has a triangular shape, as is common in Artiodactyla, and it has the spine in the middle of the blade, which is common in Suidae, but not near the anterior edge of the bone, as is common in ruminants.

Discussion

Suid material in the University of Baku comes from Units VI, V and III and that from Units V and III was assigned to *Sus scrofa* (Aliev 1969; Lioubine 2002; Rivals 2004). This material consists largely of postcrania and does not include well preserved elements that show clear *Sus scrofa* morphologies, such as the male upper and lower canines and upper fourth premolar. Nevertheless the material belongs most probably to this species, since no other species is known from the Middle Pleistocene of western Eurasia. The material from Unit I might belong to a domestic pig, but this cannot be confirmed.

Sus scrofa must have originated in eastern Eurasia and dispersed into Europe just before the Brunhes – Matuyama transition (it is present in the latest Early Pleistocene of Atapuerca TD6; Van der Made 1999). The early forms were larger than living *Sus scrofa scrofa,* but at later sites such as Mosbach and Mauer (about 0.5–0.6 Ma) and younger faunas, they are smaller. In Taubach (OIS5) they are large again, while in later faunas they are again smaller. At present there are slight geographic differences in size between Spain and Germany, while living wild boars of Israel and Georgia are larger. The female canine from Unit II must belong to such a large form. Since there are not many data on the size of this species in general, and from the Caucasus area in particular, these observations cannot be interpreted with reference to the age of the locality.

Family Cervidae Goldfuss, 1820

Capreolus aff. *pygargus* (Pallas, 1771)

New material

Unit Vm

Middle plat., cleaning 26-7-05 – right axial sesamoid behind first phalanx: DAP = 6.3, L = 10.8, DT = 4.8.

Unit II

Azokh, 18-8-06, Unit II, G-48, 202 – right astragalus: Lext ≥ 34.6.

Description of the new material and comparison

The astraglus is damaged. Its length (Lext ≥ 34.6) is comparable to the length of the astragali of *Capreolus priscus* and *Capreolus suessenbornensis* (Fig. 6.17/5). The sesamoid has the typical artiodactyl shape. Its DAP or dorso-plantar diameter is small, so it is an axial and not an abaxial sesamoid. Apart from the shape of the dorsal facet, the transverse section is nearly symmetrical, with rounded corners at the latero-plantar and medio-plantar sides. In Bovidae like *Capra*, the plantar side is markedly a-symmetrical in such a way that the two sesamoids form a gulley at the plantar side. The size of the specimen is smaller than in *Dama*, but fits *Capreolus*.

Discussion

Material from Units V and III was assigned to *Capreolus capreolus* (Aliev 1969; Lioubine 2002; Rivals 2004). The new collections include some poor specimens from Units V and II that are compatible with *Capreolus*, but this taxon is well represented in the old collections from Units VI, V and III in Baku.

Roedeer of the genus *Procapreolus* were common in Europe, but disappeared after about 3.4 Ma (Heintz 1970; Kahlke 2001). *Capreolus* evolved from that genus and first appeared with the species *Capreolus constantini* in Udunga (Siberia) and other localities in Moldavia and Slovakia with ages as old as 3.5 Ma (Vislobokova et al. 1995). The earliest West European record attributed to *Capreolus* is *C. cusanoides* from Untermassfeld (Kahlke 2001), and with an age of about 1 Ma this species retains primitive characters present in *Procapreolus* but lost already in *Capreolus constantini*, so that this species seems to be an evolutionary side branch. The first morphologically clear European *Capreolus* is from the early Middle Miocene (Voigtstedt, Süssenborn, etc.). Pfeiffer (1998) recognized three species: *Capreolus suessenbornensis*, which is replaced by *Capreolus priscus*, of similar size but of different leg proportions, while the living species *Capreolus capreolus* is smaller. This size decrease must have occurred during the Late Pleistocene in Europe as well as in the Middle East (Fig. 6.16/1).

The living roe deer were formerly considered to belong to two or three subspecies (e.g., Whitehead 1993), but the current view is that they belong to two separate species *C. capreolus* (Europe and Middle East) and *C. pygargus* (Asia; Duff and Lawson 2004). The latter species is larger, has relatively larger antlers, and differs in the morphology of the antler base. Some authors included the populations from the Caucasus in the species or subspecies "*capreolus*", while others included it in "*pygargus*". The large recent material in the GSM in Tbilisi, attributed to this species, either represents *C. pygargus*, or a larger subspecies of *C. capreolus.* In either case, the material in the GSM seems to belong to a taxon that was different from the roe deer of most of Europe and Israel since the Late Pleistocene, at least.

The material from Unit VI is very poor, but the material from Unit III is larger than *Capreolus capreolus* (at least the west European form; Fig. 6.16/1), and the phalanges from Unit V are even larger than in *C. priscus* and *C. suessenbornensis* (Fig. 6.17/1, 2). This suggests, that the species from Azokh was very large and possibly was on a different

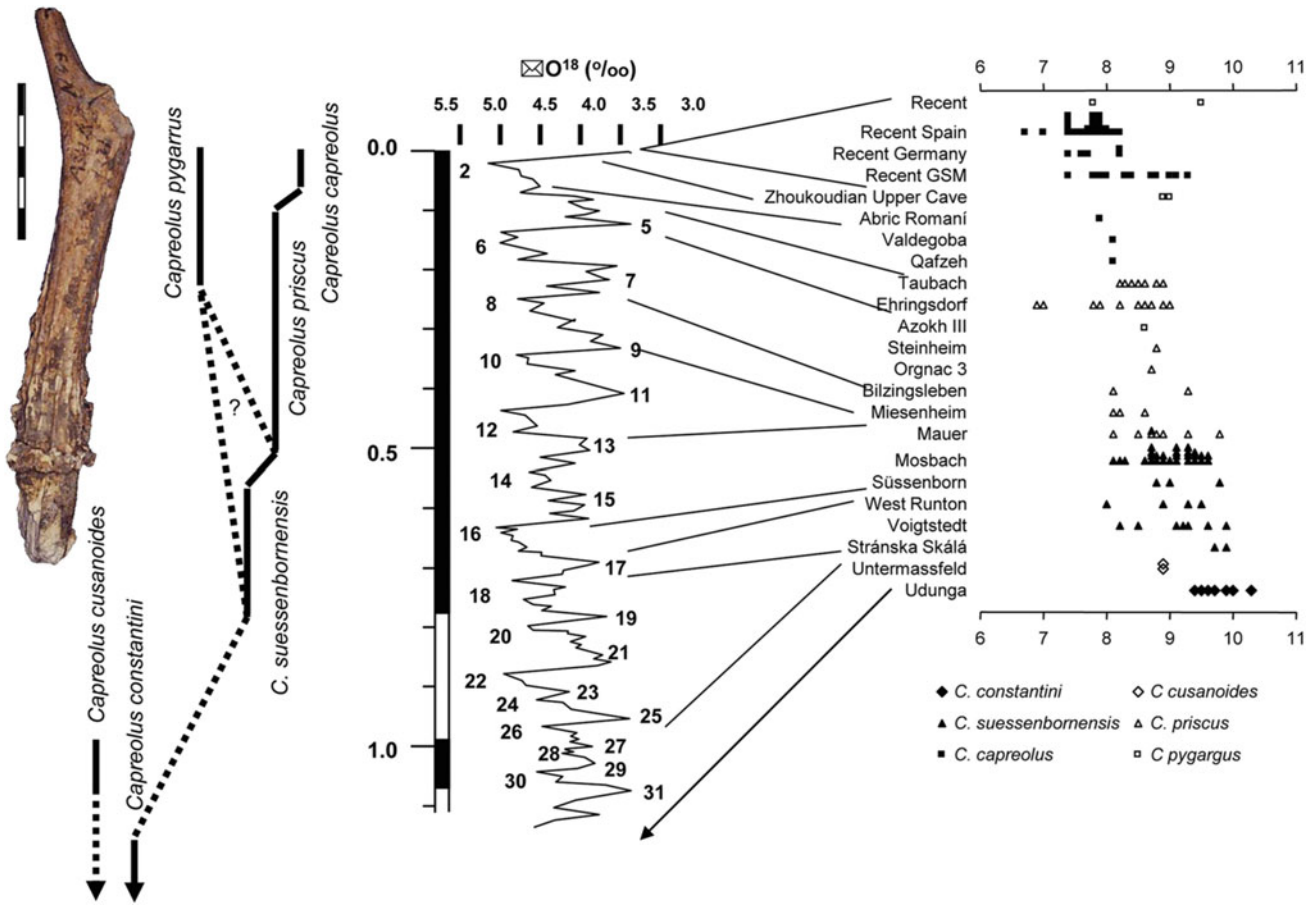

Fig. 6.16 *Left* MUB 5/277 – left antler of *Capreolus* fom Unit III. The scale bar represents 5 cm. *Right* The variation in size of *Capreolus* as indicated by the width of the first lobe (DTa) of the M_3. The localities are ordered in approximate stratigraphic order: Udunga (about 3.5 Ma; PIN, GIN), Untermassfeld (IQW), Stránska Skálá (MMB), Voigtstedt (IQW), West Runton (IQW), Süssenborn (IQW), Mosbach (NMM), Mauer (SMNS), Miesenheim (FASMN), Bilzingsleben (FBFSUJ), Orgnac 3 (MPT), Steinheim (SMNS), Unit III (MUB), Ehringsdorf (IQW), Taubach (IQW), Qafzeh (IPH), Congosto (MNCN), Valdegoba (UBU), Abric Romaní (LAUT), Zhoukoudian Upper Cave (IVPP), Recent material attributed to *Capreolus capreolus* and *Capreolus pygargus* in the GSM, Recent *Capreolus capreolus* from Germany (FASMN) and Spain (MNCN)

lineage from the west European forms; possibly it was on a lineage leading to *C. pygargus*. Some antler remains are not as large as they may be in the living species *C. pygargus* (Fig. 6.16/2), and possibly the relatively large antlers in that species are relatively recent.

Dama aff. *peloponesiaca* (Sickenberg, 1976)

New material

Unit VI

Found below the collumn of sediment, 13/09/02, VI – right D^2: DAP = 14.4, DAPb = 12.8, DTa = 8.6, DTp = 9.9.

Unit Vm

Azokh middle, 6/09/02, G-41, general finds – tip of tine of an antler: length of the fragment about 5 cm, diameters at the base of the fragment 13.9 × 11.4.

C-43, 12-8-03, general find Unit III?, northern wall – fragment of branch of an antler (brow tine?): length of the fragment >93, width 29.0.

6-9-2002, plat middle, Unit V, z = 112, F41, 2 – fragment of tine or beam of an antler.

Azokh, 15-8-03, E-40, middle platform, Unit V, 3 (z = 122) – left humerus, distal part: DTd ≥ 41.1, DTdf = 37.3, R1 = 31.1, R2 = 23.3, R3 = 25.7, R4 = 17.7, R5 = 19.0.

AZUM'02, F40, 3 – fragment shaft of metatarsal: DTmini.18.4.

Azokh Cave, F42, split sample – left ulnar: DAP = 21.7, DT = 12.2, H = 24.2, Ha = 19.3.

14-09-02, plat upper, E-44, gen. finds – various finds, including a right I_1: DT = 9.0, DMD = 7.0, DLL = 4.9, DTroot = 4.0, DLLroot = 4.9, Hli > 9.0.

Azokh 1, Unit V, 27-7-2009, I-42, 11 (z = 827) – right D^4: DAPo = 17.1, DAPb = 15.2, DTa = 15.3, DTp = 14.9.

Azokh 1, Unit V, 1-8-2009, I-42, 26 (z = 844) – right D^2: DAPo = 14.3, DAPb = 14.1, DTa = 7.8, DTp = 9.7.

Azokh 1, Unit V, 28-7-2009, I-42, 6 (z = 844) – left M^2: DAPo = 21.8, DAPb = 19.9, DTa = 21.7, DTp = 21.4.

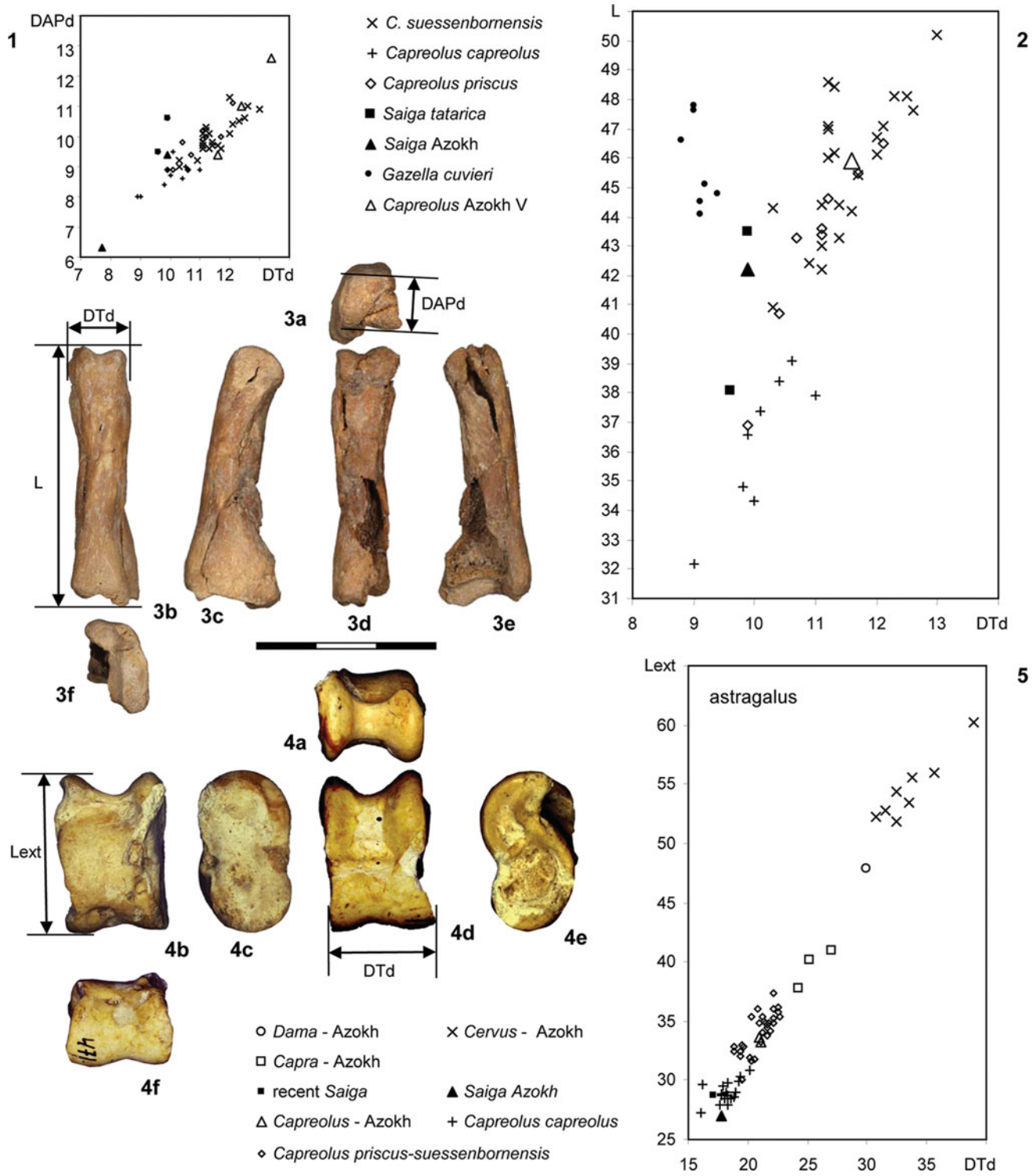

Fig. 6.17 *Capreolus* and *Saiga*. **1**, **2** Bivariate plots of the distal transverse diametre (DTd) versus the distal antero-posterior diametre (DAPd) and of the length (L) versus the DAPd of the first phalanx of *Capreolus* and *Saiga*: *C. suessenbornensis* from Süssenborn (IQW), Voigtstedt (IQW) and Koneprusy (NMP); *C. priscus* from Miesenheim (FASMN), Ehringsdorf (IQW) and Grotte des Cèdres (MRA), *C. capreolus* from Can Rubau (CIAG) and Cueva Morín (MNCN), *Capreolus* cf. *pygargus* from Unit V and III (MUB); the eight phalanges of of one individual of *Gazella cuvieri* (MNCN); an anterior and posterior phalanx of recent *S. tatarica* (NNML) and *Saiga* from Unit II. **3** Azokh, 18-8-06, Unit II, F-48, 94 – right first phalanx of *Saiga* from Unit II (**a**–**f** distal, dorsal, abaxial, plantar, axial, and proximal views). **4** MUB 471 – left astragalus of *Capreolus* from Unit V (**a**–**f** proximal, posterior, medial, anterior, laterla, and distal views). **5** Bivariate diagram of the lateral length (Lext) and distal width (DTd) of the astragalus of the deer and small bovids from Azokh (MUB), compared to *Capreolus suessenbornensis* and *C. priscus* (provenance of data as above) and *Capreolus capreolus* from Can Rubau and Spain (recent, MNCN). The scale bar represents 3 cm

Azokh 1, Unit V, 25-7-2009, I-42, 5 (z = 825) – right M^3: DAPo > 22.5, DAPb > 21.2, DTa = –, DTp = 22.4.
Azokh 1, Unit V, 4-8-2009, I-42, 40 (z = 848) – left M^1: DAPo = 19.5, DAPb = 17.2, DTa = 18.2, DTp = 17.9.
Azokh 1, Unit V, 1-8-2009, I-42, 25 (z = 844) – left D^4: DAPo = 16.9, DAPb = 14.0, DTa = 14.9, DTp = 14.8.
Azokh 1, Unit V, 25-7-2009, I-41, 2 (z = 857) – fragment of M^x (protocone of left M^2?).
Azokh 1, Unit V, 28-7-2009, I-41, 4 (z = 839) – right I_3: DT = 5.8, DMD = 5.0, DLL = 6.4; root: DT = 3.6, DLL = 5.2.
Unit V/VI
Azokh upper, 16/9/02, E-44, 6 (Z = 100) – left distal tibia: DAPd = 29.0, DTd = 34.9, DTfast = 24.0.

Description of the new material

Bones and teeth (Fig. 6.18/1–7) that are slightly smaller than those assigned to *Cervus elaphus* tend to have characters described by Lister (1996) as typical for *Dama*. For instance, a distal tibia has characters 3 and 4 developed as in *Dama* (Lister 1996). Though smaller than their homologues in *Cervus elaphus*, the Azokh bones and dental remains tend to be large for *Dama* and are on average larger than in any *Dama dama* and most *Dama clactoniana*.

Discussion

Material from Azokh was assigned to *Cervus (Dama)* cf. *mesopotamica* (Aliev 1969; Lioubine 2002; Rivals 2004). The new material broadly confirms the presence of *Dama*, but the old collections in Baku are much more abundant.

Basal parts of the antlers from Unit VI (Fig. 6.19/1) and Unit V (Fig. 6.20/2) have the first bifurcation (between brow tine-main beam) higher above the burr than in *Dama dama*, *Dama mesopotamica* and *Dama clactoniana* (Fig. 6.20). This bifurcation (as well as the second one) became progressively lower with time in the *Dama*-like deer, and in *Dama mesopotamica* it is particularly low and the brow tine is extremely short.

A specimen from Unit Vm (Fig. 6.19/7) consists of a large part of the palmation, which was wide and probably curved anteriorly as in *Dama dama* (the concave border of the left hand side of the photograph would then be the anterior border of the palmation). This is unlike *Dama clactoniana* and *Dama mesopotamica*. The oldest known palmate *Dama* is *Dama clactoniana,* appearing about 550 ka ago. Both *Dama mesopotamica* and *Dama dama* have more reduced brow tines, but this is especially so in the former. While *Dama dama* has a palmation that is better developed than in *D. clactoniana*, in *D. mesopotamica* it is like in the latter species, or, perhaps, even less developed. The material from Units VI and V does not seem to belong to any of these three species.

Previous to these three species, there were several "*Dama*-like deer", which have broadly similar size and morphology, but which lack a palmation. Some authors place them in *Dama* (Azzaroli 1953; Van der Made 1996, 1999b, 2001; Pfeiffer 1999), but others assign them to different genera such as *Pseudodama*, *Euraxis*, *Axis*, *Rusa*, *Metacervocerus* and *Cervus* (s.l.) (Azzaroli 1992; Di Stefano and Petronio 1998, 2002; Kahlke 2001; Croitor 2006).

Teilhard de Chardin and Trassaert (1937) described *Dama sericus* from China. It has a palmation that is different from that of *Dama dama*, *Dama mesopotamica* and *Dama clactoniana* and has a first bifurcation that is much higher. Unfortunately it is not possible to compare these palmations to those of *Dama peloponesiaca*, which will be discussed below, because only fragments are known of the latter. Nor is it possible to compare bones or teeth, since these were not described by Teilhard de Chardin and Trassaert, who indicated the age as Plio-Pleistocene, probably Zone III or Villafranchian. *Dama sericus* (or better *Dama serica*?) was considered to be related to the Mio-Pliocene genus *Cervocerus* (Qiu 1979). If this is the case, this species is not related and is separated by time and distance from *Dama* or "*Dama*-like deer".

A species which is not often discussed in the literature on Cervidae is *Dama peloponesiaca*. Sickenberg (1976) based the new name "*Cervus* (s. l.) *peloponesiacus*" on material from Megalopolis. There are older collections in the University of Athens. These collections include flattened tines, which suggest that they originated from a palmation. Because of the presence of a palmation and of other morphological similarities in antlers, teeth and bones, this species is here included in *Dama*, though the position of the first bifurcation is variable and in many cases is higher than in any *Dama dama* and *Dama clactoniana* (Fig. 6.20/1).

Dama peloponesiaca seems to be older than *Dama mesopotamica*, but its age is not exactly known. Sickenberg (1976) described material from various fossiliferous sites in the basin, but he treated it as if representing one fauna, including *Praemegaceros verticornis* and *Bubalus marathousae*. *Bubalus* is known from a number of localities in Germany, which are either OIS5 or OIS9 (Von Koenigswald 1986; Van der Made 2005b). The giant deer *Preaemegaceros verticornis* (or *Megaceroides* or *Megaloceros solilhacus*) is considered to be a "Cromerian" form, but still occurred in Atapuerca Galeria TG10, which might be as late as 300–400 ka (Berger et al. 2008). If the material from Megalopolis represents more or less one age, this age might be 300 ka (if the presence of *Bubalus* is believed to be coeval with the OIS9 dispersal of that genus), or about 400 ka (if a very young occurrence of the giant deer is not favored). In any case, it seems that *Dama peloponesiaca* is a side branch of the *Dama* lineage in the south eastern part of its area of distribution, similar to *Dama mesopotamica* in this respect, but earlier.

The material from Unit V and VI is similar in several characters to that of Megalopolis, but is clearly larger (Figs. 6.19 and 6.20). The deer from Azokh and

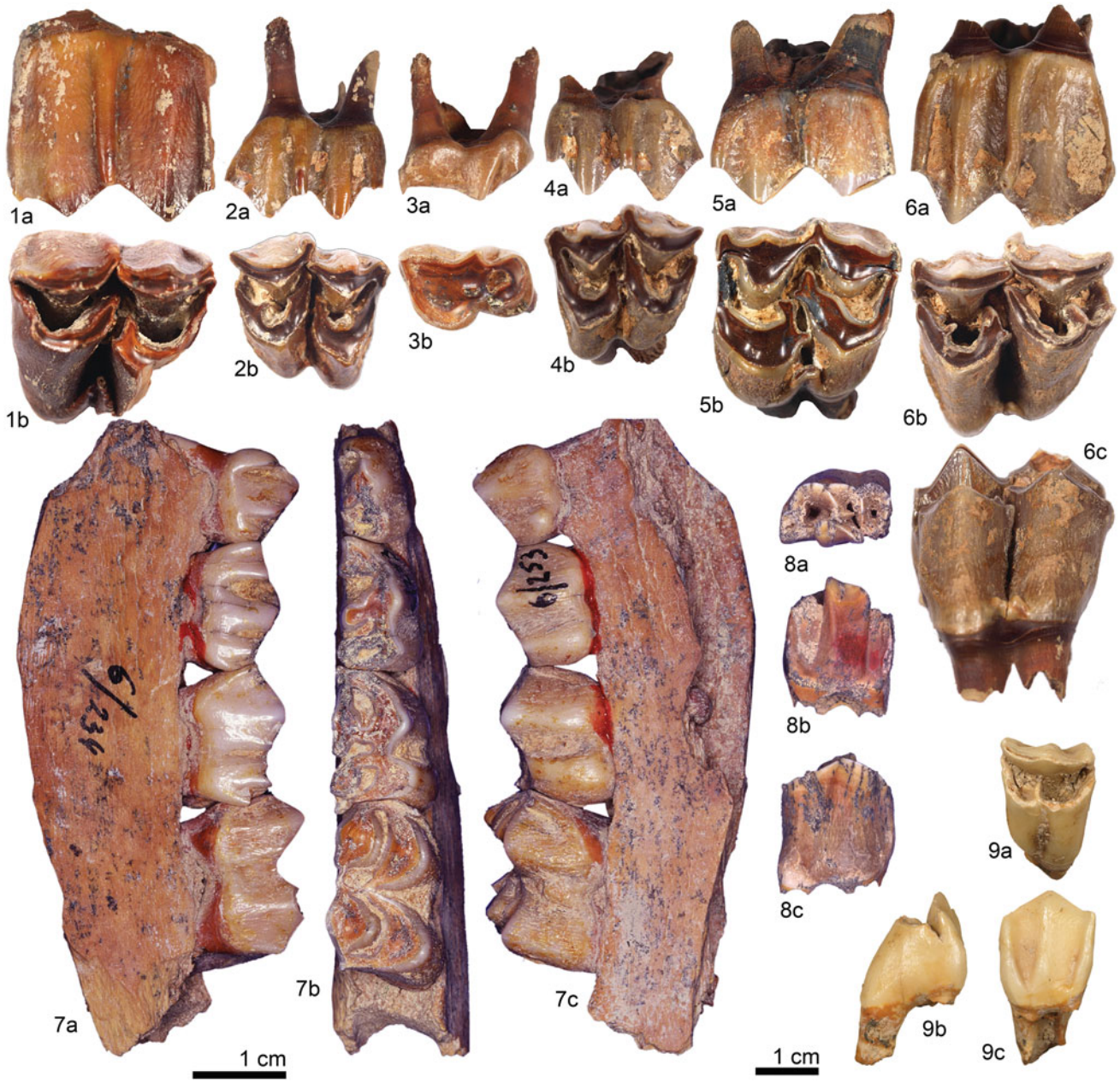

Fig. 6.18 Cheek tooth morphology in *Dama* aff. *peloponesiaca* from Unit V (figures **1**–**7**) and *Cervus elaphus* from Unit Vm (8) and from Unit II (9). **1** Azokh 1, Unit V, 28-7-2009, I-42, 6 – left M^3 (**a**, **b** buccal and occlusal views). **2** Azokh 1, Unit V, 27-7-2009, I-42, 11 – right D^4 (**a**, **b** buccal and occlusal views). **3** Azokh 1, Unit V, 1-8-2009, I-42, 26 – right D^2 (**a**, **b** buccal and occlusal views). **4** Azokh 1, Unit V, 1-8-2009, I-42, 25 – left D^4 (**a**, **b** buccal and occlusal views). **5** Azokh 1, Unit V, 4-8-2009, I-42, 40 – left M^1 (**a**, **b** buccal and occlusal views). **6** Azokh 1, Unit V, 25-7-2009, I-42, 5 – right M^2 (**a**, **b** buccal and occlusal views). **7** MUB 6/234 (=6/253) – right P_2-M_1 (**a**–**c** lingual, occlusal, and buccal views). **8** Azokh 1, Unit V, E-44, 21 – right P_4 (**a**–**c** occlusal, lingual, and buccal views). **9** Azokh 1, Unit II, N-49, 12 – right P^4 (**a**–**c** occlusal, anterior and buccal views). The left scale bar applies to figures **1**–**7** and the right one to figures **8** and **9**

Megalopolis share the combination of a primitive character in their high first bifurcation and a derived character of palmation, which is unique in *Dama*-like deer, but which differs in size. The size difference might be due to geographic or temporal separation, although the latter is perhaps more likely. These forms seem to belong to a branch or lineage that may have separated from the main west Eurasian *Dama*-lineage because of isolation in SE Europe or the Middle East. This may have happened before *Dama mesopotamica* separated from the main *Dama* lineage, which may have occured in OIS8, replacing the *Dama peloponesiaca* lineage (Fig. 6.21).

Fig. 6.19 Antlers of *Dama* aff. *peloponesiaca* (1, 3, 6-7), *Dama* sp. (2) and *Cervus elaphus* (4-5) from Azokh. **1** MUB 1/206 – right antler from Unit Vu (**a**, **b** lateral and anterior views). **2** Azokh 1, Unit II, C-46, 327 – fragment of the palmation of an antler from Unit II (**a**–**c** distal and medial views, section). **3** MUB 7/839 – left (?) antler fragment from Unit III (**a**, **b** distal section and lateral view). **4** MUB 6/95 – crown of a left (?) antler from Unit V (**a**, **b** distal and medial views). **5** MUB 6/158 – close up of the surface of a fracture at the crown of an antler from Unit V; in the left upper corner the outer surface of the antler can be seen. **6** MUB 4/406 – fragment of the palmation; from Unit V. **7** MUB 6/623 – fragment of the palmation of a left (?) antler from Unit V (lateral view). The scale bar represents 4 cm for figures **2**, **3** and **6**, **7**, and it represents 6 cm for figures **1** and **4**; figure **5** is not to scale

Dama sp. (*Dama mesopotamica*?)

There is no new material of *Dama* from Unit III, but there is some material in the older collections. The largest antler fragment from this unit (Fig. 6.19/3) has a narrower palmation (right and left hand side in the photograph are natural borders, no fractures) than in the specimen from Unit V (Fig. 6.19/7). There is a small flat process, which protrudes less than 2 cm. Such processes occur in *Dama dama* at the back of the palmation. This narrow palmation

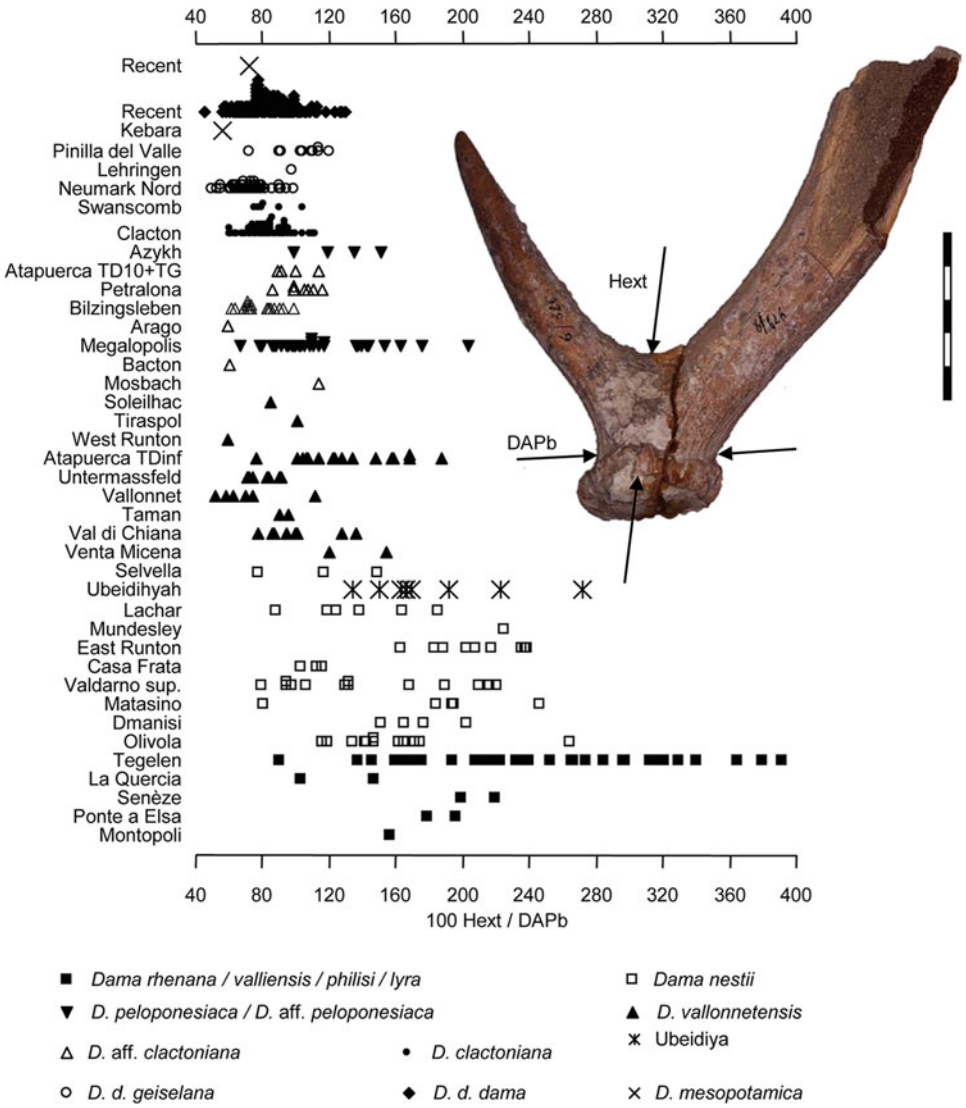

Fig. 6.20 The morphology of the basal part of the antler in the *Dama*-like deer. The variation in the height above the burr of the bifurcation of brow tine and main beam, expressed as the index 100× Hext/DAPb, in the *Dama*-like deer as shown in the picture: MUB 6/626 left shed antler of Dama aff. peloponesiaca from Azokh 1 Unit V (lateral view). The scale bar represents 5 cm. The localities in the graph are ordered in approximate stratigraphic order: Montopoli (IGF), Ponte a Elsa (IGF), Senèze (IQW), La Quercia (IGF), Tegelen (NNML, TMH, NMMa), Olivola (IGF), Dmanisi (GSM), Matasino (IGF), Valdarno sup. (IGF), Casa Frata (IGF), East Runton (NHM), Mundesley (NHM), Lachar (MNCN), Ubeidiyah (HUJ), Selvela (IGF), Venta Micena (IPS), Val di Chiana (IGF), Taman (PIN), Vallonnet (MPRM), Untermassfeld (IQW), Atapuerca TDinf (CENIEH), West Runton (NHM), Tiraspol (PIN), Soleilhac (MCP), Mosbach (NMM), Bacton (NHM), Megalopolis (NCUA, BGR), Arago (MPT), Bilzingsleben (FBFSUJ), Petralona (AUT), Atapuerca TD10+TG (CENIEH), Azokh (MUB), Clacton (NHM), Swanscombe (NHM), Neumark Nord (FBFSUJ, presenty kept in LVH), Lehringen (HMV), Pinilla del Valle (UCM), Kebara (HUJ), Recent *Dama dama* (EDB), Recent *Dama mesopotamica* (HUJ)

does not seem to be a fragment from a different position in the antler of *Dama* aff. *peloponesiaca*, because there is no space for a section with this morphology between the lower part of the antler and the palmation as in Fig. 6.19/1 and 6.19/7. It does not seem to represent a different ontogenetic stage, because it is relatively large and straight for a juvenile antler (compared to *Dama dama*, where antlers of different ages are known). Alternatively it could belong to a different species, *Dama mesopotamica*, where the palmation is narrow. The oldest clear records of *Dama mesopotamica* are also of about OIS 7-8 (excluding Ubeidiyah and Gesher Benot Ya'akov; Di Stefano 1996).

Antler fragment MUB 7/839 (Fig. 6.19/3) has part of the surface of the antler with small pores. This suggests that the antler was not fully ossified at the moment of death of that individual. Shortly after full ossification the antler is cleaned of the velvet. In *Dama dama* this cleaning occurs at the end of August and the beginning of September (Ueckermann and Hansen 2002). Possibly the individual of MUB 7/839 died during August. This feature will be discussed more in detail under *Cervus elaphus*.

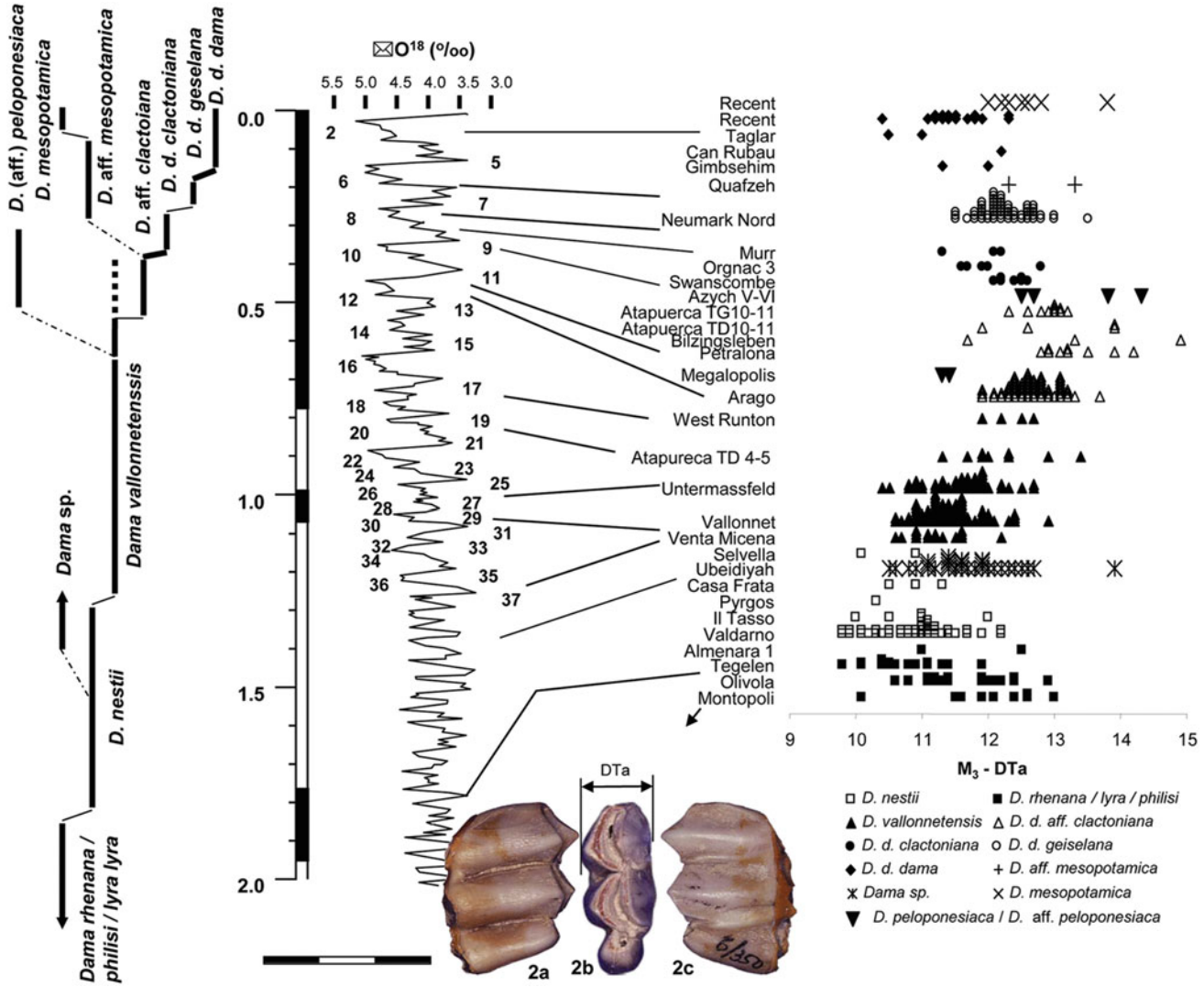

Fig. 6.21 The third lower molar in *Dama*-like deer. **1** The variation in size of the *Dama*-like deer as indicated by the width of the first lobe (DTa) of the M_3. The localities are ordered in approximate stratigraphic order: Montopoli (IGF), Tegelen (NNML, TMH, NMMa), Olivola (IGF), Almenara 1 (SIAP), Valdarno sup. (IGF), Il Tasso (IGF), Pyrgos (IVAU), Casa Frata (IGF), Ubeidiyah (HUJ), Selvella (IGF), Venta Micena (IPS; presently kept in the village of Orce), Vallonnet (MPRM), Untermassfeld (IQW), Atapuerca TDinf (CENIEH), West Runton (NHM), Megalopolis (NCUA, BGR), Arago (MPT), Bilzingsleben (FBFSUJ), Petralona (AUT), Azokh (MUB), Atapuerca TD10 & TG10-11(CENIEH), Orignac 3 (MPT), Swanscombe (NHM), Murr (SMNS), Neumark Nord (FBFSUJ, presently LVH), Qafzeh (IPH), Gimbsheim (NMM), Can Rubau (CIAG), Taglar (MUB), Recent Spain (MNCN). **2** MUB 6/350 – left M_3 of *Dama* aff. *peloponesiaca* from Azokh 1 Unit V (**a**–**c** bucal, occlusal, and lingual views). The scale bar represents 3 cm

Dama sp. (*Dama dama*?)

New material

Unit II

Azokh 1, Unit II, 03-8-08, C46, 327 (z = 119) – antler fragment (of a left antler?), including part of the palmation and the basis of a tine: diameters near the base of the tine 34.2 × 16.4.

Azokh uppermost, 11-9-03, D-45, rescue, 17 (Z = 130) – tip of the tine of an antler: length of the fragment about 10 cm, diametre at the base of the framgent 27.9 × 18.8.

Azokh uppermost, 16-8-03, D-45, 2 (Z = 132) – right calcaneum, juvenile: DAPn = 17.7, DTn = 11.0, DAPsf = 23.8, DTsf = 21.4.

Azokh 1, Unit II, J-48, 6 (z = 101, 8-8-2008) – right mandible with P_{3-4} (much worn) and alveoles of the P_2; P_3: DAP = 9.8, DTa = 6.3, DTp = 6.9; P_4: DTa = 7.9.

Unit I

Azokh 1, 4-8-06, unit I, F51, 12 (z = 36) – condyle of a right mandible. Probably juvenile and might belong to other ruminants as well (e.g., *Capra, Cervus*?). Condyle DT = 20.1.

Azokh, Unit I, subunit c, 20-7-07, D-48, 16 (z = 201) – left magnum: DAP = 17.0, DT = 14.7, H = 10.9, h = 8.6.

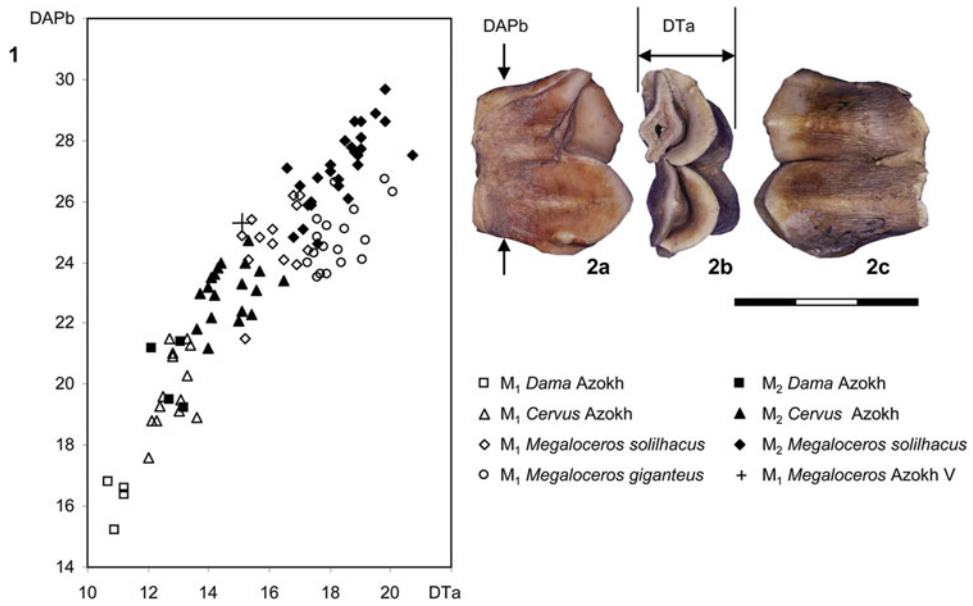

Fig. 6.22 **1** Bivariate plot of the first and second lower molar comparing *Dama* from Units III, V and VI (MUB), *Cervus elaphus* from Units III, V and VI (MUB), *Megaloceros solilhacus* from Pakefield (NHM), Voigtstedt (IQW, SMS), Süssenborn (IQW), West Runton (NHM), Mosbach (NMM), Megalopolis (NCUA, BGR), Atapuerca TG (CENIEH), Unit V (MUB), and *Megaloceros giganteus* from the Late Pleistocene Rhine sediments (NMM). **2** MUB 6/315 right M_1 of *Megaloceros solilhacus* from Azokh 1 Unit V (**a**–**c** lingual, occlusal, and buccal views). The scale bar represents 3 cm

Description of the new material

The antler fragment number 327 from Unit II (Fig. 6.19/2) contains part of the palmation and the beginning of a short tine. Another fragment of a tine of an antler (no. 17), also from Unit II, is flattened at the base, suggesting that it originated from a wide palmation, wider than in *Dama mesopotamica*.

Discussion

Within the Azokh sequence, the antler material from Unit II (Fig. 6.19/2) suggests again a wider palmation than in Unit 3, more like in the species from Unit V and *Dama dama*. Good antler bases are diagnostic between *Dama peloponesiaca* and *Dama dama*, but none have yet been recovered from Units II and I. *Dama dama* appeared not later than in OIS 7 (or about 220 ka) and at present extends its range into Anatolia. It is not impossible that the material from Units I and II belongs to *Dama dama*.

Megaloceros solilhacus (Robert, 1829)

Aliev (1969) assigned a number of fossils from Azokh to *Megaloceros giganteus*, but no material from recent excavations can be assigned to this species or genus. Aliev's material includes fragments of large antler, but we have found that all these antler fragments belong either to *Cervus elaphus* or to *Dama*. All the bones and teeth we have studied are smaller than in *Megaloceros giganteus*, but one tooth, a lower first or second molar from Unit V, belongs to a large deer (DAP = 30.9, DAPb = 25.3, DTa = 15.1, DTp = 15.0) (Fig. 6.22/2). Its size dimensions, however, are within the upper range of the M_2 of *Cervus elaphus* from Azokh (Fig. 6.22/1). It is unworn, but the tip of the metaconid is broken off, so the standard measurement for crown height cannot be taken. At the entoconid, the height is 24.9 mm, which is relatively low for a *Cervus elaphus* M_2. In the morphology of the styles at the lingual side, the tooth differs from *Cervus*, but recals *Megaloceros*. It is smaller than the M_1 of *Megaloceros giganteus*, but it is in the ranges of the lower molars of deer of the type of *Megaloceros solilhacus*.

Deer of this type appeared in localities such as Pietrafitta and Ubeidiyah, with estimated ages around 1.4 Ma and are assigned to *M. boldrini* or *M. obscurus*. By the early Middle Pleistocene they had evolved into *M. solilhacus*. (Some authors recognize *M. verticornis* and *M. dawkinsi* as different species, and some authors place all of them in *Megaceroides* or *Praemegaceros*.) The last occurrence of that species in Western Europe is in Atapuerca TG10a (base of unit GIIb), which recently has been redated in the range 422–466 ka (Berger et al. 2008). Other late occurrences are in Petralona (probably OIS11 on the basis of biochronology) and Megalopolis (see discussion of the age of this locality under *Dama* aff. *peloponesiaca*). A *Megaloceros* sp. cited from Kudaro I-5b (Lioubine 2002) either belongs to this species or to *Megaloceros giganteus*. *Megaloceros solilhacus* is closely related to the highly modified species *M. algericus*, which appeared during the Late Pleistocene in

North Africa. Thus a large part of the evolution of this branch of cervids is unkown and this new late record suggests that they may have lived in SW Asia immediately prior to their dispersal into northern Africa.

Cervus elaphus Linnaeus, 1758

New material

Unit Vm

Azokh upper, D-43, Unit V, 12 (z = 105) – left metacarpal: L = 253.6, L_{III} = 245.5, L_{IV} = 246.7, DAPp = 30.5, DTp = 42.0, DAPpf = 25.3, DTpf = 39.4, DAPm = 21.6, DTm = 27.1, DTd = 43.6, DAP_{III} = 28.9, DT_{III} = 19.9, DAP_{IV} = 29.5, DT_{IV} = 20.4.

Azokh middle, G-40, 7/9/02, Unit bag – fragment of shaft of metatarsal.

Azokh middle platform, Unit V, 17-8-03, E-41, 2 (z = 110) – right P^3: DAP = 16.2, DAPb = 15.1.

Azokh'03, middle platform, D-42, 20-8-03, 11 (z = 92) – right P^3: DAP = 17.5, DAPb = 15.8, DTa = 17.1, DTp = 17.8.

Azokh middle platform, Unit V, E-41, 22-8-03, 11 (z = 122) – right magnum: DAP = 21.8, DT = 22.1, H = 14.7, h = 10.0.

Azokh mid. platf. D41, 16-08-03, disturbed – left first phalanx: DAPd = 14.6, DTd = 17.2.

Azokh'03, Middle platform, Unit V, 19-8-03, F-42, 5 (z = 118) – left distal articulation of metacarpal: DT ≥ 20.2.

Azokh, plat. middle, 3-8-05, Unit V, F-40, 4 (Z = 137) – left scaphoid: DAP = 35.5, DT = 22.4, Ha = 25.1.

Unit Vu

Azokh upper, 17/9/02, E-44, 21 (Z = 92) – right P_4: DAPo = 18.2, DAPb = 16.5, DTa = 11.9, DTp = 11.1.

Azokh Cave, 5/09/02, nivel IV, C-42, pared norte – fragment of branch of an antler: width of the fragment 27.2.

Azokh upper, 16/09/02, E-43, 2 (Z = 113) – right M_2: DAP = 22,9, DAPb = 22.8, DTa = 14.8, DTp = 15.5, Ta = 0.9.

Azokh 1, Unit IV, D45, 10 (z = 24, 6-8-08) – right navicocuboid: DAP = 37.3, DT = 41.7, DTfast = 33.6.

Unit III

AZUM'03, D46, 151 – left I_1: DLL = 8.4, DMDroot = 6.0, DLLroot = 6.2.

Unit 3/II

AZUM'03, D46, 72 – right distal humerus: DTd = 61.3, DTdf = 55.2, R1 = 44.8, R2 = 32.5, R3 = 36.1, R4 = 27.7, R5 = 29.8.

Unit II

Azokh 1, Unit II, 5-8-08, H-49, no. 12, z = 113 – right P^4: DAP = 15.3, DAPb = 13.1, DT = 20.7.

Azokh 1, Unit II, 25-7-08, C45, 2 (z = 56) – left distal tibia: DAPd = 43.6.

Azokh uppermost, 15-08, D-46, 32 (Z = 108) – fragment of left distal tibia.

Azokh 1, Unit II, C-46, 232 (z = 97, 1-8-2007) – juvenile phalanx 1 without proximal articulation: DAPd = 14.1, DTd = 14.9.

Azokh, plat. uppermost, Unit II, 2-8-05, surface find, no. A – fragment of a right astragalus: DTd = 32.7.

Unit I

Azokh 1, Unit I, 7-8-06, D-51, 68 (z = 103) – right distal tibia: DAPd = 40.9, DTd = 54.4, DTdfast = 37.8.

Overburden

7-9-02, F-41, overburden – left third phalanx: L ≫ 40.

Description of the new material and taxonomic classification

A group of bones and teeth of cervid morphology larger than those of *Dama* and smaller than what is expected for *Megaloceros* (or *Megaceroides*, *Praemegaceros*), tend to have morphologies that are similar to those in *Cervus elaphus*. The metacarpal has a morphology that is typical of *Cervus elaphus* (characters 1 and 3–7 of Lister 1996; Fig. 6.23/2). It is small for fossil *Cervus elaphus* and approaches the size of large *Dama* (6.24/2). The navicocuboid has characters 1 and 2 of Lister (1996) as in *Cervus* and unlike in *Dama*. The profile of the lingual wall of the upper premolars, as seen in anterior or posterior view, has a convex upper profile (Fig. 6.18/9b), as in *Cervus* and unlike in *Dama*, where the lower part is convex and the upper part concave. This feature corresponds approximately to character 3 of Lister (1996) for the upper premolars.

Discussion

Aliev (1969) assigned material to *Cervus elaphus* from the collection in Baku, which includes basal antler fragments with a bez tine, and various fragments of a crown (Fig. 6.19/4). Both characters are very typical of *Cervus elaphus*. The new material confirms the presence of this species.

Cervus elaphus entered western Europe just before the Brunhes-Matuyama limit (Atapuerca TD4, Dorn Dürkheim; Van der Made 1996; Franzen et al. 2000). The earliest forms were large (Fig. 6.24/1) and lacked a crown, but they became smaller in Mosbach, where the subspecies *Cervus elaphus acoronatus* is defined (some authors consider this a separate species). This locality is about 600 or 500 ka old. In Mauer (with a range of dates around 500–600 ka for most of the section – Wagner et al. 2010), where the subspecies *C. e. priscus* is defined, there is still not a well developed crown. Possibly both subspecies are identical. Fully coronate antlers appeared about 400 ka ago (subspecies *C. e. angulatus*). The species became large again in OIS7 until OIS5 (*C. e. spelaeus*), and then late in OIS5 it became small again. In OIS 2, it became large and at present it is small again (*C. e. elaphus*). These size fluctuations seem to be independent of glacial-interglacial changes, since the species is large in Germany

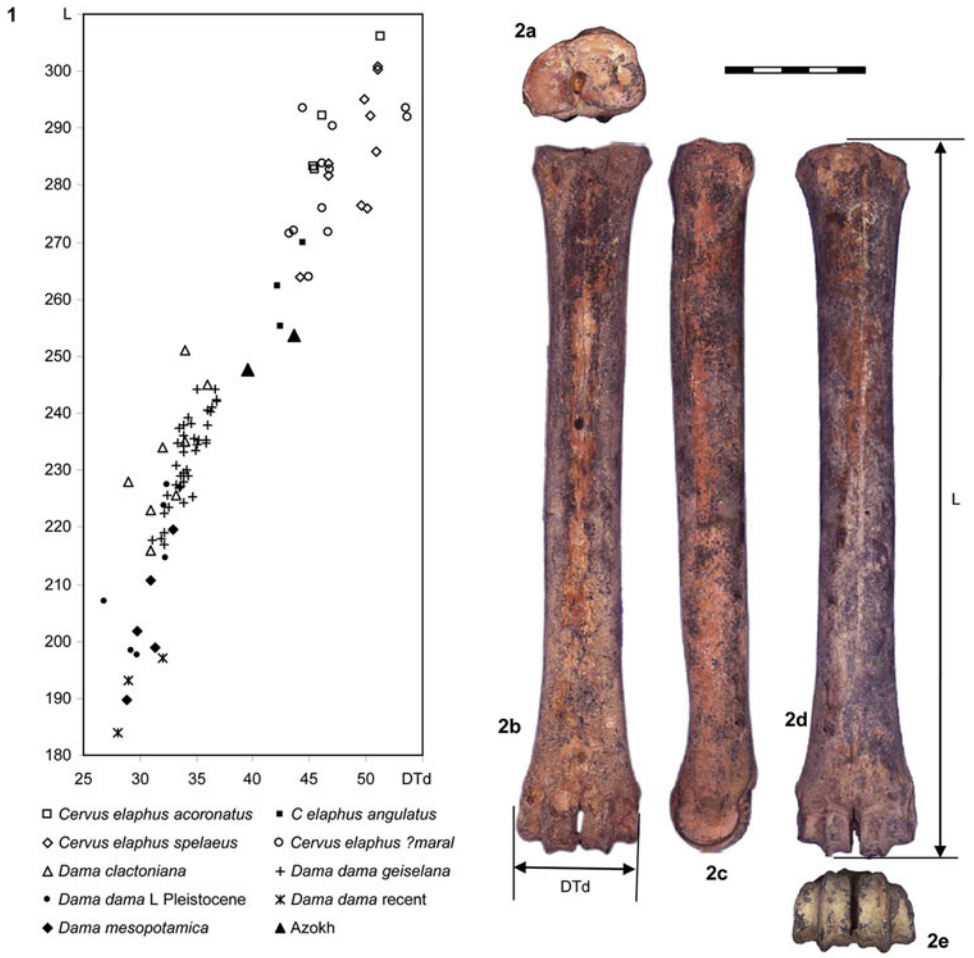

Fig. 6.23 **1** Bivariate diagram of the metacarpal comparing distal width (DTd) and length (L) in *Cervus elaphus* and *Dama*: *Cervus elaphus acoronatus* from Voigtstedt (IQW); *Cervus elaphus angulatus* from Bilzingsleben (FBFSUJ) and Petralona (AUT); *C. e. spelaeus* from Neumark Nord (FBFSUJ, presently LVH), *Cervus elaphus?maral* from Roterberg, Heiligenstadt, Tingleff, Pinne, Dobschau, Wismar-Torfmoor and an unkown locality (all MNHUB); *Cervus elaphus* from Unit III (MUB) and Unit V (ASMHCS); *Dama clactoniana* from Petralona (AUT) and Riano, Clacton and Swanscombe (all Leonardi and Petronio 1976); *D. dama geiselana* from Neumark Nord (FBFSUJ, presently LVH); *Dama dama* from the Late Pleistocene of Lehringen (HMV), Gimbsheim (NMM), Danne (MNHUB) and Steinbeck (MNHUB) and recent *D. d. dama* (Leonardi and Petronio 1976); recent *Dama mesopotamica* (HUJ). **2** Azokh upper, D-43, Unit V, 12 – left metacarpal of *Cervus elaphus* from Unit V (**a**–**e** proximal, posterior, medial, anterior and distal views). The scale bar represents 5 cm

in OIS7 (warm), OIS6 (cold) and OIS5 (warm). These size fluctuations also are much larger than contemporary geographic size differences between representatives from Germany and Spain. Living *Cervus elaphus* are small in western Europe (with minor differences between Spain and Germany), while it is larger in the Caucasus area (subspecies *C. e. maral*).

Changes in body size of *Cervus elaphus* occured also in the Caucasus area: the species was small in Azokh VI, V and III, large in Binagadi (believed to be of Eemian age; e.g., Eisenmann and Mashkour 1999), small in Taglar and Ortvala and at present it is large (Fig. 6.24/1). Evidently, the Holocene size decrease did not occur in this area, although other size changes might have been synchronous with western Europe. If this is the case, the small size in Unit VI–III, in combination with well developed crowns, present in Unit V, indicates an age in the range OIS12 to 8 or late OIS5 to OIS3 for Units V–III, while Unit VI, from which no crown is known, might be as old as OIS13 or 14 (Fig. 6.24).

Some antler fragments from Azokh have porous outer bone, whereas antlers normally have compact bone at the outer surface. This compact bone is about 4–5 mm thick and below it the inner part of the antler is made up of spongeous bone with large pores. In deer living at middle and high latitudes, the antler cycle is determined by seasonal variation in the intensity of the light. Antlers are shed once a year, and when they grow again, they are made of cartilage initially, but within less than a month they are ossified. Antlers that are fossilized in the middle of the process of ossification give a relatively precise indication of the month in which the individual died. Ossification occurs from proximal to distal

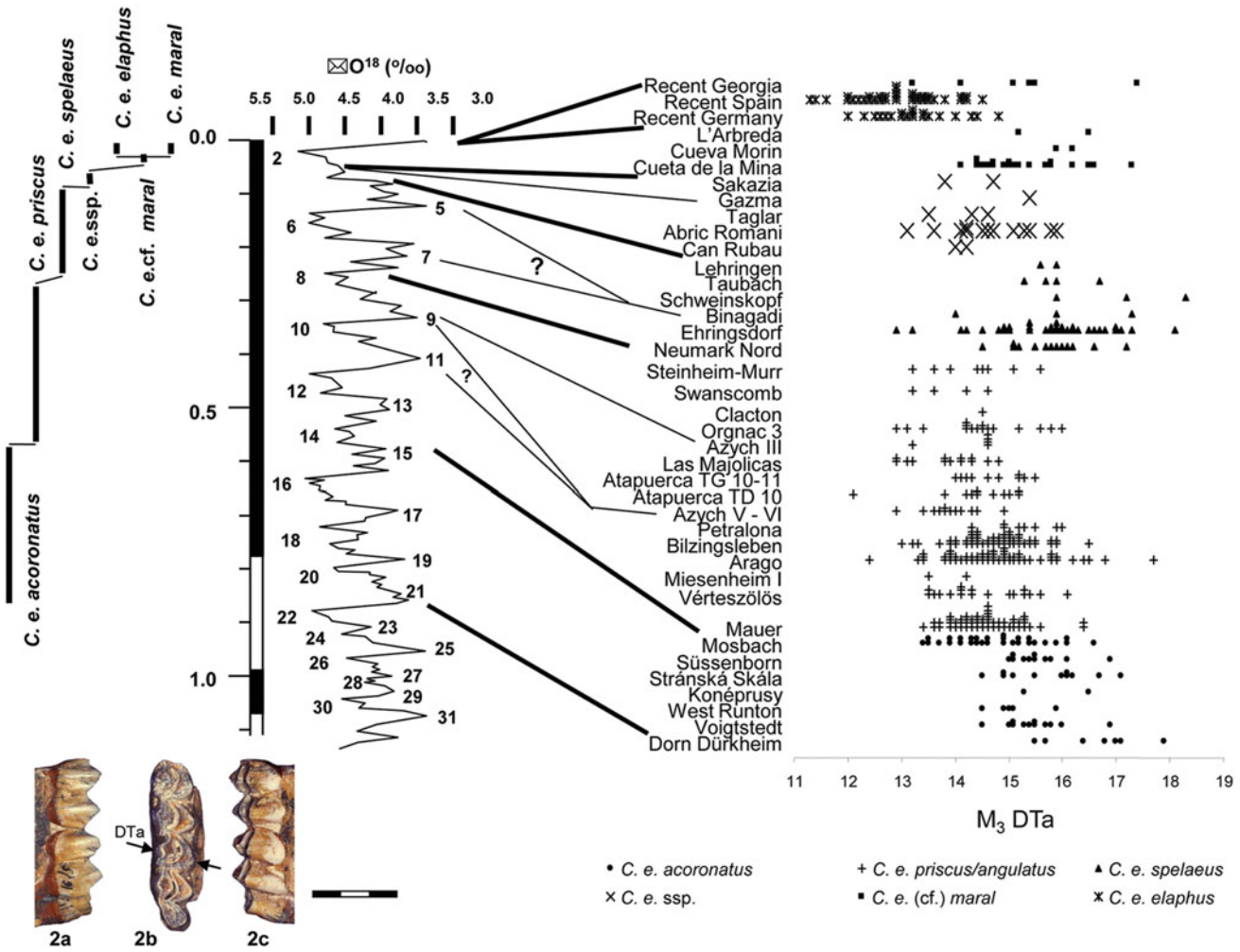

Fig. 6.24 **1** The variation in size of *Cervus elaphus* as indicated by the width of the first lobe (DTa) of the M_3. The localities are ordered in approximate stratigraphic order: Dorn Dürkheim (FISF), Voigtstedt (IQW), West Runton (NHM), Koneprusy (NMP), Stránska Skálá (MMB), Süssenborn (IQW), Mosbach (NMM), Mauer (SMNK), Vérteszölös (HGSB), Miesenheim (FASMN), Arago (MPT), Bilzingsleben (FBFSUJ), Petralona (AUT), Azokh (MUB), Atapuerca TD10 & TG10-11 (CENIEH), Orignac 3 (MPT), Clacton (NHM), Swanscombe (NHM), Steinheim – Murr (SMNS), Neumark Nord (FBFSUJ, presently LVH), Ehringsdorf (IQW), Binagadi (NHMB), Schweinskopf (FASMN), Taubach (IQW), Lehringen (HMV), Can Rubau (CIAG), Abric Romaní (LAUT), Taglar (MUB), Sakazia (GSM), Cueto de la Mina (MNCN), Cueva Morin (MNCN), L'Arbreda (CIAG), Recent Germany (FASMN), Recent Spain (EBD, MNCN), Recent Georgia (GSM). **2** MUB 5/91 – right $M_{2\text{-}3}$ from Azokh 1 Unit III (**a**–**c** lingual, occlusal, and buccal views). The scale bar represents 3 cm

and the compact bone layer is initially spongeous with pores that are finer than those of the inner part of the antler. Figure 6.19/5 shows a detail of a crown (MUB 6/158), that is not fully mineralized: the spongeous inner bone is seen in the lower part of the photograph, then there is a layer of bone with finer pores reaching the outer surface in the upper part of the photograph. Some fragments of the lower part of the antler also show porous bone reaching the surface at different places. This is the case in MUB7/883 and in an un-numbered specimen kept with MUB 6/18 and 6/26. The latter is the tip of a tine, which is broken at its base, where at some places porous bone reaches the surface. When mineralisation of the antler is complete, the velvet dies off and the antler is cleaned. In *Cervus elaphus* this occurs in August (Lincoln et al. 1982), suggesting that the specimens from Unit V described above, belonged to individuals that died in August or the end of July.

Family Bovidae Gray, 1821
Bison schoetensacki Freudenberg, 1914
Bos/*Bison* sp.

New material

Unit III

Azokh 1, Rescue, Unit III, 1.046 (?), 12 (z = 173(?), 24-7-2008) – right maleolar bone: DAP = 54.5, DT = 28.3, H > 33.4.

Unit II

Azokh 1, Unit II, 2-8-05, E-48, section cleaning – left cuneiform II-III: DAP > 43.7, DT = 26.9.

Azokh 1, Unit II, C-46, 70 (Z = 70, 8-10-08) – right astragalus: Lext > 84.4, Lm = 68.6, Lint > 78.3, DTp = 50.4.

Description of the new material

Fossil bones from Unit II have the morphology and size of a large ruminant. The massiveness of the cuneiform and maleolar (Fig. 6.25/3) suggest they belong to a bovine. Heintz (1970) indicated that in the Bovidae, the large cuneiform (II + III) has a vertical facet on its lateral side for articulation with the cuboid part of the navicocuboid, where it is well developed unlike the conditionwhile in the Cervidae where it is reduced or absent. Though this side of the bone is partially eroded, a relatively large part of such a facet remains, indicating again that the fossils correspond to a bovid.

There are no good morphological characters to separate cervid and bovid astragali (Heintz 1970). Bovini have very stout limb bones and the slenderness of the astragalus suggested that it might belong to a large cervid and not to a bovine. However, a metrical comparison of *Bos*, *Bison* and *Megaloceros* astragali (Fig. 6.25/1) does not show that these Bovini to have stouter astragali than a large cervid. The astragalus from the recent excavations (Fig. 6.25/4) is close in size to one recovered from the previous excavations at Azokh (Fig. 6.25/1), and both are larger than the astragali of large cervids of the type of *Megaloceros soleilhacus* (or *Megaceroides*, *Praemegaceros*, *M. verticornis*, *M. dawkinsi*) and *M. boldrini* (or *M. obscurus*).

Discussion

Material from Azokh Unit VI was assigned to *Bison* sp. or *Bison schoetensacki* (Aliev 1969; Lioubine 2002; Rivals 2004). The assignment of bones and teeth to *Bos* or *Bison* and in particular to different species of *Bison* is a dificult task. Some fragments of horn cores in the old collections from Azokh V have a surface with deep groves as occurs in the lower side and near the base of the horn cores of *Bison*. Likewise, distal articulations of metapodials from Unit III (and VI?) indicate the same genus.

The species of *Bison* differ in characters of the skull and horn cores, but also in the robusticity of the metapodials. The horn cores of *Bison schoetensacki* tend to be flattened (they have a relatively small transverse diameter in comparison to the anteroposterior diameter), while this tends to be less the case in *Bison priscus*. A relatively complete specimen from the old collections of Unit V has this "flattened" morphology. We follow the original assignment of the bovine material from Azokh to *Bison schoetensacki*. For the material from Unit II, which is much younger, other possibilities like *Bison priscus* or *Bos primigenius* are not to be excluded.

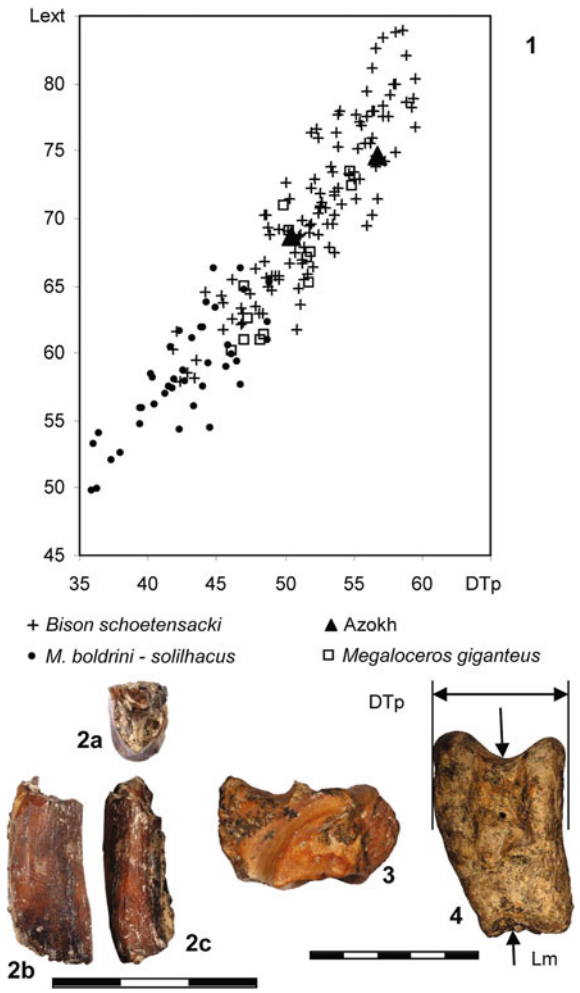

Fig. 6.25 **1** Bivariate diagram of the astragalus comparing axial length (Lm) and proximal width (DTp) in: *Megaloceros boldrini* and *M. solilhacus* from Ubeidiyah (HUJ), Bacton (NHM), Voigtstedt (IQW), Süssenborn (IQW), East Runton (NHM), West Runton (NHM) and Petralona (AUT); *Megaloceros giganteus* from Steinheim (SMNS) and Ireland (NHM); *Bison schoetensacki* from Vallonnet (MPRM), Akhalkalaki (GSM), Apollonia 1(AUT), Koneprusy (NMP), Pakefield (NHM), Vérteszölös (GSB), Süssenborn (IQW), Soleilhac (MCP), Mauer (SMNK), Jockgrim (SMNK), Bacton (NHM), Mundesley (NHM), Bilzingsleben (FBFSUJ), and Petralona (AUT); *Bos primigenius* from Miesenheim (FASMN), Megalopolis (AUT), Neumark Nord (FBFSUJ, presently LVH) and Lehringen (HMV) and "Azokh" including *Bison schoetensacki* from Unit V and cf. *Bison schoetensacki* from Unit II. **2** Azokh 1, Rescue, Bed II, 1.046 (?), 12 – right maleolar bone of cf. *Bison schoetensacki* from Azokh II (medial view). **3** Azokh 1, unit II, C-46, 70 – right astragalus of cf. *Bison schoetensacki* from Azokh II (anterior view). **4** AZM'05, E38, 3 – protocone of left upper molar of Bovidae indet. from Azokh 1 Unit V. The scale bars represent 3 cm (tooth) and 5 cm (bones)

The origin of the genus *Bison* was probably in the plains of Asia. In western Europe there may have been three lineages: the *Bison menneri-B. voigtstedtensis* lineage (large, slender metapodials, narrow skulls) had an age range of about 1.2–0.5 Ma; the *B. degiulii- B. schoetensacki* lineage (initially small, increasing in size, and with robust metapodials and wide

skulls) ranged about 1–0.1 Ma; and *B. priscus* (relatively small, with robust metapodials and wide skulls) might be related to the living *B. bonasus* (Van der Made 2005a). The moment of entry of *B. priscus* or related forms is interesting here, but the date is not well known beyond the notion that it was during the late Middle Pleistocene. The presence of *B. schoetensacki* in Azokh broadly confirms a Middle Pleistocene (or early Late Pleistocene) age for Unit II.

Saiga tatarica (Linnaeus, 1766)

New material

Unit Vm
?Middle plat., cleaning 26-7-05 – left first phalanx distal part: DAPd = 6.3, DTd = 7.7.
Unit II
Azokh, 18-8-06, Unit II, F-48, 94 (z = 75) – right first phalanx: DAPp.15.3, L = 42.2, DAPd = 9.4, DTd = 9.9.

Description of the new material and taxonomic classification

The first phalanx from Unit II (Fig. 6.16/3) is damaged and its proximal morphology is unclear. It is smaller, however, and more slender and elongate than that of *Capra*, but proximally it is not as narrow or elongate as in *Gazella* (Fig. 6.16/2). It appears more gracile than the *Capreolus* phalanges (especially those of the manus) and this is confirmed to some extent by the measurements. It is much smaller than the *Capreolus* phalanges from Unit V and it is relatively elongate compared to the phalanges of *C. priscus* and *C. capreolus*. The dorsal surface of the proximal end is flatter than it tends to be in *Capreolus*. In size and proportions it is similar to phalanges of recent *Saiga tatarica*.

The phalanx from Unit Vm is fragmentary, but the remaining morphology is that of a ruminant. It is very small and even much smaller than the phalanx from Unit II (Fig. 6.16/1).

Discussion

Aliev (1969) assigned a horn core from Unit V to *Gazella* cf. *subguturosa* (see also list by Rivals 2004), but this taxon was absent from the list given by Lioubine (2002). Horn core MUB 209 (Fig. 6.26) originates directly above the orbit and curves backwards. The rugose part (the part that was in contact with the keratine sheath) has relatively deep grooves. The section is oval, with a slight bulge just posterior of the middle at the medial side. The horn core is wider than is the case in male gazellas, and it is larger than in female gazellas. Morphologically and metrically it is close to a saiga fossil from Pahren described by Kahlke (1990).

The phalanx from Unit II has more resemblance to *Saiga* than to *Gazella* or *Capreolus*. Though from a different Unit, the horn core again resembles *Saiga*. We assume the presence of saiga antelopes in Units II and V. *Saiga* is an antelope that at present lives in a restricted area of the steppes north of the Himalayas. During the last two cold periods it extended its range into western Europe (Kahlke 1990, 1994) and even reached the north of Spain (Altuna and Mariezkurrena 1996).

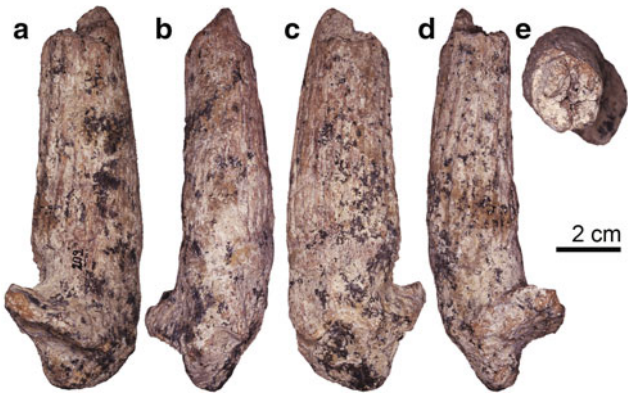

Fig. 6.26 *Saiga tatarica* from Unit V: MUB 209 – left horn core (**a**–**e** medial, anterior, lateral, posterior, and apical views)

Ovis ammon Linnaeus, 1766

New material

Unit Vm
?AZM'05, E38, 3 – fragment of a left upper molar.
Unit I
Azokh 1, Unit Ib, 21-7-07, B51, 8 (z = 99) – right proximal metatarsal: DAPp = 26.9, DTp = 25.7, DAPpf = 25.8, DTpf = 24.9, DTmini = 17.5, L ≫ 132.

Description of the new material and taxonomic classification

On the proximal surface of the metatarsal from Unit I (Fig. 6.27/1), the posterior facet for the navico-cuboid is narrow and elevated at the medial end, as typical in Bovidae (and unlike the condition in Cervidae). The posterior area comprising this facet and the facet for the first cuneiform is narrow in comparison to the width at the major (anterior) facets. This is more evident in *Alcelaphus* (cited as far to the north as Ksâr'akil in Hooijer 1961), where the facet for the small cuneiform is situated on a pointed posterior extension. In most Caprinae, this area is wide, though it is not so wide in *Ovis* and *Rupicapra*.

The proximal articulation and a major part of the shaft of the metatarsal are preserved. The distal part lacks widening, so the metatarsal must have been a long one, much longer than in *Capra* and most other Caprinae, save for *Ovis* and *Rupicapra*, which among the Caprinae are the animals with the most elongate metapodials.

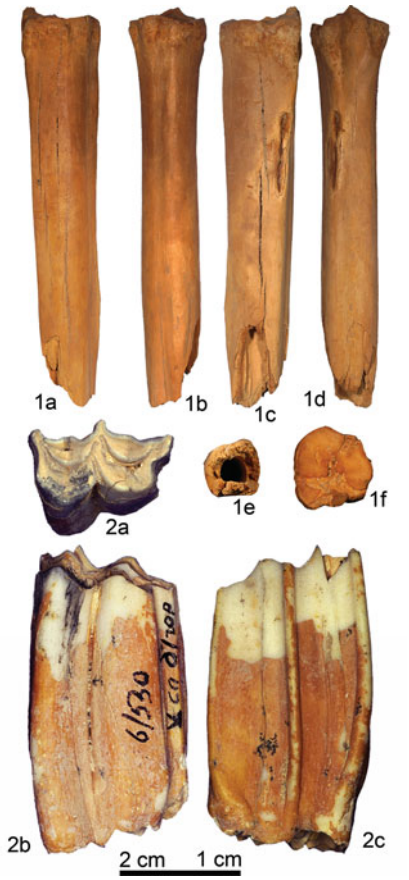

Fig. 6.27 *Ovis ammon* from Unit I and V. **1** Azokh 1, Unit Ib, 21-7-07, B51, 8 (z = 99) – right proximal metatarsal (**e**, **f** lateral, anterior, medial, posterior, distal and proximal views). The scale bar represents 2 cm. **2** MUB 6/530 – left M^3 (**a**–**c** occlusal, buccal and lingual views). The scale bar represents 1 cm

The anterior side of the bone lacks a clear furrow between the third and fourth metatarsals. Such a furrow is seen in Cervidae and some Bovidae, but it is lacking in Caprinae and some other Bovidae, where there is only a shallow depression. There is no clear longitudinal depression on the posterior side of the shaft.

In the morphology described above, the bone shows some similarities to the metatarsal of *Saiga*, but it is larger and the shaft is more robust. The closest resemblance is to the metatarsals of *Ovis antiqua* from Arago (MPT) and Bammenthal (SMNK), but it is a little smaller. It is larger than the metatarsal of *Ovis vignei* (NNML).

The molar fragment from Unit Vm consists of the protocone and part of the paracone. The preserved height of the protocone is 28 mm, but it must have been greater before it was worn. Wear was possibly not much advanced, and the paracone is higher than the protocone. The enamel is rugose, as is the case in the Bovini and some other Bovidae, like Alcelaphini and Hippotragini. In other bovids, like Caprinae, the enamel surface tends to be smooth.

The base of the protocone curved backwards, and the angle between the anterior side of the tooth, and what is preserved of the occlusal surface, both suggest that the tooth is an M^3. However, the facet on the protocone may occasionally be inclined, so this observation may not be valid. The anteroposterior diameter of the protocone is about 10 mm, suggesting that the DAP of the complete tooth was about 20 mm. This is small for *Bison schoetensacki*, if the tooth is an M^3. The estimated size of the specimen is not unlike in *Ovis ammon*.

The anterior and posterior crests of the protocone are straight, forming a smooth crescent, which limits a cresent shaped fossa. In living species of Alcelaphini and Hippotragini, there is a secondary crest on the inner sides of the anterior and of the posterior crest, resulting in a fossa with a more complex shape. These bovids also tend to have a well developed interlobular column, a minute additional fossa between the anterior and posterior lobes, and a flat occlusal surface. In all these characters they differ from the tooth fragment from Azokh.

Discussion

Ovis was not cited in early reports from Azokh (Aliev 1969; Lioubine 2002; Rivals 2004, p. 20). Rivals (2004, p. 31, Fig. 37, Table 6.9) assigned specimen MUB6/530 from Unit V (Fig. 6.27/2) to *Ovis ammon antiqua*. In size it is close to the specimen described above. A fragment of a large humerus from Unit III (MUB 5/48) has a distal articulation that is nearly cylindrical, not conical, and which has a small radius. It is large for *Capra* and might also represent *Ovis ammon*.

The metatarsal from Unit I is recent and could be from the wild species of *Ovis* that lives at present in the area. The recent species from this area is indicated as *Ovis aries* (Wilson and Reeder 1993), *Ovis orientalis* (Duff and Lawson 2004) or *Ovis gmelini* (Rivals 2004), and there does not seem to be any consensus on their names. The name *Ovis aries* is now applied to the domestic form. *Ovis orientalis* was cited at Mezmerskaya (Golanova et al. 1999) and *Ovis ammon* or *Ovis* cf. *ammon* was cited at Ortvala Klde, Tsona and Kudaro (Lioubine 2002; Rivals 2004, p. 20). The latter species is large, while *Ovis orientalis* and *Ovis vignei* are small (Rivals 2004). The bone from Unit I seems to belong to *Ovis ammon*.

Ovis ammon lives in an area extending from east Kazakhstan to south Siberia, Mongolia and northern China in the east and to northern Pakistan and northern India in the south. During the Early Pleistocene and again during the Middle Pleistocene, some 500 ka ago, it dispersed into western Europe, where the fossils are known as *Ovis antiqua* or *Ovis ammon antiqua* (Rivals 2004; Crégut-Bonnoure 2006).

Capra aegagrus Erxleben, 1777

New material

Unit Vm

Azokh'03, middle platform, Unit V, 17-8-03, 1 (Z = 117) – left $M^{1/2}$: DAP = 20.1, DAPb = 14.9, H ≫ 30.

Azokh, 28-7-05, plat middle, Unit V, F-39, 3 (z = 139) – left $M^{1/2}$: DAPo = 16.5, DAPb = 15.4, DTa = 14.9, DTp = 14.2.

Azokh, 8-9-02, plat. middle, F-43, 2 (z = 90) – right scapula: DAPn = 15.8, DTn = 11.8.

Azokh 1, Unit V, 4-8-2009, I-42, 39 (z = 860) – left M^1: DAPo = 14.4, DAPb = 11.1, DTa = 10.7, DTp = 10.3.

Unit Vm-IV

17-9-02, plat north, E44, gen finds – very rolled antero-proximal fragment of a metatarsal (?)

Azokh upper, 14/9/02, F-43, general finds – right P^4: DAP ≥ 10.2, DAPb ≥ 8.6, DT = 12.6.

Azokh, 13-9-02, F-44, dry sieve – sesamoid behind phalanx 1, right axial: L = 15.3, DAP = 8.8, DT = 9.5.

Azokh 1, Unit V, 27-7-2009, E-39, 8 (z = 871) – left ulnar: DAP = 16.7, DT ≥ 14.2, H > 22.2, Ha ≥ 16.5.

Unit Vu

Azokh 1, Unit IV, 7-8-08, O45, 31 (z = 60) – left lower molar (M_1 or M_2): DAP = 17.7, DAPb = 16.6, DTa = 9.7, DTp = 10.1.

Azokh upper, 17/9/02, D-45, 5 (Z = 73) – left distal articulation of metapodial, juvenile: DAP = 22.1, DT = 17.2.

Unit II

Azokh uppermost, 21-8-03, D-45, 16 (Z = 174) – right M^3: DAPo = 24.3, DAP = 26.2, DAPb = 22.5, DTa = 14.7, DTp = 12.3.

Description of the new material and taxonomic classification

The molars have high crowns, smooth enamel and lack interlobular columns. The lower molars have a caprine fold and relatively flat lingual walls (Fig. 6.28/6). The upper molars have marked styles on the buccal walls, but the buccal walls are flat or concave buccally on the tips of the para- and meta-cones (Fig. 6.28/3). A third upper molar has a posterior expansion at the base of the postero-buccal corner, which is typical in *Capra* (Fig. 6.28/4).

A distal articulation of a metapodial has the typical caprine morphology with the abaxial part of the condyle small in diameter and a dorsal surface that is horizontal or slightly elevated at the abaxial side.

Discussion

Material from Units V and III was assigned to *Capra aegagrus* (Aliev 1969; Lioubine 2002; Rivals 2004). The collections in Baku also include *Capra* from Unit VI. These collections include fragments of very large horn cores (e.g., Fig. 6.28/5). We have not had the opportunity to study horn cores of adult males of most species of *Capra* and therefore cannot fully evaluate the information the specimens from Unit VI contain.

The number of living species of *Capra* recognized varies from author to author. *Capra aegagrus* is the wild ancestor of the domestic *Capra hircus* (Duff and Lawson 2004), and in some literature it was included in the latter species (e.g., Wilson and Reeder 1993). It occurs in a wide area including Crete, Turkey and the area from the Caucasus to Pakistan. *Capra cylindricornis* and *Capra caucasica*, which for some are a single species, occur also in the Caucasus. During the late Pleistocene, the latter gave rise to *Capra pyrenaica* (Crégut-Bonnoure 1992). Material from Tsona, Ortvala and Sakazia is believed to represent *Capra caucasica* (Lioubine 2002; Touchabramichvili 2003; Rivals 2004), but is much larger than the recent species (e.g., compare recent *Capra caucasica* in Fig. 6.28/1 with Tsona, which is the largest specimen in the group "Tsona-Akhalkalaki"). There must have been a considerable size decrease in the latter species, as was also the case in *C. ibex*. *Capra ibex* dispersed some 400 ka ago into Europe.

A metacarpal from Unit V (Fig. 6.28/2) is robust, much larger than recent *Capra cylindricornis* and close in size to recent *Capra caucasica* and a little smaller and more gracile than specimens from Akhalkalaki and Tsona (Fig. 6.28/1). It is in the lower range of *Capra ibex* from Petralona. The phalanges (Fig. 6.29/2–4) are more abundant than complete metacarpals. Some first phalanges from Unit V reach larger sizes than those of *Capra ibex* from Petralona (Fig. 6.29/1), suggesting that this might be the case also with the metacarpal, if that sample would be larger. The phalanges of *Hemitragus* show a wider range of variation in robusticity than those of *Capra*; possibly this is due to a greater difference between anterior and posterior phalanges. The phalanges from Azokh Unit V are similar in size and proportions to those from Tsona, Sakazia and Ortvala.

?*Capra hircus* Linnaeus, 1758

New material

Unit I

Azokh 1, Unit I, subunit c, 20-7-07, D48, 4 – right I_1: DT = 5.3, DLL > 5.4.

Azokh 1, Unit I, passage, 22-7-07, C51, 57 (z = 124) – buccal side of left upper molar, probably M^2: DAP = 17.7, DAPb = 16.6.

Azokh 1, Unit I, 4-8-06, F-51, 3 (z = 29) – fragment buccal cusp upper molar.

Azokh 1, Unit I, E-51 4-8-06, 25 (z = 39) – right M_3: DAP = 32.4, DAPb = 30.5, DTa = 9.1, DTp = 9.8, DTpp = 6.5.

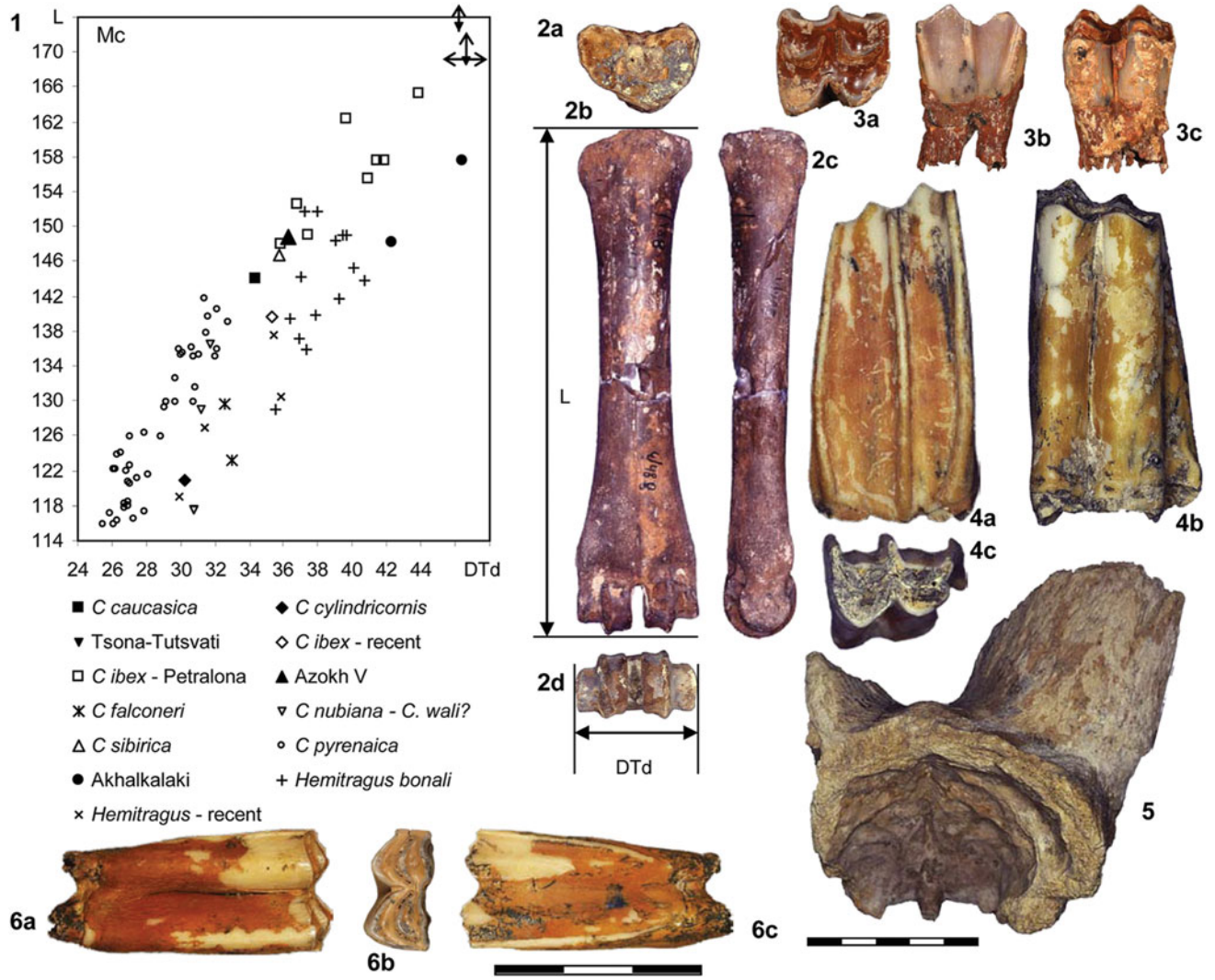

Fig. 6.28 **1** Bivariate diagram of the distal width (DTd) and length (L) of the metacarpal of *Capra*: *Capra* from Unit V, *C. causasica* from Tsona (GSM), Akhalkalaki (GSM) and Tsona (GSM); recent *C. cylindricornis* (GSM); *C. ibex* recent (LPT) and from Petralona (AUT); recent *C. falconeri* (NMB), recent *C. nubiana* (NMB), recent *C. sibirica* (NMB), recent *C. pyrenaica* (MNCN), recent *C. ?wali* (NHM). *Capra* from Azokh 1 Unit V: **2** MUB 4/488 – right Mc (**a**–**d** proximal, anterior, medial, and distal views). **3** AZM'05, F39, 3 – left M^1 (**a**–**c** occlusal, buccal and lingual views). **4** MUB 1/473 – left M^3 (**a**–**c** buccal, lingual, and occlusal views). **5** MUB 6/354 – skull fagment (posterior view). **6** Azokh 1, Unit V, O45, 31 – left M_2 (**a**–**c** buccal, occlusal and lingual views). The scale bars represent 5 cm (Mc and skull) and 3 cm (teeth)

Azokh 1, Unit I, 4-8-06, E-51, 46 (z = 44) – left ulna, juvenile (?): DAPmax = 27.2, DTupperfacet = 8.7, DAPmini = 16.4, DTmax = 16.9.

?Azokh 1, Unit I, 4-8-06, E-51, 45 (z = 46) – left femur, juvenile.

Azokh 1, Unit J, 6-8-06, D-51, 31 (z = 64) – left first phalanx: DAPp = 17.4/16.6, DTp = 14.4, L = 43.5, DAPd = 11.5, DTd = 13.2.

Azokh 1, Unit I, subunit b, 21-7-07, B51, 10 (z = 102) right P4: DAP = 8.3, DAPb = 7.4, DT = 10.1; M^1: DAP = 11.3, DAPb > 11.3, DTa = 12.3, DTp = 13.5; M^2: DAP = 17.5, DAPb = 16.1, DTa ≥ 14.2, DTp = 13.1; M^3: DAPo = 24.4, DAPmax = 27.4, DAPb = 26.1, DTa = 13.4, DTp = 11.4; Left P^3: DAP = 8.1, DAPb = 7.7, DT = 9.5; P^4: DAP = 7.9, DAPb = 7.7, DT ≥ 8.8; M^1: DAP = 10.6, DAPb > 10.6.

Description of the new material and taxonomic classification

The teeth from Unit I have typical caprine morphology as described above. The ulna is much expanded laterally at the level of the facets with the radius, which is typical in the Caprini. It is not fused to the radius. In adult *Capra ibex*, the two bones tend to be fused, while they tend to remain separate in other genera of Caprini, such as the closely related *Hemitragus*. The ulna might be from a juvenile individual. A first

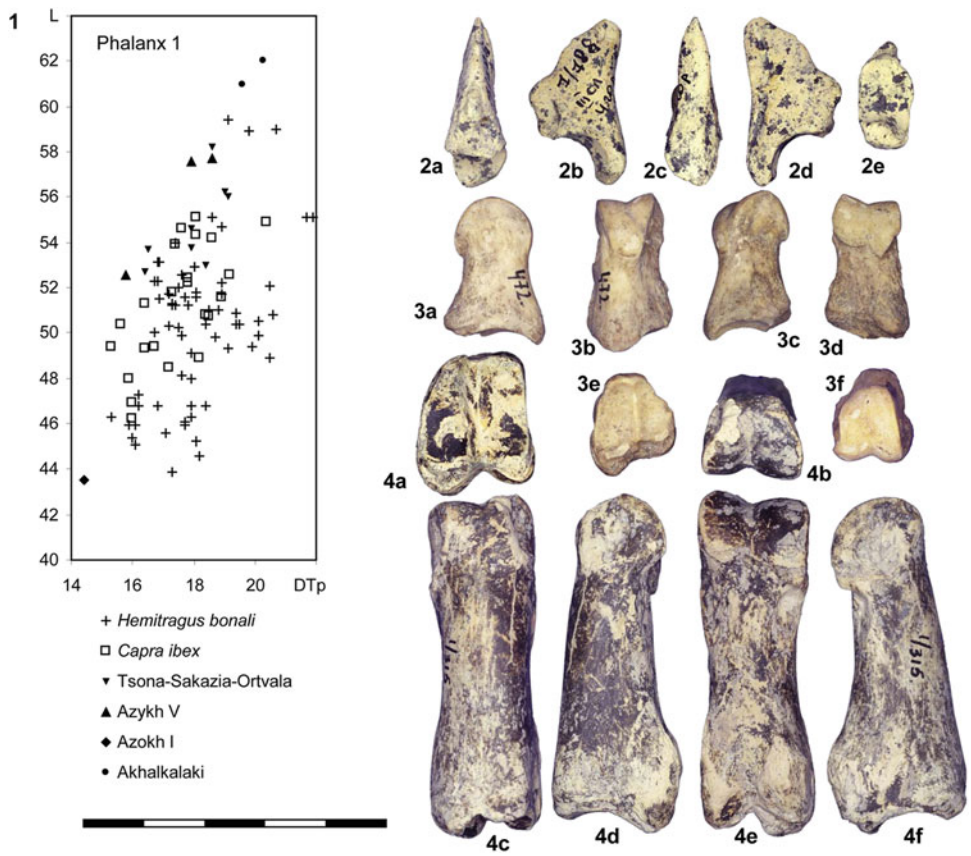

Fig. 6.29 **1** Bivariate diagram of the proximal width (DTp) and length (L) of the first phalanx of *Capra* and *Hemitragus*: *H. bonali* from Hundsheim (IPUW) and L'Escale (Bonifay 1975b), *C. ibex* from Petralona (AUT), *Capra* from Tsona (GSM), Sakazia (GSM), Ortvala (GSM), *Capra* from Azokh 1 Unit V (MUB) and *Capra hircus* from Unit I. **2** MUB 7/788 – left third phalanx of *Capra* from Unit III (**a–e** dorsal, abaxial, axial, plantar, and proximal views). **3** MUB 472 – left second phalanx of *Capra* from Unit V (**a–f** abaxial, dorsal, axial, plantar, proximal, and distal views). **4** MUB 1/315 – left first phalanx of *Capra* from Unit V (**a–f** proximal, distal, dorsal, axial, plantar, and abaxial views. The scale bar represents 5 cm

phalanx of caprine morphology from Unit I is very small (Fig. 6.29/1). It might represent the domestic *Capra hircus*.

General Discussion and Conclusions

Aliev (1969) described the large mammals from Azokh recovered at that time. Rivals (2004) gave a composite faunal list based on Aliev (1969), while Lioubine (2002) gave faunal lists per unit and incorporated later work. Our updated faunal lists are based on these publications, with additions of new material and discussed modifications; if we did not consult the original material and do not have new material, we have not changed the original determination. The updated lists of large mammals from different Units from Azokh are diplayed in Table 6.7.

One of the most striking things about the Azokh large mammal fauna is that in the old collections, large mammals were only recovered from Units VI, V and III, while in the new collections they are also recovered from Unit II. In the most recent excavation, Unit V was separated into upper and middle levels (abbreviated here as Vm and Vu). In Table 6.7, Unit V of the earlier excavations is grouped with Unit Vm of the excavation and Unit Vu is given in a separate column. Observing the lists, it is striking that carnivore remains come mainly from Unit V, while the other units have mainly ungulates. This is probably a genuine result, because the most extensive collections were made from Unit V in the old seasons, and because fossils from the old seasons were dug from the entrance of the cave and the most recent excavations come from the rear of the cave.

Animals that tend to be typical of closed environments dominate the faunas of all units, while animals more typical of open environments are less common. They are present, however, and Caprinae species adapted to mountainous, rocky or arid environments also occur. All units contain taxa that are commonly associated with interglacial environments (*Stephanorhinus kirchbergensis*, *Sus scrofa*, *Dama*), and with the possible exception of *Saiga*, none contains taxa that are clearly associated to glacials. This suggests that the climate was temperate, either interglacial or of a glacial

Table 6.7 Reviewed taxonomic identifications of Azokh Cave of material deposited in Baku (from the 1960 to 1989 seasons lead by Huseinov), and faunal list of large mammal fossils recovered from excavations 2002 to 2009

	VI	V/Vm	Vu	III	II	I
Vulpes vulpes	X				X	
Canis lupus		cf	cf		X	
Canis aureus		X				
Meles meles		X	X			
Martes cf. *foina*		X				
Crocuta crocuta		X	X			
Lynx sp.		X				
Felis chaus		X				
Panthera pardus		X		X	X	
Ursus spelaeus	X	X	X	X	X	
Ursus sp. (*U. thibetanus*?/*U. arctos*?)	X				X	
Equus hydruntinus	X	X		X		
Equus asinus						cf
Equus ferus	X	X				
Equus caballus						cf
Stephanorhinus hemitoechus	X	X	?	X		
Stephanorhinus kirchbergensis	X	X	?			
Sus scrofa	X	X		X	X	
Sus scrofa – domestic						X
Capreolus pygargus		X		X	X	
Dama aff. *peloponesiaca*	X	X	?			
Dama sp. (*Dama mesopotamica*?)				X		
Dama sp. (*Dama dama*?)					X	X
Megaloceros solihacus		X				
Cervus elaphus	X	X	X	X	X	X
Bison schoetensacki	X	X		cf		
Bos/Bison					X	
Ovis ammon		X		X		X
Capra aegagrus		X	X	X	X	
Capra hircus						cf
Saiga tatarica		X			X	

refugium. The area south of the Caucasus may have been a refugium for "interglacial" species during glacial times. However, during glacial times, the altitude of Azokh Cave (926 m above sea level) would result in a harsh environment in the immediate surroundings of the locality.

Figure 6.30 shows the faunas from the different levels of Azokh in a wider context, compared with other faunas of the region. A comparison is made with the stratigraphic distribution of the same taxa of Europe (solid lines). In the case of taxa not present in Europe, a comparison is made with the stratigraphic distribution in Africa and the Indian Subcontinent. The first observation that can be made is that most taxa present in the region are also present in Europe. Towards the south, European affinities decrease, but remain important. This pattern seems to be more or less constant in the time considered here. The faunas studied are biogeographically part of Western Eurasia, though African, Indian and central Asian elements are present.

Many of the localities and units in Fig. 6.30 are dated by some physical method (references in the figure caption), while some of the levels not yet dated form part of a sequence that includes dated levels. In a few cases, a site with a particular taxon in the study area has an age outside the temporal range for that taxon in Europe. These exceptions are: *Ovis ammon*, *Megaloceros solilhacus,* and *Cervus elaphus maral*, which all survived longer in the area, and *Bos primigenius* and *Vulpes vulpes*, which were present earlier than in Europe. The Holocene size decrease in *Cervus elaphus* that is so well known in Western Europe, did not occur here. The late occurrence of *Megaloceros solilhacus* is discussed under that species and there is no reason to believe that it is not a real result. The remains from Unit I show that *Ovis ammon* persisted in the area until the Present. *Bos primigenius* was present at Gesher Benot Ya'akov before it appeared in Europe. As discussed under *Cervus elaphus*, it seems that size changes south of the Caucasus follow those in western and central Europe, save for the Holocene. Leaving aside these exceptions, we can attempt to position the Units from Azokh in this scheme and thus estimate their ages on the basis of biochronology (Fig. 6.30).

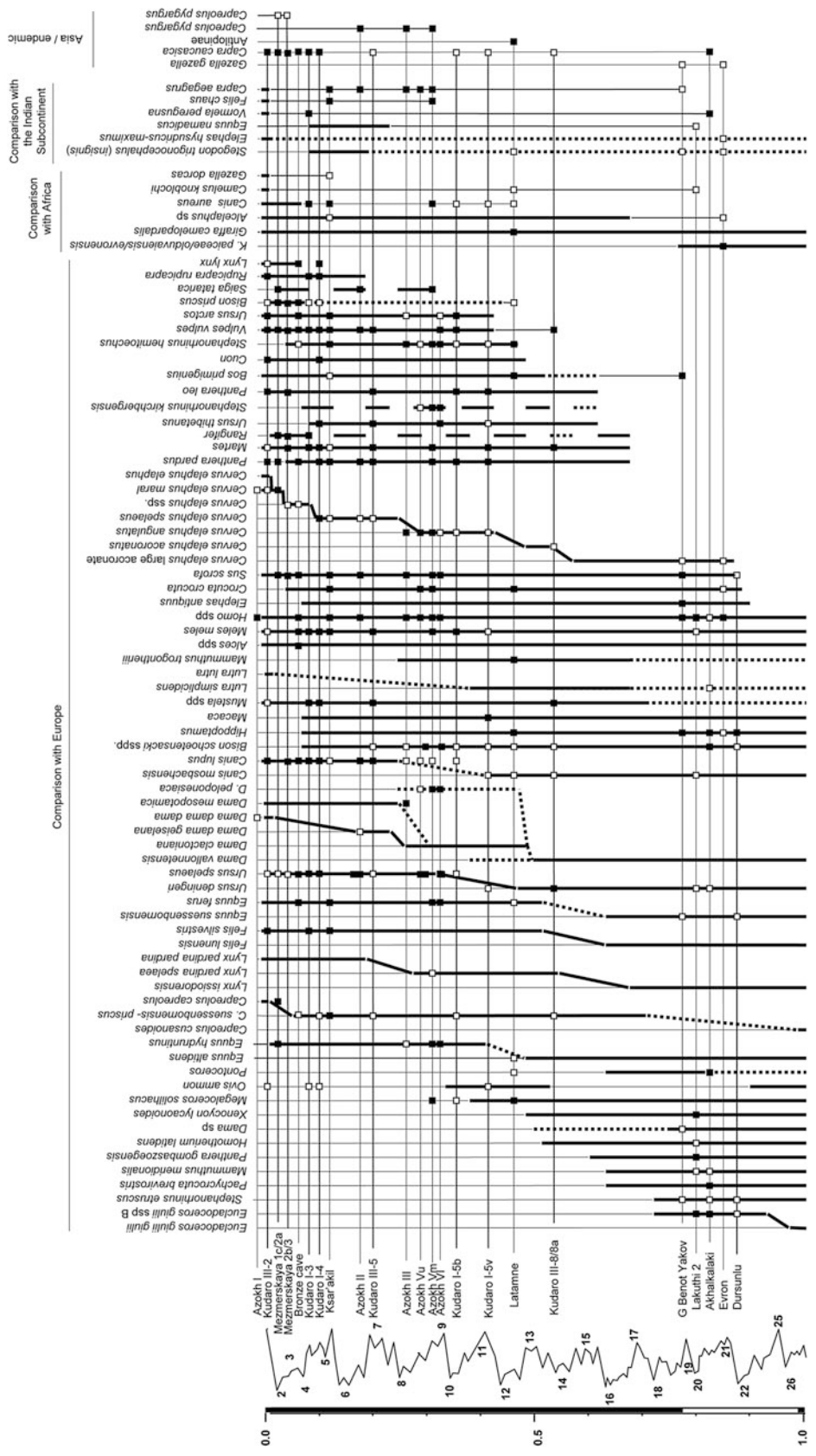

Fig. 6.30 The fauna from Azokh in the stratigraphic context of SW Asia (modified after Van der Made 2005a, b and based on the present study and the literature, principally: Lioubine 2002; Golanova et al. 1999; O'Regan et al. 2005; Tchernov et al. 1994; Ron et al. 2003; Hooijer 1961; Sharapov 1986; Janashvili 1978; Sotnikova and Vislobokova 1990; Vekua 1986, 1995). Solid squares indicate the presence of a taxon in the localities, open squares indicate "cf.", "aff.", "sp." or "?". In the cases of *Cervus elaphus*, *Capreolus*, *Ursus* and *Canis*, the information in the publications is insufficient to asses the grade of evolution of (sub)species and open squares are used. The fat vertical solid lines indicate the stratigraphic ranges of the taxa in Europe (left part of the figure), Africa and Asia (after Van der Made 2005b). Vertical fat dashed lines indicate uncertainty on the stratigraphic ranges. Fat oblique lines indicate phylogenetic relationships and dashed fat lines indicate assumed or possible relationships

The small sized *Cervus elaphus* identified in Units VI to IV marks a maximum age of 500–550 ka (OIS13 or 14), while the presence of well developed crowns of the antlers in Unit V indicates a maximum age of about 450–400 ka (OIS 11 or 12) for that and overlying units. The presence of *Equus ferus* and *E. hydruntinus* indicate maximum ages of about 500 ka (OIS13) for Units V and VI, but the material that we studied is too poor for certain identification. *Stephanorhinus hemitoechus* is identified in Units VI and V and indicates a maximum age of about 450 ka (or OIS12; see details on the temporal distribution in the discussion of the species). This species is assumed to have evolved outside western Europe and to have dispersed into Europe (Guérin 1980; Van der Made 2010a; Van der Made and Grube 2010a). *Ursus spelaeus* is present in Units VI, Vm, Vu, III, and II. It is assumed to have evolved from *Ursus deningeri* not later than 300 ka ago. In the period between about 450–240 kyr, the small *Canis mosbachensis* was replaced by the somewhat larger *C. lupus lunellensis*, which evolved into the large sized *C. lupus*. However, the material we studied from Units V and VI is to poor for assesing the grade of evolution. These data suggest a maximum age of around 300 ka for Unit VI and the overlying units. *Dama peloponesiaca* is an offshoot of the *Dama* lineage in the southeastern part of the geographical range of the genus and probably it was replaced there by *Dama mesopotamica*, when this species arose possibly during OIS8. This is in accordance with the small size of *Cervus* in Units VI–Vu (which in western Europe became large in OIS7). These data suggest that Units VI–Vu have ages between about 300 and 240 ka (corrseponding to OIS10-8). In the case of Unit VI this is based on the bear material, which we did not study, and which was deposited with fluvial sediments (Murray et al. 2016). If the presence of "interglacial" taxa is taken as indicative, these units are to be correlated with OIS9. Radiometric dating indicates ages of about 300 ka for Unit Vm and 200 ka for Unit Vu (see Appendix, ESR), which is compatible with a correlation of Units VI and Vm to OIS9, while it suggests a younger age for Unit Vu.

Unit III has a fauna that is poorer but similar to that of the underlying units. The main difference is that there is a fragment of antler of *Dama*, which might belong to *Dama mesopotamica*. The material is not very abundant nor the character very clear, but if this attribution is correct, it suggests a younger age and correlation to OIS8 or more recent. Unit III also has a small *Cervus elaphus*, which in western Europe occurs until OIS9 or 8, and again from late OIS5 to OIS3. Radiometric dates of 200 ka from the underlying Unit Vu and of 185 ka from the bottom of the ovelying Unit II (see Appendix, ESR, and Murray et al. 2016), leaves a short time span for Units IV and III. If these dates are correct, size changes in *Cervus* in this area, do not follow the trend in western Europe. This would not be surprising, even though in several other localities sizes are in accordance with those in western Europe.

Unit II has rather poor faunal remains. Its main difference from Unit III is the indication of cervids with wide antler palmation, which suggests *Dama dama* rather than *Dama mesopotamica*. The material of *Cervus* is too poor to assess its evolutionary grade. The bottom of this unit has been dated around 185 ka and the top around 100 ka (Appendix, ESR), which is compatible with the biochronological data from this unit.

Unit 1 has remains of domestic animals. This suggests a Holocene age, which is compatible with a datation of 157 years BP (Appendix, radiocarbon).

Acknowledgements In the context of the project INTAS AO1051S, directed by H. de Lumley, JvdM had the opportunity to study collections in Baku and Tbilisi, in the care of S.D. Aliev and D. Lordkipanidze and benefitted from discussions with F. Rivals, P.E. Moullé, and A. Arellano. In addition JvdM received support by projects CGL2006-13532-C03-03 and CGL2008-03881 and YFJ by CGL 2007-66231 and CGL2010-19825 projects of the Spanish Ministerio de Ciencia y Inovación.The following persons allowed access to material for comparison: F. Alférez Delgado, J. Barreiro, J.M. Bermúdez de Castro, C. Brauckmann, P. Cabot, E. Carbonell, E. Cioppi, E. Crégut-Bonnoure, G. Bossinski, A Currant, M. Dermitzakis, M. Esteban, O. Feifar, E. Frey, late J. Gibert, E. Gröning, J. H. Grünberg, F. Gusi, O. Hampe, W.-D. Heinrich, C. Heunisch, N. Ibañez, J. Jagt, R.D. Kahlke, F. Lacombat, L. Kordos, G. Koufos, D. Lordkipanidze, H. de Lumley, H. Lutz, G. Lyras, D. Mania, H. Meller, A. M. Moigne, W. Munk, R. Musil, M. Patou-Mathis, E. Pons, D. Reeder, J. Rodríguez, L. Rook, B. Sánchez Chillón, C. Smeenk, late P.Y. Sondaar, M. Sotnikova, U. Staesche, late E.Tchernov, Tong Haowen, E. Tsoukala, E. Turner, K. Valoch, I. Vislobokova, J. de Vos, R. van Zelst, R. Ziegler.

References

Adam, K. D. (1975). Die mittelpleistozäne Säugetier-Fauna aus dem Heppenloch bei Gutenberg (Württemberg). *Stuttgarter Beiträge zur Naturkunde, Serie B, 3*, 1–245.

Aliev, S. D. (1969). *Fauna Azikhskoy paleolitcheskoy stoyanki*. Baku.

Aliev, S. D. (1989). Referred in Lioubine (2002).

Aliev, S. D. (1990). Referred in Lioubine (2002).

Altuna, J., & Mariezkurrena, K. (1996). Primer hallazgo de restos óseos de antílope Saiga (*Saiga tatarica* L) en la Península Ibérica. *Munibe (Anthropologia-Arkeologia), 48*, 3–6.

Andrews, P., & Turner, A. (1992). Life and death of the Westbury bears. *Annales Zoologici Fennici, 28*, 139–149.

Appendix: Fernández-Jalvo, Y., Ditchfield, P., Grün, R., Lees, W., Aubert, M., Torres, T., et al. (2016). Dating methods applied to Azokh Cave sites. In Y. Fernández-Jalvo, T. King, L. Yepiskoposyan & P. Andrews (Eds.), *Azokh Cave and the Transcaucasian Corridor* (pp. 321–339). Dordrecht: Springer.

Argant, A. (1996). Sous-famille des Felinae. In C. Guérin & M. Patou-Mathis (Eds.), *Les grands mammifères Plio-Pléistocènes d'Europe* (pp. 200–215). Paris, Milan & Barcelona: Masson.

Azzaroli, A. (1953). The deer of the Weybourn Crag and Forest Bed of Norfolk. *Bulletin of the British Museum, Natural History, 2*(1), 1–96.

Azzaroli, A. (1962). Validitá della species *Rhinoceros hemitoechus* Falconer. *Palaeontographica Italica, 57*, 21–33, pls. 16–20.

Azzaroli, A. (1990). The genus *Equus* in Europe. In E. H. Lindsay, V. Fahlbusch & P. Mein (Eds.), *European Neogene Mammal Chronology* (pp. 339–356). New York: Plenum Press.

Azzaroli, A. (1992). The cervid genus *Pseudodama* n.g. in the Villafranchan of Tuscany. *Palaeontographia Italica, 79*, 1–41.

Baryshnikov, G. F. (1991). *Ursus mediterraneus* v Pleistocene Caucasa i zamechania po istorii melkih medvedey Eurasii. Palaeoteriologicheskie issledovania fauny SSSR. *Trudy Zoologischekoo Instituta AN SSSR, 238*, 3–60.

Baryshnikov, G. F. (1998). Cave bears from the paleolithic of the Greater Caucasus. In J. J. Saunders, B. W. Styles & Baryshnikov (Eds.), *Quaternary Paleozoology in the Northern Hemisphere. Illinois State Museum Scientific Papers, 27*, 69–118.

Baryshnikov, G. F. (2006). Morphometrical variability of cheek teeth in cave bears. *Scientific Annals, School of Geology Aristotle University of Thessaloniki, Special volume 98*, 81–102.

Berger, G. W., Pérez-González, A., Carbonell, E., Arsuaga, J. L., Bermúdez de Castro, J.-M., & Ku, T.-L. (2008). Luminescence chronology of cave sediments at the Atapuerca paleoanthropological site, Spain. *Journal of Human Evolution, 55*, 300–311.

Bonifay, M. F. (1971). Carnivores Quaternaires du sud-est de la France. *Mémoires du Museúm National d'Histoire Naturelle, novelle série, Série C, 21(2)*, 43–377, 27 pls.

Bonifay M. F. (1975a). Les Ursidés du gisement des Abimes de la Fage a Noailles (Corrèze) (*Ursus deningeri* von Reichenau). *Nouvelles Archives Musée. Histoire Naturelle. Lyon, 13*, 21–28.

Bonifay, M. F. (1975b). "*Hemitragus bonali*" Harlé et Stehlin, "Caprinae" de la Grotte de l'Escale (Saint-Estève-Janson, Bouches du Rhône). *Quaternaria, 18*, 215–302.

Burchak-Abramovitch, N. I., & Aliev, S. D. (1989). Iskopaemaya ornitofauna paleolitcheskoy stoyanki Azikhskoy peschery na Malom Caucase v Azerbaidjane (Chast I). *Materialy po ekologii jivotnih v Azerbaidjane: Temat sbornik*. Baku, 72–80.

Burchak-Abramovitch, N. I., & Aliev, S. D. (1990). Iskopaemaya ornitofauna paleolitcheskoy stoyanki Azikhskoy peschery na Malom Caucase v Azerbaidjane (Chast I). *Materialy po ekologii jivotnih v Azerbaidjane: Temat sbornik*. Baku, 44–57.

Cerdeño, E. (1990). *Stephanorhinus hemitoechus* (Falc.) (Rhinocerotidae, Mammalia) del Pleistoceno medio y superior de España. *Estudios Geológicos, 6*, 465–479.

Crégut-Bonnoure, E. (1992). Les Caprinae (Mammalia, Bovidae) du Pléistocène dÉurope: Intérêt biostratigraphique, peléoécologique et archéozoologique. *Mémoires de la Société géologique de France, n. s., 160*, 85–93.

Crégut-Bonnoure, E. (1996). Ordre des Carnivores. In C. Guérin & M. Patou-Mathis (Eds.), *Les grands mammifères Plio-Pléistocènes d'Europe* (pp. 155–230). Paris, Milano & Barcelona: Masson.

Crégut-Bonnoure, E. (2006). European Ovibovini, Ovini and Caprini (Caprinae, Mammalia) from the Plio-Pleistocene: New interpretations. *Courier Forschungsinstitut Senckenberg, 256*,139–158.

Croitor, R. (2006). Early Pleistocene small-sized deer of Europe. *Hellenic Journal of Geosciences, 41*, 89–117.

Croitor, R., & Brugal, J. F. (2010). Ecological and evolutionary dynamics of the carnivore community in Europe during the last 3 million years. *Quaternary International, 212*, 98–108.

de Vos, J., Leinders, J. J. M., & Hussain, S. T. (1987). A historical review of the Siwalik Hyaenidae (Mammalia, Carnivora) and description of two new finds from the upper Siwalik of Pakistan. *Proceedings of the Koninklijke Nederlandse Akademie van Wetenschappen, Series B, 90*(4), 333–369.

Di Stefano, G. (1996). The Mesopotamian fallow deer (*Dama*, Artiodactyla) in the Middle East Pleistocene. *Neues Jahrbuch für Geologie und Paläontologie Abhandlungen, 199*(3), 295–322.

Di Stefano, G., & Petronio, C. (1998). Origin of and relationships among *Dama*-like cervids in Europe. *Neues Jahrbuch für Geologie und Paläontologie Abhandlungen, 207*(1), 37–55.

Di Stefano, G., & Petronio, C. (2002). Systematics and evolution of the Eurasian Plio-Pleistocene tribe Cervini (Artiodactyla, Mammalia). *Geologica Romana, 36*, 311–334.

Doronichev V. B. (2000). Lower paleolithic occupation on the northern Caucasus. In D. Lordkipanidze, O. Bar-Josef & M. Otte (Eds.), *Early Humans at the Gates of Europe. Études et Recherches Archéologiques de l'Université de Liège, 92*, 67–77.

Duff, A., & Lawson, A. (2004). *Mammals of the world: A checklist*. London: A & C Black.

Dufour, R. (1989). *Les carnivores Pléistocènes de la Caverne de Marlarnaud (Ariège)*. Bordeaux: Museum d'Histoire Naturelle de Bordeaux.

Eisenmann, V. (1991). Les chevaux Quaternaires européens (Mammalia, Perissodactyla). Taille, typologie, biostratigraphie et taxonomie. *Geobios, 24*(6), 747–759.

Eisenmann, V., Alberdi, M. T., de Giuli, C., & Staesche U. (1988). Volume 1: Methodology. In M. Woodburne & P. Sondaar (Eds.), *Studying Fossil Horses* (pp. 1–71). Leiden: E.J. Brill.

Eisenmann, V., & Mashkour, M. (1999). The small equids of Binagady (Azerbaidjan) and Qazvin (Iran): *E. hemionus binagadensis* nov. subsp. and *E. hydruntinus*. *Geobios, 32*(1), 105–122.

Fernández-Jalvo, Y., King, T., Andrews, P., & Yepiskoposyan, L. (2016). Introduction: Azokh Cave and the Transcaucasian Corridor. In Y. Fernández-Jalvo, T. King, L. Yepiskoposyan & P. Andrews (Eds.), *Azokh Cave and the Transcaucasian Corridor* (pp. 1–26). Dordrecht: Springer.

Forsten, A. (1988). Middle Pleistocene replacement of stenonid horses by caballoid horses – ecological implications. *Palaeogeography, Palaeoclimatology, Palaeoecology, 65*, 23–33.

Forsten, A. (1992). Early *Equus* dispersal and taxonomy: Conflicting opinions. *Courier Forschungsintsitut Senckenberg, 153*, 171–176.

Forstén, A., & Ziegler, R. (1995). The horses (Mammalia, Equidae) from the early Wuermian of Villa Seckendorff, Stuttgart-Bad Cannstatt, Germany. *Stuttgarter Beiträge zur Naturkunde, Serie B* (*Geologie und Paläontologie*)*, 224,* 1–22.

Fortelius, M., Mazza, P., & Sala, B. (1993). *Stephanorhinus* (Mammalia: Rhinocerotidae) of the western European Pleistocene, with a revision of *S. etruscus* (Falconer, 1868). *Palaeontographia Italica, 80*, 63–155.

Franzen, J. L., Gliozzi, E., Jellinek, T., Scholger, R., & Weidenfeller, M. (2000). Die spätaltpleistozäne Fossillagerstätte Dorn-Dürkheim 3 und ihre Bedeutung für die Rekonstruktion der Entwicklung des rhenischen Flusssystems. *Senckenbergiana Lethaea, 80*(1), 305–353.

Gadziev, D. V., Guseinov, M. M., Mamedov, A. V., & Shirinov, N Sh. (1979). Kratkie rezul'taty complexnih issledovaniy Azikhskoy drevnepaleoitcheskoy stoyanki. *Izvestia AN AzSSR, seriya nauk o zemle, 3*, 10–16.

García, N., & Arsuaga, J. L. (1999). Carnivores from the Early Pleistocene hominid-bearing Trinchera Dolina 6 (Sierra de Atapuerca, Spain*). Journal of Human Evolution, 37*(3/4), 415–430.

García, N., Arsuaga, J. L., & Torres, T. (1997). The carnivore remains from the Sima de los Huesos Middle Pleistocene site (Sierra de Atapuerca, Spain). *Journal of Human Evolution, 33*(2/3), 130–154.

Golanova, L. V., Hoffecker, J. F., Kharitonov, V. M., & Romanova, G. P. (1999). Mezmerskaya Cave: A Neanderthal occupationin the Northern Caucasus. *Current Anthropology, 40*(1), 77–86.

Guérin, C. (1980). Les Rhinoceros (Mammalia, Perissodactyla) du Miocène terminal au Pléistocène Supérieur en Europe occidentale. Comparaison avec les espèces actuelles. *Documents des Laboratoires de Géologie Lyon, 79(1–3)*, 1–1185.

Guérin, C., & Barychnikov, G. F. (1987). Le rhinocéros acheuléen de la gotte Koudaro I (Georgie, URSS) et le problème des espèces relictes du Pléistocène du Caucase. *Geobios, 20*(3), 289–396.

Heintz, E. (1970). Les cervidés Villafranchiens de France et d'Espagne. *Mémoires du Muséum National d'Histoire Naturelle, nouv. sér., série C, Sciences de la Terre, 22*, 1–303, 40 pls., 319 figs., 131 tables.

Hemmer, H. (2001). Die Feliden aus dem Epivillafranchium von Untermassfeld. In R. D. Kahlke (Ed.), *Das Pleistozän von Untermassfeld bei Meinignen (Thüringen). Teil 2* (pp. 699–782, pls. 132–143). Bonn: Dr. Rudolf Habelt GMBH.

Hooijer, D. A. (1961). The fossil vertebrates of Ksâr'akil, a palaeolithic rock shleter in the Lebanon. *Zoologische Verhandelingen, 49*, 1–67, pls. 1–2.

Janashvili, R. (1978). The fauna of the caves. In *Exploration of Caves in Colchis*. Tbilisi 94–126.

Kahlke, H. D. (2001). Neufunde von Cerviden-Resten aus dem Unterplesitozän von Untermassfeld. In R. D. Kahlke (Ed.), *Das Pleistozän von Untermassfeld bei Meinigen (Thüringen), Teil 2. Römisch-Germanisches Zentralmuseum Forschungsinstitut für Vor- und Frühgeschichte. Monographiën 40(2),* 461–482, pls. 72–76.

Kahlke, R. D. (1990). Der Saiga-Fund von Pahren. Ein Beitrag zur Kenntnis der paläarktischen Verbreintungsgeschichte der Gattung *Saiga* Gray 1843 unter besonderer Berücksichtigung des Gebietes der DDR. *Eiszeitalter und Gegenwart, 40*, 20–37.

Kahlke, R. D. (1994). Die Entstehungs-, Entwicklungs- und Verbreitungsgeschichte des oberpleistozänen *Mammuthus-Coelodonta*-Faunenkomplexes in Eurasien (Grossäuger). *Abhandlungen der Senckenbergischen Naturforschenden Gesellschaft, 546*, 1–164.

Knapp, M., Rohland, N., Weinstock, J., Baryshnikov, G., Sher, A., Nagel, D., et al. (2009). First DNA sequences from Asian cave bear fossils reveal deep divergences and complex phylogeographic patterns. *Molecular Ecology, 18*, 1225–1238.

Koby, F. E. (1951). Les dimensions maxima et minima del os longs d'*Ursus spelaeus*. *Eclogae Geologicae Helvetiae, 43*(2), 287.

Kurten, B. (1955). Sex dimorphism and size trends in the cave bear. *Acta Zoologica Fennica, 90*, 1–47.

Kurten, B., & Poulianos, A. (1977). New stratigraphical and faunal material from Petralona cave with special reference to the carnivores. *Anthropos, 4*, 47–130.

Leonardi, G., & Petronio, C. (1976). The fallow deer of European Pleistocene. *Geologica Romana, 15*, 1–67.

Lincoln, G. A., Fraser, H. M., & Fletcher, T. J. (1982). Antler growth in male red deer (*Cervus elaphus*) after active immunization against LH-RH. *Journals of Reproduction and Fertility, 66*, 703–708.

Lioubine, V. P. (2002). L'Acheuléen du Caucase. *Études et Reschrches Archéologiques de l'Université de Liège, 93*, 1–140.

Lister, A. M. (1996). The morphological distinction between bones and teeth of fallow deer (*Dama dama*) and red deer (*Cervus elaphus*). *International Journal of Osteoarchaeology, 6*, 119–143.

Loose, H. (1975). Pleistocene Rhinocerotidae of W. Europe with reference to the recent two-horned species of Africa and S.E. Asia. *Scripta Geologica, 33*, 1–59.

Madurell-Malapeira, J., Alba, D. M., & Moyá-Solá, S. (2009). Carnivora from the Late Early Pleistocene of Cal Guardiola (Terrassa, Vallès-Penedès, Catalonia, Spain). *Journal of Paleontology, 83*(6), 969–974.

Marin-Monfort, M. D., Cáceres, I., Andrews, P., Pinto, A. C., & Fernández-Jalvo, Y. (2016). Taphonomy and site formation of Azokh 1. In Y. Fernández-Jalvo, T. King, L. Yepiskoposyan & P. Andrews (Eds.), *Azokh Cave and the Transcaucasian Corridor* (pp. 211–249). Dordrecht: Springer.

Markova, A. K. (1982). Microteriofauna iz paleoliticheskoy peschernoy stoyanki Azikh. *Palaeontoligischeskoy sbornik, 19*, 14–28.

Morales, J., Soria, D., Montoya, P., Pérez, B., & Salesa, M. J. (2003). *Caracal depereti* nov. sp. y *Felis* aff- *silvestris* (Felidae, Mammalia) del Plioceno Inferior de Layna (Soria, España). *Estudios Geológicos, 59*, 229–247.

Murray, J., Lynch, E. P., Domínguez-Alonso, P., & Barham, M. (2016). Stratigraphy and Sedimentology of Azokh Caves, South Caucasus. In Y. Fernández-Jalvo, T. King, L. Yepiskoposyan & P. Andrews (Eds.), *Azokh Cave and the Transcaucasian Corridor* (pp. 27–54). Dordrecht: Springer.

Musil, R. (1969). Die Equiden-Reste aus dem Pleistozän von Süssenborn bei Weimar. *Paläontologische Abhandlungen, Abteilung A Paläozoologie, 3(3–4)*, 617–666, pls. 37–45.

Musil, R. (1977). Die Equidenreste aus den Travertinen von Taubach. *Quartärpaläontologie, 2*, 237–264.

O'Regan, H. J., Bishop, L. C., Lamb, A., Elton, S., & Turner, A. (2005). Large mammal turnover in Africa and the Levant between 1.0 and 0.5 Ma. In M. J. Head & P. L. Gibbard (Eds.), *Early-Middle Pleistocene transitions: The land-ocean evidence. Geological Society, London, Special Publications 247*, 231–249.

Pfeiffer, T. (1998). *Capreolus suessenbornensis* Kahlke 1956 (Cervidae, mammalia) aus den Mosbach-Sanden (Wiesbaden, Biebrich). *Mainzer naturwissenschaftliches Archiv, 36*, 47–76.

Pfeiffer, T. (1999). Die Stellung von *Dama* (Cervidae, Mammalia) im system pleisometacarpaler Hirsche des Pleistozäns. Phylogenetische Reconstruktion – Metrische Analyse. *Courier Forschungsinstitut Senckenberg, 211*, 1–218.

Qiu, Z. (1979). Some mammalian fossils from the Pliocene of Inner Mongolia and Gansu (Kansu). *Vertebrata PalAsiatica, 17*(3), 222–235.

Rabeder, G., Hofreiter, M., & Withalm, G. (2004). The systematic position of the cave bear from Potocka zijalka (Slovenia). *Mitteilungen der Kommission für Quartärforschung der Österreichischen Akademie der Wissenchaften, 13*, 197–200.

Rabeder G., Pacher M., & Withalm G. (2010). Early Pleistocene bear remains from Deutsch-Altenburg (Lower Austria) *Mitteilungen der Kommission für Quartarforschung der Österreichischen Akademie der Wissenchaften, 17,* 1–135.

Rivals, F. (2004). Les petits bovidés (Caprini et Rupicaprini) pléistocènes dans le bassin méditerranéen et le Caucase. Étude paléontologique, biostratigraphique, archéozoologizue et paléoécologique. *British Archaeological Reports International Series, 1327*, 1–252.

Rohland, N., Knapp, M., Weinstock, J., Baryshnikov, G., Sher, A., Nagel, D., et al. (2008). The complex biogeography of extinct Eurasian Cave bears. Society for Molecular Biology and Evolution Meeting 5–8 June, Spain.

Ron, H., Porat, N., Ronen, A., Tchernov, E., & Horwitz, L. K. (2003). Magnetostratigraphy of the Evron Member – Implications for the age of the Midle Acheulian site of Evron Quarry. *Journal of Human Evolution, 44*, 633–639.

Schmid, E., & O. Garraux (1972). *Atlas of animal bones for prehistoirans, archaeologists and Quaternary geologists* (pp. 1–159). Amsterdam, London & New York: Elsevier.

Sharapov, S. (1986). *The Kurksay complex of Upper Pliocene Mammalian of Afghan-Tadjik Depression* (pp. 1–269). Academy of Sciences of the Tadjik SST, Dushanbe.

Sickenberg, O. (1976). Eine Säugetierfauna des tieferen Bihariums aus dem becken von Megalopolis (Peloponnes, Griechenland). *Annales Géologiques des Pays Helléniques, 1e série, 27*, 25–73, pls. 6–10.

Soergel W. (1926). Der Bär von Suszenborn. Ein beitrag zur näheren Kenntinis der diluvialen Bären. *Zeitschrift Deustchen Geologischen Gesellschaft, 77 Abteilung B (Geologie und Paläontologie)*, 115–156.

Sotnikova, M. V., & Vislobokova, I. A. (1990). Pleistocene mammals from Lakhuti, southern Tajikistan, U.S.S.R. *Quartär-Paläontologie, 8*, 144–237.

Tchernov, E., Kolska Horwitz, L., Ronen, A., & Lister, A. (1994). The faunal remains from Evron Quarry in Relation to other Lower Palaeolithic hominid sites in the southern Levant. *Quatenary Research, 42*, 328–339.

Teilhard de Chardin, P., & Trassaert, M. (1937). The Pliocene Camelidae, Giraffidae, and Cervidae of South Eastern Shansi. *Palaeontologia Sinica, new series C, 1*, 1–56, pls. 1–6.

Torre, D. (1967). I cani villafranchani della Toscana. *Palaeontographia Italica, 63*, 113–138, pls. 10–19.

Torres, T. (1978). Estudio comparativo de las mandíbulas de *Ursus spelaeus* Ros.-Hein. *Ursus deningeri* von Reich. y *Ursus arctos* Linn. *Boletín Geológico y Minero, 89(3)*, 203–222.

Torres, T. (1989). *Estudio de la filogenia, distribución estratigráfica y geográfica y análisis morfológico y métrico de esqueleto y dentición de los osos (Mammalia, Carnivora, Ursidae) del Pleistoceno de la Península Ibérica (*U. deningeri *Von Reichenau,* Ursus spelaeus *Rosenmüller-Heinroth,* Ursus arctos *Linneo).* Madrid: Publicación Especial Instituto Geológico y Minero de España.

Torres T., & Cervera, J. (1992). Análisis Multivariante de la morfología dental de los Ursidos del Plio-Pleistoceno, con algunas consideraciones sobre la posición filogenética de *Ursus deningeri* von REICHENAU de Cueva Mayor (Sima de los Huesos), Atapuerca-Burgos. In. E. Aguirre, E. Carbonell & J. M. Bermúdez de Castro (Eds.), *Evolución Humana en Europa y las Yacimientos de la Sierra de Atapuerca, 1* (pp. 123–135). Valladolid: Junta de Com. Castilla-León.

Torres T., & Guerrero P. (1993). Análisis multivariante de la morfología de los metápodos de osos espeloides del Pleistoceno Ibérico (*Ursus deningeri* von Reichenau y *Ursus spelaeus* Rosenmüller-Heinroth). Abstracts de las IX Jornadas de Paleontología, Málaga 49–54.

Torres, T., Nestares, T., Cobo, R., Ortiz, J. E., Cantero, M. A., Ortiz, J., et al. (2001). Análisis morfológico y métrico de la dentición y metapodios del oso de Deninger (*Ursus deningeri* Reichenau) de la cueva Santa Isabel de Ranero. *Aminocronología (Valle de Carranza-Vizcaya-País Vasco), 51*, 107–141.

Torres, T., Ortiz, J. E., Llamas, J. F., Canoira, L., Juliá, R., & García de la Morena, M. A. (2002). Cave bear dentine aspartic acid racemization analysis, proxy for Pleistocene Cave infills dating. *Archaeometry, 44*(3), 417–426.

Torres, T., Ortiz, J. E., Cobo, R., Julià, R., Camacho, A., Puch, C., & Llamas, J. F. (2006). Presence of two cave bear species in La Lucia cave (Lamasón, Cantabria, N Spain): *Ursus deningeri* von Reichenau and *Ursus spelaeus* Rosenmüller-Heinroth. *Munibe, 57*(1), 103–122.

Touchabramichvili, N. (2003). Les industries du Paléolithique inférieur dans le Caucase méridional. *L'Anthropologie, 107*, 565–576.

Turner, A. (1990). The evolution of the guild of larger terrestrial carivores during the Plio-Pleistocene in Africa. *Geobios, 23*(3), 349–368.

Ueckermann, E., & Hansen, P. (2002). *Das Damwild. Biologie, Hege und Jagd.* Kosmos, Stuttgart 1–327.

Van der Made, J. (1996). Listriodontinae (Suidae, Mammalia), their evolution, systematics and distribution in time and space. *Contributions to Tertiary and Quaternary Geology 33(1–4)*, 3–254, microficha 54 pp.

Van der Made, J. (1999). Ungulates from Atapuerca-TD6. *Journal of Human Evolution, 37*(3–4), 389–413.

Van der Made, J. (2000). A preliminary note on the rhinos from Bilzingsleben. *Praehistoria Thuringica, 4*, 41–62.

Van der Made, J. (2001). Les ongulés d'Atapuerca. Stratigraphie et biogéographie. *L'Anthropologie, 105*, 95–113.

Van der Made, J. (2005a). La fauna, Capítulo 3 – Asia; Sección 3.4. In E. Carbonell (Ed.), *Homínidos: Las primeras ocupaciones de los continentes* (pp. 270–306). Barcelona: Ariel.

Van der Made, J. (2005b). La fauna del Pleistoceno europeo, Capítulo 4 – Europa; Sección 4.4. In E. Carbonell (Ed.), Homínidos: Las primeras ocupaciones de los continentes (pp. 394–432). Barcelona: Ariel.

Van der Made, J. (2010a). The rhinos from the Middle Pleistocene of Neumark Nord (Saxony-Anhalt). *Veröffentlichungen des Landesamtes für Archeologie, 62*, 432–527.

Van der Made, J. (2010b). Biostratigraphy – "Large Mammals". In D. Höhne & W. Schwarz (Eds.), "Elefantentreich – Eine Fossilwelt in Europa". Landesamt für Denkmalpflege und Archälogie Sachsen-Anhalt & Landesmuseum für Vorgeschichte, Halle 82–92.

Van der Made, J., & Grube, R. (2010). The rhinoceroses from Neumark-Nord and their nutrition. In D. Höhne & W. Schwarz (Eds.), *Elefantentreich – Eine Fossilwelt in Europa* (pp. 383–394). Halle: Landesamt für Denkmalpflege und Archälogie Sachsen-Anhalt & Landesmuseum für Vorgeschichte.

Van der Made, J., & Tong, H. W. (2008). Phylogeny of the giant deer with palmate brow tines *Megaloceros* from west and *Sinomegaceros* from east Eurasia. *Quaternary International, 179*, 135–162.

Vekua, A. (1986). The lower Pleistocene Mammalian Fauna of Akhalkalaki (southern Georgia, USSR). *Palaeontographia Italica, 74*, 63–96.

Vekua, A. (1995). Die Wirbeltierfauna des Villafranchium von Dmanisi und ihre biostratigraphische Bedeutung. *Jahbuch des Römisch-Germanischen Zentralmuseums Mainz, 42*, 77–180, pls. 7–54.

Velichko, A. A., Antonova, G. V., Zelikson, E. M., et al. (1980). Paleogeographia stoyanki Azikh – drevnejshego poselenia pervobytnogo cheloveka na territorii SSSR. *Izvestia AN SSSR, seria geograph, 3*, 20–35.

Vislobokova, I., Dmitrieva, E., & Kalmykov, N. (1995). Artiodactyls from the Late Pliocene of Udunga, western Trans-Baikal, Russia. *Journal of Vertebrate Paleontology, 15*(1), 146–159.

von Koenigswald, W. (1986). Beziehungen des pleistozänen Wasserbüffels (*Bubalus murrensis*) aus Europa zu den asiatischen Wasserbüffeln. *Zeitschrift für Säugetierkunde, 51*(5), 312–323.

Wagner, G. A., Krbetschek, M., Degering, D., Bahain, J. J., Shao, Q., Falguères, C., et al. (2010). Radiometric dating of the type-site for *Homo heidelbergensis* at Mauer, Germany. *Proceedings of the National Academy of Sciences, 107(46)*, 19726–19730.

Whitehead, G. K. (1993). *The Whitehead Encyclopedia of Deer*. Shrewsbury: Swan Hill Press.

Wilson, D. E., & Reeder, D. A. M. (1993). *Mammal species of the world – a taxonomic and geographic reference* (2nd ed.). Washington & London: Smithsonian Institution Press.

Wolsan, M. (2001). Remains of *Meles hollitzeri* (Carnivora, Mustelidae) from the Lower Pleistocene site of Untermassfeld. In R. D. Kahlke (Ed.), *Das Pleistozän von Untermassfeld bei Meinigen (Thüringen), Teil 2. Römisch-Germanisches Zentralmuseum Forschungsinstitut für Vor- und Frühgeschichte. Monographiën 40(2)*, 659–671.

Xue X., & Zhang Y. (1991). Chapter 10. Quaternary mammalian fossils and fossil human beings. In Z. Zhang, S. Shao, G. Tong & J. Cao (Eds.), *The Quaternary of China* (pp. 307–374). Beijing: China Ocean Press.

Zapfe, H. (1946). Die altplistozänen Bären von Hundsheim in Niederösterreich. *Jahrbuch der Geologischen Bundesanstalt, 3–4*, 95–164.

Chapter 7
Rodents, Lagomorphs and Insectivores from Azokh Cave

Simon A. Parfitt

Abstract Azokh Cave in the Karabakh range of the Lesser Caucasus has yielded one of the richest small mammal assemblages yet reported from the entire Caucasus region. Over 2770 dental and cranial remains from at least 24 taxa of insectivore, rodent and lagomorph have been studied from the Middle/Late Pleistocene (Units II–V) and Holocene (Unit 1) deposits at Azokh 1. Holocene samples were also studied from Azokh 5. The small mammal assemblages are dominated throughout by arvicoline rodents indicative of dry steppes and semi-deserts. Notable species include several regionally extinct arid-adapted or montane taxa, such as *Ochotona* (pika), *Marmota* sp. (marmot), *Spermophilus* sp. (ground squirrel), *Chionomys nivalis* (snow vole) and *Allactaga* spp. (jerboa). Hamsters (*Mesocricetus* sp., *Cricetulus migratorius*), jirds (*Meriones* spp.) and mole voles (*Ellobius* sp.) are also well represented throughout the sequence. Habitat preferences of extant representatives of the rodent and lagomorph fauna suggest that the landscape surrounding the cave was dominated by grassland/steppe interspersed with rocky ground. Small mammals that prefer more humid conditions and woodland or scrub vegetation are present as rare components of the Pleistocene fauna. Unit Vu has yielded the earliest Caucasian record of rat (*Rattus* sp.), a species previously thought to have been a relatively recent (late Holocene) introduction. Several species recovered from the Pleistocene and Holocene deposits are now scarce or no longer live in the region, adding to evidence for distributional changes of these taxa in the latter part of the Pleistocene and Holocene. The small mammal fauna shows broad similarities to those from semi-desert and steppe regions to the south, implying dispersals from the adjacent parts of Asia; there appear to be only tenuous links with the Pleistocene small mammals north of the Caucasus.

Резюме Азохская пещера, расположенная в горной цепи Карабаха (Малый Кавказ), является ключевой стоянкой для понимания развития кавказской малой фауны в эпохи плейстоцена и голоцена. Большая коллекция грызунов, зайцеобразных и насекомоядных (землеройка и крот), обнаруженная в период археологических раскопок 2002–2009 гг., включает в себя более 23 таксонов из различных горизонтов верхней части седиментной последовательности (подразделения *I–V*). Найденные образцы находятся в прямой ассоциации с останками по крайней мере двух видов гоминид (*Homo heidelbergensis* в *пласте V* и *Homo sapiens в пласте I*) наряду с мустерианскими артефактами в подразделениях *IV–II*, указывающими на возможное присутствие *H. neanderthalensis*. Проливая свет на четвертичную биогеографию различных видов мелких млекопитающих, обнаруженные образцы представляют собой прямые свидетельства экологических условий в период пребывания человека на данной стоянке.

Среди обнаруженных мелких млекопитающих доминируют грызуны подсемейства полевковых, особенно представители групп *Microtus arvalis* и *M. Socialis*, которые указывают, соответственно, на превалирование луговой и степной растительности. Наиболее распространенные виды, обнаруженные в пещере, относятся к различным, адаптированным к аридным или гористым условиям, таксонам, таким как *Ochotona* spp. (пищуха), *Marmota* sp. (сурок), *Spermophilus* sp. (бурундук), *Allocricetulus* sp. (хомяк), *Chionomys nivalis* (снеговая полевка) и *Allactaga* spp. (тушканчик). Хомяки (*Mesocricetus* sp., *Cricetulus migratorius*), песчанки (*Meriones* spp.) и слепушонки (*Ellobius* sp.) также хорошо представлены во всей последовательности отложений. Средовые предпочтения ныне живущих представителей грызунов и зайцеобразных

S.A. Parfitt (✉)
Institute of Archaeology, University College London,
31–34 Gordon Square, London WC1H 0PY, UK
e-mail: s.parfitt@ucl.ac.uk

Yolanda Fernández-Jalvo et al. (eds.), *Azokh Cave and the Transcaucasian Corridor*,
Vertebrate Paleobiology and Paleoanthropology, DOI 10.1007/978-3-319-24924-7_7

свидетельствуют о том, что в ландшафтном окружении пещеры доминировали луга и степи с вкраплением скалистых пород. У основания седиментной последовательности (подразделение *V*) находки включают мелких млекопитающих, что свидетельствует о более мезонных условиях с древесной или кустарниковой растительностью. Эти таксоны сохранились в качестве редких элементов в некоторых расположенных выше горизонтах. Пока еще невозможно определить, является ли комбинация таксонов, адаптированных к аридным или умеренным условиям, результатом гетерогенности среды или смесь отдельных групп находок появивилась по причине перемежения периодов с более теплыми/влажными и более холодными/сухими условиями.

Обнаружение останков крысы (*Rattus* sp.), представленной тремя особями из различных горизонтов подразделения *IV*, заслуживает особого внимания. Ранее считалось, что род *Rattus* появился здесь относительно недавно, но находки в Азохе доказывают его присутствие в регионе уже в эпоху среднего плейстоцена. Различные виды, найденные в плейстоценовых и голоценовых отложениях, уже не встречаются в данном регионе, что свидетельствует об изменении в структуре фауны в течение поздних фаз рассматриваемых геологических периодов. Фауна мелких млекопитающих имеет большое сходство с животным разнообразием полупустынь и степей, расположенных южнее, указывая тем самым на приход этих биологических форм из юго-западной Азии; вместе с тем отмечаются только слабые связи с плейстоценовыми мелкими млекопитающими Кавказа.

Keywords Biogeography • Lesser Caucasus • Pleistocene • Small mammals

Introduction

Small mammal research has provided significant insights into environmental and climatic history and biogeography. For example, in a number of recent studies, Quaternary small mammals have proven fundamental to achieving an understanding of the long-term history of mammalian communities (e.g., Blois et al. 2010; López-García et al. 2010; Schmitt and Lupo 2012), in reconstructing colonisation patterns and pacing (Barnes et al. 2006), to infer mode and rates of evolution (Martin 1993), and in the quantification of past changes in climate (e.g., Andrews 1990; Marean et al. 1994; Schmitt et al. 2002; Barnosky et al. 2004; Navarro et al. 2004). Small mammals are also routinely used in archaeological work to elucidate the environmental impact of early agriculture and urbanism (Tchernov 1991; O'Connor 1993; Audoin-Rouzeau and Vigne 1997; Cucci et al. 2005; Terry 2010) and to characterize the environments and landscapes in which past human activity took place (e.g., Agadjanian 2006; Cuenca-Bescós et al. 2009; Louchart et al. 2009; Rodríguez et al. 2011; Stoetzel et al. 2011). Ethnographic studies show that small mammals were commonly collected for food and pelts, and there is a growing body of archaeological evidence demonstrating that small mammals were also similarly exploited in the past (Stahl 1996; Fernández-Jalvo et al. 1999; Weissbrod et al. 2005; Jin et al. 2012).

Bones and teeth of small mammals are often abundant in a range of depositional environments (Falk and Semken 1998) and are especially common in caves occupied by predatory birds (Andrews 1990). Accurate interpretation of fossil small mammal assemblages is reliant on correct taxonomic identification of unbiased samples (usually recovered by fine-mesh sieving), combined with information on its taphonomic history (Andrews 1990; Fernández-Jalvo and Andrews 1992; Fernández-Jalvo et al. 2011).

Quaternary small mammals in the Lesser Caucasus are scarce but important for reconstructing the paleoenvironment of early humans in the region (Pinhasi et al. 2008, 2011; Dennell 2009). Only a few cave sites in the Lesser Caucasus have been sampled for small vertebrates, and most of these contain relatively short sequences, dating to the Late Pleistocene or Holocene (Vereschagin 1967; Pinhasi et al. 2008, 2011). The presence of abundant small mammal remains from Azokh Cave offers the opportunity to scrutinize the small mammal assemblages from a longer sequence that extends into the Middle Pleistocene.

Azokh Cave is situated in the foothills of the Karabakh mountain range at the south-eastern end of the Lesser Caucasus, at an elevation of about 960 m above sea level.

The site was discovered in 1960 by M.M. Huseinov and subsequently excavated by his team. These excavations led to the discovery of a stratified succession of Middle Palaeolithic and Acheulean industries with a purported 'Pebble Culture' at the base of the sequence. In addition to stone tools, the 1968 excavation recovered a mandible fragment now attributed to *Homo heidelbergensis* (King et al. 2016). The importance of the paleoenvironmental evidence at the site was recognized by Velichko et al. (1980), who collected small mammal remains from nine levels (Markova 1982). Markova recorded 12 genera of lagomorphs and rodents, noting a prevalence of steppe species throughout the sequence. Since 2002, renewed excavations have recovered a much larger small mammal assemblage, together with herpetofauna (Blain 2016), fishes, birds and bats (Sevilla 2016). As well as many of the common taxa identified by Markova (1982) the new assemblage includes at least 13 small mammal taxa not previously known from the site.

In this chapter, preliminary results from the taxonomic identification of the small mammals collected between 2002 and 2009 are outlined. The primary aim is to shed light on the environmental conditions that characterized the region during its occupation by early humans. Subsidiary aims are to investigate the shifts in geographical distribution of small mammal taxa and biogeographical composition of the assemblages through the sequence.

Materials and Methods

Small mammals were recovered from all strata in the upper sequence (Units I–V), but the lower sequence was devoid of small mammal material. The specimens were concentrated by wet-screening excavated sediment, using sieves with a 0.5 mm mesh. Most of the samples were sieved in the field by the excavation team and the resulting residues were air-dried and sorted in the site laboratory. Five hundred and sixty-seven small bags of material sorted from these residues were examined for faunal remains. Two-thirds of the bags (n = 241) derive from Unit II and 28% (n = 161) from Unit I. A further 34 (6%) derive from Unit III, 35 (6%) from Unit Vu, and 131 (23%) from Unit Vm.

In 2002, a separate series of 32 samples from Unit Vu was processed in London and the residues were meticulously sorted with the aid of a variable-magnification binocular microscope. These samples yielded particularly rich and diverse small vertebrate assemblages comprising mostly isolated teeth. Nine of these samples were selected for detailed study in order to obtain a small mammal succession covering the complete stratigraphic sequence of Unit Vu.

Every bone fragment from the sieved samples has been retained and the cranial remains cleaned and numbered sequentially. The preservation of the small mammal remains was generally good throughout, with some physical breakage, but little sign of weathering, rounding or soil corrosion (Andrews et al. 2016). However, many of the bones were partially encrusted by manganese and carbonate concretions. Where these obscured diagnostic surfaces and diagnostic features of the teeth, the specimen was cleaned using a combination of chemical (buffered dilute acetic acid) and careful mechanical preparation.

Isolated cheek teeth, mandibles and maxillae were used for taxonomic identification. Small mammal identifications were confirmed using descriptions in the literature (e.g., Kryštufek and Vohralík 2001, 2005) and direct comparison with the osteological reference collections. Ecological affinities and distributions of individual taxa were obtained from Aulagnier et al. (2009), Vereschagin (1967) and Vinogradov and Argiropulo (1968). Nomenclature and taxonomic order follows IUCN Red List of Threatened Species (IUCN 2010).

Results

In all, some 2770 small mammal cheek teeth, mandibles and maxillae from Azokh were analysed. These were picked from many thousands of unidentified rodent and insectivore post-cranial bones. The results are presented in Tables 7.1 and 7.2, and plotted graphically in Fig. 7.1, where each species is shown as a percentage of the total. In the five lithologically defined horizons, Unit Vu accounts for 75% of the identifiable elements, with 12% from Unit I, while Unit II, III and Vm had around 4% of the total assemblage each.

Table 7.1 Stratigraphical occurrence of insectivores, lagomorphs, rodents and small carnivores from Azokh 1

Unit	Vm	Vu	III	II/III	II	I
Lipotyphla						
Soricidae						
Sorex minutus group		+				
Sorex araneus group	+	+				+
Crocidura spp.	+	+	+	+		+
Talpidae						
Talpa sp.	+					
Carnivora						
Mustelidae						
Mustela nivalis		+				
Lagomorpha						
Ochotonidae						
Ochotona spp.		+	+		+	+
Leporidae						
Lepus sp.		+				+
Rodentia						
Sciuridae						
Marmota sp.					+	
Spermophilus sp.					+	
Muridae						
Cricetulus migratorius	+	+			+	+
Mesocricetus sp.		+	+		+	+
Allocricetus sp.	+	+			+	
Clethrionomys glareolus	+	+	+			
Microtus arvalis/socialis	+	+	+	+	+	+
Microtus (*Terricola*) spp.	+	+	+		+	+
Chionomys nivalis	+	+			+	+
Chionomys gud	+	+				+
Ellobius sp.	+	+	+	+	+	+
Meriones spp.		+	+	+	+	+
Apodemus spp.	+	+	+		+	+
Rattus sp.		+				
Mus cf. *macedonicus*		+	+			+
Gliridae						
Dryomys nitedula		+				
Dipodidae						
Allactaga spp.		+				+
NISP[a]	120	2065	121	17	101	346

Notes
Ochotona spp. – two or more species (including one similar to *O. rufescens* and one much larger species) are present in Unit Vu
Microtus arvalis/socialis group – Based on M_1 and M^2 morphology, members of both groups are present throughout sequence
Pine voles – Probably more than one species, but difficult to separate on basis of M_1 morphology
Meriones spp. – possibly as many as three species in Unit Vu (small, medium and large forms). Small *Meriones* also present in Units I and III, with medium-large forms in Units I, II and III
Allactaga spp. – Unit Vu, large and small forms; Unit I, large form only
[a]– Number of identified specimens based on cranio-dental elements

Unit Vm

The fine-grained silts, clays and loams (c. 4.5 m thick), immediately above the limestone floor in the interior of the cave, yielded the oldest small mammal assemblages studied here. A peculiar feature of the small mammal bones from this horizon is that a proportion of the teeth have characteristics that suggest that they have a different taphonomic history from the rest of the bones in the assemblage, possibly resulting from differences in burial environment or digestion (Andrews et al. 2016). Mostly this takes the form of the teeth being lighter in colour than other teeth from the same sample. On the whole the material was well preserved with most of the cheek teeth *in situ*. However, this may

reflect selective picking of more complete and easily recognisable specimens. Reworking or incorporation into the deposit of more recent small mammal remains can probably be excluded as the deposit has not been disturbed by burrowing. The differences in preservation may simply reflect lumping of material from different subunits within the Unit. Evidence of digestion is seen on many of the arvicolid molars with a pattern and degree of digestion suggesting that a category 1 predator (probably barn owl *Tyto alba*) was the primary agent responsible for accumulating the small mammal bones in Unit Vm (Andrews et al. 2016).

Archaeological material recovered during the recent excavations includes possible Acheulian artefacts. Unit Vm also yielded the partial human mandible found in 1968. Further indications for human activity may include evidence of burning, with some small mammals affected.

The small mammal fauna from Unit Vm is moderately diverse with at least 12 taxa, dominated by arvicoline (microtine) rodents (Table 7.1). Other rodents include hamsters, mole voles and mice; insectivores are rare, but include both red-toothed (*Sorex araneus* group) and white-toothed shrews (*Crocidura*), as well as mole (*Talpa* sp.). The arvicoline assemblage includes first lower molars of pine voles (*Microtus* (*Terricola*) spp.) and *M. arvalis* group/social voles (*Microtus arvalis/socialis*). The first lower molars (M_1) of the *arvalis* group and social voles are difficult to distinguish morphologically, but the second upper molars (M^2) can be distinguished by the presence of an extra loop, which is common in the social voles but absent in the *arvalis* group (Kryštufek and Vohralík 2005; Kryštufek and Kefelioğlu 2008). Ecologically, the distinction between these two groups is important as social voles inhabitant dry steppes and semi-deserts, whereas voles of the *arvalis* group prefer humid grassland. This is reflected in their current distributions in the southern Caucasus, where the social vole is found in steppic and semi-desert regions (e.g., Azerbaijan shrub desert and steppe, and Eastern Anatolian montane steppe), while the *arvalis* voles (*Microtus arvalis* and *M. levis*) are found throughout the 'Caucasian mixed forest' zone; Azokh Cave is located close to the boundary between these two regions (Vereschagin 1967). In the Unit Vm assemblage, a relatively high percentage of the M^2s lack an additional loop (Fig. 7.1), suggesting that the *arvalis* group was present and relatively abundant in the region when this unit was deposited. Relatively humid conditions supporting scrub and woodland may be indicated by the presence of *Apodemus*, which is also well represented in the assemblage, as well as the bank vole *Clethrionomys glareolus*.

From a zoogeographical perspective, the most significant taxon is undoubtedly *Clethrionomys glareolus*. This species is today found no closer than the 'Euxine-Colchic deciduous forest' bordering the Black Sea in Georgia and Turkey. Its preferred habitat in this region includes coniferous, mixed and deciduous woodland. Two other vole species no longer found in the Azokh region are the snow voles *Chionomys nivalis* and *Chionomys gud*, which are represented in the Unit Vm assemblage by single specimens. The European snow vole (*Chionomys nivalis*) has a patchy distribution restricted to rocky and mountainous habitats across southern Europe and Asia (Castiglia et al. 2009). It is found in the Lesser Caucasus, but its distribution does not extend as far east as Azokh (Vereschagin 1967). The Caucasian snow vole (*Chionomys gud*) is also closely associated with open rocky habitats, but it inhabits a wider range of montane habitats, including sparse fir and spruce forests, alpine meadows and in valleys with streams or small rivers. Although endemic to the Caucasus and the easternmost part of the Pontic Mountains of Turkey, it is scarce in the Lesser Caucasus and occurs no closer to Azokh than south-west Georgia.

Relatively common in the assemblage are rooted cheek teeth of mole voles *Ellobius* sp. Mole voles are highly specialized fossorial voles that feed on underground storage organs of plants and especially starchy tubers and bulbs. They are particularly common in mountain grassland and steppes, but also inhabit thin soils of rocky mountainsides and sandy semi-deserts. The only species found today in the southern Caucasus is the Transcaucasian mole vole *Ellobius lutescens*, with a distribution in arid regions bordering the Lesser Caucasus, approximately 100 km from Azokh. Another indicator of dry grassland, steppes and semi-deserts is the grey hamster *Cricetulus migratorius*, which has a strong preference for arid areas with relatively sparse vegetation; it avoids forests and damp areas.

Overall, the assemblage contains a mixture of species indicative of woodland or scrub and temperate/humid conditions, together with obligate inhabitants of arid open habitats, as well as montane species that require rocky habitats.

Unit Vu

The small mammal assemblage from this unit is by far the richest in number of remains as well as the number of taxa (Tables 7.1 and 7.2). Samples processed in London yielded nearly all the material ($n = 2022$), with only 43 identifiable cranial elements from samples processed on-site. The greater concentration of small vertebrates in the laboratory-processed samples may be due to better preservation, differences in recovery techniques or a higher concentration of small mammal bones possibly relating to proximity of the roost sites. Small mammal samples were

Table 7.2 Stratigraphical occurrence of small mammal taxa and number of specimens from Azokh 1 and 5. The Azokh 5 assemblage was obtained during preliminary sampling of the Holocene deposits (Unit A)

	Azokh 1						Azokh 5
Unit	Vm	Vu	III	II/III	II	I	Holocene
Lipotyphla							
Sorex minutus group		4					
Sorex araneus group	1	2				1	
Crocidura spp.	1	48	1	1		1	1
Soricidae gen. et sp. indet.		7				2	
Talpa sp.	1						
Carnivora							
Mustela nivalis		1					
Lagomorpha							
Ochotona spp.		37	1		3	3	
Lepus sp.		1				1	
Indeterminate lagomorph		23				3	
Rodentia							
Marmota sp.					1		
Spermophilus sp.					1		
Cricetulus migratorius	4	23			1	3	6
Mesocricetus sp.		25	1		4	25	1
Allocricetus sp.	1	2			1		
Indeterminate hamster		2				9	
Clethrionomys glareolus	1	6	1				
Microtus arvalis/socialis	41	227	25	4	17	33	11
Microtus (*Terricola*) spp.	4	15	2		2	1	
Chionomys nivalis	1	3			1	1	1
Chionomys gud	1	2				1	
Indeterminate vole	50	1152	76	9	57	211	3
Ellobius sp.	5	95	6	1	3	18	1
Meriones spp.		235	5	1	2	20	
Apodemus spp.	9	84	1		8	8	
Rattus sp.		3					
Mus cf. *macedonicus*		61	2			2	
Dryomys nitedula		1					
Allactaga spp.		2				3	
Total	120	2065[a]	121	17[b]	101	346	24

Totals include: [a]two indeterminate murid molars, fragment of insectivore tooth and an incisor fragment from a large rodent, [b]one indeterminate rodent maxilla with extremely worn M^{2-3}

analysed from nine different levels within the succession (Fig. 7.1), each with between 94 and 261 identified specimens per sample.

The preservation of the small mammals was good, although many of the bones and teeth have a coating of mineral deposits. Small mammal teeth from Unit Vu exhibit a different pattern of digestion to the other levels and include a small number of heavily digested molars and an overall pattern of alterations consistent with a category 3 predator most likely the European eagle owl *Bubo bubo* (Andrews et al. 2016). Eagle owls feed on a wider variety of prey than do barn owls and this may account for the high diversity of microvertebrate remains in this level (Table 7.2).

Rodents are by far the most numerous group (number of identified specimens (NISP) = 1931), with soricids (NISP = 73) and lagomorphs (NISP = 61) making up just 3.5 and 3% of the assemblage, respectively. A single weasel (*Mustela nivalis*) tooth represents the only identifiable small carnivore from this unit.

Shrews are represented by the *Sorex minutus* group, the *Sorex araneus* group and *Crocidura* (white-toothed shrews). *Crocidura* is by far the most common shrew and at least two species are represented. There are several unresolved taxonomic issues with this group of shrews (Kryštufek and Vohralík 2001), particularly in the Caucasus, where as many as five species have been recorded. There is very little information available regarding the distribution, habitat and ecology of several of these species, for example *Crocidura armenica*, Armenian white-toothed shrew, *Crocidura caspica*, Caspian white-toothed shrew and *Crocidura serezkyensis*, Serezkaya shrew. Diagnostic dental characters that can be used to identify fossil dental material from the

Caucasus have not yet to be described, which has made it difficult to identify the Azokh soricids. Nevertheless, it is possible to make some observations on palaeoecology. Eurasian white-toothed shrews avoid dense forest, but have wide habitat preferences that include subtropical humid lowlands, dense tall grass and rocky areas in mountains, dry Mediterranean shrubland and densely vegetated damp areas near water. In arid areas, white-toothed shrews tend to be mainly associated with humid conditions near springs and water courses. Red-toothed shrews include rare specimens of a small shrew of the *Sorex minutus* group and specimens of the larger *Sorex araneus* group (Zaitsev 1998; Zaitsev and Ospipova 2004). Caucasian red-toothed shrews, for example *Sorex volnuchini*, Caucasian pygmy shrew, *Sorex raddei*, Radde's shrew and *Sorex satunini*, Caucasian shrew, prefer humid environments with dense vegetation often in forest; they also inhabit alpine meadows.

Microtus voles are overwhelmingly the dominant small mammals in the assemblage. Voles of the *arvalis/socialis* group are particularly numerous, with a predominance of social voles indicated by M^2 morphology. Voles of the *Microtus* (*Terricola*) group are less common, and it has not been possible to identify these beyond genus level. Caucasian Pine voles are found in a range of habitats: *Microtus daghestanicus* (Daghestan pine vole) and *Microtus nasarovi* (Nasarov's pine vole) prefer pastures, alpine meadows (both mesic and dry) and steppe; *Microtus majori* (sibling vole) favours clearings in forests and shrubland, as well as alpine pastures; *Microtus schidlovskii* (Schidlovsky pine vole) is more closely associated with xerophytic steppes and meadow-steppes.

The pika, was originally identified as an element of the Azokh fauna by Markova (1982), who recorded several cheek-teeth, which she attributed to *Proochotona*. More recent work has revised the taxonomy of this material, and suggests that two species are present, including one with morphological affinities to *Ochotona rufescens* (Čermák et al. 2006). Isolated and fragmentary pika teeth are relatively common in the current sample. At the present stage of analysis it is difficult to determine the number and identity of the species represented. Today, *Ochotona rufescens* (Afghan pika) is the only pika species found in the Lesser Caucasus. The Afghan pika is a widespread species that occurs in the mountains of Pakistan, Afghanistan, parts of Turkmenistan, Iran, eastern Turkey and Armenia. Holocene subfossil finds suggest that the pika was formerly more widespread with finds from several sites in the Caucasus from southern Armenia and Georgia (Čermák et al. 2006). Pikas prefer habitats with relatively sparse vegetation cover and favour steppe, rocky deserts and mountains.

Two species of hamster, *Cricetulus migratorius* (grey hamster) and *Mesocricetus* are equally common and occur together, with much rarer material of a small hamster provisionally assigned to *Allocricetus* (see Hír 1993; Kowalski 2001 and Cuenca-Bescós 2003 for contrasting views on the validity of this genus). *Cricetulus migratorius* and *Mesocricetus* are good indicators of dry grassland, steppes and semi-deserts.

Similar habitats are indicated by *Ellobius* (mole vole) and *Meriones* (jird). The jird sample may include more than three species, however, and taxonomic identification of isolated jird teeth is notoriously difficult, so that at the current stage of analysis it is not possible to take the identifications beyond the genus level. Today, five jird species are found in the Lesser Caucasus: *Meriones Dahlia* (Dahl's jird), *Meriones lybicus* (Libyan jird), *Meriones persicus* (Persian jird), *Meriones tristrami* (Tristram's jird) and *Meriones vinogradovi* (Vinogradov's jird). Jirds are strong indicators of arid conditions and desert, semi-deserts and steppic habitats.

Mus cf. *macedonicus* (Macedonian mouse) is the dominant murid in Unit Vu. This mouse is found in a wide range of habitats, including sand dunes, Mediterranean shrubland and densely vegetated riverbanks. It is absent from dense forests, and in Mediterranean regions it is restricted to areas that receive more than 400 mm of rain per year. It is common and widespread in the southern Caucasus at the present day.

Mice of the *Apodemus* group are also present in relatively large numbers in Unit Vu. The Caucasus region is notable for its high diversity of *Apodemus* species (Filippucci et al. 1996, 2002; Frynta et al. 2001; Çolak et al. 2007), some of which are difficult to distinguish from isolated cheek teeth alone. In terms of ecology, most of the species are dependent on woodland or shrubland, but most can also be found in more open situations, including reed beds and pastures (*Apodemus agrarius*) and open grasslands (*Apodemus uralensis*), provided suitable cover is nearby.

Rare remains of a large murid indistinguishable from *Rattus* sp. (rat) are of considerable significance. The material consists of three molars (M_1, M^1 and M_3), each from different samples. The Azokh material of this rat is in the same state of preservation as the associated small mammal teeth and there is no question of modern intrusion. Although humans have unwittingly transported rats around the world, *Rattus* has been shown to be a genuine member of Pleistocene faunas in the Near East, having been recorded from Palaeolithic sites in Israel and Turkey (Santel and von Koenigswald 1998; Ervynck 2002). These finds suggest that *Rattus* colonized these regions surprisingly early, spreading naturally from its assumed area of origin in southeastern Asia during the Pleistocene.

A single tooth of *Dryomys nitedula* is the sole record of forest dormouse from Azokh Cave. Although its common name suggests a woodland animal, the species inhabits a broad variety of habitats, including broad-leaved, mixed and coniferous woodland, as well as evergreen shrubland and dense herbaceous vegetation. In mountainous areas it also lives in boulder-fields and alpine pastures. *Dryomys nitedula* inhabits the Azokh region today. Its distribution extends into the nearby steppe, where it is closely associated with densely vegetated banks of streams and rivers.

A small number of highly distinctive cheek teeth of jerboas have been found. Three species are currently found in the Caucasus, the small five-toed jerboa (*Allactaga elator*) and Williams's jerboa (*Allactaga williamsi*) are both found in the southern Caucasus, whereas the larger great jerboa (*A. major*) has a range that extends into northern foothills of the Caucasus. Jerboas are highly specialized for a saltorial way of life and are good indicators of local steppe and semi-desert with hard ground; marshy areas, dense grass and thicket vegetation are avoided.

Although there is no suggestion of any clear taphonomic change during the period when the Unit Vu sediments were accumulating, changes in faunal composition through sequence are apparent. These hint at fluctuations in local ecological conditions during the deposition of this unit, with humid conditions at the base, becoming increasingly arid, followed by a return to more humid conditions in the upper samples (Fig. 7.1).

One notable feature of the assemblage is the presence of charred and calcined bones and teeth in the upper part of the sequence (Fig. 7.1). Charcoal has also been recovered from this unit (Allué 2016). Peak values for burnt bone abundance were encountered in the middle of the sequence, with up to 6.5% of the teeth either charred or calcined. Burnt material also occurs in the upper part of the sequence, but at much lower frequencies (0.4–2.1%). The presence of butchered large mammal in this horizon suggests that the burnt small mammal material is probably linked to human activity in the cave, possibly through the lighting of fires on surfaces where bones had already accumulated.

Unit III

This unit yielded a total of 121 identifiable cranial elements (Table 7.2). Overwhelmingly the most important small mammals are voles of the *Microtus arvalis/socialis* group. All of the *Microtus* M^2s ($n = 17$) have an extra loop indicative of the social voles group. This dominance suggests steppe or semi-desert habitats were prevalent, a conclusion supported by the relatively high numbers of mole voles and jirds. The remaining taxa, represented by at most two specimens each, include white-toothed shrew (*Crocidura* sp.), pika (*Ochotona* sp.), murids (*Apodemus* sp., *Mus* cf. *macedonicus*), hamster (*Mesocricetus* sp.) and voles (*Clethrionomys glareolus*, *Microtus* (*Terricola*) spp.). The presence in this small assemblage of *Clethrionomys glareolus* is noteworthy. None of the teeth are burnt (possibly due to the small size of the sample). Digested rodent teeth are present in Unit III, but the sample is too small to identify the type of predator responsible for accumulating the small mammal bones (Andrews et al. 2016).

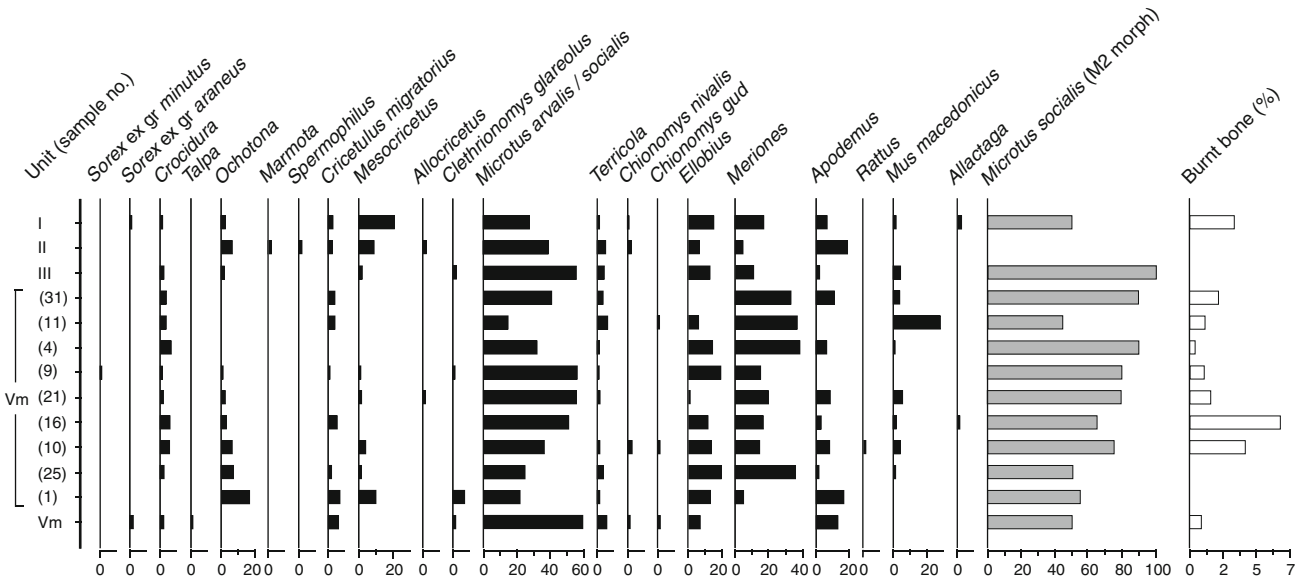

Fig. 7.1 Stratigraphical distribution and relative abundances of rodent taxa at Azokh 1. The taxa are arranged in an approximate ecological order with 'humid' taxa on the left and 'arid' taxa on the right. Values of taxonomic abundance are expressed as percentages of the total number of identified small mammal specimens, excluding all arvicoline molars other than M_1s. Alteration by burning was noted as either charred (blackened) or calcined (ash grey with flaking or mosaic cracking) as described by Preece et al. (2007). Fluctuations in the numbers of burnt bones may indicate differences in the intensity of fire use or changes in the nature of the human occupation. Fire intensity appears to vary with environmental conditions, as indicated by changes in the relative proportions of steppic voles (*M. socialis* group) and mesic grassland voles (*M. arvalis* group and *Terricola* sp.) through the sequence

Unit II

This unit is relatively poor in small mammals and only 101 identified cranial remains were recovered. The sample is noteworthy as it includes the only record of ground squirrel (*Spermophilus* sp.) from the site and the sole specimen of marmot (*Marmota* sp.) from the recent excavations (Tables 7.1 and 7.2).

Geochemical evidence suggests that the poor preservation of vertebrate fossils in this unit may be due to highly alkaline burial conditions and leaching of the organic content of the bones associated with localized accumulations of bat guano (Murray et al. 2016). On the whole, however, the small mammal material is rather well preserved with no obvious signs of post-depositional corrosion of the teeth. The pattern and degree of digestion on the small mammal teeth suggests that they were accumulated by a category 1 predator (Andrews et al. 2016).

Ecologically, the assemblage is consistent with steppe with areas of rocky ground and arid conditions. The ecological significance of *Apodemus* is unclear as the sample may include species adapted to open conditions. Rare elements, such as marmot are also closely associated a variety of open and steppic habitats. Today, marmot (*Marmota bobak*) lives no nearer than the Ukraine and southern Russia in the valley of the Don River, although isolated populations of marmot were present in the Caucasus Mountains as recently as the early 1900s (Vereschagin 1967). A more extensive distribution occurred during the Late Pleistocene, when marmots inhabited large parts of the periglacial zone in Eurasia (Zimina and Gerasimov 1973). Markova (1982) recorded a single specimen of marmot from Azokh Cave (level 10). In the northern Caucasus, marmot bones have been identified from Kudaro I (associated with Lower and Middle Palaeolithic artefacts), Akhalkalaki (Early Pleistocene), both in Georgia, and Matuzka Cave and Mezmajskaya Cave in the Krasnodar region, Russia (Nadachowski and Baryshnikov 1991). Ground squirrels also inhabit steppe, semi-deserts and rocky mountain slopes, avoiding areas with dense high grasses. Today, ground squirrels are no longer found in the Caucasus Mountains, but in the southern Caucasus region, the Asia Minor ground squirrel (*S. xanthoprymnus*) extends into northern part of the 'Eastern Anatolian Montane Steppe' to the east of Yerevan (Gür and Gür 2009).

Unit I

The Holocene sediments in Azokh 1 rest unconformably on Unit II. This unit contains much material from the burning of animal excrement and food waste when the cave was used to house livestock (Fernández-Jalvo et al. 2016). The small mammal remains are notable for the relatively high percentage (over 3%) of charred and calcined teeth. Human activity in Azokh 1 has also resulted in disturbance of the Pleistocene deposits and reworking of Late Palaeolithic stone tools, which were found together with pottery and other recent artefacts.

The Holocene levels in Azokh 1 yielded 346 identified cranial remains, and a smaller assemblage ($n = 25$) has also been recovered from Holocene deposits in Azokh 5 (Table 7.2). Overall, the small mammals are consistent with open conditions. In terms of taxonomic composition, the assemblage includes several taxa such as *Ochotona* sp., *Ellobius* sp., *Allactaga* sp., *Chionomys nivalis* and *Chionomys gud*, that appear to be absent from the environs of Azokh at the present day. Whether any of these represent reworked Pleistocene material cannot be resolved without direct dating of individual specimens. It may be significant that both *Ellobius* sp. and *Chionomys nivalis* are also present in the Holocene sediments in Azokh 5. Another small mammal that has shifted its range during the Holocene is *Ochotona*. According to Vereschagin (1967), pika is present at a number of Holocene localities in the Lesser Caucasus, where it no longer lives.

Discussion

The sequence of small mammal assemblages from Azokh Cave adds significantly to our knowledge of the Transcaucasian small mammals. There appears to be no significant turnover of rodent and insectivore taxa at any particular level, and all samples examined contained similar rodent and insectivore assemblages. At its broadest level this could signify that comparable environments existed throughout the deposition of the Middle (Unit V) to Late Pleistocene (Units III and II) sediments at Azokh, with subtle differences in faunal composition indicating changes in aridity and temperature, combined with fluctuations in woodland cover and the proximity of trees to the site. Interpretation of the Holocene small mammal assemblage from Azokh 1 is problematic as there is evidence of mixing; however, the less disturbed Holocene sediments in Azokh 5 offer the possibility of recovering a better-resolved sequence for this time period.

The Pleistocene small mammal faunas consist predominantly of species that today are associated either with open dry environments or with rocky biotopes; woodland species are rare throughout the sequence. In terms of biogeography, the fauna has a strong Asiatic aspect, with many species typical of steppe and semi-desert environments. This picture is broadly comparable to the results of earlier small mammal analyses undertaken by Markova (1982).

Taphonomic analysis of the small mammal assemblages has identified similar taphonomic trajectories for all five major stratigraphic units (Andrews et al. 2016). The results

Table 7.3 Small mammal species present in the southern Caucasus (Georgia, Armenia and Azerbaijan) and within a 50 km radius of Azokh Cave, (Y) compiled from the *IUCN Red List of Threatened Species* (IUCN 2010). Introduced species are not included

	Azokh region
Lipotyphla	
Erinaceidae	
Erinaceus concolor, eastern European hedgehog	Y
Erinaceus roumanicus, northern white-breasted hedgehog	
Hemiechinus auritus, long-eared hedgehog	Y
Soricidae	
Sorex volnuchini, Caucasian pygmy shrew	Y
Sorex raddei, Radde's shrew	
Sorex satunini, Caucasian shrew	
Neomys teres, Transcaucasian water shrew	Y
Crocidura armenica, Armenian white-toothed shrew	
Crocidura caspica, Caspian white-toothed shrew	
Crocidura leucodon, bicoloured white-toothed shrew	Y
Crocidura serezkyensis, Serezkaya white-toothed shrew	Y
Crocidura suaveolens, lesser white-toothed shrew	Y
Suncus etruscus, Etruscan shrew	Y
Talpidae	
Talpa caucasica, Caucasian mole	
Talpa levantis, Levant mole	Y
Lagomorpha	
Ochotonidae	
Ochotona rufescens, Afghan pika[a]	
Leporidae	
Lepus europaeus, brown hare	Y
Rodentia	
Sciuridae	
Sciurus anomalus, Caucasian squirrel	
Spermophilus xanthoprymnus, Asia Minor ground squirrel	
Muridae	
Cricetus Cricetus, common hamster	
Cricetulus migratorius, grey hamster	Y
Mesocricetus brandti, Brandt's hamster	Y
Mesocricetus raddei, Ciscaucasian hamster	
Clethrionomys glareolus, bank vole	
Arvicola terrestris, water vole	Y
Chionomys gud, Caucasian snow vole	
Chionomys nivalis, snow vole	
Microtus arvalis, common vole	Y
Microtus daghestanicus, Daghestan pine vole	Y
Microtus levis, sibling vole	
Microtus majori, sibling vole	Y
Microtus nasarovi, Nasarov's vole	
Microtus schelkovnikovi, Schelkovnikov's pine vole	
Microtus schidlovskii, Schidlovsky pine vole	
Microtus socialis, social vole	Y
Ellobius lutescens, Transcaucasian mole vole	
Meriones dahli, Dahl's jird	
Meriones lybicus, Libyan jird	Y
Meriones persicus, Persian jird	Y
Meriones tristrami, Tristram's jird	Y
Meriones vinogradovi, Vinogradov's jird	Y
Micromys minutus, harvest mouse	
Apodemus agrarius, striped field mouse	
Apodemus flavicollis, yellow-necked mouse	
Apodemus hyracinus, Caucasian mouse	
Apodemus mystacinus, broad-toothed mouse	
Apodemus ponticus, Black Sea mouse	Y
Apodemus uralensis, pygmy field mouse	Y
Apodemus whitherbyi, steppe field mouse	Y
Mus macedonicus, Macedonian mouse	Y
Nannospalax nehringi, Nehring's blind mole	
Gliridae	
Glis glis, fat dormouse	Y
Dryomys nitedula, forest dormouse	Y
Dipodidae	
Allactaga elater, small five-toed jerboa	?
Allactaga williamsi, Williams's jerboa	
Sicista caucasica, Caucasian birch mouse	
Hystricidae	
Hystrix indica, Indian crested porcupine	

[a]Although several authors have reported pika bones in Eagle owl pellets from the southern Caucasus region (Čermák et al. 2006), pikas have not been observed in the wild in Transcaucasia or the Armenian highlands of Turkey and Iran

suggest that most of the small mammals were brought to the site by barn owls (Units Vm, II, I and possibly III) and European eagle owls (Unit Vu), where the remains of their food were habitually deposited in regurgitated pellets around their roosts and nests. The dominant role of these two open-country hunters in accumulating the small mammal remains provides additional support for the persistence of extensive areas of open vegetation within their hunting range.

The small mammal assemblages from Azokh consist of mixtures of taxa with no modern analogue, including species which either no longer live in the region or which are extinct (i.e. *Allocricetus*). Although most of the small mammals identified from Azokh Cave inhabit the region today, the assemblage includes at least eight rodent and lagomorphs that are no longer found in the vicinity of the site (Table 7.3). These can be divided into arid-adapted species that favour steppic and semi-desert conditions, and a second group that includes mesic rodents, which inhabit high altitudes in the Caucasus region at the present day. The arid-adapted rodents include jerboas (*Allactaga*) present only in Units Vu and I. Today, jerboas are found no closer than the arid regions along the eastern and southern borders of Nagorno-Karabakh. In this region, two jerboa species are commonly found: the small five-toed jerboa *Allactaga elater*, which prefers areas with a

mixture of vegetation in deserts and semi-deserts, and Williams's jerboa *Allactaga williamsi*, which favours steppe regions with sparse vegetation. It is possible that jerboas occurred closer to the site in the recent past, before irrigation and agricultural degradation of their habitats (IUCN 2010). Mole voles, present in Units Vu, Vm, III, II and I, also favour xeric habitats, such as dry grassy habitats, meadows and semi-deserts. The nearest population of *Ellobius*, represented by the Transcaucasian mole vole *Ellobius lutescens*, is located some 70 km to the east of Azokh, but its main area of distribution is further to the south and extends as far as the Zagros Mountains in central Iran. Similar environments are also inhabited today by the ground squirrel (*Spermophilus*), which was present in Unit II. Today, the nearest population of ground squirrels to Azokh is the Asia Minor ground squirrel (*S. xanthoprymnus*), which is found no closer than the Armenian border with Turkey (Gür and Gür 2009). Another open-ground extralimital small mammal is the pika (*Ochotona*) represented in the Azokh assemblage by fossils from Units Vu, III, II and I. The identity of the *Ochotona* from Azokh is currently uncertain. Ecologically, pikas are closely associated with open landscapes, typically rocky habitats and steppe. Similar habitats are occupied by marmots (*Marmota*), which today mainly inhabit alpine meadows and steppes, from lowland plains to hills and rocky outcrops in mountains. At Azokh the single record of marmot comes from Unit II. Vereschagin (1967) noted that marmots were present in the Caucasus during historical times and suggested that the contraction in range and eventual extirpation of the Caucasian marmot may have resulted from persecution and over-hunting.

The second group of extralimital species includes the bank vole (*Clethrionomys glareolus*), which occurs only in low frequencies at Azokh. This vole, present in Units Vu, Vm and III, is a typical woodland species that is closely associated with mesic habitats and relatively low temperatures. It has a western (mainly European) Palaearctic distribution and, with the exception of the humid coastal belt to the south of the Black Sea, the northern slopes of the Taurus mountains and spruce forests of the Adzhar-Imeretian range, is absent from the southeastern Mediterranean. Vereschagin (1967, p. 323) speculated that the bank vole 'penetrated the Black Sea coast very late, during the period of maximum cooling in the Upper Pleistocene', from the southern Balkans and Asia Minor. The new records from Azokh, however, document a much earlier incursion, with a history extending at least into the Middle Pleistocene.

Finally, the two species of snow vole, *Chionomys gud* (Units Vu, Vm and I) and *Chionomys nivalis* (Units Vu, Vm, II and I), are inhabitants of humid mountains and rocky habitats. The snow vole *Chionomys nivalis* inhabits mountain forests, alpine habitats with overgrown rocky taluses and steppe meadows; it is also found amongst rocks on mountain slopes. Its current distribution includes most of the higher mountains in the Lesser Caucasus, but it does not appear to reach as far as Azokh at the present day. The distribution of the Caucasian snow vole *Chionomys gud* includes the Greater Caucasus, with isolated populations occurring in southern Georgia and northern Turkey. It prefers more humid conditions than the snow vole and is most common in the alpine or subalpine zone. Alpine meadows and rock taluses overgrown with pine, birch and willow are favoured habitats.

The occurrence of a mixture of small mammals, today found at high altitude, together those that live in mesic woodland and steppic or semi-desert environments poses interesting questions in terms of the paleoenvironmental interpretation. Several scenarios may account for such 'mixed' assemblages. For example, the assemblage may include an amalgamation of formerly stratified faunas from different habitats and climatic conditions that became mixed at death or during burial. Such assemblages can also result from time averaging where bones accumulate together over a long period of time and incorporate elements from different, temporally discrete environments. The latter factor is a particular problem during periods of rapid climatic change and in burial contexts with a low sedimentation rate (Roy et al. 1996). This situation may have pertained at Azokh Cave, where the fossiliferous deposits span at least 300,000 years, during which global temperatures alternated between relatively short interglacials and longer glacial periods, both incorporating numerous shorter (millennial, centennial or even decadal) high-amplitude climatic oscillations (Dansgaard et al. 1993; McManus et al. 1999; EPICA 2004; Jouzel et al. 2007). In Asia Minor and the Caucasus, these temperature oscillations were associated with marked changes in precipitation; as a consequence the region experienced alternating periods of aridity and increased humidity. Palaeobotoanical studies of pollen and plant macrofossils from southern Georgia (Connor 2006) and Armenia (Ollivier et al. 2010) show that the vegetation was largely controlled by aridity during the entire Pleistocene, with wetter periods supporting woodland and more arid (generally colder) conditions associated with an expansion of the steppic vegetation (Dodonov et al. 2000; Connor 2006; Markova and Puzachenko 2007; Kehl 2009; Litt et al. 2009; Ollivier et al. 2010, but see El-Moslimany 1987). Today, Azokh is located close to the boundary between a semi-arid subtropical climate characterized by semi-deserts or dry shrubland-steppe, and a region with a thermo-moderate humid climate that supports forests of hornbeam, oak and pine. Even relatively minor perturbations in rainfall and climatic fluctuations are therefore likely to have resulted in significant changes in the distribution of small mammals and other biota during the Pleistocene. At Azokh Cave, comparisons between different environmental proxies would appear to indicate a heterogeneous landscape with a mix of open-ground and woodland/mesic elements during the deposition of the fossiliferous units. The wood charcoal from Unit Vu, in particular, provides conclusive evidence that broadleaved deciduous woodland grew near the site, whereas the associated small mammals indicate an essentially open environment (Andrews et al. 2016). If these

represent contemporaneous samples of the local biota, a much steeper environmental gradient is indicated, possibly combining a relatively high biotic diversity with contrasting local ecological niches, which could have supported the non-analogue Pleistocene fauna (cf. Stafford et al. 1999).

The occurrence of other sites with a relatively good record of small mammals in the Caucasus may help to clarify aspects of the ecological background, dating and biogeographical context of early human occupations in this region. For example, the cave deposits at Hovk (Pinhasi et al. 2008, 2011), has yielded small mammals from the same horizons that contain archaeological evidence for sporadic and low-intensity human occupation during the Late Pleistocene and Holocene. Hovk-1 is located approximately 200 km to the northwest of Azokh, but at a higher altitude (2040 m above sea level). Although the climatic context of the human occupation at Hovk-1 is less clear, the nature of the archaeological record contrasts markedly with that from Azokh Cave, where the higher density of butchered bones and stone tools indicate greater continuity of human occupation, as well as more intensive use of the cave. The contrasting archaeological signature at these two cave sites suggests that in the Lesser Caucasus range conditions at higher altitudes were less favourable for human occupation than at sites located at lower elevation, bordering the Transcaucasian plain (Pinhasi et al. 2011). The Hovk-1 fauna shares many small mammal species with that of Azokh, with the notable inclusion of common hamster *Cricetus cricetus*. Today, the common hamster occupies an extensive range, stretching from Western Europe to the Altai Mountains in Asian Russia, wherever there is suitable fertile steppe or grassland. The presence of common hamster at Hovk-1 is biogeographically significant, as its current range does not cross the Greater Caucasus range. In contrast, the Azokh small mammal faunas have a stronger affinity with the region to the south of the Caucasus Mountains, with the notable presence of the bank vole suggesting earlier links with the Balkans and Asia Minor.

Although Transcaucasia is geographically at the crossroads between the Mediterranean, Europe and Asia, the Pleistocene small mammal fauna suggests that the region cannot simply be considered as a passive corridor linking these areas. Throughout much of the Pleistocene (Gabunia et al. 2000), the Greater Caucasus Mountains formed a major climatic and topographical barrier separating the east European plain to the north from the Transcaucasian highlands to the south; this separation is clearly reflected in the small mammal faunas on either side of the mountains. There is stronger evidence for refugia during Pleistocene glacial periods when the region was surrounded by 'hostile' arid, hyper-arid and periglacial landscapes, with extensive glaciation in the mountains (Hoffecker 2002; Dennell 2009). During these intensely cold periods, the region sheltered a large number of temperate plant species, including so-called 'Tertiary relics', which require warm and humid conditions to grow (Connor 2006). Pockets of relatively stable, climatically favourable conditions are also indicated by the presence of many endemic animals, including several small mammal species. Identifying the location(s) of these refugia, and their potential for sustaining early human occupation, will require the excavation and study of fossil remains from further well-dated, stratified archaeological sites in the region.

Conclusions

1. There is no significant turnover of rodent and insectivore taxa through the stratigraphic sequence of Azokh 1, and all samples examined contained broadly similar rodent and insectivore assemblages.
2. This could signify that comparable environments existed throughout the deposition of the Middle (Unit V) to Late Pleistocene (Units III and II) sediments at Azokh, with small differences in faunal composition.
3. The small mammal assemblages from Azokh consist of mixtures of taxa with no modern analogue, including species, which either no longer live in the region or which are extinct (i.e. *Allocricetus*).
4. In terms of biogeography, the fauna has a strong Asiatic aspect, with many species typical of steppe and semi-desert environments.
5. Transcaucasia is geographically at the crossroads between the Mediterranean, Europe and Asia, but the Pleistocene small mammal fauna suggests that the region acted more as a barrier to small mammal dispersal rather than as a passive corridor linking these areas.
6. The area formed refugia during Pleistocene glacial periods when the region was surrounded by arid, hyper-arid and periglacial landscapes, with extensive glaciation in the mountains.
7. Taphonomic analysis of the small mammal assemblages has identified taphonomic trajectories for all five major stratigraphic units: prey assemblages of barn owls (Units Vm, II, I and possibly III) and European eagle owls (Unit Vu).
8. There is a mixture of small mammals from different habitats: some found only at high altitude mixed with those that live in mesic woodland and steppic or semi-desert environments.
9. The small mammal faunas consist predominantly of species that today are associated either with open dry environments or with rocky biotopes; woodland species are rare throughout the sequence.
10. These differences could indicate minor changes in aridity and temperature, combined with fluctuations in woodland cover and the proximity of trees to the site.

Acknowledgments We are indebted to Glenys Salter and Lena Asryan for their meticulous sorting of the sieved residues. David Harrison is thanked for help with the identification of problematic specimens.

References

Agadjanian, A. A. (2006). The dynamic of biorescources and activity of the Paleolithic Man, using example of northwestern Altai Mountains. *Paleontological Journal, 40*, 482–493.

Allué, E. (2016) Charcoal remains from Azokh 1 cave: Preliminary results. In Y. Fernández-Jalvo, T. King, L. Yepiskoposyan & P. Andrews (Eds.), *Azokh Cave and the Transcaucasian Corridor* (pp. 297–304). Dordrecht: Springer.

Andrews, P. (1990). *Owls, caves and fossils*. London: British Museum (Natural History).

Andrews, P., Hixson Andrews, S., King, T., Fernández-Jalvo, Y., & Nieto-Díaz, M. (2016). Palaeoecology of Azokh 1. In Y. Fernández-Jalvo, T. King, L. Yepiskoposyan & P. Andrews (Eds.), *Azokh Cave and the Transcaucasian Corridor* (pp. 305–320). Dordrecht: Springer.

Audoin-Rouzeau, F., & Vigne, J.-D. (1997). Le rat noir (*Rattus rattus*) en Europe antique et médiévale: les voies du commerce et l'expansion de la peste. *Anthropozoologica, 25–26*, 399–404.

Aulagnier, S., Haffner, P., Mitchell-Jones, A. J., Moutou, F., & Zima, J. (2009). *Mammals of Europe, North Africa and the Middle East*. London: A&C Black Publishers.

Barnes, S. S., Matisoo-Smith, E., & Hunt, T. L. (2006). Ancient DNA of the Pacific rat (*Rattus exulans*) from Rapa Nui (Easter Island). *Journal of Archaeological Science, 33*, 1536–1540.

Barnosky, A. D., Bell, C. J., Emslie, S. D., Goodwin, H. T., Mead, J. I., Repenning, C. A., et al. (2004). Exceptional record of mid-Pleistocene vertebrates helps differentiate climate from anthropogenic ecosystem perturbations. *Proceedings of the National Academy of Sciences of the United States of America, 101*, 9297–9302.

Blain, H.-A. (2016). Amphibians and squamate reptiles from Azokh 1. In Y. Fernández-Jalvo, T. King, L. Yepiskoposyan & P. Andrews (Eds.), *Azokh Cave and the Transcaucasian Corridor* (pp. 91–210). Dordrecht: Springer.

Blois, J. L., McGuire, J. L., & Hadly, E. A. (2010). Small mammal diversity loss in response to late-Pleistocene climatic change. *Nature, 465*, 771–774.

Castiglia, R., Annesi, F., Kryštufek, B., Filippucci, M. G., & Amori, G. (2009). The evolutionary history of a mammal species with a highly fragmented range: The phylogeography of the European snow vole. *Journal of Zoology, 279*, 243–250.

Čermák, S., Obuch, J., & Benda, P. (2006). Notes on the genus *Ochotona* in the Middle East (Lagomorpha: Ochotonidae). *Lynx (Praha), 37*, 51–66.

Çolak, R., Çolak, E., Yiğit, N., Kandemir, I., & Sözen, M. (2007). Morphometric and biochemical variation and the distribution of the genus *Apodemus* (Mammalia: Rodentia) in Turkey. *Acta Zoologica Academiae Scientiarum Hungaricae, 53*, 239–256.

Connor, A. E. (2006). A Promethean Legacy: Late Quaternary Vegetation History of Southern Georgia, Caucasus. PhD dissertation. University of Melbourne, Australia.

Cucci, T., Vigne, J.-D., & Auffray, J.-C. (2005). First occurrence of the house mouse (*Mus musculus domesticus*) in the Western Mediterranean: A zooarchaeological revision of subfossil occurrences. *Biological Journal of the Linnean Society, 84*, 429–445.

Cuenca-Bescós, G. (2003). Análisis filogenético de *Allocricetus* del Pleistoceno (Cricetidae, Rodentia, Mammalia). *Journal of Archaeological Science, 36*, 95–114.

Cuenca-Bescós, G., Straus, L. G., González Morales, M. R., & García Pimienta, J. C. (2009). The reconstruction of past environments through small mammals: From the Mousterian to the Bronze Age in El Mirón Cave (Cantabria, Spain). *Journal of Archaeological Science, 36*, 947–955.

Dansgaard, W., Johnsen, S. J., Clausen, H. B., Dahl-Jensen, D., Gundestrup, N. S., Hammer, C. U., et al. (1993). Evidence for general instability of past climate from a 250-kyr ice-core record. *Nature, 364*, 218–220.

Dennell, R. (2009). *The palaeolithic settlement of Asia*. Cambridge: Cambridge University Press.

Dodonov, A. E., Tchepalyga, A. L., Mihailescu, C. D., Zhou, L. P., Markova, A. K., Trubikhin, V. M., et al. (2000). Last-interglacial records from central Asia to the northern Black Sea shoreline: Stratigraphy and correlation. *Netherlands Journal of Geosciences, 79*, 303–311.

El-Moslimany, A. P. (1987). The late Pleistocene climates of the Lake Zeribar region (Kurdistan, western Iran) deduced from the ecology and pollen productivity on non-arboreal vegetation. *Vegetatio, 72*, 131–139.

EPICA community. (2004). Eight glacial cycles from an Antarctic ice core. *Nature, 429*, 623–628.

Ervynck, A. (2002). Sedentism or urbanism? On the origin of the commensal black rat (*Rattus rattus*). In K. Dobney & T. O'Connor (Eds.), *Bones and the man. Studies in honour of Don Brothwell* (pp. 95–109). Oxford: Oxbow Books.

Falk, C. R., & Semken, H. A. (1998). Taphonomy of rodent and insectivore remains in North American archaeological sites: Selected examples and interpretations. In J. J. Saunders, B. W. Styles, & G. F. Baryshnikov (Eds.), *Quaternary paleozoology in the Northern Hemisphere* (vol. XXVII, pp. 285–321). Illinois State Museum Scientific Papers.

Fernández-Jalvo, Y., & Andrews, P. (1992). Small mammal taphonomy of Gran Dolina, Atapuerca (Burgos), Spain. *Journal of Archaeological Science, 19*, 407–428.

Fernández-Jalvo, Y., Andrews, P., & Denys, C. (1999). Cut marks on small mammals at Olduvai Gorge Bed-I. *Journal of Human Evolution, 36*, 587–589.

Fernández-Jalvo, Y., Scott, L., & Andrews, P. (2011). Taphonomy in palaeoecological interpretations. *Quaternary Science Reviews, 30*, 1296–1302.

Fernández-Jalvo, Y., King, T., Andrews, P., & Yepiskoposyan, L. (2016). Introduction: Azokh Cave and the Transcaucasian Corridor. In Y. Fernández-Jalvo, T. King, L. Yepiskoposyan & P. Andrews (Eds.), *Azokh Cave and the Transcaucasian Corridor* (pp. 1–26). Dordrecht: Springer.

Filippucci, M. G., Storch, G., & Michaux, J. R. (1996). Taxonomy of the genus *Sylvaemus* in western Anatolia – morphological and electrophoretic evidence. *Senckenberg Biology, 75*, 1–14.

Filippucci, M. G., Macholán, M., & Michaux, J. R. (2002). Genetic variation and evolution in the genus *Apodemus* (Muridae: Rodentia). *Biological Journal of the Linnean Society, 75*, 395–419.

Frynta, D., Mikulová, P., Suchomelová, E., Sádlová, J., Suchomelová, E., & Sádlová, J. (2001). Discriminant analysis of morphometric characters in four species of *Apodemus* (Muridae: Rodentia) from eastern Turkey and Iran. *Israel Journal of Zoology, 47*, 243–258.

Gabunia, L., Vekua, A., & Lordkipanidze, D. (2000). The environmental contexts of early human occupation of Georgia (Transcaucasia). *Journal of Human Evolution, 38*, 785–802.

Gür, M. K., & Gür, H. (2009). *Spermophilus xanthoprymnus* (Rodentia, Sciuridae). *Mammalian Species, 42*(864), 183–194.

Hír, J. (1993). *Cricetulus migratorius* (Pallas 1773) (Rodentia, Mammalia) population from the Toros Mountain (Turkey) (with special reference to the relation of *Cricetulus* and *Allocricetus* genera). *Folia Historico Naturalia Musei Matraensis, 18*, 17–34.

Hoffecker, J. F. (2002). *Desolate landscapes. Ice-age settlement in Eastern Europe*. New Brunswick, New Jersey: Rutgers University Press.

IUCN. (2010). *IUCN Red List of Threatened Species*. http://iucnredlist.org.

Jin, J. J. H., Jablonski, N. G., Flynn, L. J., Chaplin, G., Xueping, X., Zhicai, L., Xiaoxue, S., & Guihua, L. (2012). Micromammals from an early Holocene archaeological site in southwestern China: Paleoenvironmental and taphonomic perspectives. *Quaternary International* doi:10.1016/j.quaint.2012.04.012.

Jouzel, J., Masson-Delmotte, V., Cattani, O., Dreyfus, G., Falourd, S., Hoffmann, G., et al. (2007). Orbital and millennial Antarctic climate variability over the past 800,000 years. *Science, 317*, 793–796.

Kehl, M. (2009). Quaternary climate change in Iran – the state of knowledge. *Erkunde, 63*, 1–17.

King, T., Compton, T., Rosas, A., Andrews, P. Yepiskoyan, L., & Asryan, L. (2016). Azokh Cave Hominin Remains. In Y. Fernández-Jalvo, T. King, L. Yepiskoposyan & P. Andrews (Eds.), *Azokh Cave and the Transcaucasian Corridor* (pp. 103–106). Dordrecht: Springer

Kowalski, K. (2001). Pleistocene rodents of Europe. *Folia Quaternaria, 72*, 1–389.

Kryštufek, B., & Kefelioğlu, H. (2008). The social vole *Microtus socialis* in the Near East. *Mammal Review, 31*, 229–237.

Kryštufek, B., & Vohralík, V. (2001). *Mammals of Turkey and Cyprus. Introduction, Checklist, Insectivora*. Koper: Knjižnica Annales Majora.

Kryštufek, B., & Vohralík, V. (2005). *Mammals of Turkey and Cyprus. Rodentia I: Sciuridae, Dipodidae, Gliridae, Arvicolinae*. Koper: Knjižnica Annales Majora.

Litt, T., Krastel, S., Sturm, M., Kipfer, R., Örcen, S., Heumann, G., et al. (2009). 'PALEOVAN', International Continental Scientific Drilling Program (ICDP): Site survey results and perspectives. *Quaternary Science Reviews, 28*, 1555–1567.

López-García, J. M., Blain, H.-A., Allué, E., Bañuls, S., Bargalló, A., Martín, P., et al. (2010). First fossil evidence of an 'interglacial refugium' in the Pyrenean region. *Naturwissenschaften, 97*, 753–762.

Louchart, A, Wessleman H., Blumenschine, R. J., Hlusko, L. J., Njau, J. K., Black, M. T., et al. (2009). Taphonomic, avian, and small vertebrate indicators of *Ardipithecus ramidus* habitat. *Science, 326*, doi:10.1126/science.1175823.

Marean, C. W., Mudida, N., & Reed, K. E. (1994). Holocene paleoenvironmental change in the Kenyan Central Rift as indicated by micromammals from Enkapunde Ya Muto Rockshelter. *Quaternary Research, 41*, 376–389.

Markova, A. K. (1982). [Small mammals from the Palaeolithic site in Azykh Cave]. *Paleontologcheskii Sbornik, 19*, 14–28 [in Russian, with English summary].

Markova, A., & Puzachenko, A. (2007). Late Pleistocene of northern Asia. In S. A. Elias (Ed.), *Encyclopedia of Quaternary science* (Vol. 4, pp. 3158–3174). Amsterdam: Elsevier.

Martin, R. A. (1993). Patterns of variation and speciation in Quaternary rodents. In R. A. Martin & A. D. Barnosky (Eds.), *Morphological change in Quaternary mammals of North America* (pp. 226–280). Cambridge: Cambridge University Press.

McManus, J. F., Oppo, D. W., & Cullen, J. L. (1999). A 0.5 million year record of millennial-scale climate. *Science, 283*, 971–974.

Murray, J., Lynch, E. P., Domínguez-Alonso, P., & Barham, M. (2016). Stratigraphy and Sedimentology of Azokh Caves, South Caucasus. In Y. Fernández-Jalvo, T. King, L. Yepiskoposyan & P. Andrews (Eds.), *Azokh Cave and the Transcaucasian Corridor* (pp. 27–54). Dordrecht: Springer.

Nadachowski, A., & Baryshnikov, G. (1991). Pleistocene snow voles (*Chinomys* Miller, 1908) (Rodentia, Mammlia) from Northern Caucasus (USSR). *Acta Zoologica Cracoviensia, 34*, 437–451.

Navarro, N., Lécuyer, C., Montuire, S., Langlois, C., & Martineau, F. (2004). Oxygen isotope compositions of phosphate from arvicoline teeth and Quaternary climatic changes, Gigny, French Jura. *Quaternary Research, 62*, 172–182.

O'Connor, T. P. (1993). Pets and pests in Roman and Medieval Britain. *Mammal Review, 22*, 107–113.

Ollivier, V., Nahapetyan, S., Roiron, P., Gabrielyan, I., Gasparyan, B., Chataigner, C., et al. (2010). Quaternary volcano-lacustrine patterns and palaeobotanical data in southern Armenia. *Quaternary International, 223–224*, 312–326.

Pinhasi, R., Gasparian, B., Wilkinson, K., Bailey, R., Bar-Oz, G., Bruch, A., et al. (2008). Hovk 1 and the Middle and Upper Palaeolithic of Armenia: A preliminary framework. *Journal of Human Evolution, 55*, 803–816.

Pinhasi, R., Gasparian, B., Nahapetyan, S., Bar-Oz, G., Weissbrod, L., Bruch, A., et al. (2011). Middle Palaeolithic human occupation of the high altitude region of Hovk-1, Armenia. *Quaternary Science Reviews, 30*, 3846–3857.

Preece, R. C., Parfitt, S. A., Bridgland, D. R., Lewis, S. G., Rowe, P. J., Atkinson, T. C., et al. (2007). Terrestrial environments during MIS 11: Evidence from the Palaeolithic site at West Stow, Suffolk, UK. *Quaternary Science Reviews, 26*, 1236–1300.

Rodríguez, J., & 26 others. (2011). One million years of cultural evolution in a stable environment at Atapuerca (Burgos, Spain). *Quaternary Science Reviews, 30*, 1396–1412.

Roy, K., Valentine, J. W., Jablonski, D., & Kidwell, S. M. (1996). Scales of climatic variability and time averaging in Pleistocene biotas: Implications for ecology and evolution. *Trends in Ecology and Evolution, 11*, 458–463.

Santel, W., & von Koenigswald, W. (1998). Preliminary report on the middle Pleistocene small mammal fauna from Yarimburgaz Cave in Turkish Thrace. *Eiszeitalter und Gegenwart, 48*, 162–169.

Schmitt, D. N., & Lupo, K. D. (2012). The Bonneville Estates Rockshelter rodent fauna and changes in late Pleistocene – middle Holocene climates and biogeography in the Northern Bonneville Basin, USA. *Quaternary Research, 78*, 95–102.

Schmitt, D. N., Madsen, D. B., & Lupo, K. D. (2002). Small-mammal data on early and middle Holocene climates and biotic communities in the Bonneville Basin, USA. *Quaternary Research, 58*, 255–260.

Sevilla, P. (2016). Bats from Azokh Caves. In Y. Fernández-Jalvo, T. King, L. Yepiskoposyan & P. Andrews (Eds.), *Azokh Cave and the Transcaucasian Corridor* (pp. 177–189). Dordrecht: Springer.

Stafford, T. W., Semken, H. A., Graham, R. G., Klippel, W. F., Markova, A., Smirnov, N. G., & Southon, J. (1999). First accelerator mass spectrometry ^{14}C dates documenting contemporaneity of nonanalog species in late Pleistocene mammal communities. *Geology, 27*, 903–906.

Stahl, P. W. (1996). The recovery and interpretation of microvertebrate bone assemblages from archaeological contexts. *Journal of Archaeological Method and Theory, 3*, 31–75.

Stoetzel, E., Marion, L., Nespoulet, R., El Hajraoui, M. A., & Denys, C. (2011). Taphonomy and palaeoecology of the late Pleistocene to middle Holocene small mammal succession of El Harhoura 2 cave (Rabat-Témara, Morocco). *Journal of Human Evolution, 60*, 1–33.

Tchernov, E. (1991). Biological evidence for human sedentism in southwest Asia during the Natufian. In O. Bar-Yosef & F. R. Valla (Eds.), *The Natufian Culture in the Levant* (pp. 315–340). International Monographs in Prehistory, Michigan: Ann Arbour.

Terry, R. C. (2010). The dead do not lie: Using skeletal remains for rapid assessment of historical small-mammal community baselines. *Proceedings of the Royal Society B, 277*, 1193–2101.

Velichko, A. A., Antonova, G. V., Zelikson, E. M., Markova, A. K., Monoszon, M. M., Morozova, T. D., et al. (1980). Paleography of Azykh – oldest site in USSR territories. *Izvestiya Akademii Nauk SSSR. Seriya Geographicheskaya, 3*, 20–35. (in Russian).

Vereschagin, N. K. (1967). *The mammals of the caucasus. A history of the evolution of the Fauna*. Jerusalem: Israel Program for Scientific Translations. (Translated from the Russian).

Vinogradov, B. S., & Argiropulo, A. I. (1968). *Fauna of the U.S.S.R. Mammals*. Israel Jerusalem: Program for Scientific Translations. (Translated from the Russian).

Weissbrod, L., Dayan, T., Kaufman, D., & Weistein-Evron, M. (2005). Micromammal taphonomy of el-Wad Terrace, Mount Carmel, Israel: Distinguishing cultural from natural depositional agents in the Late Natufian. *Journal of Archaeological Science, 32*, 1–17.

Zaitsev, M. V. (1998). Late Anthropogene Insectivora from the south Urals, with a special reference to diagnostics of red-toothed shrews of the genus *Sorex*. In J. J. Saunders, B. W. Styles & G. F. Baryshnikov (Eds.), *Quaternary Paleozoology in the Northern Hemisphere* (vol. XXVII, pp. 145–158). Illinois State Museum Scientific Papers.

Zaitsev, M. V., & Ospipova, V. A. (2004). Insectivorous mammals (Insectivora) of the late Pleistocene in the northern Caucasus. *Zoologicheskii Zhurnal, 83*, 851–868.

Zimina, R. P., & Gerasimov, I. P. (1973). The periglacial expansion of marmots (*Marmota*) in middle Europe during Late Pleistocene. *Journal of Mammalogy, 54*, 327–340.

Chapter 8
Bats from Azokh Caves

Paloma Sevilla

Abstract Azokh Cave is well-known in the Caucasus not only for its archaeological interest, but also for sheltering large colonies of bats, some of which are rare in the region. During the summer the bat communities in the cave include individuals of at least four different species. Both the Lesser Mouse-eared Bat (*Myotis blythii*) and Schreiber's Long-fingered Bats (*Miniopterus schreibersii*) form large breeding colonies, but abandon the cave during the winter. Another two species, Mehely's Horseshoe Bat (*Rhinolophus mehelyi*) and the Greater Horseshoe Bat (*Rhinolophus ferrumequinum*), can be found roosting in the cave all year round. During the active season, the colonies of *R. mehelyi* reach several thousand individuals, being the largest grouping of this species known in the Caucasus. Excavations in the sediments preserved in the cave, dating from the late middle Pleistocene to Recent, contain evidence that the same four species have been roosting in Azokh Cave for at least the past 300 kyr, accompanied by several other species. However, species richness and relative abundances have varied during this time interval as shown by the thanatocoenosis preserved in the different layers of Azokh 1. The species represented in these assemblages differ in their habitat preferences, and have been used as a means of interpreting the changes that took place in the surrounding environment during this time, mainly concerning vegetation and forest development.

Резюме Азохская пещера хорошо известна на Кавказе не только как археологический памятник, но и по причине проживания в ней больших колоний различных видов летучих мышей, некоторые из которых являются редкими в регионе. Согласно сведениям из доступных источников, колонии из примерно 4000 особей подковоноса Мегели (*Rhinolophus mehelyi*) постоянно ночуют в пещере, а количество летучих мышей увеличивается от весны к осени за счет около 10 тыс. особей длиннопалой ночницы (*Miniopterus schreibersii*). Большая ночница (*Myotis blythii*) и меньшее количество большого подковоноса (*Rhinolophus ferrumequinum*) проживают в пещере вместе с этими двумя видами и другими формами, некоторые из которых также считаются редкими на Кавказе. Такое изобилие особей и богатство видов указывает на то, что летучие мыши региона нашли в пещере и его окружении благоприятные условия для своего проживания.

Данная обстановка имеет, по крайней мере, 280-тысячелетнюю историю – возраст наиболее древнего материала, раскопанного до сих пор в пещере, где останки летучих мышей оказались наиболее часто встречающимися формами в отложениях. К настоящему времени идентифицировано 13 видов в различных горизонтах наиболее тщательно раскопанных седиментов. Хотя основные виды, представленные в коллекции из подразделений *V–I*, относятся к гнездящимся в настоящее время в пещере, между ними все же наблюдаются различия в видовом разнообразии и относительной численности. Так, подразделения *V* и *IV* содержат большее число видов летучих мышей, которое резко уменьшается в подразделении *III*, практически стерильным для окаменелостей этих животных; в подразделениях *II* и *I* разнообразие видов умеренное, не достигая значений для наиболее древних горизонтов.

Несмотря на то, что в отложениях есть свидетельства проживания человека, наблюдаемые различия в видовом разнообразии и количестве летучих мышей, вероятнее всего, связаны с изменениями среды, имея в виду климат и окружающий пещеру ландшафт, а не с антропогенным фактором. Так, с учетом технологии собирательства, географического распределения и температурных характеристик мест гнездования видов, зарегистрированных в каждом подразделении, мы попытались объяснить эти изменения в экологических терминах. Удалось выяснить, что

P. Sevilla (✉)
Facultad de Geología, Departamento de Paleontología, Universidad Complutense de Madrid (UCM), C/ José Antonio Novais, 12, 28040 Madrid, Spain
e-mail: psevilla@ucm.es

Yolanda Fernández-Jalvo et al. (eds.), *Azokh Cave and the Transcaucasian Corridor*, Vertebrate Paleobiology and Paleoanthropology, DOI 10.1007/978-3-319-24924-7_8

незначительное похолодание в регионе с превалированием открытых ландшафтов способствовало относительно бурному развитию лесов, что могло стать причиной большего видового разнообразия летучих мышей, наблюдаемого в подразделении *V*.

Keywords Lesser Caucasus • Upper Pleistocene • Holocene • Chiroptera • Rhinolophidae

Introduction

Azokh Cave is well known as one of the largest caves in the Caucasus. A good part of it remains unexplored, and it consists of several chambers, large and small, connected by galleries that offer a good choice of roosts for cave-dwelling bats. Azokh Cave provides shelter and roosting sites for large colonies of bats, and references to this cave are common in the literature dealing with the bats from the Caucasus (see Rakhmatulina 1989, 1995a, b, 1996a, b).

Two species of horseshoe bats, *Rhinolophus mehelyi* and *R. ferrumequinum*, permanently occupy the cave at present (Fig. 8.1a, b). The colonies of the former are the largest known in the region, with numbers reaching several thousand individuals. From spring to autumn the number of bats in Azokh Cave exceeds 20,000 individuals, as *M. schreibersii* (Fig. 8.1c) and *M. blythii* settle in the cave during the breeding season. The colonies of Schreiber's Bent-winged Bats can reach close to 10,000 individuals and those of *M. blythii* are equally numerous (Rakhmatulina 1996a). Since these species build their colonies at well-exposed roosting sites, they are easily observed (Fig. 8.2). Several other species have been reported in Azokh, but they are either less numerous or roost at less conspicuous places, so that they are more difficult to observe.

A greater number of species have been roosting in Azokh Cave during the last three hundred thousand years. Reports on the excavations conducted in the cave during the 1980s already referred to the finding of fossil bones of five different species in the cave, *R. mehelyi*, *R. ferrumequinum*, *M. blythii*, *M. nattereri* and *M. schreibersii* (Rakhmatulina 1995a). With the new excavations this number has increased to 13 different

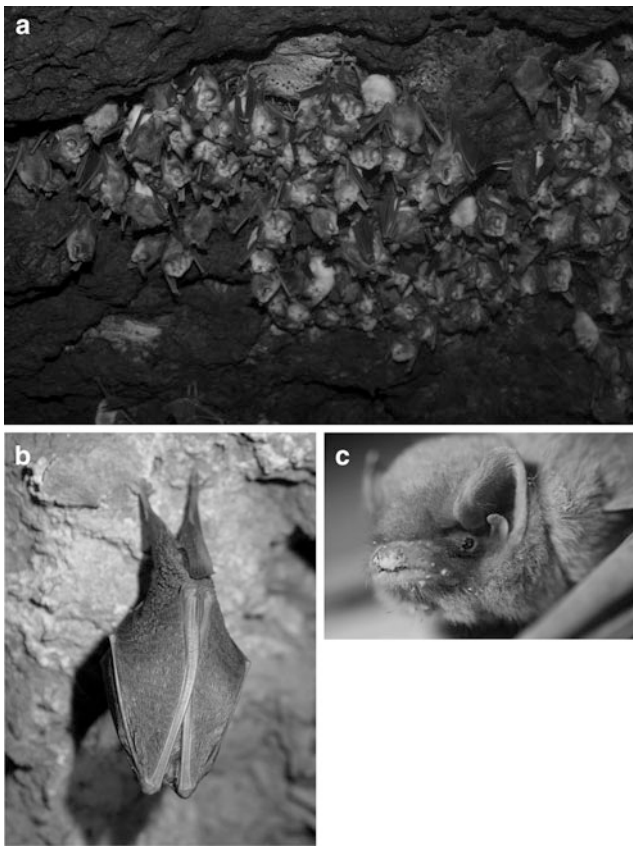

Fig. 8.1 Bats of Azokh Cave. **a** A colony of *Rhinolophus mehelyi*. **b** An isolated specimen of *Rhinolophus ferrumequinum*. **c** Detail of the head of a specimen of *Miniopterus schreibersii* found roosting near the entrance to Azokh 1 (Photographs by P. Domínguez 2004, 2005)

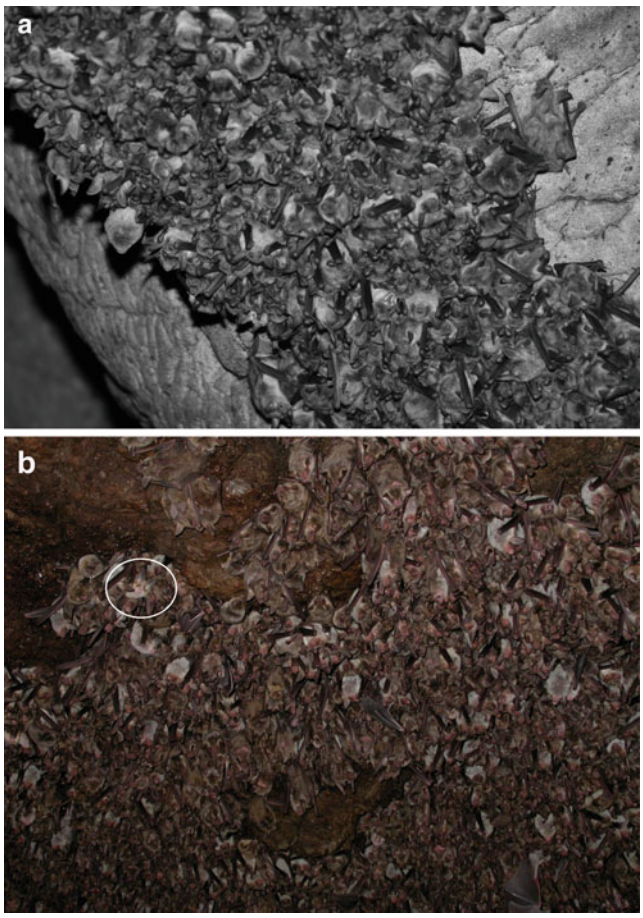

Fig. 8.2 Bats of Azokh Cave. **a** A colony of *Myotis blythii*. **b** A colony of *M. blythii* with an individual of *R. mehelyi* (circle) (Photographs by P. Domínguez 2004, 2005)

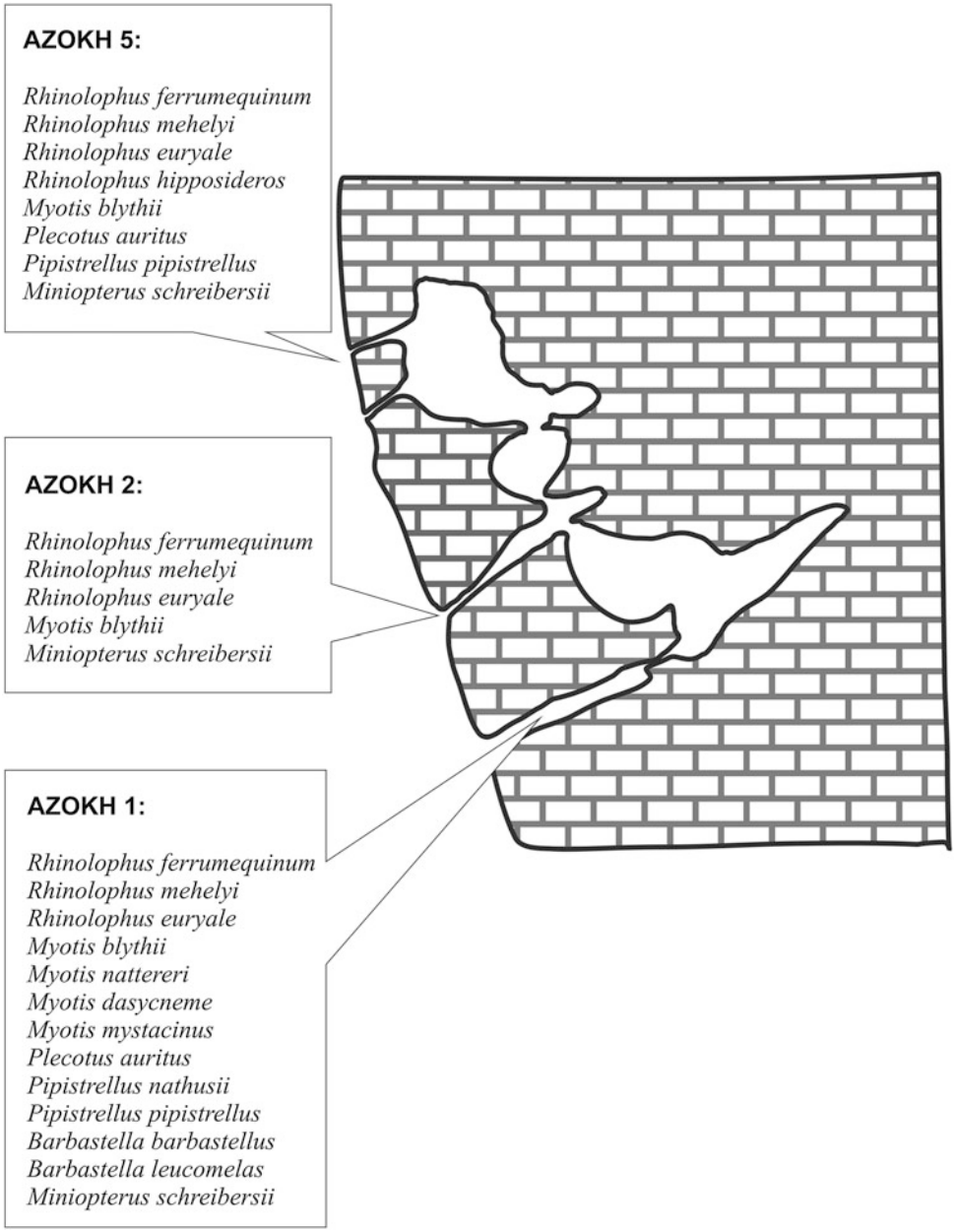

Fig. 8.3 Bat species recorded in the new excavations (2002–2009) in Azokh Cave

bat species in Azokh 1 (Fig. 8.3), and this number might increase with further excavations in other parts of the cave.

In this chapter, the numerous bat fossils found in the new excavations of Azokh Cave are described. The faunal assemblages preserved in each of the units in Azokh 1 have yielded bat bones and teeth of several different species, some of which have not been reported as roosting presently in the cave. Both the abundance of bats and the species represented in each assemblage show that the bat community roosting in Azokh Cave has varied in the last 300 kyr, according to changes that took place both within and outside the cave. Since some of the species found in Azokh Cave are considered rare or vulnerable, the study of these variations and their possible causes may be important to understand the long term dynamics of their populations.

Materials and Methods

The material studied here comes mainly from Azokh 1 (Main Entrance), Unit I (top unit in the stratigraphic succession) to Unit V (bottom unit as presently excavated). Fossil material from Azokh 2 and Azokh 5 passageways have also been examined briefly, but results from these sites

are not included in this paper. Most of the bat fossils collected in the recent excavations at Azokh 1, Azokh 2 and Azokh 5 were fragments, mainly isolated teeth, sometimes covered with a dark mineral coating (manganese oxides) that makes taxonomic determination tasks more difficult.

Fossils described here were recovered from the eight excavation seasons carried out from 2002 to 2009 (Fernández-Jalvo et al. 2010). Sediments were labelled by square and vertical coordinate (Z), and wet-sieved in the river using superimposed sieves of 2, 1 and 0.5 mm meshes. Sorting was partially done at the field laboratory, as well as at the laboratory under light microscopes.

Though some cases of exceptional preservation in bats are known, with complete skeletons and bones preserved in articulation, fossilization of bats usually implies a certain degree of disarticulation and loss of the smaller and most delicate bones. The hardest parts of a bat skeleton, such as teeth, mandibles, maxillae and humeri, are the most common anatomical elements in the fossil assemblages. Other parts of the skeleton may also be common, such as scapulae, pelves, femora, cochlea and fragments of phalanges. If preservation is good, and collecting methods are adequate, even deciduous teeth and poorly ossified bones of newly born bats can be collected, as in the case for the bat fossils in Azokh Cave.

Taxonomic determination was focused on the mandibles and maxillae, humeri (if the distal articulation is preserved) and certain teeth, mainly the molars, since these skeletal elements enable species determination. The nomenclature used in the description of the material, and the criteria for taxonomic determination, follow Menu and Sigé (1971), Felten et al. (1973), Sevilla (1986, 1988) and Menu and Popelard (1987). Wear stages to establish age of death are based on Sevilla (1986). Traits of digestion have also been analysed on cranial and/or postcranial anatomical elements according to criteria and stages set up by Andrews (1990).

Species representation was quantified using both numbers of remains and minimum numbers of individuals (MNI). To interpret the environmental conditions implied by the bat assemblage, the known ecology of the extant representatives of each species was considered. The main sources for this information were several papers from the National Bat Reports of Armenia and Azerbaijan, available at eurobats.org/documents/national reports, and the information about habitat and geographic distributions found in Campester Field Researcher's Union site and at the IUCN (2009) Red lists site. The biogeographic character of each species was considered according to Horaček et al. (2000).

Table 8.1 Differences in the representation of bat fossils in Azokh 1. (NR: number of identified remains; MNI: minimum number of individuals)

Distribution of bat remains in Azokh 1						
Azokh 1 (2002–2009)		UNIT I	UNIT II	UNIT III	UNIT Vu	UNIT Vm
Rhinolophus ferrumequinum	NR	3	3		93	14
	MNI	2	2		14	5
Rhinolophus mehelyi	NR	16		1	37	5
	MNI	6		1	6	2
Rhinolophus euryale	NR				3	1
	MNI				3	1
Myotis blythii	NR	271	23	2	2067	22
	MNI	26	7	1	123	5
Myotis nattereri/schaubi	NR				1	1
	MNI				1	1
Myotis mystacinus	NR	2			6	1
	MNI	1			2	1
Myotis dasycneme	NR		1			
	MNI		1			
Plecotus auritus/macrobullaris	NR	3			6	
	MNI	1			1	
Barbastella barbastellus	NR				2	
	MNI				1	
Barbastella leucomelas	NR				2	2
	MNI				1	1
Pipistrellus nathusii	NR					4
	MNI					2
Pipistrellus pipistrellus	NR		1		3	3
	MNI		1		2	2
Miniopterus schreibersii	NR	15	16		94	80
	MNI	6	7		18	23
Total NR		298	43	3	2314	133

Results

Table 8.1 shows the record of bats in Azokh 1, indicating the number of fossil specimens that have been identified for each species, and the minimum number of individuals (MNI) these fossils represent. Skeletal elements are relatively scarce, particularly in the upper units. This is especially evident in Unit II, where destruction of bone has been caused by heavy guano deposition which has destroyed much of the bone. The reduced fossil representation from Unit III may be a consequence of the heavily cemented sediment that hampered the sieving work, and because the only excavation performed in unit III has been restricted to a test pit of no more than 2 square metres near the cave wall.

Two families of bats are represented, the Vespertilionidae and the Rhinolophidae (Fig. 8.4). Five different genera of vespertilionids were identified, *Myotis*, *Pipistrellus*, *Barbastella*, *Plecotus* and *Miniopterus* with ten different species in the assemblages of Azokh 1. The Rhinolophidae are represented since the Quaternary by a single genus, *Rhinolophus*, with five extant species distributed in the Caucasus. Thus, a total number of 13 species of bats are represented in the material, with important differences in their relative abundances along the sequence, the meaning of which will be commented later in the discussion.

The genus *Myotis* is the most diverse in the region, with eight species distributed in the Caucasus (Fig. 8.2), and many of these are frequently found roosting in caves. Their remains are distinctive (Fig. 8.5): the humeri have distal epiphyses with a short styloid process and a shallow depression between the trochlea and the condylus; three premolars are retained in both the upper and lower tooth rows; the upper molars are robust, without a talon; the lower molars are myotodont, with a thick and well-developed labial cingulum; the third molars present an important distal reduction. The anatomical elements of the different species within the genus differ in size and in the development of particular structures in the teeth, mainly of the upper molars.

Myotis blythii, the Lesser Mouse-eared Bat is not only the best represented species of this genus in Azokh 1, but it is also more numerous than all the remaining species of the other genera, except in Unit V. Isolated teeth, mandibles, maxillae, cochlea, humeri and other bones of this species were collected in all of the five units; and even poorly ossified bones, deciduous teeth and a few mandibles with erupting permanent molars were found at certain levels. The skeletal elements of this species stand out for their large size (Fig. 8.5a–d) and are particularly abundant at Unit Vu. Even Unit III, with few bat fossils, yielded a couple of lesser Mouse-eared Bat fossils. *Myotis blythii* is a widely spread species in the Caucasus; and it is found in a variety of habitats, from humid forests to semi-desertic areas, except for alpine meadows. From a biogeographic point of view, it is a "temperate arid" species, linked to warm and dry habitats (Horaček et al. 2000). Its roosts are varied, including large and relatively warm caves. Large nursery colonies of the Lesser Mouse-eared Bat are observed today in Azokh

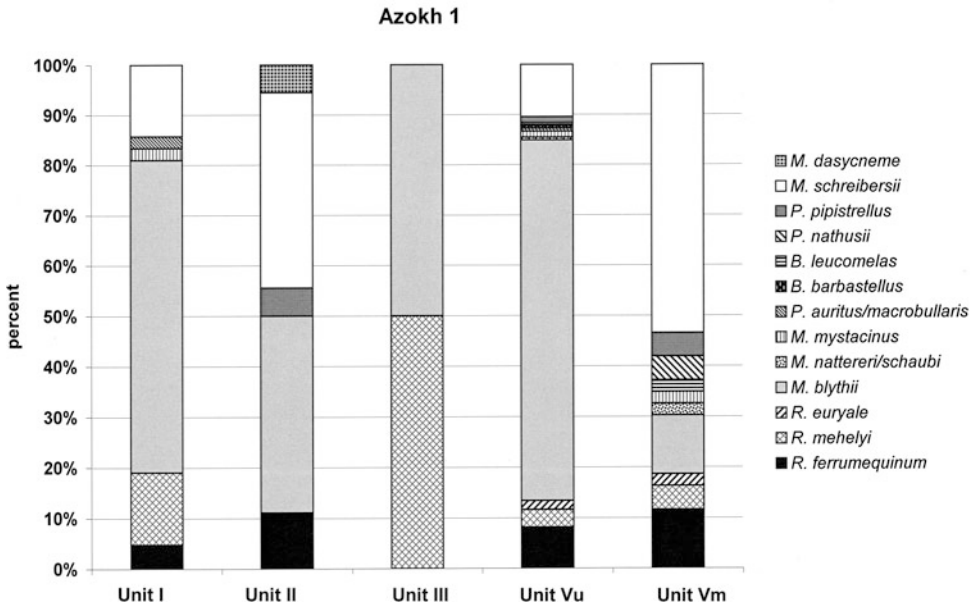

Fig. 8.4 Variation in the relative abundances of bat species in Azokh 1

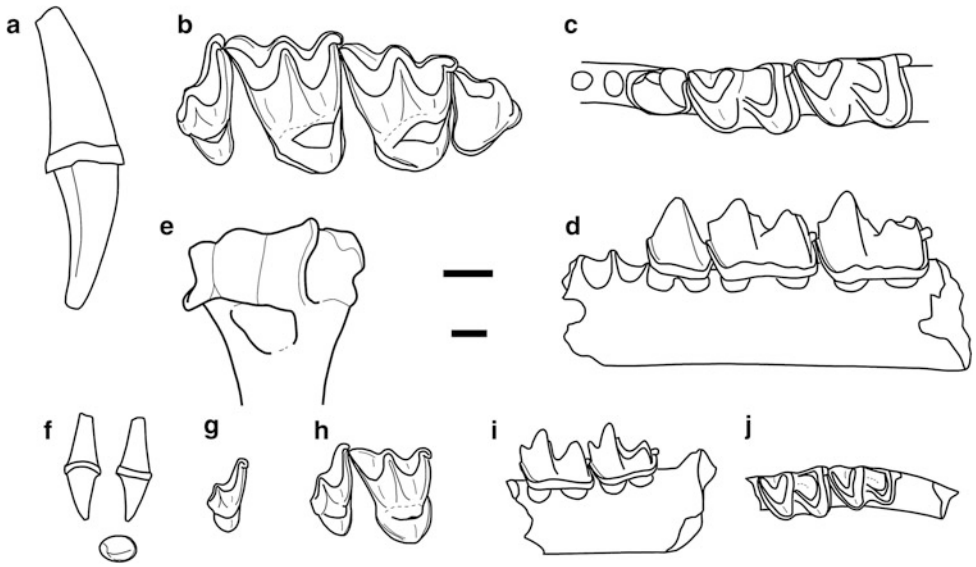

Fig. 8.5 *Myotis blythii*. **a** Right upper canine; **b** right $P^4M^1M^2M^3$; **c**, **d** fragment of left mandible with $P_4M_1M_2$. **e** Distal epiphysis of left humerus. *Myotis mystacinus*. **f** Right upper canine; **g** right M^3. *Myotis nattereri*. **h** Right M^2M^3. *Myotis dasycneme*. **i**, **j** Fragment of left mandible with M_2M_3. Scale = 1 mm. (The short bar is only for **e**)

Cave from spring to autumn, occupying exposed places on the ceiling and in wide fissures, but this species moves to another cave for hibernation. *M. blythii* is common in Quaternary fossil assemblages.

The representation of the other species of the genus *Myotis* may be considered occasional, their fossils restricted to certain units and represented by few individuals. A few teeth and a humeri of *Myotis mystacinus,* commonly known as the Whiskered Myotis, were found in Units I, Vu and Vm (Fig. 8.5f, g). It is the smallest species of the genus in the Caucasus and is considered rare. The morphology of these fossils agrees with the general morphology observed in the species within the genus *Myotis*, but its humeri are half the size of the same bone in *M. blythii*. The two first upper molars are more rectangular in outline than in the Lesser Mouse-eared Bat, and the third molar is less reduced in its distal region. It is a western Palaearctic species with a "temperate humid" pattern of distribution. It occurs in a variety of habitats and hunts exclusively near inland waters. Winter roosts may be located in caves, where they congregate in small groups.

Myotis nattereri, Natterer's Bat, was reported by Huseinov (according to Rakhmatulina 1995a) as one of the species represented in the bat assemblages from the old excavations, but only two fossils of this species were found in the recent excavations. These are maxillary teeth that were collected at Units Vm and Vu. The teeth and bones of this species are similar in morphology to, but smaller than, those of *M. blythii*, and they are distinctly larger than the Whiskered Myotis (Fig. 8.5h). *Myotis nattereri* is a western Palaearctic species, with an extensive distribution, frequent in Pleistocene fossil assemblages with bats but becoming less common in Holocene assemblages, probably due to a reduction of favourable habitats. This species is currently rare in the Caucasus. It is known to forage mainly in woodland, sometimes over water, and although it occurs both in humid and in dry areas, it depends on the presence of water bodies. Like *M. mystacinus*, it is a species with a temperate humid pattern of distribution. Summer roosts are occasionally located in underground sites, but hibernation takes place preferably in caves and in underground habitats. Its sibling species, *M. schaubi* Kormos 1934, is also distributed in the region, but poorly known. It was described first with Pleistocene fossil material from eastern Europe. It closely resembles *M. nattereri*, though it is slightly more robust, and according to the original description, differences are observed in the lower molars, which have a very weak hypoconulid. With only two fossils in our material, we cannot establish to which of the two species it might belong. New collections of *M. nattereri/schaubi* group fossils in future excavations in Azokh might help to clarify this point.

A single fossil, consisting of a fragment of a lower mandible with two molars of *Myotis dasycneme*, known as the Pond Bat, was found at Unit II (Fig. 8.5i, j). Both the morphology and the size agree with that of extant specimens of this species. It has a wide distribution that extends from

Fig. 8.6 Recent distribution of *Myotis dasycneme* (after Hutson et al. 2008) shown in in dark grey. The approximate position of Azokh Cave is marked by the symbol (*). Note the distance between the cave and the nearest areas at which *M. dasycneme* is known to live at the present time

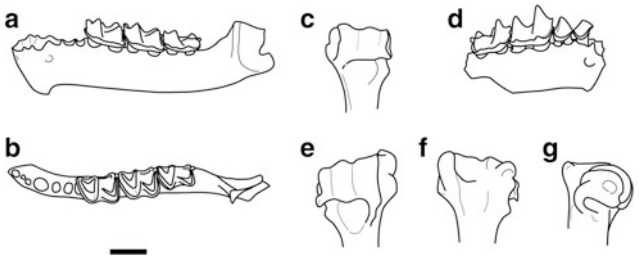

Fig. 8.7 *Pipistrellus pipistrellus*. **a**, **b** Fragment of left mandible with $M_1M_2M_3$; **c** distal epiphysis of right humerus. *Pipistrellus nathusii*. **d** Fragment of right mandible with $P_2P_4M_1M_2$; **e**, **f**, **g** distal epiphysis of left humerus. Scale: 1 mm

north-west Europe to central Russia, (Fig. 8.6), with its southernmost limits at latitude 44º N, well to the north from Azokh Cave. The Pond Bat is known to be a partial migrant; fossils of this species are known in several Holocene localities that are beyond its present range of distribution, though never reaching distances as great as Azokh Cave. It is a species linked to water habitats since it feeds mainly over open calm water, preferring water bodies with banks of open rough vegetation and no trees. It frequently hibernates in natural caves forming small colonies of a few hundred individuals.

Two species of the genus *Pipistrellus* were found in Azokh 1. A few fossils of *Pipistrellus pipistrellus*, known as the Common Pipistrelle, were collected at Units Vm and Vu and II. In Unit V fossils of another species of the genus, *Pipistrellus nathusii* were also found. The pipistrelles are small-sized bats, with a very small skeleton. Their humeri are characterized by the relatively deep fossa for the elbow joint and the hood-like styloid process. The teeth of these bats are slender, with pointed cusps; the lower molars are nyctalodont, with narrow trigonids and relatively large hypoconulids (Fig. 8.7). *P. pispistrellus* is smaller than *P. nathusii*. It is a widespread and abundant species and one of the most common bats in the Palearctic, frequent both in Mediterranean and in temperate humid regions. It forages in a wide variety of habitats including open woodland and woodland edges, Mediterranean shrubland, semi-desert, as well as anthropogenic landscapes, feeding mainly on small moths and flies. Roosts are varied, including tree holes, rock fissures and caves. Fossils of this species are known from several upper Pleistocene and Holocene localities, but never in large numbers. The other pipistrelle species found in Azokh, *P. nathusii*, is rare in the Caucasus, but widespread and abundant in other areas within its range of distribution, probably because of its preference for temperate humid regions. It is a species mainly linked to forest habitats, foraging in woodland edges, wetlands, and open parkland. It is a migratory species, sometimes covering close to 2,000 km during migration. Winter roosts include the entrance of caves, often in relatively cold, dry, and exposed sites. However, signs of digestion were observed on humeri both of *P. pipistrellus* and of *P. nathusii*, and since pipistrelles are occasional prey to owls, it seems reasonable to consider these fossils as coming from pellets from some bird of prey.

A few fossils of the two Barbastelles distributed in the Causasus were found in the lower levels of Azokh 1. A mandible and a broken humerus from Unit Vm and another two fragments of humeri from Unit Vu were identified as belonging to the Eastern Barbastelle, *Barbastella leucomelas,* while a smaller mandible with similar morphology, as well as a humerus from Unit Vu, were determined as fossils of the European barbastelle, *Barbastella barbastellus* (Fig. 8.8). The distal epiphyses of the barbastelles are very characteristic mainly for the triangular shape of the styloid process that projects inwards; the ramus in the mandibles has a relatively high and narrow coronoid process, a low articular process, and long and robust angular process, commonly broken in the fossil material. The molars are nyctalodont, elongate, with wide trigonids. The Eastern Barbastelle is somewhat larger than the European species. It extends its distribution from the Caucasus, through southern Asia to China, where it is found in forest habitats, both in moist temperate and in dry coniferous forests. It is a widespread, but infrequent, temperate arid species. It roosts in small groups both in caves and in tree hollows, or beneath the bark. The European Barbastelle on the other hand, is a temperate humid species, distributed mainly through Europe and part of the Caucasus, absent in the drier areas of its distribution. It is found linked to mountain and lowland forests; the abundance of this species depends on the

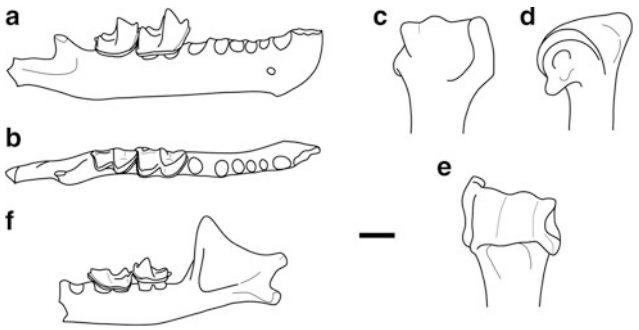

Fig. 8.8 *Barbastella leucomelas*. **a**, **b** Fragment of right mandible with M_2M_3. *Barbastella barbastellus*. **c**, **d**, **e** Distal epiphysis of right humerus; **f** fragment of left mandible with M_2M_3. Scale: 1 mm

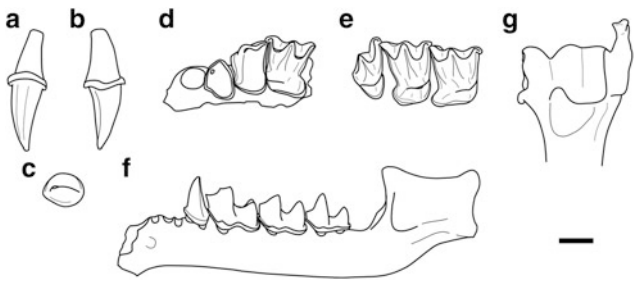

Fig. 8.10 *Miniopterus schreibersii*. **a**, **b**, **c** right upper canine. **d** fragment of left maxilla with $P^3P^4M^1$; **e** right $M^1M^2M^3$. **f** Left mandible with damage in the anterior region, broken angular process and $P^4M^1M^2M^3$ retained in alveoli. **g** Distal epiphysis of left humerus. Scale: 1 mm

presence of old and dead trees with hollows that provide the roosts used during the active season. In winter, the European Barbastelle is commonly found roosting in cold and dry caves, grottos, underground sites, and tree hollows. Though mainly a solitary species, it is sometimes found forming small groups, but a few large wintering colonies have been described. *B. barbastellus* feeds on insects with soft cuticles; it finds its prey mainly in the borders of forests or among separate groups of trees.

The Long-eared bats, genus *Plecotus*, are represented at Azokh 1 by a few teeth collected in Units Vu and I. The isolated upper molars of the species of the Long-eared bats have rounded lingual margins and low protocones with the anterior and posterior cristas evenly curved and without cuspules. The lower molars are myotodont with a clear notch in the preprotocrista. The talonid of the third lower molar is narrow but long (Fig. 8.9). Because of their similarity and the fact that they are found in similar habitats, the alpine long-eared bat, (*P. macrobullaris*) was commonly taken for *P.auritus* Linnaeus, 1758. Both species are distributed in the Caucasus, but *P. macrobullaris* is poorly known, and since no differences between them have been described, either in the dentition or the skeleton, the fossils form Azokh are referred to as *P. auritus*/*P. macrobullaris*. Both of them are linked to forest habitats, though a certain degree of habitat partitioning seems to take place where both species occur, *P. macrobullaris* being more abundant at higher altitudes. *P. auritus* has a temperate humid pattern of distribution, rather common in central Europe, but rare in the Mediterranean. It forages in forest landscapes, gleaning soft bodied insects from the foliage. It forms small colonies during the summer, located mainly in tree holes. During the winter, it is generally solitary and can be found roosting in caves, underground sites as well as in trees.

Fig. 8.9 *Plecotus auritus/macrobullaris*. **a** Fragment of left maxilla with P^4M^1. **b**, **c** Right M_1. Scale: 1 mm

Schreiber's Long-fingered Bat, *Miniopterus schreibersii* (Fig. 8.10) have been found in all units of Azokh 1 except Unit III, perhaps due to the sampling bias previously mentioned. It is the most common bat in Unit Vm, where it outnumbers the Lesser Mouse-eared Bat, *M. blythii,* which is the dominant bat species in the other units of Azokh 1. The bones and teeth of *M. schreibersii* are distinctive, even when broken. The humerus has a long, well-developed and flattened styloid process in its distal epiphysis; and the condylus and epicondylus are connected by a deep groove. The mandibles have a marked ventral bend at the connection between the body and the ramus; the coronoid and the articular process are of similar height; the lower third premolar has two roots, and the lower molars are nyctalodont, with narrow and high cusps. The upper canines are long and slender, with deep longitudinal grooves on both the lingual and labial side. The third and fourth upper premolars are large with a lingual talon, both teeth with three roots; the two first upper molars are rectangular in outline, the disto-lingual margin strong, but without a talon; the parastyle is strong and hook-like. Though previously considered the most widespread species of bat in the world, recent studies restrict the distribution of *M. schreibersii* to Northern Africa, European regions adjacent to the Mediterranean, Asia Minor, extending to the east as far as the Caucasus. The remaining distribution is now considered to correspond to several sibling species. Schreiber's Long-fingered Bat is found in a wide variety of landscapes in the Caucasus: steppes, semi-steppes and xerophytes zones, as well as in mountain and humid forests. These bats hunt in open arid landscapes and over woods, preferring mosaic habitats where there is variety and abundance of prey. They are strict cave dwellers, usually choosing cool and highly humid roosting places. Large colonies are common among these bats, sometimes even reaching numbers of several thousands

of individuals, and occasionally these colonies are mixed with other species.

Four Rhinolophid species are recorded at Azokh 1. The bones and teeth of Horse-shoe bats have the following charaters: the humerus has a distal epiphysis with a relatively long and slender styloid process; the epitrochlea is wide; a deep and wide groove separates the trochlea from the condylus and epicondylus, which projects laterally; the upper canines are strong, with a narrow crown and a sinuous, well-developed cingulum; in labial view the crown and the root of the canine form an angle; the fourth upper premolar is slender, with a well-developed talon; the first and second upper molars have a talon without a hypocone; no additional cuspules are observed in the cristas of the protocone. The third upper molar is less reduced than in other bats, the premetacrista complete or only slightly reduced. The lower dentition is also slender, and the molars present a nyctalodont pattern (Fig. 8.11).

Two species, *R. ferrumequinum* and *R. mehelyi*, are constant elements in the assemblages of Azokh 1, though numbers of specimens never exceed 20% of the bat material identified in any of the different units. The first of these species, commonly known as the Greater Horse-shoe Bat, is present in all units except for Unit III. It has a wide geographic range in temperate arid environments, extending through the South Palaearctic region from Portugal to China, including all of the Caucasus. It forages in pastures, deciduous temperate woodland, Mediterranean and sub-mediterranean shrubland and woodland. It shelters typically in large caves and underground cavities, choosing warm sites for nursery colonies and cold sites for hibernation. Colonies consist of several dozens to a few hundred individuals, often mixed with other Horse-shoe bats, Schreiber's Bent-Winged bats or the Lesser Mouse-eared Bats.

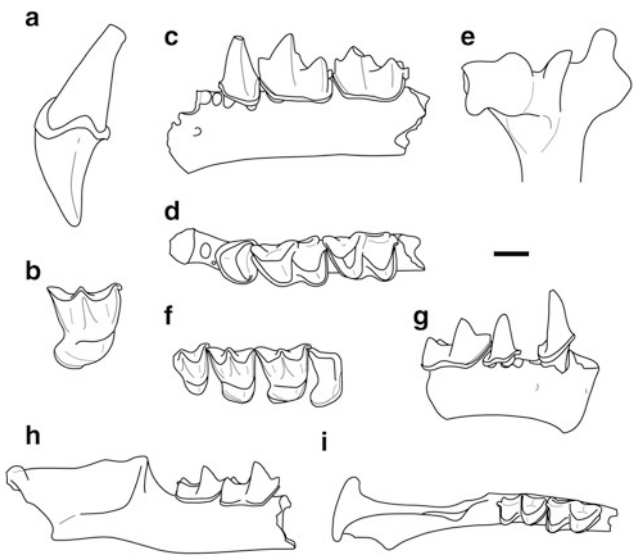

Fig. 8.11 *Rhinolophus ferrumequinum*. **a** Left upper canine. **b** Right M^1. **c**, **d** Fragment of left mandible with $P_4M_1M_2$. **e** Distal epiphysis of left humerus. *Rhinolophus mehelyi*. **f** Right $P^4M^1M^2M^3$. **g** Fragment of right mandible with canine, P_4M_1. **h**, **i** Fragment of right mandible with M_2M_3. Scale: 1 mm

The fossils of *R. mehelyi*, Mehely's Horse-shoe Bat, are similar to those of the Greater Horse-shoe Bat but distinctly smaller. They were collected in all the units of Azokh 1 except Unit II. The species has a Mediterranean distribution and forages mainly in dry shrubland and woodland, and in steppe landscapes. It is found roosting in caves and underground cavities, where it chooses colder conditions for hibernation and warmer sites for its summer roosts, but invariably in places with high humidity. Where Mehely's Horse-shoe Bat finds adequate conditions in the Caucasus region, it is found forming large colonies; this is just the case of Azokh Cave, well known in the Caucasus for sheltering the largest colonies of *R. mehelyi* in the region (Rakhmatulina 1989). Mehely's Horseshoe Bats roost in Azokh Cave the year-round; their nursery colonies are frequently mixed with other species, mainly other Horse-shoe bats, the Lesser Mouse-Eared Bat (*Myotis blythii*) and the Schreiber's Long-fingered Bat (*Miniopterus schreibersii*).

A few fossils found at Units Vm and Vu, agree with the morphology and size of a third rhinolophid species, *Rhinolophus euryale* Blasius, 1853, known as the Mediterranean Horse-shoe bat. Though practically distributed throughout the whole of Transcaucasia, it is considered a rare component of its bat fauna. It forages in Mediterranean and sub-Mediterranean shrubland and woodland. The geographic range of *R. euryale* is relatively wide, it covers forests in karst areas of North-East Africa, Southern Europe, the Caucasus, Middle East and Central Asia. It mainly roosts in caves, frequently sharing its roosts with other species. Nursery colonies comprising up to several dozens or rarely hundreds of individuals, are located in warm places.

Discussion

Caves are perhaps the most favourable environments for the preservation of fossil bats. The delicate bones of these mammals are rapidly destroyed as a result of weathering and other processes, and they are rarely found as fossils in localities even where other small vertebrates may be abundant. Additionally, since predation on bats is opportunistic, their remains are equally rare in fossil assemblages caused by predatory activity. For this reason, it is generally assumed that bones of bats preserved in cave fossil localities belong to animals that died within the cave. In caves where conditions are suitable, bats are common inhabitants, sometimes in extremely high numbers, and natural death occasionally

overcomes individuals while roosting. In this case, the possibilities that their bones may be preserved are much higher. These bones usually belong to adult and sub-adult animals that died in winter during hibernation (Kowalski 1995; Zahn et al. 2007); during the summer, the floors of the caves is covered by guano in which bone remains become totally dissolved. However, opportunistic predation on bats cannot be totally excluded as the origin of a fossil bat assemblage, especially when dealing with a mixed assemblage that includes both cave bats and other non cave dwellers such as rodents or insectivores. The signs of digestion observed in some of the teeth and bones of *Pipistrellus pipistrellus*, *Miniopterus schreibersii* and *Myotis blythii* in Azokh 1 indicates a mixed origin for the assemblages collected at Units Vm and Vu. No digestion was observed in the fossils of the Horse-shoe bats, agreeing with observations that Rhinolophidae are the bats least represented in scats and pellets (Krzanowski 1973; Chaline 1974; Aulagnier 1989). In Unit V, the abundance of unworn teeth (stage "0" in Sevilla 1986), the presence of poorly ossified bones from very young specimens of several species, and the preservation of deciduous teeth of *Myotis blythii,* all indicate that young individuals were present in the cave and support the presence of breeding colonies in it.

Fossil bats are poor biostratigraphic indicators. Since their first appearance in the fossil record, only minor changes have taken place in their morphology. In Europe, extant genera such as *Rhinolophus* or *Hipposideros* are known as fossils since the Late Eocene (more than 40 Ma) and some of the recent European species are as old as four million years (Sigé and Legendre 1983). Bats are also considered poor paleoecological indicators, since adaptations such as hibernation, flight or echolocation makes them less restricted by local conditions that otherwise control the abundance and diversity of small mammals (Feldehamer et al. 2007). It is the case, however, that some bat species are restrictive concerning their choice of roosts or of foraging grounds. For instance, the presence of strictly tree roosting bats in a fossil assemblage indicates the presence of forested landscapes, sometimes even the type of forest (deciduous, mixed, mature, etc.). Other species have clear foraging habitat preferences, hunting their prey over open landscapes, or by river banks, etc. This too can be used to infer past environments. Additionally, the recent patterns of distribution of a species can also indicate the degree of tolerance to certain environmental parameters; thus, "Mediterranean" species are restricted in their distribution to areas with short and warm winters, whereas "boreal" species have more northern distributions where the climate is cooler. Occasionally a species may be found in a fossil assemblage located beyond its recent range of distribution; this might indicate either different environmental conditions in the past, or the reduction of a previously wider range of distribution due to landscape degradation.

The density and diversity of bats roosting in a particular cave depends mainly on both temperature and humidity values within the cavity. However, the surrounding landscapes must provide adequate hunting places, and this also influences in the presence or absence of bats in a cave. Within small caves changes in temperatures and humidity may take place in response to changes in the weather and season, and where this is the case bat communities are more unstable. Contrary to this, larger caves such as Azokh Cave, shelter more stable bat communities and the long-term changes in the bats have more to do with changes outside the cave, mainly in the characteristics of the surrounding habitats used as foraging grounds.

Fossil localities with deposits in which bat fossils are well represented may be analysed in these terms to reconstruct past environments. Changes in bat abundance and composition along the fossil sequence may be used to infer past environmental changes in a similar way as rodents and insectivores are used for this purpose. Moreover, since human presence in a cave interferes with cave-roosting bats, having an influence on the communities occupying the cave regularly, intensity of human use of a cave may also be inferred from its consequences on the fossil bat assemblage (Postawa 2004; Rossina 2006; Rossina et al. 2006).

Species richness in the Caucasus is strongly linked to vegetation and availability of roosts (Rakhmatulina 1998). The richest habitats in bat species are the mountain steppes, closely followed by mountain forest habitats. The lowest values are observed in mountain grasslands, due to harder climatic conditions and the fewer available roosts in these habitats. The Karabagh uplands, where Azokh Cave is located, is characterised by arid landscapes; the development of karsts provide abundant and varied roosts that favour an important diversity of bats. Ten species are common or numerous in this part of the Caucasus, including five *Rhinolophus* species, *Myotis blythii*, *Miniopterus schreibersii*, *Pipistrellus pipistrellus*, *P. kuhlii* and *Eptesicus serotinus*. Additionally another 13 less common species are also to be found here. Eight of the ten cave-dwelling species distributed in the region have been identified in the fossil assemblages from Azokh 1: the exceptions are *R. blasii* and *R. hipposideros* (Table 8.2). The possible explanation for their absence in Azokh 1 is that these two species are both rare in the region and do not group in large colonies. (However, we have a few fossils of the latter species in Azokh 5). Occasional cave-dwellers are also represented in the material.

According to the information obtained from the bat assemblages preserved at Units I to V, a paleoecological interpretation has been carried out for each bed (Figs. 8.12 and 8.13).

Table 8.2 Roosts and faunal status of the bats in the Lesser Caucasus at the present time compared with the species recorded in Azokh 1. Roost preferences follow Rakhmatulina (1995b); Faunal status is extracted from the National Reports of Armenia (2006): numerous (++); common (+); rare (−)

Choice of roosts and status of the bat species of Azokh 1						
Bat species in the Lesser Caucasus	Caves, underground spaces	Rock fissures	Buildings or other human constructions	Trees	Faunal status	Recorded in Azokh 1
Rhinolophus ferrumequinum	+		+		+	+
Rhinolophus mehelyi	+				–	+
Rhinolophus euryale	+				–	+
Rhinolophus blasii	+				–	
Rhinolophus hipposideros	+		+		–	
Myotis blythii	+	+	+		+	+
Myotis nattereri/schaubi		+	+		–	+
Myotis mystacinus/aurascens	+		+		–	+
Plecotus auritus/macrobullaris	+	+	+		+	+
Barbastella barbastellus		+	+		–	+
Nyctalus noctula			+	+	–	
Nyctalus leisleri				+	++	
Pipistrellus pipistrellus		+	+	+	+	+
Pipistrellus kuhlii			+		+	
Hypsugo savii		+	+		–	
Eptesicus serotinus			+	+	–	
Miniopterus schreibersii	+				–	+
Tadarida teniotis		+			–	

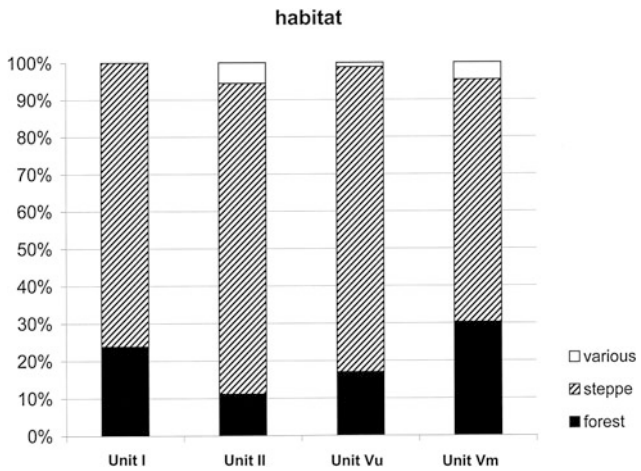

Fig. 8.12 Variation in the proportion of bat species in Azokh 1 grouped according to foraging preferences in different landscapes

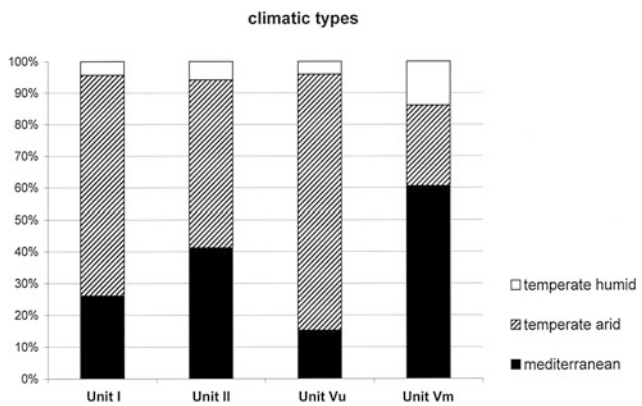

Fig. 8.13 Variation in the proportion of bat species in Azokh 1 grouped according to climatic type (after Horacek et al. 2000)

- Unit Vm is characterised by the presence of six occasional species, all of them frequently foraging in forest areas. This is the only unit where *M. schreibersii* outnumbers *M. blythii* both in number of fossils and in MNI. A dominance of Mediterranean species is observed; this unit has the highest representation of temperate humid species in the series.
- Unit Vu is the richest both in number of bat remains and species of the whole sequence of Azokh 1. The assemblage has a strong temperate arid character, as interpreted from the high predominance of *M. blythii* and the increase in the representation of the species of the genus *Rhinolophus*. A greater extent of open-steppe habitat seems most probable, with the occasional presence of trees.

Warmer temperatures and more arid conditions agree with these changes. It is also the case that this unit has by far the greatest number of small mammals (Parfitt 2016).

- Unit III can be considered practically sterile in bat fossils. The restricted area of excavation and heavily cemented sediment (see methods) might influence such a reduced record. Rodents (Parfitt 2016), for instance, also have a lower species representation at Unit III, but amphibians (Blain 2016), do not. Only the persistence in the cave of *R. mehelyi* and *M. blythii* can be ascertained. This lack of material makes an interpretation difficult, and it might hide a change in the bat community due to an environmental change or to a more permanent presence of humans in the cave.
- Unit II has slightly more bat fossils compared to Unit III. The upper part of this unit is practically sterile due to the influence of guano; this might indicate the settlement of large summer colonies of bats in the cave. The sediment is acidic because of the guano accumulation and this destroys the bones and the evidence of the species that formed these colonies. Nevertheless, the few fossil remains show the presence of three of the four constant species, with *R. mehelyi* missing. On the other hand, the pond bat, *M. dasycneme,* is present as the single occasional species of this unit. The Caucasus is well beyond the recent range of distribution of the pond bat, which has a northern distribution, and the presence of this species might be considered as indicating colder climatic conditions. The absence of *R. mehelyi,* of strict mediterranean distribution, could support this interpretation.
- Unit I has a "modern" sample of the recent community of bats roosting permanently or occasionally in the cave. The four constant species are represented in proportions that are comparable to their present abundance in the cave; two of the three additional species found at this unit are common in the region, and the third (*M. mystacinus*) is considered rare.

Since the four constant species (*M. blythii*, *R. ferrumequinum*, *R. mehelyi* and *M. schreibersii*) seem to be relatively independent of the environmental conditions, the variations in habitat were interpreted focusing attention mainly on the changes observed in the occasional species representation within each assemblage. Figures 8.12 and 8.13 show these variations based on MNI values; the species are grouped according to foraging landscape preferences and climatic type, and the variations in their relative proportions were used as the basis to interpret changes in the environment from one unit to another.

Thus, a picture of a changing landscape may be drawn from the bat fossil assemblages of Azokh 1. During the late middle Pleistocene, though open steppe habitats were common in the surroundings of the cave, a more "Mediterranean" character is inferred, with significant presence of trees and shrubs, probably favoured by a combination of slightly less arid conditions and lower temperatures. During the formation of the upper part of Unit V, these conditions changed towards an increase in open habitats with steppe vegetation, probably accompanied by an increase in temperatures favouring the presence of a higher diversity of species. The changes that might have taken place during the formation of Unit III are hidden because of the few available specimens; however a real decrease in bat abundance may have occurred due to a more intensive occupation of the cave by humans, as indicated by other remains preserved in this unit and perhaps a change in environmental conditions. The slight increase in bat representation in Unit II shows low values of diversity and hints at change towards colder conditions than at Unit V. Finally, environmental conditions similar to those of today are inferred from the assemblage preserved in Unit I.

Conclusions

1. The bat fossils preserved in the Pleistocene and Holocene sediments in Azokh Cave provide good evidence of a long-term occupation of the cave by bats for at least the last 300 kyr.
2. No major change is observed in the main components of the bat communities established in the cave during this time; *Myotis blythii*, *Miniopterus schreibersii*, *Rhinolophus mehelyi* and *Rhinolophus ferrumequinum* all occur through the sequence of Azokh 1, and are represented in all the units that contained a significant number of bat fossils. These four species constitute the main elements of the bat community presently roosting in Azokh Cave.
3. There is evidence in the lowermost units that the Lesser Mouse-eared bat (*Myotis blythii*) both wintered and bred in Azokh 1. At present, the colonies of this species move to another cave during the winter.
4. Variations in the abundance of fossil species and in the relative proportions of the species represented at each unit in Azokh 1 may be linked to changes in the vegetation in the area surrounding the cave, and more particularly to the degree of forest development.
5. There is no evidence of human occupation of the cave having a significant influence on the bat communities, except perhaps in Unit III, where practically no bat fossils are preserved.
6. The bat assemblages represented at Azokh 1 indicate that an open-ground landscape with steppe vegetation

prevailed in the region since the late middle Pleistocene. Slightly less arid conditions, favouring greater development of trees in the area might explain the higher species richness observed at the time of the Unit V faunas.

7. A shift towards a treeless, arid and cold environment could have taken place during the formation of Units III and II, slowly recovering towards more favourable conditions up through Unit II, when large amounts of bat guano accumulated.
8. The Holocene assemblage of Unit I indicates a situation similar to the present, in which mountain steppe species are well represented and dominating in the community of bats, accompanied by a few occasional species.

Acknowledgements This study has been supported with funds provided by the following institutions: Institute of Archaeology Awards (Univ. London), The Harold Hyam Wingate Trust, The Royal Society, the Spanish Ministry for Science & Technology and the BSCH-UCM Research Group n. 910607. The MNCN (Madrid), Estación Biológica de Doñana (Seville) and the Hungarian Natural History Museum (London) Collections Departments provided skulls for direct comparison at different stages of the research. The author is indebted to Dr. P. Andrews and Y. Fernández-Jalvo for their careful review of the manuscript.

References

Andrews, P. (1990). Owls, Caves and Fossils. Predation, preservation and accumulation of small mammal bones in caves, with an analysis of the Pleistocene cave faunas from Westbury-sub-Mendip. Somerset, UK: The Natural History Museum Publications. British Museum (Natural History).

Aulagnier, S. (1989). Les chauve-souris (Chiroptera) dans le régime alimentaire des rapaces nocturnes (Strigiformes) au Maroc. In V. Hanák, J. Horaček & J. Gaisler (Eds.), *European bat research symposium, 1987* (pp. 457–463). Praha: Charles University Press.

Blain, H.-A. (2016). Amphibians and squamate reptiles from Azokh 1. In Y. Fernández-Jalvo, T. King, L. Yepiskoposyan & P. Andrews (Eds.), *Azokh Cave and the Transcaucasian Corridor* (pp. 191–210). Dordrecht: Springer.

Chaline, J. (1974). *Les proies des rapaces*. Paris: Doin éditeurs.

Feldehamer, G. A., Drickamer, L. C., Vessey, S. H., Meritt, J. F., & Krajewski, C. (2007). *Mammalogy: Adaptation, diversity, ecology* (643pp). John Hopkins University.

Felten, H., Helfricht, A., & Storch, G. (1973). Die Bestimmung der Europäischen Fledermausfaunen nach der distal epyphise des Humerus. *Senckenbergiana biologae, 54*, 291–297.

Fernández-Jalvo, Y., King, T., Andrews, P., Yepiskoposyan, L., Moloney, N., Murray, J., et al. (2010). The Azokh Cave complex: Middle Pleistocene to Holocene human occupation in the Caucasus. *Journal of Human Evolution, 58*, 103–109.

Horaček, I., Hanák, V., & Gaisler, J. (2000). Bats of the Palearctic region: A taxonomic and biogeographic review. In B. W. Woloszyn (Ed.), *Proceedings of the VIIIth European bat research symposium* (pp. 11–158).

Hutson, A. M., Aulagnier, S., & Nagy, Z. (2008). *Myotis dasycneme*. In IUCN 2010. IUCN Red List of Threatened Species. Version 2010.1. www.iucnredlist.org.

IUCN (2009). IUCN Red List of Threatened Species. Version 2010. www.iucnredlist.org.

Kowalski, K. (1995). Taphonomy of bats (Chiroptera). *Geobios, 18*, 251–256.

Krzanowski, A. (1973). Numerical comparison of Vesertilionidae and Rhinolophidae (Chiroptera: Mammalia) in the owl pellets. *Acta Zoologica Cracoviensia, 18*, 133–140.

Menu, H., & Popelard, J. B. (1987). Utilisation des charactères dentaires pour la détermination des vespertilioninés de l'ouest européen. *Le Rhinolophe, 4*, 1–88.

Menu, H., & Sigé, B. (1971). Nyctalodontie et myotodontie, importants caractères de grades évolutifs chez les Chiroptères entomophages. *Comptes Rendus de l'Academie des Sciences de Paris, 272,* 1735–1738. http://www.campester.org, http://www.eurobats.org.

Parfitt, S. (2016). Rodents, Lagomorphs and Insectivores from Azokh Cave. In Y. Fernández-Jalvo, T. King, L. Yepiskoposyan & P. Andrews (Eds.), *Azokh Cave and the Transcaucasian Corridor* (pp. 161–175). Dordrecht: Springer.

Postawa, T. (2004). Changes in bat fauna during the Middle and Late Holocene as exemplified by Thanatocoenoses dated with 14C AMS from Kralów-Czestochowa Upland caves, Poland. *Acta Chiropterologica, 6*, 269–292.

Rakhmatulina, I. K. (1989). The peculiarity of bat fauna of Azerbaijan. In *European bat research, 1987* (pp. 409–414). Praha: Charles University Press.

Rakhmatulina, I. K. (1995a). Zoogeography of bats in the Eastern Transcaucasia. *Myotis, 32–33*, 135–144.

Rakhmatulina, I. K. (1995b). Bats' attachment to different shelters in the Transcaucasia. *Myotis, 32–33*, 197–202.

Rakhmatulina, I. K. (1996a). On the history of study and tendency of changes of the Eastern Transcaucasian bat fauna. *Myotis, 34*, 59–70.

Rakhmatulina, I. K. (1996b). The bat fauna of the Caucasus and problems of its study. *Myotis, 34*, 51–57.

Rakhmatulina, I. K. (1998). Bat demography in main landscapes of Eastern Transcaucasia. *Myotis, 36*, 151–157.

Rossina, V. V. (2006). Bats as an Indicator of human activity in the Paleolithic, using the example of Denisova Cave, Northwestern Altai. *Paleontological Journal, 40*, 494–500.

Rossina, V. V., Baryshnikov, G. F., & Woloszyn, B. W. (2006). Dynamics of the Pleistocene bat fauna from the Matuzca Paleolithic site (Northern Caucasus, Russia) (Chiroptera). *Lynx, 37*, 229–240.

Sevilla, P. (1986). Identificación de los principales quirópteros ibéricos a partir de sus dientes aislados. Valor sistemático de los caracteres morfológicos y métricos dentarios. Doñana. *Acta Vertebrata., 13*, 111–130.

Sevilla, P. (1988). Estudio paleontológico de los Quirópteros del Cuaternario español. *Paleontologia i evolució, 22*, 113–233.

Sigé, B., & Legendre, S. (1983). L'Histoire des peuplements de chiroptères du bassin méditerranéen: l'apport comparé des remplissages karstiques et des dépôts fluvio-lacustres. *Mémoires de Biospéleologie, 10*, 209–225.

Zahn, A., Rodrigues, L., Rainho, A., & Palmeirim, J. M. (2007). Critical times of the year for *Myotis myotis*, a temperate zone bat: Roles of climate and food resources. *Acta Chiropterologica, 9*, 115–125.

Chapter 9
Amphibians and Squamate Reptiles from Azokh 1

Hugues-Alexandre Blain

Abstract The amphibian and squamate reptile fossil remains from the 2002 to 2009 excavation campaigns in Azokh 1 Cave (Nagorno-Karabakh region) are described. The fauna includes three anurans (*Pelobates* cf. *syriacus*, *Pseudepidalea viridis* sensu lato and Ranidae/Hylidae indet.), at least five lizards (Agamidae indet., *Pseudopus apodus*, *Lacerta* sp., *Ophisops elegans* and Lacertidae indet.) and seven snakes [*Eryx jaculus*, cf. *Coronella austriaca*, cf. *Elaphe* sp. (probably *E. sauromates*), cf. "*Coluber*" sp., "Colubrinae" indet., *Vipera* sp. [*V. berus* complex (probably *V. ursinii*)], *Vipera* sp. ("Oriental vipers" complex or *Daboia*)]. Of particular relevance is the occurrence of species that currently live at high altitude in the Caucasus, such as the representatives of the *V. berus* complex and the smooth snakes cf. *Coronella austriaca*. Azokh 1 represents the first fossil evidence for their presence in the Caucasian area at around 200 ka. The other taxa have greater similarities with the fossil and extant herpetofauna of the Irano-Turanian or Mediterranean biogeographical provinces. No Middle Asian desert taxon has been found. Through the Azokh 1 chronological sequence, the evolution of the paleoherpetofaunal assemblages suggest a progressive increase in aridity between Unit Vu (late Middle Pleistocene) and Units II and I (Upper Pleistocene to subrecent) and the replacement of a meadow-steppe by an arid mountain steppe environment.

Резюме Окаменевшие останки амфибий и чешуйчатых рептилий, обнаруженные в период раскопок 2002–2009 гг. в *пещере Азох 1*, относятся к эпохе среднего плейстоцена и исследуются впервые. Поскольку остеологическое описание различных видов амфибий и рептилий, живущих на Кавказе, все еще отсутствует, проведенная нами классификация носит предварительный характер. Тем не менее, мы надеемся, что данная статья поможет сформировать общее представление о богатстве этого региона начиная с эпохи среднего плейстоцена.

Рассматриваемые нами окаменевшие останки представляют собой расчлененные элементы, которые были обнаружены в результате просеивания отложений из пещеры *Азох 1*. Все образцы седимента были скринированы под напором воды с использованием металлических сеток с 10-, 5- и 0,5-мм ячейками и помещены в отдельные пакеты с обозначением координат раскопок. В последующем микроокаменелости были визуально рассортированы и классифицированы в большие таксоны. Остатки костей амфибий и чешуйчатых рептилий содержат около 800 элементов, представляющих по меньшей мере 14 таксонов, включая жаб, лягушек, агамовых, ящериц и различных змей. Материал распределен неравномерно между различными секциями пещеры *Азох 1:* подразделение *1* представляет 54% всех находок, верхние уровни подразделения *V* – 34%, подразделения *II* и *III* – менее 10% и средние горизонты подразделения *V* – только 0,7%.

Список представителей фауны в *Азох 1* включает три вида бесхвостых земноводных (*Pelobates* cf. *syriacus, Pseudepidalea viridis* sensu lato и *Ranidae/Hylidae indet.*), по меньшей мере 5 ящериц (*Agamidae indet., Pseudopus apodus, Lacerta* sp., *Ophisops elegans* и *Lacertidae indet.*) и 7 змей: *Eryx jaculus*, cf. *Coronella austriaca*, cf. *Elaphe* sp. (возможно, *E. sauromates*), cf. "*Coluber*" sp., "*Colubrinae*" indet., *Vipera* sp. [*V. berus* complex (возможно, *V. ursinii*)], *Vipera* sp. ("*Oriental vipers*" *complex* или *Daboia*)].

Главные выводы проведенного исследования:

1. Герпетофауна *Азох 1* состоит исключительно из сохранившихся до наших дней родов и видов, большинство из которых относится к теплолюбивым и сухоустойчивым формам (например, *Pelobates*

H.-A. Blain (✉)
IPHES, Institut Català de Paleoecologia Humana i Evolució Social, Zona Educacional 4, Campus Sescelades URV (Edifici W3), 43007 Tarragona, Spain
e-mail: hablain@iphes.cat
and
Àrea de Prehistòria, Universitat Rovira i Virgili (URV), Avinguda de Catalunya 35, 43002 Tarragona, Spain

Yolanda Fernández-Jalvo et al. (eds.), *Azokh Cave and the Transcaucasian Corridor*, Vertebrate Paleobiology and Paleoanthropology, DOI 10.1007/978-3-319-24924-7_9

syriacus, Agamidae, *Pseudopus apodus, Ophisops elegans, Eryx jaculus, Elaphe sauromates*, etc.).
2. Большинство таксонов характеризуется выраженной восточносредиземноморской или турано-средиземноморской биогеографией (например, *P. syriacus, P. apodus, O. elegans, E. sauromates*), в то время как некоторые другие формы имеют более широкую область распространения, включающую турано-средиземноморский регион (*P. viridis* и *E. jaculus*).
3. Заметным исключением является присутствие *C. austriaca* и представителей комплекса *V. berus*, имеющих европейское и сибирско-европейское происхождение. В *Азох 1* впервые найдены свидетельства их присутствия на территории Кавказа около 200 тыс. лет назад (подразделение *III* и верхние горизонты подразделения *V*).
4. С хронологической точки зрения, европейские и турано-средиземноморские виды присутствуют здесь по меньшей мере с эпохи среднего плейстоцена (верхние горизонты подразделения *V*), в то время как никаких характерных представителей среднеазиатских пустынь в *Азох 1* не обнаружено, поскольку не было выяснено происхождение мелких форм лацертидных и агамидных ящериц. Тем не менее, заслуживает внимания тот факт, что они появляются в подразделении *I* (т.е. недавно) и это может быть связано с тем, что аридный климат на территории Нагорного Карабаха появился после оледенения, что подтверждено палинологическими свидетельствами.
5. С палеоэкологической точки зрения, экология в верхних горизонтах подразделения *V* более всего соответствует степнолуговой, в то время как в подразделениях *III*, *II* и особенно в подразделении *I* она могла быть засушливой и похожей на сухие горные степи (в настоящее время встречающиеся на более низких уровнях, чем степнолуговые ландшафты). Климат в окрестностях пещеры, по-видимому, всегда был относительно теплый.

Keywords Amphibia • Squamata • Middle Pleistocene to Holocene • Nagorno-Karabakh • Southern Caucasus

Introduction

We describe here the amphibian and squamate reptile fossil remains coming from the 2002 to 2009 excavations campaigns of Azokh 1 Cave. Because osteological descriptions of many of the species of amphibians and reptiles living in the Caucasus are still not available, taxonomic attributions are tentative. However we hope that this paper will give an overview of the richness of this area since the late Middle Pleistocene.

The herpetofauna in the Northeastern part of the Armenian Plateau includes eight amphibian species. Most of these species are generally widespread (European marsh frog, *Pelophylax ridibundus*; brusa frog, *Rana macrocnemis*; European green toad, *Pseudepidalea viridis*; European tree frogs, *Hyla arborea shelkovnikovi*, and *H. savigni*), along with the Syrian spadefoot toad (*Pelobates syriacus*). Also this area is recognized too as having one of the most interesting reptile faunas with a total of 53 reptiles, many of which are both endemic and threatened (Ministry for Nature Protection 1999).

These high levels of diversity are supported by the complex relief and different altitudes producing a high diversity of ecosystems and microclimates, ranging from steppe on the Kura lowland through dense forests of oak, hornbeam and beech on the lower mountain slopes to birch and alpine meadows higher up. High biodiversity is also supported by the biogeographical position of Armenia, and its diversity is outstanding compared to other countries of the region. Many of the species that occur are at the edge of their range, or in disjunct populations, and they are therefore of particular interest for zoologists (Ministry for Nature Protection 1999).

Materials and Methods

The amphibian and squamate fossil remains used for this study consist of disarticulated elements collected by wet-screening the sediments obtained during the archaeological excavation of the site during the field campaigns of the years 2002–2009. All the sediment was wet-screened using superimposed 10, 5 and 0.5-mm-mesh screens and bagged by square, layer and excavation sub-levels. In subsequent years, the microfossils were processed, sorted and classed in broad categories. The amphibian and squamate bone remains include around 800 elements representing at least 14 taxa, including toads and frogs, agamid, lacertid and anguid lizards and several snakes (Table 9.1). The material is not homogeneously distributed between the different units of Azokh 1 cave: Unit I has 54% of the remains, Unit Vu 34%, Units II and III less than 10% and finally Unit Vm only 0.7%.

Dating by ESR shows that Unit Vm is approximately 300 ka and Unit Vu around 200 ka. There are no dates for Unit IV and III. Unit II has values between 185 ka near the bottom to about a 100 ka on top, in contact with Unit I (dated by Radiocarbon to 157 years BP) (see Appendix, radiocarbon).

Taxonomic nomenclature basically follows Speybroeck et al. (2010). The osteological nomenclature mainly follows Szyndlar (1984), Bailon (1991), Barahona and Barbadillo (1997), Sanchiz (1998), and Blain (2005). The distribution

Table 9.1 Distribution of amphibians and squamate reptiles remains from Azokh 1 by units

AZOKH 1	Unit I	Unit II	Unit III	Unit V-upper	Unit V-middle
Pelobates cf. *syriacus*		■			
Pseudepidalea viridis sensu lato	■	■		■	
Ranidae/Hylidae indet.				■	
Agamidae indet.	■				
Pseudopus apodus	■	■		■	
Lacerta sp.	■	■	■	■	■
Ophisops elegans	■	■			
Lacertidae indet.	■				
Eryx jaculus	■	■	■	■	■
cf. *Coronella austriaca*	■	■		■	
cf. *Elaphe* sp. (probably *E. sauromates*)	■	■		■	
cf. "*Coluber*" sp.	■	■	■	■	
"Colubrinae" indet.				■	
Vipera sp. (*V. berus* complex)	■		■		
Vipera sp. ("Oriental vipers" or *Daboia*)	■				

and habitat data mainly comes from Ananjeva et al. (2006), Ministry of Nature Protection (1999) and Williams et al. (2006). Measurements have been made with scaled drawings made under binocular with camera lucida.

Systematic Descriptions

Class Amphibia Gray, 1825
Order Anura Fischer von Waldheim, 1813
Family Pelobatidae Bonaparte, 1850
Genus *Pelobates* Wagler, 1830
Pelobates cf. *syriacus* Boettger, 1889 (Fig. 9.1a)

A single fused sacrum and urostyle assigned to *Pelobates* has been documented in Unit II from Azokh 1 cave. The sacrum possesses an anterior cotyle and the sacral diapophyses are antero-posteriorly spread, which is characteristic of the genera *Pelobates* and *Pelodytes*. According to its size (maximal width = 12.0 mm) this element is more consistent with *Pelobates* because all modern and fossil representatives of *Pelodytes* have a smaller size (Sanchiz 1998). Moreover, in our fossil, the incomplete urostyle is fused to the sacrum as in *Pelobates fuscus* and *Pelobates syriacus,* whereas in *Pelobates cultripes* and *Pelobates varaldi* these two elements are frequently dissociated (Bailon 1991, 1999; B. Sanchiz, personal communication). In addition, it differs from *P. fuscus*, which has the prezygapophyses generally more developed and circular (Böhme 1977; Bailon 1999; Blain and Villa 2006) whereas here the prezygapophyses are smaller and oval.

The Syrian spadefoot (*P. syriacus*) ranges from the Balkan Peninsula to Central Asia (Turkey, Israel, Lebanon, North of Syria and Iran), as well as in an area located between the

Black Sea and the Caspian Sea (Nöllert and Nöllert 2003). It is currently present in Armenia (Tadevosyan 2004–2009). It lives in steppe areas as well as in coastal sand dunes or agricultural regions. *P. syriacus* also frequents woodland and rocky areas. During its breeding period, it prefers generally clean and deep waters with sparse aquatic vegetation.

P. syriacus has been mentioned in the Middle to Late Pleistocene fossil record of Karain E (Turkey; S. Bailon personal communication) and in the Holocene-Middle Pleistocene of Israel and Greece (Sanchiz 1998; Martín and Sanchiz 2010). It is also known in Western and Central Europe from the Early Miocene to the Late Pleistocene (Sanchiz 1998; Martín and Sanchiz 2010) and in the Late Pliocene (MN15) of Southern Ukraine (Ratnikov 2001c; 2009).

Family Bufonidae Gray, 1825

Genus *Pseudepidalea* Laurenti, 1768 Frost, Grant, Faivovich, Bain, Haas, Haddad, De Sà, Channing, Wilkinson, Donnellan, Raxworthy, Campbell, Blotto, Moler, Drewes, Nussbaum, Lynch, Green & Wheeler, 2006

Pseudepidalea viridis sensu lato

The former large genus *Bufo* is now frequently divided into at least four genera (Frost et al. 2006): *Pseudepidalea* for *P. viridis* sensu lato, *P. raddei* and *P. brongersmai*; *Amietophrynus* for *A. mauritanicus* and *A. regularis*; *Epidalea* for *E. calamita* and *Bufo* sensu stricto for *B. bufo*, *B. gargarizans* and *B. verrucosissimus*. Note that *P. viridis* sensu lato is used here in the old sense, encompassing *P. balearicus*, *P. siculus*, *P. boulengeri*, *P. viridis* sensu stricto and *P. variabilis* (Stöck et al. 2006, 2008), because while molecular biology separates these species in the western part of the distribution area, the osteology of these newly created species and subspecies has not yet been distinguished.

The green toad is the best represented anuran in Azokh 1, with most of its skeleton preserved: squamosal, mandible, sacra, vertebrae, ilia, humeri, scapulae, radioulnae, tibiofibulae and phalanges (Fig. 9.1b–f). All fossil bones have the osteological characteristics of genera *Bufo*, *Pseudepidalea* and *Epidalea* (formerly *Bufo* sensu lato). We do not list these general characteristics in detail, for they may be found in other works. Detailed descriptions of species discussed below may be found in Böhme (1977), Sanchiz (1977), Hodrova (1986), Bailon (1991, 1999), Venczel and Sen (1994), Hossini (2001, 2002), Ratnikov (2001a), Blain (2005) and Delfino et al. (2009). Attribution of fossil material to *P. viridis* sensu lato is mainly based on the morphology of sacrum, scapula and ilium.

The sacrum (Fig. 9.1b) has an anterior cotyle and two posterior condyles. Sacral diapophyses are moderately antero-posteriorly spread, with the presence of a laterally opened fossa at the base of the diapophyses as in *P. viridis*, *P. raddei*, *A. mauritanicus*, *P. brongersmai* and *E. calamita,* whereas in *B. bufo*, *B. gargarizans* and *B. verrucosissimus* there is no (or lesser developed) fossa. According to Bailon (1999) this fossa opens more laterally in *P. viridis* than in *E. calamita*. This characteristic seems to be quite variable in *P. brongersmai* (Delfino et al. 2009).

The scapula is longer than wide, with a *processus glenoidalis* separated from the bone and clearly visible in dorsal view (Fig. 9.1f). The *pars acromialis* and the *processus glenoidalis* are robust with a sinuous concave anterior margin like *P. viridis* whereas in all other species but *B. verrucosissimus* it is convex. A shallow supraglenoidalis fossa is present as in *P. viridis*, *E. calamita*, *A. mauritanicus* and *A. regularis*.

The ilium lacks a dorsal crest (Fig. 9.1c, d), the superior tubercle is low and with a round and uni- or bi-lobated dorsal edge as in *P. viridis*, *P. raddei*, *A. regularis*, *P. brongersmai* and *A. mauritanicus,* whereas in *E. calamita* and *B. bufo* it is always unilobated. A well developed preacetabular fossa is present as in *P. viridis*, *A. mauritanicus*, *A. regularis*, *P. brongersmai* and *P. raddei*. Fossil ilia do not show any latero-ventral outgrowth ("calamita ridge") on the ilial shaft contrary to *E. calamita* and *P. raddei*. The *pars descendens* is poorly developed and does not have the markedly convex outline seen in *P. brongersmai* (Delfino et al. 2009) and *A. regularis* (Hossini 2001, 2002), where the angle between the *pars cylindriformis* and the *pars descendens* is close to 90°. *A. mauritanicus* generally reaches a larger size than the Azokh fossil material.

The green toad (*P. viridis* sensu lato) ranges in Central Europe, Central Asia, Arabia and the northernmost part of Africa. In Russia, the northern limit of its distribution area lies between the parallels 59° and 55° (Nöllert and Nöllert 2003; Stöck et al. 2006, 2008). *P. viridis* is reputed to be a typical steppe species not very sensitive to dryness, to warmth or to cold. It is found up to an altitude of 4,500 m. It is currently present in Armenia, including close to Azokh village (excavation team, personal communication).

P. viridis has been mentioned in numerous localities of the former U.S.S.R. since the Late Pliocene (MN16) (Ratnikov 2009): Early Pleistocene of Dmanisi (Georgia; M. Delfino in Lordkipanidze et al. 2007); Pleistocene or Holocene of Devichi Skaly and in the Holocene of Talgar (Azerbaijan; in Sanchiz 1998). It is also mentioned in the Pliocene of Çalta (Turkey; Rage and Sen 1976); the Middle Pleistocene of Emirkaya-2 (Turkey; Venczel and Sen 1994) and in the Middle to Late Pleistocene of Karain E (Turkey; S. Bailon, personal communication). *P. viridis* was the only anuran recorded in the earlier excavations at Azokh cave (Azykh in Sanchiz 1998). Most of the reliable finds of *P. viridis* in the Russian Platform are restricted to the Late Pleistocene-Holocene according to Ratnikov (1996, 2009), whereas in the Late Pliocene-Middle Pleistocene, *P. raddei* is

found persistently. In the Late Pliocene, the Mongolian toad seems to have occupied a vast area, including, besides its recent natural habitat, the southern Russian Platform, where it had persisted up to the Middle Pleistocene. The green toad has been present in Eastern Europe since the Late Miocene (Sanchiz 1998; Martín and Sanchiz 2010), while it appeared only recently in the Late Pleistocene in the Russian Platform, at the same time as the distribution area of the Mongolian toad reduced. This is in accordance with the presence of the green toad (*P. viridis*) in Azokh cave probably since the Unit Vu (with an age between 200 and 300 ka, see Appendix ESR, racemization) and the absence of *P. raddei*.

Family Hylidae Rafinesque, 1815
Family Ranidae Rafinesque-Schmaltz, 1814
Ranidae or Hylidae indet (Fig. 9.1g)

An unidentified frog is represented in the Unit Vu by a single maxilla. The maxilla is elongated and bears numerous teeth (unlike in all Bufonidae which are toothless), and although partially hidden by concretion the labial surface lacks dermal ornamentation (unlike genus *Pelobates*). Although incomplete, the *processus palatinus* does not seem to have been well developed (unlike genus *Discoglossus*). The lamina anterior is broken but is relatively low, and the presence of a well individualized frontal process is consistent with genera *Hyla*, *Rana* and *Pelophylax* (Bailon 1999).

Class Reptilia Laurenti, 1768
Order Squamata Oppel, 1811
Family Agamidae Spix, 1825
Agamidae indet (Fig. 9.2a–c)

Agamid lizards are represented in Azokh cave (Unit I) mainly by maxillae, dentaries and few caudal vertebrae. The fossil maxillae and dentaries, all incomplete, are characterized by an acrodont dentition fixed on the lingual surface and not strictly on the dorsal margin as in chameleons (Moody and Roček 1980). These acrodont teeth are laterally flattened and mostly have a triangular shape. The medial surface of the teeth is slightly convex. The teeth are more or less packed, with the posterior part overlapping the anterior part of the following tooth. Some fossils

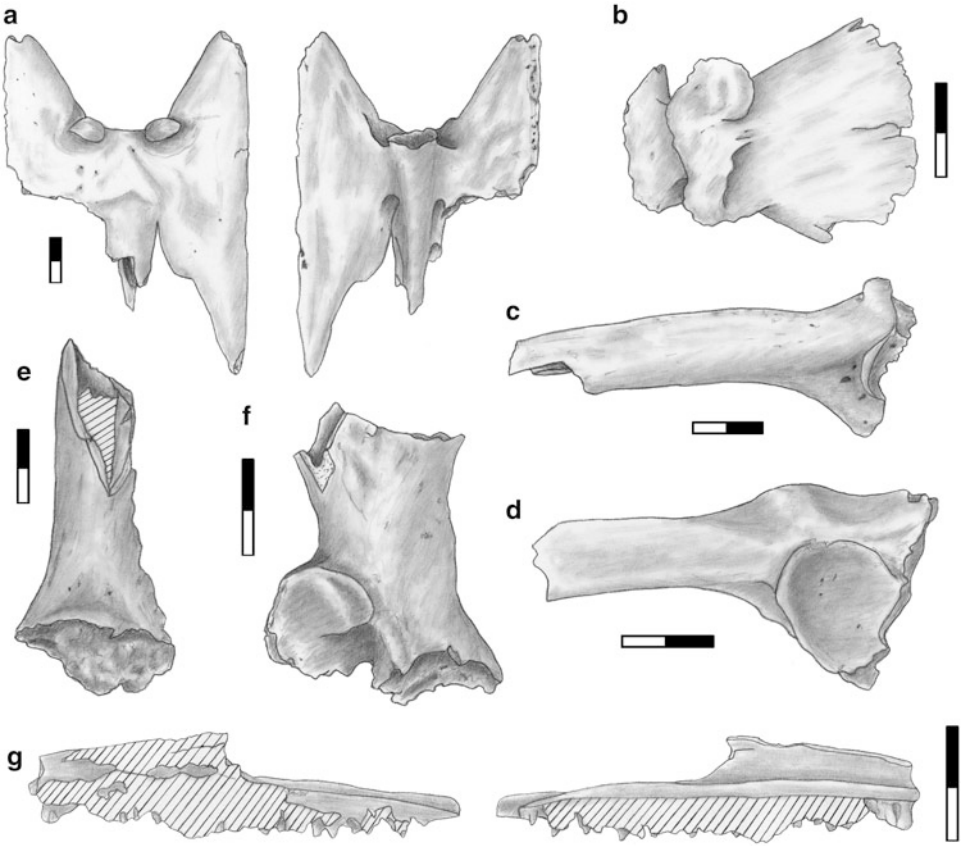

Fig. 9.1 **a** *Pelobates* sp., sacrum, dorsal and ventral views; **b–f** *Pseudepidalea viridis* sensu lato, **b** sacrum, dorsal view, **c** and **d** left ilium, lateral views, **e** left humerus of female, ventral view, **f** right scapula, dorsal view, **g** Ranidae/Hylidae indet., maxilla, labial and lingual views. All scales = 2 mm

have preserved the more anterior teeth or tooth positions (two in number) that are pleuroacrodonts, caniniforms and with a widened base. On one specimen (Fig. 9.2c) a third supplementary small pleurodont (but not caniniform) tooth is present posteriorly: it is probably a teratological character. Such a set of characteristics is typical of the family Agamidae in comparison with all other squamates (Moody 1980; Ananjeva 1981; Bailon 1991; Delfino et al. 2008).

The caudal vertebrae are elongated and show a centrum with a long haemal keel, narrow in its anterior half but posteriorly large. The neural spine is rather long, thin and low and is prolonged by an interzygapophyseal tip that does not reach the posterior limit of the postzygapophyses.

With the exception of the supplementary third pleurodont tooth on a dentary, the fossil material from Azokh 1 cave is most similar to the African-West Asian agamid clade Agaminae (sensu Macey et al. 2000; Group VI of Moody 1980; Maul et al. 2011) in possessing "only" two anterior pleuroacrodont caniniform teeth on the dentary. The tooth morphology of simple unicuspid crowns with a triangular labial and lingual profile and lacking significant longitudinal grooves or irregularities is derived in the same manner as in Agaminae.

Today, only genera *Laudakia*, *Trapelus* and *Phrynocephalus* are present in Northern Eurasia (Ananjeva et al. 2006), where they live in savannahs, steppes and deserts, with a way of life always linked with warm arid areas in rocky or sandy environments. According to Tadevosyan (2004–2009), only *Laudakia caucasia* and *Phrynocephalus persicus* are currently represented in Armenia.

In the Pleistocene fossil record of the Levant and Eastern Europe, agamid lizards have been mentioned in the Early Pleistocene of Ubeidiya (*Laudakia stellio*; Haas 1966, 1968) and in the Middle Pleistocene of Qesem cave (*Laudakia* sp.; Maul et al. 2011), both in Israel, in the Middle to Late Pleistocene of Karain E, Turkey (*Laudakia stellio*; S. Bailon, personal communication), and in the Late Pleistocene of Wezmeh cave, Iran (*Laudakia* sp.; Mashkour et al. 2009).

Family Anguidae Gray, 1825
Genus *Pseudopus* Merrem, 1820
Pseudopus apodus (Pallas, 1775) (Fig. 9.2d–h)

The glass lizard is represented in Units I, II and Vu mainly by maxillae, dentaries, vertebrae and by numerous osteoderms. Dentaries and maxillae (Fig. 9.2d, e) are incomplete but bear subpleurodont, monocuspid and cylindrical teeth with a bulbous apex. In the dentary, the anterior teeth are smaller and become progressively larger posteriorly. Large foramina are present on the labial side of the maxillae and dentaries.

Trunk vertebrae are procoelous, relatively strong, wider than long and dorsoventrally flattened. In ventral view, the centrum is triangular and flat, with lateral margins well defined, straight and anteriorly divergent. There is no precondylar constriction (unlike in Varanidae; e.g., Rage and Sen 1976; Bailon 1991), and the subcentral foramina are small and rarely visible. The postzygapophyseal articular surfaces are rectangular-shaped and elongated laterally. In dorsal view, the trunk vertebrae have a pronounced interzygapophyseal constriction. In lateral view, the neural spine is rather high on its posterior half. The condyle and cotyle are dorsoventrally flattened.

The caudal vertebrae are longer than wide. Hemapophyses are always fused to the posterior half of the centrum, and posteriorly the neural spine ends in a long tip. Transverse processes are dorsoventrally flattened, located under the prezygapophyses and oriented antero-ventrally.

The osteoderms are simple and have a dermal ornamentation of vermiculated type. Most of them correspond to mediodorsal osteoderms (bearing a longitudinal carina) whereas the laterodorsal and lateroventral osteoderms (that do not have carina) are fewer in number.

The fossil material from Azokh cave clearly pertains to a large anguid lizard whose tooth morphology is consistent with *Pseudopus*, differing from *Anguis* and *Dopasia,* which have caniniform curved teeth (e.g., Klembara 1979, 1981). A longitudinal carina on the mediodorsal osteoderms is present in genus *Dopasia* and *Pseudopus* but lacking in genus *Anguis* (Hoffstetter 1962). The centrum length of the trunk vertebrae, no greater than 5 mm, is consistent with an attribution to the current species *P. apodus,* whereas the extinct European species *P. pannonicus* from the Pliocene, and *P. laurillardi* from the Miocene, generally reach a larger size (up to 10 mm; see Blain 2005 and Klembara et al. 2010) and *Dopasia* and *Anguis* are smaller (less than 4 mm).

The only living representative of the genus, the glass lizard (*Pseudopus apodus*) is widely distributed from the Balkan Peninsula, Asia Minor and Middle East in the west, to Iraq and Iran in the east. In North Eurasia it occurs on the southern coast of the Crimea, on the coast of the Black Sea, in submontane Dagestan, eastern Chechnya, southern Kalmykia and the countries of Transcaucasia-Azerbaijan, Georgia and Armenia (Tadevosyan 2004–2009; Ananjeva et al. 2006). It is a species that lives in dry and bushy environments, sometimes in open woodlands but avoids dense forest areas (Matz and Weber 1983).

In the Russian Platform, fossil records of *P. apodus* have been mentioned in the Pliocene of South Ukraine and in the Late Pleistocene of Phatmai (near Baku) in Azerbaijan (Ratnikov 2009). In Turkey it has been mentioned in the Middle to Late Pleistocene of Karain E (S. Bailon, personal communication) and in the Middle Pleistocene of Emirkaya-2 (Venczel and Sen 1994), whereas *Pseudopus* sp. has been reported in the Late Pliocene of Çalta (Rage and Sen 1976). In Israel *Pseudopus* sp. is cited in the Middle Pleistocene of Qesem Cave (Maul et al. 2011). In Europe the

genus is known by *Pseudopus moguntinus* since the Late Oligocene whereas the extant species *P. apodus* is known since at least the Late Pliocene of Poland (Klembara 1981, 1986; Bailon 1991).

Family Lacertidae Oppel, 1811

In the fauna of North Eurasia lacertid lizards are currently represented by 54 species belonging to eight genera (Ananjeva et al. 2006). According to Tadevosyan

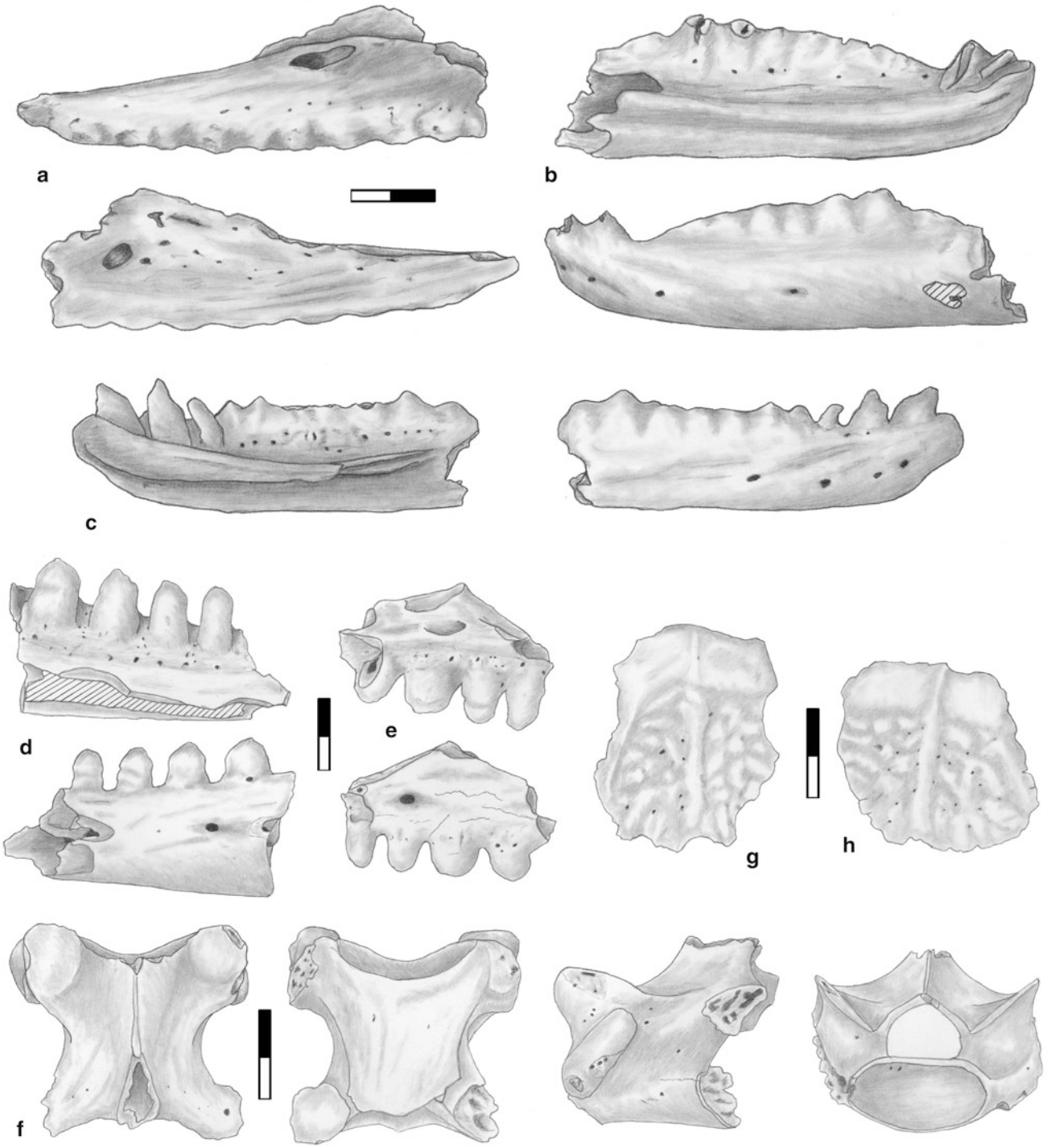

Fig. 9.2 **a–c** Indeterminate agamid lizard. **a** maxilla, lingual and labial views, **b** and **c** left and right dentaries, lingual and labial views. **d–h** *Pseudopus apodus*. **d** left dentary, lingual and labial views, **e** left maxilla, lingual and labial views, **f** trunk vertebra, dorsal, ventral, left lateral and anterior views, **g** and **h** medio-dorsal osteoderms, dorsal views. All scales = 2 mm

(2004–2009) such lizards are currently only represented in Armenia by four genera: *Darevskia*, *Eremias*, *Lacerta* and *Ophisops*. Among the Azokh fossil material, three different morphologies are present. In addition to genus *Ophisops*, the smaller one may be compared with those found in genus *Eremias* and *Podarcis* (osteological characteristics of *Darevskia* remain unknown) whereas the larger one is more consistent with genus *Lacerta*.

Genus *Lacerta* Linnaeus, 1758
Lacerta sp. (Fig. 9.3a–e)

Numerous bones pertain to juveniles or subadults of a rather large form in Units I to Vm: they are mainly composed by maxillae, dentaries, jugal, quadrate and vertebrae. The teeth on the maxillae and dentaries are large, packed, pleurodont and mainly bicuspids. The anterior edge of the maxilla ascends abruptly. A sculptured band extends along the upper edge of the bone (Fig. 9.3a), as in *Lacerta agilis* (Rauscher 1992; Ratnikov 2001b). The postfrontal is not fused with the postorbital and bears a reduced anteromedial process, expanded as it is in subadult and adult specimens of genera *Lacerta* and *Timon* (Barahona and Barbadillo 1997). The jugal has a well developed quadratojugal process and no evidence of a medial process on the palatal shelf. By its morphology, ornamentation on lingual side, and size, it fits well with genus *Lacerta* and differs from other smaller size genera like *Acanthodactylus*, *Podarcis* and *Psammodromus* (jugal of *Ophisops* still remains undescribed).

The trunk vertebrae are procoelous. The centrum is convex and shows on its ventral side a haemal keel more or less developed. The anterior margin of the neural arch has a deep emargination, and the neural crest is strongly extended backwards and upwards. Although often worn, a zygosphene-zygantrum articulation can be seen on most of the vertebrae. The condyle is large and the cotyle is rather deep.

The size and morphology of the bones are consistent with an attribution to genus *Lacerta* that corresponds in North Eurasia to large lizards with body lengths between 70 and 160 mm (Ananjeva et al. 2006). The fauna of North Eurasia contains four species: *Lacerta agilis*, *Lacerta media*, *Lacerta strigata* and *Lacerta viridis*. With the exception of *L. viridis* all are well represented today in Armenia (Tadevosyan 2004–2009). Fossil material from Azokh 1 cave is similar to material described by Ratnikov (2001b) and attributed to *Lacerta* cf. *agilis*; *L. viridis* being of larger size. The osteology of the other *Lacerta* species from Armenia is still unknown so that a more precise determination is not possible at present.

In the fossil record, attributions have been made at family level (Lacertidae indet.) in the Late Pliocene of Çalta, Turkey (Rage and Sen 1976), and in the Middle to Late Pleistocene of Karain E, Turkey (S. Bailon, personal communication); attributions at genus level have been made (*Lacerta* sp.) in the Middle Pleistocene of Emirkaya-2, Turkey (Venczel and Sen 1994). In the Russian Platform, *L. agilis* is known since the Miocene (MN5) and *L. viridis* since the Pliocene (MN16) (Ratnikov 2009). In Georgia, *Lacerta* ex. gr. *viridis* has been mentioned in the Early Pleistocene of Dmanisi (M. Delfino in Lordkipanidze et al. 2007). In Europe, *L. agilis* is known since the Early Pleistocene from Poland, Germany, Croatia and Serbia; and *L. viridis* since the Late Pliocene from Italy, Hungary, Poland, Croatia and Serbia (Holman 1998).

Genus *Ophisops* Ménétries, 1832
Ophisops elegans Ménétries, 1832 (Fig. 9.3f, g)

One dentary and two fused frontals are attributed to the snake-eyed lacertid (*O. elegans*) in Units I and II. The dentary is small-sized, elongated and rather slender and bears pleurodont and bicuspid teeth. Like the morphology in lacertids, the Meckelian groove is open on its whole length and the impression of the coronoid is present on the posterodorsal limit of the bone. The dentary has more projecting and slightly more slender and separated teeth than is present on fossil dentaries of the previous taxa (*Lacerta* sp.).

The frontals are fused together and show a strong medial constriction which is unique to the species *Ophisops elegans* (Rauscher 1992 and personal observations). The posterior edge has interdigitations visible on the ventral side that are not present on the comparative specimens we have examined at the Anatomie Comparée collections, Muséum national d'Histoire naturelle de Paris or in published illustrations (Rauscher 1992) of *O. elegans*.

O. elegans is widely distributed in the northeast of the Balkan Peninsula, some islands of the Aegean and Mediterranean Seas, Sinai Peninsula, Asia Minor, Middle East and the Caucasus to Pakistan and north-western India in the east. In North Eurasia it occurs in the Caucasus in Azerbaijan, Armenia and eastern Georgia, extending west approximately to the city Tbilisi (Ananjeva et al. 2006). *O. elegans* is a ground-dwelling species usually inhabiting open arid plains with sparse vegetation and rocky substrates.

The only fossil citation for the species has been made from the Early Pleistocene of Bad Deutsch-Altenburg (Austria) (Rauscher 1992; Böhme and Ilg 2003).

Lacertidae indet (Fig. 9.3h)

One vertebra is attributed to an indeterminate small-sized lizard recovered from Unit I. Unlike the trunk vertebrae

previously attributed to genus *Lacerta,* this vertebra is characterized by a low neural crest. The anterior emargination of the neural arch is rounded and the ventral keel is distinct, widened posteriorly and flattened. Although slightly worn, a zygosphene-zygantrum articulation is present. Such a vertebral morphology is commonly found (or as far as our current knowledge goes) in the genus *Eremias* (*E.* aff. *arguta* in Ratnikov 2002, Fig. 4) and *Podarcis* (e.g., Delfino 2002, Fig. 31). Since osteological descriptions of the lacertid genera from Asia Minor are still unknown, no more precise attribution is possible at present.

The genus *Eremias* (racerunners or desert lacertas) is widely distributed from south-eastern Europe and western Asia to Korea and north-eastern China. The diversity of this group of lizards in North Eurasia is very high; of approximately 25 known species, 20 occur in North Eurasia (Ananjeva et al. 2006). The genus *Podarcis* (wall lizards) are distributed mainly in the Mediterranean countries in the south of Europe. Of 15 known species, one is present in North Eurasia (*P. taurica*) (Ananjeva et al. 2006) and another one (*P. muralis*) is known in Northwestern Anatolia (Sindaco et al. 2000).

In the North Eurasian fossil record, *Podarcis taurica* has been mentioned in the Pliocene of the Crimean Peninsula, and *Eremias arguta* is known from the Pliocene in the Russian Platform (Ratnikov 2009).

Suborder Serpentes Linnaeus, 1758
Family Boidae Gray, 1825
Subfamily Erycinae Bonaparte, 1831
Genus *Eryx* Daudin, 1803
Eryx jaculus (Linnaeus, 1758) (Fig. 9.4)

The sand boa is represented by cervical, trunk and caudal vertebrae. The trunk vertebrae are small (maximal centrum length <5 mm). In dorsal view the vertebrae are wider than long and show a well marked interzygapophyseal constriction. The neural spine is relatively strong, and it is low and long. The zygosphene is wide and possesses a concave anterior margin. The articular surface of the prezygapophyses is well developed and more or less oval-shaped. The prezygapophyseal processes are short, ending in a blunt point. In ventral view, the centrum, is anteriorly wide, short and convex. The haemal keel is wide with lateral margins poorly marked. A small subcentral foramen is often present on each side of the haemal keel. In anterior view, the cotyle is slightly flattened dorso-ventrally. There is no evidence of paracotylar foramina. The prezygapophyses lie upward and the neural canal is wide and roughly trapezoidal-shaped. In lateral view, the vertebra is relatively short. The margo lateralis is well developed. The diapophyses are protruding and more developed than the parapophyses.

The cervical vertebrae have a rather similar morphology to those of the trunk vertebrae, being wide and short, but they are characterized by the presence of a small hypapophysis. In ventral view, the haemal keel is slender and well delimited laterally and ends in a short and relatively robust hypapophysis with a sigmoid ventral margin in lateral view.

The caudal vertebrae are characterized by the presence of secondary bony expansions with a degree of increasing complexity in posterior caudal vertebrae. The posterior caudal vertebrae (Fig. 9.4c) are complex, short and high with numerous bony expansions. The neural spine is high, strong and dorsally forked. In lateral view, on each lateral branch, the neural spine has an overhanging small anterior point. The pterapophyses topping the postzygapophyseal wings are well developed and separated. In anterior view, the pleurapophyses are long and oriented latero-ventrally. The neural canal has a more or less circular shape and the condyle and cotyle are small and laterally flattened. The more anterior caudal vertebrae have less developed bony expansions (Fig. 9.4b). They are less high and longer than the caudal vertebrae described previously (Fig. 9.4c). The neural spine is moderately high, strong and dorsally forked. In all the posterior caudal vertebrae, the postzygapophyseal wings are never fused anteriorly with the prezygapophyses.

Small sized trunk vertebrae, wider than long, characterize the Erycine snakes, in combination with low neural arches, a flattened haemal keel, wide and sometimes very diffuse, and caudal vertebrae with supplementary bony expansions (Hoffstetter and Rage 1972; Rage 1984; Bailon 1991; Szyndlar 1991a; Szyndlar and Schleich 1994; Delfino 2002).

The genus *Eryx* differs from other Erycinae in having trunk vertebrae with a long, slender and low neural spines, and caudal vertebrae with strong neural spines that are generally dorsally forked. In the genera *Bransateryx* (from the Late Oligocene and Early Miocene of Western Europe), *Albaneryx* (from the Miocene of France and Ukraine) and *Gongylophis* (living genus from the Indian Peninsula), the trunk vertebrae have a wider neural spine in dorsal view (Szyndlar 1991a). Moreover in *Gongylophis* the trunk vertebrae differ from *Eryx*, except for living *Eryx colubrinus* from Africa, by the presence of a distinct haemal keel (Szyndlar 1991a). In the genera *Charina* (living genus from North America known since the Early Miocene of California; Holman 2000), *Calabaria* (living genus from Western Africa) and *Bransateryx,* the neural spine of posterior caudal vertebrae is higher than in *Eryx* (except in extant *Eryx johni* from Southern Asia), and in *Gongylophis* the neural spine is relatively lower than in *Eryx* (Szyndlar 1991a).

Eryx jaculus is considered to be the most primitive among the living members of the genus based on its caudal osteology (Szyndlar and Schleich 1994). According to these

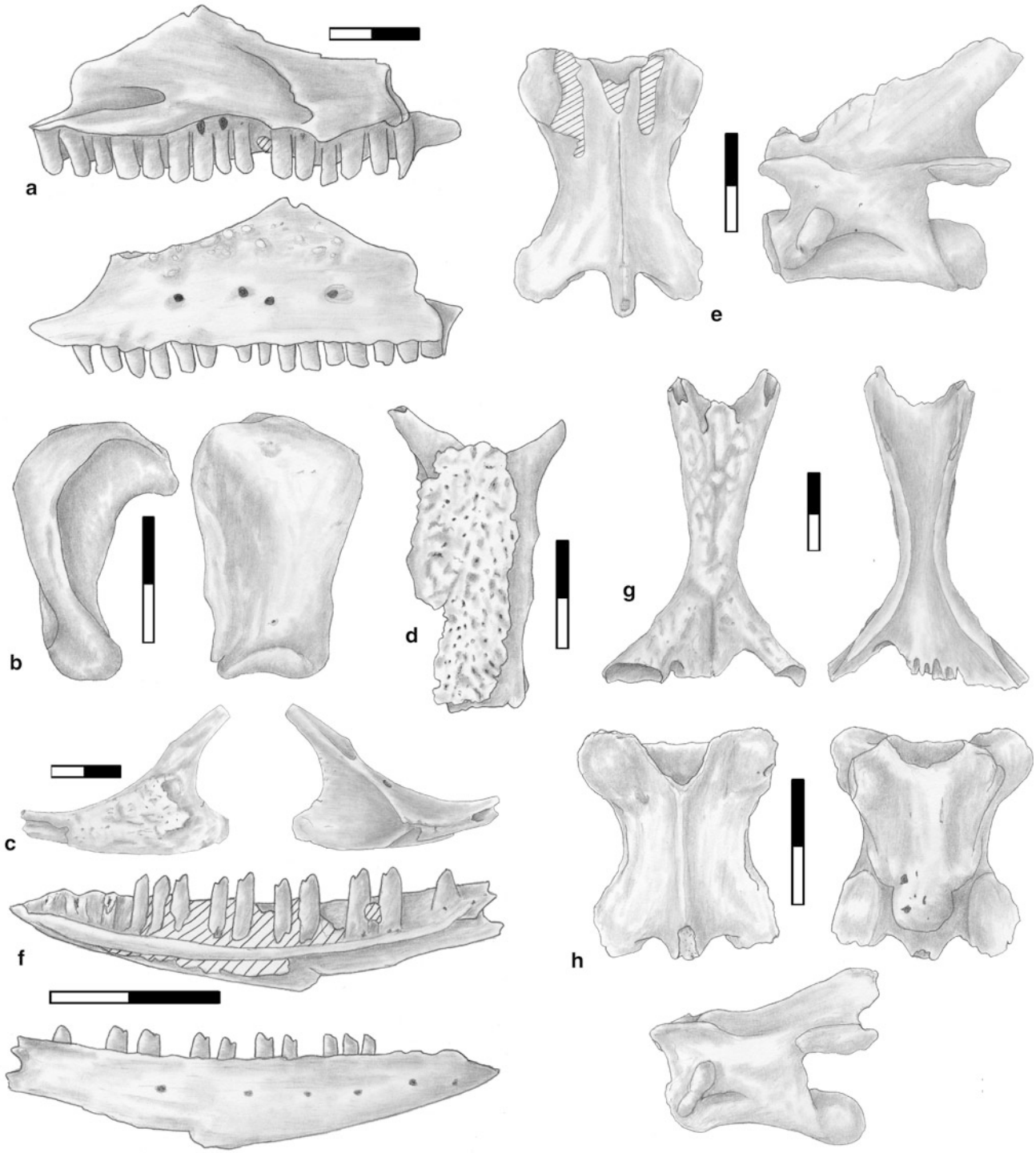

Fig. 9.3 **a–e** *Lacerta* sp. **a** left maxilla, lingual and labial views, **b** quadrate, medial and posterior views, **c** left jugal, lateral and medial views, **d** right postfrontal, dorso-lateral view, **e** vertebra, dorsal and lateral views. **f, g** *Ophisops elegans* **f** right dentary, lingual, labial and dorsal views, **g** frontal, dorsal and ventral views, **h** Lacertidae indet., vertebra, dorsal, ventral and lateral views. All scales = 2 mm

authors the most important feature differentiating *E. jaculus* from other living species is that in its posterior caudal vertebrae the postzygapophyseal wings are not fused anteriorly with the prezygapophyses. It differs from the fossil *Eryx primitivus* from the Middle/Late Pliocene of Spain (Szyndlar and Schleich 1994) by pterapophyses distinctly separated, postzygapophyseal wings in adults and longer pleurapophyses (Szyndlar and Schleich 1994). In conclusion the

Erycine fossil vertebrae from Azokh 1 cave clearly pertain to the living species *Eryx jaculus*.

Genus *Eryx* contains 10 species inhabiting south-eastern Europe, western and southern Asia from the Arabian Peninsula up to India and Pakistan, and northern Africa from Morocco up to Egypt. The fauna of North Eurasia contains six species (Ananjeva et al. 2006). According to Tadevosyan (2004–2009), only *Eryx jaculus* is currently present in Armenia, whereas *Eryx miliaris* has a northern distribution along the shore of the Caspian Sea (Ananjeva et al. 2006). The sand boa (*E. jaculus*) is distributed in northern Africa, in the north of the Arabian Peninsula, in Asia Minor, Syria, Iran, Iraq and Palestine. In southern Europe it is known from the Balkan Peninsula. In the Caucasus it is recorded in southern Armenia, eastern Georgia and Azerbaijan (Ananjeva et al. 2006). It is a fossorial animal that inhabits open dry steppes and semi-deserts. It prefers clayish and stony soils, and more rarely it is encountered on stabilized hillock sands, in vineyards and gardens. In the Caucasus it reaches altitudes from 1500 up to 1700 m above sea level along the river valleys. On the northern border of its distribution range in southern Russia it is recorded from the sheep's-fescue--sagebrush steppe. Habitats everywhere are associated with arid landscapes (Ananjeva et al. 2006; Bruno and Maugeri 1992).

In the fossil record, the extant species *E. jaculus* has been mentioned in the Late Miocene (MN13) of Salobreña, Spain (*E.* cf. *jaculus*; Szyndlar and Schleich 1994), the Late Miocene of Cava Monticino, Italy (*E.* cf. *jaculus*; Delfino 2002), the Late Pliocene (MN16) of Balaruc II, France (*E.* cf. *jaculus*; Bailon 1991; Szyndlar and Schleich 1994), the subrecent layers of Pili B, Greece (Szyndlar 1991a; Szyndlar and Schleich 1994), and in the Middle to Late Pleistocene of Karain E, Turkey (S. Bailon, personal communication). In the Eastern part of its distribution, records are known of genus *Eryx* since the Late Miocene in Ukraine and the Early to Middle Pliocene in Greece and Turkey (Rage and Sen 1976; Szyndlar and Schleich 1994).

Family Colubridae Oppel, 1811

Family Colubridae is a family of snakes distributed all over the world with high species diversity. There are more than 2000 recent species and about 300 genera of colubrids (Ananjeva et al. 2006). Colubrid snakes are represented by a wide variety of ecological forms, in particular by fossorial, arboreal, terrestrial and semi-aquatic species. In Eurasia they reach the Arctic Circle, and in the southern hemisphere their distribution range reaches the Cape of Good Hope in Africa (Ananjeva et al. 2006). In the fauna of North Eurasia there are currently 21 genera and 45 species (Ananjeva et al. 2006). As not all species currently present in the Caucasian area have been osteologically described, taxonomic attribution of fossils is made very tentatively. "Colubrinae" type differs from Elapidae, Viperidae and "natricines" by the absence of a hypapophysis on the trunk vertebrae. The "colubrines" are represented in Azokh Cave mainly by small-sized vertebrae with a centrum length smaller than 5 mm (Fig. 9.5).

Genus *Coronella* Laurenti, 1768

cf. *Coronella austriaca* Laurenti, 1768 (Fig. 9.5a)

The smooth snake is represented by trunk vertebrae in Units I, II and Vu. The genus *Coronella* is characterized by small-sized trunk vertebrae (centrum length is 2.61 ± 0.51 mm; min 1.71 mm; max 3.45 mm), with a strongly depressed neural arch, and very short prezygapophyseal processes (two to three times shorter than the prezygapophyseal facets). The haemal keel is usually weakly developed and, in dorsal view, the trunk vertebrae are strongly narrowed in the middle of the centrum length (Szyndlar 1984, 1991a). Moreover the precondylar constriction is generally well marked in genus *Coronella* unlike in juveniles of other larger colubrine snakes (Blain 2005). *C. austriaca* differs from *C. girondica* by the basal portion of prezygapophyses being more strongly built and the parapophyses longer than diapophyses (Szyndlar1984; Bailon 1991; Blain 2005). The fossil material from Azokh 1 differs from the morphologically close genus *Telescopus* by having the parapophyses well defined and not as long as the diapophyses, as it is the case in *Telescopus* (Szyndlar 1991a).

The distribution range of the smooth snake (*C. austriaca*) covers nearly all the territory of Europe, except for Ireland, a part of England and northern Scandinavia, as well as the central and southern parts of the Iberian Peninsula and the islands of the Mediterranean Sea (Ananjeva et al. 2006). It is found in deciduous, coniferous and mixed forests, usually preferring woodland edges warmed by the sun. In the Caucasus it is known in rocky mountainous-xerophytic steppe and stony slopes with bush vegetation. Smooth snakes penetrate into the meadow and subalpine zones of mountainous regions, up to elevations of 3000 m above sea level. In the eastern Transcaucasia, it is found as a rule at altitudes above 1100–1200 m above sea level (Ananjeva et al. 2006).

C. austriaca is reported in the fossil record in the Late Pliocene of Eastern Europe (Szyndlar 1991a) and the Early Pleistocene in South Ukraine and Russia (Ratnikov 2009). It appears that the fossils from Azokh may represent the south-easternmost record for this species, although they are

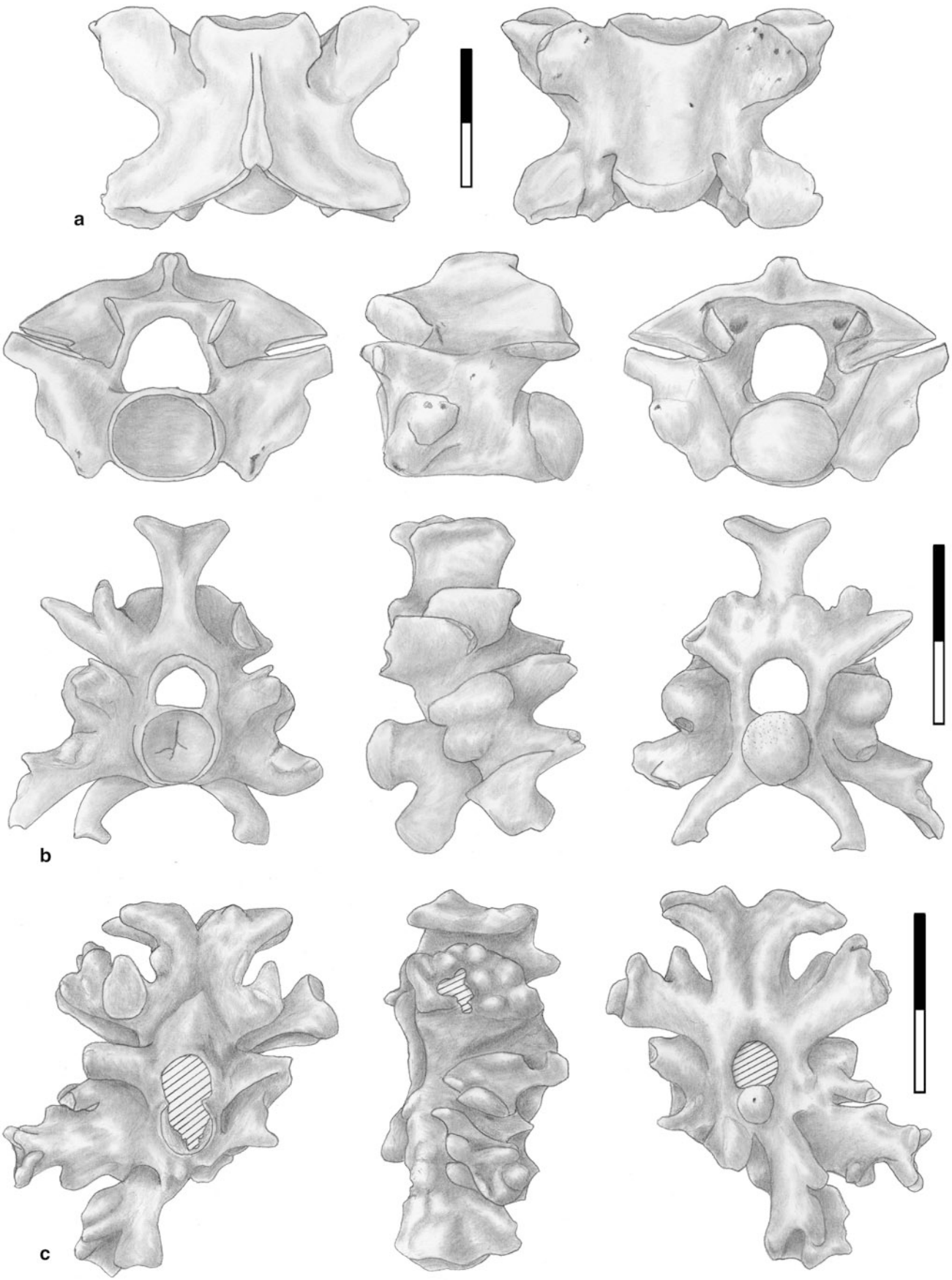

Fig. 9.4 **a–c** *Eryx jaculus*. **a** trunk vertebra, dorsal, ventral, anterior, left lateral and posterior views, **b** and **c** caudal vertebrae, anterior, right lateral and posterior views. All scales = 2 mm

within its present range: *C. austriaca* currently occurs in Armenia (Ananjeva et al. 2006; Tadevosyan 2004–2009).

Genus *Elaphe* Fitzinger in Wagler, 1833
cf. *Elaphe* sp. (probably *E. sauromates*) (Fig. 9.5b, c)

A probable ratsnake is represented by one cervical vertebra and a few trunk vertebrae in Units I, II and Vu. The incomplete cervical vertebra has the centrum preserved and part of the hypapophysis, whose base is orientated forward (Fig. 9.5b). *Elaphe quatuorlineata*, *E. sauromates* and *E. schrenckii* (unlike *E. longissima* and *E. situla*) are known to have the hypapophysis directed forward and not backward on cervical vertebrae (Szyndlar 1984, 1991a; Venczel and Sen 1994). *E. schrenckii* is currently distributed in the easternmost part of Northern Eurasia: northern and north-eastern China and Korea, eastern Mongolia and easternmost Russia (Ananjeva et al. 2006), and it can be excluded for biogeographical reasons. Until recently *Elaphe sauromates* was considered as one of the subspecies of the four-lined ratsnake *Elaphe quatuorlineata* (Ananjeva et al. 2006). Consequently because *E. quatuorlineata* is currently absent from Northern Eurasia and Near East region (Sindaco et al. 2000; Ananjeva et al. 2006), we assume that available osteological descriptions of this snake in this area refer very probably to the former eastern representatives of *E. quatuorlineata* now called *E. sauromates*. Because osteological descriptions of the cervical vertebrae of other Eurasian ratsnakes (like *E. persica*, *E. hohenackeri* and *E. dione*) are lacking, no more precise attribution of these fossils is possible.

The trunk vertebrae are small (centrum length = 4.08 ± 0.38 mm; min = 3.36 mm; max = 4.81 mm), with a vaulted neural arch and long (quite as long as the prezygapophyseal facets) and acute prezygapophyseal processes. The haemal keel is narrow and usually well developed. The centrum is long and triangular (centrum length/width is 1.34 ± 0.10; min 1.16 mm; max 1.50 mm). The interzygapophyseal constriction is well marked and half way along the length of the vertebra. In dorsal view, the zygosphene is concave with a small median tubercle. The paradiapophyses are large and project laterally.

In the literature the description of the trunk vertebrae of *E. quatuorlineata* varies slightly. According to Szyndlar (1991a), the trunk vertebrae are characterized by a strongly flattened haemal keel, a concave zygosphene and a very short prezygapophyseal process (half the length of the prezygapophyseal facets). However, according to Ratnikov (2004), a large and flattened haemal keel is only present on the anterior trunk vertebrae, whereas in middle- and posterior-trunk vertebrae the haemal keel is narrower, the zygosphene is concave or with a small median tubercle, and the prezygapophyseal processes are long and usually pointed. In a similar way, the fossils from Azokh 1 are concordant in size with living specimens of *E. quatuorlineata* (centrum length = 4.35 to 4.55 mm in Szyndlar 1984, 1991a; 4.4–6.2 mm in Ratnikov 2004) but differ from Szyndlar's measurements for their centrum length/width (1.12 ± 0.33; min 1.09 mm; max 1.16 mm). They are consistent with Ratnikov's measurements (min 1.23 mm; min 1.50 mm), and in accordance with the characters described by Ratnikov (2004), the fossil trunk vertebrae from Azokh 1 Cave may be the only representative of the genus *Elaphe* currently living in Armenia, *E. sauromates*.

The distribution range of the blotched snake (*E. sauromates*) covers eastern Europe: Bulgaria and Romania (to the east from Danube and Prut rivers), Moldova, the south of Ukraine, the steppes of the southern Russia and Ciscaucasia. In Asia *E. sauromates* is distributed in eastern Georgia, Armenia, Azerbaijan, the eastern part of Turkey, northwestern Iran, the extreme north-west of Turkmenistan and western Kazakhstan eastwards to the Aral Sea. It is normally found in arid landscapes, in steppes and semi-deserts, as well as in the forest-steppe zone (both on the plains and in the foothills), on areas of stony and sandy semi-desert, on the slopes with bush vegetation and with rocky outcrops, on forest edges, and in open steppe and tugai forests. In Transcaucasia it goes up to 2500 m above sea level (Ananjeva et al. 2006).

E. quatuorlineata (sensus lato) has been mentioned in the fossil record from the Early Pleistocene of Dmanisi, Georgia (cf. *E. quatuorlineata*; M. Delfino in Lordkipanidze et al. 2007) on the basis of a fragmented cervical vertebra (M. Delfino, personal communication). It is also recorded from the Middle Pleistocene of Emirkaya-2, Turkey, on the basis of a cervical and some trunk vertebrae (*E.* cf. *quatuorlineata*; Venczel and Sen 1994), and in Central and Eastern Europe it is known since the Late Pliocene (Szyndlar 1991a; Venczel and Várdai 2000; Delfino 2002).

cf. "*Coluber*" sp. (small-sized) (Fig. 9.5d)

A small colubrid snake is represented by various trunk vertebrae in Units I to Vu. The trunk vertebrae differ from the previous form (cf. *Elaphe* sp.) in being smaller (centrum length is 3.19 mm; min 2.59 mm; max 3.70 mm), a higher centrum length/width ratio (centrum length/width = 1.54 ± 0.18 mm; min 1.26 mm; max 1.88 mm) and prezygapophyseal processes directed more anteriorly. The anterior cotyle is more dorso-ventrally flattened and the posterior condyle is smaller. In dorsal view, the zygosphene is widened posteriorly. A smaller size together with a more elongated centrum is consistent with an attribution to a small colubrid from genera *Platyceps* or *Hemorrhois* (formerly forming part of the genus *Coluber* sensu lato together with *Hierophis*). In *Hierophis gemonensis*, the centrum length/width is smaller (from 1.29 to 1.50; Szyndlar 1991a).

Today, the Dahl's whip snake (or olive slender racer; *Platyceps najadum*), the coin-marked snake (or leaden colored racer; *Hemorrhois nummifer*) and the spotted whip snake (or

variegated racer; *Hemorrhois ravergieri*) are present in the Transcaucasian area (Ananjeva et al. 2006). They are eurytopic species which prefer xerophytic landscapes and are usually found on the open parts of stony semi-desert and steppe, among rocky outcrops and stones. Their habitats are the slopes of foothills and mountains covered with bush vegetation and woods. They range in altitude up to 2200–2300 m above sea level (Ananjeva et al. 2006).

In the fossil record, small-sized vertebrae have been described in the Middle Pleistocene of Emirkaya-2, Turkey (Venczel and Sen 1994) as *Coluber* sp. (i.e. *P. najadum*, *P. rubriceps* or *H. gemonensis*) and Colubrinae indet. (i.e. "several small members of the genus *Coluber* (e.g., *C. ravergieri*").

"Colubrinae" indet. (Fig. 9.5e)

Another "colubrinae" specimen, probably from a juvenile individual, is represented by two trunk vertebrae in Unit Vu. The trunk vertebrae are small (best preserved vertebra centrum length is 2.97 mm) but the centrum is elongated (centrum length/width is 1.33 mm). In ventral view, the haemal keel is thin along its length with lateral edges well defined. The prezygapophyseal processes, although broken, seem to have been relatively long and acute. In dorsal view, the zygosphene is straight with two small lobes. In posterior view, the dorsal margins of the highly vaulted neural arch are straight and form an angle around 100° as in the genus *Malpolon* (Bailon 1991). Nevertheless the poor preservation of these two vertebrae, as well as the fact that they probably pertain to a juvenile specimen, do not permit a clear assignation.

Family Viperidae Oppel, 1811
Genus *Vipera* Laurenti, 1768

The genus *Vipera* sensu lato unites about 30 species inhabiting northern Africa, Europe and Asia (Ananjeva et al. 2006). As stressed by Bailon et al. (2010) the systematics, taxonomy and phylogeny of Viperidae is controversial. Traditionally, paleontologists separate a number of groups within the genus *Vipera* (sensu lato) on the basis of morphological differences in trunk vertebrae (Szyndlar and Rage 1999; Bailon et al. 2010): (1) the "European vipers" including the *V. berus* and *V. aspis* complexes; (2) the "Oriental vipers" complex (except *Daboia*) and (3) *Daboia* consisting of the extant *D. russelii* and the fossil *D. maxima* from the Pliocene of Spain (Szyndlar 1988).

Vipera berus complex (probably *V. ursinii*)
[= Subgenus *Pelias* in Nilson and Andrén 1997] (Fig. 9.6a–c)

A small-sized viper is represented in Units I and III from Azokh 1 by some trunk and cervical vertebrae and a venom fang. The venom fang is a slender empty tube (preserved length 2.7 mm) with a narrow and elongated aperture at the apex that serves to discharge the venom. Only three families of snakes have a tubular venom fang: Atractaspididae, Elapidae and Viperidae (Jackson 2003). In the Elapidae (*Naja*) and Atractaspididae, the suture corresponding to the venom canal is visible on the anterior side of the fang at all stages of ontogeny (Jackson 2002). On the Azokh specimen, the canal is closed and there is no visible groove along the surface of the fang. In addition, the fang in Elapidae is hooked and possesses a strongly widened base (Kuch et al. 2006), but the Azokh specimen is poorly curved as in Viperidae. Venom fangs do not provide any taxonomic information within the family.

The trunk vertebrae show typical characters of Viperidae: presence of a straight hypapophysis, a posteriorly depressed neural arch, a ventrally convex cross section of the centrum with indistinct lateral margins, a large condyle and cotyle, and zygapophyseal articular surfaces inclined above the horizontal (Szyndlar 1984; 1991b). The elongation of the centrum, the flattened neural arch that bears a low neural spine and the acute morphology of the hypapophysis are more consistent with V. *berus* and *V. ursinii* whereas *V. aspis* and *V. seoanei* have a shorter elongation of the trunk vertebrae and distinctly relatively higher neural spines and stronger hypapophysis (Szyndlar 1984; Szyndlar and Rage 1999).

The cervical vertebrae are incomplete but show a hypapophysis that seems to be shorter than the centrum and slightly curved backward as in *V. aspis*, *V. seoanei*, *V. ursinii* and *V. berus*, whereas in *V. ammodytes* and *V. latastei* the hypapophysis of cervical vertebrae is longer and straight.

In conclusion, the fossil material from Azokh 1 cave resembles extant *V. berus* and *V. ursinii* and differs from *V. latastei*, *V. seoanei* and *V. ammodytes*. Because there are no caudal vertebrae, distinction between *V. berus* and *V. ursinii* cannot be made, although *V. ursinii* is much smaller than *V. berus*. According to their size the fossils from Azokh 1 cave are more consistent with the *V. ursinii* represented in Armenia by *V.* (*Pelias*) *eriwanensis*; nevertheless attribution is carefully made at level of *V. berus* complex only.

V. berus inhabits large parts of Europe and Asia and is distributed in Europe between 68° N and 45° N (Ananjeva et al. 2006) i.e. further north than Armenia (41–39° N). On the other hand, the range of *V. ursinii* is in the southeastern regions of Europe, in central Italy, south-eastern France, Austria, the countries of the Balkan Peninsula, Romania, Hungary and Moldova. Both species have in common that they are cold-adapted or mountainous vipers. Today only *V. darevskii* and *V. eriwanensis* live in Armenian mountainous area (Tadevosyan 2004–2009). Until the osteology

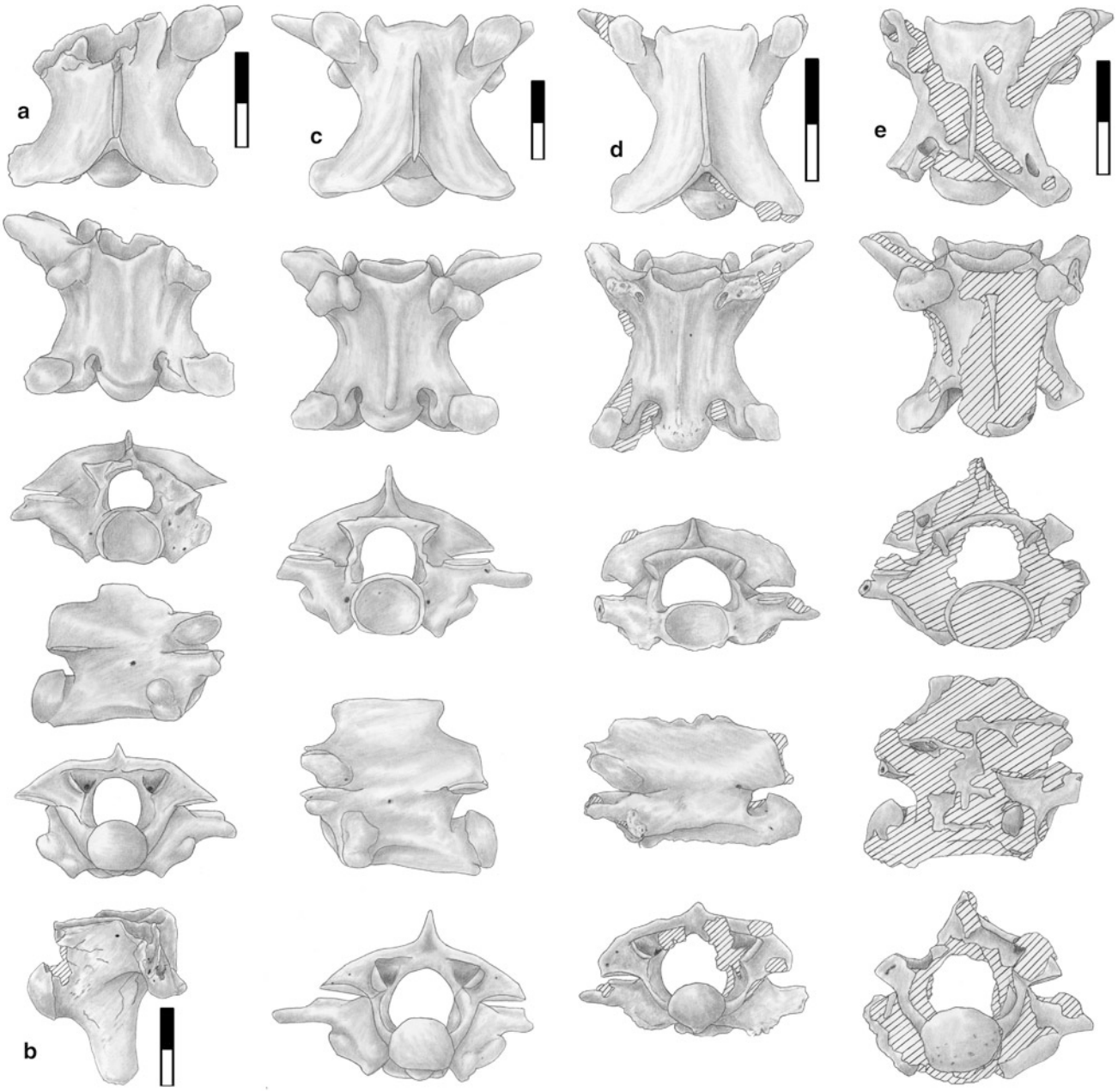

Fig. 9.5 **a** cf. *Coronella austriaca*, trunk vertebra, dorsal, ventral, anterior, right lateral and posterior views. **b, c** cf. *Elaphe* sp. (probably *E. sauromates*), **b** cervical vertebra, right lateral view, **c** trunk vertebra, dorsal, ventral, anterior, left lateral and posterior views. **d** cf. "*Coluber*" sp., trunk vertebra, dorsal, ventral, anterior, left lateral and posterior views. **e** "Colubrinae" indet., trunk vertebra, dorsal, ventral, anterior, right lateral and posterior views. All scales = 2 mm

and systematic affinities of these two species, as well as other Caucasian-Russian small vipers (*V. kaznakovi, V. dinniki, V. lotievi, V. magnifica, V. nickolskii* and *V. orlovi*), are better known, no more precise attribution of the fossils can be made.

Extant small-sized *Vipera* from Armenia are considered to be mountain snakes (Ananjeva et al. 2006). The Darevsky's viper (*V. darevskii*) is a high-mountain snake that inhabits rocky screes and steep (35–45°) detrital slopes with extensive large-sized volcanic rocks. It is found in restricted areas in northern Shirak province in Armenia. This population is known in the subalpine and alpine meadows of Legli Mountain at an altitude 2600–3000 m above sea level on the Armenian-Georgian border. The Erivanian meadow viper (*V. eriwanensis*, formerly considered as a subspecies of *V. ursinii*; Sindaco et al. 2000) is found in the Kars and

Erzurum Provinces in north-eastern Turkey and mountain-steppe regions of Armenia at an altitude of 1000–2200 m above sea level. It is a mountain-steppe species that inhabits dry slopes of mountains, rocky mountain-steppes, and banks of canyons overgrown with bush vegetation. It grows up to 50 cm in length.

In the fossil record, the *V. berus* complex is known since at least the Late Miocene of Central and Eastern Europe (Szyndlar 1991b). In the Russian Platform, *V. berus* is known since the Early Pleistocene and *V. ursinii* since the Late Pliocene (MN16) (Ratnikov 2009). Until now, no small viper has been mentioned in the fossil record of the Transcaucasian region, and consequently the remains from the Unit III (dated around 200 ka) of Azokh 1 are very interesting and may represent the first evidence of the presence of the *V. berus* complex (probably *V. ursinii*) in the Caucasian area.

Vipera sp. ("Oriental vipers" complex or *Daboia*) (Fig. 9.6d)

Two fragments of vertebrae from Unit I are larger in size consistent with an attribution to the "Oriental vipers" complex and genus *Daboia*. Because of the incompleteness of Azokh fossils (in particular the development of the neural spine can not be judged) no more precise attribution can be made.

Currently in Armenia two large-sized vipers are known: the Armenian viper (*Vipera raddei*) and the blunt-nosed viper (*Vipera lebetina*) (Tadevosyan 2004–2009). The blunt-nosed viper, which may reach up to 2 m in length, is found in the diverse desert and mountain-steppe biotopes. It typically inhabits slopes with abundant rocky outcrops, boulders and scree, sparsely covered with xerophilous trees and scrub, as well as rocky semi-deserts, orchards and vineyards. In Armenia on the mountain Dorakh in the

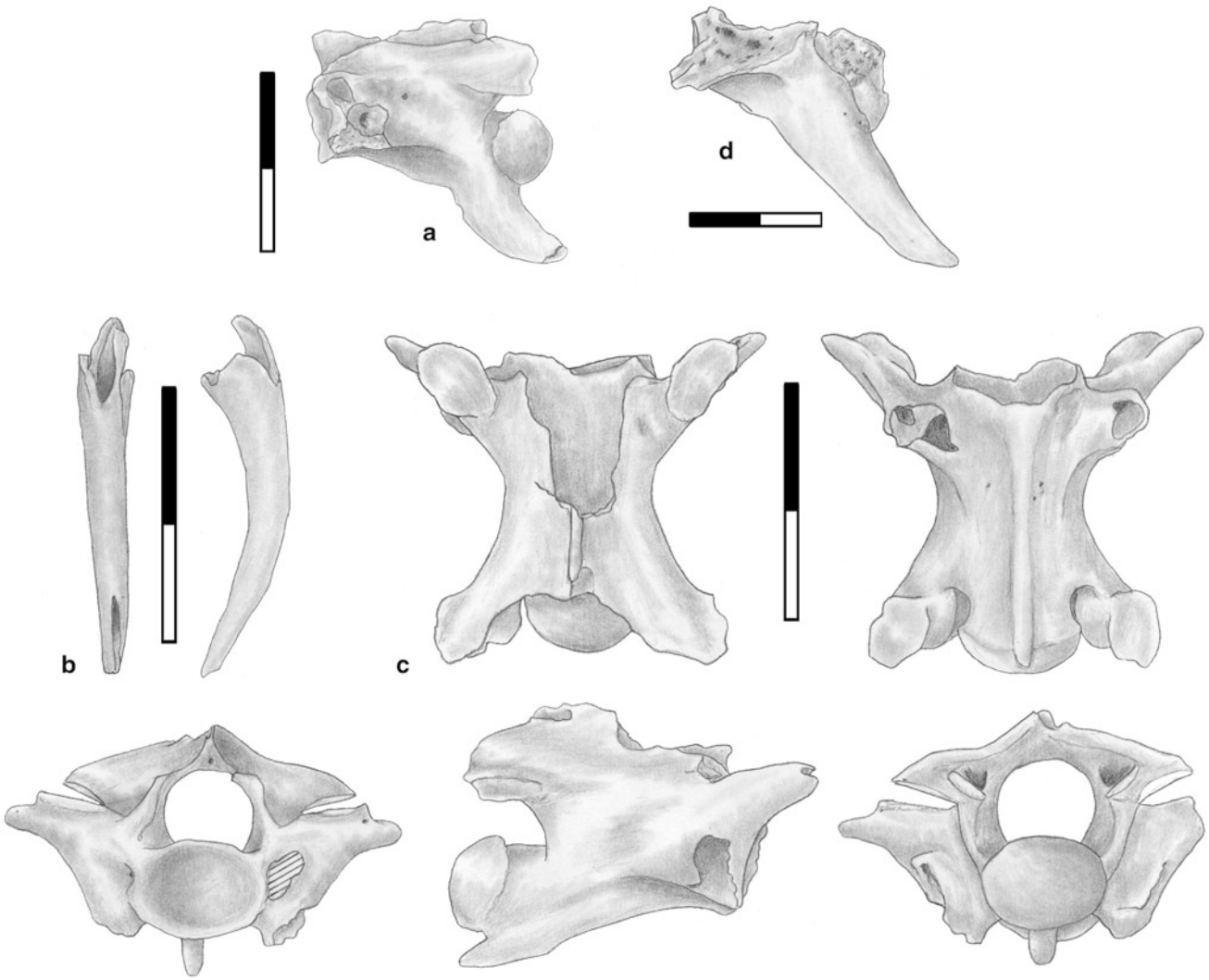

Fig. 9.6 **a**–**c** *Vipera* sp. [*V. berus* complex (probably *V. ursinii*)], **a** cervical vertebra, lateral view, **b** venom fang, anterior and lateral views and **c** trunk vertebra, dorsal, ventral, anterior, right lateral and posterior views. **d** *Vipera* sp. ("Oriental vipers" complex or *Daboia*), cervical vertebra, lateral view. All scales = 2 mm

Khosrovsky reservation, and in Turkmenistan on the mountain Dushack in the central Kopetdag, blunt-nosed vipers are found at the altitude up to 2000 m above sea level. On the Pamir, at the altitude 2500 m above sea level, populations from even higher mountains are known (Ananjeva et al. 2006). The Armenian viper, which can be over 1 m in length, occurs at the altitude 1000–2700 m above sea level in mountain-xerophytic vegetation, in particular oak forests, in the juniper open woodlands, on the rocky slopes of the mountains with sparse bush vegetation, and in the mountain steppes. The type of biotope distribution on the southern spurs of the mountain ranges of the Lesser Caucasus corresponds to the mosaic availability of suitable biotopes (Ananjeva et al. 2006).

In the Miocene, "Oriental vipers" were widely distributed in the entire southern half of Europe and survived until the end of the Pliocene in the Mediterranean area and in Eastern Europe until at least the Middle Pleistocene (Szyndlar 1991b). In Asia Minor *Vipera lebetina* is known in the Middle to Late Pleistocene of Karain E, Turkey (S. Bailon, personal communication) and in the Late Pleistocene from Wezmeh Cave, Iran (Mashkour et al. 2009). An "Oriental viper" (*Vipera* sp.) has been mentioned too in the Middle Pleistocene of Emirkaya-2, Turkey (Venczel and Sen 1994).

Paleobiogeographical Data

Some Palearctic regions were particularly important as corridors for invasions. Trans-Caucasia was repeatedly affected by fauna and flora exchanges because it is situated at the interface of the European, Asian and African biomes from where it experienced repeated invasions since the Late Oligocene (Veith et al. 2003). According to Sindaco et al. (2000), this area is currently characterized by a high number of endemic reptile taxa bearing an "Armenian" pattern of distribution, which usually includes species inhabiting mountains or plateaux and usually adapted to steppe or rocky habitats. Excluding these endemic species, three chorotypes are dominant: the Southwestern-Asiatic, the Eastern-Mediterranean and the Turano-Mediterranean.

According to ecologists and biologists (Ministry of Nature Protection 1999), a series of climatic modifications have played an important role in determining the current landscapes, ecosystems and biodiversity of the Caucasus region. During the Late Pliocene and Pleistocene, a series of glaciations occurred which affected the existing ecosystems, resulting in reductions in primary subtropical forests, and growth in secondary habitats typical of the temperate zone. During cold phases, reptiles of European origin, such as the meadow viper (*Vipera ursinii*), grass snake (*Natrix natrix*), sand lizard (*Lacerta agilis*), and meadow lizard (*L. praticola*) migrated into the Armenian Plateau. During temperate or warm phases, the flora and fauna became dominated by taxa adapted to xerophilous conditions (probably with an Eastern-Mediterranean origin), as more arid-zone habitats emerged. A number of reptiles may also have reached the Armenian Plateau from the Middle Asian deserts, including the race runner (*Eremias arguta*), pond turtle (*Mauremys caspica*), and toadhead agama (*Phrynocephalus persicus*).

Most of the taxa represented in Azokh 1 have clear Eastern-Mediterranean or Turano-Mediterranean affinities (like *P. syriacus*, *P. apodus*, *O. elegans*, *E. sauromates*), whereas some others have a wider distribution area but always including in the Turano-Mediterranean area (*P. viridis* and *E. jaculus*). As an exception *C. austriaca* and the representatives of the *V. berus* complex have a more European or Sibero-European distribution and may constitute a special case for the Caucasian area which served as a refuge during the Pleistocene coldest periods.

European and Turano-Mediterranean species have been present at least since the Middle Pleistocene (Unit III). Only Mediterranean amphibians and reptiles are represented in the Early Pleistocene of Dmanisi, Georgia (Delfino in Lordkipanidze et al. 2007) and some Sibero-European taxon (*Lacerta* cf. *agilis* and *Natrix* cf. *natrix*) have been mentioned during or before the Pliocene in the South of the Russian Platform (Ratnikov 2009). On the contrary no clear Middle Asian desert taxa have been found in Azokh 1, but this may be partly the result of the lack of evidence for the systematic position of the small lacertid and agamid lizards, which does not allow us to see if any of the lizards had middle Asian affinities. Nevertheless, it is noteworthy that they only appear in Unit I (i.e. very recently), which may be due to the fact that more arid-zone habitats only emerged after glaciation.

Paleoclimatological and Paleoenvironmental Inferences

Before completing a quantitative reconstruction of the environment, the origin of the small vertebrate accumulation (i.e. taphonomy) must be understood. During the systematic descriptions, strong evidence of digestion has been seen, in particular on some trunk vertebrae of erycine snake, suggesting predation by a small carnivore. However some preliminary remarks can be made.

The herpetofauna of Azokh 1 is composed exclusively of extant genera and species, the majority of them belonging to thermophilous and xerophilous forms (e.g., *Pelobates syriacus*, Agamidae, *Pseudopus apodus*, *Ophisops elegans*, *Eryx jaculus*, *Elaphe sauromates*, etc.). The anuran *Pseudepidalea*

viridis is a form with a wide ecological tolerance. Many of the taxa of Azokh 1 may frequent open wooded or bushy areas. Moreover high mountainous taxa are well represented, with the presence of a representative of the *V. berus* complex (probably *V. ursinii*) and the small colubrine *Coronella austriaca*. There are two high altitude mountains (around 2000–2500 m) within 6–10 km of Azokh, but the site itself is at less than 1000 m and the surrounding mountains barely reach 1500 m (P. Andrews 2010, personal communication). Through the sequence, the faunas from Units I to II appear to represent the driest period with the exclusive presence of agamid lizards and *P. syriacus*, whereas the unit Vu fauna seems to indicate "moister" conditions due to the presence of a larger number of *C. austriaca* remains. Moreover in the Unit Vu fauna, there are no species present that avoid forest environments, such as *P. syriacus* and the small vipers. So the environment in Unit Vu seems to be more consistent with a meadow-steppe whereas in Units III, II and particularly Unit I, the environment seems to have been more xeric corresponding to an arid mountain steppe (now occurring at lower elevations than meadow-steppes). Here is a case that demonstrates that need to understand the taphonomy, for if the herpetofauna represents mountain steppe, it must have been transported from considerable distances and it needs to be shown how it reached the cave. The small mammal fauna shows a similar range of ecological adaptations, but it has been shown to have been transported to the cave by predatory birds, which can easily travel these distances (Andrews et al. 2016). The climate seems to have been always relatively warm-temperate.

Conclusions

1. The amphibian and squamate reptile fossil fauna from the 2002–2009 excavations of Azokh 1 is composed of 14 taxa made up of three anurans (*Pelobates* cf. *syriacus*, *Pseudepidalea viridis* and Ranidae/Hylidae indet.), at least fave lizards (Agamidae indet., *Pseudopus apodus*, *Lacerta* sp., *Ophisops elegans* and Lacertidae indet.) and seven snakes [*Eryx jaculus*, cf. *Coronella austriaca*, cf. *Elaphe* sp. (probably *E. sauromates*), cf. "*Coluber*" sp., "Colubrinae" indet., *Vipera* sp. [*V. berus* complex (probably *V. ursinii*)], *Vipera* sp. ("Oriental vipers" complex or *Daboia*)].
2. The herpetofauna of Azokh 1 cave is composed exclusively of extant genera and species, the majority of them belonging to thermophilous and xeric- adapted forms.
3. Most of the taxa have clear Eastern-Mediterranean or Turano-Mediterranean affinities, whereas some others have a larger distribution area but always including in the Turano-Mediterranean region.
4. A notable exception is the presence of *C. austriaca* and the representatives of the *V. berus* complex that have European or Sibero-European affinities. Azokh 1 represents the first fossil evidence for their presence in the Caucasian area at around 200 ka (Units III and V-upper).
5. From a chronological point of view, European and Turano-Mediterranean species are present at least since the Middle Pleistocene (Unit Vu) whereas no clear Middle Asian desert taxon has been found in Pleistocene levels at Azokh 1 (since the small lacertids and agamid lizard systematic affinities have yet to be elucidated). They only appear in Holocene deposits of Unit I (i.e. very recently), and this may be due to the fact that more arid-zone habitats emerged in the Armenian Plateau after the last glaciation.
6. From a paleoenvironmental point of view, the environment at the time of Unit Vu is consistent with a meadow-steppe environment, whereas in Unit III, II and particularly in Unit I, the environment may have been more xeric corresponding to an arid mountain steppe (now occurring at lower elevations that meadow-steppe). The climate seems always to have been relatively warm-temperate.

Acknowledgements We are deeply grateful to Dr. Prof. Vyacheslav Yu. Ratnikov (State University of Voronezh, Russia), Dr. Prof. Zbigniew Szyndlar (Institute of Systematics and Evolution ofAnimals of the Polish Academy of Sciences, Krakow, Poland), Dr. Salvador Bailon (MNHN, Paris, France), Dr. Massimo Delfino (University of Turin, Italy), Dr. Jean-Claude Rage (MNHN, Paris, France), Dr. Marton Venczel (Museul Tárii Crisurilor, Oradea, Romania), Dr. Borja Sanchiz (MNCN, Madrid, Spain), Dr. Yolanda Fernández-Jalvo (MNCN, Madrid, Spain) and to Dr. Peter Andrews (The Natural History Museum, London, UK) for providing us bibliography and/or unpublished information. Dr. José Enrique González and Dr. Salvador Bailon permitted us to consult the osteological material for comparison respectively from the Amphibians and Reptiles collections of the *Museo Nacional de Ciencias Naturales* in Madrid and from the Anatomie Comparée collections of the *Muséum national d'Histoire naturelle* in Paris. We want to thank Dr. Prof. Paloma Sevilla (Universidad Complutense de Madrid, Spain), Lena Asryan and Sandra Bañuls (IPHES, Tarragona, Spain) for continuous encouragement and pleasant discussions on Azokh localities and Armenia. Dr. Marton Venczel, Dr. Prof. Zbigniew Szyndlar and Dr. Salvador Bailon as well as two of the editors Dr. Yolanda Fernández-Jalvo and Dr. Peter Andrews improved this manuscript by their comments.

References

Ananjeva, N. B. (1981). Structural characteristics of skull, dentition and hyoid of lizards of the genus *Agama* from the fauna of the USSR. In *Academy of Sciences of the USSR, Proceedings of the Zoological Institute, 101*, 3–20. [in Russian].

Ananjeva, N. B., Orlov, N. L., Khalikov, R. G., Darevsky, I. S., Ryabov, S. A., & Barabanov, A. V. (2006). *The Reptiles of Northern Eurasia, taxonomic diversity, distribution, conservation status*. Zoological Institute, Russian Academy of Sciences. Pensoft Series Faunistica (Vol. 47, p. 245). Sofia, Bulgaria: Pensoft Publishers.

Andrews, P., Hixson-Andrews, S., King, T., Fernandez-Jalvo, Y., & Nieto-Díaz, M. (2016). Paleoecology of Azokh 1. In Y. Fernández-Jalvo, T. King, L. Yepiskoposyan & P. Andrews (Eds.), *Azokh Cave and the Transcaucasian Corridor* (pp. 305–320). Dordrecht: Springer.

Appendix: Fernández-Jalvo, Y., Ditchfield, P., Grün, R., Lees, W., Aubert, M., Torres, T., et al. (2016). Dating methods applied to Azokh cave sites. In Y. Fernández-Jalvo, T. King, L. Yepiskoposyan & P. Andrews (Eds.), *Azokh Cave and the Transcaucasian Corridor* (pp. 321–339). Dordrecht: Springer.

Bailon, S. (1991). Amphibiens et reptiles du Pliocène et du Quaternaire de France et d'Espagne: mise en place et évolution des faunes. PhD dissertation, Université de Paris VII, pp. 499, 89 pls.

Bailon, S. (1999). Différenciation ostéologique des Anoures (Amphibia, Anura) de France. In J. Desse & N. Desse-Berset (Eds.), *Fiches d'ostéologie animale pour l'archéologie, Série C: varia* (p. 38). Centre de Recherches Archéologiques-CNRS: Valbonne.

Bailon, S., Bover, P., Quintana, J., & Alcover, J. A. (2010). First fossil record of *Vipera* Laurenti 1768 "Oriental vipers complex" (Serpentes: Viperidae) from the Early Pliocene of the western Mediterranean islands. *Comptes Rendus Palevol, 9*, 147–154.

Barahona, F., & Barbadillo, L. J. (1997). Identification of some Iberian lacertids using skull characters. *Revista Española de Herpetología, 11*, 47–62.

Blain, H.-A. (2005). Contribution de la paléoherpétofaune (Amphibia & Squamata) à la connaissance de l'évolution du climat et du paysage du Pliocène supérieur au Pléistocène moyen d'Espagne. PhD dissertation, Muséum national d'Histoire naturelle, Département de Préhistoire, pp. 402, 67 pls.

Blain, H.-A., & Villa, P. (2006). Amphibians and squamate reptiles from the early Upper Pleistocene of Bois Roche Cave (Charente, southwestern France). *Acta Zoologica Cracoviensia, 49A*, 1–32.

Böhme, G. (1977). Zur Bestimmung quartärer Anuren Europas an Hand von Skelettelementen. *Wissenschaftliche Zeitschrift Humbold-Universität Berlin (Math.-Nat. Reihe)*, *36*, 283–300.

Böhme, M., & Ilg, A. (2003). fosFARBase: http://www.wahre-staerke.com/ (site consulted in January 2011).

Bruno, S., & Maugeri, S. (1992). *Guía de las Serpientes de Europa* (p. 223). Barcelona: Ediciones Omega.

Delfino, M. (2002). Erpetofaune italiane del Neogene e del Quaternario. PhD dissertation, Università degli Studi di Modena e Reggio Emilia. pp. 382, 15 fig., 13 tab., 43 pls.

Delfino, M., Doglio, S., Roček, Z., Seglie, D., & Kabiri, L. (2009). Osteological Peculiarities of *Bufo brongersmai* (Anura: Bufonidae) and Their Possible Relation to Life in an Arid Environment. *Zoological Studies, 48*, 108–119.

Delfino, M., Kotsakis, T., Arca, M., Tuveri, C., Pitruzzella, G., & Rook, L. (2008). Agamid lizards from the Plio-Pleistocene of Sardinia (Italy) and an overview of the European fossil record of the family. *Geodiversitas, 30*, 641–656.

Frost, D. R., Grant, T., Faivovich, J., Bain, R. H., Haas, A., Haddad, C. F. B., et al. (2006). The amphibian tree of life. *Bulletin of the American Museum of Natural History, 297*, 1–370.

Haas, G. (1966). On the Vertebrate Fauna of the Lower Pleistocene Site 'Ubeidiya. *Publications of the Israel Academy of Sciences and Humanities*, Jerusalem, Israel, pp. 70, 14.

Haas, G. (1968). On the Fauna of 'Ubeidiya. The Israel Academy of Sciences and Humanities. *Proceedings* (Section of Sciences, n 7, p. 14), Jerusalem, Israel: Israel Academy of Sciences and Humanities Publisher.

Hodrova, M. (1986). Find of *Bufo raddei* in the Upper Pliocene Bural-Obo locality (Mongolia). *Acta Universitatis Carolinae (Geologica) Spinar 2*, 17l–186.

Hoffstetter, R. (1962). Observations sur les ostéodermes et la classification des Anguidés actuels et fossiles (Reptiles, Sauriens). *Bulletin du Muséum National d'Histoire Naturelle, 34*, 149–157.

Hoffstetter, R., & Rage, J.-C. (1972). Les Erycinae fossils de la France (Serpents, Boidae). Compréhension et histoire de la sous-famille. *Annales de Paléontologie (Vertébrés), 63*, 161–190.

Holman, J. A. (1998). *Pleistocene amphibians and reptiles in Britain and Europe*. Oxford Monographs on Geology and Geophysics (Vol. 38, p. 254). New York and Oxford: Oxford University Press

Holman, J. A. (2000). *Fossil snakes of North America: Origin, evolution, distribution, paleoecology* (p. 371). Bloomington, Indiana: Indiana University Press.

Hossini, S. (2001). Les Anoures (Amphibiens) du Pléistocène inférieur ("Villafranchien") du Jebel Irhoud (carrière "Ocre"), Maroc. *Annales de Paléontologie, 87*, 79–97.

Hossini, S. (2002). La faune d'Anoures marocains du Miocène au Pléistocène et ses rapports avec celle de la meme époque au Sud-Ouest Européen: hypotheses sur l'origine des Anoures au Maroc. PhD dissertation, Université Moulay Ismail, Faculté des Sciences de Meknes, pp. 243, 56 figs.

Jackson, K. (2002). How tubular venom-conducting fangs are formed. *Journal of Morphology, 252*, 291–297.

Jackson, K. (2003). The evolution of venom-delivery systems in snakes. *Zoological Journal of the Linnean Society, 137*, 337–354.

Klembara, J. (1979). Neue Funde der Gattungen *Ophisaurus* und *Anguis* (Squamata, Reptilia) aus dem Untermiozän Westböhmens (CSSR). *Věstnik Ústřednho ústavu geologickhélo, 54*, 163–169.

Klembara, J. (1981). Beitrag zur Kenntnis der Subfamilie Anguinae (Reptilia, Anguidae). *Acta Universitatis Carolinae (Geologica) Spinar 2*, 121–168.

Klembara, J. (1986). New Finds of the Genus *Ophisaurus* (Reptilia, Anguidae) from the Miocene of Western Slovakia (Czechoslovakia). *Acta Universitatis Carolinae, Geologica, Spinar, 2*, 187–203.

Klembara, J., Böhme, M., & Rummel, M. (2010). Revision of the Anguine lizard *Pseudopus laurillardi* (Squamata, Anguidae) from the Miocene of Europe, with comments on paleoecology. *Journal of Paleontology, 84*, 159–196.

Kuch, U., Müller, J., Mödden, C., & Mebs, D. (2006). Snake fangs from the Lower Miocene of Germany: evolutionary stability of perfect weapons. *Naturwissenschaften, 93*, 84–87.

Lordkipanidze, D., Jashashvili, T., Vekua, A., Ponce de León, M. S., Zollikofer, C. P. E., Rightmire, G. P., et al. (2007). Postcranial evidence from early *Homo* from Dmanisi, Georgia. *Nature, 449*, 305–310.

Macey, J. R., Schulte, J. A., Larson, A., Ananjeva, N. B., Wang, Y., Pethiyagoda, R., et al. (2000). Evaluating trans-Tetys migration: An example using acrodont lizard phylogenetics. *Systematic Biology, 49*, 233–256.

Martín, C., & Sanchiz, B. (2010). Lisanfos KMS. Version 1.2. Online reference accessible at http://www.lisanfos.mncn.csic.es/. Museo Nacional de Ciencias Naturales, CSIC. Madrid, Spain. (site consulted in January 2011).

Mashkour, M., Monchot, H., Trinkaus, E., Reyss, J.-L., Biglari, F., Bailon, S., et al. (2009). Carnivores and their Prey in the Wezmeh Cave (Kermanshah, Iran): A Late Pleistocene Refuge in the Zagros. *International Journal of Osteoarchaeology, 19*, 678–694.

Matz, G., & Weber, D. (1983). *Guide des Amphibiens et Reptiles d'Europe, Les 173 espèces européennes* (p. 292). Delachaux & Niestlé éditeurs: Lausanne.

Maul, L. C., Smith, K. T., Barkai, R., Barash, A., Karkanas, P., Shahack-Gross, R., & Gopher, A. (2011). Of Men and Mice at Middle Pleistocene Qesem Cave, Israel: small vertebrates, environment and biostratigraphy. *Journal of Human Evolution, 60*, 464–480.

Ministry of Nature Protection (1999). Republic of Armenia First National Report to The Convention on Biological Diversity incorporating A Country Study on the Biodiversity of Armenia, Republic of Armenia – National Report, Yerevan, March 1999, 104 pp. http://www.cbd.int/doc/world/am/am-nr-01-en.pdf.

Moody, S. M. (1980). Phylogenetic and historical biogeographical relationships of the genera in the family Agamidae (Reptilia: Lacertilia). PhD dissertation, University of Michigan. pp. 373.

Moody, S., & Roček, Z. (1980). *Chamaeleo caroliquarti* (Chamaeleonidae, Sauria): A new species from the Lower Miocene of central Europe. *Věstník Ústředníko ústavu geologického, 55*, 85–92.

Nilson, G., & Andrén, C. (1997). Evolution, systematics and biogeography of Palaeartic vipers. In R. S. Thorpe, W. N. Wüster, A. Malhotra (Eds.), *Venomous snakes: Ecology, evolution and snakebite*, Symposium of the Zoological Society of London (Vol. 70, pp. 31–42).

Nöllert, A., & Nöllert, C. (2003). *Guide des amphibiens d'Europe, Biologie, Identification, Répartition* (p. 383). Delachaux et Niestlé Ed., Paris.

Rage, J.-C. (1984). Serpentes. *Handbuch der Paläoherpetologie*, part. 11, Gustav Fischer, Stuttgart, xii + 80 p.

Rage, J.-C., & Sen, S. (1976). Les amphibiens et les reptiles du Pliocène supérieur de Çalta (Turquie). *Géologie méditerranéenne, 3*, 127–134.

Ratnikov, V. Yu. (1996). On the Finds of Green Toads (*Bufo viridis* Complex) in the Late Cenozoic of the East-European Platform. *Palaeontological Journal, 30*, 225–231.

Ratnikov, V. Yu. (2001a). Osteology of Russian toads and frogs for paleontological researches. *Acta Zoologica Cracoviensia, 44*, 1–23.

Ratnikov, V. Yu. (2001b). Herpetofauna from Cherny Yar Sands of the Cherny Yar-Nizhnee Zaimishche Section, Lower Povolzhye (Volga Region). *Paleontological Journal, 35*, 635–640.

Ratnikov, V. Yu. (2001c). Pliocene anurans of East-European Platform. *Russian Journal of Herpetology, 8*, 171–178.

Ratnikov, V. Yu. (2002). Muchkapian (Early Neopleistocene) amphibians and reptiles of the East-European Plain. *Russian Journal of Herpetology, 9*, 229–236.

Ratnikov, V. Yu. (2004). Identification of some Eurasian species of *Elaphe* (Colubridae, Serpentes) on the basis of vertebrae. *Russian Journal of Herpetology, 11*, 91–98.

Ratnikov, V. Yu. (2009). Fossil remains of modern amphibian and reptile species as the material for studing of their areas history. *Science Research Works of the Geological Institute of Voronezh*, 59, 91 p. [in Russian].

Rauscher, K. L. (1992). Die Echsen [Lacertilia, Reptilia] aus dem Plio-Pleistozän von Bad Deutsch-Altenburg, Niederösterreich. *Beiträge zur Paläontologie Österreich-Ungarns und des Orients, 17*, 81–177.

Sanchiz, F. B. (1977). La familia Bufonidae (Amphibia, Anura) en el Terciario Europeo. *Trabajos Neogeno-Cuaternario* 75–111.

Sanchiz, B. (1998). Salientia. In *Handbuch der Paläoherpetologie*, tome 4, München, pp. 275, 153 figs., 12 pls.

Sindaco, R., Venchi, A., Carpaneto, G. M., & Bologna, M. A. (2000). The reptiles of Anatolia: a checklist and zoogeographical analysis. *Biogeographia, 21*, 441–554.

Speybroeck, J., Beukema, W., & Crochet, P.-A. (2010). A tentative species list of the European herpetofauna (Amphibia and Reptilia) – an update. *Zootaxa, 2492*, 1–27.

Stöck, M., Moritz, C., Hickerson, M., Frynta, D., Dujsebayeva, T., Eremchenko, V., et al. (2006). Evolution of mitochondrial relationships and biogeography of Palearctic green toads (Bufo viridis subgroup) with insights in their genomic plasticity. *Molecular Phylogenetics and Evolution, 41*, 663–689.

Stöck, M., Sicilia, A., Belfiore, N. M., Buckley, D., Lo Brutto, S., Lo Valvo, M., & Arculeo, M. (2008). Post-Messinian evolutionary relationships across the Sicilian channel: mitochondrial and nuclear markers link a new green toad from Sicily to African relatives. *BMC Evolutionary Biology, 8*, 56.

Szyndlar, Z. (1984). Fossil snakes from Poland. *Acta zoologica cracoviensia, 28*, 1–156.

Szyndlar, Z. (1988). Two new extinct species of the genera *Malpolon* and *Vipera* (Reptilia, Serpentes) from the Pliocene of Layna (Spain). *Acta zoologica cracoviensia, 31*, 687–706.

Szyndlar, Z. (1991a). A review of Neogene and Quaternary snakes of Central and Eastern Europe. Part I: Scolecophidia, Boidae, Colubrinae. *Estudios Geologicos, 47*, 103–126.

Szyndlar, Z. (1991b). A review of Neogene and Quaternary snakes of Central and Eastern Europe. Part II: Natricinae, Elapidae, Viperidae. *Estudios Geologicos, 47*, 237–266.

Szyndlar, Z., & Rage, J.-C. (1999). Oldest Fossil Vipers (Serpentes: Viperidae) from the Old World. *Kaupia: Darmstädter Beiträge zur Naturgeschichte*, *8*, 9–20.

Szyndlar, Z., & Schleich, H. H. (1994). Two species of the genus *Eryx* (Serpentes; Boidae; Erycinae) from the Spanish Neogene with comments on the past distribution of the genus in Europe. *Amphibia-Reptilia, 15*, 233–248.

Tadevosyan, T. L. (2004–2009). Tadevosyan's Herpetological Resources. http://www.herp-am.narod.ru/index.htm. Accessed March 2010.

Veith, M., Schmidtler, J. F., Kosuch, J., Baran, I., & Seitz, A. (2003). Palaeoclimatic changes explain Anatolian mountain frog evolution: A test for alternating vicariance and dispersal events. *Molecular Ecology, 12*, 185–199.

Venczel, M., & Várdai, G. (2000). The genus *Elaphe* in the Carpathian Basin: fossil record. *Nymphaea, Folia Naturae Bihariae, 28*, 65–82.

Venczel, M., & Sen, S. (1994). Pleistocene amphibians and reptiles from Emirkaya-2, Turkey. *Herpetological Journal, 4*, 159–165.

Williams, L., Zazanashvili, N., & Sanadiradze, G. (Eds.). (2006). *Ecoregional Conservation Plan for the Caucasus* (2nd edn.), May 2006, Tbilisi, Countur Ltd. pp. 222. http://www.wwf.de/fileadmin/fm-wwf/pdf_neu/Kaukasus_OEkoregionaler_Naturschutzplan_May06.pdf.

Chapter 10
Taphonomy and Site Formation of Azokh 1

M. Dolores Marin-Monfort, Isabel Cáceres, Peter Andrews, Ana C. Pinto-Llona, and Yolanda Fernández-Jalvo

Abstract This chapter aims to describe the complete scenario that existed during the Middle Pleistocene in Azokh Caves and the Lesser Caucasus area from the evidence provided by the fossil assemblages recovered from excavations between 2002 and 2009. In the case of Azokh 1, taphonomic studies are particularly relevant since there is no such information from the early phase of excavations (1960–1980), during which much of the sediment was removed. This study, based on the taphonomy of large mammals, has allowed us to distinguish two sources of the large mammal fauna. Cave bear remains accumulated as a result of hibernation, and some of the carcasses were butchered by hominins *in situ*. The other faunal remains, mainly herbivores, were brought by hominins, but butchering took place somewhere else, not at the rear of the cave where they have been found. There is no evidence for simultaneous occupation of the cave by bears and hominins. There is also no evidence of human occupation at the rear of the cave, and they may have occupied the mouth of the cave during summer time. Cave bears could enter in winter-spring and occupied the rear of the cave. When the cave sediments reached close to the cave roof, bats occupied areas previously inhabited by bears and visited by hominins. Minerals neo-formed in fossils and sediments indicate seasonal changes in humidity and temperature inside the cave during the Pleistocene. Bat guano and corrosive fluid percolation caused strong corrosion on fossils after burial, damaging bones to such an extent that some of them could not be recovered. Bat guano was especially harmful to collagen, which is not preserved in most bones. Finally, during the Holocene, the top of the sequence was eroded by high energy water that removed the upper part of the sediments and opened the cave again to humans and animals.

Резюме Тафономия представляет собой исследование процессов фоссилизации и "истории жизни" окаменелостей. Она изучает, в частности, причины смерти животных, каким образом их останки сохранились до наших дней и как расшифровать информацию, находящуюся на поверхности костей, в тканях, гео- и биохимическом составе. Расшифрованная информация рассказывает нам об экологических условиях прошлого, о вымерших животных и растениях и, в целом, о природе и изменениях в древних экосистемах и климате. Таким образом, тафономия является наукой, которая использует закодированную информацию и сохранившиеся следы деятельности человека для описания естественной "жизни" окаменелостей и восстановления объективной палеобиолого-палеоэкологической и другой палеонтологической информации с целью детальной реконструкции прошлого.

Целью данной главы является, в частности, описание максимально полного сценария событий, имевших место в течение среднего плейстоцена в Азохской пещере. Тафономические исследования на данной стоянке направлены на восстановление исходной информации с ранних фаз раскопок (1960–1980 гг.), в течение которых бóльшая часть седиментов была перемещена из пещеры.

M.D. Marin-Monfort · Y. Fernández-Jalvo (✉)
Museo Nacional de Ciencias Naturales (CSIC), José Gutiérrez Abascal, 2, 28006 Madrid, Spain
e-mail: yfj@mncn.csic.es

M.D. Marin-Monfort
e-mail: dores@mncn.csic.es

I. Cáceres
Àrea de Prehistòria, Universitat Rovira I Virgili (URV), Avinguda de Catalunya 35, 43002 Tarragona, Spain
e-mail: icaceres@iphes.cat
and
IPHES, Institut Català de Paleoecologia Humana I Evolució Social, Zona Educacional 4, Campus Sescelades URV (Edifici W3), 43007 Tarragona, Spain

P. Andrews
Natural History Museum, Cromwell Road, London SW7 5BD, UK
e-mail: pjandrews@uwclub.net

A.C. Pinto-Llona
Instituto de Historia (CCHS-CSIC), Albasanz 26-28, 28037 Madrid, Spain
e-mail: acpinto@ih.csic.es

Yolanda Fernández-Jalvo et al. (eds.), *Azokh Cave and the Transcaucasian Corridor*, Vertebrate Paleobiology and Paleoanthropology, DOI 10.1007/978-3-319-24924-7_10

Сегодня мы обладаем ограниченными данными (иногда они полностью отсутствует) для выяснения контекстовых и постседиментных процессов, а также о том, каким образом формировалась пещера. Данное исследование, основанное на тафономии крупных млекопитающих, позволило нам выделить два источника происхождения этих форм животных. Причиной многочисленных останков пещерных медведей является их спячка, и в ряде случаев их туши были разделаны *in situ*. Другие останки фауны, относящиеся главным образом к травоядным, были привнесены гоминидами, но разделка туш происходила не у задней стены пещеры, где были обнаружены кости. Никаких следов проживания человека не было найдено в тыльной части стоянки; люди, возможно, находились у входа в пещеру главным образом в летнее время. Гигантский пещерный медведь (*Ursus spelaeus*) проживал в пещере в зимне-весенний период, занимая ее тыльную часть.

После того как отложения достигли потолка пещеры, летучие мыши заняли пространство в ее задней части, ранее принадлежащее медведям и время от времени посещаемое человеком. Новые формы минералов в окаменелостях и седиментах указывают на сезонные изменения во влажности и температуре внутри пещеры в эпоху плейстоцена. Но гуано и просачивание едкой жидкости вызвало сильное разъедание останков после их погребения, и некоторые из них сегодня невозможно восстановить. Особенно вредным было воздействие гуано на коллаген. И наконец, в эпоху голоцена поверхность седиментной последовательности подверглась эрозии за счет высокой энергии водных потоков, которые вымыли верхние слои седиментов и снова открыли пещеру людям и животным.

Keywords Large mammal taphonomy • Lesser Caucasus • Bat guano • Fossilization • *Ursus spelaeus* • Pleistocene • Fossil humans

Introduction

Fossils are direct witnesses of past life forms that have reached the present through fossilization. Fossil sites cannot be considered as a snapshot of the past (Shipman 1981); on the contrary, they provide a record of the biotic and abiotic sequences of events extending over space and time and may not be an original image of the past (Fernández-López 1991). Ivan A. Efremov observed that species recovered from fossil sites were often not part of living associations but were brought together in specific locations, forming fossil accumulations due to thanatocoenoses (death associations) in alien surroundings. Efremov (1940) observed that this situation was especially prevalent in terrestrial environments and had special relevance to paleoecological interpretations. Efremov (1940, 1950) proposed a new discipline to investigate the transition of past biological entities from the biosphere to the lithosphere in order to ensure paleoecological interpretations and other paleontological reconstructions were as accurate as possible. Efremov named this new discipline *Taphonomy*.

Taphonomy provides information on past contemporaneous organisms (with ethological implications), and their associations with past environments, climates and ecosystems. Taphonomy may also inform us about fossilization environments, and provide evidence of possible mixtures of more modern fossils combined with older fossils by reworking of sediments. In summary, taphonomy is an integrative and multidisciplinary investigation that aims to reconstitute the past in all details. It is often the case that scarcity or poor preservation of fossils may limit paleontological studies, but from a taphonomic viewpoint, even poor preservation provides much information.

Taphonomy investigates fossils for information gained from past processes, both biotic, for example modifications left by saprophagous fungi or bacteria, root-marks made by plants, butchery marks or cooking by humans, tooth marks and digestion traces by carnivores, and abiotic, for example weathering and breakage. These processes may act before or after burial. Taphonomy also investigates the traces recorded on fossils and on the sediment in which they are preserved, for example fossilized burrows or nests of underground animals and plants, or traces left by unknown predators on the bones of their prey (Fernández-López 2000). These traces provide information about the activity of past contemporaneous organisms that interacted with the sediment or animal carcasses and give evidence of their behavior, living strategies and paleoecology (Andrews et al. 2016). All this informs us about conditions during decay, the types of environment to which remains were exposed, diagenetic processes and modifications forced by seasonal/climatic changes. In summary, all processes that give rise to fossils provide information about past organisms and allow us to gain information about their paleobiology, way of living and evolutionary traits (Fernández López 1981, 1991, 1995, 2006).

Taphonomic Agents

Taphonomic modifications occur at death or soon after (Weigelt 1927). The earliest stage of surface modification that can be recognized is predation, as indicated by skeletal representation, breakage and digestion, as well as by superficial modifications. Taphonomic effects of predation have been extensively studied by various authors (Behrensmeyer and Hill

1981; Brain 1981; Bunn 1983; Haynes 1983; Andrews 1990; Pobiner 2008; Egeland et al. 2008; Martin 2008), and some aspects relate to human and carnivore competition (e.g., Blumenschine and Selvaggio 1988; Selvaggio 1994, 1998; Blumenschine 1995; Capaldo 1995, 1997, 1998; Domínguez-Rodrigo 1997, 1999; Selvaggio and Wilder 2001; Domínguez-Rodrigo and Barba 2006). Signs of carnivore action are seen as tooth marks, bone breakage, digestion and, in the case of humans, cut marks. Differences between predation and scavenging are shown by which anatomical elements show signs of carnivore activity, as there is a sequence of access that may distinguish between primary (usually predators) or secondary (usually scavengers) access to dead animals. Sometimes, the distinction between primary and secondary access by carnivores (humans included) is complex and predation versus scavenging may not be distinguished.

Whether predation is involved or not, decay of carcasses results in the loss of soft tissues (Weigelt 1927). Environmental conditions (e.g.,: humidity, temperature, fluid percolation, acidity/alkalinity) have a strong influence on the decay sequence by biotic agents, as well as secondary mineral growth and corrosion (Fernández-Jalvo et al. 2010a). Microorganisms (Nabaglo 1973; Korth 1979) or insect action (Dodson 1973; Behrensmeyer 1978; Kitching 1980; Smith 1986; Britt et al. 2005, 2008; Fernández-Jalvo and Marin-Monfort 2008; Hutchet et al. 2011) are ubiquitous processes, and the sequence of activity has important forensic value when soft tissues are still present. The action of these organisms can also have physical effects on the bone hard tissues (Wedl 1864; Hackett 1981; Bell 1990; Bell et al. 1996) as well as chemical (see Smith et al. 2016). Forensic studies (Bell et al. 1996) suggest that when carcasses are not affected by predation or scavenging, the body's own indigenous bacterial gut flora are responsible for decay and may affect the bone through the vascular network.

Bone remains lying on the surface of the ground, may be exposed to weathering, trampling and abrasion by wind or water. Weathering on bones is identified as cracks, fissures and exfoliation of the surface of the remains (Behrensmeyer 1978). Weathering comprises all effects on bone by subaerial agents due to changes in temperature, humidity and sun exposure (Behrensmeyer 1978), with different effects in tropical savannah (Behrensmeyer 1978), temperate (Andrews and Cook 1985; Andrews 1990), desert (Andrews and Whybrow 2005) or tropical forest habitats (Tappen 1994). Depending on the habitat and, therefore, and on the intensity of environmental or weathering agents, the time span of bone modifications varies.

Trampling produces scratches on the bone surface, breakage, bone dispersal and abrasion (Andrews and Cook 1985; Behrensmeyer et al. 1986; Fiorillo 1989; Andrews 1990; Lyman 1994; Blasco et al. 2008). Distinction between striations by trampling and cut marks has been a controversial subject, as they strongly mimic each other (Andrews and Cook 1985; Behrensmeyer et al. 1986; Olsen and Shipman 1988; Domínguez-Rodrigo et al. 2009). Rounding affects broken edges as well as anatomical protuberances and it may be the result of trampling, abrasion by water or wind, and digestion (Behrensmeyer 1975; Korth 1979; Boaz 1982; Shipman and Rose 1983, 1988; Denys et al. 1995, 2007; Fernández-Jalvo and Andrews 2003; Thompson et al. 2011). The effects of these processes is seen as macro- and micro-scopic alteration on fossil bone and bone surface texture modifications that distinguish each process (Fernández-Jalvo and Andrews 2003; Fernández-Jalvo et al. 2010a).

After burial, bones are protected from the worst effects of surface weathering and trampling, but they are still in a biologically active environment. The pH of soils where bones are initially buried has been shown to be an important taphonomic agent (Gordon and Buikstra 1981). Some soils produce strong chemical corrosion, even destruction of bones, both by extreme acidity or alkalinity. Bone corrosion by acidic soils in wet and sheltered conditions in open air environments has been observed by Andrews (1995), who noted that corrosion affected articular eminences in such a way as to mimic carnivore activity that is classified as 'hollowing out' or 'scooping out' (Sutcliffe 1970; Haynes 1980, 1983; Binford 1981). The main difference between bone corrosion and carnivore action is that salient angles in contact with the soil are the only parts affected by corrosion, while carnivores may alter any surface and leave tooth marks on the bone surface (Fernández-Jalvo et al. 2010a). Acid soils produce etching of tooth enamel, and in extreme cases of bone as well. High alkalinity produces superficial desquamatory or exfoliation of surface bone (Fernández-Jalvo et al. 1998, 2002), similar in appearance to late stages of weathering, but differing from it by the fact that weathered bones are cracked and split before exfoliation (Behrensmeyer 1978; Andrews 1990). Root marks may form on the surfaces of bone, and may cause corrosion in association with fungi or bacteria. Fungal and bacterial activity in the soil continues to break down the bone tissue. All these agents produce distinct and localized modifications that may affect any area of the surface.

During the stages reported above, some molecular changes occur in the original bone (*bone diagenesis*). Preservation/destruction of bone histology, organic (collagen, DNA) or mineral (bioapatite and stable isotopes) components of bone are related to the environment both before and after burial (Tütken and Vennemann 2011). Structural changes of bone tissues contribute to understanding modifications by biotic and abiotic agents (such as microorganisms, hydrolysis, pH, humidity, temperature, or fluid percolations) that may influence changes in organic and mineral bone bioapatite composition. Bone changes in organic composition related to weathering have been observed by Trueman et al. (2004). These authors

demonstrated how the destruction of the organic matrix of bone (collagen) with extensive surface weathering facilitates dissolution and remineralization. Once the bones are buried these changes are more dramatic, with the original mineral of the skeleton being affected by secondary minerals of apatite (brushite, Molleson 1990), $CaCO_3$, Fe_2O_3 and/or SiO_3, and filling empty spaces in its molecular structure (Wyckoff 1972; Francillon-Vieillot et al. 1989).

These modifications have been examined for the fossils from Units I to Vm in Azokh 1. Accumulation and preservation of bones in caves limits some types of modification but increases others; for example Smith et al. (2016) report that the bone the Azokh is poorly preserved, with no collagen preservation and extensive mineral alteration; and similarly, Bennett et al. (2016) show that no DNA could be amplified from any of the Azokh fossils. The present analysis will therefore concentrate on the surface modifications found on the large mammal fossils recovered from Azokh 1. The small mammal taphonomy of the site is described by Andrews et al. (2016).

Materials and Methods

The fossil collections studied here come from the excavations and prospection work carried out in Azokh 1 Cave between 2002 and 2009. The total number of fossils studied here is 1879 specimens (Table 10.1). The fossils analyzed here all come from the back of the Azokh 1 passageway (see Murray et al. 2016). A test trench of 2 × 2 m was dug in 2003 to establish the limits between stratigraphic units, as well as to confirm lithic and fossil content richness. This test trench was made from mid Unit II to the limit of Unit III to IV. Due to the unstable sediments, the bottom of the trench did not properly reach Unit IV, which has yet to be excavated. Huseinov's excavation team indicated that Unit IV only contained microfauna (*Ellobius lutescens* and *Microtus sociales*; Markova 1982). We, however, may confirm the presence of cave bear fossils in Unit IV, for during the clearing of wall sediment from this unit, fossil teeth and bones of cave bears and other mammalian species were recovered. Finally, material recovered from the middle part of Unit V, Unit Vm, comes from an excavation area exposed by previous excavations. The lower part of Unit V, which is very thick, has not yet been reached.

Unit II is currently under excavation, with an area of 40 m^2, but some of the Unit II fossils also come from the test trench described above. Unit III is restricted to the 2 × 2 m test trench. Fossils from Unit Vu come from a small excavation mainly done in the 2002 and 2008 seasons covering 8 m^2. Unit Vm has been exposed over an area of 24 m^2 and has yielded both stone tools and fossil bones. Units Vm to II at Azokh 1 date from 300 to 100 ka, with Holocene periods recorded in Unit I.

Taxonomic faunal identifications by Van der Made et al. (2016) may slightly differ from those identified here, because small broken fragments that could only provide a rough taxonomic identification (order – family level) or only anatomical identification and animal size as well as unidentified bone splits are also included in this study.

All fossils were analyzed using a 6.3x to 50x stereoscopic light microscope (Leica MZ 7.5). A selection of these fossils (N = 22) was also analyzed using a scanning electron microscope (SEM). Two SEM microscopes were used – a QUANTA 200 Environmental SEM and a FEI-INSPECT Low Vacuum SEM – and both of them are housed at the Laboratory of Non-Invasive Techniques of the Museo Nacional de Ciencias Naturales of Madrid. SEM detectors were used in backscattered electron (BSE) mode combined with secondary electron (SE) emission mode, at 20–30 kV, 0.6–0.33 Torr. Both types of microscopes enable specimens to be directly analyzed at high magnification and high resolution with no necessity for coating or any other pre-treatment. Histological analyses to establish the presence of bacterial attack or any other modification in the interior of the bone were carried out on sectioned bones (N = 53). Oxford energy dispersive spectrometry (EDS) detectors provided the chemical element composition of specific areas of interest. Some samples were analyzed by X-ray diffraction (Philips PW-1830) to obtain their mineral composition (N = 26).

Anatomical Elements and Species Identification

Fossils were identified by Species; Body part; Segment and Portion (diaphysis, proximal and distal end; complete; lateral; body, process; arch). Dental eruption and wear, epiphyseal fusion and bone texture determined age (immature – infant or juvenile- or adult). We distinguished (see Supplementary Information) between number of remains (NR), number of identified specimens (NISP), minimum number of elements (MNE) and minimum number of individuals (MNI), in accordance with the criteria suggested in Lyman (1994). NR covers all recognized fragments, while NISP covers identifiable specimens. MNE was calculated taking into account age, portion, and size. Calculations of survival rate (Brain 1969) or Relative Abundance (Andrews 1990) refer to the value that may be expected in the light of their MNI ($\%\text{Relative Abundance}_i = \text{MNE} \times 100/\text{number of element i in the animal skeleton} \times \text{MNI}$).

The skeletal proportions recovered from archaeological sites depend on the bias caused by the agents involved in the formation of the deposit (e.g., Lyman 1984). In order to check differential preservation arising from the intrinsic nature of fossil bones, we compared Relative Abundances of each bone element with its density obtained by photon densitometry (Lyman 1984). Specimens attributed to large species and sizes were compared with the values obtained for Bison (Kreutzer 1992), medium-sized species with data for reed deer (Hillson 1992) and small sizes with those of sheep (Lyman 1984). Lam et al. (1998) recorded bone mineral density values of long bones using computed tomography. The technique is more accurate than photon densitometry, but both methods show values that correlate well ($R^2 = 0.47$ and $r_s = 0.68$).

Correlations between density of the anatomical element (Ei) and the Relative Abundance (Ri) was statistically analyzed by means of the Spearman's correlation coefficient (r Spearman). The significance level used was $p = 0.05$. Differential conservation of the anatomical element was identified by a significant correlation. The high breakage observed at Azokh 1 results in restricted taxonomic and anatomical identifications. Different anatomical categories have been distinguished taking into considerations cranial skeleton (skull, mandible and isolated teeth) axial skeleton (vertebrae, ribs), including girdles (scapulae and pelves), and major long bones (humerus, radius, ulna, femur, tibia, fibula).

We also distinguished weight size groups according to the classifications of Rodríguez (1997) and Blumenschine (1986), according to species present in the site (see Van der Made et al. 2016):

- Large sized: >300 kg includes adults and immature individuals of *Ursus spelaeus* and rhinoceros (*Stephanorhinus hemitoechus*, *S. kirchbergensis*), as well as adults of *Equus ferus* and *Equus caballus*, and *Bison schoetensacki*.
- Medium sized: 100–300 kg includes Cervidae (immature *Cervus elaphus* and adult *Dama* sp.), adult *Sus scrofa*, immature *Equus ferus* and *Equus* caballus, both adults and immature individuals of *Equus asinus*, and small bovids (*Ovis*, adults).
- Small sized: <100 kg. Adult and immature *Capreolus pygargus, Capra* and *Saiga*. Immature *Dama*, *Sus* and *Ovis*, and all carnivores identified in Azokh 1: canids (*Vulpes vulpes*, *Canis lupus*, *Canis aureus*), hyenid (*Crocuta crocuta*), felids (*Panthera pardus*) and mustelids (*Meles meles*).

Carnivores are mainly restricted to Unit V (Vu and Vm), except for canids and panther that are also present in Unit II. Identifications by Van der Made et al. (2016) include the fossil collections from previous excavations. These identifications include all species from Unit VI that have not been excavated by the present excavation team, except for dental remains of *Dama* aff. *peloponesiaca* found during geological sampling of this unit. The following species from Unit V also were identified from previous excavations: *Meles meles, Martes* cf. *foina*, *Lynx* sp., *Felis chaus*, *Panthera pardus*, *Equus hydruntinus* and *Megaloceros*. Similarly, the following species from Unit III came from earlier excavations: *Equus hydruntinus*, *Stephanorhinus hemitoechus, Capreolus pygargus*, *Dama mesopotamica*, *Ovis ammon*, *Capra aegagrus.*

Shape, Size and Fracture

Length/Width/Thickness were measured on every fossil with micrometric calipers. Lineal dimensions (mm) were classified according to Cáceres (2002) who uses the following four categories: A >2 cm, B 2–5 cm, C 5–10 cm, D >10 cm. Three orthogonal dimensions were also used to characterize the shape of the fossils (D1 length, D2 width, D3 thickness). Based on the original work of Wentworth (1919) to characterize the morphology of sedimentary particles, Frostick and Reid (1983) applied this methodology to fossils, and Blott and Pye (2008) increased the numbers of shape categories to eight. This is a bi-variant approach that relates D2/D1 in ordinates and D3/D2 in abscissas, and it shows the variety of shapes found in fossils ranging from those that are laminar/blade in form (Category 1) to those that are the most rounded/spheroid (Category 8). This approach is useful to analyse shape selection, absent, for example, if all shape categories are present, and it is usually related to hydrologically transported fossils. Similarly, Voorhies groups (Voorhies 1969) also discriminate between potentially transported fossils, this time based on the original (hydrological) shape and weight of anatomical elements which distinguishes those fossils on the basis of their potential for being transported. Other authors (Behrensmeyer 1975; Boaz and Behrensmeyer 1976; Korth 1979) repeated experiments initiated by Voorhies to obtain a more comprehensive classification.

The methodology to determine breakage patterns suggested by Bonnichsen (1979) and Bunn (1983) and completed by Villa and Mahieu (1991) was used and the following traits were recorded:

(1) Number of fractures.
(2) Fracture angle: oblique/right/mixed
(3) Fracture outline: transverse/curved-V-shaped/intermediate.
(4) Fracture edge: smooth/jagged.
(5) Shaft circumference: 1 = circumference is <1/2 of the original; 2 = circumference is >1/2 of the original; 3 = complete.

(6) Shaft fragmentation: 1 = shafts <1/4 of original length; 2 = length between 1/4 and 1/2 of original length 3 = length between 1/2 and 3/4 of original length 4 = length >3/4 of original length (complete).

Villa and Mahieu (1991) compared three different French sites, Fontbrégoua a Neolithic site (4000 BC), and the collective burials of Bezouce and Sarrians (Late Neolithic, 2500 BC). At Fontbrégoua there is evidence of cannibalism and hence frequent traces of long bone breakage when the bone was still green or fresh (Villa et al. 1986). At Bezouce, the sub-fossil bones were broken by impact, and at Sarrians fossil bones were broken by sediment pressure.

Surface Modification Related to Breakage

- Peeling, a term coined by White (1992), defines a roughened surface with parallel grooves or fibrous texture produced when fresh bone is fractured and peeled apart, similar to bending a small fresh twig with two hands. Peeling was recorded as present/absent for each fossil.
- Percussion pits: These are of variable size and depth on the side of the bone opposite to where impact scars and the resulting fracture were produced. Friction of the bone against the surface on which it was resting when struck (see Blumenschine and Selvaggio 1988) produces a series of pits and scratches identified as "rebound points" by Johnson (1985), "Percussion striae" by White (1992), "contrecoup" by Leroi-Gourhan and Brezillon (1972) or the most used term "hammerstone/anvil scratches" by Turner (1983). These pits and scratches were recorded as present/absent.
- Adhering flakes: These are bone flakes that adhere to the fracture surface of a specimen. These flakes are caused by curving incipient fracture lines, often hairline, which are sub-parallel to the fracture edge. These were recorded as present/absent.
- Conchoidal percussion scars: Following Blumenschine (1988), we distinguished between *notches*: arcs on the bone edge; and *flakes*: bone fragments splintered off by the impact.

Tool-Induced Surface Modifications

- Morphology, emplacement and distribution of striations distinguish between incisions (slicing marks and sawing marks), chop marks and scraping marks. Each type of mark results from the different application of a tool on the bone or a combination for different purposes (defleshing, dismembering or grease removal). Striation distribution (isolated marks/grouped/widespread) and orientation (oblique/transversal/longitudinal) was described for each cut mark, chop mark or scrape mark, according to the size of the mammal species. Striation length was also measured (maximum and minimum lengths when sets of cuts occurred).
- Incisions: These are long striations of variable length and width characterized by a transversal V-shape section, internal microstriations and lateral roughness (Hertzian cones, Bromage and Boyde 1984). Similarly, saw marks (Noe-Nygaard 1989) are produced by a repetitive and bi-directional motion.
- Scrapes: These are shallow subparallel multiple cut marks (Noe-Nygaard 1989) caused when a stone tool is dragged transversally along the length of the bone. It is traditionally assumed that this removes periosteal and grease. Some authors (Binford 1981) suggest that scraping marks are caused by the removal from the bone surface of any substance that may absorb the blow when breaking the bone to extract marrow.
- Chops: These marks are the result of striking the bone surface with a sharp stone tool, leaving deep, wide and V-shaped scars. The action may be related to cutting strong muscle attachments or dismembering. They also may have internal microstriations.

Tooth Marks

Tooth marks were described and measured separately for all anatomical items following Andrews and Fernández-Jalvo (1997) and modified (written below in italic) in Fernández-Jalvo and Andrews (2016):

a = Shallow pits on diaphyses of limb bones (minimum dimension);
a1 = Deep perforations on shafts of limb bones[1];
b = linear marks on surface of bone (transverse measurement of grooves, minimum dimension)
b1 = linear marks on ends of bones[1]
b2 = linear marks on articular bone[1]
c = Deep perforations on articular ends of bones;
d = Deep perforations on the edges of spiral breaks;
e = Deep perforations on the edges of transverse breaks;
f = Deep perforations along edges of split bones;

[1]These modifications were not recognized in our initial classification because they were not present in the original classification by Andrews and Fernández-Jalvo 1997.

g = Multiple perforations on the bone surface made by multi-cusped teeth;
h = Deep perforations on anatomical edges;
i = Double arched puncture marks on crenulated edges.[2]

Punctures on spiral breaks (category d) are related to carnivore breakage, and they also depend on the size or type of the anatomical element (e.g., femur vs. radius, and flat vs. long bone) and the size of the prey (large, medium, small sized animals). Breakage category 'e' may not be produced by carnivores, but may be the result of a relatively deep puncture mark on diaphysis (category a) that facilitates post-depositional or diagenetic breakage. This has been seen at Sima de los Huesos site (Andrews and Fernández-Jalvo 1997) where single bones with two fragments having transversal breakage have a puncture mark at the break recorded on both fragments. Bones chewed by hominins have been identified at Azokh Cave (Fernández-Jalvo and Andrews 2011).

These categories have been adapted to other types of measurements of tooth marks taken by different authors investigating modern carnivore tooth marks (Selvaggio and Wilder 2001; Dominguez-Rodrigo and Piqueras 2003; Pobiner 2008; Delaney-Rivera et al. 2009) as follows:

- pc: puncture marks on compact bone (category a, pits on diaphyses, and punctures on broken edges: categories d, e, f, i)
- pac: puncture marks on cancellous or articular surfaces (category c, pits on epiphyses)
- gc: grooves on compact bone (category b, scores on diaphyses)
- gac: grooves on cancellous or articular surfaces (category b1/b2, scores on epiphyses).

We use these four categories, and sizes of tooth marks have been shown graphically in box plot diagrams. This shows the median that separates the higher half of the sample (upper quartile) from the lower half of the sample (lower quartile), as well as the range of measurements (sample minimum and sample maximum) and outliers (data exceeding the data represented in boxes). Following Andrews and Fernández-Jalvo (1997) methodology, the smaller dimension of pits and scores was always measured, which is equivalent to 'minor axis' for Delaney-Rivera et al. (2009), or 'breadth' for Domínguez-Rodrigo and Piqueras (2003) and Pobiner (2008) tooth marks produced by modern carnivores. Measurements obtained by Pinto and Andrews (2004), Pinto et al. (2005) and Rabal-Garcés et al. (2011) have been applied or adapted to the categories of Andrews and Fernández-Jalvo (1997) for cave bear fossil sites.

[2]This category has been proposed in Fernández-Jalvo and Andrews 2011.

Other Surface Modifications

- Cracking: three different categories were distinguished under the light microscope: a0–1 very superficial and very thin cracking; f2–3: fissures, wider and deeper cracks; e4–5: exfoliation of cracked surface following stages described by Behrensmeyer (1975). We also distinguished cracks that show raised or warped-up ridges similar to mud-cracks that contrast with weathering cracks where the edges are just separated. These cracks differ from those produced by weathering, the edges of which are even. They were recorded as presence/absence.
- Concretions: cemented sediment heavily attached to the fossil, sometimes with manganese dioxide stains.
- Rodent gnawing marks, trampling marks, polishing, rounding, root-marks, and soil corrosion. Distribution of these disturbances on the fossils was described as isolated (I: a single mark), clustered (C: in patches or on a particular area on the fossil) or widespread (W: almost covering the whole fossil surface).
- Sediment friction marks refer to processes that entail movement of bone against a rocky/sandy substrate or friction of rocks falling on bones causing multiple randomly dispersed scratch marks, usually transverse to the length of the bone, as the bones are rubbed against the stones. These marks are also described as trampling marks by animals (Andrews and Cook 1985), including humans (Domínguez-Rodrigo et al. 2009) due to bones pressed into the rocky substrate. In archaeological contexts, trampling marks strongly mimic cut marks made by stone tools, and distinction between them is especially relevant. Criteria used to distinguish cuts by stone tools from scratches due to trampling are based on orientation and location of striations on anatomical areas (near articular ends, muscle insertions or tendon attachments), which are congruent with butchering purposes (disarticulation, defleshing, skinning off or cleaning the bone from fat).
- Abrasion (by water or wind) may also produce scratches, although striations are microscopic in size (Fernández--Jalvo and Andrews 2003). Rounding affects broken edges as well as anatomical protuberances.
- Root-marks (linear marks on bones) are the result of roots of vascular plants in symbiosis with fungi or bacteria, and marks are commonly divided into branches and show signs of chemical corrosion at their interior. There are no fossils affected by root-marks at Azokh 1.
- Soil corrosion on bone surfaces indicates the side of the bone that has been in direct contact with an acidic ground under constant humidity. When lifted from the sediment during excavation, fossils were marked with a permanent marker placed on the side that had been in contact with the soil.

- Manganese dioxide deposits are common at Azokh 1 in agreement with a karstic damp environment. The presence of manganese deposition is related to environmental condition characterized by high wet, mildly alkaline and oxidizing (López-González et al. 2006). Manganese dioxide is insoluble and tends to form crusts and coatings in caves (Karkanas et al. 2000).

Histology

We have followed sample preparation methods described by Fernández-Jalvo et al. (2010a) and criteria to identify microscopic focal destruction (MFD). The histological modification according to Hackett (1981) is divided into Wedl and Non-Wedl foci (i.e. Hackett's "linear longitudinal, lamellate and budded foci"). Hacket's non-Wedl MFD is associated with the activity of bacteria. Bacterial attack can be recognized in the BSE-SEM (backscattered electron mode SEM) as a brighter rim (i.e. more compact and dense bone mineral) that is reprecipitation of amorphous hydroxylapatite surrounding the MFD destructive foci (small pores and thin channels 0.1–2.0 microns in diameter). The Oxford Histological Index established by Hedges et al. (1995) from OHI 5 unmodified histology to OHI 0 with no original features identifiable, was used to characterize the general histological preservation of the bone. Tunnelling between 5 and 15 microns is usually assigned to fungal activity following Wedl (1864) and named "Wedl tunnelling" (see also Trueman and Martill 2002; Jans et al. 2002; Jans 2005).

Results

Skeletal Element Representation

Of the 1879 fossils examined from Azokh only 462 fossils (24.6%) could be taxonomically or anatomically identified due to the high frequency of breakage in the sample (Table 10.1).

With regard to family (Fig. 10.1) or order taxonomic identifications (Fig. 10.2), Unit I differs from the other units with a higher percentage of Bovidae. Unit I is associated with a fumier (manure hearth) from occupation of the cave by people who entered with livestock (Fernández-Jalvo et al. 2010b). In contrast Units II to V are Pleistocene in age and have a predominance of cave bear in the mammalian fauna. Among these Pleistocene deposits, Units II and III are similar to each other and slightly

Table 10.1 Fossil identifications from each fossiliferous unit of Azokh 1. NR, number of remains(fossils). %t, partial percentage referred to the total number of fossils per unit. %Az, percentage referred to the total number of fossils (1879) from Azokh1

Levels of identification	Units											
	Unit I		Unit II		Unit III		Unit Vu		Unit Vm		Total	
	NR	%t	NR	%t	NR	%t	NR	%t	NR	%t	NR	%Az
Taxonomic	20	11.8	258	24.6	52	36.4	52	30.2	80	23.3	462	24.6
Anatomic	41	24.1	213	20.3	43	30.1	37	21.5	68	19.8	402	21.4
Unidentified	109	64.1	579	55.1	48	33.6	83	48.3	196	57.0	1015	54.0
Total (%Az)	170	9.1	1050	55.9	143	7.6	172	9.2	344	29.1	1879	100.0
Fossil size												
Fossil size <2 cm	26	15.3	101	9.6	3	2.1	11	6.4	52	15.1	193	10.3
Fossil size 2–5 cm	93	54.7	435	41.4	76	53.2	95	55.2	209	60.8	908	48.33
Fossil size 5–10 cm	39	22.9	370	35.2	51	35.7	50	29.1	72	20.9	582	31.0
Fossil size >10 cm	12	7.1	144	13.7	13	9.1	16	9.3	11	3.2	196	10.4

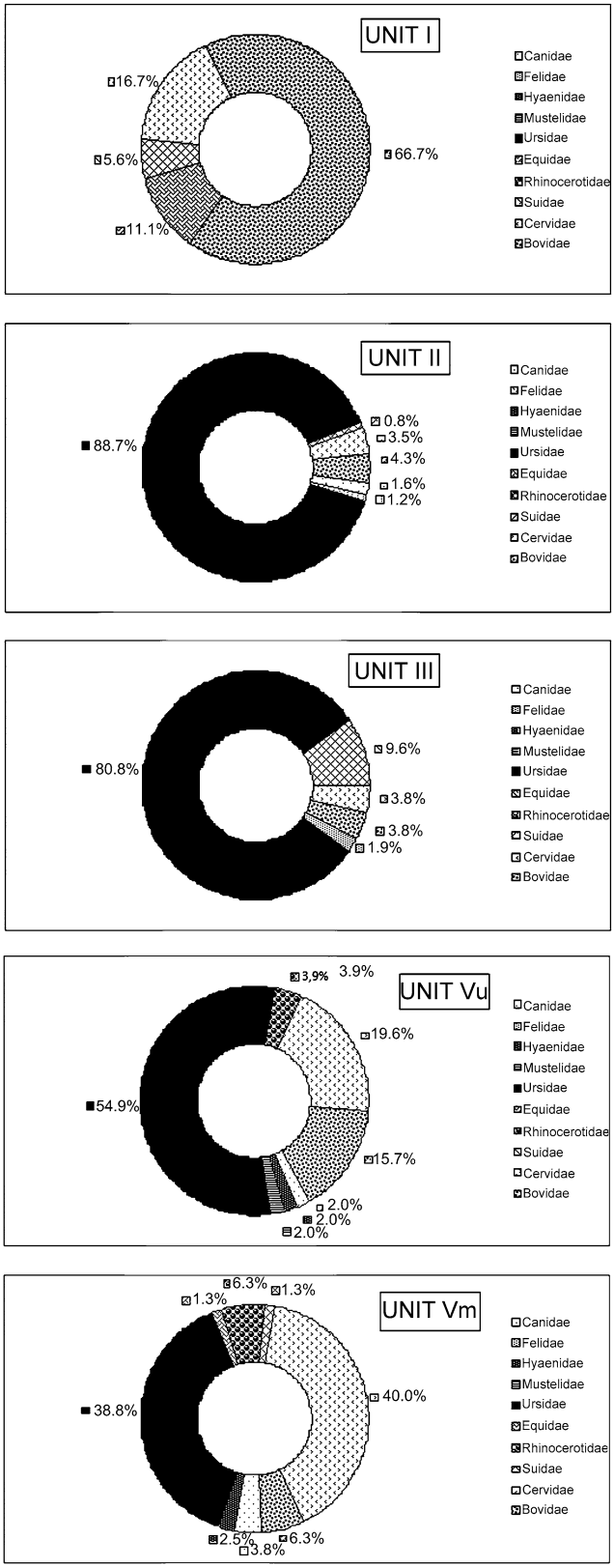

Fig. 10.1 Percentages of different families identified from each stratigraphic unit from Azokh 1 (obtained from the number of remains, NR)

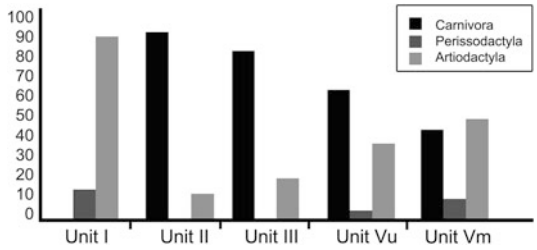

Fig. 10.2 Percentage of macromammal orders (Carnivora, Perisodactyla and Artiodactyla) from Azokh 1 stratigraphic units (obtained from the number of remains, NR)

Table 10.2 Levels of identification. NR, number of remains; NISP, number of identified specimens; MNE, minimum number of elements; MNI, minimum number of individuals

	Unit I	Unit II	Unit III	Unit Vu	Unit Vm
NR	170	1050	143	172	344
NISP	54	417	81	85	133
MNE	39	280	61	71	95
NISP:NR	0.3	0.4	0.6	0.5	0.4
MNE:NISP	0.7	0.7	0.8	0.8	0.7
MNI Carnivores	0	9	4	5	6
MNI Ungulates	10	10	4	7	11

different from Units Vu and Vm, which have higher abundances of taxa other than ursids. The classification by size of mammals in Azokh 1 gives percentages of 36.93% for the large sized animals, 25.55% for medium sized and 13.41% for small sized (24.11% could not be assigned to any of these size classes). The size classification by units shows a higher abundance of medium sized animals in Units I, Vu and Vm, while Units II and III have higher percentages of large sized mammals (cave bears).

The minimum number of identified elements (MNE) is lower than the number of fossils (NR) or the number of identified specimens (NISP) because of the high degree of breakage, which restricts their identification to skeletal element (Table 10.1). This table also includes indices comparing NISP/NR and MNE/NISP that, according to Lyman (1994), provide an indication of completeness. These indices are low showing the high breakage rates of these fossil assemblages. The minimum number of individuals is also given in Table 10.2, with carnivores and ungulates shown separately.

Skeletal elements that could be anatomically identified provide a total percentage in Azokh 1 of 7% for vertebrae, 6.6% for ribs, 6.8% for isolated teeth, 4.5% for phalanges 3.8% for metapodials with the rest of the skeleton elements below 2%. Hyoid bone and baculum, which are uncommon in fossil sites, have been recovered from Units II and III. Comparing skeletal abundances of anatomical elements per unit, most fossils could only be assigned to indeterminate long bones (non-assigned to fore or hind limbs). This is

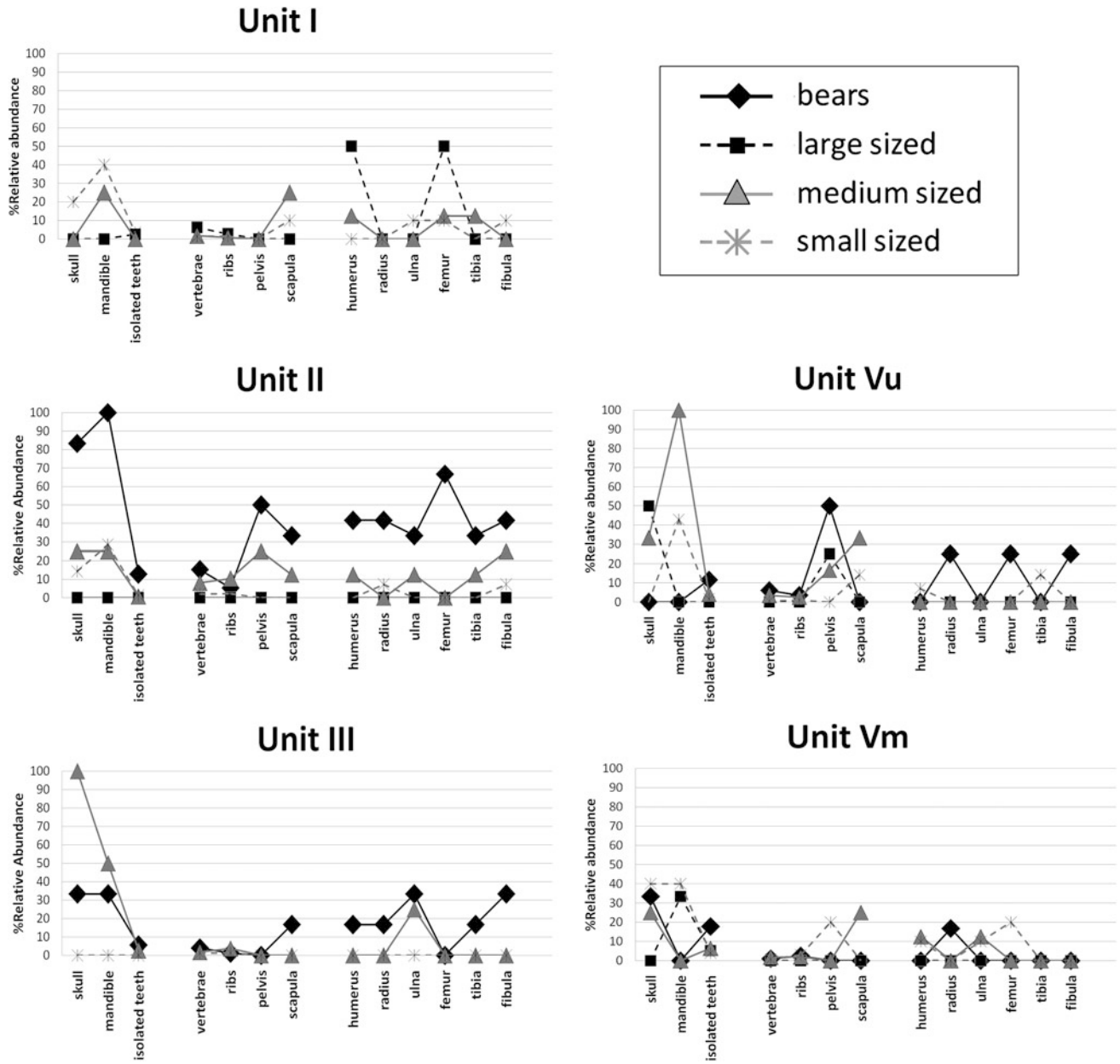

Fig. 10.3 Relative abundances (Ri) of major cranial and postcranial elements identified from five stratigraphic units of Azokh 1

common to all units, and next most abundant in all units are axial elements, particularly of juvenile individuals. Units Vu and Vm have greater numbers of cranial elements compared with other units. Main anatomical skeletal elements of bears and large, medium and small sized animals have been compared per stratigraphic unit (Fig. 10.3) showing an uncommon pattern of human occupation. Small sized animals may be transported complete, but in general the proportion of these animals in most units is low. Similarly, medium and large sized animals are less abundant and less well represented when compared to bears at this part of the cave.

Ages of individuals could be identified in many cases, and there is a high predominance of adults in all units of Azokh 1. Based on dental elements, *Ursus spelaeus* is the only taxon that has a range of ages, with adults, juveniles and old individuals in Units II and Vm. This could suggest that in these two levels the cave was occupied by female bears with their young (Kurten 1958; Andrews and Turner 1992), while at other levels, where only adult specimens have been found, the evidence may suggest that males only were living in the cave, but the interpretation is complicated both by the low numbers of individuals in all units (Table 10.2), and by the fact that cut marks are present on

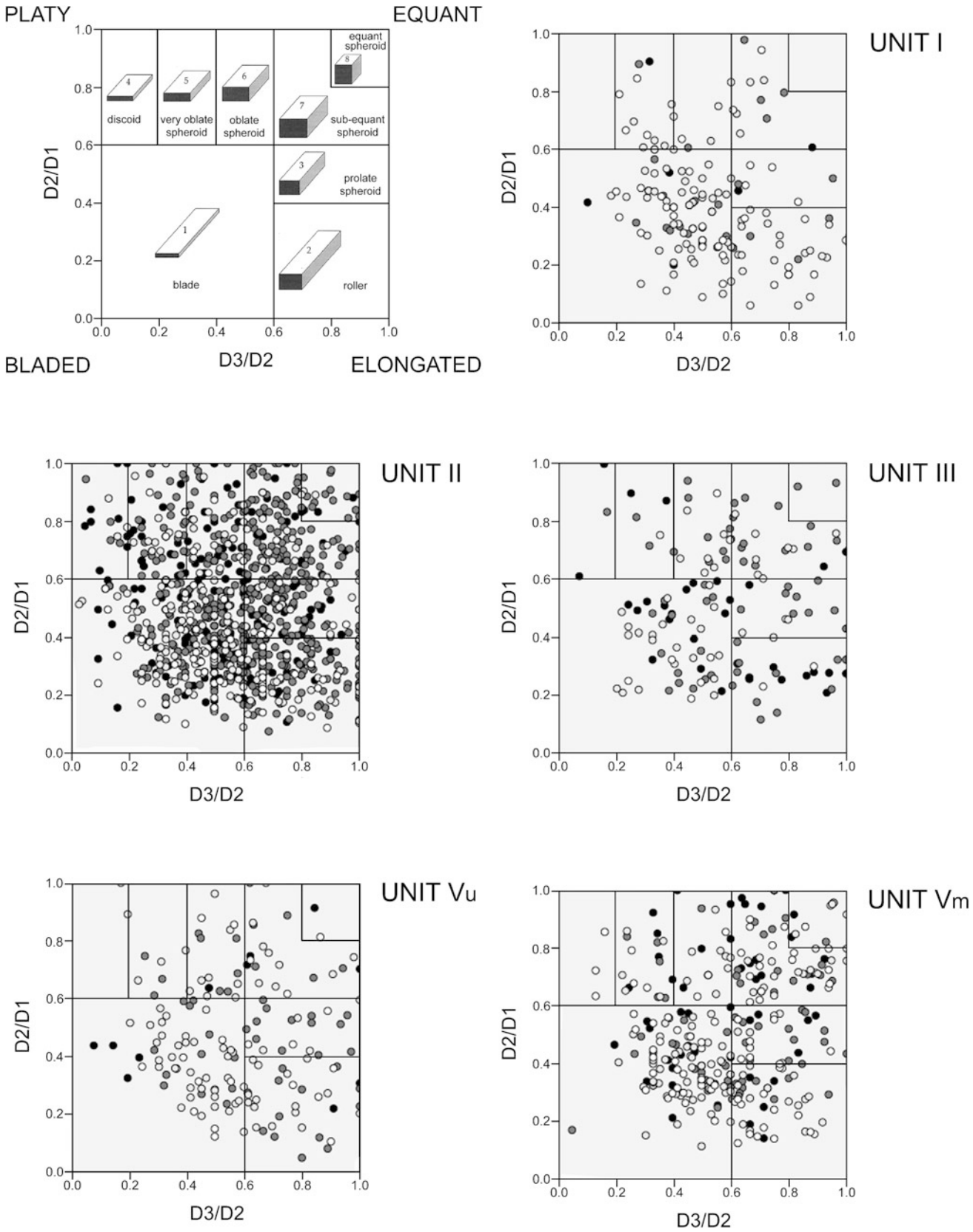

Fig. 10.4 Shape categories established by Blott and Pye (2008) showing the different shapes: elongation, flatness and sphericity. These diagrams represent orthogonal dimensions of fossils from Units I to Vm of Azokh 1. The ratio between width (D2) and length (D1) is shown on the vertical axis and the ratio between thickness (D3) and width (D2) on the horizontal axis. These diagrams characterize predominance of fossil shapes selected by hydrology or gravitational agents. In Azokh 1 the shape of the fossils are randomly dispersed in all categories indicating the absence of fossil shape selection. Black circles: unidentified fossil bone fragments; grey circles: large sized animals; white circles: medium and small sized animals.

Table 10.3 Correlation through *Rho Spearman* between the structural bone density and the relative abundance of different skeletal elements of fossils from each unit of Azokh1

	Density bison	Large sized					Density cervid	Medium sized					Density sheep	Small sized				
		Ri						Ri						Ri				
		Unit I	Unit II	Unit III	Unit Vu	Unit Vm		Unit I	Unit II	Unit III	Unit Vu	Unit Vm		Unit I	Unit II	Unit III	Unit Vu	Unit Vm
Mandible	79.0	0.0	42.9	12.5	0.0	8.3	61.0	12.5	10.0	16.7	50.0	0.0	62.0	20.0	14.3	0.0	21.4	20.0
Vertebrae	62.0	3.1	13.4	3.1	3.1	0.5	30.0	1.8	6.4	1.2	3.6	1.4	26.0	1.4	2.0	0.9	0.5	0.7
Rib	57.0	1.4	3.6	0.7	1.4	0.9	40.0	1.0	8.5	2.6	2.6	1.5	37.0	1.5	2.2	1.0	1.1	3.1
Scapula	50.0	0.0	28.6	25.0	0.0	0.0	49.0	25.0	10.0	0.0	0.0	0.0	20.0	10.0	0.0	0.0	0.0	0.0
Pelvis	55.0	0.0	42.9	25.0	0.0	0.0	49.0	0.0	20.0	0.0	33.3	20.0	49.0	0.0	0.0	0.0	14.3	0.0
Humerus	48.0	25.0	35.7	12.5	0.0	0.0	63.0	12.5	10.0	0.0	0.0	10.0	42.0	0.0	0.0	0.0	7.1	10.0
Radius	62.0	0.0	35.7	12.5	12.5	8.3	68.0	0.0	0.0	0.0	0.0	0.0	57.0	0.0	7.1	0.0	0.0	0.0
Ulna	69.0	0.0	28.6	25.0	0.0	0.0	45.0	0.0	10.0	16.7	0.0	10.0	28.0	10.0	0.0	0.0	0.0	10.0
Femur	45.0	25.0	57.1	0.0	12.5	0.0	57.0	12.5	0.0	0.0	0.0	0.0	36.0	10.0	0.0	0.0	0.0	20.0
Tibia	76.0	0.0	28.6	12.5	0.0	0.0	74.0	12.5	10.0	0.0	0.0	0.0	59.0	0.0	0.0	0.0	14.3	0.0
Carpal/ Tarsal	51.0	0.0	19.2	6.7	2.9	1.3	81.0	3.9	1.5	1.3	2.6	1.5	65.5	0.0	2.2	0.0	0.0	0.8
Metapodial	61.0	0.0	85.7	43.8	25.0	8.3	73.0	12.5	15.0	8.3	25.0	20.0	67.5	5.0	7.1	0.0	3.6	5.0
Phalanx	42.0	8.3	41.7	8.3	14.6	9.7	39.0	0.0	1.7	6.9	0.0	2.5	42.3	0.8	1.2	1.0	0.0	3.3
r Spearman		−0.61	−0.17	0.23	−0.31	0.07		0.40	0.05	−0.21	−0.01	−0.13		42.53	0.57	−0.30	0.41	0.03
P-level		0.03	0.58	0.44	0.30	0.82		0.17	0.88	0.49	0.97	0.67		0.27	0.04	0.32	0.17	0.93

Table 10.4 Abundance and proportions of fossils according to the groups proposed by Voorhies (1969) for each unit of Azokh1. NR, Number of fossils. A%, percentage of elements identified in Azokh1 according to the Voorhies skeletal elements; column B%, shows skeletal elements included by Voorhies (1969) plus other authors (Behrensmeyer 1975; Boaz and Behrensmeyer 1976; Korth 1979)

Voorhies groups	Unit I			Unit II			Unit III			Unit Vu			Unit Vm		
	NR	A (%)	B (%)	NR	A (%)	B (%)	NR	A (%)	B (%)	NR	A (%)	B (%)	NR	A (%)	B (%)
Group I	17	37.8	27.9	153	43.1	32.5	29	42.7	30.5	27	43.6	30.3	30	37.0	20.3
Group I–II	10	22.2	16.4	70	19.7	14.9	13	19.1	13.7	10	16.1	11.2	18	22.2	12.2
Group II	13	28.9	21.3	99	27.9	21.0	15	22.1	15.8	16	25.8	18.0	19	23.5	12.8
Group II–III	3	6.7	4.9	17	4.8	3.6	4	5.9	4.2	6	9.7	6.7	5	6.2	3.4
Group III	2	4.4	3.3	16	3.4	3.4	7	10.3	7.4	3	4.8	3.4	9	11.1	6.1
Total %	101			355			68			62			81		

Table 10.5 Number of large mammals fossils and coprolites, and fossil richness content (fossil/cubic metre of sediment) for each unit at Azokh 1. [1]NR includes fossils and coprolites making a total number of 1935

Unit	NR	Thickness (m)	Area (m^2)	Volume (m^3)	Fossil richness (fossils/m^3)
I	203	1.1	17.4	18.2	11.2
II	1052	0.5	32.7	17.4	60.5
III	143	0.9	3.0	2.7	53.0
Vu	187	0.7	6.2	4.4	42.5
Vm	350	0.6	18.0	10.8	32.4
Total	1935[1]	3.8	77.3	53.5	36.2

some of the bear bones, indicating possible human activity in the accumulation of the bones (see below).

Fossil Size, Shape and Density

Most fossils recovered from Azokh 1 measure between 2 and 10 cm long, with about 10% of remains being larger than 10 cm or smaller than 2 cm (Table 10.1). With regard to the shape of these fossils, we have applied the eight categories established by Blott and Pye (2008). All eight shape categories have been recognized in nearly all units of Azokh 1 (Fig. 10.4). Unit I has no fossils in either category 4 (discoid) or category 8 (equant-spheroid), which are also scarce in the rest of the units (Fig. 10.4).

Correlations between the structural bone density of fossils from Azokh 1 and their relative abundance (Ri), have provided negative values or insignificant correlations. Spearman correlation is sensitive to non-linear relationships between variables, so that if only a slight correlation exists between two variables, r Sperman will show this better than Pearson's correlation. Results obtained from Azokh 1 shown in Table 10.3 suggest that skeletal elements present from these units lack differential preservation due to the density or strength (robustness) of the skeletal element.

Finally, with regard to the transport groups established by Voorhies (1969), the five groups are all well represented in all units of Azokh 1 (Table 10.4), indicating that there is no preferential accumulation of more easily transported skeletal elements. This suggests that there is no evidence of transport in the fossil assemblage of Azokh 1. This is also in agreement with field data/observations indicating the lack of any preferential orientation of fossils, and the horizontal position that most fossils were found resting in within the sediment. It has also been possible to refit fossils within most units (Units II, III and Vu), indicating lack of reworking. Reworking has only been seen in Unit I, but this was modern reworking by burrowing animals.

The abundances of fossils from each unit, and the richness per unit volume of sediment, are shown in Table 10.5. This does not take into account variations across units, and we have found that all units have higher abundances of fossils at certain parts of the excavation area. In Units II and III these coincide with stone tool spatial abundance (Fig. 10.5).

Results of breakage (Fig. 10.6) following Villa and Mahieu's (1991) methodology show predominance of mixed angles, curved-Vshape outline and smooth edges. Most fossils have circumference1 (C1 < 1/2 of the original) and length1 (L1 < 1/4 of original length). Complete bones (C3/L4) appear more abundant in Units Vu, III and II, and very scarce in Units I and Vm, and in general breakage is high in all units.

Surface Modifications

The number of fossils that show carnivore tooth marks is low (120 fossils, and 6.4% of total NR in Azokh 1, Table 10.6) and there is a low frequency of bone splinters. Unit II yielded the highest number (NR) of chewed fossils (76), but the relative number of fossils showing carnivore damage is highest in Unit I (12.9%, see Table 10.6). The distribution of chewing categories seen in Unit I fossils also differs from the rest of the units of Azokh 1, and especially from Units III and Vm ($X^2 = 26.043$; $p < 0.05$; $df = 4$).

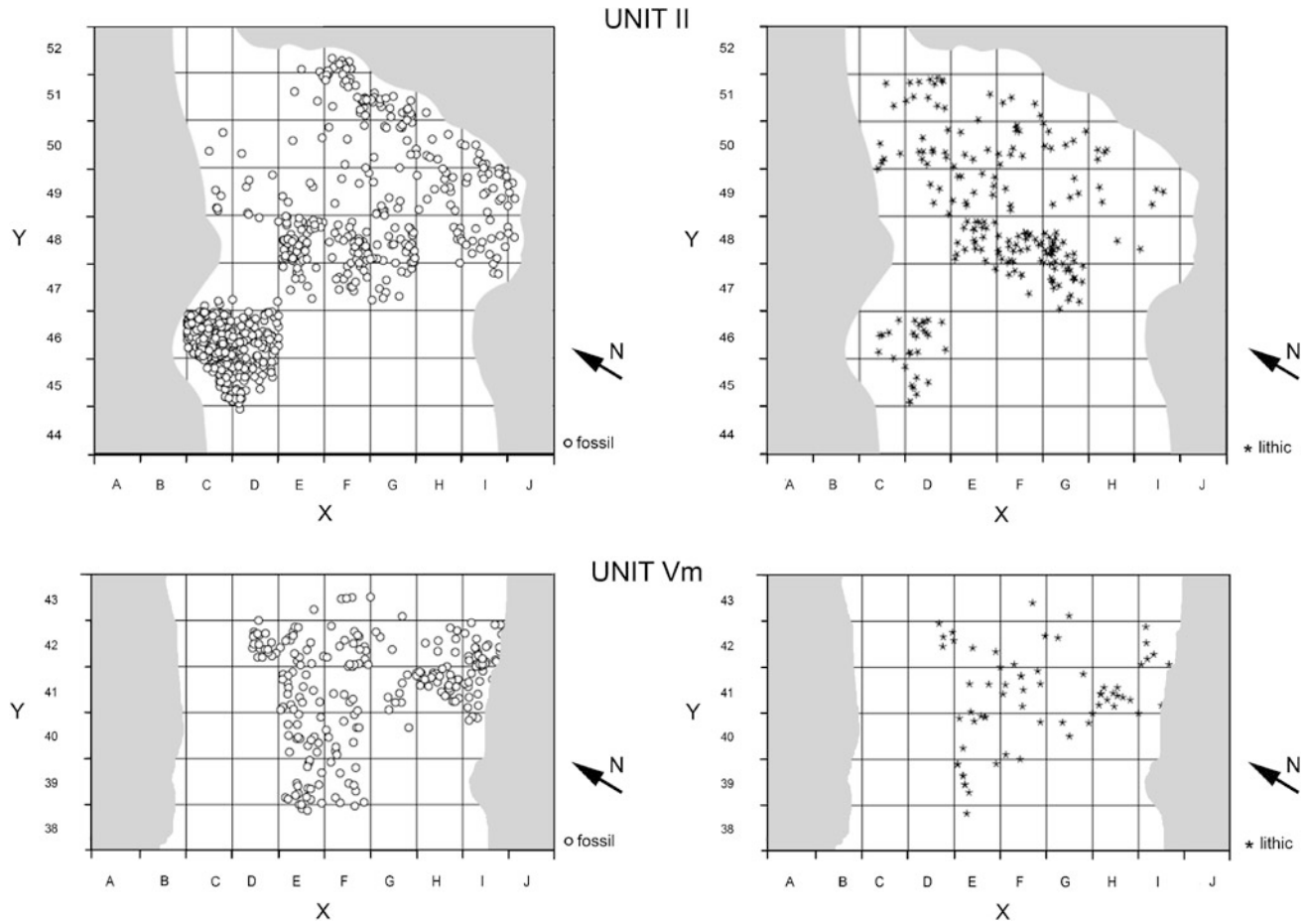

Fig. 10.5 Surface plans of spatial distributions fossils and lithics in Unit II and Unit Vm. These two units have excavated areas large enough to show dispersal patterns

The high post-depositional damage (mainly trampling, see below) has also damaged the edges of tooth marks, which hindered measurement of many of them. The total number of tooth marks that could be measured was 199, and the measurements provided in Table 10.6 distinguish the place on the bone where the tooth marks are located (Andrews and Fernández-Jalvo 1997). Most tooth marks are less than 4 mm wide in all categories, but there are also some tooth marks larger than 7 mm in Unit II and Unit Vu. Tooth marks linked to breakage (on spiral breaks category d, transversal break category e, or splinters category f) are scarce or absent (Unit III). Category d (tooth marks on spiral breaks) is most characteristic of predator size, but it is especially rare at Azokh 1, only present at Unit I and II on one and two specimens respectively. The most abundant damage in all units is grooves on diaphysis (compact bone, category b). These are predator-specific as well, but because the diaphyses bone is compact and the marks may have been made by anterior teeth (such as incisors) as well as posterior ones, the sizes of the grooves are generally small, even when made by large body-size carnivores. Tooth prints made by multi-cusped teeth (category g) have only been recovered from Unit II, the measurements of which (length × breadth of both cusps, and distance between cusps) are as follows:

- (4.5 × 2.2) (7.4 × 3.0) d 8.9
- (3.9 × 1.76) (2.9 × 1.45) d 8.4
- (2.84 × 3.53) (3.73 × 4.80) d 7.5
- (17 × 8.7) no clear distance can be measured
- (16.1 × 5.92) d 11.82.

The last two multi-cusped prints above 15 mm in length, have been recorded on both sides of a *Panthera pardus* calcaneus (Fig. 10.7a, b). The large size of these prints may be influenced by their location on thin cortical bone and the small dimension of the anatomical element. However, the size of the tooth printed on this bone indicates the size of the carnivore animal that produced it.

The size distributions of these tooth marks based on the four chewing categories are presented graphically in box plot diagrams, showing the range of measurements (max and min), the median and the distribution of measurements (Fig. 10.8). Some outliers are present (from Unit II), shown

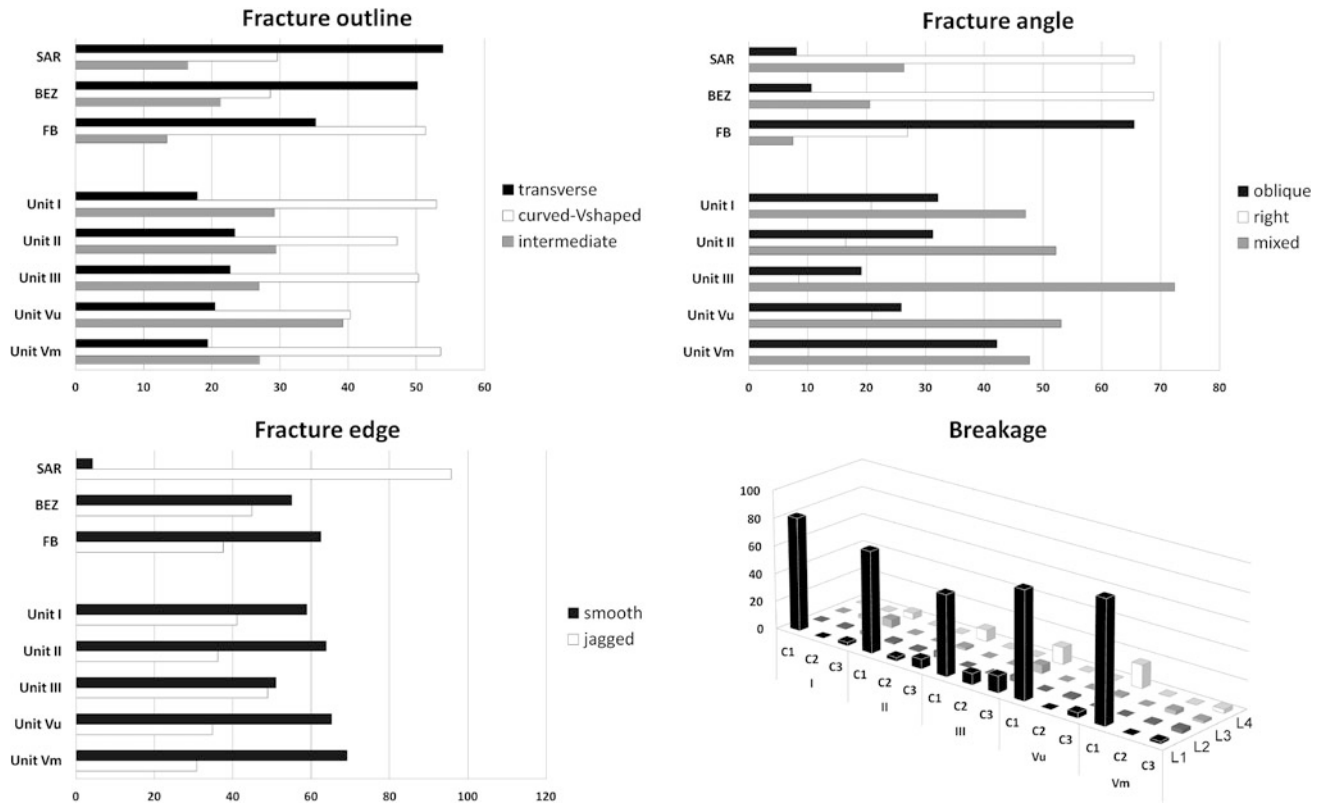

Fig. 10.6 Breakage typology according to Villa and Mahieu (1991) applied to fossils from five stratigraphic units at Azokh 1: **a** fracture outline, **b** fracture angle, **c** fracture edge and **d** circumference versus length. Diagrams **a**, **b** and **c** compare Azokh units with the French sites (SAR = Sarrians, BEZ = Bezouce and FB = Fontbrégoua) studied by these authors. Fracture outline shows similarities between Azokh 1 and Fontbrégoua (butchery site). Fracture edge patterns from Bezouce (sub-fossil bones broken by stone fall impact) and Fontbrégoua are similar to those seen at Azokh 1. The breakage pattern of fossils from Sarrians (fossil bones broken by sediment pressure) differs from all Azokh 1 units. Fracture angle from Azokh 1, however, is different from the French sites, with a high abundance of mixed angles

on the general overview in Fig. 10.8f, but they have been excluded from the single unit figures. The lowest values have been recorded in Unit I. Units II and Vu show the largest tooth marks and the most diverse tooth mark sizes, especially pits on compact bones (pc). The median values are not high, in part due to the low number of marks recorded on these fossils, but the maximum show large sizes that exceed values obtained in modern chewing cases. This is especially significant as measurements taken in Azokh correspond to breadth or minor axis taken at the narrower part of the pit or the groove. Finally fossils bearing tooth marks are dispersed over the excavation surface at each unit, except the central area of excavation in Unit II, where poor fossil preservation has obscured the evidence (see below, histological analyses).

A rib fragment from Unit I (Holocene) has the ventral end bent at the edge of the rib, which is characteristic of human chewing (see the Fig. 10.4a in Fernández-Jalvo and Andrews 2011). This is the only evidence that we have found so far at Azokh that can be assigned to human chewing.

Few fossils in Azokh 1 have rodent tooth marks (NR = 16, 0.85%). Fossils from Unit I and II have small gnawing marks (between 0.18 and 0.40 mm width). Unit III has not yielded fossils with rodent tooth marks and those from Unit Vu could not be measured. Unit Vm fossils have larger marks in a range of medium (1–2 mm) and large sized marks (3–4 mm) respectively. The latter are characteristic of porcupine (Tong et al. 2008).

Tool induced damage on fossils from Azokh 1 affect 135 fossils (7.2%) showing evidence of cut marks. Unit I exhibits the highest relative percentage (14.7%) of tool marked fossils (Table 10.7) and Unit Vm the lowest (3.8%). The most abundant types of damage recorded are cut marks (incisions) and scraping marks, although the Unit I fossils have few scraping marks. Only a small number of fossils showing stone tool marks could be taxonomically identified (41 specimens), and of these 37 were *Ursus spelaeus*, mainly from Units II, III and Vu. The rest were *Capra hircus* and *Cervus elaphus* from Units I, II and Vm. Incisions identified on these fossils are related to specific anatomical areas, such as joints or ligament/muscle attachments (even in unidentified bone fragments) and most of them appear oblique to the

Table 10.6 Types of tooth marks distinguished in Azokh 1 (see methods). NRtm, Number of fossils bearing tooth marks; Ntm, Number of tooth marks; %tm, percentage of tooth marks (in square brackets, size ranges in mm, in brackets individual measurements, shown in bold are the outliers); %tAz, percentage of tooth marks compared to the total number of tooth marks in Azokh1

Units	Unit I (NRtm = 22)			Unit II (NRtm = 76)			Unit III (NRtm = 4)			Unit Vu (NRtm = 10)			Unit Vm (NRtm = 8)			TOTAL (NRtm = 120)	
	%NRtm I = 12.9			%NRtm II = 7.24			%NRtm III = 2.8			%NRtm Vu = 5.8			%NRtm Vm = 2.33			%NRtm Az = 6.4	
Categ.	Ntm	%tm	%tAz	Ntm	%tm	%tAz	Nmm	%tm	%Az	Ntm	%tm	%tAz	Ntm	%tm	%tAz	Ntm	%tAz
a/PC	13 [0.7–3.0] (**4.4**)	25.0	6.5	16 [0.3–2.5/ 3.1–4.0/ 4.6–5.5/ 6.6–8.1]	15.7	8.0	1 (4.0)	7.7	0.5	0	–	–	1 (5.0)	5.6	0.5	31	15.6
b/GC	25 [0.2–1.0] (**1.5**)	48.1	12.6	39 [0.3–2.5] (**11.2**)	38.2	19.6	3 [1.8–2.5]	23.1	1.5	5 [0.6–1.7]	35.7	2.5	14 [0.2–1.0]	77.8	7.0	86	43.2
c/PAC	4 [0.7–1.2]	7.7	2.0	13 [1.5–2.5/ 3.1–5.0]	12.8	6.5	8 [1.2–3.0/ 4.0–5.4/ 6.6–7.0]	61.5	4.0	2 (4.0; 8.0)	14.3	1.0	1 (6.0)	5.6	0.5	28	14.1
d/PC	1 (2.6)	1.9	0.5	2 (0.9; 5.8)	2.0	1.0	0	–	–	0	–	–	0	–	–	3	1.5
e/PC	5 [1.8–2.9]	9.6	2.5	6 [3.4–6.6]	5.9	3.0	0	–	–	4 (2.9; 5.4; 7.6; 8.8)	28.6	2.0	0	–	–	15	7.5
f/PC	2 (2.6; 2.9)	3.9	1.0	6 [0.4–3.6] (5.3)	5.9	3.0	0	–	–	3 (3.26;3.31; 4.98)	21.4	1.5	1 (3.3)	5.6	0.5	12	6.0
g/PC	0	–	–	4 [1.5–3.0]	3.9	2.0	0	–	–	0	–	–	0	–	–	4	
g/PAC	0	–	–	4 (3.5; 4.8; 5.9; **8.7**)	3.9	2.0	0	–	–	0	–	–	0	–	–	4	
h/PC	0	–	–	4 [1.3–4.5]	3.9	2.0	0	–	–	0	–	–	1 (0.9)	5.6	0.5	8	
h/PAC	2 (2.9; 3.5)	3.9	1.0	0	–	–	1 (6.6)	7.7	0.5	0	–	–	0	–	–		4.0
b2/GAC	0	–	–	8 [1.5–4.0]	7.8	4.0	0	–	–	0	–	–	0	–	–	8	4.0
Total tm	52	100	26.1	102	100	51.3	13	100	6.5	14	100	7.0	18	100	9.1	199	100

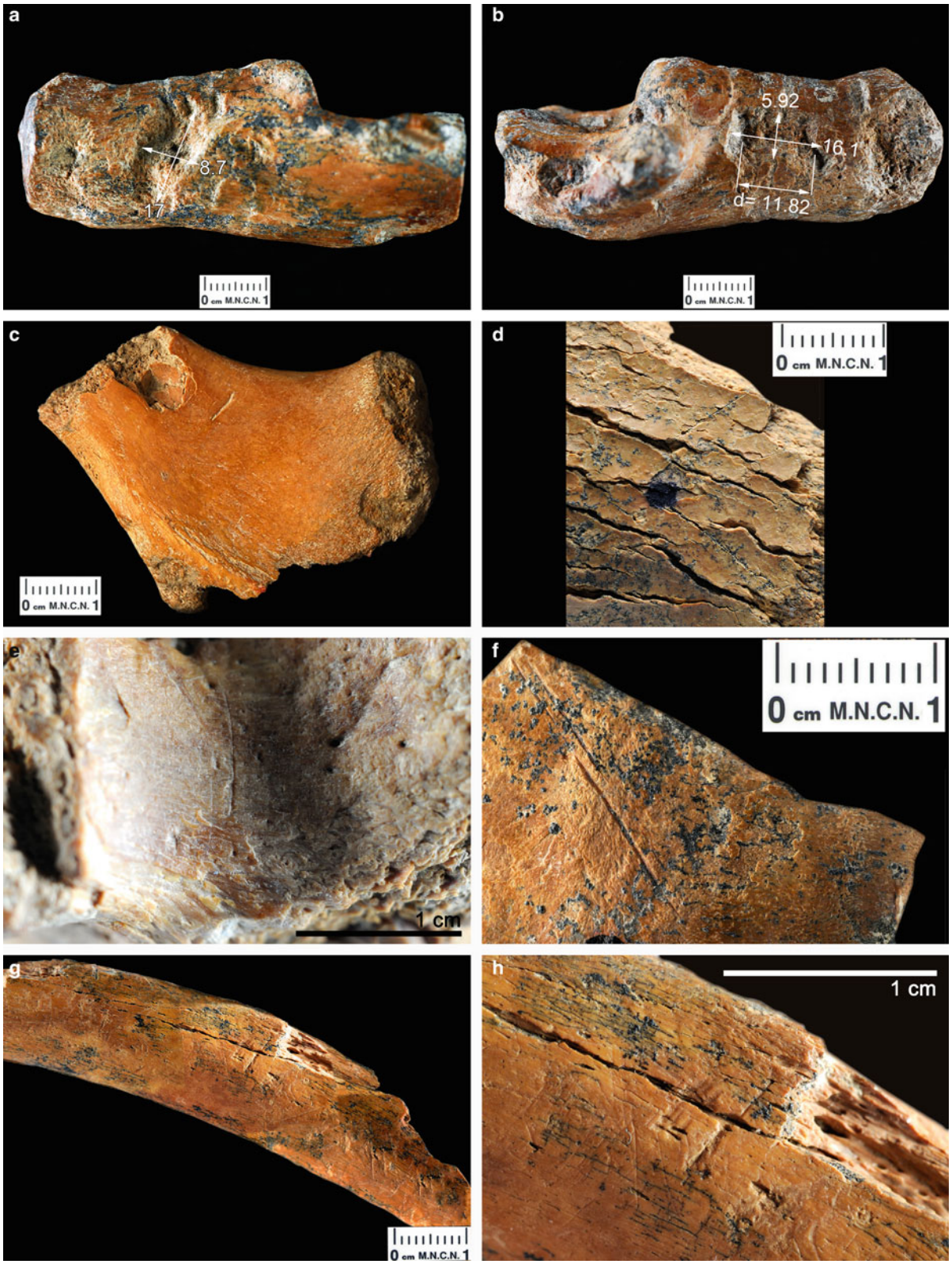

Fig. 10.7 **a**, **b** Calcaneus of panther showing tooth prints on both sides of the fossil. **c** Fragment of pelvis bearing tooth marks on the surface and on the edges, both anatomical and broken edges. **d** Cracking showing warped up edges; the blue point marks the side of the fossil that was in contact to the substrate. **e** Very thin cut mark in a concave surface. **f** Thick cut mark on the fossil surface. **g** Fragment of rib intensively marked by trampling. **h** Detail of previous fossil showing an apparent gnawing mark similar to rodent tooth marks, located in the central part of the rib. Rodents can gnaw the edges (anatomical or broken edges) but the occurrence of this mark in the central part of the rib suggests similarities with descriptions by Haynes (1980) due to bear chewing

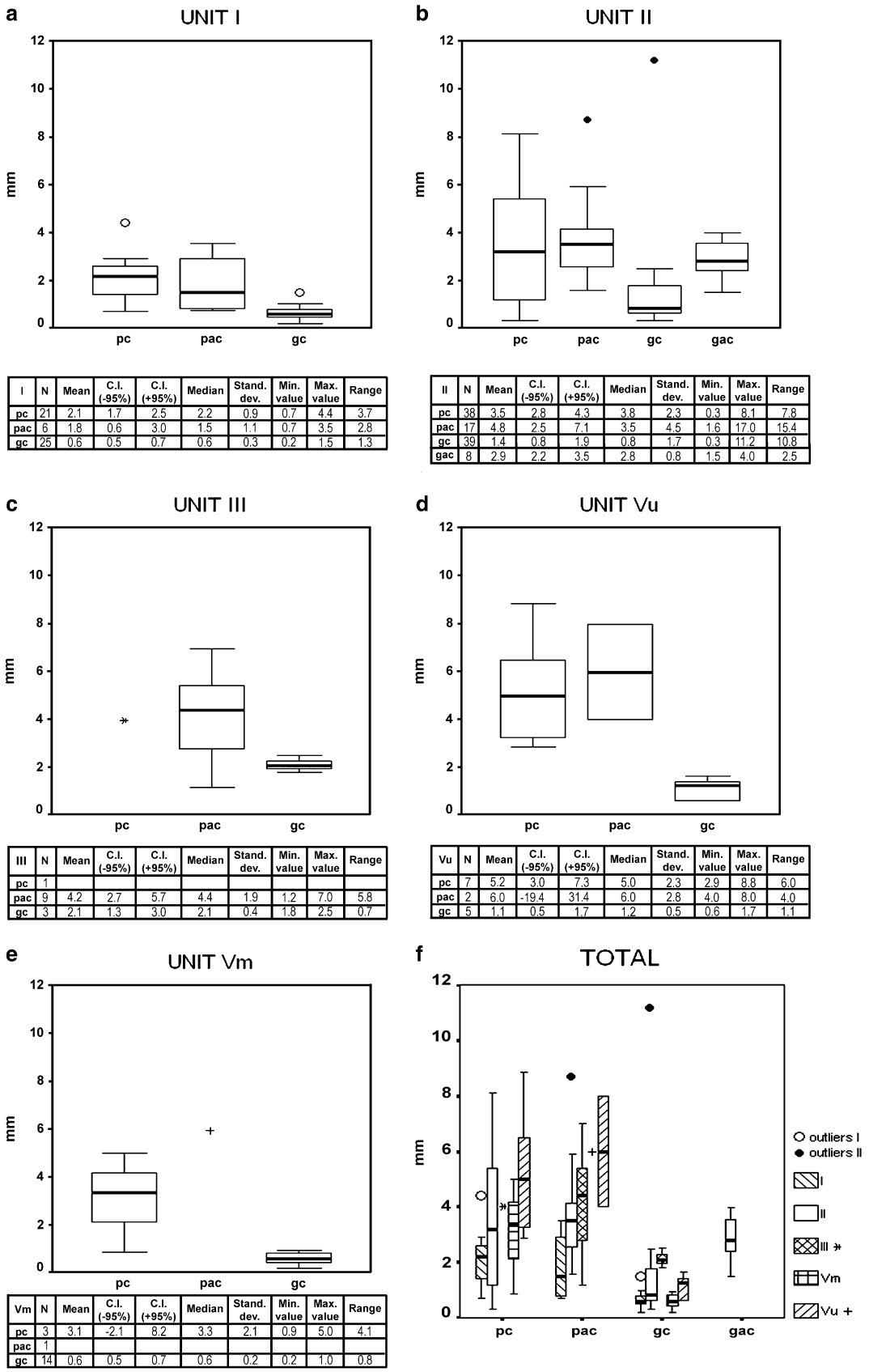

I	N	Mean	C.I. (-95%)	C.I. (+95%)	Median	Stand. dev.	Min. value	Max. value	Range
pc	21	2.1	1.7	2.5	2.2	0.9	0.7	4.4	3.7
pac	6	1.8	0.6	3.0	1.5	1.1	0.7	3.5	2.8
gc	25	0.6	0.5	0.7	0.6	0.3	0.2	1.5	1.3

II	N	Mean	C.I. (-95%)	C.I. (+95%)	Median	Stand. dev.	Min. value	Max. value	Range
pc	38	3.5	2.8	4.3	3.8	2.3	0.3	8.1	7.8
pac	17	4.8	2.5	7.1	3.5	4.5	1.6	17.0	15.4
gc	39	1.4	0.8	1.9	0.8	1.7	0.3	11.2	10.8
gac	8	2.9	2.2	3.5	2.8	0.8	1.5	4.0	2.5

III	N	Mean	C.I. (-95%)	C.I. (+95%)	Median	Stand. dev.	Min. value	Max. value	Range
pc	1								
pac	9	4.2	2.7	5.7	4.4	1.9	1.2	7.0	5.8
gc	3	2.1	1.3	3.0	2.1	0.4	1.8	2.5	0.7

Vu	N	Mean	C.I. (-95%)	C.I. (+95%)	Median	Stand. dev.	Min. value	Max. value	Range
pc	7	5.2	3.0	7.3	5.0	2.3	2.9	8.8	6.0
pac	2	6.0	-19.4	31.4	6.0	2.8	4.0	8.0	4.0
gc	5	1.1	0.5	1.7	1.2	0.5	0.6	1.7	1.1

Vm	N	Mean	C.I. (-95%)	C.I. (+95%)	Median	Stand. dev.	Min. value	Max. value	Range
pc	3	3.1	-2.1	8.2	3.3	2.1	0.9	5.0	4.1
pac	1								
gc	14	0.6	0.5	0.7	0.6	0.2	0.2	1.0	0.8

Fig. 10.8 Distribution of tooth marks on fossils from five stratigraphic units of Azokh 1 graphically represented in boxplots. pc = punctures/pits on compact bone; pac = punctures/pits on articular/cancellous bone. gc = grooves/scores on compact bone; gac = grooves/scores on articular/cancellous bone. Measurements of pits and grooves follow the methodology of Andrews and Fernández-Jalvo (1997), measured across the breadth or minor axis

Table 10.7 Tool induced damage at each stratigraphic unit of Azokh 1. NR, number of cut fossils; %t, percentage of damaged fossils per unit; %tm, percentage compared to the tool marked fossils of Azokh1 (NR = 135). %Az, Percentage compared to the total number of fossils recovered from Azokh1 (NR = 1879)

Tool marks	Units																	
	Unit I			Unit II			Unit III			Unit Vu			Unit Vm			Total		
	NR	%t	%Az	NR	%t	%Az	NR	%t	%Az	NR	%t	%Az	NR	%t	%Az	NR	%tm	%Az
Incisions	23	13.5	1.2	40	3.8	2.1	9	6.3	0.5	10	5.8	0.5	11	3.2	0.6	93	68.9	5.0
Saw marks	1	0.6	0.1	0	0.0	0.0	1	0.7	0.1	1	0.6	0.1	2	0.6	0.1	5	3.7	0.3
Scrape marks	2	1.2	0.1	34	3.2	1.8	6	4.2	0.3	4	2.3	0.2	1	0.3	0.1	47	34.8	2.5
Chop marks	1	0.6	0.1	2	0.2	0.1	0	0.0	0.0	0	0.0	0.0	0	0.0	0.0	3	2.2	0.2
Total*	25	14.7	1.3	67	6.4	3.6	16	11.2	0.9	14	8.1	0.8	13	3.8	0.7	135	100.0	7.2

*Some of these fossils are simultaneously damaged by more than one type of tool mark

Table 10.8 Fossils with evidence of trampling and associated damage by abrasion, and breakage referred to other modifications, e.g., human activity, burning or carnivore tooth marks at each unit of Azokh1. NR, number of remains (fossils). %t, percentage of the total number of fossils per unit. %Az, percentage of the total number of fossils recovered from all units of Azokh1. %Azbrk, percentage of total number of broken fossils of Azokh1

	Units																	
	Unit I			Unit II			Unit III			Unit Vu			Unit Vm			Total		
	NR	%t	% Az	NR	%t	% Az	NR	%t	% Az	NR	%t	% Az	NR	%t	% Az	NR	% Azbrk	**% Az**
Total trampling	25	14.7	1.3	255	24.3	13.6	20	14.0	1.1	16	9.3	0.9	25	7.3	1.3	341	21.1	18.1
Trampling + abrasion	5	2.9	0.3	64	6.1	3.4	3	2.1	0.2	1	0.6	0.1	1	0.3	0.1	74	2.6	3.9
Total abrasion	16	9.4	0.9	134	12.8	7.1	13	9.1	0.7	3	1.7	0.2	8	2.3	0.4	174	10.7	9.3
Brkg + trampling	25	14.7	1.3	221	21.0	11.8	16	11.2	0.9	14	8.1	0.7	24	7.0	1.3	300	18.5	16.0
Brkg + human activ.	21	12.4	1.1	44	4.2	2.3	23	16.1	1.2	16	9.3	0.9	21	6.1	1.1	125	7.7	6.7
Brkg + burning	72	42.4	3.8	10	1.0	0.5	0	0.0	0.0	0	0.0	0.0	4	1.2	0.2	86	5.3	4.6
Brkg + carnivores	7	4.1	0.4	15	1.4	0.8	2	1.4	0.1	5	2.9	0.3	1	0.3	0.1	30	1.9	1.6
Total breakage	160	94.1	8.5	915	87.1	48.7	113	79.0	6.0	135	78.5	7.2	296	86.0	15.8	1619	100.0	86.2

length of the bone. They are rarely transversal and only one case from Unit Vm has a longitudinal incision. In contrast, scraping marks usually run longitudinally to the length of the bone, rarely transversal. Although all types of anatomical elements have been affected to some extent by stone tool marks, the most abundant are limb bones with the locations of the marks indicating defleshing processes. There is also evidence of disarticulation and skinning, especially on *Ursus spelaeus*. Only eight fossils have surface stone tool damage (scraping) directly related to breakage for marrow extraction (four of these were on *U. spelaeus*). Most fossils between 2 and 10 cm long were cut marked, but in units Vu and Vm cut marks are more frequent on fragments between 2 and 5 cm, while in Units I, II, and III they are present on fragments between 5 and 10 cm. Cut bone fragments larger than 10 cm are present in all units but in low percentages. Remains of animals that have been butchered are dispersed over the excavation area, except for the areas close to the walls.

Raw materials used for stones tools are chert, limestone, basalt, hornfelts, schist, obsidian and a range of siliceous and volcanic materials from nearby river gravels (Asryan et al. 2016). Obsidian is a hard vitreous and easy to knap raw material, but exotic to the area. Obsidian stone tools can be made with durable and thin edges, leaving thin cut marks on bone surfaces, and this sometimes makes it difficult to distinguish between trampling and cut marks as they strongly mimic each other.

Trampling striations occur over the whole bone surfaces. Trampling marks are present on fossils from all units in Azokh 1, with a higher abundance on those from Unit II and less than 10% at Unit Vu and Vm (Table 10.8). The X^2 test shows significant differences between trampling recorded from both parts of Unit V (Vu and Vm) and the other units of Azokh 1, especially between them and Unit II ($X^2 = 66.128$; $p < 0.05$; df = 4). On bones with a long axis, trampling marks usually run transversal to the long axis of the bone, affecting salient angles and rarely concave areas. Apart from striations, trampling may also produce rounding, breakage and dispersal of bones (Olsen and Shipman 1988; Andrews 1990; Fernández-Jalvo and Andrews 2016). The breakage traits of broken fossils bearing trampling marks, analyzed according to Villa and Mahieu's (1991) methodology, shows predominance of mixed angles, although mixed angles are also predominant on all broken fragments at Azokh 1 (Fig. 10.6). Fossils showing

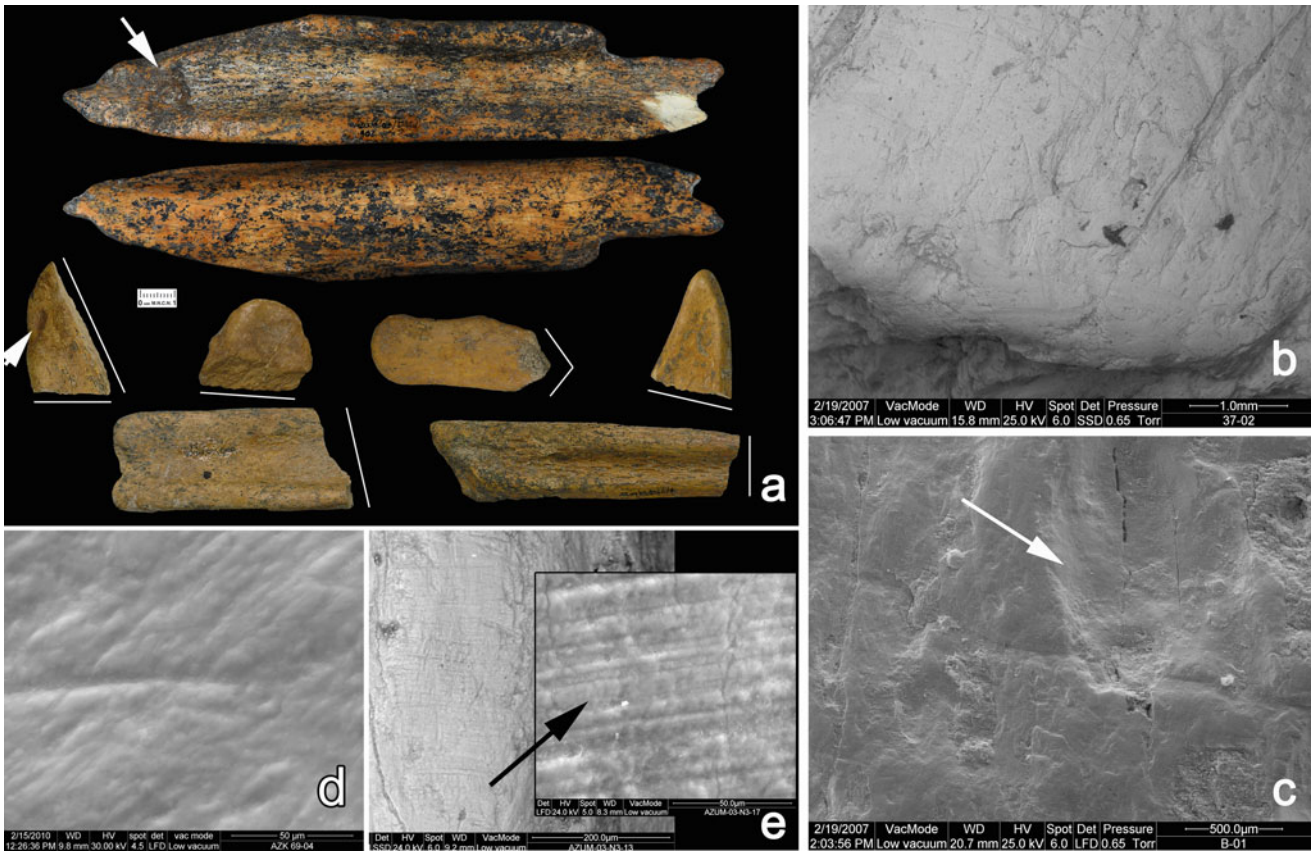

Fig. 10.9 Azokh 1 has yielded some fragments of highly rounded fossils mixed with more abundant non-rounded fossils. **a** Rarely, these rounded fossils appear complete (rounded and smooth all over) as shown at top: both sides photographed. Most frequently, rounded fragments have an old non-rounded broken edge, outlined below by white lines, which may have been broken by trampling. **b** SEM microphotograph showing more numerous striations produced by trampling on the surface than on the rounded edge. **c** SEM microphotograph of a rounded and smooth groove or score covered by a non-rounded transversal scratch by trampling. **d** SEM microphotograph of some of the fossils displayed on top left, showing a smooth surface, but no signs of sediment abrasion or digestion that could cause rounding. **e** A peculiar pattern of parallel fine striations differs from the marks made by trampling or abrasion and may be the result of licking (saliva enzyme rounding and tongue). The small inset shows a higher magnification of these striations the edges of which are also smoothed

signs of trampling are dispersed over the excavation areas with no particular pattern.

Rounding is also produced by biotic agents such as digestion and licking by carnivores. Digestion produces bone polishing and rounding that differs from sediment abrasion (dry or wet) by distinct ultramicroscopic features (Andrews 1990; Fernández-Jalvo and Andrews 2003, 2016). Digested fossil bones have been recovered from Azokh 1, but in relatively low proportions (<10%). In addition, some fossils from Units II, III and Vu have extremely rounded edges and elongated shape (Fig. 10.9a). These fossils could be mistaken for highly abraded bones, but this possibility is incongruent with taphonomic traits and geological evidence from the site. Evidence of transport has only been distinguished in Unit VI (Murray et al. 2016). Trampling scratches are not any more abundant on the rounded edges than on the rest of the bone surfaces (Fig. 10.9b). Tooth grooves or scores produced by carnivores appear smooth and rounded (Fig. 10.9c). Sharper scratches by trampling are superimposed on the smooth and rounded edges (Fig. 10.9d). A peculiar pattern of microstriations observed on some of these fossil bones also have rounded edges (Fig. 10.9e). Several of these fragments also show more recent breakage, probably by trampling, with no rounding affecting broken edges (Fig. 10.9a).

Most fossils from Azokh 1 are broken (86%). Table 10.8 shows surface modifications of known taphonomic agents on broken fragments (trampling, abrasion, human action, carnivores or fire). Carnivore tooth marks on broken fragments are not abundant (1.6%). Similarly, tool induced damage and human action related to breakage (adhered flakes, impact and percussion marks and peeling) only affects 6.7% of broken bones. Many of the complete bones have low nutritional content (e.g., ulnae or radius). Fire could influence breakage (in fact, all burnt fossils are broken), for fire increases the likelihood of breakage, but the incidence of

burning is low at Azokh 1 (Table 10.8). The highest number of fossils affected by fire is observed in Unit I (a manure hearth), and low frequencies of burnt bones have been recovered from Units II and Vm (10 and 4 respectively) and none from Units III and Vu. Although the percentage of fossils bearing trampling marks is low (18% of total fossils from Azokh 1), this is the main agent of breakage on broken fossils (16%, see Table 10.8). Breakage due to diagenetic compression such as sediment compaction would occur *in situ* with both fragments lying close each other.

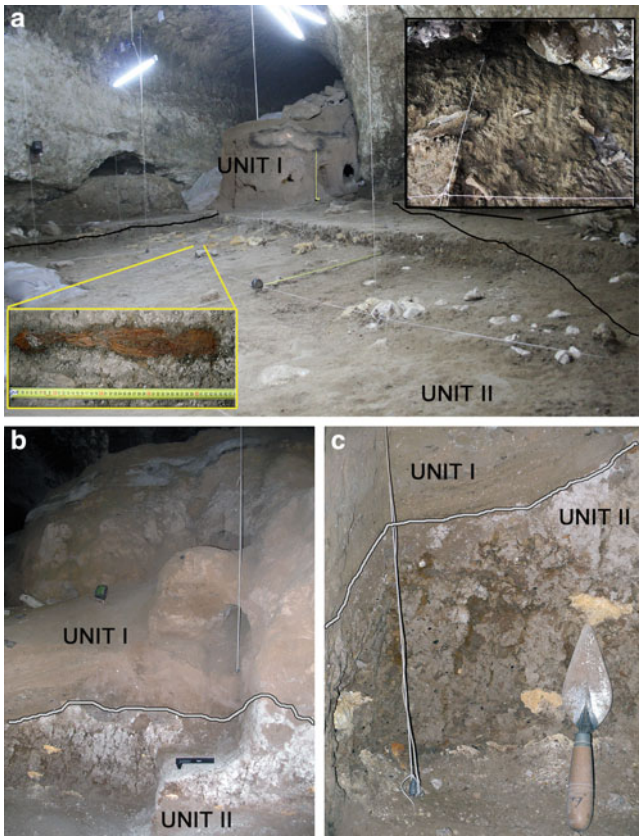

Fig. 10.10 **a** General view of the excavation area of Unit II, and the remains on the left of the fumier of Unit I. Note modern burrows in the section of Unit I, some of them also affecting the top of Unit II, that caused reworking of fossils and stone tools. The black lines along the sides of the excavation area of Unit II show the limit of crumbly grey sediment in the center and the reddish non-crumbly texture of the sediment next to the cave wall. The small inset bottom left shows the characteristic heavy corrosion of fossils recovered from the central area embedded in the crumbly grey sediment. The small inset top right shows fossils structurally undamaged near the cave wall, embedded in unaltered sediment. Note stones in the central area have a yellow color (and soft texture), white colored stones are less damaged. **b** Section of Unit II showing the grayish-crumbly sediment and the erosive contact between Unit II and I. **c** Detail of previous showing the crumbly texture of the Unit II sediment containing soft-yellow stones. Note the laminar sedimentation of Unit I at the erosive contact with Unit II

Fossils recovered from Azokh 1 show cracks with raised or warped up ridges (13.8%) similar in shape to mud-cracks in fine substrates (Fig. 10.7d). This type of cracking has been observed on fossils deep inside caves or in continental aquatic environments (lakeshores), suggesting its relationship with changes in humidity in a damp environment (Díez et al. 1999; Pesquero et al. 2010; Fernández-Jalvo and Andrews 2016). A high abundance of manganese deposits cover these fossils (57%) (Table 10.9).

Highly corroded bones have been observed at Unit II in the central area of excavation. At the same level, but near the cave walls, there is less to no corrosion, and undamaged fossils have been recovered (Fig. 10.10a). The corrosion is observed as heavy cracking, producing a laminated effect and with flaky and dusty surfaces (Fig. 10.10a). Corroded fossil bones are very fragile and require consolidants before they can be removed from the sediments. This corrosion also affects the sediment that is grayish and crumbly towards the central area of excavation, while sediment close to the cave walls is reddish and lacks this crumbly texture. In addition, stones (originally limestone and chert) found in the central part of the excavation are soft and yellow-white in color ('decayed stones', Fig. 10.10b, c), and when analyzed by XR-diffraction (Table 10.10) and EDS, inclusions of tinsleyite, apatites and other minerals are seen.

Corrosion and Chemical Composition (Histological Analysis)

Histological analyses of 53 fossils analyzed show either heavy bacterial attack (OHI = 0) or bone unmodified by microorganisms (OHI = 5). Intense bacterial attack has only been found in Unit II affecting six of the 22 fossils that were histologically analyzed from this unit. Bacterial colonies in these fossils from Unit II are organized around canals of Havers in a characteristic way (encircling osteones, Fig. 10.11a) that suggests that bacteria acted during the body's decay (Bell 1990). Bacterial attack can be recognized in the BSE-SEM (backscattered electron mode SEM) as more dense (hypermineralized) zones containing small pores and thin channels 0.1–2.0 microns in diameter. Superimposed generations of bacterial attack on some of these specimens (Fig. 10.11b) have been observed, suggesting fluctuation in the environmental conditions. These more dense areas (re-precipitation of amorphous calcium phosphate) have 'resisted' destructive effects of bone corrosion that have literally 'eaten away' remains of bone between bacteria colonies (Fig. 10.11a). Canaliculi (histological canals interconnecting osteocytes/lacunae) are enlarged mainly on the most external cortical layer (Fig. 10.11c).

Table 10.9 Fossils cracked and bearing manganese from each unit of Azokh1. NR, number of remains (fossils). %t, partial percentage of the total number of fossils per unit. %Az, percentage of the total number of fossils recovered from all units of Azokh1

	Units																
	Unit I			Unit II			Unit III			Unit Vu			Unit Vm			Total	
	NR	%t	%Az	NR	%t	%Az	NR	%t	%Az	NR	%t	%Az	NR	%t	%Az	NR	%Az
Total cracking humidity	12	7.06	**0.6**	148	14.1	**7.8**	31	21.7	**1.6**	23	13.4	**1.2**	48	14.0	**2.5**	262	**13.8**
Total manganese	77	45.3	**4.1**	573	54.6	**30.5**	119	83.2	**6.3**	143	83.1	**7.6**	156	45.4	**8.3**	1068	**56.8**

In contrast to Unit II, light bacterial attack has been detected in one fossil from Unit III, based on a sample of five from this Unit. Microbial damage is so mild that has not affected the general histology of this bone (OHI is still 5). No bacterial attack has been observed on fossils from Units I, Vu and Vm. Fungal action has been found on fossils from Units III and Vm affecting 1 and 3 fossils respectively (Fig. 10.11d).

In addition to bacterial attack, Unit II has the heaviest corrosion observed in Azokh 1. No specific histological damage has been observed that may explain this heavily flaked and laminated texture that also affects the inner layers of the compact bone (Fig. 10.11e). Fossils contain secondary deposits of tinsleyite minerals ($KAl_2(PO_4)_2(OH)\cdot 2(H_2O)$), confirmed by XRD. Crumbly sediment and flaked fossils also have tinsleyite in their composition (Table 10.10). Soft 'decayed' stones have a highly porous texture and have been transformed into calcium phosphate (Fig. 10.11f), identified as hydroxylapatite by XRD (Table 10.10, stub sample #110). Local deposits of barite [$Ba(SO_4)$] have also been detected by EDS in Unit II fossil bones, as well as gypsum [$Ca(SO_4)\cdot 2(H_2O)$] and bassanite [$2(Ca)2(SO_4)\cdot(H_2O)$] identified by diffraction spectrometry (XRD).

Hydroxylapatite [$Ca_5(PO_4)_{2.5}(CO_3)_{0.5}(OH)$] is the most thermodynamically stable mineral of this group, and it forms in a short time. Brushite [$Ca(HPO_4)\cdot 2(H_2O)$] is stable in conditions of high acidity ($pH < 6$) and damp conditions, but it loses water readily, converting to monetite [$Ca(HPO_4)$]. The formation of gypsum [$Ca(SO_4)\cdot 2(H_2O)$] is common in the processes of decomposition of bat guano, where sulfur comes from organic matter and the calcium from the dissolution of the calcareous rock (or fossils). Ardealite [$Ca_2(SO_4)(HPO_4)\cdot 4(H_2O)$] can also be formed in caves in the presence of guano, and this mineral together with gypsum often appear in dry caves. Sepiolite [$Mg_4Si_6O_{15}\cdot 6(H_2O)$] is an authigenic mineral of caves associated with conditions of filtration of water rich in magnesium followed by extreme aridity, while pyrolusite [MnO_2] and oxides of manganese are frequent in damp caves. Several of these minerals (hydroxylapatite or series of apatite, gypsum, sepiolite and tinsleyite) have been detected by XR diffraction or by EDS analysis of the Azokh 1 fossils, indicating fluctuations of arid conditions and high humidity.

Unit Vm has also yielded laminated and flaky fossils (Fig. 10.11g). EDS analyses of these fossil bones shows a high proportion of phosphorous that anomalously exceeds the amount of calcium for the basic bone mineral composition of hydroxylapatite. None of the samples from Unit Vm analyzed by XRD yielded tinsleyite, which was observed in Unit II and which could explain the cracked-laminated surfaces. These XRD analyses, however, show the presence of sepiolite minerals [$Mg_4Si_6O_{15}\cdot 6(H_2O)$] both in fossils and sediment/stones.

Some fossils from Azokh 1 have a 'stone-like' texture to the naked eye, and while most of them come from Unit Vm, some also are known from Units II and Vu. These fossils show a heavy microscopic cracking (Fig. 10.11h) and anomalous quantities of chemical elements detected by EDS spectrometry. Some fossils have enrichment in phosphate and others in calcium, as well as sulfur, potassium or silica. Sediment attached or underneath these fossils are enriched in phosphorous. An amorphous secondary deposit infilling histological features (canals of Havers or Volkmann's) of some fossils is mainly calcium phosphate (brushite, apatite or hydroxylapatite) sometimes with sulfur (possibly ardealite, monetite). Element composition obtained by EDS is not sufficiently conclusive to identify the type of mineral or substance that might deposit on these fossils. XRD analysis of one of these 'stone like' fossils provides 100% of hydroxylapatite. The only conclusive result that may be proposed for this peculiar heavy microscopic cracking and 'stone-like' texture is chemical, but it is unclear what the exact chemical process was, or which minerals were responsible for the damage to these fossils. Limestone blocks from the central area of Unit II excavation are also structurally and chemically altered. These stones have enormously increased porosity, and the original calcareous or siliceous composition (limestone or chert) has been transformed to calcium phosphate.

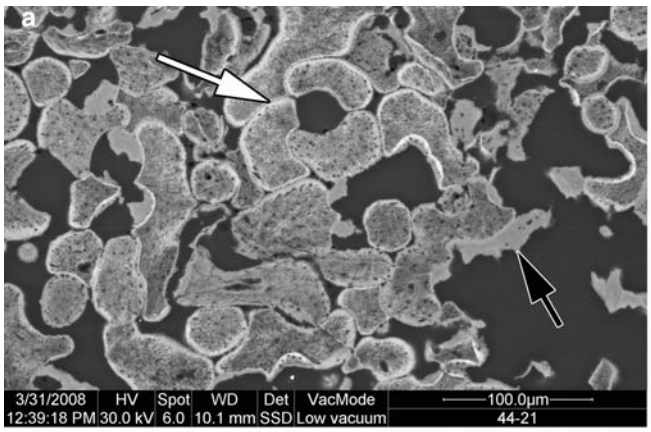

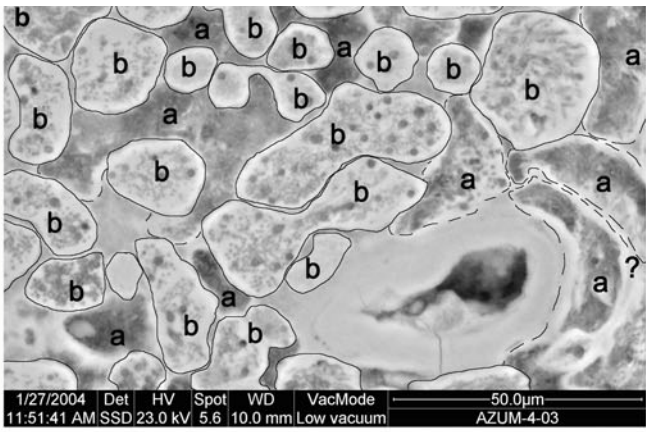

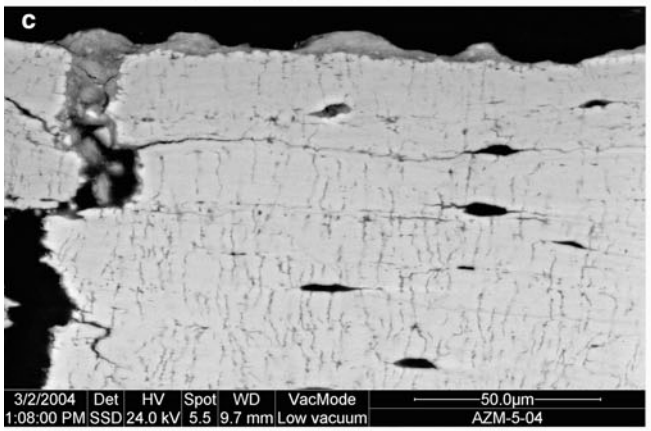

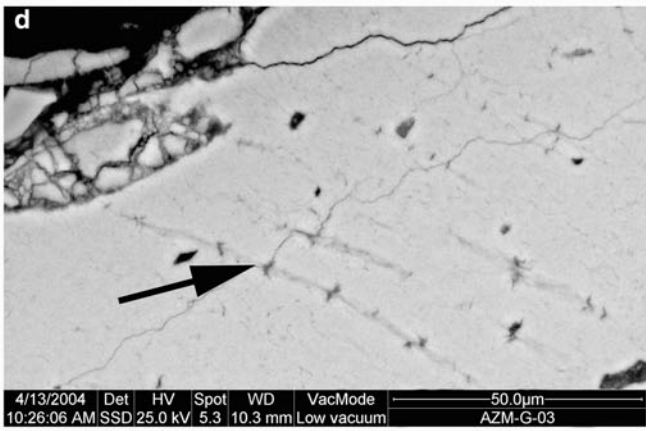

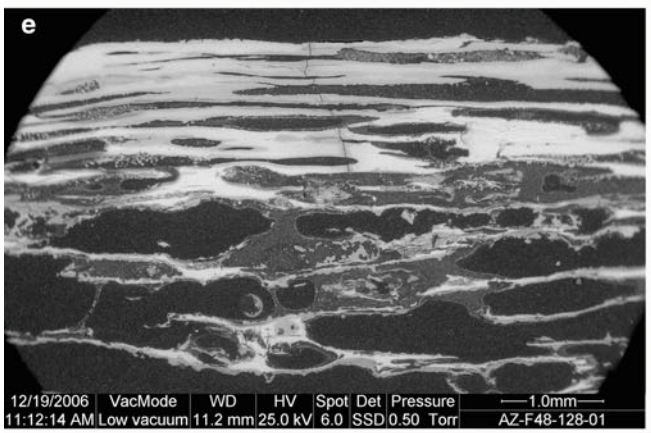

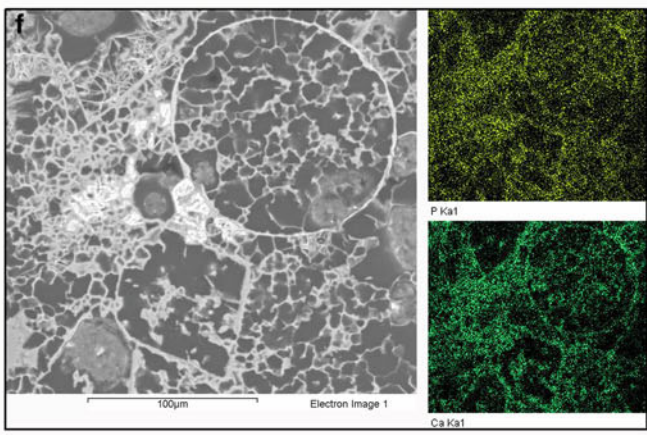

Element	Weight%
E42 15	Bone
O K	40.27
Mg K	0.21
Al K	1.66
Si K	3.37
P K	27.04
S K	0.93
K K	0.51
Ca K	23.57
Fe K	2.44
Totals	100.00

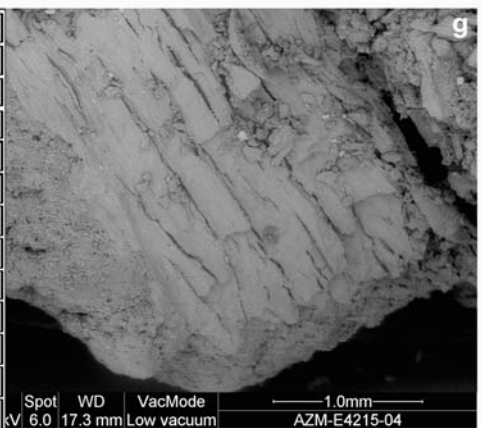

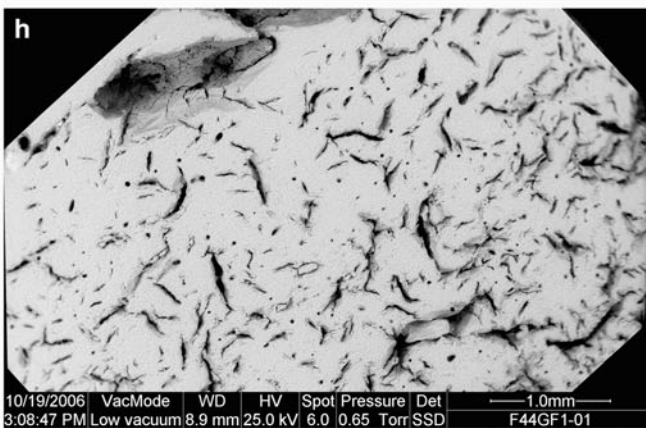

◀ **Fig. 10.11** SEM microphotographs of histological sections of fossils from Azokh 1: **a** fossil from Unit II intensively attacked by bacteria characteristic of natural body decomposition (surrounding osteones, white arrow). This specimen has also been intensively corroded by acid fluids and only the remains of bacteria colonies (microscopic focal destruction, MFD) have remained with some pieces of bone attached (black arrow). **b** Fossil from Unit II intensively attacked by bacteria showing at least two generations of bacteria superimposed. **c** Fossil from Unit Vm where canaliculli are enlarged on the outer side of the cortical surface. **d** Fossil from Unit Vm showing Wedl microtunneling produced by fungi. **e** Heavily laminated and flaky fossil from Unit II showing no histological damage except for the heavy laminar texture. **f** Yellow-soft 'decayed stone' from Unit II showing the high porosity texture. The small insets on the right show EDS mapping spectrometry of high content of phosphorus (top) and calcium (bottom). **g** Fossil with highly laminated surface from Unit Vm. The small inset on the left shows the EDS table of chemical element composition, note the high content of phosphorus that should be no more than half that of the calcium in a normal bone analysis. **h** SEM microphotograph of a histological section of a heavily cracked texture of a 'stone like' fossil

Discussion

Presence of Humans in Azokh 1 Cave

Evidence for the presence of humans is recorded in all levels of the excavation in Azokh 1. Fragmentary human fossils have been found of *H. heidelbergensis* from Unit V and *H. neanderthalensis* from Unit II (King et al. 2016), and lithic implements made by humans have also been recovered from all levels of this site (Asryan et al. 2016) together with stone tool induced damage on some of the fossil bone.

Carcasses of animals were dismembered and butchered (cut, sawn and scraped). Once animals were free of meat and skin, bones were broken to extract the marrow. Signs of this human induced breakage are cut marks, impact and percussion marks, peeling, conchoidal scar and adhered bone flakes, and these affect 125 fossils (6.7% of total NR in Azokh 1). The few complete fossils found at the site are skeletal elements with low marrow content, and these were left unbroken by humans. The complete sequence of butchering has been observed on cave bears at Unit II. Higher abundances of cut marks have been distinguished on limbs and axial skeleton. Butchering has also been observed on medium sized animals, but small sized animals have less stone tool induced damage. Burnt bones may be assumed to be the result of human action in Azokh 1, because the excavation area from where the burnt fossils have been recovered is far from the cave entrance and they would be unlikely to have been burnt by natural fires. Unit 1 yielded 72 burnt bones, with 10 burnt in Unit II and five in Unit Vm, making 4.6% of the total NR for the site as a whole.

Chewing by humans was found on a single rib fragment from Unit I (Fernández-Jalvo and Andrews 2011). The ends of the rib were bent during human chewing by pushing up or down on the ends of the bone with the hands and holding the ends between the teeth. This type of damage was named as fraying by Pobiner et al. (2007) and experimentally reproduced in humans (Saladié 2009; Fernández-Jalvo and Andrews 2011; Saladié et al. 2013) and chimpanzees (Pickering and Wallis 1997; Plummer and Stanford 2000).

Carnivore Damage

Carnivore tooth marks have been identified on 120 fossils from Azokh 1 (6.4%), but only 30 of them have tooth marks on their broken edges, which suggests that carnivore action was unimportant in producing the breakage at the site. Pinto and Andrews (2004) and Pinto et al. (2005) have done an extensive study of various sites in the Iberian Peninsula with *Ursus spelaeus* and *Ursus arctos* as part of the faunas. These authors investigated sites that yielded only cave bears (Troskaeta, Tito Bustillo, Eirós, named monospecific) and compared them with sites where other carnivores were found together with bears (cave bears at Arrikrutz and brown bears in a modern natural trap, Sima de los Osos from Somiedo). Rabal-Garcés et al. (2011) applied the same methodology to the site Coro-Tracito (Huesca, Spain) that is also monospecific.

Two of the monospecific sites, Tito Bustillo and Cova Eiros, have been distinguished as denning areas for female cave bears with young (Pinto et al. 2005), and the bones from these two caves have few small chewing marks, but a range of sizes to over 7 mm (Fig. 10.12). A similar pattern is seen for Coro Tracito (Rabal-Garcés et al. 2011), but Troskaeta has a more uniform distribution, although still with many marks greater than 7 mm. Comparison of these sites with Azokh 1 (Fig. 10.12) shows a lower intensity of tooth marks and more limited range of sizes in the Azokh 1 fossil assemblages. Unit I has not yielded any fossil carnivores (except for reworked bear fossils from Unit II brought into Unit I by modern burrowers), but it has provided the highest abundance of chewing marks which are all smaller than 4 mm. This is similar to the fox-ravaged assemblage from Neuadd (Wales) described by Andrews and Armour-Chelu (1998). Unit I has been compared with Atapuerca TD6, where a small canid of similar size to foxes was identified by Díez et al. (1999), although the species may be different. It is likely that the type of carnivore responsible for the chewed bones in Unit I, at that late stage of the cave infilling, was either dogs of the people that inhabited the cave, or wild jackals or foxes which still live in the area today.

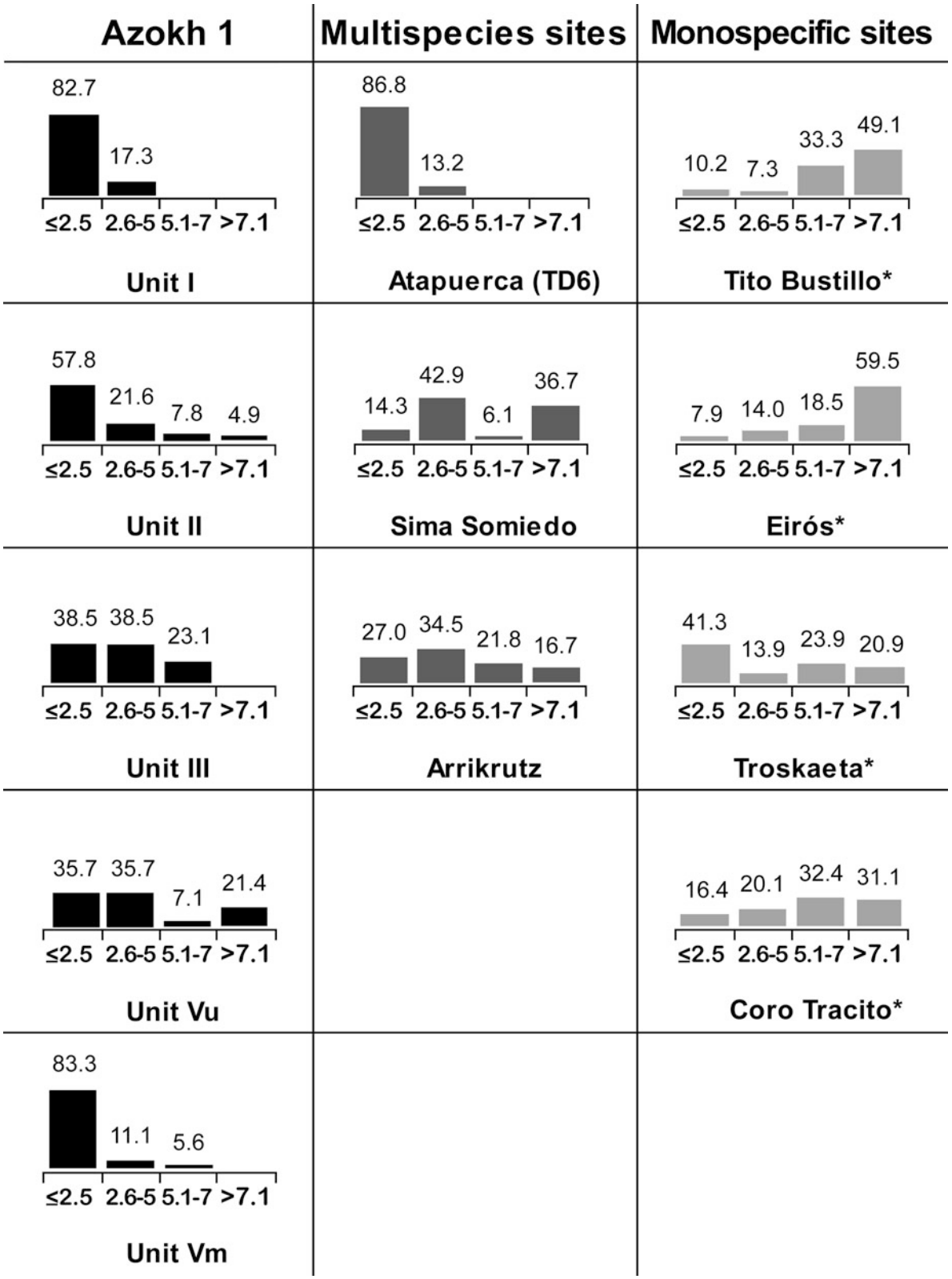

Fig. 10.12 Percentages and size of carnivores tooth marks (width in mm) on fossils from the five stratigraphic units of Azokh 1 compared with different sites from the Iberian Peninsula. Asterisk (*) shows MONOSPECIFIC deposits of *Ursus spelaeus* exclusively. Multispecies sites contains *Ursus spelaeus* and other carnivore species. Data from Iberian sites taken from Díez et al. (1999), Pinto et al. (2005) and Rabal-Garcés et al. (2011)

Table 10.10 XR diffraction results of sediment and fossils. Fossil samples are highlighted in italics

Unit	Stub	Label and remarks	Hydroxylapatite/ (apatites)	Q	Gypsum + bassanite	Calcite	Tinsleyite	Feldspar	Mica	Sepiolite	Amorph
II	110	E48 blackened decayed stone Z = –247	49.00	9.30	–	4.10	–	3.60	3.80	–	30.20
II	111	E48 _crumbly sediment. Z = –247	–	30.80	–	–	28.20	15.20	25.50	–	0.30
II	112	G47 26 Z = –297_crumbly sediment	–	30.60	–	6.40	16.40	18.10	24.40	–	4.10
II	*113*	*G47 26 Z = –297_dusty surface*	*60.50*	*2.50*	*3.30*	*3.80*	–	*7.40*	*5.70*	–	*16.80*
II	115	E48 73 Z = –294_decayed stone	59.80	2.30	–	2.30	–	3.70	4.50	–	27.40
II	116	F47 Z = –277_grey crumbly sediment	–	30.30	–	–	22.20	20.20	24.10	–	3.30
II	117	E47 11 Z = –293 decayed stone	2.00	0.50	–	96.70	–	–	–	–	0.90
II		D46 78 Z = –377 sediment underneath cave bear ulna	27.59	40.13		–		10.05		Sepiolite < 5 – smectite < 5 – Illite 10.05	
II		D45R20 (sediment underneath tooth) Z = –330	–	36.31		30.29		13.29		Sepiolite < 4 – smectite < 3 – Illite 14.13	
II	120	E48 64–75 Z = –295 grey sediment	33.00	2.10	–	49.50	–	2.70	6.70	–	6.10
II	*121*	*F47 34 Z = –287 fossil: brown colour/flaky*	*45.60*	*2.30*	*14.40*	–	*11.40*	*4.70*	*6.10*	–	*15.60*
II	*123*	*F48 128 Z = –290 fossil: flaky surface*	*33.00*	*15.50*	–	–	*13.80*	*12.70*	*14.20*	–	*10.80*
II	*124*	*F47 43 Z = –289 fossil: flaky surface*	*48.50*	*6.80*	*4.00*	–	*10.70*	*5.50*	*9.70*	–	*14.80*
III		D45 54 Z = –495 limestone cave wall	–	<4		96.99		–		–	
III	119	Mixed block sediment rescue 29/07/05–10/08/05 Z = –330 approx	42.80	0.80	–	1.50	–	6.60	4.80	–	43.50
Vu		*E43 GF Z = –624_fossil*	*100*	–		–		–		–	
Vm		E42 11 Z = –846 sediment underneath cervid premolar	21.83	62.97		–		10.57		<5	
Vm		D42 GF Z = –790 sediment block	–	13.79		81.91		–		<5	
Vm	114	F40 8 Z = –850 cave crust	16.80	39.90	–	–	–	7.30	31.80	–	4.20
Vm		E42 9 Z = –845 sediment underneath damaged fossil	<5	90.84		–		–		<5	
Vm	118	F39 7 Z = –857 _28/07/05	31.10	32.00	–	1.90	–	11.60	10.00	11.80	1.60
Vm		*G43 GF Z = –850_fossil*	*100*	–		–		–		–	
Vm		*G43 GF Z < –850 fossil*	*74.81*	*19.94*		–		–		*<5*	
Vm	*122*	*E38 2 Z = –856 fossil: transparent. brown colour*	*56.80*	1.50	–	*4.80*	–	*7.30*	*6.70*	–	*22.80*
Vm		*G40 GF Z < –845_ fossil*	*91.27*	*5.17*		–		–		*<4*	
Vm		*G42 GF Z < –850_ fossil*	*92.24*	*<5*		–		–		*<4*	

With regard to lower units of Azokh 1 (II to Vm), the range of sizes of puncture marks and grooves is diverse (Fig. 10.8), with minimum values (smaller than 4 mm) on compact bone and larger than 7 mm on cancellous tissues. This may be due to either other carnivores involved in the site (felids, canids, or even mustelids, all of which are recorded in the fossil fauna) or to the presence of different sizes of cave bears: adult males are much bigger than females, and juveniles. Azokh 1 puncture marks have a lower abundance and smaller sizes than those recorded at monospecific *U. spelaeus* sites (Pinto and Andrews 2002; Pinto et al. 2005; Rabal-Garcés et al. 2011). The minimum dimension of puncture marks on diaphyses, 'category a' (Fig. 10.8, 'pc'), have mean values ranging from 2.6 to 5.5 mm and maximum values between 4.0 and 8.8 mm. These punctures on diaphyses or compact bone are larger than those produced by any extant carnivore including hyenas (mean 1.5–2.24 and max 2.1), lions (mean 1.1–2.2 and max 2.3) or panthers. On the contrary, pit breadth on epiphyses of the Azokh 1 fossil assemblage (pac 'punctures on articular or on cancellous tissues') and score/groove breadth (gc or gac, minor axis measured in Azokh 1) provide similar or even smaller values than modern lions or hyenas. The maximum size of punctures recorded from Azokh 1 fossils (minor axis/breadth) is 8.8 mm for puncture marks on diaphyses (pc) and 8.7 mm for those on cancellous bone

(pac). A major axis/length of 17 mm was recorded for one tooth print (Fig. 10.7a). These dimensions are too large for lions, for which the maximum records of punctures are 6.3 mm on epiphyses – minor axis – and 8.16 mm on metaphyses – major axis – (Delany-Rivera et al. 2009).

At Azokh 1, the low number of fossils with carnivore chewing marks, the low proportions bone splinters, and low breakage associated with tooth marks all reject the involvement of carnivore bone breakers such as hyenas or wolves at any level of Azokh 1. Lions are not bone crushers. They leave relatively low numbers of tooth marks on bone, produce few bone splinters, and in particular they leave almost no marks on the limbs of the carcasses of their prey (Dominguez-Rodrigo 1999). Cave bears are also not bone crushers. Bone accumulations, documented by Pinto and Andrews (2004) and Pinto et al. (2005), that are comprised solely of cave bears showed percentage completeness ranging from 42 to 84% (Pinto and Andrews 2004). Furthermore, Haynes (1983) observed that bears could occasionally use their cheek teeth and leave characteristic scratches on the shaft resembling those made by rodents: *short and parallel, shallow etched straight score lines* (Haynes 1983, p. 169). Some grooves observed on some fossils from Azokh 1, too far from the edge to be rodent made tooth marks (Fig. 10.7), may fit with this description.

Some differences in the tooth mark sizes can be observed in units from Azokh 1 (Fig. 10.12). Unit Vu in particular is the only unit at Azokh 1 that has a high proportion (21.4%) of tooth marks greater than 7.1 mm, and the distribution of tooth mark sizes is similar to those of Troskaeta and Coro Tracito (Fig. 10.12), which are monospecific sites of cave bears. Unit III has similarities to Arrikrutz (although tooth marks larger than 7.1 mm have not been observed). Arrikrutz is a site where there were mixtures of different sized carnivores chewing the bones, including bears (Pinto and Andrews 2004; Pinto et al. 2005). Units II and Vm (the former with 4.9% of tooth marks greater than 7.1 mm, have distributions of tooth mark sizes similar to that of Unit I with the largest sized tooth marks present, and like Unit I, it is likely that the fossils from Units II and Vm had been chewed by a small carnivores like a fox or jackal and possibly by cave bears as well.

This brings to a controversial subject with regard to the diet of *U. spelaeus*. Physiological studies based on skull, mandible and tooth morphology have inferred a largely herbivorous diet for this cave bear (Kurtén 1976; Mazza et al. 1995; Mattson 1998; Grandal d'Anglade and López-González 2005). Figueirido et al. (2009), however, showed indications of omnivorous diet based on morphometric analyses of the skull and dentition of *U. spelaeus*. Several studies based on isotopic signals (e.g., Bocherens et al. 1994; Fernández 1998; Vila Taboada et al. 1999, 2001; Fernández et al. 2001) provided strong evidence that *Ursus spelaeus* was highly herbivorous. Brown bears, on the other hand, have isotopic signals of pure carnivory in spite of their observed omnivorous diet (Bocherens et al. 1997, 2006). In an analysis of cave bear from a cave in Romania, Richards et al. (2008) found that the cave bear teeth of Pestera cu Oase had higher nitrogen isotope values than seen in herbivores, and they could therefore be considered omnivorous. Dental microwear has also provided evidence of an omnivorous diet before dormancy (Pinto et al. 2005; Peigné et al. 2009). Finally there is the evidence discussed here of cave bear sites which have bones preserved with carnivore tooth marks larger than those of any of the usual makers of tooth marks, such as hyenas and wolves, and which lack evidence of other carnivores being present.

The low rates of chewing marks and near absence of bone splinters excludes hyenas or any other bone crusher carnivore being active at Azokh 1. The large size of tooth marks on bone diaphyses also excludes small carnivores and larger species such as lions, which even though they are not bone breakers, produce smaller sized tooth marks on the bones of their prey. These results from Azokh 1, as well as from other sites that only yielded cave bears, leaves little margin for doubt that in some cases cave bears eat meat and chew bones. Environment impoverishment, extreme climate conditions or just population variability might affect the extent to which cave bears have this behavior in the different sites where *U. spelaeus* is present. Finally, even strict herbivores, such as deer, reindeer, cows or camels, may also chew bones (Sutcliffe 1973, 1977; Brothwell 1976; Johnson 1985), and some populations of deer and fallow deer may do so intensively (Cáceres et al. 2011). This behavior in ungulates stems from nutritional deficiencies in the environment (Grasman and Hellgren 1993). In the case of *U. spelaeus*, even if they are more herbivorous in some areas (e.g., Bocherens et al. 1994; Fernández 1998; Vila Taboada et al. 1999, 2001; Fernández et al. 2001) than others (Pinto and Andrews 2004; Pinto et al. 2005; Rabal-Garcés et al. 2011; Richards et al. 2008), they are less restricted by their dental morphology than deer to a herbivorous diet. Less work has been done on the Middle Pleistocene cave bear (*U. deningeri*), but we have shown that it too probably chewed bones and may have been an habitual scavenger (Andrews and Fernández-Jalvo 1997).

Some fossils from Units II, III and Vu are extremely rounded (Fig. 10.9). Fossil size, shape (Fig. 10.4), orientation, skeletal elements (Voorhies groups, Table 10.4) and bone density (Table 10.3) all exclude transport of bones into

or within the cave. Although friction against the sediment (i.e. trampling) may produce rounding, this occurs in dry conditions and does not smooth the bone edges to the extent seen in these specimens. Trampling may also be discarded because trampling marks are not more abundant on these highly rounded and smoothed edges than on the rest of the bone surfaces (Fig. 10.9b). We have observed, in fact, that earlier modifications, such as tooth mark grooves, have also been smoothed or rounded (white arrows in Fig. 10.9a, c), and so the chewing predated the rounding. Trampling, on the other hand, occurred after the rounding and produced scratches on the rounded surfaces (Fig. 10.9d) and breakage (Fig. 10.9a). Two factors emerge: firstly, examination of the rounded surfaces under high magnification microscopy showed that some areas of these highly rounded bones have a peculiar pattern of parallel microscopic striations (different from microstriations produced by friction against sediment, Fernández-Jalvo and Andrews 2003); and secondly, many of the highly rounded fossils are too large to be ingested. Our interpretation is that these fragments were abraded by oral enzymes and tongue abrasion, and that the rounding could have been the result of bear licking.

Post-Depositional Damage

The most characteristic trait of the Azokh 1 fossil assemblage is breakage, affecting 1619 fossils (86.2% of the fossils from Azokh 1). Breakage has hampered higher taxonomic (even anatomical) identifications and increased the numbers of small fragments (Table 10.1). However, biological agents such as humans or carnivores did not cause this high breakage rate. Neither of these agents has produced a high impact on the fossil assemblages of Azokh 1, as indicated by little evidence of breakage by humans (see Tables 10.6, 10.7 and 10.8) (6.7%) or by carnivores (1.6%). Fire may also contribute to bone breakage (Shipman et al. 1984; Stiner et al. 1995; Mayne 1997; Cáceres et al. 2002), but fire is infrequent at Azokh 1 (4.6%), although all burnt fossils are broken. Trampling has the highest incidence at Azokh 1, although marks on surfaces of fossils have only affected 18.1% of the fossils and 21.1% of broken fossils (Table 10.8).

Post-depositional environmental conditions indicated by mineral deposits (e.g., manganese) and surface modifications (warped-up cracking) on these fossils suggest a damp environment (see below). This is in agreement with the low number of fossils gnawed by rodents in Azokh 1 (NR16, 0.85%). Porcupines chew hard surfaces, such as plastics (Kibii 2009) and bones when they are dry and have lost the greasy periosteum (Brain 1981), and they do this to wear out their ever-growing teeth or to gain minerals from the bone in the same way that herbivores do, but when bone is wet it does not produce the same effect. The location of these marks has no relation to muscle insertions (Rabinovich and Horwitz 1994; Klippel and Synstelien (2007).

Damp environments, high relative humidity and mild temperatures generally are characteristic of inner parts of caves, and these conditions persist today in Azokh 1. Measurements in summer of temperature and relative humidity inside and outside the cave gave a high relative humidity (average 80% compared with 32% outside), but the temperature does not vary, especially sediment temperatures (constantly 19 °C). High humidity may increase the effects of trampling, leaving bones more susceptible to breakage, but we have not investigated this yet. Traits of breakage following Villa and Mahieu's (1991) methodology show high percentages of curved-Vshape outline and smooth edges (Fig. 10.6). These two traits would suggest breakage when bones were fresh (as shown by Villa and Mahieu 1991, for Fontbrégoua site). However, Azokh 1 fossils have a higher abundance of mixed angles on the broken edges that does not fit with Fontbrégoua, Bezouce or Sarrians sites. Broken fragments that have trampling marks have also been analyzed with the same methodology showing high predominance of mixed angles, as well as, curved and smooth edges.

The best explanation for the high breakage recorded in Azokh 1 is tentatively taken to be the combination of high humidity and trampling by large sized animals (*Ursus spelaeus*).

Pre- and Post-Burial Environmental Conditions of Azokh 1 Fossils

Bacterial attack may also increase the fragility of bones. Forensic studies (Bell et al. 1996) indicate that removal of soft parts of the body by scavenging or predation reduces indigenous bacterial attack, stopping or slowing down the dispersal of bacteria through the vascular network. Histological analyses of fossils from Azokh 1 have showed either a very intense bacterial attack (Unit II), or, more frequently, reduced/absent microbial activity. The bacterial attack observed in Unit II (OHI = 0, no original features identifiable other than Haversian canals) has a characteristic organization pattern around histological features (Fig. 10.11a),

which is typical of decay processes. This would suggest that, at least in Unit II, there were intact carcasses that were not eaten by carnivores or butchered by humans. Large bones were found almost complete in some areas (e.g., bear femora), but they were not articulated with the rest of the skeleton but found isolated, often close to cave walls, together with stone tools. Bacteria are absent in fossils from Units I, Vu or Vm, whether as a result of consumption of the carcasses by carnivores or humans, or by the action of fire (in Unit I). On the other hand, Units III, and Vm show evidence of corrosion by fungi.

Some indications about the cave environment may be discerned through histological modifications, although the histological studies have been carried out in a small number of fossils. Successive generations of bacterial colonies have been distinguished in some fossil bones from Unit II that provide some evidence of change in environment in Azokh 1. This succession of bacterial generations has been observed in modern bones monitored in Neuadd (UK) resting in a seasonal river (Fernández-Jalvo et al. 2010a). In the case of Azokh today, there are important variations in the water rate of the cave, becoming extremely humid in summer after the rains and very dry in winter (Domínguez-Alonso, personal communication). Another type of histological damage observed in fossils from Units I, II and Vm affect the canaliculi (histological channels of connection between osteocytes/lacunae). Several fossils from Azokh 1 show enlarged canaliculi, an alteration that has been described by Jans (2005) in a medieval settlement in Moorend farm (UK). Similarly, enlarged canaliculi have also been found in modern bones monitored in open air environments (Fernández-Jalvo et al. 2010a) resting in highly acid soils (pH < 6) under constant high humidity and extensive vegetation (moss and algae). These previous cases of what has now been also observed in Azokh 1 suggest that the histological damage of enlarged canaliculli is related to acidic fluids that penetrate the cortical bone, dissolving the walls of the canaliculi.

In the case of Azokh 1, the site has an acidic environment through the combination of the urea from the bat guano, the high relative humidity in the cave and the damp ground. Fossils from Unit II (central area of excavation) are heavily corroded (flaky and heavily cracked-laminated texture) that affects the entire compact bone. The sediment also has a characteristic crumbly texture and grayish color. Fossils (flaky) and sediment (crumbly) share the presence of tinsleyite in their composition (see Table 10.10). The formation of tinsleyite has been related to the presence of bat guano (Magela da Costa and Rúbia Ribeiro 2001; Marincea et al. 2002; White and Culver 2012). The formation of a wide variety of minerals of the apatite group is frequent in caves and related to urea and bat guano (White and Culver 2012). The presence of brushite has also been mentioned as neoformed mineral by bone decay (Molleson 1990). According to this author, the hydroxylapatite (bone mineral component) is unstable in conditions of high acidity and transform into brushite during decay. The effect of this transformation is very destructive, for brushite occupies a space much larger than the crystals of hydroxylapatite, so when this transformation occurs, the original molecular structure suffers a physical destruction (Molleson 1990). The formation of barite [$Ba(SO_4)$] is also common in conditions of high acidity and associated with microbial activity. Its formation is less destructive to bone because barite fills histological empty spaces, or secondary porosity.

A common feature of fossils from Azokh 1, Azokh 2 and Azokh 5 is the absence of collagen (Smith et al. 2016). This absence has been observed even in bone remains from Holocene periods in Unit I, which did not contain enough carbon to be dated by ^{14}C (Ditchfield, personal communication, see Appendix, radiocarbon). The destruction of collagen at Azokh 1 (Smith et al. 2016) occurs according to a model described by Smith et al. (2002), characterized by a high bone crystallinity, almost no histological damage, but sudden removal of collagen in a very short time. The cause of such destruction of collagen is not known (Smith et al. 2002), but in the case of Azokh it also seems to affect DNA preservation, or lack of it. Indeed, as mentioned by Bennett et al. (2016), attempts to PCR amplify DNA from many fossils and sediment samples from all units of the sites Azokh 1, 2 and 5 have failed. The common element in all these areas of the cave system is the presence of guano and, at least in the case of Azokh, the explanation for this widespread loss of collagen appears to be due to this agent.

The distribution of areas of alteration in the center of the Unit II is seen today in the interior of the cave inhabited by bats. This distribution suggests that populations of bats occupied areas closer to the entrance of the cave, and conditions would have resembled those we find today in the interior of the gallery where bats live permanently, with thick accumulations of guano may reach up to 3 m thick. Water filtering through cracks of the cave carried highly acidic fluids, rich in phosphates, sulfates and carbonates dissolved from the guano, through the sediments. Depending on the conditions of the cave (moments of aridity vs. increase in humidity), different sets of minerals would be formed, some of them very aggressive to the hydroxylapatite mineral component of the bone. Brushite, for instance, is one of the most common cave minerals in guano deposits, formed at low pH by reaction of phosphate-rich solutions

with calcite, clay and bone. Its formation affects the bone structure, and we have also seen that tinsleyite, and probably sepiolite, may also destroy the bone structure. High humidity and guano has produced the conditions for the high corrosion observed in these fossils, especially at Unit II.

The duration of these sealed conditions that led to the occupation of populations of bats in this part of the cave cannot be established, but it was long enough to allow fluid percolation, mineralization and corrosion took place, reaching several meters deep through the sediment. Evidence of corrosive fluids percolation is still recorded in the section on top of Unit II (Fig. 10.8b). The time gap between Unit II (Pleistocene ~100 kyr) and Unit I (Holocene) and the laminar sedimentation observed on the limit between these two units (Fig. 10.8c) suggest the involvement of water erosion that ended by flooding the substrate. It is likely that an episode of heavy rains and flash floods, removed the upper part of the Pleistocene sediments by erosion. This event opened the cave again to the outside environment, and allowed the entry and cave occupation by animals and humans during Holocene.

Human occupations of caves are usually more frequent near cave entrances, and bears are more frequent at the back of the cave where they may hibernate. Sediments closer to the entrance had already been excavated, however, and no information was available to us. On the other hand, the back area of the cave is a more suitable area for bear hibernation, and bear fossils are more abundant in this part of the cave than at the cave entrance and were exposed to the damp acidic conditions. This situation suggests to us that the actual butchery processes were concentrated on bears, while other large mammal carcasses could also be butchered, but not in this part of the cave.

This opens an interesting discussion about the behavior and type of occupation of these extinct cave bears (*Ursus spelaeus*), whether for example they lived more permanently in the cave than only during hibernation. Probably, bears were not in the cave during summer, as the cave becomes wetter during this period after the rains. Humans could then shelter in the cave at the entrance in summer time and eventually penetrate into the cave interior. Another question is the capacity of bears to scavenge other bear remains or at least to chew bones. Chewing marks on the fossils of Azokh 1 and breakage by carnivore action are scarce, and there is no taphonomic evidence of hyenas taking any part of the bone accumulations. The maximum size of puncture marks on diaphyses/compact bone in two units of Azokh 1 exceeds any recorded chewing by larger carnivores, such as lions (Pinto et al. 2005; Domínguez-Rodrigo and Piqueras 2003; Pobiner 2008). These are Unit II and Unit Vu, and in the absence of a better candidate, we propose that cave bears have damaged and chewed other bones during deposition of these two units. Unit I, on the other hand, lacks large chewing marks (<4 mm) and have a pattern suggesting scavenging by a small carnivore such as a fox or jackal. Unit Vm fossils have tooth marks larger than 4 mm, but with a similar pattern to those in Unit I, and the pattern in Unit III is close to the multispecies site of Arrikrutz (see Fig. 10.12). These patterns would suggest that together with cave bears, smaller carnivores were scavenging.

Another possibility is that bears carried bones from previous human occupations at the entrance, where abandoned bone remains were lying on the floor, into the rear of the cave where the bears were living. Comparing the rear of the cave environment in the past to what it is like today suggests that the back of the cave had almost permanent high relative humidity and seasonally (summer-autumn) damp substrate. Seasonal dampness in the cave is indicated by the formation of cave minerals characteristic of both wet and dry caves, modifications observed on the surface of the fossils (cracks by humidity) and successive stages of bacterial attack. In this context, trampling under wet conditions could greatly increase breakage. If the cave was dry in winter, as seen today, the intense trampling observed on bones (as well as on lithics, see Asryan et al. 2016), and the resulting high breakage rate, suggests that bears were occupying the cave for longer periods than just while hibernating, extending the occupation to autumn and spring. With further analysis and larger samples, it may be possible to investigate the nature of the cave bears populations, whether all males, or females with their young, were alternately using the cave as a den: there is an indication from variations in tooth mark sizes (Fig. 10.10) that it was occupied by both at different times, the presence of very large tooth marks being the product of male-only occupation, and variation in size being the product of females with yearling young (Kurten 1958; Andrews and Turner 1992).

Conclusions: Site Formation and Background Scenario

1. The location of the fossiliferous sediments studied here is at the back of the Azokh 1 cave entrance, about 40 meters from the contact with the open air. This situation limits the taphonomic history typical taphonomic karstic agents.

2. Large mammal fossils, other than bears, recorded at the back of the cave show signs of human activity, but do not show a clear pattern that may indicate which type of human occupation took place.
3. Small and medium sized animal skeletons are sparse and incomplete, suggesting an anomalous carcass selection, skin removal and butchery technique. More complete and typical sequences of butchery have been observed on bear fossils, but even here many parts of the skeleton are absent and large bones unbroken.
4. Human occupations of caves are usually more frequent near cave entrances, and bears are more frequent at the back of the cave where they may hibernate. Sediments closer to the entrance had already been excavated, however, and no information was available to us. On the other hand, the back area of the cave is a more suitable area for bear hibernation, and bear fossils are more abundant in this part of the cave than at the cave entrance. This situation suggests to us that the actual butchery processes were concentrated on bears, while other large mammal carcasses could also be butchered, but not in this part of the cave.
5. Chewing marks on the fossils of Azokh 1 and breakage by carnivore action are scarce, and there is no taphonomic evidence of hyenas taking any part of the bone accumulations. The maximum size of puncture marks on diaphyses/compact bone in two units of Azokh 1 exceeds any recorded chewing by other large carnivores, and it is likely that cave bears have damaged and chewed other bones during deposition of Units II and Vu.
6. Unit I, on the other hand, lacks large chewing marks and have a pattern suggesting scavenging by a small carnivore such as a fox or jackal. Unit Vm fossils have tooth marks larger than 4 mm, but with a similar pattern to those in Unit I, and the pattern in Unit III is close to the multi-species site of Arrikrutz (see Fig. 10.12). These patterns would suggest that together with cave bears, smaller carnivores were scavenging the bones in these units.
7. The cave bears may have carried bones from previous human occupations at the entrance to the rear of the cave.
8. Seasonal dampness in the cave is indicated by the formation of cave minerals characteristic of both wet and dry caves, modifications observed on the surface of the fossils (cracks by humidity) and successive stages of bacterial attack. In this context, trampling under wet conditions could greatly increase breakage.
9. The distribution of areas of alteration in the center of the Unit II is seen today in the interior of the cave inhabited by bats. Accumulations of guano in a damp environment would produce highly acidic fluids (rich in phosphates, sulfates and carbonates dissolved from the guano) percolating through the sediments. Several minerals identified in fossils, sediments and stones are associated with guano breakdown (e.g., brushite, monetite, ardealite, gypsum, sepiolite, tinsleyite).
10. Depending on the conditions of the cave (moments of aridity vs. increase in humidity), different sets of minerals could be formed, some of them very aggressive to the hydroxylapatite mineral component of the bone. High humidity and guano has produced the conditions for the high corrosion observed in these fossils, especially at Unit II.
11. The time gap between Unit II (Pleistocene $\sim$100 kyr) and Unit I (Holocene) and the laminar sedimentation observed on the limit between these two units (Fig. 10.8c) suggest the involvement of water erosion that ended by flooding the substrate. It is likely that an episode of heavy rains and flash floods, removed the upper part of the Pleistocene sediments (formerly deposited almost reaching the roof of the cave) by erosion. This event opened the cave again to the outside environment, and allowed the entry and cave occupation by animals and humans during the Holocene.
12. With further analysis and larger samples, it may be possible to investigate if cave bears males and females with their young were alternately using the cave as a den: there is an indication from variations in tooth mark sizes (Fig. 10.10) that it was occupied by all male groups in some cases, and by females with young in others (Kurten 1958; Andrews and Turner 1992).

Acknowledgements This chapter is based in part on the PhD Thesis investigation by DMM. We are deeply grateful to the authorities of Nagorno-Karabakh for the support and permissions to work at Azokh Caves and to analyze these fossils. We are grateful to Manuel Nieto who has greatly helped with the statistical treatments of this extensive data base, as well as to M.D. Pesquero for taphonomic discussions. Thanks also to Jesús Muñoz and Fernando Señor of the Photo Unit of the Museo Nacional de Ciencias Naturales. We also thank the EMUnit, Laura Tormo, Marta Furió, and Alberto Jorge, as well as Rafael Gómez (XRD analyses) for their professional work and deep involvement in the analysis of some of these samples. The authors are grateful for constructive comments from the three anonymous reviewers and the editor in charge (Tania King) which greatly improved this chapter. These taphonomic investigations have been made possible through funded research projects by the Spanish Ministry of Science (BTE2000-1309, BTE2003-01552, BTE 2007-66231 and CGL2010-19825).

Supplementary Information

S.I. Table 10.1 Anatomical elements per animal sized groups in Unit I, plus 20 unidentified fragments that cannot be even assigned to animal size. Two fossils of *U. spelaeus* (one incisor (I3) and a femur fragment) were recovered from the modern burrows in Unit I that originated from Unit II

Unit I	Large sized				Medium sized				Small sized			
	NR	NISP	NME	Ri	NR	NISP	NME	Ri	NR	NISP	NME	Ri
Horns/Antlers					1	1	1	16.7				
Skull + maxilla									2	2	1	20.0
Mandible					1	1	1	25.0	2	2	2	40.0
Isolated teeth									6	6	6	3.5
Hyoid												
Vertebrae	2	2	2	6.3	3	3	2	1.7	3	3	2	1.4
Rib	3	3	1	2.8	1	1	1	0.9	5	5	2	1.5
Sternum												
Clavicle												
Scapula					5	5	2	25.0	1	1	1	10.0
Pelvis												
Baculum												
Humerus	1	1	1	50.0	1	1	1	12.5				
Radius												
Ulna									1	1	1	10.0
Femur					1	1	1	12.5	1	1	1	10.0
Patella												
Tibia					1	1	1	12.5				
Fibula									1	1	1	10.0
Carpal/Tarsal					2	2	2	2.2				
Metapodial					4	4	2	12.5	3	3	1	3.1
Phalanx	2	2	2	16.7					1	1	1	0.7
Malleolus												
Sesamoid												
Long bone	15				56				21			
Flat bone	1											
Articular bone					1							
Total	24	8	6	3.3	77	20	14	1.9	47	26	19	1.9
MNI	1				4				5			

NR = number of remains; NISP = number of identified specimens; MNE = minimum number of elements; Ri = relative abundance per element (i); MNI = minimum number of individuals (* includes unidentified MNI, that make extra individuals from the taxonomically identified assigned individuals)

S.I. Table 10.2 Anatomical elements per animal sized groups in Unit II, plus 336 unidentified fragments that cannot be assigned to animal size

Unit II	Large sized				Medium sized				Small sized			
	NR	NISP	NME	Ri	NR	NISP	NME	Ri	NR	NISP	NME	Ri
Horns/Antlers					4	4	1	16.7				
Skull + maxilla	13	13	5	71.4	1	1	1	25.0	1	1	1	12.5
Mandible	14	14	6	85.7	1	1	1	25.0	3	3	2	25.0
Isolated teeth	32	32	23	10.8	1	1	1	0.7	3	3	3	1.1
Hyoid	2	2	1	14.3					1	1	1	12.5
Vertebrae	52	52	30	13.3	16	16	9	8.0	4	4	4	1.8
Rib	21	21	9	4.6	27	27	11	10.4	10	10	4	1.9
Sternum												
Clavicle												
Scapula	6	6	4	28.6	1	1	1	12.5				
Pelvis	5	5	3	42.9	2	2	1	25.0				
Baculum	3	3	6	50.0								
Humerus	10	10	5	35.7	2	2	1	12.5				
Radius	7	7	5	35.7					1	1	1	6.3
Ulna	10	10	4	28.6	2	2	1	12.5				
Femur	14	14	8	57.1								
Patella	4	4	4	28.6					1	1	1	6.3
Tibia	13	13	4	28.6	1	1	1	12.5				
Fibula	12	12	5	35.7	2	2	2	25.0	1	1	1	6.3
Carpal/Tarsal	35	35	35	18.4	2	2	2	2.1	4	4	4	2.1
Metapodial	26	26	24	19.4	3	3	3	10.7	3	3	2	2.5
Phalanx	37	37	35	9.7	2	2	2	1.7	2	2	2	0.7
Malleolus												
Sesamoid												
Long bone	142				99				40			
Flat bone	5				6							
Articular bone	3								2			
Total	466	316	216	12.1	172	67	38	4.6	76	34	26	1.5
MNI	7				4 (1*)				8			

NR = number of remains; NISP = number of identified specimens; MNE = minimum number of elements; Ri = relative abundance per element (i); MNI = minimum number of individuals (* includes unidentified MNI, that make extra individuals from the taxonomically identified assigned individuals)

S.I. Table 10.3 Anatomical elements per animal sized groups in Unit III, including 34 unidentified fragments that cannot be assigned to animal size

Unit III	Large sized				Medium sized				Small sized			
	NR	NISP	NME	Ri	NR	NISP	NME	Ri	NR	NISP	NME	Ri
Horns/Antlers					1	1	1	50.0				
Skull + maxilla	1	1	1	25.0	2	2	2	100.0				
Mandible	1	1	1	25.0	1	1	1	50.0				
Isolated teeth	5	5	5	4.1	2	2	2	2.6				
Hyoid	1	1	1	25.0								
Vertebrae	10	10	4	3.1	1	1	1	1.8	1	1	1	1.2
Rib	2	2	1	0.9	7	7	2	3.7	5	5	1	1.3
Sternum	1	1	1	25.0								
Clavicle												
Scapula												
Pelvis	3	3	1	25.0								
Baculum	1	1	1	33.3								
Humerus	1	1	1	12.5								
Radius	1	1	1	12.5								

(continued)

S.I. Table 10.3 (continued)

Unit III	Large sized				Medium sized				Small sized			
	NR	NISP	NME	Ri	NR	NISP	NME	Ri	NR	NISP	NME	Ri
Ulna	2	2	2	25.0	1	1	1	25.0				
Femur												
Patella					1	1	1	25.0				
Tibia	1	1	1	12.5								
Fibula	3	3	2	25.0								
Carpal/Tarsal	7	7	7	6.6	1	1	1	1.9				
Metapodial	7	7	7	10.9	2	2	1	5.0				
Phalanx	4	4	4	2.1	3	3	3	4.2	3	1	1	0.8
Malleolus	1	1	1	50.0								
Sesamoid												
Long bone	10				15				1			
Flat bone												
Articular bone												
Total	62	52	42	4.3	37	22	16	3.6	10	7	3	0.4
MNI	4				2 (1*)				2 (1*)			

NR = number of remains; NISP = number of identified specimens; MNE = minimum number of elements; Ri = relative abundance per element (i); MNI = minimum number of individuals (* includes unidentified MNI, that make extra individuals from the taxonomically identified assigned individuals)

S.I. Table 10.4 Anatomical elements per animal sized groups in Unit Vu, plus 18 unidentified fragments that cannot be assigned to animal size

Unit Vu	Large sized				Medium sized				Small sized			
	NR	NISP	NME	Ri	NR	NISP	NME	Ri	NR	NISP	NME	Ri
Horns/Antlers					2	2	1	16.7		0	0	0.0
Skull + maxilla	1	1	1	33.3	1	1	1	33.3				
Mandible					3	3	3	100.0	3	3	3	42.9
Isolated teeth	7	7	7	8.3	4	4	4	4.2	4	4	4	1.7
Hyoid												
Vertebrae	6	6	4	4.2	4	4	3	3.6	1	1	1	0.5
Rib	4	4	2	2.2	6	6	2	2.6	5	5	2	1.1
Sternum												
Clavicle												
Scapula	2	2	2	33.3	1	1	1	16.7				
Pelvis					1	1	1	33.3	1	1	1	14.3
Baculum												
Humerus									1	1	1	7.1
Radius	1	1	1	16.7								
Ulna												
Femur	1	1	1	16.7								
Patella												
Tibia									2	2	2	14.3
Fibula	1	1	1	16.7								
Carpal/Tarsal	3	3	3	3.5	2	2	2	3.0				
Metapodial	4	4	4	7.4	4	4	3	25.0	1	1	1	1.3
Phalanx	7	7	7	4.7								
Malleolus												
Sesamoid	1	1	1	0.8	1	1	1	1.4				
Long bone	15				45				8			
Flat bone					1							
Articular bone												
Total	53	38	34	4.5	75	29	22	4.0	26	18	15	1.0
MNI	3				2 (1*)				7			

NR = number of remains; NISP = number of identified specimens; MNE = minimum number of elements; Ri = relative abundance per element (i); MNI = minimum number of individuals (* includes unidentified MNI, that make extra individuals from the taxonomically identified assigned individuals)

S.I. Table 10.5 Anatomical elements per animal sized groups in Unit Vm, plus 82 unidentified fragments that cannot be even assigned to animal size

Unit Vm	Large sized				Medium sized				Small sized			
	NR	NISP	NME	Ri	NR	NISP	NME	Ri	NR	NISP	NME	Ri
Horns/Antlers					3	3	1	12.5				
Skull + maxilla	2	2	1	16.7	1	1	1	20.0	5	5	2	33.3
Mandible	1	1	1	16.7					4	4	2	33.3
Isolated teeth	25	25	21	11.8	13	13	9	5.2	7	7	7	3.3
Hyoid												
Vertebrae	1	1	1	0.5	5	5	2	1.4	1	1	1	0.6
Rib	4	4	2	1.0	7	7	2	1.5	12	12	4	2.5
Sternum												
Clavicle												
Scapula									2	2	2	16.7
Pelvis					1	1	1	20.0				
Baculum												
Humerus	2				1	1	1	10.0	1	1	1	8.3
Radius	1	1	1	8.3								
Ulna					1	1	1	10.0	1	1	1	8.3
Femur									2	2	2	16.7
Patella												
Tibia												
Fibula												
Carpal/Tarsal	2	2	2	1.2	2	2	2	1.7	1	1	1	0.7
Metapodial	3	3	2	2.2	5	5	4	12.5	3	3	1	1.4
Phalanx	7	7	7	2.8	3	3	3	2.1	4	4	4	1.7
Malleolus												
Sesamoid	1	1	1	0.5	1	1	1	0.7				
Long bone	20				61				38			
Flat bone					1				2			
Articular bone	2								3			
Total	71	47	39	2.7	105	43	28	2.8	86	43	28	2.1
MNI	6				5 (1*)				6			

NR = number of remains; NISP = number of identified specimens; MNE = minimum number of elements; Ri = relative abundance per element (i); MNI = minimum number of individuals (* includes unidentified MNI, that make extra individuals from the taxonomically identified assigned individuals)

References

Andrews, P. (1990). *Owls, caves and fossils*. London: Natural History Museum.

Andrews, P. (1995). Experiments in taphonomy. *Journal of Archaeological Science, 22*, 147–153.

Andrews, P., & Armour-Chelu, M. (1998). Taphonomic observations on a surface bone assemblage in a temperate environment. *Bulletin of the Geological Society of France, 169*, 433–442.

Andrews, P., & Cook, J. (1985). Natural modifications to bones in a temperate setting. *Man (N.S.) 20*, 675–691.

Andrews, P., & Fernández-Jalvo, Y. (1997). Surface modifications of the Sima de los Huesos fossil humans. *Journal of Human Evolution, 33*, 191–217.

Andrews, P., & Turner, A. (1992). Life and death of the Westbury bears. *Annales Zoologici Fennici, 28*, 139–149.

Andrews, P., & Whybrow, P. (2005). Taphonomic observations on a camel skeleton in a desert environment in Abu Dhabi. *Palaeontologia Electronica*. http://palaeo-electronica.org/paleo/2005_1/andrews23/issue1_05.htm.

Andrews, P., Hixson A. S., King, T., Fernández-Jalvo, Y., & Nieto-Díaz, M. (2016). Palaeoecology of Azokh 1. In Y. Fernández-Jalvo, T. King, L. Yepiskoposyan & P. Andrews (Eds.), *Azokh Cave and the Transcaucasian Corridor* (pp. 305–320). Dordrecht: Springer.

Appendix: Fernández-Jalvo, Y., Ditchfield, P., Grün, R., Lees, W., Aubert, M., Torres, T., et al. (2016). Dating methods applied to Azokh cave sites. In Y. Fernández-Jalvo, T. King, L. Yepiskoposyan & P. Andrews (Eds.), *Azokh Cave and the Transcaucasian Corridor* (pp. 321–339). Dordrecht: Springer.

Asryan, L., Moloney, N., & Ollé, A. (2016). Lithic assemblages recovered from Azokh 1. In Y. Fernández-Jalvo, T. King, L. Yepiskoposyan & P. Andrews (Eds.), *Azokh Cave and the Transcaucasian Corridor* (pp. 85–101). Dordrecht: Springer.

Behrensmeyer, A. K. (1975). The taphonomy and paleoecology of Plio-Pleistocene vertebrate assemblages east of Lake Rudolf, Kenya. *Bulletin of the Museum of Comparative Zoology, 146*, 473–578.

Behrensmeyer, A. K. (1978). Taphonomic and ecologic information from bone weathering. *Paleobiology, 4*, 150–162.

Behrensmeyer, A. K., & Hill, A. (1981). *Fossils in the making*. Chicago: University Chicago Press.

Behrensmeyer, A. K., Gordon, K. D., & Yanagi, G. T. (1986). Trampling as a cause of bone surface damage and pseudo cutmarks. *Nature, 319*, 768–771.

Bell, L. S. (1990). Paleopathology and diagenesis: An SEM evaluation of structural changes using backscattered electron imaging. *Jorunal of Archaeological Science, 17*, 85–102.

Bell, L. S., Skinner, M. F., & Jones, S. J. (1996). The speed of postmortem change to the human skeleton and its taphonomic significance. *Forensic Science International, 82*, 129–140.

Bennett, E. A., Gorgé, O., Grange, T, Fernández-Jalvo, Y., & Geigl, E. M. (2016) Coprolites, paleogenomics and bone content analysis. In Y. Fernández-Jalvo, T. King, L. Yepiskoposyan & P. Andrews (Eds.), *Azokh Cave and the Transcaucasian Corridor* (pp. 271–286). Dordrecht: Springer.

Binford, L. R. (1981). *Bones, ancient men and modern myths*. New York: Academic Press.

Blasco, R., Rosell, J. Fernández, Peris, J., Cáceres, I., & Vergès, J. M. (2008). A new element of trampling: An experimental application on the Level XII faunal record of Bolomor Cave (Valencia, Spain). *Journal of Archaeological Science, 35*, 1605–1618.

Blott, S. J., & Pye, K. (2008). Particle shape: A review and new methods of characterization and classification. *Sedimentology, 55*, 31–63.

Blumenschine, R. J. (1986). *Early Hominid Scavenging Opportunities: Implications of Carcass Availability in the Serengeti and Ngorongoro Ecosystems*. International Series *283*. Oxford: British Archaeological Reports.

Blumenschine, R. J. (1988). An experimental model of the timing of hominid and carnivore influence on archaeological bone assemblages. *Journal of Archaeological Science, 15*, 483–502.

Blumenschine, R. J. (1995). Percussion marks, tooth marks, and experimental determinations of the timing of hominid and carnivore access to long bones at FLK *Zinjanthropus*, Olduvai Gorge, Tanzania. *Journal of Human Evolution, 29*, 21–51.

Blumenschine, R. J., & Selvaggio, M. M. (1988). Percussion marks on bone surfaces as a new diagnostic on hominid behavior. *Nature, 333*, 763–765.

Boaz, N. T. (1982). American research on australopithecines and early Homo, 1925–1980. In F. Spencer (Ed.), *A history of american physical anthropology, 1930–1980* (pp. 239–260). New York: Academic.

Boaz, N. T., & Behrensmeyer, A. K. (1976). Hominid taphonomy: Transport of human skeletal parts in an artificial fluviatile environment. *American Journal of Physical Anthropology, 45*, 53–60.

Bocherens, H., Fizet, M., & Mariotti, A. (1994). Diet, physiology and ecology of fossil mammals as inferred from stable carbon and nitrogen isotope biogeochemistry: Implications for Pleistocene bears. *Palaeogeography, Palaeoclimatology, Palaeoecology, 107*, 213–225.

Bocherens, H., Billiou, D., Patou-Mathis, M., Bonjean, D., Otte, M., & Mariotti, A. (1997). Paleobiological implications of the isotopic signatures (^{13}C,^{15}N) of fossil mammal collagen in Scladina Cave (Sclayn, Belgium). *Quaternary Research, 48*, 370–380.

Bocherens, H., Drucker, D. G., Billiou, D., Geneste, J.-M., & van der Plicht, J. (2006). Bears and Humans in Chauvet Cave (Vallon-Pont-d'Arc, Ardèhe, France): Insights from stable isotopes and radiocarbon dating of bone collagen. *Journal of Human Evolution, 50*, 370–376.

Bonnichsen, R. (1979). *Pleistocene bone technology in the beringian refugium*. *Mercury series 89*. Ottawa: National Museum of Man.

Brain, C. K. (1969). The contribution of Namib desert Hottentots to an understanding of australopithecine bone accumulations. *Scientific Papers of the Namib Desert Research Station, 39*, 13–22.

Brain, C. K. (1981). *The hunters or the hunted? An introduction to African Cave taphonomy*. Chicago: University of Chicago Press.

Britt, B. B., Scheetz, R. D., & Dangerfield, A. (2005) Jurassic dinosaurs and insects: The paleoecological role of Termites as carcass feeders. *Geological Society of America* 2005 Salt Lake City Annual Meeting (October 16–19, 2005).

Britt, B. B., Scheetz, R. D., & Dangerfield, A. (2008). A suite of dermestid beetle traces on dinosaur bone from the Upper Jurassic Morrison Formation, Wyoming, USA. *Ichnos, 15*, 59–71.

Bromage, T. G., & Boyde, A. (1984). Microscopic criteria for the determination of directionality of cutmarks on bone. *American Journal of Physical Anthropology, 65*, 357–366.

Brothwell, D. (1976). Further evidence of bone chewing by ungulates: The sheep of North Ronaldsay, Orkney. *Journal of Archaeological Science, 3*, 179–182.

Bunn, H. T. (1983). Evidence on the diet and subsistence patterns of Plio-Pleistocene hominids at Koobi Fora, Kenya, and Olduvai Gorge, Tanzania. In J. Clutton-Brock & C. Grigson (Eds.) *Animals and Archaeology* (Vol. 163, pp. 21–30). International Series. Oxford: British Archaeological Reports.

Cáceres, I. (2002). Tafonomía de yacimientos antrópicos en Karst. Complejo Galería (Sierra de Atapuerca, Burgos), Vanguard Cave (Gibraltar) y Abric Romaní (Capellades, Barcelona). PhD dissertation, Universitat Rovira i Virgili.

Cáceres, I., Bravo, P., Esteban, M., Expósito, I., & Saladié, P. (2002). Fresh and heated bones breakage. An experimental approach. In M. De Renzi, M.V. Pardo Alonso, M. Belinchón, E. Peñalver, P. Montoya, A. Márquez-Aliaga (Eds.), *Current Topics on Taphonomy and Fossilization* (pp. 471–479). Valencia: Ayuntamiento de Valencia.

Cáceres, I., Esteban-Nadal, M., Bennàsar, M., & Fernández-Jalvo, Y. (2011). Was it the deer or the fox? *Journal of Archaeological Science, 38*, 2767–2774.

Capaldo, S. D. (1995). Inferring hominid and carnivore behaviour from dual patterned archaeofaunal assemblages. PhD dissertation, Rutgers University, New Brunswick, New Jersey.

Capaldo, S. D. (1997). Experimental determinations of carcass processing by Plio-Pleistocene hominids and carnivores at FLK 22 (*Zinjanthropus*), Olduvai Gorge, Tanzania. *Journal of Human Evolution, 33*, 555–597.

Capaldo, S. D. (1998). Methods, marks, and models for inferring hominids and carnivore behavior. *Journal of Human Evolution, 35*, 323–326.

Delaney-Rivera, C., Plummer, T. W., Hodgson, J. A., Forrest, F., Hertel, F., & Oliver, J. S. (2009). Pits and pitfalls: Taxonomic variability and patterning in tooth mark dimensions. *Journal of Archaelogical Science, 36*, 2597–2608.

Denys, C., Fernández-Jalvo, Y., & Dauphin, Y. (1995). Experimental taphonomy: Preliminary results of the digestion of micromammal bones in laboratory. *Comptes Rendues de l'Academie Scientifique*, série II a (Paris), *321*, 803–809.

Denys, C., Schuster, M., Guy, F., Mouchelin, G., Vignaud, P., Viriot, L., et al. (2007). Taphonomy in present day desertic environment: The case of the Djourab (Chad) Plio-Pleistocene deposits. *Journal of Taphonomy, 5*, 177–204.

Díez, J. C., Fernández-Jalvo, Y., Rosell, J., & Cáceres, I. (1999). Zooarchaeology and taphonomy of Aurora stratum (Gran Dolina, Sierra de Atapuerca, Spain). *Journal of Human Evolution, 37*, 623–652.

Dodson, P. (1973). The significance of small bones in paleoecological interpretation. *Contributions to Geology, University of Wyoming, 12*, 15–19.

Domínguez-Rodrigo, M. (1997). Meat-eating by early hominids at the FLK 22 Zinjanthropus site, Olduvai Gorge (Tanzania): An experimental approach using cut-mark data. *Journal of Human Evolution, 33*, 669–690.

Domínguez-Rodrigo, M. (1999). Flesh availability and bone modifications in carcasses consumed by lions: Palaecological relevance in

hominid foraging patterns. *Palaeogeography, Palaeoclimatology, Palaeoecology, 149*, 373–388.

Domínguez-Rodrigo, M., & Barba, R. (2006). New estimates of tooth mark and percussion mark frequencies at the FLK Zinj site: The carnivore-hominid-carnivore hypothesis falsified. *Journal of Human Evolution, 50*, 170–194.

Domínguez-Rodrigo, M., & Piqueras, A. (2003). The use of tooth pits to identify carnivore taxa in tooth-marked archaeofaunas and their relevance to reconstruct hominid carcass processing behaviours. *Journal of Archaelogical Science, 30*, 1385–1391.

Dominguez-Rodrigo, M., de Juana, S., Galan, A., & Rodriguez, M. (2009). A new protocol to differentiate trampling marks from butchery marks. *Journal of Archaeological Science, 36*, 2643–2654.

Efremov, I. A. (1940). Taphonomy: New branch of paleontology. *Pan-American Geologist, 74*, 81–93.

Efremov, I. A. (1950). Taphonomy and geological annals. Book 1. Burial of terrestrial fauna in the Paleozoic. *Trudy Paleontologicheskogo instituta AN SSSR*, vol. 24, pp. 1–177. (*in Russian*). Translated in 1953 in *Annales du Centre d'Études et de Documentation Paléontologiques*, *4*, 1–196.

Egeland, A. G., Egeland, C. P., & Bunn, H. T. (2008). Taphonomic analysis of a modern spotted hyena (*Crocuta crocuta*) den from Nairobi. *Kenya. Journal of Taphonomy, 6*(3–4), 301–335.

Fernández, D. (1998). Biogeoquímica isotópica (^{13}C, ^{15}N) del *Ursus Spelaeus* del yacimiento de Cova Eiró s, Lugo. *Cadernos do Laboratorio Xeolóxico de Laxe, 23*, 237–249.

Fernández, D., Vila, M., & Grandal, A. (2001). Stable isotopes data (delta ^{13}C, delta ^{15}N) from the cave bear (*Ursus spelaeus*): A new approach to its palaeoenvironment and dormancy. *Proceedings of the Royal Society of Biological Sciences, 268B*, 1159–1164.

Fernández-Jalvo, Y., & Andrews, P. (2003). Experimental effects of water abrasion on bone fragments. *Journal of Taphonomy, 1*(3), 147–163.

Fernández-Jalvo, Y., & Andrews, P. (2011). When humans chew bones. *Journal of Human Evolution, 60*, 117–123.

Fernández-Jalvo, Y., & Andrews, P. (2016). *Atlas of Taphonomic Identifications.* Dordrecht: Springer.

Fernández-Jalvo, Y., & Marin-Monfort, M. D. (2008). Experimental taphonomy in museums: Preparation protocols for skeletons and fossil vertebrates under the scanning electron microscopy. *Geobios, 41*(1), 157–181.

Fernández-Jalvo, Y., Denys, C., Andrews, P., Williams, C. T., Dauphin, Y., & Humphrey, L. (1998). Taphonomy and palaeoecology of Olduvai Bed-I (Pleistocene, Tanzania). *Journal of Human Evolution, 34*, 137–172.

Fernández-Jalvo, Y., Sánchez Chillón, B., Andrews, P., Fernández-López, S., & Alcalá Martínez, L. (2002). Morphological taphonomic transformations of fossil bones in continental environments, and repercussions on their chemical composition. *Archaeometry, 44*(3), 353–361.

Fernández-Jalvo, Y., Andrews, P., Pesquero, D., Smith, C., Marin-Monfort, D., Sánchez, B., et al. (2010a). Early bone diagenesis in temperate environments part I: Surface features and histology. *Palaeogeography, Palaeoclimatology, Palaeoecology, 288*, 62–81.

Fernández-Jalvo, Y., King, T., Andrews, P., Yepiskoposyan, L., Moloney, N., Murray, J., et al. (2010b). The Azokh Cave complex: Middle Pleistocene to holocene human occupation in the Caucasus. *Journal of Human Evolution, 58*, 103–109.

Fernández-Jalvo, Y., Valli, A. M. F., Marin-Monfort, D., & Pesquero M. D. (submitted). The taphonomy of Senèze. In E. Delson, M. Faure & C. Guérin (Eds). *Senèze: Life in central france two million years ago*. New York: Springer.

Fernández-López, S. R. (1981). La evolución tafonómica (un planteamiento neodarwinista). *Boletín de la Real Sociedad Española de Historia Natural, 79*, 243–254.

Fernández-López, S. R. (1991). Taphonomic concepts for a theoretical biochronology. *Revista Española de Paleontología, 6*, 37–49.

Fernández-López, S. R. (1995). Taphonomie et interprétation des paléoenvironnements. *Geobios, 18*, 137–154.

Fernández-López, S. R. (2000). *Temas de tafonomia*. Madrid: Universidad Complutense de Madrid.

Fernández-López, S. R. (2006). Taphonomic alteration and evolutionary taphonomy. *Journal of Taphonomy, 4*, 111–142.

Figueirido, B., Palmqvist, P., & Pérez-Claros, J. A. (2009). Ecomorphological correlates of craniodental variation in bears and paleobiological implications for extinct taxa: An approach based on geometric morphometrics. *Journal of Zoology, 277*, 70–80.

Fiorillo, A. R. (1989). An experimental study of trampling: Implications for the fossil record. In R. Bonnichsen & M. H. Sorg (Eds.), *Bone modification* (pp. 61–71). Orono: University of Maine Center for the Study of the First Americans.

Francillont-Viellot, H., Buffrenil, V. D. E., Castanet, J., Geraudie, J., Meunier, F. J., Sire, J. Y. et al., (1989) Microstructure and mineralization of vertebrate skeletal tissues. In J.G.Carter (Ed.), *Skeletalb biomineralization: Patterns, processes and evolutionary trends* (pp. 175–234). Washington D.C.: American Geophysical Union.

Frostick, L., & Reid, I. (1983). Taphonomic significance of sub-aerial transport of vertebrate fossils on steep semi-arid slopes. *Lethaia, 16*, 157–164.

Gordon, C. C., & Buikstra, J. E. (1981). Soil pH, bone preservation and sampling bias at mortuary sites. *American Antiquity, 46*, 566–571.

Grandal d'Anglade, A., & López-González, F. (2005). Sexual dimorphism and autogenetic variation in the skull of the cave bear (*Ursus spelaeus* Rosenmüller) of the European upper pleistocene. *Geobios*, *38*, 325–338.

Grasman, B. T., & Hellgren, E. C. (1993). Phosphorus-nutrition in white-tailed deer nutrient balance, physiological-responses, and antler growth. *Ecology, 74*, 2279–2296.

Hackett, C. J. (1981). Microscopical focal destruction (tunnels) in excavated human bones. *Medicine, Science and Law, 21*, 243–265.

Haynes, G. (1980). Evidence of carnivore gnawing on Pleistocene and recent mammalian bones. *Paleobiology, 6*, 341–351.

Haynes, G. (1983). A guide for differentiating mammalian carnivore taxa responsible for gnaw damage to herbivore limb bones. *Paleobiology, 9*, 164–172.

Hedges, R. M., Millars, A. R., & Pike, A. W. G. (1995). Measurements and relationships of diagenetic alteration of bone from three archaeological sites. *Journal of Archaeological Science, 22*, 201–209.

Hillson, S. (1992). *Mammal bones and teeth: An introduction guide methods of identification*. London: Institute of Archaeology, University College London.

Huchet, J.-B., Deverly, D., Gutierrez, B., & Chaucha, C. (2011). Taphonomic evidence of a human skeleton gnawed by termites in a Moche-civilisation grave at huaca de la luna, Peru. *International Journal of Osteoarchaeology, 21*, 92–102.

Jans, M. M. E. (2005). *Histological characterization of diagenetic alteration of archaeological bone* (vol. 4). Geoarchaeological and bioarchaeological studies. Amsterdam: Institute for Geo and Bioarchaeology, Vrije Universiteit.

Jans, M. M., Kars, H., Nielsen-Marsh, C. M., Smith, C. I., Nord, A. G., Arthur, P., et al. (2002). *In situ* preservation of archaeological bone: A histological study within multidisciplinary approach. *Archaeometry, 44*(3), 343–352.

Johnson, E. (1985). Current developments in bone technology. In M. B. Schiffer (Ed.), *Advances in archaeological method and theory* (Vol. 8, pp. 157–235). New York: Academic Press.

Karkanas, P., Bar-Yosef, O., Goldberg, P., & Weiner, S. (2000). Diagenesis in prehistoric caves: The use of minerals that form *in situ* to assess the completeness of the archaeological record. *Journal of Archaeological Science, 27*, 915–929.

Kibii, M. J. (2009). Taphonomic aspects of African porcupines (Hystrix cristata) in the Kenyan Highlands. *Journal of Taphonomy, 7*, 21–27.

King, T., Compton, T., Rosas, A., Andrews, P. Yepiskoyan, L., & Asryan, L. (2016). Azokh Cave hominin remains. In Y. Fernández-Jalvo, T. King, L. Yepiskoposyan & P. Andrews (Eds.), *Azokh Cave and the Transcaucasian Corridor* (pp. 103–106). Dordrecht: Springer.

Kitching, J. W. (1980). On some fossil arthropoda from the limeworks Makapansgat, Potgietersrus. *Palaeontologica Africana, 23*, 63–68.

Klippel, W. E., & Synstelien, J. A. (2007). Rodents as taphonomic agents: Bone gnawing by brown rats and gray squirrels. *Journal of Forensic Science, 52*, 765–773.

Korth, W. W. (1979). Taphonomy of microvertebrate fossil assemblages. *Annals of the Carnegie Museum, 48*, 235–285.

Kreutzer, L. A. (1992). Bison and deer bone mineral densities: Comparisons and implications for the interpretation of archaeological faunas. *Journal of Archaeological Science, 19*, 271–294.

Kurtén, B. (1958). Life and death of the Pleistocene cave bear. *Acta Zool. Fennica, 95*, 1–59.

Kurtén, B. (1976). *The cave bear story*. New York: Columbia University Press.

Lam, Y. M., Chen, X., Marean, C. W., & Frey, C. J. (1998). Bone density and long bone representation in archaeological faunas: Comparison results from CT and photon densitometry. *Journal of Archaeological Science, 25*, 559–570.

Leroi-Gourhan, A., & Brezillon, M. (1972). *Fouilles de Pincevent: Essay d'analyse ethnographique d'un habitat Magdalénien*. VIII (Supplement): Gallia-Préhistoire.

López-González, F., Grandal-d'Anglade, A., & Ramón Vidal-Romaní, J. (2006). Deciphering bone depositional sequences in caves through the study of manganese coating. *Journal of Archaeological Science, 33*, 707–717.

Lyman, R. L. (1984). Bone density and differential survivorship of fossil classes. *Journal of Anthropological Archaeology, 3*, 259–299.

Lyman, R. L. (1994). *Vertebrate taphonomy*. Cambridge: Cambridge University Press.

Magela da Costa, G., & Rúbia Ribeiro, V. (2001). The occurrence of tinsleyite in the archaeological site of Santana do Riacho, Brazil. *Mineralogical Society of America, 86*, 1053–1056.

Marincea, S., Dumitras, D., & Gibert, R. (2002). Tinsleyite in the "dry" Cioclovina Cave (Sureanu Mountains, Romania): The second occurrence. *European Journal of Mineralogy, 14*, 157–164.

Markova, A. K. (1982). Microteriofauna iz paleoliticheskoy peschernoy stoyanki Azikh. *Palaeontoligischeskoy sb.-k Moskwa, 19*, 14–28. (In Russian).

Martin, F. M. (2008). Bone crunching felids at the end of the Pleistocene in Fuego-Patagonia. *Chile Journal of Taphonomy, 6*(3–4), 337–372.

Mattson, D. J. (1998). Diet and morphology of extant and recently extinct northern bears. *Ursus, 10*, 479–496.

Mayne, P. M. (1997). Fire modification of bone: A review of the literature. In W. D. Haglund & M. H. Sorg (Eds.), *Forensic taphonomy: The postmortem fate of human remains* (pp. 275–293). Boca Ratón: CRC Press.

Mazza, P., Rustioni, M., & Boscagli, G. (1995). Evolution of ursid dentition; with inferences on the functional morphology of the masticatory apparatus in the genus Ursus. In J. Moggi-Cecchi (Ed.), *Aspects of dental biology: Palaeontology, anthropology and evolution* (pp. 147–157). Florence: International Institute for the study of man.

Molleson T. (1990). The accumulation of trace metals in bone during fossilization. In N.D.Priest & F.L.Van der Vyver (Eds.), *Trace Metals and Fluoride in Bones and Teeth* (pp. 341–365). Boca Ratón: C.R.C. Press.

Murray, J., Lynch, E. P., Domínguez-Alonso, P., & Barham, M. (2016). Stratigraphy and sedimentology of Azokh Caves, South Caucasus. In Y. Fernández-Jalvo, T. King, L. Yepiskoposyan & P. Andrews (Eds.), *Azokh Cave and the Transcaucasian Corridor* (pp. 27–54). Dordrecht: Springer.

Nabaglo, L. (1973). Rats in the diet of the Barn owl. *Journal of Zoology of London, 189*, 540–545.

Noe-Nygaard, N. (1989). Man-made trace fossils on bones. *Human Evolution, 4*, 461–491.

Olsen, S. L., & Shipman, P. (1988). Surface modification on bone: Trampling versus butchery. *Journal of Archaeological Science, 15*, 535–553.

Peigné, S., Goillot, C., Germonpré, M., Blondel, C., Bignon, O., & Merceron, G. (2009). Predormancy omnivory in European Cave bears evidenced by a dental microwear analysis of Ursus spelaeus from Goyet, Belgium. *Proceedings of the National Academy of Sciences USA, 106*, 15390–15393.

Pesquero, M. D., Ascaso, C., Alcalá, L., & Fernández-Jalvo, Y. (2010). A new taphonomic bioerosion in a Miocene lakes hore environment. *Palaeogeography, Palaeoclimatology, Palaeoecology, 295*, 192–198.

Pickering, T., & Wallis, J. (1997). Bone modifications resulting from captive chimpanzee mastication: Implications for the interpretation of Pliocene archaeological faunas. *Journal of Archaeological Science, 24*, 1115–1127.

Pinto, A. C., & Andrews, P. (2002). *Taphonomy and palaeocology of quaternary bears from Northern Spain*. Oviedo: FAO, NHM & DuPont/Grafisa.

Pinto, A. C., & Andrews, P. J. (2004). Scavenging behaviour patterns in cave bears *Ursus spelaeus*. *Revue de Paléobiologie, 23*, 845–853.

Pinto Llona, A. C., Andrews, P. J., & Etxebarría, F. (2005). *Tafonomía y paleoecología de Úrsidos cuaternarios cantábricos*. Oviedo: Fundación Oso de Asturias.

Plummer, T. W., & Stanford, C. B. (2000). Analysis of a bone assemblage made by chimpanzees at Gombe National Park, Tanzania. *Journal of Human Evolution, 39*, 345–365.

Pobiner, B. (2008). Paleoecological information in predator tooth marks. *Journal of Taphonomy, 6*, 373–397.

Pobiner, B. L., DeSilva, J., Sanders, W. J., & Mitani, J. C. (2007). Taphonomic analysis of skeletal remains from chimpanzee hunts at Ngogo, Kibale National Park, Uganda. *Journal of Human Evolution, 52*, 614–636.

Rabal-Garcés, R., Cuenca-Bescós, G., Canudo, J. I., & Torres, T. (2011). Was the European bear an occasional scavenger? *Lethaia, 45*(1), 96–108.

Rabinovich, R., & Horwitz, L. K. (1994). *An experimental approach to the study of porcupine damage to bones. Taphonomie/Bone Modification*. Treignes (Belgium): Editions du CEDARC.

Richards, M. P., Pacher, M., Stiller, M., Quilès, J., Hofreiter, M., Constantin, S., et al. (2008). Isotopic evidence for omnivory among European cave bears: Late Pleistocene Ursus spelaeus from the

Peştera cu Oase, Romania. *Proceedings of the National Academy of Sciences of the United States of America, 105*, 600–604.

Rodríguez, J. (1997). Análisis de la estructura de las communidades de maníferos del Pleistoceno de la Sierra de Atapuerca. Revisión de metodologías. PhD dissertation. Universidad Autónoma de Madrid.

Saladié, P. (2009). Experimental Chewing and Gnawing of Humans and Other Primates Compared to Canids, Suids and Felids. PhD dissertation. Universitat Rovira i Virgili (Tarragona, Spain).

Saladié, P., Rodríguez-Hiraldo, A., Díez, C., Martín-Rodríguez, P., & Carbonell, E. (2013). Range of bone modifications by human chewing. *Journal of Archaeological Science, 40*, 380–397.

Selvaggio M. M. (1994). Evidence from carnivore tooth marks and stone-tool-butchery marks for scavenging by hominids at FLK Zinjanthropus Olduvai Gorge, Tanzania. PhD dissertation, Rutgers University, New Brunswick.

Selvaggio, M. M. (1998). Concernig the three stage model of carcass processing at FLK Zinjanthropus: A reply to Capaldo. *Journal of Human Evolution, 35*, 319–321.

Selvaggio, M. M., & Wilder, J. (2001). Identifying the involvement of multiple carnivore taxa with archaeological bone assemblages. *Journal of Archaeological Science, 28*, 465–470.

Shipman, P. (1981). *Life History of a Fossil: An introduction to taphonomy and paleoecology*. Cambridge: Harvard University Press.

Shipman, P., & Rose, J. (1983). Early hominid hunting, butchering, and carcass-processing behaviors: Approaches to the fossil record. *Journal of Anthropological Archaeology, 2*, 57–98.

Shipman, P., & Rose, J. J. (1988). Bone tools: An experimental Approach. In S. Olsen (Ed.), *Scanning electron microscopy in archaeology* (pp. 303–335). Oxford: British Archaeological Reports International Series *452*.

Shipman, P., Foster, G., & Schoeninger, M. (1984). Burnt bones and teeth: An experimental study of color, morphology, crystal structure and shrinkage. *Journal of Archaeological Science, 11*, 307–325.

Smith, K. G. V. (1986). *A manual of forensic entomology*. London: British Museum (Natural History) Publications.

Smith, C. I., Faraldos, M., & Fernández-Jalvo Y. (2016). Bone diagenesis at Azokh Caves. In Y. Fernández-Jalvo, T. King, L. Yepiskoposyan & P. Andrews (Eds.), *Azokh Cave and the Transcaucasian Corridor* (pp. 251–269). Dordrecht: Springer.

Smith, C. I., Nielsen-Marsh, C. M., Jans, M. M. E., Arthur, P., Nord, A. G., & Collins, M. J. (2002). The strange case of Apigliano: Early 'fossilization' of medieval bone in southern Italy. *Archaeometry, 44*, 405–415.

Stiner, M. C., Weiner, S., Bar-Yosef, O., & Kuhn, S. L. (1995). Differential burning, recrystallization and fragmentation of archaeological bone. *Journal of Archaeological Science, 22*, 223–237.

Sutcliffe, A. J. (1970). Spotted hyaenas: Crusher, gnawer, digester and collector of bones. *Nature, 227*, 1110–1113.

Sutcliffe, A. J. (1973). Similarity of bones and antlers gnawed by deer to human artefacts. *Nature, 246*, 428–430.

Sutcliffe, A. J. (1977). Further notes on bones and antlers chewed by deer and other ungulates. *Deer, 4*, 73–82.

Tappen, M. (1994). Bone weathering in the tropical rain forest. *Journal of Archaeological Science, 21*, 667–673.

Thompson, C. E. L., Ball, S., Thompson, T. J. U., & Gowland, R. (2011). The abrasion of modern and archaeological bones by mobile sediments: The importance of transport modes. *Journal of Archaeological Science, 38*, 784–793.

Tong, H. W., Zhang, S., Chen, F., & Li, Q. (2008). Rongements sélectifs des os par les porcs-épics et autres rongeurs: Cas de la grotte Tianyuan, un site avec des restes humains fossiles récemment découvert près de Zhoukoudian (Choukoutien). *L'Anthropologie, 111*, 353–369.

Trueman, C. N., & Martill, D. M. (2002). The long-term survival of bone: The role of bioerosion. *Archaeometry, 44*, 371–382.

Trueman, C. N. G., Behrensmeyer, A. K., Tuross, N., & Weiner, S. (2004). Mineralogical and compositional changes in bones exposed on soil surfaces in Amboseli National Park, Kenya: Diagenetic mechanisms and the role of sediment pore fluids. *Journal of Archaeological Science, 31*, 721–739.

Turner, A. (1983). The quantification of relative abundances in fossil and subfossil bone assemblages. *Annals of the Transvaal Museum, 33*, 311–321.

Tütken, T., & Vennemann, T. W. (2011). Fossil bones and teeth: Preservation or alteration of biogenic compositions? *Palaeogeography, Palaeoclimatology, Palaeoecology, 310*, 1–8.

Van der Made, J., Torres, T., Ortiz, J. E., Moreno-Pérez, L., & Fernández-Jalvo, Y. (2016). The new material of large mammals from Azokh and comments on the older collections. In Y. Fernández-Jalvo, T. King, L. Yepiskoposyan & P. Andrews (Eds.), *Azokh Cave and the Transcaucasian Corridor* (pp. 117–159). Dordrecht: Springer.

Vila Taboada, M., Fernández Mosquera, D., López González, F., Grandal d'Anglade, A., & Vidal Romaní, J. R. (1999). Paleoecological implications inferred from stable isotopic signatures (d13C, d15 N) in bone collagen of *Ursus spelaeus* ROS.-HEIN. *Cadernos do Laboratorio Xeolóxico de Laxe*, *24*, 73–87.

Vila Taboada, M., Fernández Mosquera, D., & Grandal d'Anglade, A. (2001) Cave bear's diet: A new hypothesis based on stable isotopes. *Cadernos do Laboratorio Xeolóxico de Laxe*, *26*, 431–439.

Villa, P., & Mahieu, E. (1991). Breakage patterns of human long bones. *Journal of Human Evolution, 21*, 27–48.

Villa, P., Bouville, C., Courtin, J., Helmer, D., Mahieu, E., Shipman, P., et al. (1986). Cannibalism in the Neolithic. *Science, 233*, 431–436.

Voorhies, M. R. (1969). Taphonomy and population dynamics of an early Pliocene vertebrate fauna Knox County, Nebraska. *Contributions to Geology, University of Wyoming Special Paper, 1*, 1–69.

Wedl, C. (1864). Uber einen im Zahnbein und Knochen keimenden Pilz. Akademi der Wissenschaften in Wien. Fitzungsbereichte Naturwissenschaftliche ABI. *Mineralogi, biologi erdkunde, 50*, 171–193.

Weigelt, J. (1927). Resente *Wirbeltierleichten und ihre Paläobiologische Bedeutung*. Max Weg Verlag, Leipzig, p. 227. Translated in 1989 *Recent Vertebrate Carcasses and their Paleobiological Implications.* Chicago: University Chicago Press.

Wentworth, C. K. (1919). A laboratory and field study of cobble abrasion. *Journal of Geology, 27*, 507–521.

White, T. D. (1992). *Prehistoric Cannibalism at Mancos 5MTUMR-2346*. Princeton: Princeton University Press.

White, W. B., & Culver, D. C. (2012). *Encyclopedia of caves*. Dordrecht: Springer.

Wyckoff, R. W. G. (1972). *The biochemistry of animal fossils*. Bristol: Scientechnica Ltd.

Chapter 11
Bone Diagenesis at Azokh Caves

Colin I. Smith, Marisol Faraldos, and Yolanda Fernández-Jalvo

Abstract Bone diagenesis is a set of processes by which the organic and mineral phases and the structure of bone are transformed during fossilization. To understand how these processes have affected skeletal material recovered from Azokh Caves (particularly the organic preservation), we measured 'diagenetic parameters' of skeletal material from Holocene, Late Pleistocene and Middle Pleistocene deposits from Azokh Caves. Additionally, we used this study to further test the application of both nitrogen adsorption isotherm analysis and mercury intrusion porosimetry for measuring the porosity of fossil bone. The skeletal material from the Pleistocene layers of Azokh Caves can be characterized as generally poorly preserved (especially collagen preservation). Porosity values of the bones are lower than might be expected as many bones show evidence of extensive infilling of the pores with secondary minerals. The pore infilling in the Middle Pleistocene layers is most extensive and this type of preservation has not previously been described in archaeological material.

Резюме Диагенез костей – это совокупность процессов, в результате которых органические и минеральные составляющие структуры кости трансформируются благодаря распаду и фоссилизации. Чтобы понять, как эти процессы воздействовали на скелетный материал, обнаруженный в Азохской пещере (и, в частности, оценить степень сохранности органических веществ в костях), были измерены определенные "диагенетические параметры" скелетного материала. Тридцать три кости из трех главных участков Азохской пещеры были исследованы для выяснения степени сохранности в зависимости от места находки и возраста образца. Голоценовый материал из *Азох 2* был сопоставлен с костями из *Азох 1* (подразделения *II–III* – поздний плейстоцен и средние горизонты подразделения *V* – средний плейстоцен).

Мы оценили количество коллагена, оставшегося в костях после деминерализации, и степень сохранности минералов с использованием метода FTIR (инфракрасная спектроскопия на основе преобразования Фурье). Изменения на поверхности костей и гистологическая структура поперечного сечения были исследованы с помощью обычного светового и сканирующего электронного микроскопов с электронной информационной системой (EDS). Степень гистологической сохранности была оценена с использованием шкалы *Oxford Histological Index*. Изменения в пористости костей были измерены с помощью изотермального анализа поглощения азота (NAIA) и ртутной интрузионной порометрии (HgIP), а результаты этих двух методов в дальнейшем были сопоставлены.

Согласно величинам "диагенетических параметров", материал из *Азох 2* представлял собой смесь из хорошо сохранившегося материала и костей, которые лишились коллагена химическим путем, а также некоторых костей, потерявших коллаген из-за микробного воздействия. Мы объясняем этот конгломерат различных типов сохранности как возможный результат смешения современного и ископаемого материала на поверхностных слоях *Азох 2*. Скелетный материал из плейстоценовых слоев *Азох 1* в целом плохо сохранился. Содержание коллагена бедное, с большими изменениями в кристалличности структуры. Результаты гистологического исследования и анализа на пористость показывают, что во многих случаях кости лишились коллагена по причине химической деградации, хотя

C.I. Smith (✉)
Department of Archaeology and History, La Trobe University, Melbourne, VIC 3086, Australia
e-mail: Colin.Smith@latrobe.edu.au

M. Faraldos
Instituto de Catálisis Y Petroleoquímica (CSIC), Marie Curie 2, Campus de Cantoblanco, 28049 Madrid, Spain
e-mail: mfaraldos@icp.csic.es

Y. Fernández-Jalvo
Museo Nacional de Ciencias Naturales (CSIC), José Gutiérrez 2, 28006 Madrid, Spain
e-mail: yfj@mncn.csic.es

Yolanda Fernández-Jalvo et al. (eds.), *Azokh Cave and the Transcaucasian Corridor*, Vertebrate Paleobiology and Paleoanthropology, DOI 10.1007/978-3-319-24924-7_11

потеря коллагена, вызванная микробами, также может быть значительной, особенно в подразделениях *II–III*. Степень пористости костей оказалась ниже, чем ожидалось, учитывая показатели потери коллагена и микробного воздействия. Многие кости имеют обширную заполненность пор вторичными минералами. Содержание пор в среднеплейстоценовых горизонтах наиболее экстенсивное, и данный тип сохранности ранее не был описан в археологическом материале.

Обнаруженные уровни коллагена как показателя сохранности органического материала свидетельствуют о низком содержании древней ДНК (*aDNA*) в пещере; более того, сильно измененные минералы костей также оставляют мало надежд на сохранность *aDNA*.

Данное исследование представляет собой интересный пример сравнения двух методов измерения пористости. Оно показало, что поры диаметром ниже порога чувствительности метода HgIP, но исследованные с помощью NAIA (с диаметром пор меньше 0,1мкм), возникли по причине потери коллагена; они заполняются таким же образом, как и поры диаметром 0,01–0,1мкм.

Keywords Diagenetic parameters • Mercury intrusion porosimetry • Nitrogen adsorption isotherm analysis • Collagen • Histology • Fossilization

Introduction

Diagenesis is the process of physical, chemical, and biological changes of sediments after their deposition. The term can also be applied to bones as part of a soil component deposited at an archaeological or paleontological site and the term 'Bone diagenesis' can be used to describe specifically the changes that bones undergo during fossilization. Bone is a composite biological material with a complex structure and is composed principally of bone mineral (bio-apatite) and the tough fibrous protein collagen (about 25% by weight in fresh bone). Typical diagenetic changes include the degradation and loss of organic matter such as collagen and DNA, changes in the bone mineral, and often microbial destruction of the morphological structure (which also alters the organic and mineral components) (Collins et al. 2002). Increases in the bone porosity are also common as a result of these diagenetic changes (Hedges et al. 1995).

It is important to understand how and why diagenetic changes take place, as they control the formation of the archaeological and fossil record as a whole. Understanding the reasons why bones do or do not survive in particular sites helps to improve site prediction and detection, and can help develop *in situ* heritage site protection strategies (Kars and Kars 2002). Moreover, archaeological bones are used for laboratory analyses such as radiocarbon dating, stable isotope analysis and ancient DNA studies, and it is imperative to understand how diagenetic changes affect the quality of this data.

There are many factors that influence the types and rates of diagenetic changes to bone (Hedges 2002). The intrinsic factors (the properties of the bone itself) need to be considered; for example different skeletal elements have different structural properties (and these vary with species, sex and age) and will have different proportions of collagen and mineral at a micro-scale. The soil environment in which the bone is deposited will also have a major influence on the diagenetic processes. Sediment conditions, such as, soil chemistry, pH, redox potential of the soil, and temperature as well as water interaction with the bone especially site hydrology (Hedges and Millard 1995), are major factors. The results of bone degradation vary from complete destruction, to fossilization where the organic material is degraded and the mineral heavily altered. Between these two extremes is a spectrum of preservation types that depends on the factors mentioned above, history of deposition and age of the material.

The number of factors that influence diagenetic processes and the length of time that they take means that they cannot be easily replicated in laboratory conditions or field experiments, so often the process of studying bone diagenesis relies on the examination of the properties of the bones excavated from sites and relating these to the properties of the sediments and history of the site.

A popular mode of investigation has been to measure 'diagenetic parameters' of bones in order to characterize the physical and chemical characteristics of the material, i.e.; mineral alteration, collagen loss, micromorphological preservation and pore structure changes of bone (e.g., Hedges et al. 1995; Colson et al. 1997; Gutierrez 2001; Trueman et al. 2004; Smith et al. 2007). These parameters can be compared with each other in order to observe how the different aspects of bone degradation are related. Furthermore, the characteristics of bones from a site can be compared with each other, and with bones from other sites, and these can also be related to the specific depositional contexts and histories of the bones in order to build models of diagenetic trajectories and processes (Hedges 2002).

Building on the diagenetic parameter approach pioneered by Hedges et al. (1995), Smith et al. (2007) described four major types of bone preservation in European Holocene deposits, based on their diagenetic parameter values (see also Nielsen-Marsh et al. 2007). Figure 11.1 displays example pore structures (a plot of pore volume against pore diameter, determined by mercury intrusion porosimetry) as well as typical diagenetic parameter values of the main diagenetic types (after Smith et al. 2007). In brief the 'Well Preserved Bone' category has diagenetic parameter values similar to those of modern bones. A second category of bones are those

that have undergone 'Accelerated Collagen Hydrolysis' (ACH), where the bones have only small amounts of collagen remaining and often extreme mineralogical changes, but no evidence of histological damage caused by microbes. Notably these bones have a significant increase in their pore volume in the smallest pore range (~0.01–0.1 μm diameter). Bones that have undergone 'Microbial Attack' have porosity increases in the >0.1 <10 μm diameter pore range and damage to the histological structure of the bone caused by microbes and fungi (semi quantified in a histological index, from 5-unaltered to 0-heavily damaged). Collagen yields of the microbially damaged bone vary ranging from 0 to 20% by weight and there are some mineralogical changes. It should be noted that the ACH type and microbial attack appear to be mutually exclusive pathways of diagenesis.

A fourth type of preservation described is bone that is undergoing 'Catastrophic Mineral Dissolution'. These bones tend to be poorly preserved in most aspects with large pore structures, low collagen yields and high levels of mineral alteration, but with variable levels of histological damage. This research has indicated that some bone degradation processes such as microbial attack (Jans et al. 2004) or accelerated collagen loss (Smith et al. 2002) can occur rapidly post-mortem and that these processes can lead to extensive changes in the diagenetic state of the bone in a short period of time. In contrast, under other circumstances very little change can occur over hundreds or even thousands of years and the bone remains in the 'Well Preserved' state. It is also important to be aware that these early stages of bone diagenesis can affect subsequent longer-term changes that occur in bone fossilization (Trueman and Martill 2002; Smith et al. 2007; Marin-Monfort et al. 2016). Besides helping us to understand the processes of fossilization and the formation of the archaeological record (at a site level and more generally), understanding diagenetic changes to the mineral and organic fraction of bone helps us to understand how these changes can affect the biogenic signals that they contain (i.e. isotopic and DNA data) and inform us as to where and for how long such information might be preserved in bone.

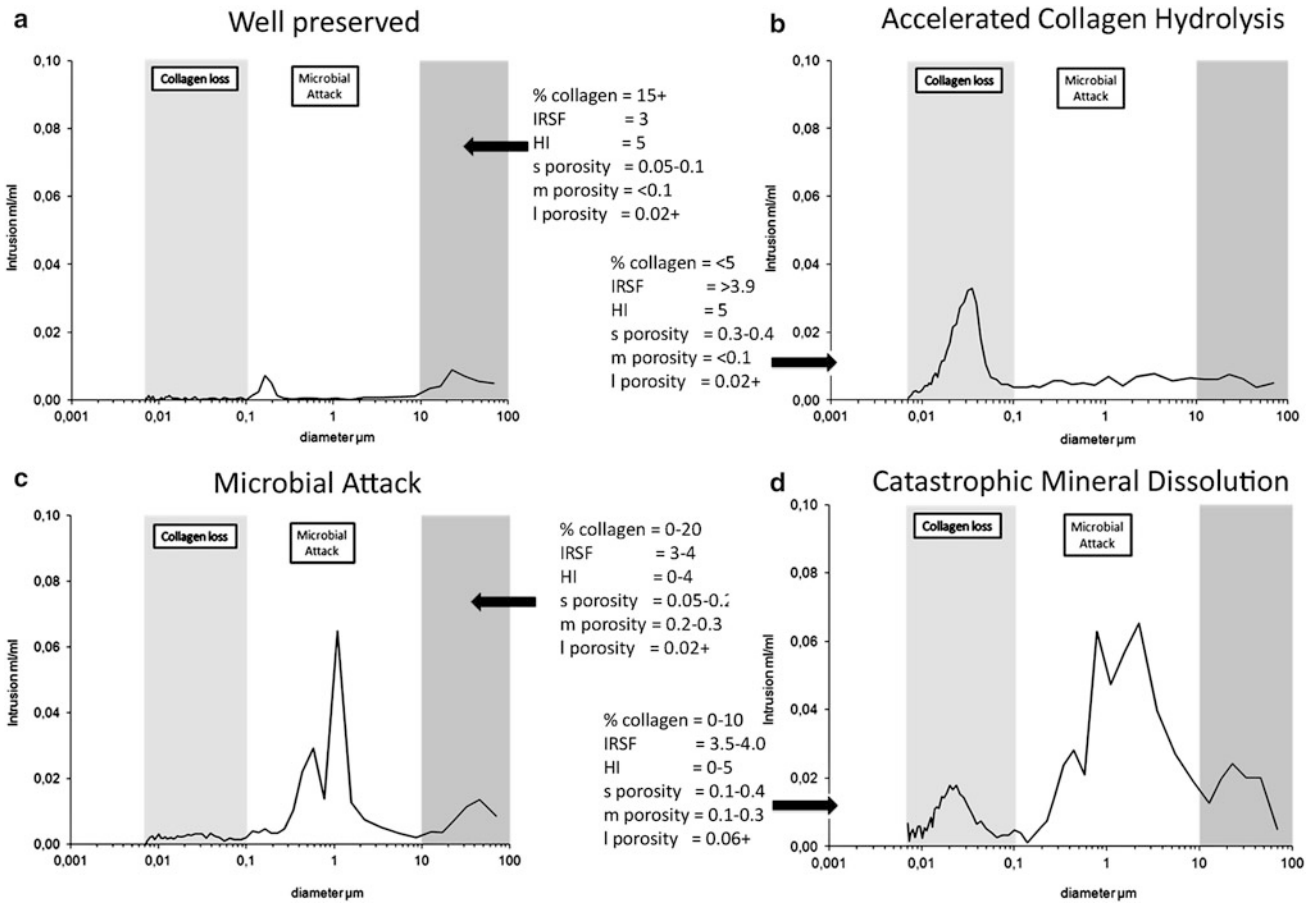

Fig. 11.1 Examples of typical pore size distributions (measured by mercury intrusion porosimetry) of four types of archaeological bone. **a** "Well preserved bone". **b** Accelerated collagen hydrolysis, **c** Microbially Attacked bone and **d** Catastrophic Mineral Dissolution (After Smith et al. 2007 and Nielsen-Marsh et al. 2007). Typical diagenetic parameter values are also given

Porosity as a Diagenetic Indicator

Measuring the porosity using mercury intrusion porosimetry (HgIP) has become a valuable tool in determining diagenetic changes, as plotting the pore size distribution provides a clear visual way of comparing bones and reveals the signature pore structures of the preservational types (see Fig. 11.1). HgIP does, however, have some disadvantages; firstly the minimum pore diameters that HgIP can measure are limited to around 0.005–0.01 μm and bone has a significant amount of porosity in pores of smaller diameter (Robinson et al. 2003), secondly, HgIP fills the bone sample with toxic mercury and is thus, in effect, destructive. A complementary method of porosity analysis that has been applied to archaeological bone is that of Nitrogen Adsorption Isotherm Analysis (NAIA) (Robinson et al. 2003; Smith et al. 2008; Bosch et al. 2011). This method is capable of measuring the volume in pores with sub nanometer diameters and leaves the sample of bone intact so that it can be used for subsequent analysis (e.g., HgIP, histological examination or sub sampling for other diagenetic parameters). NAIA is not useful for measuring the larger pore diameters associated with microbial attack, however it has been used to measure pores between approximately 0.0005–0.1 μm in a limited archaeological bone data set and shown that it also records changes occurring in ACH bone in the 0.01–0.1 μm range (Smith et al. 2008). NAIA has yet to be applied extensively to archaeological and paleontological bone but holds great potential in investigating changes in sub nanometer pore sizes that have yet to be explored in detail.

Bone Diagenesis at Azokh Caves

Azokh Caves site is located in the Lesser Caucasus (Fernández-Jalvo et al. 2010a). Azokh 1 yielded a Middle Pleistocene human mandible discovered in the 1960s (Kasimova 2001; King et al. 2016), and it was accompanied by an abundant contemporaneous fauna and human made tools. Detailed sedimentology and stratigraphy has been described by Murray et al. (2010, 2016). In 2002 excavation at the site was resumed by an international team which discovered two new entrances (Azokh 2 and Azokh 5), and which has extended the research into this interesting western Eurasian area from Holocene to middle Pleistocene (Fernández-Jalvo et al. 2016; see also Appendix of this volume).

Bone diagenesis at Azokh Caves was investigated in order to understand the general level of bone preservation at the site and to help to establish how this can contribute to the discussion about the poor aDNA preservation at Azokh (see Bennett et al. 2016). In addition it presented an opportunity to measure material from a Pleistocene cave site using the same parameters used by Smith et al. (2007). Smith et al. (2007) tested mainly Holocene open air European sites, so the characterization of diagenesis at Azokh is a useful addition to compare preservation at an older and contextually different site. Moreover, material was analyzed from Holocene, late Pleistocene and Middle Pleistocene layers from the site giving an overview of diagenesis over a period of approximately 300 kyr. It also enabled further testing and evaluation of a new method of investigating pore size distribution in archaeological bone with the application of combined nitrogen adsorption isotherm analysis with subsequent mercury intrusion porosimetry on the same sub-sample of bone. As mentioned above, this approach was first implemented by Smith et al. (2008) but has yet to be fully employed in diagenetic investigations.

Materials Analyzed

The skeletal material analyzed here was excavated from Azokh Caves during the 2003 field season (Fernández-Jalvo et al. 2010b, 2016). The material available for analysis was comprised of mainly unrecognizable fragments of bone (i.e. unknown species or element), so as not to destroy useful material that could be identified to species level using morphological characteristics. In addition some more complete bone pieces were also analyzed for diagenetic parameters as they were also analyzed for ancient DNA. There was no obvious macroscopic difference between fragmentary or more complete bones in terms of preservation (Marin-Monfort et al. 2016), and so we believe that the bones represent a faithful sample of the overall assemblage. Fossil bones were collected from three main parts of the site. In Azokh 1, Units II and III represent Late Pleistocene layers which date from around 100 ka to less than 200 ka (see Appendix, ESR). Bone was also excavated from Unit Vm from Azokh 1, which is a Middle Pleistocene layer and probably dates to approximately 300 ka. Bone from Unit Vm appears to be heavily fossilized. Bone was also sampled from the initial excavation of the surface layers at Azokh 2 (another entrance to the Azokh Cave system). Bone found on the surface of Azokh 2, or in the first 30–50 cm of test pit excavations, was also taken for analysis. Whilst anticipating that the majority of the material from Azokh 2 (from the 2003 season) is of recent modern origin, it was noted that some appeared to be heavily fossilized and it is believed that the top layers of the site are a mixture of recent and fossil material, where fossil material may have become mixed as the result of geomorphological cave collapses, producing a sediment mixture of different strata (Fernández-Jalvo et al. 2010b; Domínguez-Alonso et al. 2016; Murray et al. 2016). One sample was taken from the section between Unit III and Unit Vm (i.e. Unit Vu) from Azokh 1. Further descriptions of the material are given in Table 11.1.

Methods

Diagenetic Parameters

The material was analyzed using a suite of diagenetic parameters to measure collagen preservation (% 'collagen'), mineral alteration (IRSF and carbonate phosphate ratio), histological preservation (Oxford Histological Index), (Hedges et al. 1995; Smith et al. 2007 and references therein).

% 'Collagen'

Bone shards of known weight (<60 mg) were demineralized in 2 mls of 0.6 M HCl overnight in Eppendorf tubes. The tubes were centrifuged (at 6000 rpm for 5 min), the acid decanted, and the remaining acid insoluble residue was washed three times in 2 mls of distilled water under centrifugation. The acid insoluble fraction was then oven dried overnight at 65 °C, and weighed. Elemental analysis was carried out in duplicate to obtain the % carbon and nitrogen values to calculate the C:N ratio (molar ratio) to assess if the insoluble fraction is collagen (DeNiro 1985) with values between 2.9 and 3.6 being acceptable collagen values.

Crystallinity Index and Carbonate Phosphate Ratio

The crystallinity index and carbonate phosphate ratio of the mineral fraction was measured using infrared spectroscopy of hand ground bone powder crushed into a potassium bromide (KBr) pellet. The crystallinity index or Infrared Splitting Factor (IRSF) was calculated using the splitting ratio of the phosphate $\nu 4$ doublet at 567 and 605 cm^{-1} in the infrared spectrum following Weiner and Bar-Yosef (1990). The carbonate:phosphate ratio was calculated using the peaks at 1415 cm^{-1} (CO_3^{2-}), and 1035 cm^{-1} (PO_4^{3-}). It should be noted however that this measurement is only semi-quantitative as it can be interfered with by collagen that also absorbs in the 1415 cm^{-1} region of the spectrum.

Surface Modifications and Histological Analysis

Surface modifications were recorded with the naked eye and by examination using a binocular light microscope (10× to 80× magnification), and with an environmental scanning electron microscope (ESEM) QUANTA 200 housed at the Museo Nacional de Ciencias Naturales. Observations were made in backscattered electron mode, combined with secondary electron emission mode, at 20–30 kV, 0.6–0.33 Torr (Fernández-Jalvo et al. 2010a). Histological sections were prepared in the manner described by Fernández-Jalvo et al. (2010a) to produce polished sections of bone (fragile samples were embedded in resin while harder samples were polished without the need for resin support). The sections were examined using ESEM in backscatter mode to determine the extent of damage to the original bone histology caused by microscopic focal destructions and assigned a histological index score (Hedges et al. 1995; Millard 2001; Jans et al. 2004). Other observations were also noted (Table 11.2) and some areas were analyzed using energy dispersive x-ray spectroscopy (EDS) to determine the composition of inclusions or other notable features. Using the elemental compositions from the EDS analysis, possible secondary minerals were suggested in Table 11.2.

Pore Size Analysis Using Nitrogen Adsorption Isotherm Analysis and Mercury Intrusion Porosimetry

Samples of bone (approximately 1 g chunks) were cut from the main sample using an electrically powered circular hand saw at its slowest speed. Porosity analysis was carried out by nitrogen adsorption isotherm analysis (NAIA), which is non-destructive, and then by mercury intrusion porosimetry on the same piece of bone. The following pre-treatment was carried out so that the sample was dry prior to analysis. The samples were frozen at −20 °C for 18–24 h and then lyophilized (for at least 18 h), no more than 48 h prior to the analysis. After lyophilization the samples were stored in an airtight container until required. Immediately before analysis samples were degassed in a Micromeritics VacPrep 061 system for 20 h.

Nitrogen adsorption isotherm analysis was carried out at 80 K in a Micromeritics Tristar 3000 automatic system dosing nitrogen following a custom made pressures table. Equilibrium time and other parameters were optimized to assure the best assay reproducibility. Nitrogen adsorption isotherm analysis works by applying nitrogen to a sample, which adsorbs to the pore walls in a theoretical monolayer. Adsorbed nitrogen does not contribute to the pressure in the system and thus adsorption results in a pressure change. Changes in the partial pressure of nitrogen can be monitored and related to the surface area covered by the nitrogen. Larger pores are filled by increasing the partial pressure of nitrogen and thus at each pressure increment the volume of pores at a certain diameter can be calculated. Following B.J.H. theory (Barrett et al. 1951), the

pore size distribution and specific surface area can be calculated by knowing the volume of nitrogen adsorbed and its relative pressure. Using this technique we were able to measure the BET Surface Area m^2/g and the pore volume (cm^3/g) contained in pores of 0.001–0.1 μm diameters. Further descriptions of the technique and its application to bone porosity measurements can be found in Robinson et al. (2003) and Smith et al. (2008).

Following the non-destructive nitrogen adsorption isotherm analysis, mercury intrusion porosity analysis was carried out. No additional pre-treatment was required other than maintaining dry storage of the samples. A Micromeritics 9320 Poresizer was used for mercury intrusion porosimetry analysis, the volume of mercury intruded was measured following a customized pressure table from 0 to 30 000 Psi (0–2000 MPa). Mercury intrusion porosimetry has been used extensively to investigate bone diagenetic changes and details of the method can be found in Nielsen-Marsh and Hedges (1999), Smith et al. (2002, 2008), among others. Calculations were made using a mercury-apatite contact angle of 163.1° after Joscheck et al. (2000), and a mercury surface tension of 485 dyn/cm. The analysis produces bulk density values (density including pore space) and apparent (skeletal) density (density of the structure excluding pore space). The pore size distribution can be calculated indicating the volume of pore space within certain pore diameters. Table 11.1 gives the values for certain pore diameter ranges relevant to bone diagenesis after Smith et al. (2007).

Results and Discussion

The diagenetic parameter results can be seen in Tables 11.1 and 11.2. Diagenetic changes to bone can be compared with the typical values of modern bone in the tables.

Table 11.1 Surface modifications, collagen and mineral diagenetic parameter values of fossil bones from Azokh Cave

	Sample code	Site	Skeletal element	% Collagen (mean)	% Collagen (s.d.)	C:N ratio of 'collagen'	Crystallinity index (IRSF)	Carbonate: phosphate ratio (by IRSF)
Typical modern values								
	Typical modern bone	N/A	N/A	20–25%	2.0	3.2	2.8	0.40
Azokh 1 Units II–III	AZUM D46 181	Azokh 1 Units II–III	Calcaneous *Ursus spelaeus* (no apparent damage on surface)	0.0	N/A		3.4	0.30
	AZUM D46 2	Azokh 1 Units II–III	Long bone fragment	31.8	10.8	6.3	3.4	0.19
	AZUM D46 3	Azokh 1 Units II–III	Long bone fragment	0.1	0.4		4.3	0.03
	AZUM D45 25	Azokh 1 Units II–III	Radius *Ursus spelaeus*	0.8	0.3		3.6	0.25
	AZUM D45 4	Azokh 1 Units II–III	Long bone fragment	0.4	0.1		3.9	0.20
	AZUM D45 42	Azokh 1 Units II–III	Radius *Ursus spelaeus* (Mn deposit on fractures and bone/sediment surface)	0.2	0.0		2.9	0.47
	AZUM D45 9	Azokh 1 Units II–III	Calcaneous *Ursus spelaeus*	2.1	0.4	7.0	3.3	0.51
	AZUM-D46G	Azokh 1 Units II–III	Several fragments of various bones [Mn staining/carbonatic crust]	0.6	0.4		3.0	0.38
	AZUM-D46G 27 A	Azokh 1 Units II–III	Several fragments of various bones [Mn staining/carbonatic crust]	2.4	0.1	6.3	3.0	0.33
	AZUM-D46G 27 B	Azokh 1 Units II–III	Fragments	1.4	0.0	5.9	3.5	0.25
	AZUM-D46G 19-A	Azokh 1 Units II–III	Several fragments of various bones many 3–5 cm long [Mn staining and trampling]	1.4	0.9	8.7	3.0	0.33
	AZUM-D46G 19-B	Azokh 1 Units II–III	Fragments [trampling marks]	0.1	0.1		3.4	0.28
	AZUM-D46G 19-C	Azokh 1 Units II–III	Fragments	0.0	0.0		3.3	0.24
	AZUM-D46G 19-D	Azokh 1 Units II–III	Fragments [trampling, rounding, Mn staining]	2.6	1.4	7.0	3.5	0.24

(continued)

Table 11.1 (continued)

	Sample code	Site	Skeletal element	% Collagen (mean)	% Collagen (s.d.)	C:N ratio of 'collagen'	Crystallinity index (IRSF)	Carbonate: phosphate ratio (by IRSF)
Azokh 1 Unit Vu	AZU-Section	Azokh 1 Unit Vu	Long bone fragment [black staining, mainly trabecular bone]	0.0	0.3		3.5	0.26
Azokh 1 Unit Vm	AZM E39 1	Azokh 1 Unit Vm	Long bone fragment	0.9	0.5	6.1	3.4	0.20
	AZM E41 4	Azokh 1 Unit Vm	Long bone fragment	0.5	0.1		3.6	0.20
	AZM-E40G	Azokh 1 Unit Vm	Fragments [fibrous texture]	0.7	0.2	6.1	3.3	0.23
	AZM-E41G	Azokh 1 Unit Vm	Fragment of Mandible(?) [splitting and exfoliation on surface]					
	AZM-F42 9	Azokh 1 Unit Vm	Long bone (fragment) [heavily mineralized, fibrous surface]	0.6	0.3		3.9	0.17
	AZM-G41 5	Azokh 1 Unit Vm	Fragments	0.5	0.2		3.9	0.18
Azokh 2	AZN P11	Azokh 2		16.9	1.3	3.3	3.8	0.25
	AZN-Q10	Azokh 2	Long bone [modern root marking, shallow trampling marks]	7.5	0.8	3.3	2.9	0.43
	AZN-SL-HDU	Azokh 2	Metapodial [some skin still present, cut marks, one side weathered, the other not]	23.1	0.2	3.2	3.7	0.36
	AZN-SL-HWU	Azokh 2	Metapodial [surface corroded]	18.7	0.0	3.2	3.3	0.32
	AZN-SL-HDW	Azokh 2	Metapodial [moderately weathered, cracked surface]	21.7	0.1	3.2	3.4	0.31
	AZN-SL-HWW	Azokh 2	Metapodial	21.4	0.4	3.2	3.4	0.28
	AZN-SL-A	Azokh 2	Fragments [root marks]	0.9	0.1		3.4	0.34
	AZN-SL-B	Azokh 2	Epifysis [spots of gypsum and Mn stains]	2.6	0.1	7.1	3.5	0.32
	AZN-SL-C	Azokh 2		0.3	0.1		3.7	0.27
	AZN-SL-D	Azokh 2	Tibia/Fibia proximal end (?) epifysis [heavily mineralized corroded surface]	0.1	0.1		3.4	0.30
	AZN-SL-F	Azokh 2	Fragments of long bone [heavily mineralized, root marks]	0.8	0.1		3.4	0.31
	AZN-SL-G	Azokh 2	Fragments of long bone	0.3	0.1		3.4	0.28

Azokh 1 Units II–III

Units II–III at Azokh 1 are represented by heavily degraded bone, with low levels of organic preservation (none of which displays a collagen like C:N ratio (see DeNiro 1985)) and with the exception of a few samples can be characterized as having highly altered mineral (IRSF values are typically 3.4 or above and C:P values typically less than 0.3). It should be noted that a critical error appears to have occurred in the collagen extraction from sample AZUM-D46-2 that had two disparate values from the duplicate analysis, so this value should be ignored, as it is unreliable. The histological preservation varies in these deposits with some bones showing signs of extensive microbial attack (Histological

Table 11.2 Histological and Porosity values of fossil bones from Azokh Caves

Sample code	Site	Oxford Histological Index and Histology notes	BET Surface Area m^2/g (by N_2 Porosimetry)	Volume (cm^3/g) between 0.001 and 0.1 μm (N_2 porosity)	Volume (ml/ml) in pores <0.1 μm (Hg porosity)	Volume (ml/ml) in pores <10 >0.1 μm (Hg porosity)	Volume (ml/ml) in pores >10 μm (Hg porosity)	Total Porosity (ml/ml) (Hg porosity)	Bulk Density g/ml (Hg porosity)	Skeletal Density g/ml (Hg porosity)
Typical modern values										
Typical Modern Bone	N/A	OHI 5	0.2–1.4	0.002–0.008	0.05	0.02	0.0200	0.0900	1.90	2.10
Azokh 1 Units II–III										
AZUM D46 181	Azokh 1 Units II–III	OHI 5 Microfissures, most infilled by Mn. Sediment illite	101.4	0.2123	0.1791	0.0052	0.1472	0.3314	1.61	2.41
AZUM D46 2	Azokh 1 Units II–III		23.0	0.0993	0.1185	0.2710	0.0652	0.4547	1.01	1.85
AZUM D46 3	Azokh 1 Units II–III	OHI 5 Intense cracking. Abundant secondary osteons (pathology?) Canals filled by sediment	89.3	0.2880	0.3633	0.0417	0.0382	0.4432	1.28	2.29
AZUM D45 25	Azokh 1 Units II–III	OHI 5 Enlarged canaliculi, possibly mineralised by Mn	77.5	0.1964	0.2251	0.0225	0.0481	0.2957	1.63	2.31
AZUM D45 4	Azokh 1 Units II–III	OHI 0 Areas of organised and areas of chaotic bacterial attack all over. Radial and peripheral tubes on bacterial corroded areas (fungi?)	35.6	0.1133	0.1445	0.2518	0.0601	0.4564	1.39	2.56
AZUM D45 42	Azokh 1 Units II–III	OHI 4 Initial bacterial attack. Canals infilled by illite rich in carbonates, and also sulphur detected? gypsum? $Ca(SO_4) \cdot 2(H_2O)$	87.5	0.1958	0.2222	0.0072	0.0225	0.2519	1.74	2.33
AZUM D45 9	Azokh 1 Units II–III	OHI 5 Some osteones are infilled carbonatic minerals (calcite) and minerals enriched in phosphorous and sulphur related to bat guano breakdown. Corrosion of the cortical area	65.4	0.1290	0.1153	0.0524	0.1025	0.2702	1.73	2.37
AZUM-D46G	Azokh 1 Units II–III	OHI 5 Canals partially infilled clayish sediment rich in phosphorous	84.7	0.1715	0.1945	0.0075	0.0274	0.2294	1.92	2.49

(continued)

Table 11.2 (continued)

Sample code	Site	Oxford Histological Index and Histology notes	BET Surface Area m^2/g (by N_2 Porosimetry)	Volume (cm^3/g) between 0.001 and 0.1 μm (N_2 porosity)	Volume (ml/ml) in pores <0.1 μm (Hg porosity)	Volume (ml/ml) in pores <10 >0.1 μm (Hg porosity)	Volume (ml/ml) in pores >10 μm (Hg porosity)	Total Porosity (ml/ml) (Hg porosity)	Bulk Density g/ml (Hg porosity)	Skeletal Density g/ml (Hg porosity)
AZUM-D46G 27 A	Azokh 1 Units II–III	OHI 5 Porous bone with good histology. Mn infilling osteocites, also Ni has been detected with Mn(EDS)	80.6	0.1752						
AZUM-D46G 27 B	Azokh 1 Units II–III	OHI 5 Porous bone, osteocytes and small cracks infilled with Mn (EDS)	76.9	0.1529						
AZUM-D46G 19-A	Azokh 1 Units II–III	OHI 5 Porous bone though good histology. EDS sediment Illite	54.8	0.0705	0.0324	0.0042	0.0475	0.0841	2.22	2.42
AZUM-D46G 19-B	Azokh 1 Units II–III	OHI 0 Bacterial MFD surround Haversian canals at the outer cortical layer chaotic distribution. Radial and peripheral microtunnelling	33.7	0.0897	0.1235	0.0125	0.0288	0.1648	2.01	2.41
AZUM-D46G 19-C	Azokh 1 Units II–III	OHI 0 Similar to B, microtunnelling damaging bacterial attack (fungi?), peripherally dispersed	36.6	0.0933	0.0883	0.0034	0.0171	0.1088	2.14	2.40
AZUM-D46G 19-D	Azokh 1 Units II–III	OHI 2 Histological traits partially disappear, radial distribution of small tubes, fungi? from Haversian canals. EDS Barium sulfate (Barite), and illite (sediment). Enlarged canaliculi, mineralised	48.6	0.0647	0.0416	0.0127	0.0552	0.1096	2.31	2.60
Azokh 1 Unit Vu										
AZU-Section	Azokh 1 Unit Vu	OHI 5 Some canals infilled with clayish sediment rich in phosphorous	80.7	0.2268	0.2674	0.0124	0.0435	0.3233	1.44	2.13
AZM E 39 1	Azokh 1 Unit Vm	OHI 5 Mineralized osteons. Sediment (illite), manganese, Sn and Ti are also present. Mineral "acicular" shape with illites, Mn and unknown minerals with Zn, Ni. (EDS)	31.6	0.0378						

(continued)

Table 11.2 (continued)

Sample code	Site	Oxford Histological Index and Histology notes	BET Surface Area m^2/g (by N_2 Porosimetry)	Volume (cm^3/g) between 0.001 and 0.1 μm (N_2 porosity)	Volume (ml/ml) in pores <0.1 μm (Hg porosity)	Volume (ml/ml) in pores <10 >0.1 μm (Hg porosity)	Volume (ml/ml) in pores >10 μm (Hg porosity)	Total Porosity (ml/ml) (Hg porosity)	Bulk Density g/ml (Hg porosity)	Skeletal Density g/ml (Hg porosity)
AZM E41 4	Azokh 1 Unit Vm	OHI 5 Strong cracking on the outer and inner cortical area. Enlarged canaliculi	33.3	0.0437	0.0104	0.0005	0.0153	0.0262	2.47	2.53
AZM-E40G	Azokh 1 Unit Vm	OHI 4–5 Good histology except in a lateral side that has localized corrosion and enlarged canaliculi	55.8	0.0687	0.0254	0.0089	0.0186	0.0529	2.33	2.46
AZM-E41G	Azokh 1 Unit Vm	OHI 5 ESEM surface of rounded holes, of unknown cause. Nodules of Si (EDS). Heavily cracked	30.7	0.0376	0.0000	0.0000	0.0694	0.0694	2.11	2.27
AZM-F42 9	Azokh 1 Unit Vm	OHI 5 Haversian canals are infilled with secondary minerals of apatite. Enlarged canaliculi	4.2	0.0074	0.0000	0.0000	0.0515	0.0515	3.08	3.25
AZM-G41 5	Azokh 1 Unit Vm	OHI 4–5 Some strong and localized cracking, mainly at the outer cortical area, unknown origin, maybe mineral loss, Sediment illites and Mn Enlarged canaliculi on cortical	36.7	0.0461	0.0244	0.0378	0.0683	0.1305	2.44	2.80
Azokh 2										
AZN P11	Azokh 2	OHI 0 Chaotic distribution of bacterail attack. Slightly enlarged canaliculi	22.1	0.0678	0.0927	0.1515	0.1159	0.3602	1.30	2.05
AZN-Q10	Azokh 2		18.6	0.0486	0.0714	0.0108	0.0173	0.0994	1.76	1.96
AZN-SL-HDU	Azokh 2	Surface analysis, bacterial attack apparent	0.6	0.0026	0.0155	0.0239	0.0000	0.0393	1.91	1.99
AZN-SL-HWU	Azokh 2	OHI 4 Bacterial attack on the outer cortical, very incipient. Deep cracks < 2 mm deep. Enlarged canaliculi	0.1	0.0012	0.0000	0.0000	0.0503	0.0503	2.13	2.24

(continued)

Table 11.2 (continued)

Sample code	Site	Oxford Histological Index and Histology notes	BET Surface Area m^2/g (by N_2 Porosimetry)	Volume (cm^3/g) between 0.001 and 0.1 μm (N_2 porosity)	Volume (ml/ml) in pores <0.1 μm (Hg porosity)	Volume (ml/ml) in pores <10 >0.1 μm (Hg porosity)	Volume (ml/ml) in pores >10 μm (Hg porosity)	Total Porosity (ml/ml) (Hg porosity)	Bulk Density g/ml (Hg porosity)	Skeletal Density g/ml (Hg porosity)
AZN-SL-HDW	Azokh 2	OHI 5 Deep cracking >2 mm deep of weathering. Wedl tunneling dispersed. Most lacunae infilled	1.9	0.0097	0.0303	0.0230	0.0746	0.1279	1.95	2.24
AZN-SL-HWW	Azokh 2		4.6	0.0134	0.0396	0.0341	0.0000	0.0737	1.95	2.10
AZN-SL-A	Azokh 2	OHI 5 Surface affected by root marks, histology is not etched. EDS sediment rich in Fe and Mn	109.4	0.2324	0.2659	0.0226	0.0228	0.3113	1.52	2.21
AZN-SL-B	Azokh 2	The white dots contain gypsum (EDS)	87.9	0.2038	0.2313	0.0442	0.1175	0.3930	1.37	2.26
AZN-SL-C	Azokh 2	OHI 0 Completely invaded by bacteriae. EDS Barium sulfate (Barite) crystals	48.3	0.1153	0.1035	0.2624	0.0109	0.3768	1.47	2.37
AZN-SL-D	Azokh 2	OHI 4 Pitted periosteal cortical layer, possibly fungi								
AZN-SL-F	Azokh 2	OHI 5 ESEM surface analysis, root marks. Good histology, no evidence of root etching in section	102.0	0.1961	0.1603	0.0231	0.0123	0.1957	1.34	1.66
AZN-SL-G	Azokh 2	OHI 5 Root marks on surface. Section: Good histology, no evidence of root etching. Barite deposits	105.5	0.2238	0.2581	0.0303	0.0521	0.3404	1.48	2.25

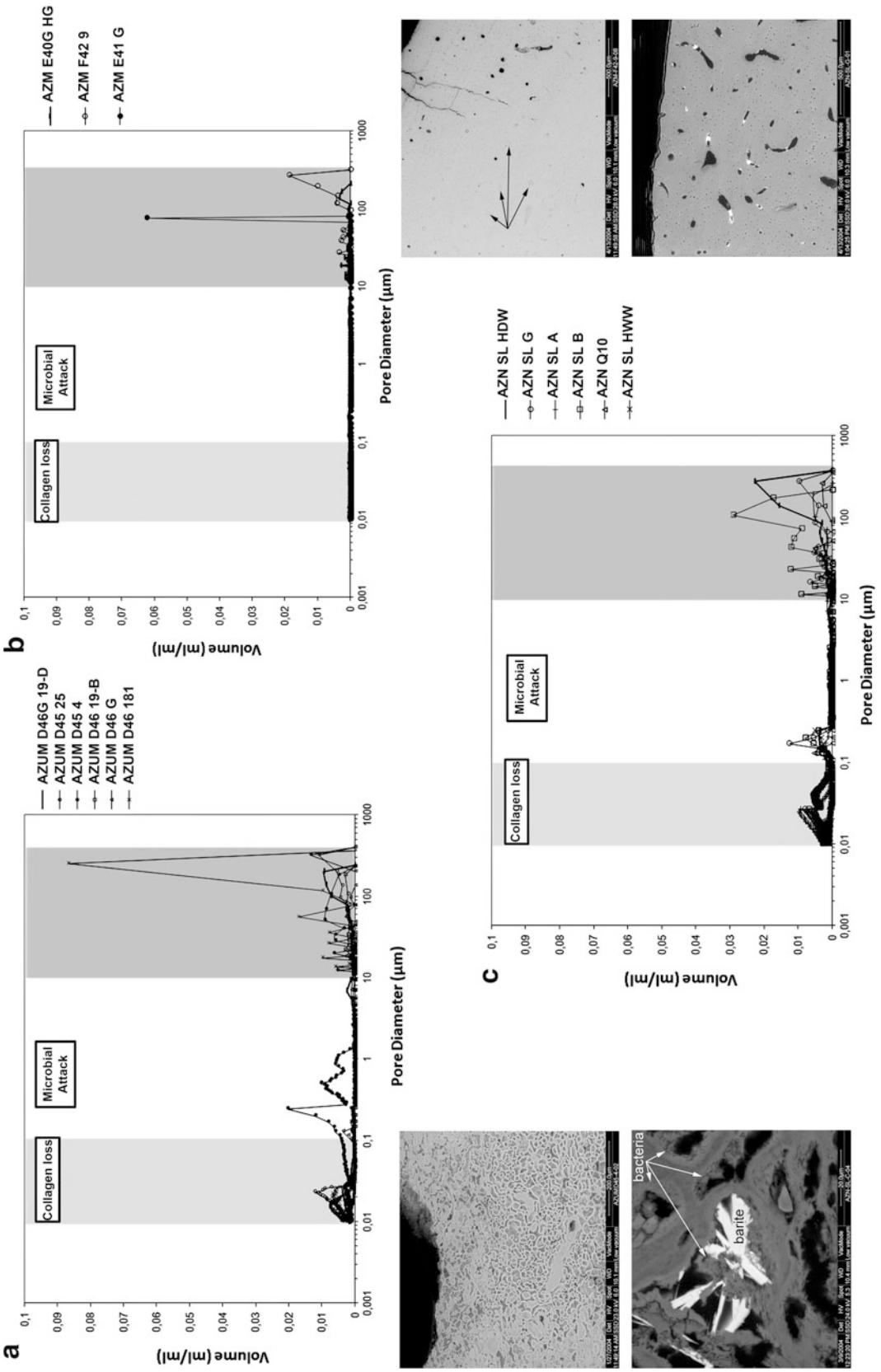

Fig. 11.2 Pore size distributions of Azokh fossil bone samples measured by mercury intrusion porosimetry. **a** Units II–III (inset middle left, AZUM D45 4 SEM microphotograph showing intense bacterial attack), **b** Unit Vm (inset middle right: AZM F42 9 SEM microphotograph showing Canals of Havers filled by calcareous secondary minerals, black arrows), **c** Azokh 2 (inset bottom left: AZN SL C SEM microphotograph showing bacterial attack and barite ($BaSO_4$ identified by EDS) damaging bacteria colonies [microscopic focal destruction, MFD], so bacteria predated secondary growth of minerals; inset bottom right: SEM microphotograph of AZN SL G with histological cavities filled by secondary minerals, see Marin-Monfort et al. 2016)

Index 0) and others none (Histological Index 5). The pore structure of bone from these units (Fig. 11.2a) is somewhat unusual, but it is most similar to that of bone recovered from Etton Causewayed Enclosure (Brock et al. 2010). Such material is similar to those having undergone accelerated collagen hydrolysis (ACH) (Smith et al. 2002, 2007), i.e. it has a significant increase in the porosity in pores of less than 0.1 μm, however there is less volume in this pore space. This pore space is interpreted as the pore space that remains after collagen loss but is only apparent following non-microbially mediated loss of collagen, i.e. it occurs when the collagen is chemically removed. This collagen loss can occur rapidly and has been observed in bones as young as 700 years (Smith et al. 2002), however, the bones from Units II–III in Azokh 1 are likely to be around 100–200 ka (see Appendix, ESR). This Azokh material and that from Etton Causewayed Enclosure (Brock et al. 2010) differs from that of ACH bone as the pore volume is smaller and the pore space is distributed in smaller pores within this range. The smaller pore volume and smaller diameter pore range in the Azokh and Etton Causewayed Enclosure material, compared to that of previously published material from European deposits and boiled bone (Smith et al. 2002, 2007; Roberts et al. 2002; Turner-Walker et al. 2002), is probably the result of some pore infilling during deposition. This observation is supported in the Azokh material by observations under ESEM of bone sections where secondary mineralization can be observed (Table 11.1), suggesting exogenous mineral sources related to cave environments and decay (calcite, tinsleyite, barite, brushite), are contributing to the infilling (Marin-Monfort et al. 2016; Murray et al. 2016).

There are two probable scenarios as to how these bones have been preserved in this state. They either underwent a rapid phase of degradation, like ACH bone during early diagenesis, remaining stable for the following millennia with some pore infilling. Or the observed changes occurred slowly over the whole taphonomic history of the fossils, so that bones with characteristics similar to those of ACH bone can be formed by an alternative slower process.

AZUM D45 4 16/8/3 is a sample that shows extensive histological damage and displays the characteristic increase in porosity (Fig. 11.2a) in pores of diameter 0.1–10 μm (Jans et al. 2004). Samples AZUM-D46G 19- B, C and D also have a low histological index, but do not show this increase in porosity. Indeed they display very low porosity considering that they have no collagen and evidence of microbial attack. This again must be attributed to the pores being in-filled during deposition.

Azokh 1 Unit Vm

The material from Unit Vm, the oldest part of the Azokh 1 sequence excavated so far, is heavily fossilized. The samples analyzed had no collagen preserved (and have yielded no DNA, Geigl 2012 personal communication). They have highly altered mineral (IRSF ranges from 3.3 to 3.9 and C:P ratio 0.26–0.17) and good histological preservation (Histological Index 4 or 5). They have little porosity in the detectable range of mercury porosimetry (on average ~6%) and high density values (both bulk and skeletal). As stated earlier, when collagen is lost from the bone, the porosity of the bone increases (in pores less than 0.1 μm diameter) and there is a concomitant decrease in bulk density and an increase in apparent skeletal density. In the fossil bone from Unit Vm there is a small pore volume in the <0.1 μm diameter pore range (Fig. 11.2b), but it is much smaller than that observed in ACH bone (see Smith et al. 2002) and that observed in bones from Units II–III of Azokh 1 and Etton Causewayed Enclosure (Brock et al. 2010). Even though the fossil bone from Unit Vm of Azokh 1 has lost its collagen, its density is greater than that of fresh modern bone (e.g., Nielsen-Marsh and Hedges 1999), suggesting that the pore space has been in filled with material denser than collagen.

This type of preservation is not prevalent in European Holocene bone (Smith et al. 2007), but the pore structure and lack of collagen is similar to that of dinosaur fossils measured by Trueman and Tuross (2002, in particular Fig. 1 therein). We can speculate about the processes that have formed this material from Unit Vm as being similar to those that may have occurred to the bones in Units II–III. Possible initial ACH type bone may have been formed with subsequent infilling of the pore space, or a different process, where the collagen is slowly degraded and replaced with mineral.

Azokh 2

Interpretation of the samples from Azokh 2 is difficult as the bones are probably a mixture of both modern and fossil material. Based on appearance and diagenetic parameter values the modern bones are represented by AZN P11, AZN Q10 and four samples from the same metapodial AZN H- DU, DW, WW, WU. Four samples were taken from this one metapodial as the bone exhibited an obviously weathered side and an unweathered side. Furthermore, the effect of rudimentary cleaning of the

bone (dry brushing and wet brushing) was also tested on this one specimen, giving four parameters: DU, dry/unweathered, DW, dry/weathered, WW, wet/weathered and WU, wet/unweathered. In general the modern bones show high levels of collagen remaining with the exception of AZN Q10, which has only a moderate amount of collagen. AZN P11 has lost some collagen and has evidence of microbial attack (0 histological index and increased porosity in the 0.1–10 μm pore diameter range). Although the AZN H metapodial is differentially weathered and has been cleaned differently there is little difference in the diagenetic parameters of the four samples. The bone is "well preserved" in terms of collagen preservation although the mineral component of the bone is heavily altered (IRSF 3.3 or above and C:P ratio ranging from 0.36 to 0.28). Interestingly, the surfaces of the un-weathered side show signs of some microbial attack, which is absent in samples taken from the weathered (exposed) side. In general the porosity of the modern samples from Azokh 2 is low (as would be expected), with the exception of sample AZN P11, mentioned above.

The other samples recovered from Azokh 2, probably represent either; rapidly degraded modern samples or, more likely, semi-fossil material that has been transported from inside the cave and deposited in the top layers at the cave entrance during the sedimentation of the cave (Fernández-Jalvo et al. 2010b; Murray et al. 2016). They are typically ACH type bone, with low levels of collagen, and high levels of mineral alteration and porosity in the <0.1 μm diameter pores (Fig. 11.2c), although it should be noted that AZN SL C has been heavily microbially attacked (evidenced by increased porosity in the 0.1–10 μm pore diameter range). They are from a diagenetic perspective similar to the material from Azokh 1 Units II–III.

Assessment of Nitrogen Adsorption Isotherm Analysis and Mercury Intrusion Porosimetry

The investigation of pore structure using both nitrogen adsorption isotherm analysis (NAIA) and mercury intrusion porosimetery (HgIP) worked well in this sample set. The majority of the samples retained little collagen so that they were easy to dry and outgas and amenable to analysis. HgIP

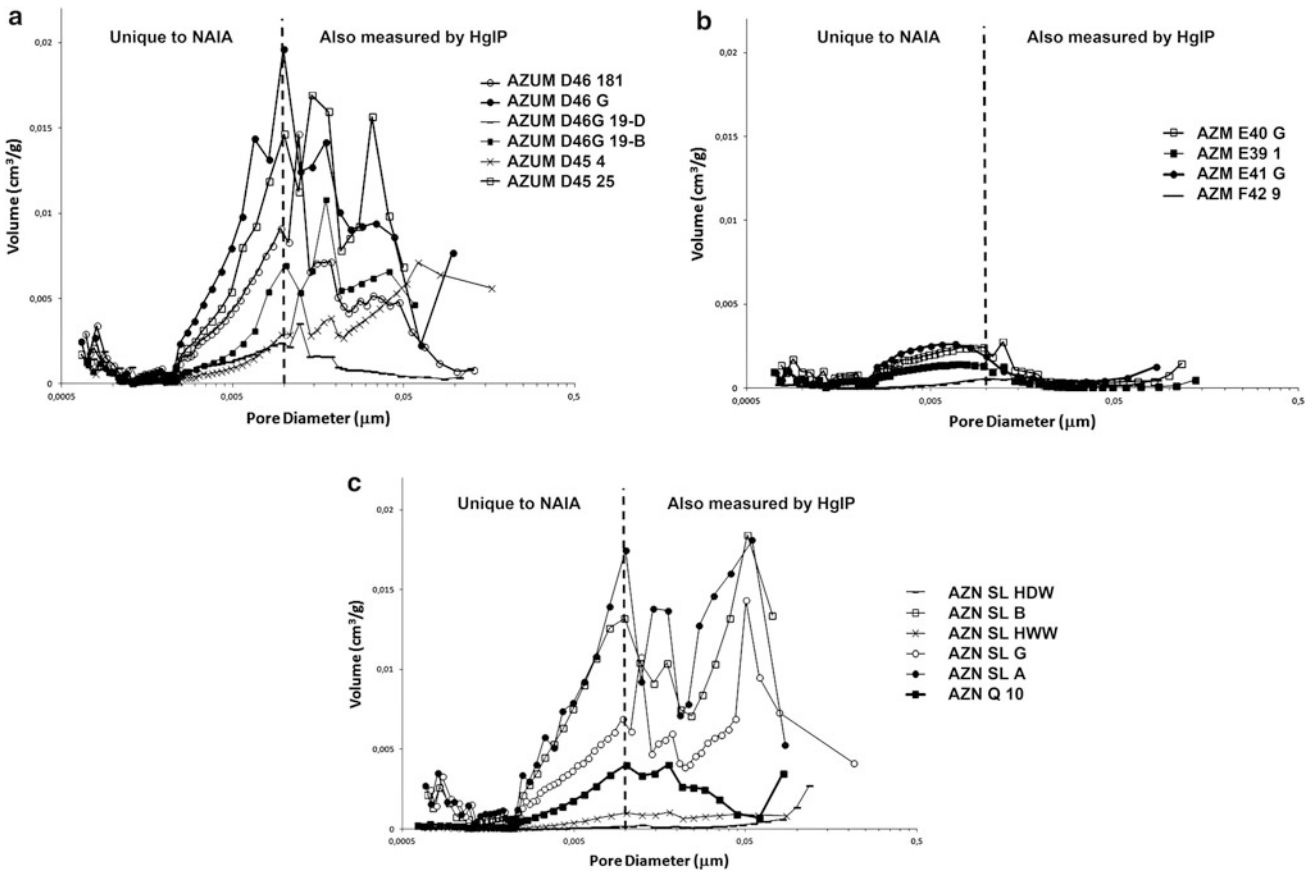

Fig. 11.3 Pore size distributions of Azokh fossil bone samples measured by Nitrogen adsorption isotherm analysis. **a** Azokh 1, Units II–III, **b** Azokh 1, Unit Vm, **c** Azokh 2

has been used to analyze archaeological bone porosity on numerous occasions (e.g., Nielsen-Marsh and Hedges 1999; Smith et al. 2002, 2008) but NAIA has not been used as comprehensively.

In this data set, when measured using HgIP most of the bones have either a large pore space associated with collagen loss or have little collagen but lack this pore space. Presumably, in the latter case, this pore space has been opened with the loss of collagen but subsequently re-filled by exogenous mineral. A similar pattern is true for the pores measured by NAIA in the 0.001–0.1 μm pore diameter range; with bone from Azokh 1 Units II–III (Fig. 11.3a) having the largest NAIA pore volume, and the heavily in filled and fossilized bones from Unit Vm showing low NAIA pore volumes (Fig. 11.3b).

There is a strong relationship between the pore volumes measured by the two techniques in the smallest pore range (Fig. 11.4), with both measurements responding in the same way to the diagenetic processes in the bone. There is some overlap in the two pore ranges measured by the different methods (HgIP in the smallest pores is approximately 0.01–0.1 μm but with NAIA from 0.001 to 0.1 μm), but this common pore volume measured does not appear to be completely responsible for this relationship. It is clear that the sub 0.01 μm pores measured *only* by NAIA are mimicking what is happening in larger pores. The sub 0.01 μm pores are increasing in volume with collagen loss (Fig. 11.3a, c) and also being infilled (Fig. 11.3b).

Although the pore space measured by NAIA in samples from Azokh 1 Vm is small in comparison to other samples, where large amounts of collagen have been lost, there is some evidence that this small pore volume is indeed what has been suggested above: the pores opened by collagen loss have subsequently been refilled. Figure 11.5 shows the same data as Fig. 11.3b with a smaller *y-axis* to accentuate the pore volume. In addition the "well preserved (collagen rich) bones" from Azokh 2 are included and AZUM D46G 19-D is included for comparison, as the sample from Units II–III with the smallest volume in this pore range. At this scale it is clear that the pore volume in the Unit Vm bones is significantly larger than that found in the "well preserved bones" that have >20% collagen, with the exception of AZM F42 9. AZUM D46G 19-D has a similar pore size distribution to the Unit Vm material and can clearly be seen to be a filled in bone. Interestingly AZM F42 9 has a low pore volume in this pore range, similar to the "well preserved bones"; the reason for this is not clear, and it was noticed that many of the haversian structures and other pore spaces visible under ESEM were infilled with mineral, indicating extensive infilling.

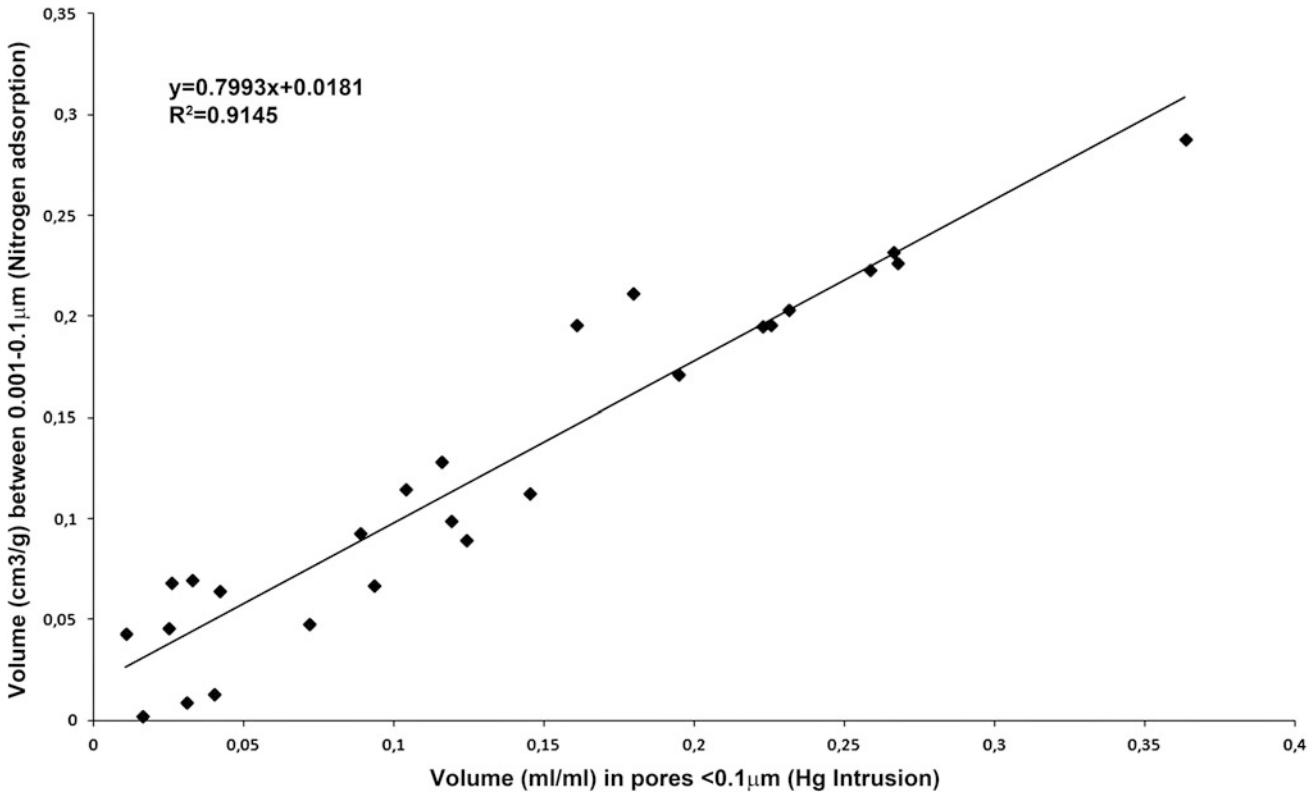

Fig. 11.4 Pore volume comparison: nitrogen adsorption isotherm analysis volume versus mercury intrusion porosimetry volume on the same bone specimen for pores <0.1 μm

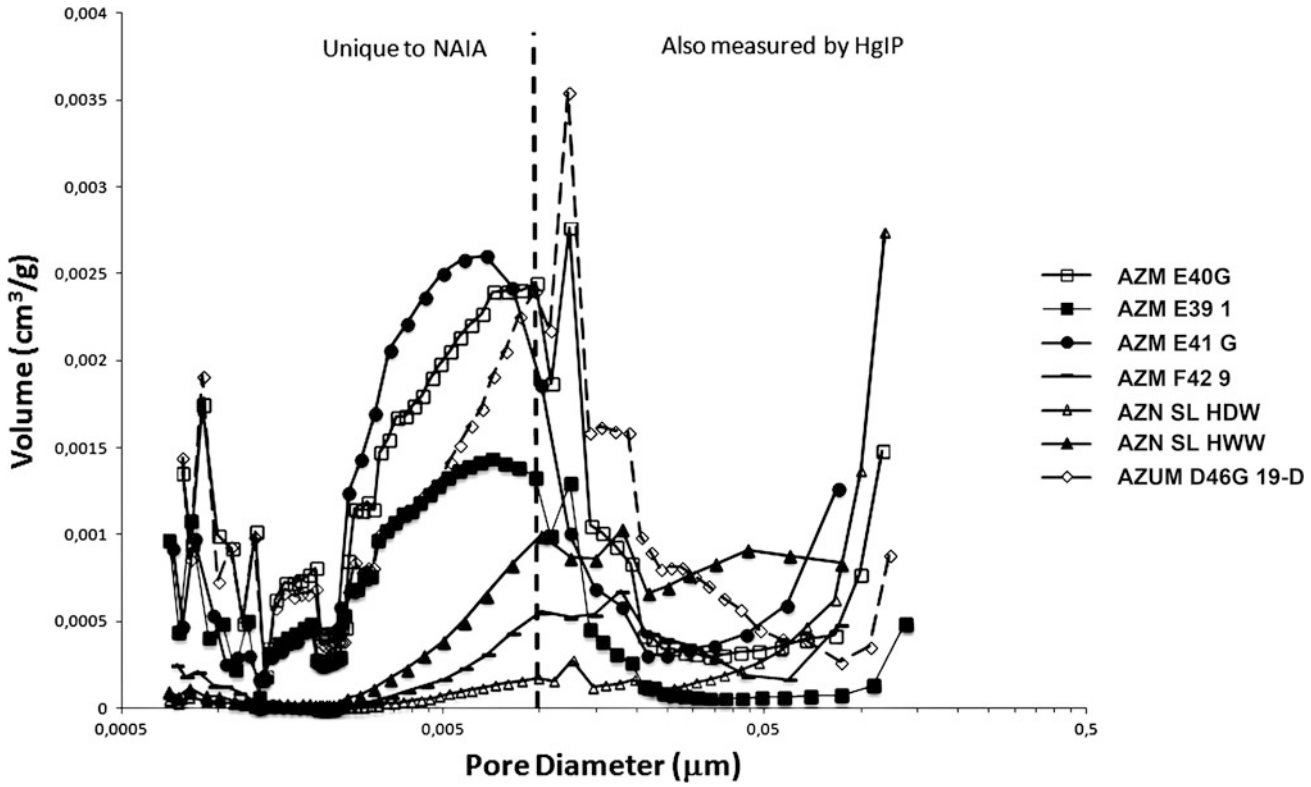

Fig. 11.5 Detailed pore size distributions of Azokh fossil bone samples measured by nitrogen adsorption isotherm analysis. Note that the *y-axis* is much smaller than in Fig. 11.3

When observing the pore structures at this fine scale there is certainly evidence to suggest that this pore space is opened via collagen loss (like the 0.01–0.1 μm range observed using HgIP) and subsequently (although not completely) refilled. This process generally leaves a different porosity pattern to "well preserved bone" that has not lost collagen. Further studies are needed to make this pattern clearer, but from the data from the Azokh material we can suggest that this is the case. It appears that in this data set NAIA is providing similar information to that given by HgIP, as the smaller pores seem to reflect the loss of collagen from the bone. In this sense it appears that NAIA could be used as a non-destructive tool to investigate non-microbial collagen loss in archaeological bone. However, as NAIA cannot be used to measure the larger pores that indicate microbial loss it cannot provide all the information that HgIP can.

Of note is the role of infilling of the pores at this site and how this obscures some of the interpretations that might easily be made using HgIP. Previous studies have suggested that HgIP can be used to identify distinct types of preservation; i.e. ACH, microbially attacked bone, "well preserved bone" and bone undergoing mineral dissolution (Nielsen-Marsh et al. 2007; Smith et al. 2007). In this data set, although microbial attack has been identified in some bones, the characteristic pore structure caused by this (porosity in the 0.1–10 μm pore diameter range) is not obvious. Similarly many of the bones analyzed here have undergone collagen loss without microbial attack and we might expect to observe pore increases in the <0.1 μm pore diameter range. Again this information has been obscured by infilling. In data sets where pore infilling is prevalent it becomes imperative to do histological examinations to determine the role of microbial attack in the diagenetic histories of the bones, as HgIP cannot be used to make distinctions between bones with and without microbial damage. Moreover, NAIA should be used to investigate porosity changes in such data sets as it can provide some information on collagen loss and infilling and would be non-destructive.

A Model of Bone Diagenesis at Azokh Caves

Bones from dead animals that enter the fossil record start out in the "well preserved bone" category (i.e. recently living tissue). From the surface exposed bones tested from Azokh 2, we can presume that bone can remain relatively unmodified for at least a few years or decades. Some changes do

occur, in initial diagenesis at the site with the modern material showing weathering and in some cases substantial mineral degradation, and some microbial attack.

Fossil bone in Units II–III at Azokh 1 is most similar to bone described by Brock et al. (2010) recovered from Etton Causewayed Enclosure. This appears to be similar to the ACH bone found in European Holocene sites (Smith et al. 2002, 2007; Nielsen-Marsh et al. 2007), but with infilling of the pore space (evident in the Azokh material from the porosity and histological analysis). Bone from Unit Vm is heavily fossilized and the pore structure is extensively in-filled, so that the bone is not porous but dense. This latter type of preservation is not typical of those described in European Holocene deposits (Smith et al. 2007; Brock et al. 2010), because of the extensive infilling of the pore structure.

Given the main features of the ancient material in Azokh 1 (predominantly ACH or Etton Causewayed Enclosure type bone in Units II–III and heavily infilled bone Unit Vm), it seems reasonable to suggest a model of bone diagenesis at Azokh Cave proceeding as follows. The initial phases of degradation at the site lead to some ACH bone and microbially attacked bone, with the cave providing a relatively stable environment where the pore space is infilled with exogenous or authigenic mineral over time. The evidence from the measurements suggests that this process takes hundreds of thousands of years at Azokh as the material from oldest layers measured here (Unit Vm) is heavily mineralized, where as the younger bones (Units II–III) still retain some pore space, although there is evidence that this has been partially filled. The rate of the initial collagen loss cannot be known at Azokh, but it has been observed within 700 years at Apigliano in Italy (Smith et al. 2002), and we can speculate that at Azokh it could have occurred over a similar time span. Afterwards, the process of pore infilling was probably gradual and the conditions for bone preservation were generally benign. In this model it seems that the type of preservation found in Unit Vm is the natural progression of bone that has passed through an early stage like that in Units II–III.

Alternatively, it is of course quite possible that both units had quite different modes of diagenesis, as the initial conditions are thought to be very important in determining the later stages of diagenesis (Trueman and Martill 2002; Jans et al. 2004; Smith et al. 2007; Nielsen-Marsh et al. 2007). The two strata measured here are separated by 100–200 ka, and environmental conditions (for example temporal variation in precipitation) could have been different for bones at these two different times, or subsequent burial depth could play a part in the differing diagenetic pathways. Thus we could speculate on a model where ACH occurred only in Units II–III, while in Unit Vm diagenesis could have occurred without an ACH phase, but with a slow rate of collagen loss and slow rate of pore infilling.

It is interesting to note is that the conditions in the cave deposits appear to be benign for both ACH bone and microbially attacked bone, with both types of bone appearing in the deposits and both undergoing infilling, although it should be noted that there is only sparse evidence of microbial attack (some bones with histological index 4–5) in Azokh 1 Unit Vm. This indicates that once bone passes through the initial phases of degradation, the Azokh sediments provide a stable and largely benign environment for bone preservation, at least macroscopically.

Prospects for Molecular Preservation

The ancient bone material from Azokh Caves presents the characteristics of heavily altered bone, with or without mineral infilling in the pore spaces. Collagen preservation is exceptionally poor in all the ancient material, with low ‘collagen’ yields and none of the acid insoluble material recovered giving good collagen C:N ratios. Previous studies have indicated that the best preserved material (i.e. with higher collagen levels, and less microbial attack) is the best material for DNA amplification (Colson et al. 1997; Haynes et al. 2002; Gilbert et al. 2005). Pruvost et al. (2007) showed that DNA could be retrieved from fossil bones heavily attacked by bacteria, suggesting that bacterial attack may not be the only reason for DNA degradation. The age of the fossils studied by these authors, however, is much younger (Holocene) than those of Azokh. Given the poor organic preservation observed in Azokh Caves sites, even in modern (Holocene) bones, it seems likely that ancient DNA preservation will be equally poor in the Azokh material. One proposed mechanism of DNA survival in ancient bone is via adsorption to the surface of the bone mineral crystals (Tuross 1993; Götherström et al. 2002) or molecular ‘niches’ within the histological structure (Geigl 2002), but given the highly altered mineral of the bones at Azokh Cave, survival of ancient DNA via these mechanisms also seems unlikely.

Conclusions

1. The fossil bone from the site of Azokh Caves is in general poorly preserved with no collagen preservation observed and in most cases with extensive mineral alteration.
2. Histological examination reveals that some bones have undergone microbial attack and that many show evidence of exogenous minerals embedded in the histological structure. Using collagen as a guide for organic preservation it is unsurprising that aDNA preservation at

the site is so poor; moreover the heavily altered mineral of the bones would also provide little hope for aDNA preservation.

3. There are distinct types of preservation for the bones in the three areas analyzed. Modern material from the surface of Azokh 2 shows diagenetic parameters characteristic of "well preserved bone", although this material is mixed with poorly preserved material (Holocene), that in general has ACH like preservation.
4. The material from Azokh 1 Units II–III shows typical ACH bone and microbial attacked bone, but both types have some infilling of the pore space with the ACH type bone giving similar diagenetic parameter and HgIP traces to bone from Etton Causewayed Enclosure (Brock et al. 2010).
5. Material from Unit Vm is heavily fossilized with extensive pore infilling and high density values. This kind of heavily infilled fossil preservation has been observed in Dinosaur fossils previously (Trueman and Tuross 2002) but not in archaeological material, so Azokh Caves represents the first time this type of preservation has been observed in Pleistocene material.
6. Azokh also presents two variables that were not present in previous studies of bone diagenesis using this diagenetic parameter approach (e.g., Smith et al. 2007). One factor is the cave environment and the other is that the material in Azokh is much older than that measured by Smith et al. (2007). One or both of these factors could be important in creating the type of bone preservation at Azokh Unit Vm and making it different from those of previous studies.
7. The use of nitrogen adsorption isotherm analysis and mercury intrusion porosimetry to measure the pore structure of the bones at Azokh was particularly successful, especially as the collagen preservation was so poor that it enabled the samples to be dried and outgassed easily. This aided the comparison of the two techniques when applied to the same bone sample and revealed that the two techniques appear to be measuring similar aspects of bone degradation. HgIP shows an increase in porosity in the small pores when collagen is lost from the bone non-microbially i.e. ACH bone). NAIA shows a similar pattern and that small pores below the range of HgIP are also affected by this non-microbial collagen loss. In Azokh 1 Unit Vm HgIP shows no increase (presumably because the pores that were opened through collagen loss have been filled in with mineral). The pores measured using NAIA, do show extensive infilling, but this is not complete. When observed at a finer scale, there is a difference between the pore structures of the Unit Vm material that has undergone chemical collagen loss and collagen rich bones, even when there has been some infilling of the pores in the first group. It appears that the pores measured by both techniques (HgIP and NAIA) are responding in the same manner to the same processes, in that pore space is opening with collagen loss and becoming infilled.
8. The study of pore structures at Azokh also provides a cautionary tale for the use of mercury intrusion porosimetry. Whilst this technique has provided a powerful way to distinguish between different early taphonomic bone types based on characteristic pore size distributions (Smith et al. 2007); the infilling of pores (e.g., in Azokh Unit Vm) obscures this detail, making such distinctions impossible. Thus when analyzing such heavily fossilized bone it becomes imperative to analyze histological sections to determine the role of microbial attack in the role of bone degradation at the site.

Acknowledgements This investigation was carried out as part of a Marie Curie Training Fellowship awarded to CS (Contract Number: HPMF-CT-2002-01605), and has benefited from funding from two research projects of the Spanish Ministry of Science (BTE2003-01552 and CGL2007-66231). Nitrogen adsorption isotherm analysis and mercury intrusion porosimetry, and FTIR analysis were carried out at the Unidad de Apoyo a la Investigación del Instituto de Catálisis y Petroleoquímica and C:N analyses were undertaken at the Facultad de Ciencias at the Universidad Autónoma de Madrid. Thanks to the technicians of the Electron Microscopy Unit of the Museo Nacional de Ciencias Naturales.

References

Appendix: Fernández-Jalvo, Y., Ditchfield, P., Grün, R., Lees, W., Aubert, M., Torres, T., et al. (2016). Dating methods applied to Azokh cave sites. In Y. Fernández-Jalvo, T. King, L. Yepiskoposyan & P. Andrews (Eds.), *Azokh Cave and the Transcaucasian Corridor* (pp. 1–26). Dordrecht: Springer.

Barrett, E. P., Joyner, L. G., & Halenda, P. P. (1951). The determination of pore volume and area distributions in porous substances. I. Computations from nitrogen isotherms. *Journal of the American Chemical Society, 73*, 373–380.

Bennett, E. A., Gorgé, O., Grange, T., Fernández-Jalvo, Y., & Geigl, E.-M. (2016). Coprolites, paleogenomics and bone content analysis. In Y. Fernández-Jalvo, T. King, L. Yepiskoposyan & P. Andrews (Eds.), *Azokh Cave and the Transcaucasian Corridor* (pp. 271–286). Dordrecht: Springer.

Bosch, P., Alemán, I., Moreno-Castilla, C., & Botella, M. (2011). Boiled versus unboiled: A study on Neolithic and contemporary human bones. *Journal of Archaeological Science, 38*, 2561–2570.

Brock, F., Higham, T., & Bronk Ramsey, C. (2010). Pre-screening techniques for identification of samples suitable for radiocarbon dating of poorly preserved bones. *Journal of Archaeological Science, 37*, 855–865.

Collins, M. J., Nielsen-Marsh, C. M., Hiller, J., Smith, C. I., Roberts, J. P., Prigodich, R. V., et al. (2002). The survival of organic matter in bone: A review. *Archaeometry, 44*, 383–394.

Colson, I., Bailey, J. F., Vercauteren, M., Sykes, B., & Hedges, R. E. M. (1997). The preservation of ancient DNA and bone diagenesis. *Ancient Biomolecules, 1*, 109–117.

DeNiro, M. J. (1985). Postmortem preservation and alteration of in vivo bone collagen isotope ratios in relation to palaeodietary reconstruction. *Nature, 317*, 806–809.

Domínguez-Alonso, P., Aracil, E., Porres, J. A., Andrews, P., Lynch, E. P., & Murray, J. (2016). Geology and geomorphology of Azokh Caves. In Y. Fernández-Jalvo, T. King, L. Yepiskoposyan & P. Andrews (Eds.), *Azokh Cave and the Transcaucasian Corridor* (pp. 55–84). Dordrecht: Springer.

Fernández-Jalvo, Y., Andrews, P., Pesquero, D., Smith, C., Marin-Monfort, D., Sánchez, B., et al. (2010a). Early bone diagenesis in temperate environments Part I: Surface features and histology. *Palaeogeography, Palaeoclimatology, Palaeoecology, 288*, 62–81.

Fernández-Jalvo, Y., King, T., Andrews, P., Yepiskoposyan, L., Moloney, N., Murray, J., et al. (2010b). The Azokh Cave complex: Middle Pleistocene to Holocene human occupation in the Caucasus. *Journal of Human Evolution, 58*, 103–109.

Fernández-Jalvo, Y., King, T., Yepiskoposyan, Y., & Andrews, P. (2016). Introduction: Azokh Cave and the Transcaucasian Corridor. In Y. Fernández-Jalvo, T. King, L. Yepiskoposyan & P. Andrews (Eds.), *Azokh Cave and the Transcaucasian Corridor* (pp. 1–26). Dordrecht: Springer.

Geigl, E.-M. (2002). On the circumstances surrounding the preservation and analysis of very old DNA. *Archaeometry, 44*, 337–342.

Gilbert, M. T. P., Rudbeck, L., Willerslev, E., Hansen, A. J., Smith, C., Penkman, K., et al. (2005). Biochemical and physical correlates of DNA contamination in archaeological human bones and teeth excavated at Matera, Italy. *Journal of Archaeological Science, 32*, 785–793.

Götherström, A., Angerbjorn, A., Collins, M. J., & Liden, K. (2002). Bone preservation and DNA amplification. *Archaeometry, 44*, 395–404.

Gutierrez, M. A. (2001). Bone diagenesis and taphonomic history of the Paso Otero 1 Bone Bed, Pampas of Argentina. *Journal of Archaeological Science, 28*, 1277–1290.

Haynes, S., Searle, J. B., Bertman, A., & Dobney, K. M. (2002). Bone preservation and ancient DNA: The application of screening methods for predicting DNA. *Journal of Archaeological Science, 29*, 585–592.

Hedges, R. E. M. (2002). Bone diagenesis: An overview of processes. *Archaeometry, 44*, 319–328.

Hedges, R. E. M., & Millard, A. R. (1995). Bones and groundwater: Towards the modelling of diagenetic processes. *Journal of Archaeological Science, 22*, 155–164.

Hedges, R. E. M., Millard, A. R., & Pike, A. W. G. (1995). Measurements and relationships of diagenetic alteration of bone from three archaeological sites. *Journal of Archaeological Science, 22*, 201–209.

Jans, M. M. E., Nielsen-Marsh, C. M., Smith, C. I., Collins, M. J., & Kars, H. (2004). Characterisation of microbial attack on archaeological bone. *Journal of Archaeological Science, 31*, 87–95.

Joschek, S., Nies, B., Krotz, R., & Gopferich, A. (2000). Chemical and physico-chemical characterization of porous hydroxy-apatite ceramics made of natural bone. *Biomaterials, 21*, 1645–1658.

Kars, E. A. K., & Kars, H. (2002). *The degradation of bone as an indicator in the deterioration of the European Archaeological Heritage – Final Report*. (ISBN 90-5799-029-6).

Kasimova, R. M. (2001). Anthropological research of Azykh Man osseous remains. *Human Evolution, 16*, 37–44.

King, T., Compton, T., Rosas, A., Andrews, P. Yepiskoyan, L., & Asryan, L. (2016). Azokh cave Hominin Remains. In Y. Fernández-Jalvo, T. King, L. Yepiskoposyan & P. Andrews (Eds.), *Azokh Cave and the Transcaucasian Corridor* (pp. 103–106). Dordrecht: Springer.

Marin-Monfort, M. D., Cáceres, I., Andrews, P., Pinto, A. C., & Fernández-Jalvo, Y. (2016). Taphonomy and site formation of Azokh 1. In Y. Fernández-Jalvo, T. King, L. Yepiskoposyan & P. Andrews (Eds.), *Azokh Cave and the Transcaucasian Corridor* (pp. 211–249). Dordrecht: Springer.

Millard, A. R. (2001). Deterioration of bone. In D. Brothwell & A. M. Pollard (Eds.), *Handbook of archaeological sciences* (pp. 633–643). Chichester: Wiley.

Murray, J., Domínguez-Alonso, P., Fernández-Jalvo, Y., King, T., Lynch, E. P., Andrews, P., et al. (2010). Pleistocene to Holocene stratigraphy of Azokh 1 Cave, Lesser Caucasus. *Irish Journal of Earth Sciences, 28*, 75–91.

Murray, J., Lynch, E. P., Domínguez-Alonso, P., & Barham, M. (2016). Stratigraphy and sedimentology of Azokh Caves, South Caucasus. In Y. Fernández-Jalvo, T. King, L. Yepiskoposyan & P. Andrews (Eds.), *Azokh Cave and the Transcaucasian Corridor* (pp. 27–54). Dordrecht: Springer.

Nielsen-Marsh, C. M., & Hedges, R. E. M. (1999). Bone Porosity and the use of Mercury intrusion porosimetry in bone diagenesis studies. *Archaeometry, 41*, 165–174.

Nielsen-Marsh, C. M., Smith, C. I., Jans, M., Nord, A., Kars, H., & Collins, M. J. (2007). Bone diagenesis in the European Holocene II: Taphonomic and environmental considerations. *Journal of Archaeological Science, 34*, 1523–1531.

Pruvost, M., Schwarz, R., Bessa Correia, V., Champlot, S., Braguier, S., Morel, N., et al. (2007). Freshly excavated fossil bones are best for amplification of ancient DNA. *Proceedings of the National Academy of Sciences USA, 104*, 739–744.

Roberts, S. J., Smith, C. I., Millard, A. R., & Collins, M. J. (2002). The taphonomy of cooked bone: Characterising boiling and its physico-chemical effects. *Archaeometry, 44*, 485–494.

Robinson, S., Nicholson, R. A., Pollard, A. M., & O'Connor, T. P. (2003). An evaluation of nitrogen porosimetry as a technique for predicting taphonomic durability in animal bone. *Journal of Archaeological Science, 30*, 391–403.

Smith, C. I., Nielsen-Marsh, C. M., Jans, M. M. E., Arthur, P., Nord, A. G., & Collins, M. J. (2002). The Strange case of Apigliano: Early 'Fossilisation' of medieval bone in southern Italy. *Archaeometry, 44*, 405–415.

Smith, C. I., Nielsen-Marsh, C. M., Jans, M. M. E., & Collins, M. J. (2007). Bone diagenesis in the European Holocene I: Patterns and mechanisms. *Journal of Archaeological Science, 34*, 1485–1493.

Smith, C. I., Faraldos, M., & Fernández-Jalvo, Y. (2008). The precision of porosity measurements: Effects of sample pre-treatment on porosity measurements of modern and archaeological bone. *Palaeogeography, Palaeoclimatology, Palaeoecology, 266*, 175–182.

Trueman, C. N., & Martill, D. M. (2002). The long-term survival of bone: The role of bioerosion. *Archaeometry, 44*, 371–382.

Trueman, C. N., & Tuross, N. (2002). Trace elements in recent and fossil bone apatite. *Reviews in Mineralogy and Geochemistry, 48*, 489–521.

Trueman, C. N. G., Behrensmeyer, A. K., Tuross, N., & Weiner, S. (2004). Mineralogical and compositional changes in bones exposed on soil surfaces in Amboseli National Park, Kenya: Diagenetic mechanisms and the role of sediment pore fluids. *Journal of Archaeological Science, 31*, 721–739.

Turner-Walker, G., Nielsen-Marsh, C. M., Syversen, U., Kars, H., & Collins, M. J. (2002). Sub-micron spongiform porosity is the major ultra-structural alteration occurring in archaeological bone. *International Journal of Osteoarchaeology, 12*, 407–414.

Tuross, N. (1993). The other molecules in ancient bone: Noncollagenous proteins and DNA. In J. B. Lambert & G. Grupe (Eds.), *Prehistoric human bone: Archaeology at the molecular level* (pp. 275–292). Dordrecht: Springer.

Weiner, S., & Bar-Yosef, O. (1990). States of preservation of bones from prehistoric sites in the Near-East: A survey. *Journal of Archaeological Science, 17*, 187–196.

Chapter 12
Coprolites, Paleogenomics and Bone Content Analysis

E. Andrew Bennett, Olivier Gorgé, Thierry Grange, Yolanda Fernández-Jalvo, and Eva-Maria Geigl

Abstract Coprolites are fossil scats and provide indirect witness of the activity of past animals of a given area, whether or not fossil bones of these animals are present in the site. The shape, size, inclusions and geo- and bio-chemical composition are criteria for identification of the animal that left the coprolite. Unit II from Azokh 1 has yielded two complete undamaged coprolites one of which contained partially digested fossil bones. Taphonomic and taxonomic indications from this coprolite could not conclusively identify the origin of the coprolites. Analysis of targeted mitochondrial DNA, performed on one of the coprolites, has provided evidence for the presence of hyena DNA, but this finding was not supported by further investigation using next-generation high throughput sequencing. The most parsimonious interpretation of the results of the genetic analyses is that the highly sensitive PCR assay reveals contamination of the coprolite with minute amounts of modern brown hyena DNA presumably originating from brown hyena scats sampled recently in South Africa.

Резюме Следы активности травоядных и плотоядных животных главным образом распознаются по отпечаткам конечностей и экскрементам. Стоянки с хорошей сохранностью древних останков могут содержать копролиты (окаменелые экскременты животных) и следы троп травоядных и плотоядных, как это наблюдается в плио-плейстоценовой стоянке Летоли (Танзания). Наиболее часто, однако, встречаются копролиты плотоядных (среди них, главным образом, гиен), чем травоядных. Первые грызут и поедают кости, включая тем самым фосфат кальция в органические остатки фекалий, в то время как последние поедают растительные волокна и семена, которые разлагаются намного легче. Форма, размер, включения, гео- и биохимический состав являются основными критериями для идентификации животного, оставившего эти фекалии. В подразделении II из *Азох 1* найдены два неповрежденных копролита. Тафономические и таксономические признаки не были достаточно убедительными для надежного установления их происхождения. При проведении сайт-специфичной реакции полимеразной цепи (РПЦ) в одном из копролитов обнаружены последовательности митохондриальной ДНК бурой гиены (*Hyaena brunnea*). Последующее секвенирование не выявило значительного присутствия эндогенной ДНК хищника; в основном были найдены бактериальные последовательности со следами человеческой ДНК – возможно, по причине контаминации. Наибоее простым объяснением результатов генетического анализа является то, что чувствительный метод РПЦ идентифицирует контаминацию копролитов ничтожно малым количеством ДНК бурой гиены, привнесенным, возможно, из современных экскрементов данного вида, собранных в Южной Африке. Высокопроизводительное секвенирование не обнаружило эндогенной ДНК хищника. В целом, несохранность эндогенной ДНК характерна для всех биологических останков в Азохской пещере, проанализированных до настоящего времени, поскольку мы не смогли найти данный субстрат и в многочисленных костях пещерного медведя.

Keywords Fossil scats • Taphonomy • Lesser Caucasus • Ancient DNA • Paleogenetics • Diffraction • Fluorescence

E.A. Bennett · O. Gorgé · T. Grange · E.-M. Geigl (✉)
Institut Jacques Monod. Laboratoire "Epigénome et Paléogénome", 15, Rue Hélène Brion, 75013 Paris, France
e-mail: eva-maria.geigl@ijm.fr

E.A. Bennett
e-mail: Andrew.BENNETT@ijm.fr

O. Gorgé
e-mail: gorge.olivier@ijm.univ-paris-diderot.fr

T. Grange
e-mail: thierry.grange@ijm.fr

Y. Fernández-Jalvo (✉)
Museo Nacional de Ciencias Naturales (CSIC), José Gutiérrez Abascal, 2, 28006 Madrid, Spain
e-mail: yfj@mncn.csic.es

Yolanda Fernández-Jalvo et al. (eds.), *Azokh Cave and the Transcaucasian Corridor*, Vertebrate Paleobiology and Paleoanthropology, DOI 10.1007/978-3-319-24924-7_12

Introduction

Azokh 1 has yielded several coprolites from Units II, III and V, but two complete and undamaged coprolites were found on the top of Unit II (dated by ESR to around 100 ka, see Appendix, ESR). These two entire and unbroken coprolites (5153 and 5246) were chosen to investigate micro-plant remains after failed attempts to obtain pollen grains from these sediments (see Scott et al. 2016). One of these complete coprolites contained two small pieces of fossil bone. Bone inclusions indicate a carnivorous (or omnivorous) diet of the animal that produced the coprolites.

Taphonomic and genetic analyses of this coprolite were carried out in order to investigate the species that produced it. Azokh 1 Cave has yielded a low number of hyenid fossil bones in Units Vu and Vm (older than Unit II), which were identified as *Crocuta crocuta* by Van der Made et al. (2016). So far, hyena fossil remains are absent in Unit II. Other potential carnivores recorded in the site, more specifically in Unit II, are leopards (*Panthera pardus*), wolves (*Canis lupus*) and foxes (*Vulpes vulpes*). Scats of other carnivores such as, panthers, wolves, foxes or lions have a different size and shape (Walker 1993; Macdonald and Barrett 1993; Stuart and Stuart 1994; Harrison 2011). Lion bones (*Panthera leo*) are absent in the whole sequence of Azokh 1 (Van der Made et al. 2016). The most abundant species of Carnivora recorded in Unit II, with 88.7% of fossils taxonomically identified, is the cave bear, *Ursus spelaeus*, but there have been many studies indicating that it was herbivorous (Kurtén 1976; Bocherens et al. 1994; Mazza et al. 1995; Fernández 1998; Mattson 1998; Vila Taboada et al. 1999, 2001; Fernández et al. 2001; Grandal d'Anglade and López-González 2005); and some suggesting it was at least partly carnivorous (Richards et al. 2008; Figueirido et al. 2009; Peigné et al. 2009). Therefore, taxonomic identification of species recorded in Unit II does not indicate the most obvious predator that produced the coprolite.

Coprolites can be very informative when analyzed paleogenetically. Indeed, animal scats contain huge amounts of cell debris shed from the mucous membrane of the intestinal tract (Albaugh et al. 1992). The gut epithelium has a high rate of renewal, which matches an equally high rate of shedding. Conservation biologists take advantage of this fact by genetically analyzing scats from rare and endangered species in order to reveal the identity of the animal that produced them (e.g., Dalen et al. 2004; Miotto et al. 2007; Shezad et al. 2012). In the scats of predators, DNA from prey species is highly degraded due to the acidic gastric juice and intestinal nucleases. As a consequence, almost all of the recovered DNA sequences come from the predator and the identity of the prey species can only be determined when the host's DNA is masked, for example through blocking primers (Shezad et al. 2012). When DNA in coprolites is analyzed, as reported for example for ground sloth, human, and hyena coprolites (Poinar et al. 1998; Gilbert et al. 2008; Bon et al. 2012, respectively), a similar situation is found. Indeed, in coprolites of cave hyenas roughly ten times more DNA of cave hyena than of reindeer was found using high throughput sequencing (Bon et al. 2012).

With the aim of investigating the animal that produced the coprolite from Azokh Unit II, a paleogenetic and paleogenomic analysis was performed in the core facility of paleogenomics and molecular taphonomy of the *Institut Jacques Monod* in Paris by amplifying targeted diagnostic sequences using qPCR and shotgun sequencing.

Materials and Methods

Coprolite/Scat Morphometry

The two complete coprolites recovered from Unit II (lab. no. 5153, AZ1'08 II-I50#12 and lab. no. 5246, AZ1'08 I-H49#4, Fig. 12.1), as well as a large number of modern and fossil hyena scats were measured using calipers. These comparative samples include modern and fossil African hyenas of brown and spotted hyena (L. Scott collection), coprolites from Laetoli (Tanzania), produced by hyena and by other carnivores (Harrison 2011), coprolites from European sites (West Runton Norfolk, Larkin et al. 2000; La Roma, Pesquero et al. 2011) as well as spotted hyena scats from Colchester Zoo (UK, Larkin et al. 2000) making a total of 216 coprolites and modern scats.

Ursus spelaeus is an extinct species and modern representatives of bear are different species the scats of which cannot be directly compared for morphometric or paleogenetic analyses.

Scats and coprolites are measured taking the maximum diameter of the transversal section. The second diameter is taken at right angles to the maximum diameter, but it is not strictly the minimum diameter. We then named 'minor axis' to the perpendicular diameter of the maximum dimension, which is here named 'major axis' as the reciprocal word of minor. Orthogonally to these axes is the length of the scat or coprolite.

Bone Observations

During plant microfossil extraction, one small fossil bone fragment (6 mm long) was found in one of the coprolites (5153) after HCl (10%) treatment. Another small piece of fossil bone (5 mm long) was found in the residues that came from sawing and cleaning the coprolite 5153. In order to avoid interpretations on the bone that could have been altered by HCl during pollen preparation, only the observations of the surface conditions of the latter bone fragment are considered here to

look for evidence of gastric digestion. This bone fragment was analyzed, along with 15 bones from modern hyena scats as controls, by means of a FEI Inspect Low Vacuum scanning electron microscope (SEM), which is housed at the Museo Nacional de Ciencias Naturales. Observations were done in backscattered electron mode, combined with secondary electron emission mode, at 30 kV, 0.6–0.33 Torr. This type of SEM enabled us to analyze specimens directly with no coating or any other pre-treatment.

Chemical Analysis of the Coprolites

Both coprolites from Azokh 1 Unit II were chemically analyzed at the MNCN laboratories. Sample labeled 5153A corresponds to the outer layer of the coprolite with sediment attached to the surface (residue from pollen cleaning) and 5153B contains exclusively the inner part of the coprolite (also paleogenetically analyzed here). Coprolite 5246 was taken as a whole and the analyzed sample is a mixture of the outer and inner layers of the coprolite. A modern hyena scat (2160) from Burungi (Tanzania) was analyzed as control. All samples were ground to a fine powder using an agate pestle and mortar to be chemically analyzed. These samples were analyzed for X-Ray Diffraction (XRD, Philips PW-1830) and X-Ray Fluorescence measurements (XRF, Philips PW-1404) to obtain their mineral and element compositions respectively.

Paleogenetics and Paleogenomics

The intact half of the coprolite 5153 that was not used for the plant microfossil studies, has been subject to a paleogenetic and paleogenomic analysis. The pre-PCR experiments were carried out in the high containment laboratory of the *Institut Jacques Monod* (http://www.ijm.fr/ijm/plates-formes/pole-paleogenomique/), the post-PCR experiments in a series of separated laboratories of the *Institut Jacques Monod* designed to minimize carry-over contamination as described previously (Bennett et al. 2014). The surface of the coprolite was removed to reduce contamination with exogenous, environmental DNA and the quantity of inhibitors that can be enriched on the surface. Removal of the outer layer was performed with a sterile scalpel and 583 mg recovered from the inner part of the coprolite with a slowly moving drill. The powder was extracted in 10 ml extraction buffer (0.5 M EDTA pH 8.0, 0.25 M potassium dihydrogenphosphate, 0.14 M beta-mercaptoethanol) and purified over silica columns (Qiagen) as described (Charruau et al. 2010). The total DNA quantity (measured on a Qubit® 2,0 Fluorometer and comprising environmental and endogenous DNA) was 0.93 ng/µl. The purified DNA was amplified via quantitative real-time PCR (Pruvost and Geigl 2004).

Several procedures to prevent contamination were implemented in the protocol, such as elimination of contamination due to carry-over (Pruvost et al. 2005) and to reagents (Champlot et al. 2010). The extract strongly inhibited the polymerase in the polymerase chain reaction (PCR) with a 5 cycle delay at 10% reaction volume, 2.8 cycle delay at 5% reaction volume, and 0.1 cycle delay at 2.5%. Two PCR primer pairs targeting a 111 bp and a 84 bp (Bon et al. 2012) fragment of the mitochondrial cytochrome B region of the hyaenidae were used. When the primer sequences are removed from the PCR product sequences, the 84 bp and the 111 bp leave 43 bp and 64 bp, respectively, of informative sequence. Moreover, two primer pairs were designed that targeted 103 and 106 bp regions of the hypervariable region of *Ursus spelaeus*. In addition, a third primer pair was designed to amplify an 88 bp region of the NADH dehydrogenase 2 gene (ND2) with equal efficiency between both *Ursus* and Hyaenidae, the 36 bp internal sequence of which would differentiate between the two.

When using the hyena-specific primers, PCR products of 84 bp and 111 bp were obtained from the extracts at 2.5%, 5%, and 10% of reaction volume (20 µl total volume reactions), despite the inhibition with the larger extract volumes. A single 88 bp product was amplified using the universal bear-hyena primers. No product was obtained when using the bear-specific primer pairs. The PCR products were directly sequenced after purification.

In order to compare the obtained sequences with those of the three extant hyena species, DNA from the hair of two male brown hyenas from the Zoo "Fauverie du Mont Faron", France, was extracted as described previously (Charruau et al. 2010) and analyzed using the same primers and PCR conditions as described above, but in a laboratory of the "Institut Jacques Monod" where modern DNA is analyzed. For next-generation high throughput sequencing, a library was prepared in the high-containment laboratory using the double-stranded DNA procedure as described in Bennett et al. (2014). The size-selected library was then amplified and sequenced on an Illumina MiSeq with paired-end 100 bp-long reads, using the manufacturer's workflow.

Results

Bone and Coprolite Morphometry

The two complete and undamaged coprolites (5153 and 5246) measure 50 × 49 × 33 mm and 48 × 47 × 30 mm (major axis by minor axis by length) respectively. Coprolite

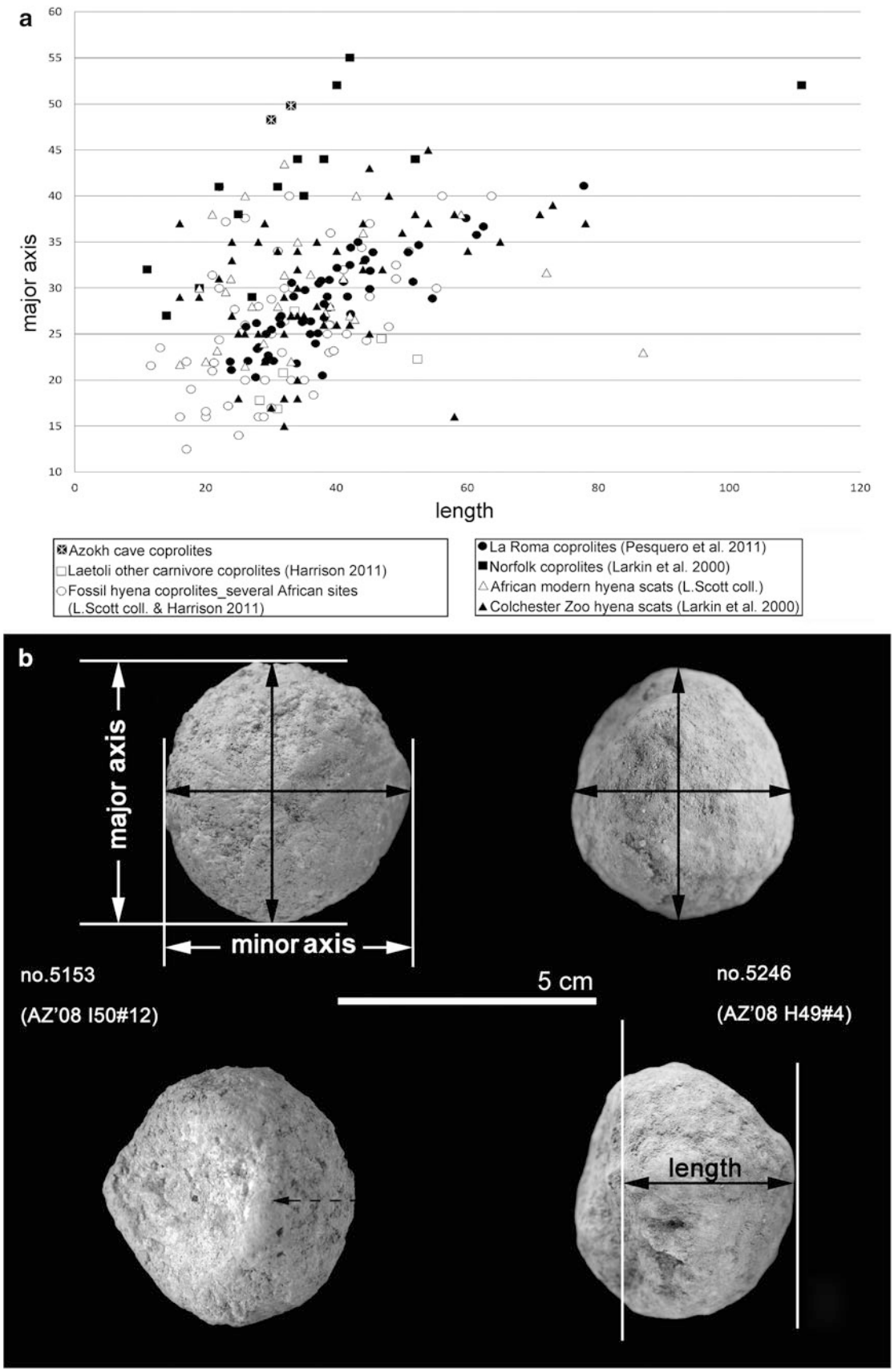

Fig. 12.1 **a** The two Azokh Cave coprolites have been measured and compared with modern hyena scats and fossil coprolites. **b** The two Azokh Cave coprolites (5153 and 5246) are photographed in sagittal or upper view (top pictures) and laterally (bottom pictures). Explanation of the measurement criteria of coprolites and scats is described in the text. The major axis is the maximum diameter of the scat's circumference and the minor axis is taken perpendicularly to the maximum diameter. Orthogonal to the previous axes is the length. Note coprolite 5153 lateral view (bottom left picture) is not showing the complete length (dashed arrow)

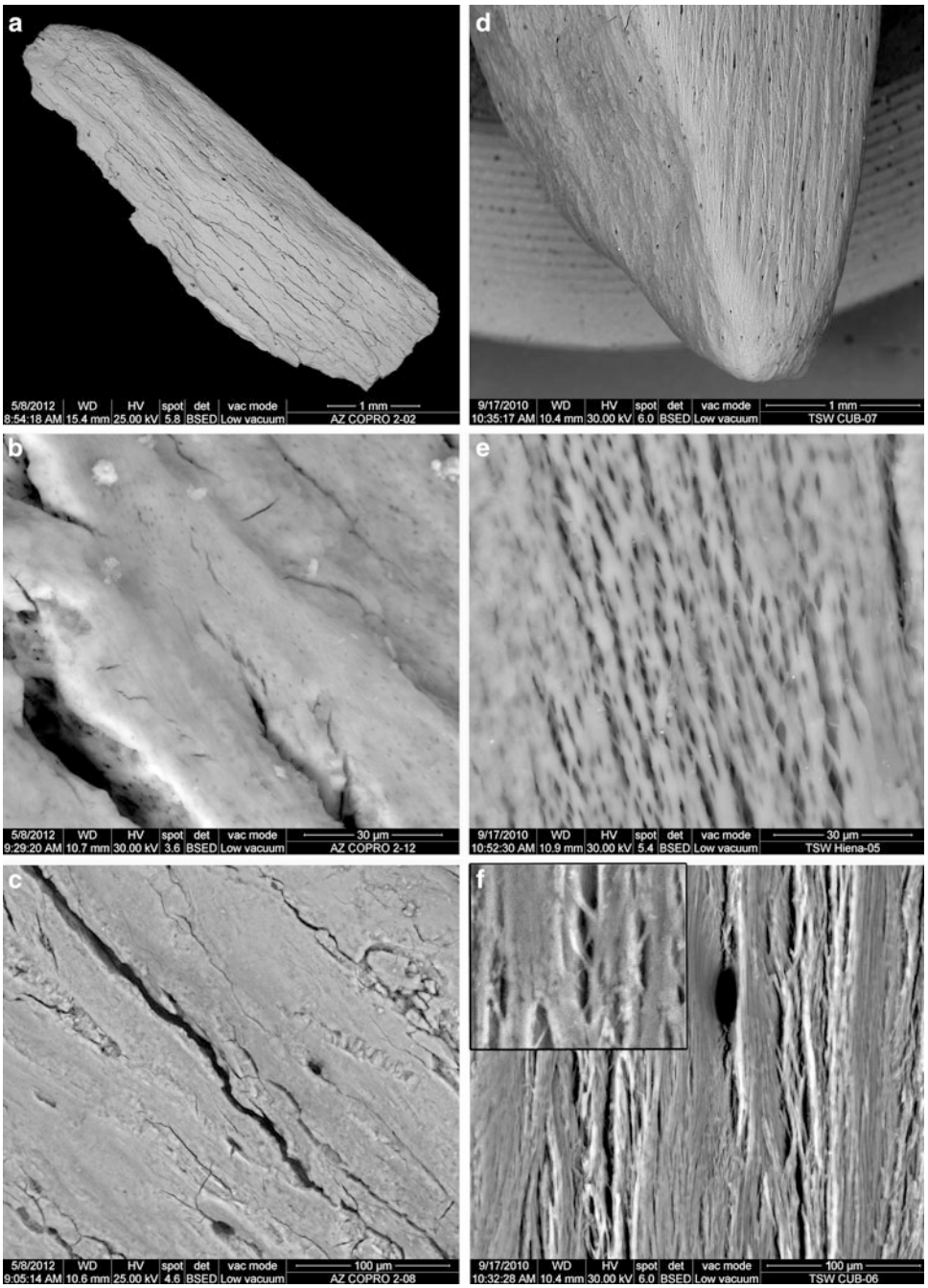

Fig. 12.2 Scanning electron micrographs. Bone fragment from Azokh coprolite (5153) (**a**) and its smooth surface at higher magnification (**b**). The bone surface shows strong post-depositional cracking with sharp edges (**c**). Characteristic damage on another piece of bone surface caused by gastric acids (**d**). Detail of cracked surface at similar magnification to (**b**) showing enlargement of the bone porosity due to digestion (**e**). Bone surface showing a characteristic "torn-like" damaged surface (**f**). Fibers attached to both edges of the crack produce the "torn-like" damaged surface, as seen in the small inset on top left (width field of the small inset = 50 microns). Note this "torn" aspect is not observed in (**c**), where cracks are post-depositional and edges are well defined

sizes were compared to modern and fossil scats of spotted hyena (*Crocuta crocuta*) and brown hyena (*Hyaena brunnea*) by Fernández-Jalvo et al. (2010a). We added the raw values of modern spotted hyena scats from Colchester Zoo and hyena coprolites from European sites (Larkin et al. 2000; Pesquero et al. 2011), as well as more measurements from hyena and other carnivore coprolites from Laetoli (Tanzania) measured by Harrison (2011) see Fig. 12.1a.

The fossil bone fragment found in the residues from sawing and cleaning the coprolite 5153 is 5 mm long and,

therefore, taxonomically unidentifiable. The small piece of fossil bone shows signs of moderate digestion (Andrews 1990), with slightly rounded edges (Fig. 12.2a) and a smooth surface (Fig. 12.2b), and in addition there is heavy diagenetic cracking on the bone surface (Fig. 12.2c). In contrast, bones contained in modern hyena scats (both spotted and brown hyenas) have higher degrees of rounding (Fig. 12.2d), enlarged bone porosity (Fig. 12.2e) and a characteristic "torn-like" damaged surface (Fig. 12.2f).

Chemical Analyses of Coprolites and Modern Scat

The XRD diagrams provide information of the mineral content in the sample and crystalline traits. Broadness of the peaks indicates low crystalline structure of the mineral content (Kolska Horwitz and Goldberg 1989; LeGeros 1994; Mulla et al. 2012). Diagrams of XRD shown in Fig. 12.3 have broad and irregular curves for the coprolites and modern scat and indicate that none of these samples are highly crystalline.

Amorphous phases obtained by XRD (Table 12.1) mainly refer to poor-crystallized minerals, but it may also be influenced by organic matter or volatile content. Azokh samples have higher amorphous content, especially sample 5153B (17.1% inner coprolite), than the modern scat (Table 12.1). The Loss on Ignition (LOI, Table 12.2) is the weight loss before and after heating. LOI values are also closely correlated to the organic matter and volatiles content in the sample (Heiri et al. 2001). Chemical analysis by XRD of the recent scat has yielded only hydroxyapatite from bones ingested by modern hyenas; amorphous phases are absent and the LOI is relatively high. Azokh coprolites have a low LOI compared to modern scats and moderately high amounts of amorphous phase (especially sample 5153B with 17.1% inner coprolite). Samples 5153A and 5246 have also calcium phosphate content as well as other minerals (feldspars and micas) from the surrounding sediment attached to the coprolites, but sample 5153B (cleaned inner layer of the coprolite) mainly contains hydroxyapatite (72.9%) and quartz (10.1%). However, influence of neo-formed minerals from the diagenetic processes cannot be fully discarded (see discussion).

Fluorescence results are displayed in Table 12.2. The XRF analysis has yielded similar results in all samples (fossil and modern scats). Some differences are observed with regard to silica and some elements, such as aluminum or potassium (components of feldspars) that are more abundant in Azokh coprolites. Trace elements, such as strontium, are more abundant in modern scat. The low value of Loss on Ignition (LOI) from Azokh coprolites (below 16.2%) indicates low proportions of organic materials and/or volatiles.

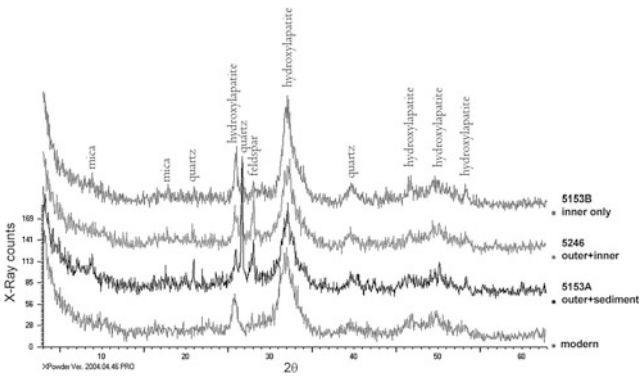

Fig. 12.3 X-Ray diffraction diagram of modern scat (below), Azokh coprolite 5153 fraction from outer layers and sediment attached (5153A). Azokh coprolite 5246 including both outer and inner layers. Azokh coprolite inner fraction of 5153 is the top XRD profile. Note hydroxyapatite peaks at 2q 44–54 region show some double simultaneous peaks (close to hydroxyapatite and fluorapatite), although in most cases the peak corresponds to the hydroxyapatite mineral

Paleogenetic Analysis of the Coprolite

In five out of eighteen attempts, PCR amplification of the coprolite extract yielded products of the 84 bp long mitochondrial DNA fragments of the cytochrome B. The longer, 111 bp fragment, however, yielded only non-specific amplifications of modern human contaminants. Depending on primer specificity, amplification of human sequences is an expected result, due to the low copy number and size degradation characteristic of targeted ancient DNA, as well as the ubiquity of modern human DNA in reagents and samples, particularly those that have not been aseptically excavated. One of nine attempts to amplify the 88 bp universal bear/hyena sequence of the ND2 gene was successful.

The sequences obtained for the 84 bp hyena-specific fragment were unambiguous and identical. Their comparison with the mitochondrial cytochrome B sequences in GenBank (NCBI Blast search) showed that the closest match was the cytochrome B sequence of the hyena (Rohland et al. 2005), rather than that of the cave bear (Krause et al. 2008). As a precaution, the sequences obtained were also compared with bovine (*Bos taurus*) and human sequences, the DNA of which can often contaminate ancient DNA analysis through reagents and handling. These sequences showed no similarity to either of these potential contaminants. The sequence from the ND2 gene fragment amplified with bear/hyena universal primers was also determined to be hyena sequence. Since the informative sequences of the coprolite obtained with the 84 bp CytB fragment most closely matched the brown hyena (*Hyaena brunnea*) and no ND2 sequences for

Table 12.1 Diffraction (XRD) results from Azokh coprolites and modern scat (HAP = hydroxyapatite, Q = quartz)

Sample	Max.counts	HAP	Q	Feldspar	Micas	Amorphous
Azokh 5153-B (inner)	160	72.90	10.10	–	–	17.10
Azokh 5246 (all)	139	63.30	6.40	15.60	5.60	9.10
Azohk 5153-A (outer)	188	40.30	33.00	15.70	3.50	7.50
Modern Scat	170	100.00	–	–	–	–

brown hyena were available in Genbank, we subsequently determined the sequence of the analyzed ND2 gene fragment from modern brown hyena using hair samples from two brown hyenas from a zoo (Fauverie du Mont Faron, France). We also amplified and sequenced the two CytB fragments from these individuals, and their sequences were identical to the brown hyena sequences deposited in Genbank. Alignments of both the CytB and ND2 fragments were concatenated, compared to those of extant bears, the extinct cave bear *Ursus spelaeus*, the cheetah (*Acinonyx jubatus*), the tiger (*Panthera tigris*), and to the different extant hyena species and the extinct cave hyena (Fig. 12.4a). A maximal likelihood phylogenetic tree was constructed using PHYML (Guindon & Gascuel 2003) (Fig. 12.4b).

Table 12.2 Fluorescence (XRF) results from Azokh coprolites and modern scat

Element	Azokh 5153-A	Azokh 5153-B	Azokh 5246	Modern scat
SiO_2	14.05	5.95	6.52	2.16
Al_2O_3	4.43	1.77	2.38	0.79
Fe_2O_3 (total)	2.15	0.72	1.27	0.43
MnO	0.33	0.18	0.04	0.00
MgO	0.90	0.83	0.81	1.23
CaO	30.66	37.52	36.14	32.79
Na_2O	0.77	0.58	0.93	0.55
K_2O	1.09	0.38	0.52	0.16
TiO_2	0.17	0.05	0.09	0.01
P_2O_5	31.77	35.81	38.64	36.87
LOI	13.68	16.22	12.67	24.61
Traces	ppm	ppm	ppm	ppm
Zr	3	–	7	–
Y	8	4	4	3
Rb	13	–	8	–
Sr	118	93	109	430
Cu	36	50	17	–
Ni	161	183	131	1
Co	5	10	3	9
Ce	5	26	4	27
Ba	–	129	–	–
F	963	897	1151	1440
S	1754	1129	1955	2637
Cl	901	205	1008	360
Cr	74	80	32	17
V	35	20	21	2
Th	1	3	–	3
Nb	–	–	–	–
La	2	2	3	2
Zn	350	127	350	69
Cs	–	52	5	–
Pb	1	–	–	–

It can be seen from both the alignment and the tree that the DNA sequences recovered from the coprolite using the highly sensitive targeted PCR approach clearly belong to *Hyaena brunnea* and can be unambiguously distinguished from the other hyena species as well as from other Feliformia. The Ursidae sequences are even more distantly related.

To explore the possibility that the coprolite could contain DNA sequences from other organisms that were not targeted with the directed PCR approach used, we constructed a library from the total DNA extracted from the coprolite and sequenced a subset of this library using the Illumina Miseq platform. High throughput sequencing is an ideal approach to analyze the DNA composition of environmental samples (Shokralla et al. 2012), including feces (Murray et al. 2011). Shotgun next-generation sequencing was performed allowing the DNA molecule present in the extract to be randomly sequenced. This approach has two advantages: first, it provides an unbiased view of the DNA sequence composition of a fossil bone extract; second, it provides sequence information of very short DNA sequences that are too short to be analyzed with the targeted PCR approach. The disadvantage of this approach is that it does not discriminate between environmental and endogenous DNA and it can generate only minute amounts of sequencing data from endogenous DNA because of the pervasive nature of environmental DNA contamination. We analyzed the sequences of 619,848 fragments from a subset of the library of the Azokh coprolite (Fig. 12.5a). Of these, only 81,063 (13.7%) sequencing reads could be uniquely mapped to sequences present in databases (Fig. 12.5b). The vast majority of these uniquely mapped sequences, i.e. 95.6%, are of bacterial, archaeal or viral origin. The sequencing reads were also mapped to the human, cat, dog, and cow genomes, as well as the cave bear and striped hyena mitochondrial genomes. None of these attempted mappings revealed any appreciable presence of mammalian DNA, apart from the low level human sequences (0.4%), which are expected background contaminants with standard excavation techniques and non-decontaminated reagents. This

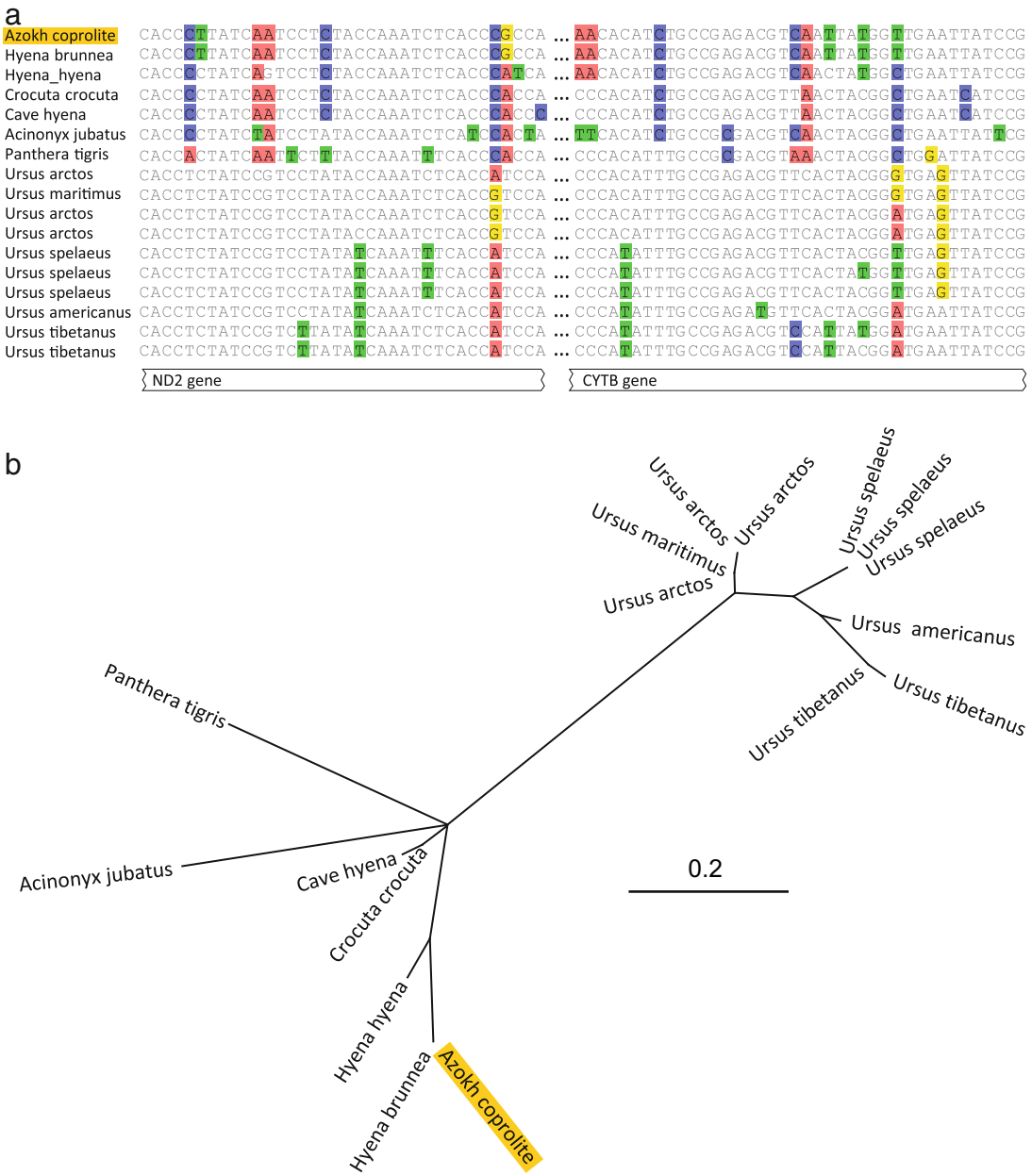

Fig. 12.4 **a** DNA sequence alignment of the concatenated sequences of mitochondrial cytochrome B (88 bp) and NADH hydrogenase 2 gene (111 bp) fragments from various Felidae and Ursidae. We present for each sequence a single sequence if all other sequences in the database were identical for the regions analyzed. **b** Phylogenetic tree: A maximum likelihood tree of the concatenated 199 bp cytb and NADH2 sequences analyzed here is drawn using PHYML showing for bears (*Ursus arctos, Ursus americanus, Ursus thibetanus, Ursus spelaeus*), the cheetah (*Acinonyx jubatus*), the tiger (*Panthera tigris*), extant hyenas and the extinct cave hyena. The scale indicates 0.2 nucleotide substitutions per site

result argues in favor of poor DNA preservation since the extract contains no detectable endogenous DNA from any of the likely scat producers, and indeed, no vertebrate DNA at all was detected (at least not in the 619,848 reads analyzed) beyond trace sequences that cannot be excluded from common biological reagent and handling contaminants. It is concluded that if any endogenous sequences are still preserved in this sample, they are too rare to be detected using a global approach without prior enrichment.

In contrast to the targeted PCR approach, which is highly sensitive to longer, targeted sequencing reads, no sequencing reads indicating the presence of *Hyaena brunnea* were obtained via next-generation sequencing. It is noteworthy that the human mitochondrial DNA sequence obtained with the PCR approach does not match any individual working in the paleogenomics laboratory in Paris indicating that human contamination occurred most likely upstream to this analysis, or was introduced by reagents.

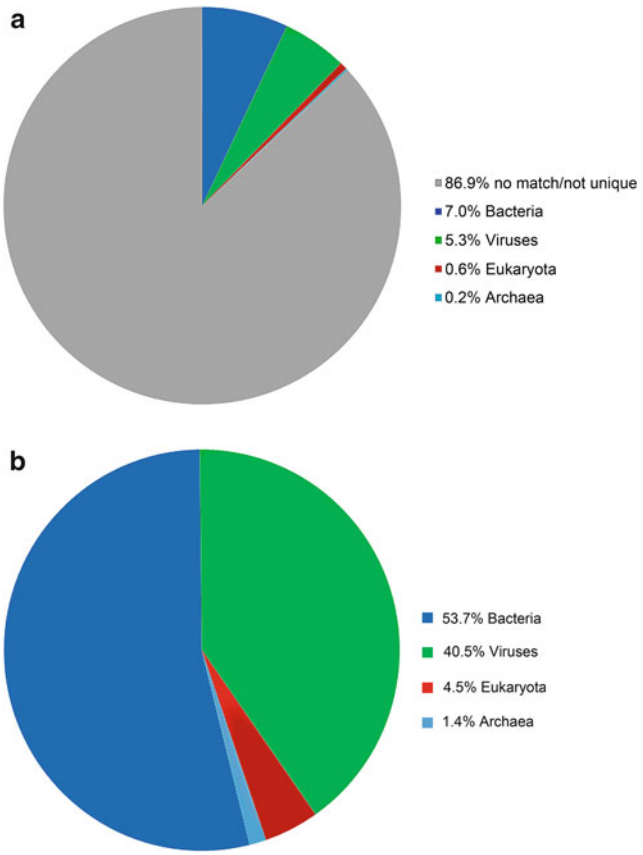

Fig. 12.5 **a** Distribution of sequence matches in 619,848 reads analyzed from high throughput sequencing of the Azokh coprolite extract. **b** Distribution of the mapped reads of the same sequencing experiment

Discussion

Bone and Coprolite Morphometry

Digestion observed in the fossil bone fragment from coprolite 5153 is no higher than moderate in Andrews' (1990) classification. Although this author did not include hyenas, bears or any other omnivorous predators in his study, experimental work on these predators (Denys et al. 1995; Matthews 2000, 2006; Mondini 2002; Montalvo et al. 2007) indicates that they produce highly digested bones, showing a "torn-like" damaged surfaces when exposed to strong gastric acids (Andrews and Fernández-Jalvo 1998). Effects of digestion on bones ingested and regurgitated by *Crocuta crocuta* show rounding of the broken edges of digested bone fragments and the characteristic "torn-like" damaged surface (Fernández-Jalvo et al. 2010b). Similar damage is observed on bones digested and excreted by *Hyaena brunnea* in Fig. 12.2d–f, but it is absent in the smooth surface bone from 5153 (Fig. 12.2b). Since we did not have bone specimens ingested by striped hyena (*Hyaena hyaena*), we could not analyze the effects of its digestion under high magnification electron microscopy (3,000×). Lower grades of digestion in the only bone that could be studied from the coprolite of Azokh1 Unit II could be pointing to an animal with weaker gastric action than hyenas, but differences in the degree of bone digestion may occur simultaneously during digestion depending on the position that the bone had in the stomach (Andrews 1990). The absence of a "torn-like" damaged surface is, however, unexpected, but further studies are needed using bones digested by *Hyaena hyaena* at high magnification electronic microscopy.

Kolska Horwitz (1990) observed signs of digestion on large mammal bones from recent striped hyena scats as well as coprolites from Kebara and Fazel 6 Levant sites. This author provided a size range of bone chips and splinters from 17 to 3 mm (62% smaller than 2 mm long). The small bone fragments found in the Azokh coprolite (6 and 5 mm long) fall within this range. However, higher abundance of bone splinters and larger pieces than the bones in the Azokh coprolites have been found in hyena scats/coprolites (Kolska Horwitz and Goldberg 1989; Kolska Horwitz 1990). Similarly, other carnivore feces referred to by Binford (1980), Haynes (1980), Maguire et al. (1980), Payne and Munson (1985) contain small sized bone splinters showing heavier signs of digestion. This is not the case with the small piece of fossil bone from 5153, in which digestion is moderate.

Kolska Horwitz and Goldberg (1989) indicate the breadth measurement (maximum diameter) of the scat may distinguish between spotted and brown hyena, with that of the spotted hyena being significantly wider. *Crocuta crocuta* is the largest extant hyaenid with a weight ranging between 45 and 85 kg. *Hyaena brunnea* weighs on average around 45 kg with exceptional cases reaching up to 72.6 kg (Roberts 1954), and *Hyaena hyaena* weighs between 30 and 35 kg. The major and minor diameters are the most consistent measurements, because length depends on the number of segments attached (see Fig. 12.1b). Most authors, however, refer to the length and maximum diameter (major axis) and we have used these dimensions to include most coprolite and modern scat measurements available. The results of these measurements are plotted in Fig. 12.1a. Unfortunately, other papers display results of coprolite measurements as average and range values of length and width which cannot be included here.

The larger Azokh coprolites (Fernández-Jalvo et al. 2010a) are still smaller than three of the coprolites from the West Runton Freshwater Bed site in Norfolk (WRFB-UK) measured by Larkin et al. (2000). Parfitt and Larkin (2010) mention an Early Pleistocene site (Untermassfeld, Germany, Keiler 2001) where the dimensions of the coprolites are even larger than those from Norfolk. The exceptionally large coprolites from Untermassfeld, which exceed the dimensions

Fig. 12.6 Modern brown bear (*Ursus arctos*) and scats produced by them have strong similarities with exceptionally large coprolites from Norfolk (see Fig. 2b in Larkin et al. 2000). Courtesy of Pablo Silva and Nigel Larkin

of modern and fossil hyena scats are considered by Keiler (2001) to have been produced by adults, whilst the smaller and more abundant coprolites derive from hyena pups. However, this would suggest that all coprolites found in other sites (see Table 12.1) are produced by pups and this would need further study. In addition, the size of modern brown hyena scats is also subject to individual diversity (E. M.G. and personnel from the "Fauverie du Mont Faron", personal observation). On the other hand, the shape of the large coprolites from Norfolk (see Fig. 2b in Larkin et al. 2000) and modern bear (*Ursus arctos*) scats are alike, both being segmented (Fig. 12.6), and, there is fossil evidence of the presence of *Ursus* sp. at West Runton (see bear taxonomic discussion in Lewis et al. 2010). Therefore, coprolite morphometry is indicative, but is not conclusive.

In this respect, there is the contention that *Ursus spelaeus* cannot produce the coprolites because hibernation and fasting would limit bear scats in caves (Nelson et al. 1973; Fernández et al. 2001; Grandal d'Anglade and Fernández-Mosquera 2008). However, we find evidence in the site that bears were not only hibernating in Azokh 1, but living for longer periods in the cave (Marin-Monfort et al. 2016, see also discussion on *Ursus spelaeus* diet in that chapter). The fossil bones recovered from Unit II show no characteristic crushed bone hyena traits, nor do they have extensive gnawing or intensive bone digestion (Marin-Monfort et al. 2016). Bone splinters and breakage linked to chewing is low in Azokh 1. Chewing affected only 6.4% of the total number of fossils of Azokh1 and 7.24% in Unit II. These values seem too low for hyena (Skinner et al. 1998; Pickering 2002; Pokines and Peterhans 2007; Pobiner 2008; Diedrich 2012). The maximum size of tooth marks recorded on bones from Unit II is much larger than those of (known) hyenas, or even lions (Selvaggio and Wilder 2001; Domínguez-Rodrigo and Piqueras 2003; Pobiner 2008; Delaney-Rivera et al. 2009, see discussion in Marin-Monfort et al. 2016).

Chemical Analyses of the Coprolites

Results from XRD and XRF chemical analyses of coprolites obtained by other authors (Kolska Horwitz and Goldberg 1989; Larkin et al. 2000; Lewis 2011; Pesquero et al. 2011) are similar to those obtained here from Azokh coprolites (Tables 12.1 and 12.2, and Fig. 12.3). Percentages of the amorphous phase, however, are higher in Azokh coprolites than in other sites (see Pesquero et al. 2011). Most coprolites and modern hyena scats analyzed by Kolska Horwitz and Goldberg (1989) contained apatite minerals (except two, likely to have been produced by striped hyena). Poor crystallization and better crystallized apatites were indistinctly obtained from both modern and fossil specimens. Coprolites analyzed from West Runton Norfolk and Boxgrove sites give peaks of calcium phosphate in similar proportions to recent *Crocuta crocuta* scats from Colchester Zoo, all of which were chemically analyzed in Larkin et al. (2000) and Lewis (2011). Other elements (Fe, Mn, Al, Si) detected in these two

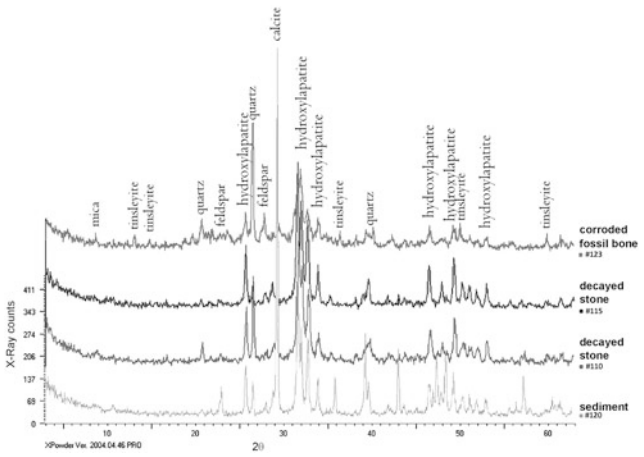

Fig. 12.7 X-Ray diffraction diagram obtained from the sediment of Unit II of Azokh cave site (#120), two decayed stones found in Unit II (#110 and 115), and a corroded fossil bone from Unit II (#123) all of them affected by diagenesis probably caused by bat guano deposits (see Marin-Monfort 2016, label # refers to the stub number shown in Table 10.10)

British fossil sites are probably due to diagenetic alteration of the host sediment. Similarly, La Roma site (Pesquero et al. 2011) shows hydroxyapatite below 50%, with other minerals (calcite, quartz, gypsum and moscovite) formed in the calcareous marginal lake environment of this site. The sample from the interior of the coprolite (5153B-inner) contains hydroxyapatite (72.9%), and quartz (10.1%) and other minerals obtained from the other portions or coprolites from Azokh show the influence of the host sediment. Lewis (2011) observed a shift between the hydroxyapatite and fluorapatite phases in the range between 2q 44–54 region of the XRD coprolite diagrams. This shift was interpreted as result of diagenetic alterations frequently occurring in hydroxyapatite minerals. Some of the double peaks observed in this 2q region in Fig. 12.3 may suggest some influence of similar diagenetic alteration, though standard hydroxyapatite positions are better conformed in Azokh coprolites than in coprolites analyzed by Lewis (2011). Therefore, the diagenetic historical context has to be considered when analyzing the chemical composition of fossil materials.

Hydroxyapatite found in Azokh coprolites could in principle come from bones ingested by the animal that produced these coprolites. However, we cannot assert that hydroxyapatite identified in coprolites is exclusively the result of digested bones because Azokh Unit II has been intensively affected by diagenesis due to fluid percolation enriched in acidic bat guano. A wide variety of secondary minerals are associated to bat guano diagenesis in caves, and hydroxyapatite is the most common and stable neo-formed mineral, which has actually been formed in the geological materials of Unit II, such as stones and sediments (Tables 12.3 and 12.4). Hydroxyapatite together with quartz and tinsleyite have been identified as neo-formed (secondary) minerals in Azokh 1 (see Marin-Monfort et al. 2016, Table 10.10 and discussion in that chapter, and Murray et al. 2016). The peaks of samples analyzed in Fig. 12.7 are less broad than in coprolites, but still form short (except for the sediment) and irregularly shaped curves. As said above, the higher and thinner the peak of a mineral is, the better crystallized it is. Thus, the short, broad and irregular peaks suggest poor crystallinity in stones, which is abnormal and indicates the presence of abundant secondary minerals due to diagenesis. The percentages of amorphous phases in these highly diagenetically altered samples, are higher than in coprolites (up to 30%) and the LOI is variable with high values in fossil and sediment and low values in decayed stones.

In this context, the relative high abundance of amorphous phase in Azokh coprolites (above 7% up to 17.1%, Table 12.1), absent in modern scats, suggest the presence of poor-crystallized minerals rather than organic matter content, which may agree better with secondary neo-formed minerals during diagenesis. This is also in agreement with the bone diagenesis results obtained by Smith et al. (2016) who concluded that fossil materials from Azokh 1 (Units II and III) show typical ACH (Accelerated Collagen Hydrolysis), with only small amounts of collagen remaining and often extreme mineralogical changes. Similarly, no preserved DNA could be PCR-amplified from any of the numerous bones analyzed from various locations and layers in Azokh (Bessa-Correia and Geigl, unpublished results).

Table 12.3 Diffraction (XRD) results from fossil and damaged (decayed) stone from Azokh 1 Unit II (HAP = hydroxiapatite, Q = quartz)

Sample	Max. counts	HAP	Q	Calcite	Tinsleyite	Feldspar	Micas	Amorphous
Azokh corroded fossil bone (123)	407	33.00	15.50	–	13.80	12.70	14.20	10.80
Azokh decayed stone (115)	457	59.80	2.30	2.30	–	3.70	4.50	27.40
Azokh decayed stone (110)	389	49.00	9.30	4.10	–	3.60	3.80	30.20
Azokh Unit II sediment (120)	1124	33.00	2.10	49.50	–	2.70	6.7	6.10

Table 12.4 Fluorescence (XRF) results from fossil and damaged (decayed) stone and sediment from Azokh 1 Unit II

Element	Azokh corroded fossil bone (123)	Azokh decayed stone (110)	Azokh decayed stone (115)	Azokh Unit II sediment (120)
SiO_2	20.41	3.39	1.52	1.58
Al_2O_3	5.83	0.64	0.22	0.21
Fe_2O_3 (total)	2.97	0.37	0.15	0.17
MnO	0.18	1.08	0.50	0.47
MgO	0.43	0.75	0.86	0.57
CaO	19.03	52.10	68.67	45.08
Na_2O	0.43	0.54	0.46	0.50
K_2O	2.36	0.42	0.07	0.01
TiO_2	0.28	0.01	–	–
P_2O_5	20.38	28.59	16.58	27.91
LOI	27.70	12.12	10.97	23.50
Traces	ppm	ppm	ppm	ppm
Zr	–	–	–	–
Y	–	–	–	–
Rb	–	–	–	–
Sr	–	–	–	–
Cu	–	–	–	–
Ni	–	–	–	–
Co	–	–	–	–
Ce	–	–	–	–
Ba	–	–	–	–
F	1891	463	549	447
S	1445	1557	687	1352
Cl	250	383	251	337
Cr	–	–	–	–
V	–	–	–	–
Th	–	–	–	–
Nb	–	–	–	–
La	–	–	–	–
Zn	–	–	–	
Cs	–	–	–	
Pb	–	–	–	

Paleogenetic and Paleogenomic Analyses

The paleogenetic analysis of the coprolite using a targeted, highly sensitive quantitative PCR approach revealed the presence of hyena DNA. The mitochondrial cytochrome B/ND2 gene sequences obtained matched those that were produced from modern brown hyena hair (*Hyaena brunnea*, formerly *Parahyaena brunnea)* rather than the extant spotted hyena (*Crocuta crocuta*) or the extinct cave hyena (*Crocuta crocuta spelaea*). Brown hyenas have never been recorded outside of Southern Africa, and it appears surprising and highly unlikely that the range of this species could have extended 100,000 years ago as far as to the Caucasus without any prior evidence of the past presence of this species on a wide geographical area (Rohland et al. 2005). Before proposing a profound reappraisal of the past distribution of brown hyenas, it is worthwhile to consider an alternative hypothesis: sample contamination.

There are several arguments in favor of contamination: first, the cytochrome B/ND2 sequences of the Azokh coprolite are identical to those of modern brown hyenas that presently show a reduced diversity of the cytochrome B gene. It would be surprising that the putative brown hyenas that would have lived in the Caucasus 100,000 years ago would have had a mitochondrial DNA identical to extant brown hyenas from South Africa. Indeed, a past population size that would cover such a wide geographical range should have a higher genetic diversity. Second, high throughput sequencing revealed that the coprolite contains essentially environmental DNA and traces of contaminating human DNA. Thus, the DNA from the scat producer is extremely rare, if present at all. The traces of human DNA having a higher mean fragment size than the bulk of DNA can most confidently be attributed to contamination. Indeed, the coprolite was identified as cave bear or hyena scat and originally intended to be solely subject to pollen and taphonomic analyses. Therefore, no contamination prevention procedures were applied. In contrast, the coprolite was extensively manipulated prior to the genetic analysis. In the high throughput next-generation sequencing data, there is no evidence of DNA from another species. This indicates that the hyena DNA sequences obtained in the PCR approach correspond to minute traces of DNA that can be detected only due to the high sensitivity that PCR can achieve when it is optimized. When downstream procedures of high sensitivity must be used, one must ensure that extreme precautions of contamination prevention are used at every stage of the analysis, especially upstream of the high sensitivity analyses, starting from sample collection in the field. These precautions were not applied to this sample prior to the paleogenetic analysis.

It is particularly striking that the hyena species that was identified via a genetic analysis is present only in Southern Africa where the sample was prepared for pollen analysis. Contamination occurred most likely at this stage of the analysis. Contamination in the paleogenomics laboratory in Paris is unlikely since contamination prevention is routinely practiced at all stages of sample analyses: strict physical separation of the different experimental steps in positive air pressure laboratories, as well as multiple contamination prevention procedures, carry-over contamination prevention and reagent decontamination that have been developed and optimized in the laboratory and are used without exception (Pruvost et al. 2004, 2005; Champlot et al. 2010). Furthermore, in the paleogenomics laboratory no hyena DNA of any species had ever been analyzed

prior to this study and all genetic data from the coprolite were obtained prior to the analyses of modern hyena samples, which were performed later in the modern DNA laboratory.

The contamination of the coprolite may have occurred in South Africa, for the Azokh coprolite was sawed for pollen analysis in the same laboratory room in Bloemfontein in which 10 days before fresh brown hyena scats had been cleaned. Thus, in spite of careful preparation to avoid pollen contamination, residues might have contaminated the coprolite before it was returned to the sample bag immediately after sawing. We believe therefore that the most likely explanation for the presence of brown hyena DNA sequences in the Azokh coprolite is that it had been contaminated with modern brown hyena DNA through secondary contact (bench surface, saw etc.) or residues produced in the Bloemfontein laboratory. This explanation is more parsimonious than would be the reappraisal of past brown hyena distribution with a range extending up to Nagorno-Karabakh. The fact that, apart from brown hyena, no other carnivore sequences were obtained via the targeted PCR approach, and that no indication of the producer's species was found in the genomic data set, taken together with our previous investigations of numerous cave bear bones from the Azokh cave from which no PCR product was obtained, argue in favor of poor endogenous DNA preservation in the fossil remains of the Azokh cave. Samples with poor DNA preservation, however, are particularly prone to produce artifactual results in paleogenetic studies. The present study highlights the importance of addressing the problems of contamination starting at the very early stages of sample collection during field work when a paleogenetic analysis of the samples is considered. Taken together with our previous demonstration of the importance of early sample treatment to favor optimal DNA preservation (Pruvost et al. 2007) our work reveals the importance of a close collaboration between molecular geneticists and archaeologists or paleontologists.

Conclusions

1. Two coprolites recovered from Azokh 1, Unit II have been studied.
2. Their size and form are comparable to hyena scats, but there is no indication in the form of bone crushing or tooth marks that hyenas were present. No hyena fossils have been recovered from Unit II so far, but they are known in underlying deposits in Unit V.
3. The most abundant species in this site is the cave bear (*Ursus spelaeus*), an extinct species whose dietary and living behaviors have been considered to be different (though still controversial) to modern bears.
4. The much larger body size of *U. spelaeus* compared to the largest sized hyena recorded in the site, should have produced larger sized coprolites. Indeed, comparisons with hyena coprolites from other fossil sites show that bear coprolites are larger than the Azokh coprolites. Coprolite morphomotry has not been conclusive. However, the involvement of hyenas with no further taxonomic remains or taphonomic evidence of their presence, except for their coprolites, appears dubious.
5. Chemical analyses of the coprolites by diffraction and fluorescence suggest the possibility of hyenas as the coprolite producer by the presence of the bone mineral (hydroxylapatite). However, hydroxyapatite is the most common and stable neo-formed mineral derived from bat guano diagenesis, which is very intense in Unit II, and has actually been identified in geological materials of Unit II, such as stones and sediments.
6. Relatively high content of amorphous phases and low crystallinity in both geological (stones and sediments) and biological (coprolites) samples may agree with neo-formed minerals, excluding the influence of any organic content in Azokh materials. However, further investigations using other techniques and a higher number of samples are needed.
7. The paleogenetic analysis of the coprolite yielded mitochondrial sequences identical to those of modern brown hyena (*Hyaena brunnea*) while the paleogenomic analysis did not reveal any indication for DNA sequences of a potential predator.
8. Brown hyenas are today and for their known history restricted to southern Africa, and it is unlikely that their range ever extended into Eurasia. The most parsimonious explanation for this result is contamination of the coprolite from fresh brown hyena scats that were treated in the University of the Free State laboratory in Bloemfontein prior to the opening of the coprolite.
9. In summary, none of the methods applied here has provided conclusive indication of the species that produced these coprolites. None of the results obtained could support or discard bears vs. hyenas as the taphonomic agent. Thus, the producer's species cannot be defined at this time.

Acknowledgements We are grateful to the authorities of Nagorno-Karabakh for permissions to work on these specimens. We thank the Electron Microscopy Unit of the Museo Nacional de Ciencias Naturales for their careful and professional work, Teresa Sanz for pictures taken of the coprolites before processing and Pablo Silva for pictures of modern bears. The authors are also grateful to M.D. Pesquero for providing coprolite measurements from La Roma site. We thank Corinne Esser from the Zoo Fauverie du Mont Faron, France, for providing hair and scats of brown hyenas. The authors are grateful to comments from Mark Lewis, Nigel Larkin, the three anonymous reviewers and the editor in charge (Peter Andrews) who greatly improved this chapter.

References

Albaugh, G. P., Iyengar, V., & Lohani, A. (1992). Isolation of exfoliated colonic epithelial cells, a novel non-invasive approach to the study of cellular markers. *International Journal of Cancer, 52*, 347–350.

Andrews, P. (1990). *Owls, caves and fossils*. London: Natural History Museum.

Andrews, P., & Fernández-Jalvo, Y. (1998). 101 uses for fossilized faeces. *Nature, 393*, 629–630.

Appendix: Fernández-Jalvo, Y., Ditchfield, P., Grün, R., Lees, W., Aubert, M., Torres, T., Ortiz, J.E., Díaz Bautista, A. & Pickering, R. (2016). Dating methods applied to Azokh cave sites (Appendix). In Y. Fernández-Jalvo, T. King, L. Yepiskoposyan & P. Andrews (Eds.), *Azokh Cave and the Transcaucasian Corridor* (pp. 321–339). Dordrecht: Springer.

Bennett, E. A., Massilani, D., Lizzo, G., Daligault, J., Geigl, E.-M., & Grange, T. (2014). Library construction for ancient genomics: Single strand or double strand? *Biotechniques*, *56*, 289–300.

Binford, L. S. (1980). *Bones: Ancient men and modern myths*. Dordrecht: Academic Press.

Bocherens, H., Fizet, M., & Mariotti, A. (1994). Diet, physiology and ecology of fossil mammals as inferred from stable carbon and nitrogen isotope biogeochemistry: Implications for Pleistocene bears. *Palaeogeography, Palaeoclimatology, Palaeoecology, 107*, 213–225.

Bon, C., Berthonaud, V., Maksud, F., Labadie, K., Poulain, J., Artiguenave, F., et al. (2012). Coprolites as a source of information on the genome and diet of the cave hyena. *Proceedings of Biological Science, 279*(1739), 2825–2830.

Cáceres, I., Esteban-Nadal, M., Bennàsar, M., & Fernández-Jalvo, Y. (2011). Was it the deer or the fox? *Journal of Archaeological Science, 38*, 2767–2774.

Champlot, S., Berthelot, C., Pruvost, M., Bennett, E. A., Grange, T., & Geigl, E.-M. (2010). An efficient multistrategy dna decontamination procedure of PCR reagents for hypersensitive PCR applications. *PLoS ONE, 5*(9), e13042.

Charruau, P., Fernandes, C., Orozco-Ter Wengel, P., Peters, J., Hunter, L., Ziaie, H., et al. (2010). Phylogeography, genetic structure and population divergence time of cheetahs in Africa and Asia: Evidence for long-term geographic isolation. *Molecular Ecology, 20*, 706–724.

Dalen, L., Götherström, A., & Angerbjörn, A. (2004). Identifying species from pieces of faeces. *Conservation Genetics, 5*, 109–111.

Delaney-Rivera, C., Plummer, T. W., Hodgson, J. A., Forrest, F., Hertel, F., & Oliver, J. S. (2009). Pits and pitfalls: Taxonomic variability and patterning in tooth mark dimensions. *Journal of Archaeological Science, 36*, 2597–2608.

Denys, C., Fernández-Jalvo, Y.. & Dauphin, Y. (1995). Experimental Taphonomy: Preliminary results of the digestion of micromammal bones in laboratory. *Comptes Rendues de l'Academie des Sciences*, *321* (série II): 803–809.

Diedrich, C. J. (2012). Cave bear killers and scavengers from the last ice age of central Europe: Feeding specializations in response to the absence of mammoth steppe fauna from mountainous regions. *Quaternary International, 255*, 59–78.

Domínguez-Rodrigo, M., & Piqueras, A. (2003). The use of tooth pits to identify carnivore taxa in tooth-marked archaeofaunas and their relevance to reconstruct hominid carcass processing behaviours. *Journal of Archaeological Science, 30*, 1385–1391.

Fernández, D. (1998). Biogeoquímica isotópica (^{13}C, ^{15}N) del *Ursus Spelaeus* del yacimiento de Cova Eiró s, Lugo. *Cadernos do Laboratorio Xeolóxico de Laxe, 23*, 237–249.

Fernández, D., Vila, M., & Grandal, A. (2001). Stable isotopes data (delta ^{13}C, delta^{15}N) from the cave bear (*Ursus spelaeus*): A new approach to its palaeoenvironment and dormancy. *Proceedings of the Royal Society B: Biological Sciences, 268*, 1159–1164.

Fernández-Jalvo, Y., Scott, L., Carrión, J. S., Gil-Romera, G., Brink, J., Neumann, F., & Rossouw, L. (2010a). Pollen taphonomy of hyaena coprolites: an experimental approach. In E. Baquedano & J. Rosell (Eds.), *Zona Arqueológica. Actas de la 1ª Reunión de científicos sobre cubiles de hiena (y otros grandes carnívoros) en los yacimientos arqueológicos de la Península Ibérica* (pp. 148–156). Alcalá de Henares: Museo Arqueológico Regional.

Fernández-Jalvo, Y., Andrews, P., Pesquero, D., Smith, C., Marin-Monfort, D., Sánchez, B., et al. (2010b). Early bone diagenesis in temperate environments Part I: Surface features and histology. *Palaeogeography, Palaeoclimatology, Palaeoecology, 288*, 62–81.

Fernández-Jalvo, Y., King, T., Andrews, P., Yepiskoposyan, L. (2016). Introduction: Azokh Cave and the Transcaucasian Corridor. In Y. Fernández-Jalvo, T. King, L. Yepiskoposyan & P. Andrews (Eds.), *Azokh Cave and the Transcaucasian Corridor* (pp. 1–26). Dordrecht: Springer.

Figueirido, B., Palmqvist, P., & Pérez-Claros, J. A. (2009). Ecomorphological correlates of craniodental variation in bears and paleobiological implications for extinct taxa: An approach based on geometric morphometrics. *Journal of Zoology, 277*, 70–80.

Gilbert, M. T. P., Jenkins, D. L., Götherstrom, A., Naveran, N., Sanchez, J. J., Hofreiter, M., et al. (2008). DNA from Pre-Clovis Human Coprolites in Oregon, North America *Science*, *320* (5877), 786–789.

Grandal d'Anglade, A., & López-González, F. (2005). Sexual dimorphism and autogenetic variation in the skull of the cave bear (*Ursus spelaeus* Rosenmüller) of the European Upper Pleistocene. *Geobios*, *38*, 325–338.

Grandal d'Anglade, A., & Fernández-Mosquera, D. (2008). Hibernation can also cause high δ15 N values in cave bears: A response to Richards et al., *Proceedings of The National Academy of Sciences of the USA*, *105*, 11.

Guindon, S., & Gascuel, O. (2003). A simple, fast, and accurate algorithm to estimate large phylogenies by maximum likelihood. *Systematic Biology, 52*(5), 696–704.

Harrison, T. (2011). Coprolites: Taphonomic and paleoecological implications. In T. Harrison (Ed.), *Paleontology and Geology of Laetoli: Human Evolution in Context* (Vol. 1, pp. 279–292). Geology, Geochronology, Paleoecology and Paleoenvironment Dordrecht: Springer.

Haynes, G. (1980). Prey bones and predators: potential ecologic information from analyses of bone sites. *OSSA, 7*, 75–97.

Heiri, O., Lotter, A. F., & Lemcke, G. (2001). Loss on ignition as a method for estimating organic and carbonate content in sediments: Reproducibility and comparability of results. *Journal of Paleolimnology, 25*, 101–110.

Krause, J., Unger, T., Nocon, A., Malaspinas, A. S., Kolokotronis, S. O., Stiller, M., et al. (2008). Mitochondrial genomes reveal an explosive radiation of extinct and extant bears near the Miocene-Pliocene boundary. *BMC Evolutionary Biology, 8*, 220.

Keiler, J.A., 2001. Die koprolithen aus dem Unterpleistozän von Untermaßfeld. In R.-D. Kahlke (Ed.), *Das Pleistozän von Untermaßfeld bei Meiningen (Thüringen)*, (pp. 691–698) Teil 2. Dr. Rudolf Habelt GMBH, Bonn

King, T., Compton, T., Rosas, A., Andrews, P. Yepiskoyan, L., & Asryan, L. (2016). Azokh Cave Hominin Remains. In Y. Fernández-Jalvo, T. King, L. Yepiskoposyan & P. Andrews

(Eds.), *Azokh Cave and the Transcaucasian Corridor* (pp. 103–106). Dordrecht: Springer.

Kolska Horwitz, L. (1990). The origin of partially digested bones recovered from archaeological contexts in Israel. *Paléorient, 16*, 97–106.

Kolska Horwitz, L., & Goldbergb, P. (1989). A study of Pleistocene and Holocen hyaena coprolites. *Journal of Archaeological Science, 16*, 71–94.

Kurtén, B. (1976). *The cave bear story*. Dordrecht: Columbia University Press.

Larkin, N. R., Alexander, J., & Lewis, M. (2000). Using experimental studies of recent faecal material to examine hyaena coprolites from the West Runton Freshwater Bed, Norfolk, U.K. *Journal of Archaeological Science, 27*, 19–31.

LeGeros, R. Z. (1994). Biological and Synthetic Apatites. In P. W. Brown & B. Constantz (Eds.), *Hydroxyapatite and Related Materials* (pp. 3–28) Boca Raton: CRC Press.

Lewis, M. (2011). Pleistocene hyaena coprolite palynology in Britain: implications for the environments of early humans. In N. M. Ashton, S. G. Lewis & C. B. Stringer (Eds.), *The Ancient Human Occupation of Britain* (pp. 263–278). Amsterdam: Elsevier

Lewis, M., Pacher, M., & Turner, A. (2010). The larger carnivora of teh West Runton Freshwater Bed. *Quaternary International, 228*, 116–135.

Macdonald, D. W., & Barrett, P. (1993). *Field Guide of Mammals*. Britain and Europe London: HarperCollins.

Maguire, J. M., Pemberton, D., & Collett, M. H. (1980). The Makapansgat limeworks grey breccia: Hominids, hyaenas, hystricds or hillwash? *Paleontologia Africana, 23*, 75–98.

Marin-Monfort, M. D., Cáceres, I., Andrews, P., Pinto, A. C., & Fernández-Jalvo, Y. (2016). Taphonomy and Site Formation of Azokh1. In Y. Fernández-Jalvo, T. King, L. Yepiskoposyan & P. Andrews (Eds.), *Azokh Cave and the Transcaucasian Corridor* (pp. 211–249). Dordrecht: Springer.

Matthews, T. (2000). Predators, prey and the palaeoenvironment. *South African Journal of Science, 96*, 23–24.

Matthews, T. (2006). Taphonomic characteristics of micromammals predated by small mammalian carnivores in South Africa: Application to fossil accumulations. *Journal of Taphonomy, 4*, 143–160.

Mattson, D. J. (1998). Diet and morphology of extant and recently extinct northern bears. *Ursus, 10*, 479–496.

Mazza, P., Rustioni, M., & Boscagli, G. (1995). Evolution of ursid dentition; with inferences on the functional morphology of the masticatory apparatus in the genus Ursus. In J. Moggi-Cecchi (Ed.), *Aspects of dental biology: palaeontology, anthropology and evolution* (pp. 147–157). Florence: International Institute for the Study of Man.

Miotto, R. A., Ciocheti, G. Rodrigues, F. P., & Galetti, Jr. P. M. (2007). Identification of pumas (*Puma concolor* (Linnaeus, 1771) through faeces: A comparison between morphological and molecular methods. *Brazilian Journal of Biology*, *67* (4, Suppl.), 963–965.

Mondini, M. (2002). Carnivore Taphonomy and the Early Human Occupations in the Andes. *Journal of Archaeological Science, 29*, 791–801.

Montalvo, C. I., Pessino, M. E. M., & González, V. H. (2007). Taphonomic analysis of remains of mammals eaten by pumas (Puma concolor Carnivora, Felidae) in central Argentina. *Journal of Archaeological Science, 34*, 2151–2160.

Mulla, S. M., Phale, P. S., Saraf, M. R. (2012). Use of X-Ray diffraction technique for polymer characterization and studying the effect of optical accesories. AdMet 2012 Paper No. OM006, 1–6.

Murray, D., Bunce, M., Cannell, B. L., Oliver, R., Houston, J., White, N. E., et al. (2011). DNA-based faecal dietary analysis: A comparison of qPCR and high throughput sequencing approaches. *PLoS ONE, 6*, 25776.

Murray, J., Lynch, E. P., Domínguez-Alonso, P., & Barham, M. (2016). Stratigraphy and Sedimentology of Azokh Caves, South Caucasus. In Y. Fernández-Jalvo, T. King, L. Yepiskoposyan & P. Andrews (Eds.), *Azokh Cave and the Transcaucasian Corridor* (pp. 27–54). Dordrecht: Springer.

Nelson, R. A., Wahner, H. W., Fones, J. J., Ellefson, R. D., & Zollman, P. E. (1973). Metabolism of bears before, during and after winter sleep. *American Journal of Physiology, 224*, 491–496.

Parfitt, S., & Larkin, N. R. (2010). Appendix. Exceptionally large hyaena coprolites from West Runton and the possible presence of the giant short-faced hyaena (Pachycrocuta brevirostris). *Quaternary International, 228*, 131–135.

Payne, S., & Munson, P. J. (1985). Ruby and how many squirrels? The destruction of bones by dogs. In N. R. J. Fieller, D. D. Gilbert-Sov & N. G. A. Ralph (Eds.), *Paleobiological Investigations* (pp. 31–46). BAR Int. Ser. *266*, Oxford.

Peigné, S., Goillot, C., Germonpré, M., Blondel, C., Bignon, O., & Merceron, G. (2009). Predormancy omnivory in European cave bears evidenced by a dental microwear analysis of Ursus spelaeus from Goyet, Belgium. *Proceedings of the National Academy of Sciences USA, 106*, 15390–15393.

Pesquero, M. D., Salesa, M. J., Espílez, E., Mampel, L., Siliceo, G., & Alcalá, L. (2011). An exceptionally rich hyaena coprolites concentration in the Late Miocene mammal fossil site of La Roma 2 (Teruel, Spain): Taphonomical and palaeoenvironmental inferences. *Palaeogeography, Palaeoclimatology, Palaeoecology, 311*, 30–37.

Pickering, T. R. (2002). Reconsideration of criteria for differentiating daunal assemblages accumuulated by hienas and hominids. *International Journal of Osteoarchaeology, 12*, 127–174.

Pobiner, B. (2008). Paleoecological information in predator tooth marks. *Journal of Taphonomy, 6*, 373–397.

Poinar, H. N., Hofreiter, M., Spaulding, W. G., Martin, P. S., Stankiewicz, B. A., Bland, H., et al. (1998). Molecular coproscopy: dung and diet of the extinct ground sloth *Nothrotheriops shastensis*. *Science, 281*, 402–406.

Pokines, T. T., & Peterhans, J. C. K. (2007). Spotted hyena (Crocuta crocuta) den use and taphonomy in the Masai Mara National Reserve, Kenya. *Journal of Archaeological Science, 34*, 1914–1931.

Pruvost, M., & Geigl, E.-M. (2004). Real-time quantitative pcr to assess the authenticity of ancient DNA. *Journal of Archaeological Science, 31*, 1191–1197.

Pruvost, M., Grange, T., & Geigl, E.-M. (2005). Minimizing DNA-contamination by using UNG-coupled quantitative real-time PCR (UQPCR) on degraded DNA samples: Application to ancient DNA studies. *BioTechniques, 38*, 569–575.

Pruvost, M., Schwarz, R., Bessa Correia, V., Champlot, S., Braguier, S., Morel, N., et al. (2007). Freshly excavated fossil bones are best for ancient DNA amplification. *Proceedings of the National Academy of. Science USA, 104*(3), 739–744.

Roberts, A. (1954). The mammals of South Africa. 2nd ed. Trustees of, The mammals of South Africa Book Fund, Johannesburg.

Rohland, N., Pollack, J. L., Nagel, D., Beauval, C., Airvaux, J., Pääbo, S., & Hofreiter, M. (2005). The population history of extant and extinct hyenas. *Molecular Biology and Evolution, 22*, 2435–2443.

Richards, M. P., Pacher, M., Stiller, M., Quilès, J., Hofreiter, M., Constantin, S., et al. (2008). Isotopic evidence for omnivory among European cave bears: Late Pleistocene Ursus spelaeus from the Peştera cu Oase, Romania. *Proceedings of the National Academy of Sciences of the USA, 105*, 600–604.

Scott, L., Rossow, L., Cordova, C., & Risberg, J. (2016). Palaeoenvironmental Context of Coprolites and Plant Microfossils from Unit II. Azokh 1. In Y. Fernández-Jalvo, T. King, L. Yepiskoposyan & P. Andrews (Eds.), *Azokh Cave and the Transcaucasian Corridor* (pp. 287–295). Dordrecht: Springer.

Selvaggio, M. M., & Wilder, J. (2001). Identifying the involvement of multiple carnivore taxa with archaeological bone assemblages. *Journal of Archaeological Science, 28*, 465–470.

Shehzad, W., Riaz, T., Nawaz, M. A., Miquel, C., Poillot, C., Shah, S. A., et al. (2012). Carnivore diet analysis based on next-generation sequencing: Application to the leopard cat (*Prionailurus bengalensis*) in Pakistan. *Molecular Ecology, 21*, 1951–1965.

Shokralla, S., Spall, J. L., Gibson, J. F., & Hajibabaei, M. (2012). Next-generation sequencing technologies for environmental DNA research. *Molecular Ecology, 21*, 1794–1805.

Skinner, J. D. (1976). Ecology of the brown hyena Hyaena brunnea in the Transvaal with a distribution map for southern Africa. *South African Journal of Science, 72*, 262–269.

Skinner, J. D., Haupt, M. A., Hoffmann, M., & Dott, H. M. (1998). Bone collection by brown hyaenas *Hyaena brunnea* in the Namib Desert: Rate of accumulation. *Journal of Archeological Science, 25*, 69–71.

Smith, C. I., Faraldos, M., & Fernández-Jalvo, Y. (2016). Bone Diagenesis at Azokh Caves. In Y. Fernández-Jalvo, T. King, L. Yepiskoposyan & P. Andrews (Eds.), *Azokh Cave and the Transcaucasian Corridor* (pp. 251–269). Dordrecht: Springer.

Stuart, C., & Stuart, T. (1994). *A field guide to the tracks and signs of southern and east african wildlife*. Cape Town: Southern Book Publishers.

Van der Made, J., Torres, T., Ortiz, J. E., Moreno-Pérez, L., & Fernández-Jalvo, Y. (2016). The new Material of Large Mammals from Azokh and Comments on the Older Collections. In Y. Fernández-Jalvo, T. King, L. Yepiskoposyan & P. Andrews (Eds.), *Azokh Cave and the Transcaucasian Corridor* (pp. 117–159). Dordrecht: Springer.

Vila Taboada, M., Fernández Mosquera, D., López González, F., Grandal d'Anglade, A., & Vidal Romaní, J. R. (1999). Paleoecological implications inferred from stable isotopic signatures (d13C, d15 N) in bone collagen of *Ursus spelaeus* ROS.-HEIN. *Cadernos do Laboratorio Xeolóxico de Laxe*, *24*, 73–87.

Vila Taboada, M., Fernández Mosquera, D., & Grandal d'Anglade, A. (2001). Cave bear's diet: A new hypothesis based on stable isotopes. *Cadernos do Laboratorio Xeolóxico de Laxe*, *26*, 431–439.

Walker, C. (1993). *Signs of the wild*. Cape Town: Struik Publishers.

Chapter 13
Palaeoenvironmental Context of Coprolites and Plant Microfossils from Unit II. Azokh 1

Louis Scott, Lloyd Rossouw, Carlos Cordova, and Jan Risberg

Abstract Poor pollen preservation in cave deposits is due to oxidation and increasing scarcity of pollen with distance from the cave entrance. After an attempt to obtain pollen grains from the sediments in Azokh 1 (Lesser Caucasus) failed, two coprolites from Unit II were investigated for their microfossil contents. They contained few diatoms (including the rare *Pliocaenicus*), even less pollen but numerous phytoliths that were compared with those in selected levels of cave deposits and modern soil from outside. Grass silica short cell phytoliths give evidence of vegetation typical of a temperate climate for Unit II, which included C_3 grasses. Not only the coprolites from Azokh are useful but the whole sequence of deposits has good potential for palaeoclimatic reconstruction based on for phytolith studies. The diatoms observed indicate feeding from a relatively moist terrestrial environment and availability of lake and/or running water.

Резюме Для изучения экологической ситуации в процессе возникновения отложений в пещере *Азох 1* (Малый Кавказ) химическому анализу были подвергнуты два образца копролитов. Исследование было предпринято после попытки получения пыльцы из мелкозернистого седимента, которая окончилась неудачей по причине продолжительной оксидации и разложения в условиях постоянного изменения влажности в пещере, а также возрастающей нехватки переносимой по воздуху пыльцы от входа в глубь пещеры. В качестве альтернативного источника пыльцы и других микроископаемых элементов были исследованы два копролита, обнаруженных в подразделении *II*. Они содержали редко встречающиеся виды диатомеи, включая *Pliocaenicus* sp., немного пыльцы и большое количество фитолитов. Фитолиты в копролитах были сопоставлены с образцами, отобранными из нескольких слоев отложений внутри и из современной почвы за пределами пещеры. Различные типы фитолитов рода *Poaceae* (силицированные короткие клетки травы) в пределах подразделения *II* указывают на типичную для умеренного климата растительность, которая включает C_3 травы и несколько отличается от современной смешанной флоры. Плотность лесного покрова не может быть определена без дальнейшего изучения нетравяных фитолитов в копролитах и седименте. Последние указывают на то, что мелкозернистая седиментная последовательность в *Азох 1* имеет одинаково хороший потенциал для анализа фитолитов в копролитах и, следовательно, для палеоэкологической реконструкции всей последовательности отложений, в том числе и для более обширного региона. Обнаруженные диатомовые водоросли свидетельствуют об относительно влажной почве и наличии озерной или речной воды в качестве источника питания.

Keywords Fossil scats • Phytoliths • Diatoms • MIS 5 • Lesser Caucasus

L. Scott (✉)
Department of Plant Sciences, University of the Free State,
PO Box 339,Bloemfontein 9300, South Africa
e-mail: scottl@ufs.ac.za

L. Rossouw
Department of Archaeology, National Museum,
PO Box 266,Bloemfontein 9300, South Africa
e-mail: lloyd@nasmus.co.za

C. Cordova
Department of Geography, Oklahoma State University,
Stillwater, OK 74078, USA
e-mail: carlos.cordova@okstate.edu

J. Risberg
Department of Physical Geography, Stockholm University,
106 91 Stockholm, Sweden
e-mail: jan.risberg@geo.su.se

Yolanda Fernández-Jalvo et al. (eds.), *Azokh Cave and the Transcaucasian Corridor*,
Vertebrate Paleobiology and Paleoanthropology, DOI 10.1007/978-3-319-24924-7_13

Introduction

The primary way of reconstructing past vegetation and environments is usually by means of pollen analysis of lakes and swamps but this method is not regularly used in caves. Fine-grained cave deposits often provide little or no information about past climates because concentrations of aerially introduced material like pollen, which is introduced as dust in the cave by air currents or other means, is usually not high. The influx of transported microscopic particles declines progressively deeper into a cave and beyond 20 to 30 m it is very low (Coles and Gilberstone 1994; Navarro et al. 2001; Hunt and Rushworth 2005). Conditions for preservation are often not ideal on cave floors, and considering these constraints both for pollen and phytoliths in fine-grained cave sediments, richer alternative sources may be needed.

Our first attempt at Azokh 1 in the Lesser Caucasus to extract pollen from sediments of Units I and V, at depths of 77 cm and lower in the Azokh cave system, was unsuccessful. After exposure for more than 20 years sediments near the cave opening became dry, crumbly, cracked, bioturbated and oxidized (Fernández-Jalvo et al. 2010) and therefore not suitable for pollen analysis. Other plant microfossil research may still be feasible, and initial investigations indicated that sediments potentially contain phytoliths and starch inclusions (Fernández-Jalvo et al. 2010). A further possible reason for the lack of pollen may be the 40 m distance of the present excavation area to cave entrance, which is removed from aerial pollen sources. Although air currents are relatively active today (Y. Fernandez-Jalvo, personal communication 2006), we do not have evidence that this was the case in the past. Preservation qualities may not be ideal and pollen could also have been destroyed by a combination of highly oxidizing conditions and microbial action in acidic bat guano rich in phosphates, which is present throughout the cave sequence, and by wet-dry cycles in the cave such as recognized in Unit II (Marin-Monfort et al. 2016). Fresh bat guano is rich in pollen, but in fossil layers it could have been decomposed over time (Carrion et al. 2006). Extensive carbonate cementation occurs in some parts of the Azokh 1 excavation, mainly in levels closer to the limestone cave walls, as result of seasonal and drip-water flows, and this could also have played a role in destroying pollen grains. It has been reported that damp areas near cave walls have poorer pollen preservation (Navarro et al. 2001; Carrion et al. 2006).

In view of the paucity of pollen in the Azokh deposits and in order to obtain additional dietary or environmental data, we turned our attention to the coprolites to search for pollen and phytoliths in them for comparison with phytoliths in the surrounding deposits. Coprolittes are biogenic inclusions that trap plants from outside the cave (Thompson et al. 1980; O'Rourke and Mead 1985; Scott 1987), and they can be useful alternatives as sources for micro-plant remains because their inclusions are sealed off and protected more effectively from adverse sedimentary conditions such as dampness and oxidation. In the long run these conditions, if severe enough can destroy pollen anywhere, also in coprolites, but the chances are that they will survive longer inside a coprolite than in unconsolidated deposits (Navarro et al. 2001; Scott et al. 2003). Coprolites in caves can therefore shed light on prehistoric conditions not only because their shape, size and structure represent prehistoric fauna, but also because their microscopic contents provide clues about past vegetation and climate. Apart from research on hyrax dung deposits in Africa and the Middle East, previous studies of coprolites in Africa and Europe were often based on hyena coprolites (Scott 1987; Carrión et al. 2007) because these coprolites are more frequently found in caves than those of other animals, for example badgers, which are less frequent (Carrion et al. 2005).

Plant microfossils in a coprolite can be derived from an animal's diet, it's drinking water, ingested dust, or that which became attached to the dung via air currents soon after defecation. Dung usually traps a representative assemblage of pollen and organic and siliceous dust derived from wide surroundings where the animals were roaming. Dung pellets fossilize in caves to become solid coprolites that preserve their micro-contents under more stable conditions than those in the surrounding fine, looser deposits, which experience local variations of humidity and temperature. As long as coprolites do not disintegrate, their slightly acidic conditions are not necessarily harmful to microscopic inclusions. Coprolites therefore prevent decomposition and destruction of organics, but this can be temporary because the microscopic contents can be lost in the long run if local conditions deteriorate (Scott et al. 2003).

Because significant differences occur in the morphology of microscopic phytolith types produced by the main Poaceae subfamilies (or grass silica short-cell types (GSSC)) (Twiss et al. 1969; Brown 1984; Mulholland 1989; Fredlund and Tieszen 1994), these microfossils in coprolites promised to be an informative tool. Despite the prevalence of 'multiplicity' and 'redundancy' in GSSC assemblages (Rovner 1971, 1983), i.e. the occurrence of a variety of types in one grass taxon as well as the occurrence of the same type in different taxa, fluctuations in the frequencies of certain types can be still be used to distinguish between the grass subfamilies (Fredlund and Tieszen 1994; Rossouw 2009).

Coprolite fragments of unidentified origin have been found at Unit II and Vu of Azokh 1. Unit II also yielded two complete coprolites (no's 5153 and 5246) of which 5246, and some obviously derived stone artifacts together with fossils typical of Unit II, were apparently displaced in Unit I

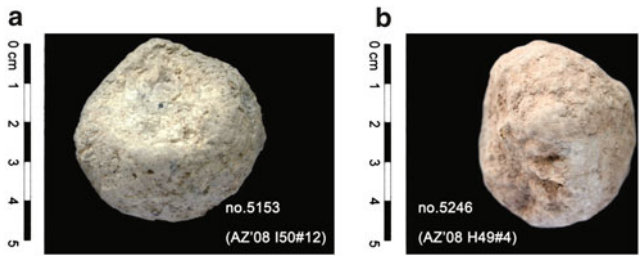

Fig. 13.1 The two studied coprolites 5153 (**a**) and 5246 (**b**) from Azokh I, Unit II

through modern bioturbation (Murray et al. 2016; Marin-Monfort et al. 2016). During extraction of palaeobotanical remains, a bone fragment was recovered indicating a carnivorous (or omnivorous) diet of the animal that produced the coprolites. Although several other coprolite fragments are available in different layers, only these two were complete and undamaged and were used for plant microfossil extraction.

This paper deals with the extraction of microfossils from the two coprolites in Azokh Cave. With the aim of shedding light on possible environmental conditions that existed during their formation, we investigate the potential of microfossils in the coprolites and discuss them in the context of other fossils and the reconstruction of faunal paleoecology and charcoal that have been found in the deposits from where the coprolites came (Andrews et al. 2016).

Environment Around the Cave

The cave at Azokh (39° 37′ 9.17″ N, 46° 59′ 18.59″ E) is in the Lesser Caucasus at 962 m elevation and the environment is described in this volume (Andrews et al. 2016; Fernández-Jalvo et al. 2016). The rainfall is approximately 600 mm/year, falling mainly in May–June and September–October, while the driest month is January (Republic of Armenia 1999). The faunal contents in the sequence of 300 kyr in the Azokh Cave sedimentary sequence show some variations but are typical of steppe, arid conditions or deciduous woodlands (Andrews et al. 2016). Evidence of the surrounding vegetation in the past can be derived from charcoal in Unit II and Unit Vu, consisting mainly of *Prunus* (80%) that was probably the most abundant tree species and could have been gathered by humans as firewood while fruits were probably dispersed around the cave (Allué 2016; Andrews et al. 2016).

According to descriptions of present vegetation and plant communities in the Caucasus region it can broadly be divided into three zones: foothill grassland, lower-mountain mixed hardwood forest, and mountain subalpine grassland (Sharrow 2007). According to global grass distribution maps, this part of the Caucasus consists mainly of species of the Pooideae (c. 300 species), which dominate over other groups like Chloridoideae (17), Paniceae (13), Andropogoneae (6) and Arundinoideae (6). The subfamily Pooideae is the premier group of grasses occupying cool temperate and boreal regions (Cross 1980; Clayton and Renvoize 1986).

Azokh Cave falls in the lower mountain mixed hardwood forest which is generally found at 600–1,100 m elevation (Gulisashvili et al. 1975; Sharrow 2007). At present, most land suitable for farming has been ploughed, and areas suitable for grazing have been grazed. Moderate slopes have often been cleared for use as crop or hay fields, forming large openings in the forest, but areas of forest still exist on steep slopes (Sharrow 2007). The vegetation on the slopes in the vicinity of the cave are currently grassy woodland vegetated by *Carpinus*, *Quercus* (probably *Q. iberica*), *Tilia* and *Fraxinus* with an understory of *Prunus*, *Cornus*, *Corylus*, *Crataegus* and *Paliurus spina-christi* (Andrews et al. 2016). In the general surroundings *Paliurus* and *Ziziphus* is common in "shibliak" (i.e. secondary woodland that develop after forest clearing) (Gabrielian and Fragman-Sapir 2008).

The grasslands of lower elevations once occupied the generally eastern facing foothills and lower slopes of the mountains at about 300–600 m elevation with an annual precipitation of approximately 250–400 mm (Sharrow 2007). Further, cool-season grasses occur with several types of woody species and herbaceous sagebrush in the more xeric areas while shrubs such as buckthorn, hawthorn, and black-wood are found in the more mesic areas.

Materials and Methods

Pollen, Phytolith and Diatom Extraction

The two coprolites (No.'s 5153 = AZ1'08 II-I50#12 and 5246 = AZ1'08 I-H49#4) (Fig. 13.1), which measured 50 × 49 × 33 and 48 × 47 × 30 mm respectively, were sawed in half. One half of each was saved and the other processed for plant microfossil extraction. The studied halves were cleaned by removing the outside 1 to 2 mm layers, which were also saved together with the dust obtained from sawing. They were cleaned further by water to remove dust and then treated in 10% HCl, and cleaned by centrifuging several times using water. Mineral separation was then performed by floating the silica and organic fraction on sodium polytungstate solution (S.G. 2.3) and washing in a centrifuge. Microscope slides were mounted in glycerine jelly and investigated under light microscope, using up to 100× oil

Table 13.1 Samples of Azokh Cave coprolites and deposits

Lab no.	Unit	Depth cm	Type	Age	MIS
5360			Modern soil outside		
5306	Unit I	80	Cave sediment	<200 yrs	1
5246	Unit II/I	224, reworked, in burrow	Coprolite # 0804	?	5
5153	Unit II	233	Coprolite # 0812	c. 100 kyrs	5
5302	Unit II	238.5	Cave sediment close to 5153	c. 100 kyrs	5
5304	Unit II	278.5	Cave sediment	100–130 kyrs	5 or 6
5305	Unit II or III	337	Cave sediment	130–160-kyrs	6

immersion magnification. Five sediment samples for comparison were also chemically processed in the same way as the coprolites for phytolith investigation (Table 13.1).

Criteria for the Identification of Phytolith Types

Nine different grass silica short cell (GSSC) phytoliths were classified morphologically following the International Code for Phytolith Nomenclature (ICPN Working Group et al. 2005). Four different morphological variations of the bilobate morphotype within the Poaceae are recognized in this study (Rossouw 2009). Variant 1 possesses orbicular lobes that are symmetrical in planar view, and it has a central portion or neck equal or greater than one third of total length of body. Variant 2 has a comparatively short central portion with orbicular to ovate lobes that are symmetrical in planar view and with the length of its central portion equal to or less than one third of total length of body. Variant 3 is always asymmetrical in planar view with the length of its central portion less than one third of total length of body. This type is comparable to the irregular complex dumbbell types recognized by Twiss et al. (1969) and the 'Other lobate' category in Fredlund and Tieszen (1994). The fourth variant, or *Stipa*-type bilobate, is a predominantly pooid morphotype, which appear trapezoidal or tabular in side view with generally ovate to scutiform lobes (Mulholland 1989; Fredlund and Tieszen 1994; Rossouw 2009).

Other GSSC-phytoliths that were identified include polylobates, commonly produced by the C_3 Pooideae subfamily and C_3 Panicoid species as well as cross and saddle morphotypes, which are primarily produced in the C_3/C_4 Panicoideae and C_4 Chloridoideae subfamilies, respectively. Trapezoidal, rondel and oblong morphotypes are largely produced by the C_3 Pooideae and Danthionoideae subfamilies. Trapezoids are six-sided, square or rectangular silica bodies with few sides parallel (Rossouw 2009). Planar margins are angular and not medially constricted. The trapezoid category is equivalent to types 1b, 1d and 1f in Twiss et al. (1969), the rondel types described by Mulholland (1989), the conical and pyramidal types in Fredlund and Tieszen (1994) and rondel types g, h and i in Thorn (2004). The rondel is cylindrical or semi-cylindrical, tapers distally, and resembles a truncated cone (Mulholland 1989). It is circular, elliptical or acicular in planar view (Rossouw 2009). This morphotype compares to type 1a in Twiss et al. (1969) and the conical type in Fredlund and Tieszen (1994). The oblong morphotype includes six-sided silica bodies that are at least twice as long as broad with parallel or nearly parallel sides. Oblong-shaped phytoliths are defined as having smooth, sinuous or crenate planar edges and trapezoidal cross-sections (Rossouw 2009). It corresponds with types 1c, 1g and 1h in Twiss et al. (1969), and the "longer forms with more polygonal cross-sections" in Mulholland (1989, p. 495). There are also elongated long-cell morphotypes as well as acicular (trichome) and bulliform morphotypes. All other unidentified morphotypes, which represent a variety of plant families that include dicotyledons or gymnosperms, were classified as "indeterminate". In this provisional study we did not attempt to identify this group because we did not have reference material from the local plants.

Results

Diatoms

Less than one diatom per gram was obtained from only one of the coprolites and a single diatom was found in 5 g of deposits of Unit I. The following species were among the diatoms recorded: *Hantzschia amphioxys* (Fig. 13.2a), *Pinnularia borealis* (Fig. 13.2b) and *Nitzschia* sp. (Fig. 13.2c). Both *H. amphioxys* and *P. borealis* are aerophilic taxa (preferring shallow or running water) and therefore indicative of moist conditions e.g., lake shores, ground water springs, wetlands or wet soils (Denham et al. 2009).

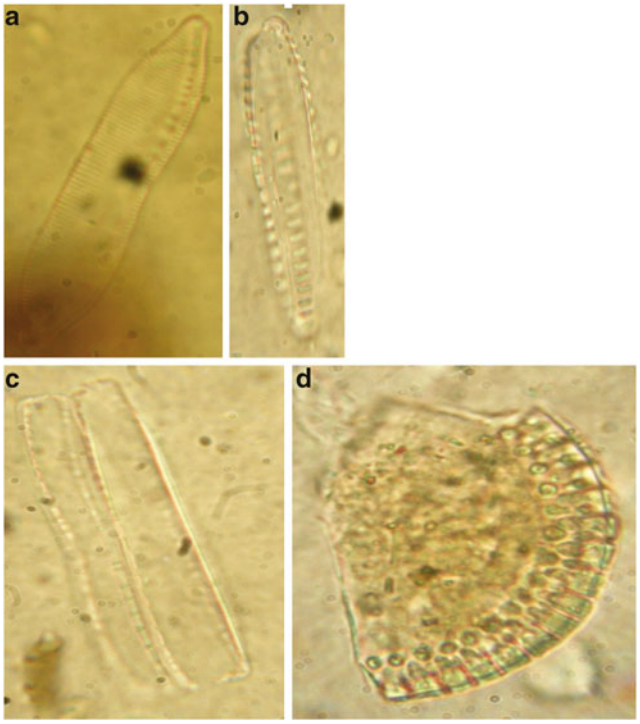

Fig. 13.2 Diatoms recorded in the two Azokh Cave coprolites, *Hantzschia amphioxys* (44 μm) (a), *Pinnularia borealis* (31 μm) (b), *Nitzschia* sp. (54 μm) (c) and *Pliocaenicus* (44 μm) (d)

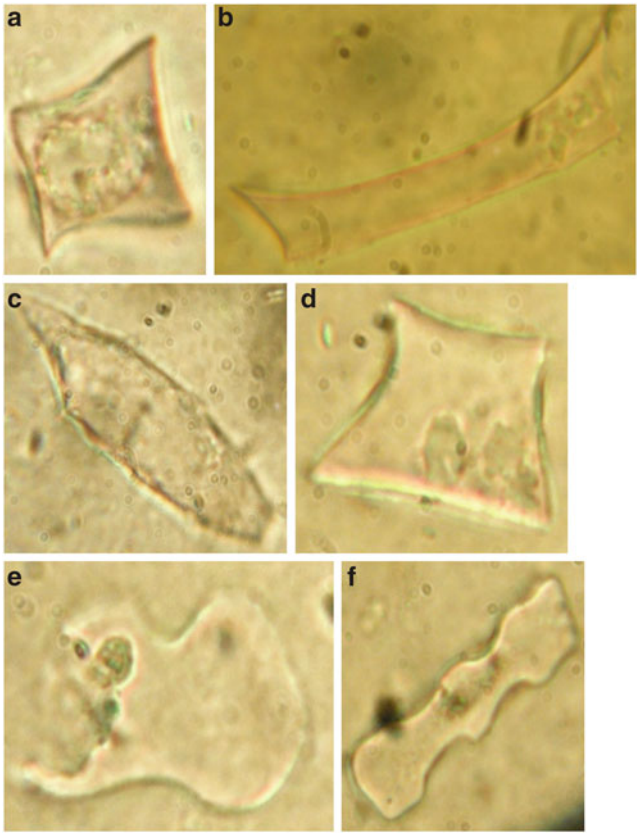

Fig. 13.3 Some phytolith types from the Azokh coprolites: Trapezoid (14 μm) (**a**); Oblong (32 μm) (**b**); Basal view of trichome (42 μm) (**c**); Rondel (20 μm) (**d**); Bilobate Variant 2 (24 μm) (**e**); Polylobate (26 μm) (**f**)

A fourth diatom type represents *Pliocaenicus* (Fig. 13.2d), a genus which has been recorded from a Tertiary freshwater environment in China (Stachura-Suchoples and Jahn 2009). The diatom specimen from the Unit 1 is obscured by sediment but could tentatively be *Achnanthes* sp., a genus which may be found in a large variety of environments and therefore least informative.

Phytoliths

Both the coprolites and studied cave deposits were very rich in siliceous phytoliths ranging from well preserved to broken, etched and damaged. Phytoliths in the coprolite 5246 were more corroded than 5153, while those deposits of Unit II (5302) from which the latter was derived were better preserved in comparison with other levels. Examples of the recorded phytoliths are shown in Fig. 13.3a–f. Counts show that GSSC-phytoliths (grass silica short cell phytoliths) make up more than 60% of the total number of phytoliths counted in coprolite 5153, while 5246 has a lower percentage (Fig. 13.4a). The rest consist of indeterminate phytoliths of various plants which could include a variety of unidentified dicotyledonous and gymnosperm species and include hair bases (Fig. 13.3c), trichomes and phytoliths of leaves, branches or fruits. In view of this high proportion of unidentified forms we cannot make an accurate reconstruction of the vegetation without further research on these types. The GSSC-phytoliths are composed of several types (Fig. 13.4b) that include comparatively few bilobate morphotypes (Fig. 13.3e) representing less than 2% of the GSSC-component. Polylobate morphotypes (Fig. 13.3f) account for less than 3% of the total number of GSSC-phytoliths counted. The highest frequencies of epidermal short cells in the coprolites are represented by trapezoidal, rondel and oblong morphotypes (totalling c. 90%) (Fig. 13.3 a, b and d).

Pollen and Other Microfossils

The coprolites were poor in pollen and there was not enough for determining past vegetation composition. Only two pollen grains and some possible spores were found in coprolite 5153. One is Asteraceae, most probably belonging to *Artemisia* (not illustrated) of which the morphology is

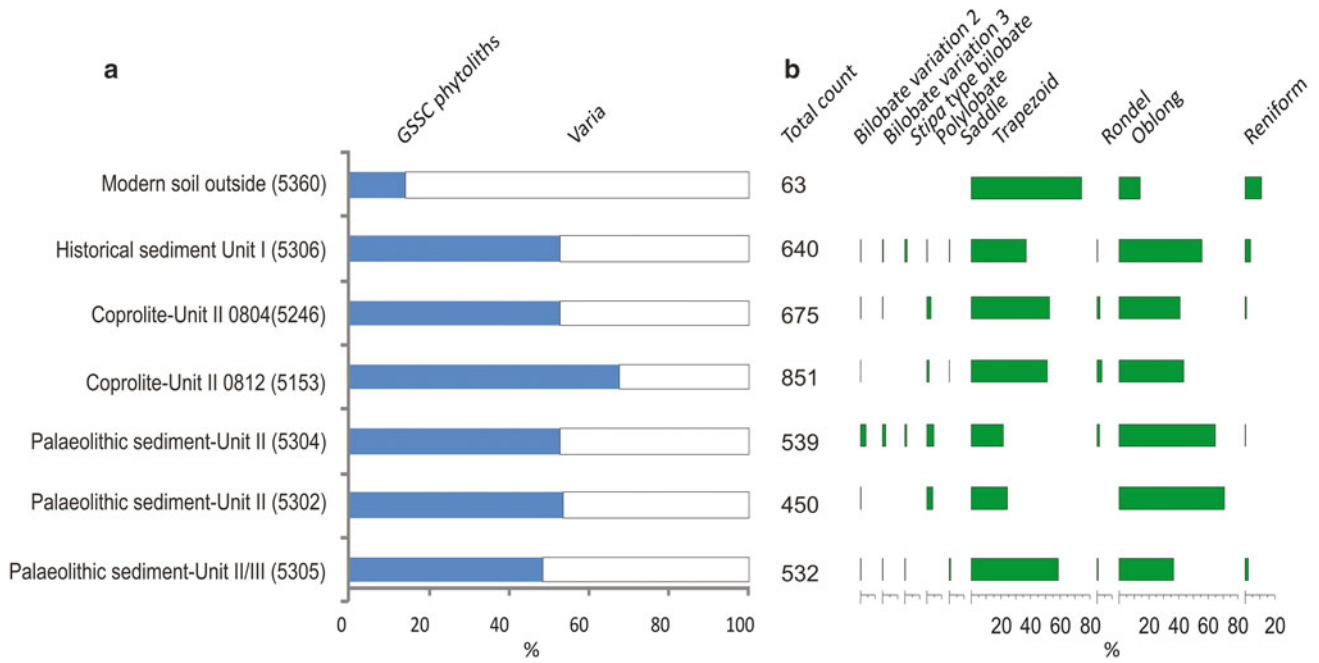

Fig. 13.4 Diagrams of phytoliths from Azok Cave surface soil, coprolites and deposits showing the ratio between GSSC (grass silica short cell) phytoliths and indeterminate phytoliths (**a**), and the percentages of different types of GSSC phytolith types (**b**)

well known, but *Echinops* or *Centaurea* cannot be excluded. The second pollen type (Fig. 13.5a) is as yet unidentified. Possible fern or bryophyte spores or algae also occur. The preservation of the two pollen grains was reasonable enough to reveal their morphological characteristics suggesting that their low concentration is possibly not a result of destructive processes but due to low pollen availability. Their brownish color suggests that they are indeed fossil and not modern contaminants.

Long silica structures (longer than 200 microns) were observed in coprolite 5153. They resemble sponge spicules (Fig. 13.5b) and are indicative of flooding or could have been derived from drinking water. In soils outside caves, this is indicative of flooding from a stream. Azokh 1 is seasonally wet (Murray et al. 2016; Marin-Monfort et al. 2016), and they may have formed at this time, but when the cave is dry, they may have entered the animal's alimentary tract through drinking water. Also recorded in coprolite 5153 are comparatively large radial leaf trichomes of c. 174 and 200 micron diameters (Fig. 13.5b, c). Microscopic charcoal occurred in small numbers as brown and black woody plant remains (Fig. 13.5d) derived from occasional natural fires or fine aerial dust ingested accidentally inside or outside the cave from hearths. A spiny "corpuscle" (Fig. 13.5e) in coprolite 5153 is similar to structures that have been seen in hyena coprolites from sites in South Africa (L. Scott unpublished data), and in a picture of an unknown structure derived from a stool (http://www.dpd.cdc.gov/dpdx/html/ImageLibrary/A-F/Artifacts/body_Artifacts_il6.htm).

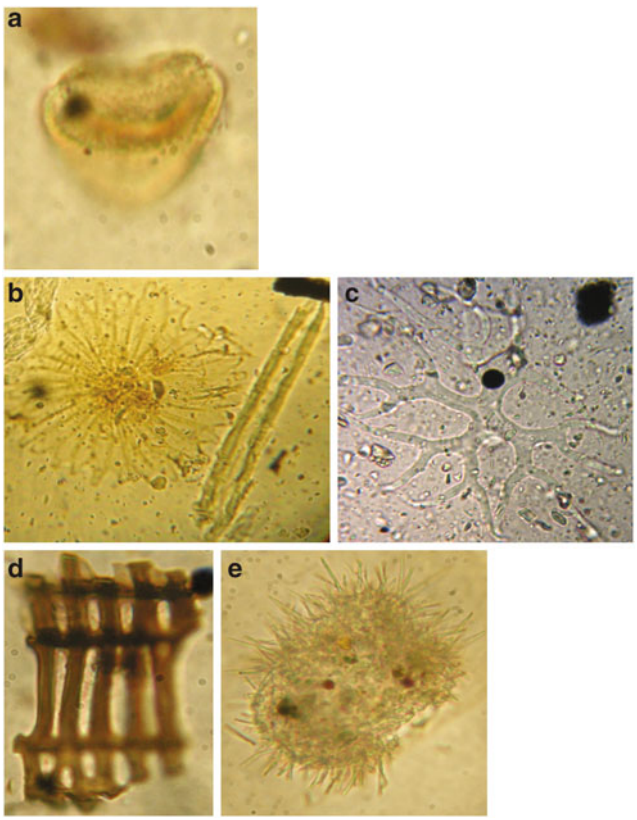

Fig. 13.5 Other microfossil types in the Azokh coprolites, unidentified pollen (22 μm) (**a**), trichome (174 μm) (left) and sponge spicule (218 μm) (right) (**b**), trichome (c. 200 μm) (**c**), woody fibre (38 μm) (**d**) and unidentified corpuscule (44 μm) (**e**)

Discussion

Unit II dates from 100 to 184 kyr according to ESR dating (see Appendix and Murray et al. 2016) covering Marine Isotope Stages 5 and 6. According to the available dates the studied coprolites are from the very top part of the unit (dated in 100 ± 7 kyr) and belong to Stage 5 (Table 13.1) but the exact age cannot be determined more precisely. They are therefore more likely to represent a warm or a stadial phase than a glacial period.

The present-day river near the area, the terraces of which indicate that it was active in the Pleistocene (Murray et al. 2016), could be a potential source of the diatoms in the one coprolite. Phytoliths in the coprolite 5246 were more corroded than those in 5153 and its associated Unit II deposits, which contained better preserved silica than other deposits. The difference in preservation quality is difficult to explain, except for the indication of guano deposits during and after burial. Corrosion might have resulted from harsh conditions in the surroundings before the phytoliths were accidentally ingested by the animal (as dust), or it might have occurred later under fluctuating water tables or dampness that affected the silica inside the coprolite in the cave. It is known that at present such fluctuations do occur, and it is likely that they also occurred in the past. Corrosion could have been enhanced further by the corrosive qualities of bat guano. Indications of guano and damp/dry fluctuations at the cave interior is indicated by secondary mineral formation, such as tinsleyite, sepiolite, gypsum, ardelite or brushite (Magela da Costa and Rúbia Ribeiro 2001; Marincea et al. 2002; White and Culver 2012) detected by X-ray fluorescence (XRF) and X-ray diffraction (XRD) in both the sediment and the fossils (Marin-Monfort et al. 2016).

Habitat structure inferred through a comparison of the contribution from GSSC phytoliths versus non-grass phytoliths (e.g., Alexandre et al. 1997; Bremond et al. 2005) points to grassy conditions in the region at the time when the coprolites were formed, although the density of woody components cannot be determined. However, the two coprolites differ in content, and the more non-grass inclusions in coprolite 5246 could be related to seasonal factors or could simply be due the possibility that the coprolites represent different habitats in which animals roamed (Fig. 13.4). As is indicated by the non-grass silica like epidermal cells or other round "blocky" phytoliths, several different unidentified plant types could be included in the coprolite assemblages. As can be inferred from the charcoal evidence (Allué 2016) woody species must have occurred locally, especially *Prunus*. Phytoliths of this genus, which are not produced in fruits, leaves and inflorescences of some species (Kealhofer and Piperno 1998), were not identified, partly because their morphologies are not known (Rovner 1971).

The proportion of GSSC–phytoliths versus indeterminate silica bodies in the coprolite-bearing deposits is similar to that of the Holocene deposits, but the recent soil shows a lower proportion of grasses, which is typical of an overgrazed area like that around the cave at present.

Some are taxonomically and ecologically significant. The underrepresentation of saddle and bilobate phytoliths and comparatively high frequencies of trapezoidal and oblong morphotypes recorded in Unit II clearly suggests that C_3 grassy conditions prevailed at the time when the coprolites were formed and the place where they were ingested outside the cave. This is supported by the presence of polylobates recorded throughout Unit II. Polylobates are recorded in at least 25% (n = 31) of modern Pooid species (Rossouw 2009). The phytoliths also indicate the presence of other plants which can at present not be identified.

The surrounding area at the time of the coprolite production could also have undergone dry summers resembling that of alpine meadows of the Crimean Mountains or that of the cold-dry steppe (winter-rain) of South Jordan (Cordova 2011). Because of the presence of *Stipa*-type in an area where Paniceae and Danthonioideae are rare, the occurrence of grasses of the Stipeae tribe, most of which reflect cold and dry continental climates, is suggested.

The coprolite phytolith assemblages only give a reflection of what is available in the environment and not necessarily of the actual proportions of plant types. Potential bias in ratio towards more grasses in the GSSC in relation to unidentified silica in the coprolite samples is plausible in view of possible selective consumption of grasses by carnivores as is recorded in ecological studies worldwide (Skinner 1976; de Arruda Bueno et al. 2002). However, comparison with the phytoliths in the surrounding deposits of Unit II does not suggest any marked bias. The cave deposit samples from the Unit II sediment may be a more unbiased reflection of the vegetation in the immediate surroundings than the coprolite because they do not favor behavioral selection from a wider range.

The oblong/trapezoid phytolith ratios between the coprolites and surrounding deposits differ slightly with more oblong types in the latter. This could be from widely roaming animals trapping phytoliths in their dung and not from the local slopes next to the cave (as represented by the cave deposits). In comparison to present conditions as reflected by the modern sample outside the cave, oblong types are more prominent but it is not possible to say if this is due to climate a different climate or modern grazing disturbance. The assemblages that occur in Unit I deposits during the Holocene compare well with those in Unit II, suggesting that climates did not differ markedly.

On the basis of other evidence the habitat varied (Andrews et al. 2016). The large mammals and charcoal indicate deciduous woodland while small mammals,

amphibians and reptiles indicate open steppe environments. The taphonomy of the latter group suggests that they were probably brought to the cave from a distance by predators in a setting similar to the present, where woodland occurs in the vicinity of the cave and steppe not too far away. Therefore it is not impossible that woodland existed similar to the vegetation that can potentially develop in the area today under current climatic conditions and no agricultural disturbance.

Conclusions

1. Pollen was extremely rare in the two carnivore coprolites investigated, and none was found in the sediments. The lack of pollen is probably due to environmental conditions and the location of the excavation 40 m into the Azokh 1 passageway.
2. Phytoliths were abundant in the coprolites and in the deposits of Unit II. Nine different grass silica short cell (GSSC) phytolith types were identified, and these indicate that the vegetation type was most likely a temperate C_3-grass steppe mosaic.
3. Phytoliths other than those of grasses were recorded and they could have been derived from local woodland. Caution is needed with the interpretation of the openness of the vegetation in view of the unknown degree of possible selection of phytoliths by the carnivore and due to the limitation that a large number of the phytoliths were not identified.
4. The few diatoms recovered suggest the availability of local water.
5. Long silica structures (longer than 200 microns) were observed in one of the coprolites. They resemble sponge spicules and indicate wet conditions.
6. The discovery of numerous phytoliths show that the Azokh deposits have great potential for a phytolith study and interpreting environmental conditions throughout the whole Azokh sequence. A more detailed analysis can therefore be undertaken beyond the scope of this study. The potential is demonstrated in deposits at the older Dmanisi site in the Georgian Caucasus that contain comparable phytolith assemblages indicating marked changes in water stress in the region (Messager et al. 2010).

Acknowledgments We thank Yolanda Fernández-Jalvo for providing the coprolites, initiating the study and providing relevant information. We are also grateful to the authorities of Nagorno-Karabakh for the support and permissions to work on these specimens. We are grateful to Tania King and diggers for careful work collecting these fossils, as well as field assistants for modern soil sampling on the slope of the cave. Thanks are extended to Karen Hardy for collecting sediment samples from the section of Azokh.

References

Alexandre, A., Meunier, J. D., Lezine, A. M., Vincens, A., & Schwarz, D. (1997). Phytoliths: Indicators of grassland dynamics during the late Holocene in intertropical Africa. *Palaeogeography, Paleoclimatology, Palaeoecology, 136*, 213–229.

Allué, E. (2016). Charcoal remains from Azokh 1: Preliminary results. In Y. Fernández-Jalvo, T. King, L. Yepiskoposyan & P. Andrews (Eds.), *Azokh Cave and the Transcaucasian Corridor* (pp. 297–304). Dordrecht: Springer.

Andrews, P., Hixson Andrews, S., King, T., Fernández-Jalvo, Y., & Nieto-Díaz, M. (2016). Paleoecology of Azokh 1. In Y. Fernández--Jalvo, T. King, L. Yepiskoposyan & P. Andrews (Eds.), *Azokh Cave and the Transcaucasian Corridor* (pp. 305–320). Dordrecht: Springer.

Appendix: Fernández-Jalvo, Y., Ditchfield, P., Grün, R., Lees, W., Aubert, M., Torres, T., et al. (2016). Dating methods applied to Azokh cave sites. In Y. Fernández-Jalvo, T. King, L. Yepiskoposyan & P. Andrews (Eds.), *Azokh Cave and the Transcaucasian Corridor* (pp. 321–339). Dordrecht: Springer.

Bremond, L., Alexandre, A., Peyron, O., & Guiot, J. (2005). Grass water stress estimated from phytoliths in West Africa. *Journal of Biogeography, 32*, 311–327.

Brown, D. A. (1984). Prospects and limits of a phytolith key for grasses in the central United States. *Journal of Archaeological Science, 11*, 345–368.

Carrión, J. S., Gil, G., Rodríguez, E., Fuentes, N., García-Antón, M., & Arribas, A. (2005). Palynology of badger coprolites from central Spain. *Palaeogeography, Palaeoclimatology, Palaeoecology, 226*, 259–271.

Carrión, J. S., Scott, L., & Marais, E. (2006). Environmental implications of pollen spectra in bat droppings from south-eastern Spain and potential for palaeoenvironmental reconstructions. *Review of Palaeobotany and Palynology, 140*, 175–186.

Carrión, J. S., Scott, L., Arribas, A., Fuentes, N., Gil, G., & Montoya, E. (2007). Pleistocene landscapes in Central Iberia inferred from pollen analysis of hyena coprolites. *Journal of Quaternary Science, 22*, 191–202.

Clayton, W. D., & Renvoize, S. A. (1986). *Genera Graminum. Grasses of the World*. London: Her Majesty's Stationary Office.

Coles, G. M., & Gilbertson, D. D. (1994). The airfall-pollen budget of archaeologically important sites: Creswell Crags, England. *Journal of Archaeological Science, 21*, 735–755.

Cordova, C. (2011). The *Stipa*-type short cell. What does it mean taxonomically, climatically and ecologically? *Proceedings of the 8th International Meeting on Phytolith Research*. Estes Park, Colorado, USA.

Cross, R. A. (1980). Distribution of sub-families of Gramineae in the old world. *Kew Bulletin, 35*, 279–289.

de Arruda Bueno, A., da Silva, C., Belentani, S., & Carlos Motta-Junior, J. (2002). Feeding ecology of the maned wolf, Chrysocyon brachyurus (Illiger, 1815) (Mammalia: Canidae), in the ecological station of Itirapina, Sao Paulo State. *Brazil. Biota Neotropica, 2*(2), 1–9.

Denham, T., Sniderman, K., Saunders, K. M., Winsborough, B., & Pierret, A. (2009). Contiguous multi-proxy analyses (X-radiography, diatom, pollen, and microcharcoal) of Holocene

archaeological features at Kuk Swamp, Upper Wahgi Valley, Papua New Guinea. *Geoarchaeology: An. International Journal, 24*, 715–742.

Fernández-Jalvo, Y., King, T., Andrews, P., & Yepiskoposyan, L. (2016). Introduction: Azokh Cave and the Transcaucasian Corridor. In Y. Fernández-Jalvo, T. King, L. Yepiskoposyan & P. Andrews (Eds.), *Azokh Cave and the Transcaucasian Corridor* (pp. 1–26). Dordrecht: Springer.

Fernández-Jalvo, Y., King, T., Andrews, P., Yepiskoposyan, L., Moloney, N., Murray, J., et al. (2010). The Azokh Cave complex: Middle Pleistocene to Holocene human occupation in the Caucasus. *Journal of Human Evolution, 58*, 103–109.

Fredlund, G. G., & Tieszen, L. T. (1994). Modern phytolith assemblages from the North American Great Plains. *Journal of Biogeography, 21*, 321–335.

Gabrielian, E., & Fragman-Sapir, O. (2008). *Flowers of Transcaucasus and adjacent areas: Including Armenia, Eastern Turkey, Southern Georgia, Azerbaijan and Northern Iran*. Ruggell: Gantner Verlag.

Gulisashvili, V. Z., Makhatadze, L. B., & Prilipko, L. I. (1975). *Rastitel'nost' Kavkaza*. Moskva: Nauka. *The vegetation of the Caucasus* (Trans: Russian). http://www.rusnature.info/reg/15_6.htm.

Hunt, C. O., & Rushworth, G. (2005). Airfall sedimentation and pollen taphonomy in the West mouth of the Great Cave, Niah. *Journal of Archaeological Science, 32*, 465–473.

ICPN Working Group, Madella, M., Alexandre, A., & Ball, T. (2005). International Code for Phytolith Nomenclature 1.0. *Annals of Botany*, *96* (2), 253–260.

Kealhofer, L. & Piperno, D. R. (1998). Opal *Phytoliths in Southeast Asian Flora*. Smithsonian Contributions to Botany 88, Washington, D.C. Smithsonian Institution Press.

Magela da Costa, G., & Rúbia Ribeiro, V. (2001). The occurrence of tinsleyite in the archaeological site of Santana do Riacho, Brazil. *Mineralogical Society of America, 86*, 1053–1056.

Marincea, S., Dumitras, D., & Gibert, R. (2002). Tinsleyite in the "dry" Cioclovina Cave (Sureanu Mountains, Romania): The second occurrence. *European Journal of Mineralogy, 14*, 157–164.

Marin-Monfort, M. D., Cáceres, I., Andrews, P., Pinto, A. C., & Fernández-Jalvo, Y. (2016). Taphonomy and Site Formation of Azokh 1. In Y. Fernández-Jalvo, T. King, L. Yepiskoposyan & P. Andrews (Eds.), *Azokh Cave and the Transcaucasian Corridor* (pp. 211–249). Dordrecht: Springer.

Messager, E., Lordkipanidze, D., Delhon, C., & Ferring, C. R. (2010). Palaeoecological implications of the Lower Pleistocene phytolith record from the Dmanisi Site (Georgia). *Palaeogeography, Palaeoclimatology, Palaeoecology, 288*, 1–13.

Mulholland, S. C. (1989). Phytolith shape frequencies in North Dakota grasses: A comparison to general patterns. *Journal of Archaeological Science, 16*, 489–511.

Murray, J., Lynch, E. P., Domínguez-Alonso, P., & Barham, M. (2016). Stratigraphy and sedimentology of Azokh Caves, South Caucasus. In Y. Fernández-Jalvo, T. King, L. Yepiskoposyan & P. Andrews (Eds.), *Azokh Cave and the Transcaucasian Corridor* (pp. 27–54). Dordrecht: Springer.

Navarro, C., Carrión, J. S., Munuera, M., & Prieto, A. R. (2001). A palynological study of karstic cave sediments on the basis of their potential for palaeoecological reconstruction. *Review of Palaeobotany and Palynology*, *117*, 245–265.

O'Rourke, M. K., & Mead, J. (1985). Late Pleistocene and Holocene pollen records from two caves in the Grand Canyon of Arizona, USA. *American Association of Stratigrapphic Palynologists, 16*, 169–185.

Republic of Armenia. (1999). *A country study on the biodiversity of Armenia*. First National Report to the Convention on Biological Diversity. Yerevan: Ministry of Nature Protection.

Rossouw, L. (2009). *The application of fossil grass-phytolith analysis in the reconstruction of Cainozoic environments in the South African interior*, PhD dissertation. University of the Free State, Bloemfontein.

Rovner, I. (1971). Potential of opal phytoliths for use in palaoecological reconstruction. *Quaternary Research, 1*, 343–359.

Rovner, I. (1983). Plant phytolith analysis: Major advances in archaeobotanical research. *Advances in Archaeological Method and Theory, 6*, 225–266.

Scott, L. (1987). Pollen analysis of hyena coprolites and sediments from Equus Cave, Taung, Southern Kalahari (S. Africa). *Quaternary Research, 28*, 144–156.

Scott, L., Fernández-Jalvo, Y., Carrión, J. S., & Brink, J. S. (2003). Preservation and interpretation of pollen in hyena corprolites: Taphonomical observations from Spain and Southern Africa. *Palaeontologia Africana, 39*, 83–91.

Sharrow, S. H. (2007). Natural resource management on the other side of the world: The Nagorno Karabakh Republic. *Society for Range Management February*, 1–16.

Skinner, J. D. (1976). Ecology of the brown hyena Hyaena brunnea in the Transvaal with a distribution map for southern Africa. *South African Journal of Science, 72*, 262–269.

Stachura-Suchoples, K., & Jahn, R. (2009). Middle Miocene record of *Plioaenicus changbaiense* sp nov. from Changbai (Jilin Province, China). *Acta Botanica Croatica, 68*, 211–220.

Thompson, R. S., Van Devender, T. S., Martin, P. S., Foppe, T., & Long, A. (1980). Shasta ground sloth (Nothrotheriops shastense Hoffstetter) at Shelter Cave, New Mexico: Environment, diet, and extinction. *Quaternaty Research, 14*, 360–376.

Thorn, V. C. (2004). Phytolith evidence for C_4-dominated grassland since the early Holocene at Long Pocket, northeast Queensland, Australia. *Quaternary Research, 61*, 168–180.

Twiss, P. C., Suess, E., & Smith, R. M. (1969). Morphological classification of grass phytoliths. *Proceedings of the Soil Science Society of America, 33*, 109–115.

White, W. B., & Culver, D. C. (2012). *Encyclopedia of Caves*. Dordrecht: Springer.

Chapter 14
Charcoal Remains from Azokh 1 Cave: Preliminary Results

Ethel Allué

Abstract We present here the results of the charcoal analyses from Unit II and Unit Vu from Azokh 1 Cave. The results from the anthracological study show a variable record with up to nine taxa, including variability within the identified genera or types. The most abundant taxon is *Prunus,* which represents 80% of the record in Unit II. The charcoal record from Azokh 1 shows a record including *Prunus*, *Acer*, Maloideae and *Quercus* sp. and other trees and shrubs. The taxa recorded were probably abundant in the landscape near the cave reflecting mild and humid environmental conditions. The charcoal is probably the remains of firewood used during the human occupations.

Резюме В данной статье представлены результаты анализа образцов древесного угля из седиментных подразделений *II* и *IV* пещеры *Азох 1*. Использованная методология основана на изучении фрагментов угля с целью генерации данных о формировании растительности в прошлом и ее эволюции во времени. Более того, с помощью данного анализа была получена информация о поведении человека, относящаяся к использованию им лесных ресурсов. Данное исследование основано на анализе 907 фрагментов древесного угля, которые были найдены в результате визуального сбора и влажного просеивания. До проведения идентификации образцы были вручную измельчены для отделения трех анатомических сегментов, которые позволяют описать клеточную структуру дерева. Классификация образцов древесного угля из подразделения *II* выявила разнообразный спектр видов, включающий *Prunus* (слива), *Acer* (клен), *Quercus* sp. *deciduous* (лиственный дуб), Maloideae (яблоня), *Lonicera* (жимолость), *Paliurus/Ziziphus* (терн Христа/ююба), *Celtis/Zelkova* (каркас/зелькова), *Euonymus* (бересклет) и *Ulmaceae* (семейство вязов). Наиболее обильно представлен таксон *Prunus*, который составляет 80% всех находок. *Quercus* sp. *deciduous*, *Acer* и *Maloideae* встречаются с частотой 2–4%, остальные таксоны имеют частоту менее 1%. Подразделение IV содержало меньшее количество остатков древесного угля и включало представителей трех таксонов: *Prunus, Maloideae* и *Quercus* sp. *deciduous*.

Перечень находок древесного угля из Азохской пещеры указывает на специфическое формирование растительного мира с превалированием *Prunus, Acer, Maloideae* и *Quercus* sp. *Deciduous* среди деревьев и кустарников. В ландшафте окрестностей пещеры в изобилии встречались различные таксоны, отражая тем самым особый тип формирования флоры, характеризующийся последовательностью, которая привела к появлению лиственного дубового леса. Этот растительный ландшафт свидетельствует о наличии мягких и влажных условий среды. Использование древесины в качестве топлива указывает на четко выраженную тенденцию в применении наиболее распространенных видов, при котором предпочтение отдано древесине сливовых деревьев.

Keywords Pleistocene • Southern Caucasus • Vegetation • Firewood • *Prunus*

Introduction

Anthracology is an archaeobotanical discipline based on the taxonomic identification of charcoal remains from archeological or natural deposits (see Vernet 1992; Thiébault 2002; Fiorentino and Magri 2008; Damblon and Court-Picon 2008; Badal et al. 2011). The aim of this discipline is the recog-

E. Allué (✉)
IPHES, Institut Català de Paleoecologia Humana i Evolució Social, Zona Educacional 4, Campus Sescelades URV (Edifici W3), 43007 Tarragona, Spain
e-mail: eallue@iphes.cat
and
Àrea de Prehistòria, Universitat Rovira i Virgili (URV), Avinguda de Catalunya 35, 43002 Tarragona, Spain

Yolanda Fernández-Jalvo et al. (eds.), *Azokh Cave and the Transcaucasian Corridor*, Vertebrate Paleobiology and Paleoanthropology, DOI 10.1007/978-3-319-24924-7_14

nition of past vegetation and its evolution through time, and it includes the study of firewood uses in relation to human behavior. Archeological charcoal from Paleolithic sites is often produced through the use of wood as fuel in domestic hearths; and therefore their anthropic origin has to be considered when interpreting the results. The presence of charcoal from firewood is an artifact conditioned by human choices and can be interpreted as such (Hastorf and Popper 1988; Théry-Parisot 2001; Asouti and Austin 2005; Allué and García-Antón 2006; Théry-Parisot et al. 2009). In addition, the value of charcoal analysis has been shown as a tool for paleoecological reconstruction (Western 1971; Vernet 1973, 1997; Figueiral and Mosbrugger 2000; Willis and Van Andel 2004; Théry-Parisot et al. 2010). This interpretation is based on the ecological characterization of the species and their dependence on ranges of climatic conditions, and it takes into account their diachronic evolution and cultural bias. Both aspects of the discipline depend on a fine and accurate sampling method, and both are being considered in this study.

The Caucasus has an important role in human evolution and dispersal due to its geographic position. Furthermore, concerning past vegetation, it is a key area for the understanding of change through time. Charcoal studies from the Caucasus are little known and the development of new studies concerning archaeobotany is now providing data on different topics concerning environmental change, firewood exploitation, and plant uses. Current and earlier studies in the area are based on pollen and plant macro-remains (seeds, charcoal, leaves) from different periods including the Pleistocene and Holocene archeological and natural deposits (Tumajanov 1971; Lisitsina and Prischepenko 1977; Zelikson and Gubonina 1985; Klopotovskaja von et al. 1989; Shatilova 1990 in Golovanova and Doronichev 2003; Djafarov 1999; Gabunia et al. 2000; Lioubine 2002; Gabrielian and Gasparyan 2003; Allué 2004; Connor et al. 2004; Kvavadze and Connor 2005; Hovsepyan and Willcox 2008; Messager et al. 2008; Díez et al. 2009; Joannin et al. 2010; Ollivier et al. 2010; Ghukasyan et al. 2010; Gabrielyan and Kovar-Eder 2011). During the last decades, the development of diverse interdisciplinary projects in the southern Caucasus has enlarged the archeobotanical assemblages, even if Pleistocene data are still very few (Gabrielian and Gasparyan 2003; Joannin et al. 2010; Ollivier et al. 2010; Ghukasyan et al. 2010; Gabrielyan and Kovar-Eder 2011).

The area under study is a mountainous zone bordering the Iranian, Armenian, and Azerbaijan territories (see Fernández-Jalvo et al. 2016). At present due to the vast intensity of human exploitation, forested areas in the southern Caucasus are scarce (Moreno-Sánchez and Sayadyan 2005). In the area near Azokh, landscape is dominated by *Paliurus spina-christi* due mainly to human disturbances related to wood cutting and livestock.

In this chapter, we are presenting the results from the charcoal analyses from Unit II and Unit Vu from Azokh 1 cave in order to provide new data concerning past vegetation and plant resources. Unit II has been dated by ESR from the top 100 to around 200 ka BP at the base and Unit Vu has been dated by ESR around 200 ka BP (see Appendix dating).

Materials and Methods

This study is based on 886 charcoal fragments from Unit II and 21 from Unit Vu that were recovered during the 2005–2009 field seasons, using hand collection and wet sieving. Hand collection is used particularly for Paleolithic deposits, in which the excavation technique permits the view of the charcoal fragments *in situ* (Allué 2006). For this purpose, each piece of charcoal of about 4–5 mm is extracted, wrapped in aluminum foil, and labeled. This kind of sampling should be accompanied by screening the sediment, and this was the procedure followed here.

For charcoal identification, the remains were fragmented by hand in order to obtain the three wood anatomy sections necessary for the description of the cell structure. Charcoal fragments were observed through a metallographic reflected light microscope with dark and light fields, using ×5, ×20, ×50 magnifications (Olympus BX41). The identification is supported with a reference collection and various wood anatomy atlases (Fahn et al. 1986; Schweingruber 1990; Benkova and Schweingruber 2004; Insidewood 2004; Schweingruber and Landolt 2005) and a charcoal reference collection made from the area.

The identification rank used in charcoal analyses is family, genus, type, and occasionally the species. Charcoal analysis does not always permit a species-level identification due to factors such as small size of the charcoal fragment, the cell structure modifications produced by combustion or postdepositional processes, low anatomical variability among species, or the absence within the fragment of all the characteristics which define a species.

Quantification of charcoal assemblages is usually based on numbers of fragments or the presence/absence of the different taxa. Furthermore, depending on the number of fragments a statistical approach can be made. Usually, a minimum number of fragments is necessary, and data sets of between 250 and 500 fragments per unit are required to obtain the total record (Chabal et al. 1999). However, the

variability of a charcoal assemblage depends on firewood management, type and duration of occupations, type of plant formation exploited, sampling, type of structures, etc.

Results

The charcoal record from Unit II shows a wide diversity of taxa (Table 14.1) with *Prunus* (plums), *Acer* (maple), *Quercus* sp. deciduous (deciduous oaks), Maloideae (pomes), *Lonicera* (honeysuckle), *Paliurus/Ziziphus* (Christ's thorn/jujube), *Celtis/Zelkova (Hackberry/Zelkova)*, *Euonymus* (spindle), and Ulmaceae (elm family). The most abundant taxon is *Prunus* which represents 80% of the record. *Quercus* sp. deciduous, *Acer,* and Maloideae show values between 2 and 4% and the rest of the taxa represent less than 1%. Unit Vu has yielded fewer charcoal remains with just three taxa: *Prunus*, Maloideae, and deciduous *Quercus* sp.

Some of the charcoal types include more than one species due to their similar wood anatomy. The genera *Ziziphus* and *Paliurus* share similar wood anatomy characters and they cannot be differentiated (Schweingruber 1990). *Ziziphus* and *Paliurus* grow at present in the area; nevertheless, *Paliurus* has a wider distribution (Grabrielian and Fragmar-Sapir 2008). *Celtis* and *Zelkova* show some singular characteristics that have not been clearly observable in the fragments from Azokh (Fig. 14.1a, b). According to Schweingruber and Landolt (2005), a difference can be noticed on the basis of the presence of crystals in rays in *Celtis* and their absence in

Table 14.1 Results from the anthracological analysis from Units II and Unit Vu from Azokh 1 cave

Taxa	II		V-upper
	Num. frags.	%	Num. frags.
Acer	34	3.84	
Carpinus	1	0.11	
Celtis/Zelkova	4	0.45	
Euonymus	2	0.23	
Lonicera	9	1.02	
Maloideae	23	2.60	3
Prunus	709	80.02	15
Quercus sp. decidous	28	3.16	2
Quercus/Castanea	2	0.23	
Paliurus/Ziziphus	3	0.34	
Ulmaceae	4	0.45	
cf. *Acer*	3	0.34	
cf. Maloideae	1	0.11	
cf. *Prunus*	13	1.47	
cf. *Quercus*			1
cf. Ulmaceae	1	0.11	
Undetermined angiosperm	48	5.42	
Undetermined	1	0.11	
Total number of fragments	886		21

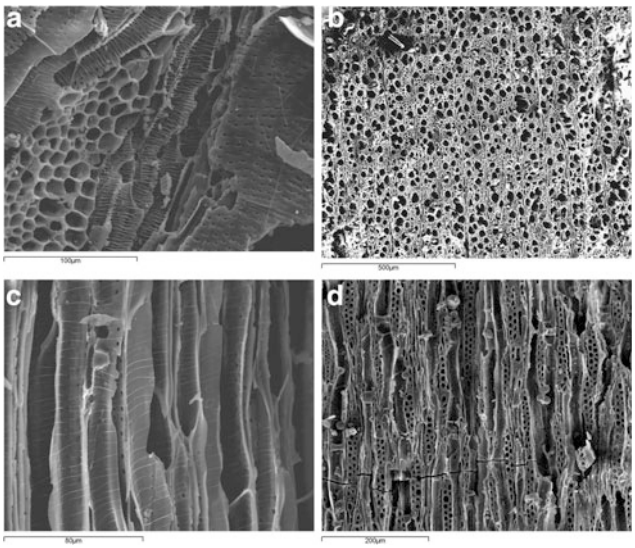

Fig. 14.1 SEM images from Azokh 1 Unit II charcoal fragments. **a** Transversal section of *Celtis/Zelkova* showing heterogeneous and sheath cells in rays. **b** Transversal section of Maloideae. **c** Tangential section of Maloideae showing spiral thickenings. **d** Tangential section of Maloideae showing bi-seriated homogeneous rays

Zelkova, but we have not been able to see this character in the charcoal fragments from Azokh. The Maloideae subfamily includes several genera such as *Crataegus*, *Sorbus*, *Malus*, *Cydonia*, etc., that share similar wood anatomy. A slight variability can be identified through the presence or absence of helical thickenings, which has been identified in several fragments; this indicates that in fossil record at Azokh there is more than one species of Maloideae present (Fig. 14.1c, d).

For the genera *Prunus*, *Cerasus,* and *Amygdalus* we use *Prunus sensu lato.* The wood anatomy of *Prunus* species is similar among all the species; but some characters are useful to group them into smaller categories. The most useful characters for European woods from the Mediterranean basin are the ones established by Heinz and Barbaza (1998). The authors described three different *Prunus* types on the basis of the number of cells in the rays. *Prunus* type 1 rays have no more than two cells; *Prunus* type 2 has between three and four cells per ray, and the *Prunus* type 3 has more than five cells. Each type would correspond to different groups, for example type 1 to *Prunus avium/padus* (cherry/European bird cherry), type 2 to *Prunus spinosa/mahaleb* (blackthorn/mahaleb cherry), and type 3 to *Prunus spinosa/amygdalus* (blackthorn/almond tree). Ntinou (2002) also uses three groups according to the species growing at present in Greece. Group I includes *P. armeriaca*, *P. dulcis*, *P. persica,* and *P. webbii*. When the rays were seven or eight seriated and have ring-porous wood they were identified as *Prunus* cf. *amygdalus*. Group II with diffuse-porous wood and two to seven cell rays, with an average of five, includes *P. domestica*, *P. padus*, *P. mahaleb*,

P. spinosa, and *P. cerasifera*. Group III with semi ring-porous wood to diffuse-porous wood and with up to four ray cells includes *P. avium* and *P. cerasus*. According to Ntinou (2002), *amygdalus* is the only *Prunus* species identified using the ring-porous wood character. Records from other sites in the surrounding areas of Turkey and Armenia often include *amygdalus* on the basis of the same character, whereas the rest of the species are grouped in the *Prunus* genus (Asouti 2003; Emery-Barbier and Thiébault 2005; Hovsepyan and Willcox 2008).

In the Azokh charcoal assemblage, we have grouped the samples according to the characters of Heinz and Barbaza (1998) based on the number of cells in the rays and the presence of ring-porous wood. In Unit II, we have been able to distinguish three different types of *Prunus* according to the former description (Table 14.2, Fig. 14.2). Most of the fragments belong to groups 2 and 3 showing multiseriate rays with more than three series and a semi ring-porous wood. Fragments from type 1 with two seriate rays are less significant, and ring-porous wood has been identified in a few fragments. Therefore, we can conclude that there were several species from this genus preserved in Azokh 1.

Table 14.2 Classification of *Prunus* fragments according to the number of cells in rays and ring porosity

Anatomy character	Types	Num.	%
Number of cells in rays	*Prunus* type 1	87	12.3
	Prunus type 2	197	27.8
	Prunus type 3	214	30.2
	Nonclassified *Prunus*	211	29.8
Ring porosity	Ring-porous *Prunus*	29	
	Ring to semi-ring porous *Prunus*	13	

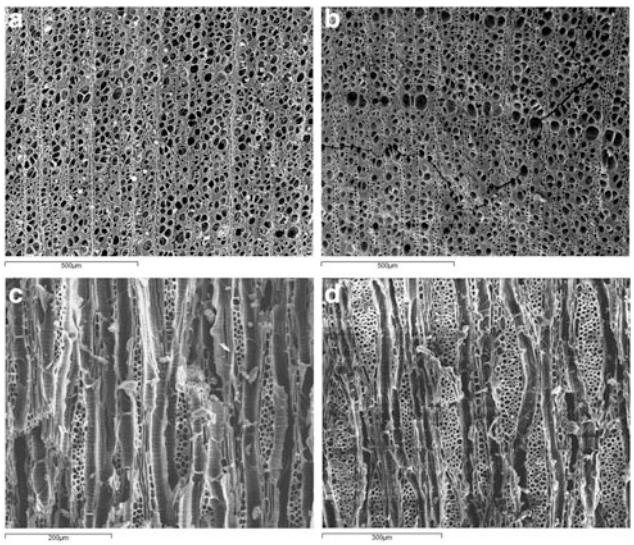

Fig. 14.2 SEM images from Azokh 1 Unit II of *Prunus* charcoal. **a** Transverse section of *Prunus* showing diffuse porosity. **b** Transverse section of *Prunus* showing slightly larger pores in early wood. **c** Tangential section of *Prunus* showing bi to tri-seriated rays. **d** Tangential section of *Prunus* showing multi-seriated rays

Discussion: Vegetal Landscapes and Firewood Uses

Charcoal analysis allows us to describe the vegetation from the local area and the firewood used in the past. For these purposes, we need to take into account the formation process of the assemblage so as to understand the origin of the charcoal assemblage. In relation to this, we are considering various aspects to understand if the charcoal remains are natural or anthropic. First, the location of these remains in the inner part of the cave, far from the entrance, indicates that they could not be naturally deposited. The size of the charcoal fragments is too large for them to have been dispersed from their original hearths suspended in the air. Secondly, the presence of charcoal is continuous in the archeological units and associated with other anthropic remains such as lithics and fauna. These materials, although they present evidence of remobilization, are *in situ* as demonstrated by the taphonomic study (see Marin-Monfort et al. 2016). Furthermore, charcoal and some cultural remains show burning marks, which indicate that there were human activities related to fire. Therefore, even though no spatial pattern indicates an anthopic organization, we consider charcoal as part of the human occupation and not the product of natural fires. In this sense, we suggest that the charcoal assemblage from Azokh is the product of the wood used as firewood by hominins.

The charcoal study shows that there was a high diversity of taxa within genera, especially concerning *Prunus*, for which our anatomical observations show that we can identify several different species. The genus *Prunus* includes at present a diversity of species within several subgenera, such as *Amygdalus*, *Cerasus*, *Laurocerasus,* and *Padus* (RBGE 1998). In the Caucasus area today, there are numerous species and subgenera including *Amygdalus fenziliana*, *A. nairica*, *Armeriaca vulgaris*, *Cerasus avium*, *C. incana*, *C. mahaleb*, *Padus racemosa*, *P. cerasifera* (Gabrielian and Fragman-Sapir 2008). At present in the Azokh area, we can find *A. fenzliana* and *P. cerasifera* the latter also growing in the yards of the village houses. In this discussion, we will use *Prunus sensu latu* when describing our results.

Archeological evidence of plum stones are rather scarce from the Epipaleolithic to the Bronze Age, whereas they increased in Roman times, probably suggesting cultivation (Zohary and Hopf 2000; Martinoli and Jacomet 2004).

Cherry stones (*P. spinosa*, *P. avium*) also appear in deposits from the Mesolithic to Neolithic. *Prunus* wood charcoal is more abundant and is present during the Middle to Upper Pleistocene in several European sequences. Its spread in anthracological records from the Mediterranean basin is clearly marked at the Late Glacial (Heinz 1990; Ntinou 2002; Allué et al. 2007), and it is related to pioneering formations that would led to the development of broad-leaved forests. In the eastern Mediterranean area, *Prunus* and *Amygdalus* are present in several Epipaleolithic and Neolithic sites showing a steppe like formation together with *Pistacia* and *Juniperus* (Asouti 2003; Emery-Barbier and Thiébault 2005). At present in the Caucasus, the different *Prunus* species grow in several plant communities. According to Gabrielian and Fragman-Sapir (2008), these species grow in different types of vegetal communities, such as deciduous forests (*Cerasus avium*), open forests (*Amygdalus fenzliana*, *Prunus cerasus*, *Cerasus mahaleb*, *Cerasus incana*), armeno-iranian phrygana (*Amygdalus fenzliana*, *Cerasus incana*), Shibliak (*Amygdalus anirica*, *A. fenzliana*, *Prunus cerasus*, *Cerasus incana*), and therefore their presence in Azokh Cave could be representing one of this communities. Taking into account the rest of the taxa from the assemblage, we would suggest an open forest being the most likely plant community.

In archeological records, charcoal from *Prunus* can be abundant, whereas *Prunus* pollen is mostly absent from palynological records due to the entomophilous character of its pollen. The same occurs for most of the significant taxa in the charcoal record from Unit II, which are generally absent in pollen records (Connor et al. 2004; Van Zeist and Bottema 2009; Joannin et al. 2010). *Prunus*, and Maloideae pollen dispersal is entomophilous and *Acer* has a low pollen production, and therefore they are usually very poorly represented or totally absent in pollen records. Other genera such as *Euonymus* or *Lonicera* are rarely identified from palynological assemblages, but they are present in charcoal record. In contrast, firewood gathering is likely to target the closest environment to the cave, and preference of the wood that is most abundant and available could cause a high significance of those taxa. The absence of these taxa in most of the pollen records might hide some local plants and their characterization.

New data from travertine deposits with leaf imprints from Pleistocene deposits in the Lesser Caucasus have yielded evidence of specific taxa, providing new light on paleoflora (Ollivier et al. 2010). This study shows the presence of a high diversity of taxa including *Prunus*, *Cerasus avium*, from the *Prunus* genus; *Crataegus*, *Malus*, *Pyrus,* and *Sorbus* from the Maloideae group and a high diversity of species from the *Acer* genus (Ollivier et al. 2010). This would confirm the importance and variability of these taxa during the early stages of the Pleistocene, giving more importance to woody plants. However, pollen data from the same sequence suggest the importance of steppe environments and suggesting in turn a cold climate (Joannin et al. 2010).

The charcoal assemblage at Azokh shows a plant record characterized by trees and shrubs growing probably in an open or semi-open environment. The presence of low values of *Quercus* and *Carpinus* and high values of other mesophilous smaller trees could indicate early stages in the spread of a forest. This vegetation type has no equivalent in the area at present, and it indicates broad-leaved forest of secondary or understory trees and shrubs. This plant community could be a pioneer succession, which based on the *Prunus* types would seem to indicate more or less humid environmental conditions. In this sense, we suggest that a climatic model signifying a recovery of the oak forest formation could be valid for Azokh's record. However, the lack of a continuous anthracological sequence does not let us have an overview of its evolution.

The former paleobotanical studies from this site, based on palynology, show the evolution and transformation of vegetal formation from earlier Pleistocene phases. The pollen record (Zelikson and Gubonina 1985; Djafarov 1999) shows different phases; corresponding to the preacheulian and acheulian layers (Zelikson and Gubonina 1985). Unit II postdates these phases and the pollen spectra show layers with an arboreal pollen spectra dominated by taxa such as *Alnus*, *Fraxinus*, *Betula*, *Ostrya*, *Carpinus,* and *Quercus,* which show fluctuations on their values. According to these authors the vegetation corresponds mainly to a forest environment that changed according to variations in humidity and aridity from low mountain forests to high altitude forests or subalpine. Nevertheless, these data should be taken carefully into account and maintained on hold until new data are available (see Scott et al. 2016).

In summary, the charcoal record from Azokh cave shows a plant community with *Prunus*, *Acer*, Maloideae among other trees and shrubs. The different taxa recorded were probably abundant in the landscape close to the cave and characterized by the dominance of plum trees together with other mesophilous taxa that were exploited for firewood. In contrast, palynological sequences from the nearest area show different forest formation dominated mainly by broad-leaved or coniferous trees according to different forest successions or more open a steppe like landscapes (Bennet et al. 1991; Denk et al. 2001; Willis and Van Andel 2004; Roucoux et al. 2008; Djamali et al. 2008; Joannin et al. 2010). These differences are probably due to the different scales in the approach of the different disciplines. In addition, evidence from the vertebrate fauna shows the presence of both broad-leaved forest and steppe environments, but the evidence for the latter is derived from small mammals,

amphibians, and reptiles that have been shown to be predator accumulations derived from species of owls that preferentially hunt over open areas (Andrews et al. 2016). Since the hunting ranges of these predators span several kilometers, it has been suggested that the steppe vegetation from which their prey came could have been some distance from the cave, while the large mammals, which indicate woodland vegetation, came from environments closer to the cave. Thus, the importance of using different approaches would provide a wider range of data in order to understand specific aspects on plant formation and plant uses among early populations. With this study, on the basis of charcoal analyses, we have obtained data based on human choices, the local vegetation, woody species, whereas pollen reflects the natural environment, regional vegetation, herbaceous and wood species, and high pollinating species. It is in fact the use of a multidisciplinary approach that will lead us to a larger comprehension of the vegetal cover.

The plant formation described above was, in short, the source for vegetal raw materials gathered by hunter-gatherers, which is characterizing their subsistence strategies. Food, tool manufacturing and firewood were probably the main objectives for wood gathering. However, we consider that these charcoal specimens were the product of combustion activities during occupation of the site; therefore they are basically related to the exploitation of firewood.

Hunter-gatherers based their exploitation for fuel on different facts such as availability and abundance of the wood in the environment, functionality and duration of the occupation, energy expenses, type of firewood (tree, shrubs, branches, trunks), and supply and type of socioeconomic organization (Théry-Parisot 2001; Allué and Garcia-Antón 2006). Despite this range of options, it is usually suggested that random wood gathering was the most common strategy (Shackelton and Prins 1992; Asouti 2003). There is an ecological conditioning which implies the use of the available species, but there is a preference for the closest trees available and those that produce the greatest amount of dead wood. The needs for fuel in short term occupations do not presuppose in any case the cutting of trees but the gathering of dead branches from the trees or from the ground. Furthermore, the strategy for firewood gathering among hunter-gatherers would not suppose intensive exploitation causing damage to a plant formation. The notable difference between *Prunus* (80%) and the rest of the taxa, suggest that there probably was a preference in wood gathering. This could be related first of the abundance in the environment described earlier in this text, and it also corresponds to the collection of the most available wood according to dead wood production.

Conclusions

1. The charcoal record from Azokh cave shows a plant community with *Prunus*, *Acer*, Maloideae among other trees and shrubs.
2. The different taxa recorded were probably abundant in the landscape close to the cave and characterized by the dominance of plum trees (80% of the sample) together with other mesophilous taxa that were exploited for firewood.
3. From the study of charcoal from Unit II and Unit Vu in Azokh 1 cave, we have contributed to the understanding of local vegetal type. The record shows highly variable spectra suggesting an open or semi-open landscape formed mainly by woody trees and shrubs.
4. The vegetal formation, dominated by pioneer species, would develop toward broad-leaved forests.
5. It is also proposed that firewood gathering based on collecting the most abundant and available species from the nearby area contributed to the plant assemblage.
6. The sequences considering earlier periods from the Lower and Middle Pleistocene from the Caucasus are very few and new contributions are essential for the comprehension of past environments and human interactions.

Acknowledgments I would like to thank Yolanda Fernández-Jalvo, Peter Andrews, and three anonymous reviewers for their comments that have helped to improve this paper. I would also like to thank Lena Asryan, Isabel Cáceres, and Norah Moloney for the helpful comments and discussions on this research during the past years.

References

Allué, E. (2004). *Report on the analyses of 15 charcoal samples from Ortvale Klde (Georgia, Caucasus)*. Tarragona: Area de Prehistòria. Universitat Rovira i Virgili.

Allué, E. (2006). Análisis antracológico. Una disciplina arqueobotánica para el conocimiento del paisaje vegetal y la explotación de los recursos forestales. In *Actas del I Congreso de Analíticas aplicadas a la arqueología* (pp. 195–218). Igualada: ArqueoCat sl.

Allué, E., & García Antón, D. (2006). La transformación de un recurso biótico en abiótico: Aspectos teóricos sobre la explotación del combustible leñoso en la prehistoria. In G. A. Martínez Fernández, M. Rodríguez & J. A. Afonso Marrero (Eds.), *Sociedades prehistóricas, recursos abióticos y territorio. III Reunión de Trabajo sobre Aprovisionamiento de Recursos Abióticos en la Prehistoria* (pp. 19–31). Loja: Fundación Ibn al-Jatib de estudios de Cooperación cultural.

Allué, E., Nadal, J., Estrada, A., & García-Argüelles, P. (2007). Los datos antracológicos de la Balma del Gai (Bages, Barcelona): Una aportación al conocimiento de la vegetación y la explotación de los recursos forestales durante el Tardiglaciar en el NE peninsular. *Trabajos de Prehistoria, 64*, 87–97.

Andrews, P., Hixson Andrews, S., King, T., Fernández-Jalvo, Y., & Nieto-Díaz, M. (2016). Palaeoecology of Azokh 1. In Y. Fernández-Jalvo, T. King, L. Yepiskoposyan & P. Andrews (Eds.), *Azokh Cave and the Transcaucasian Corridor* (pp. 305–320). Dordrecht: Springer.

Appendix: Fernández-Jalvo, Y., Ditchfield, P., Grün, R., Lees, W., Aubert, M., Torres, T., et al. (2016). Dating methods applied to Azokh Cave sites (Appendix). In Y. Fernández-Jalvo, T. King, L. Yepiskoposyan & P. Andrews (Eds.), *Azokh Cave and the Transcaucasian Corridor* (pp. 321–339). Dordrecht: Springer.

Asouti, E. (2003). Woodland vegetation and fuel exploitation at the prehistoric campsite of pınarbası, south-central Anatolia, Turkey: The evidence from the wood charcoal macro-remains. *Journal of Archaeological Science, 30*, 1185–1201.

Asouti, E., & Austin, P. (2005). Woodland vegetation and its exploitation by past societies, based on the analysis and interpretation of archaeological wood charcoal macro-remains. *Environmental Archaeology, 10*, 1–18.

Badal, E., Carrión, Y., Grau, E., Macías, M., & Ntinou, M. (Eds.). (2011). 5th international meeting of Charcoal analysis. *The charcoal as cultural and biological heritage*. Valencia, Spain, September 5th–9th 2011. *Saguntum, extra*, 11.

Bennet, K. D., Tzedakis, P. C., & Willis, K. S. (1991). Quaternary refugia of north European trees. *Journal of Biogeography, 18*, 103–115.

Benkova, V., & Schweingruber, F. H. (2004). *Russian wood anatomy*. Bern: Paul Haupt.

Chabal, L., Fabre, L., Terral, J. F., & Théry-Parisot, I. (1999). L'anthracologie. In A Ferdière (Ed.), *La Botanique* (pp. 43–104). Paris, Errance.

Connor, S. E., Thomas, I., Kvavadze, E. V., Arabuli, G. J., Avakov, G. S., & Sagona, A. (2004). A survey of modern pollen and vegetation along an altitudinal transect in southern Georgia, Caucasus region. *Review of Palaeobotany and Palynology, 129*, 229–250.

Damblon, F., & Court-Picon, M. (Eds.). (2008). *4th International Meeting of Anthracology; Charcoal and Microcharcoal; Continental and Marine records*. Abstracts. Brussels: Geological Survey of Belgium Professional Paper No. 303.

Denk, T., Frotzler, N., & Davitashvil, N. (2001). Vegetational patterns and distribution of relict taxa in humid temperate forests and wetlands of Georgia (Transcaucasia). *Biological Journal of the Linnean Society, 72*, 287–332.

Díez, F., Martínez, K., García, J., Gómez, A., Cáceres, I., Allué, E., et al. (2009). El Paleolítico medio en el Cáucaso meridional: la Cueva Doble (Valle de Tsutskhvati, República de Georgia). *Zephyrus: Revista de prehistoria y arqueología, 63*, 15–44.

Djafarov, A. G. (1999). *Crednuu maleolit atserbaudxana*. (In Russian: Middle Paleolithic from Azerbaian). Institut of archaeology and Ethnography. Baku: Akadeny nauk Azerbaian republic.

Djamali, M., de Beaulieu, J.-L., Shah-Hosseini, M., Andrieu-Ponel, V., Amini, A., Akhani, H., et al. (2008). A late Pleistocene long pollen record from Lake Urmia, NW Iran. *Quaternary Research, 69*, 413–420.

Emery-Barbier, A., & Thiebault, S. (2005). Preliminary conclusions on the Late Glacial vegetation in south-west Anatolia (Turkey): The complementary nature of palynological and anthracological approaches. *Journal of Archaeological Science, 32*, 1232–1251.

Fahn, A., Werker, E., & Baas, P. (1986). *Wood anatomy and identification of trees and shrubs from Israel and adjacent regions*. Jerusalem: The Israel Academy of Sciences and Humanities.

Fernández-Jalvo, Y., King, T., Andrews, P., & Yepiskoposyan, L. (2016). Introduction: Azokh Cave and the Transcaucasian Corridor. In Y. Fernández-Jalvo, T. King, L. Yepiskoposyan & P. Andrews (Eds.), *Azokh Cave and the Transcaucasian Corridor* (pp. 1–26). Dordrecht: Springer.

Fiorentino, G., & Magri, D. (2008). *Charcoals from the past: Cultural and palaeoenvironmental implications*. Proceedings of the Third International Meeting of Anthracology. Oxford: British Archaeological Reports 1807.

Figueiral, I., & Mosbrugger, V. (2000). A review of charcoal analysis as a tool for assessing Quaternary and Tertiary environments: Achievements and limits. *Palaeogeography, Palaeoclimatology, Palaeoecology, 164*, 397–407.

Gabrielian, E., & Fragman-Sapir, O. (2008). *Flowers of the Transcaucasus and Adjacent Areas, including Armenia, Eastern Turkey, Southern Georgia, Azerbaidjan and Northern Iran*. Germany: Gartner verlag, Institute of Botany Academy of Sciences of Armenia.

Gabrielian, I. G., & Gasparyan, B. Z. (2003). The condition of habitation of early man in the Canyon of the Vorotan River by paleontological data. (in Russian) In *International Science Conference of Archaeology, Ethnology and Folklore of Caucasus* (pp. 23–29). Yerevan.

Gabrielyan, I., & Kovar-Eder, J. (2011). The genus Acer from the lower/middle Pleistocene Sisian Formation, Syunik region, South Armenia. *Review of Palaeobotany and Palynology, 165*(3–4), 111–134.

Gabunia, L., Vekua, A., & Lordkipanidze, D. (2000). The environmental contexts of early human occupation of Georgia (Transcaucasia). *Journal of Human Evolution, 38*(6), 785–802.

Golovanova, L. V., & Doronichev, V. B. (2003). The Middle Paleolithic of the Caucasus. *Journal of World Prehistory, 17*, 71–140.

Ghukasyan, R., Colonge, D., Nahapetyan, S., Ollivier, V., Gasparyan, B., Monchot, H., & Chataigner, C. (2010). Kalavan-2 (north of lake Sevan, Armenia): A new late middle Paleolithic site in the Lesser Caucasus. *Archaeology, Ethnology and Anthropology of Eurasia, 38*, 39–51.

Hastorf, C. A., & Popper, V. S. (1988). *Current Paleoethnobotany. Analytical methods and cultural interpretations of archaeological plant remains*. Chicago: The University of Chicago Press.

Heinz, C. (1990). Dynamique des végétations holocénes en mediterrannée nord-occidentale d'après l'anthracoanalyse de sites préhistoriques methodologie and paleoécologie. *Paleobiologie Continentale, XVI*, 1–212.

Heinz, C., & Barbaza, M. (1998). Environmental changes during the Late Glacial and Post-Glacial in the central Pyrenees (France): New charcoal analysis and archaeological data. *Review of Palaeobotany and Palynology, 104*, 1–17.

Hovsepyan, R., & Willcox, G. (2008). The earliest finds of cultivated plants in Armenia: Evidence from charred remains and crop processing residues in pise from the Neolithic settlements of Aratashen and Aknashen. *Vegetation History and Archaeobotany, 17*, 63–71.

InsideWood. (2004). *Published on the Internet*. http://insidewood.lib.ncsu.edu/search (2008).

Joannin, S., Cornée, J., Münch, P., Fornari, M., Vasiliev, I., Krijgsman, W., et al. (2010). Early Pleistocene climate cycles in continental deposits of the Lesser Caucasus of Armenia inferred from palynology, magnetostratigraphy, and 40Ar/39Ar dating. *Earth and Planetary Science Letters, 291*, 149–158.

Kvavadze, E. V., & Connor, S. E. (2005). *Zelkova carpinifolia* (Pallas) K. Koch in Holocene sediments of Georgia–an indicator of climatic optima. *Review of Palaeobotany and Palynology, 133*, 69–89.

Lioubine, V. P. (2002). *L'acheuléen du caucase*. Études et Recherches Archéologiques de l'Université de Liège Liège: Eraul 93.

Lisitsina, G. N., & Prischepenko, L. V. (1977). Palaeoethnobotanickeskie Nachodki Kavkaza i Blizhevo Vostoka Izdatelstvo Nauka, Moscow. (in Russian species names in latin. Book review in Nandris J., 1977) *Journal of Archaeological Science, 4*, 296.

Marin-Monfort, M. D., Caceres, I., Andrews, P., Pinto, A. C., & Fernández-Jalvo, Y. (2016). Taphonomy and Site Formation of Azokh 1. In Y. Fernández-Jalvo, T. King, L. Yepiskoposyan & P. Andrews (Eds.), *Azokh Cave and the Transcaucasian Corridor* (pp. 211–249). Dordrecht: Springer.

Martinoli, D., & Jacomet, S. (2004). Identifying endocarp remains and exploring their use at Epipalaeolithic Öküzini in Southwest Anatolia, Turkey. *Vegetation History and Archaeobotany, 13*, 45–54.

Messager, E., Lordkipanidze, D., Ferring, C. R., & Deniaux, B. (2008). Fossil fruit identification by SEM investigations, a tool for palaeoenvironmental reconstruction of Dmanisi site, Georgia. *Journal of Archaeological Science, 35*, 2715–2725.

Moreno-Sánchez, R., & Sayadyan, H. Y. (2005). Evolution of the Forest Cover in Armenia. *International Forestry Review, 7*, 2005.

Ntinou, M. (2002). La Paleovegetación en el Norte de Grecia desde el Tardiglaciar hasta el Atlántico. Formaciones Vegetales, Recursos y Usos. British Archaeological Reports (International Series 1083) Oxford: Archaeopress.

Ollivier, V., Nahapetyan, S., Roiron, P., Gabrielyan, I., Gasparyan, B., Chataigner, C., et al. (2010) Quaternary volcano-lacustrine patterns and palaeobotanical data in southern Armenia. *Quaternary International, 223–224*, 312–326.

Roucoux, K. H., Tzedakis, P. C., Frogley, M. R., Lawson, I. T., & Preece, R. C. (2008). Vegetation history of the marine isotope stage 7 interglacial complex at Ioannina, NW Greece. *Quaternary Science Reviews, 27*, 1378–1395.

Royal Botanic Garden Edinburgh. (1998). *Flora Europaea*, http://rbg-web2.rbge.org.uk/FE/fe.html. Accessed 2009.

Shackleton, C. M., & Prins, F. (1992). Charcoal analysis and the "Principle of least effort": A conceptual model. *Journal of Archaeological Science, 19*, 631–637.

Shatilova, I. I. (1990). Rastitelnost i klimat Zapadnoi Gruzii v pozdnepleistotsenovoe vremya (Plants and climate of Western Georgia in the Upper Pleistocene time). In D. Tushabramishvili (Ed.), *Paleolit Kavkaza i sopredel'nikh territoriy* (pp. 109–111). Tbilisi, GA: Metsniereba.

Schweingruber, F. H. (1990). *Anatomie europäischer Hölzer ein Atlas zur Bestimmung europäischer Baum-, Strauch- und Zwergstrauchhölzer Anatomy of European woods an atlas for the identification of European trees shrubs and dwarf shrubs*. Stuttgart: Verlag Paul Haupt.

Schweingruber, F., & Landolt, W. (2005). http://www.wsl.ch/dendro/xylemdb/index.phpl. Swiss Federal Research Institute WSL last update 2.4.2008.

Scott, L., Rossow, L., Cordova, C., & Risberg, J. (2016). Palaeoenvironmental Context of Coprolites and Plant Microfossils from Unit II. Azokh 1. In Y. Fernández-Jalvo, T. King, L. Yepiskoposyan & P. Andrews (Eds.), *Azokh Cave and the Transcaucasian Corridor* (pp. 287–295). Dordrecht: Springer.

Théry-Parisot, I. (2001). *Économie des combustibles au Paléolithique*. Dossier de Documentation Archéologique 20 Paris: CNRS.

Théry-Parisot, I., Costamagno, S., & Auréade, H. (2009). *Gestion des combustibles au paléolithique et au mésolithique*. BAR International Series vol. 1914. London.

Théry-Parisot, I., Chabal, L., & Chrzavzez, J. (2010). Anthracology and taphonomy, from wood gathering to charcoal analysis. A review of the taphonomic processes modifying charcoal assemblages, in archaeological contexts. *Palaeogeography, Palaeoclimatology, Palaeoecology, 291*, 142–153.

Thiébault, S. (Ed.). (2002). *Charcoal Analysis. Methodological Approaches, Palaeoecological Results and Wood Uses.* Oxford: British Archaeological Reports 1063.

Tumajanov, I. I. (1971). Changes in the Great Caucasus forest vegetation during the Pleistocene and Holocene. In P. H. Davis, P. C. Harper & I. C. Hedge (Eds.), *Plant Life of South-West Asia* (pp. 73–87). Edinburgh: Botanical Society of Edinburgh.

Van Zeist, W., & Bottema, S. (2009). A palynological study of the Acheulian site of Gesher Benot Ya'aqov, Israel. *Vegetation History and Archaeobotany, 18*, 105–121.

Vernet, J. L. (1973). Étude sur l'historie de la végétation du sud-est de la France au Quaternaire, d'après les charbons de bois principalement. *Paléobiologie Continentale, IV*, 1–90.

Vernet, J. L. (1997). *L'homme et la forêt méditerranéenne de la Préhistoire à nos jours*. Paris: Errance.

Vernet, J. L. (Ed.), (1992). *Les charbons de bois, les anciens écosystèmes et le rôle de l'homme.* Actes du colloque, Montpellier. Paris: Bulletin de la Société Botanique de France 139.

Von Klopotovskaja, N., Kvavadze, E., & Lordkipanidze, D. (1989). *Vorläufige Mittelilung zur Paläobotanik. Jarhbuch RGZM, 39*, 92.

Western, C. A. (1971). The ecological interpretation of ancient charcoals from Jericho. Levant. *British School of Archaeology in Jerusalem III*, 31–40.

Willis, K. J., & Van Andel, T. H. (2004). Trees or no trees? The environment of central and eastern Europe during the Las Glaciation. *Quaternary Science Reviews, 23*, 2369–2387.

Zelikson, E. M., & Gubonina, Z. P. (1985). A displacement of altitude zonality as a basis for reconstruction of cli-matic changes in mountain states. (in Russian) In A. A. Belichko, L. P. Serebrannii, & E. E. Gurtobaia (Eds.), *Methods of climate reconstruction* (pp. 37–45). Moscow: Nauka Akademia nauk ccpp.

Zohary, D., & Hopf, M. (2000). *Domestication of plants in the Old World*. Oxford: Oxford University Press.

Chapter 15
Paleoecology of Azokh 1

Peter Andrews, Sylvia Hixson Andrews, Tania King, Yolanda Fernández-Jalvo, and Manuel Nieto-Díaz

Abstract The fauna and flora from Azokh 1 are analyzed to provide evidence on past and present environments. The large mammal fauna was accumulated by carnivore and human agents, and it is dominated by woodland species. The small mammals, amphibians and reptiles were accumulated mainly by avian predators, barn owls and eagle owls which hunt over open areas, and their prey may have been brought to the cave from some distance away. The amphibians and reptiles indicate warm dry conditions, with some taxa specific to mountainous regions and many indicating warm arid conditions. The small mammals similarly indicate mainly arid environments with minor elements from deciduous woodland. The difference between small vertebrates and large mammals is taphonomic, and all four groups indicate slight transition to more arid conditions up the section. Bats are present in all units, and it appears likely that they are derived from natural deaths within the cave. They indicate woodland conditions low in the section changing to a treeless, arid and cold environment towards the top. Plant data from charcoal indicate that the regional vegetation was broadleaved deciduous woodland with mainly small trees and shrubs. The location of the cave on the lower slopes of the mountains of the Lesser Caucasus is close to the forest/steppe boundary, with forest on the mountain slopes and steppe on the lowlands to the east, and relatively minor fluctuations in climate would shift the boundary or and down slope, towards or away from the cave, with changes in climate. It is concluded, therefore, that the large mammals and flora represent the local woodland environment, and the small mammals, reptiles and amphibians represent prey species brought from further away.

Резюме Материал по фауне и флоре из пещеры *Азох 1* проанализирован с целью получения предметных свидетельств о древней и современной экологии стоянки. В сегодняшней экофлоре окрестностей Азоха доминируют граб, дуб и ясень, которые встречаются на склонах горы, где расположена пещера; степной ландшафт находится ниже к востоку и не ближе 4–5 км к пещере. Локализация пещеры близко к краю гор Малого Кавказа указывает на то, что незначительные изменения климата могли повлиять на границу между лесом и степью по направлению к пещере или от нее.

Исследованы пять стратиграфических единиц – от подразделения *V* у основания седиментной последовательности, возрастом не более 200 тыс. лет, до недавних отложений голоцена в подразделении *I*, возрастом около 12 тыс. лет. Распределение мелких млекопитающих в отложениях *Азох 1* отличается от такового у крупных млекопитающих, указывая на различные тафономические траектории. Фауна крупных млекопитающих свидетельствует о присутствии хищников и человека; мелкие формы – земноводные и рептилии, имеющие сходное распределение в пяти стратиграфических слоях, – привнесены в пещеру главным образом хищными птицами. Фаунальные данные по земноводным и рептилиям указывают на преобладание теплых сухих условий с параллельным присутствием некоторых таксонов, специфичных для горных регионов и свидетельствующих о теплом аридном климате с небольшой тенденцией к более засушливой среде

P. Andrews (✉)
Natural History Museum, Cromwell Road, London, SW7 5BD, UK
e-mail: pjandrews@uwclub.net

S.H. Andrews · T. King
Blandford Museum, Bere's Yard, Blandford, Dorset DT11 7AZ, UK
e-mail: s.hixsonandrews@uwclub.net

T. King
e-mail: taniacking@gmail.com

Y. Fernández-Jalvo
Museo Nacional de Ciencias Naturales (CSIC). José Gutiérrez Abascal 2, 28006 Madrid, Spain
e-mail: yfj@mncn.csic.es

M. Nieto-Díaz
Molecular Neuroprotection Laboratory, Hospital Nacional de Parapléjicos (SESCAM), 45071 Toledo, Spain
e-mail: mnietod@sescam.jccm.es

Yolanda Fernández-Jalvo et al. (eds.), *Azokh Cave and the Transcaucasian Corridor*, Vertebrate Paleobiology and Paleoanthropology, DOI 10.1007/978-3-319-24924-7_15

на поверхности отложений. Присутствие мелких млекопитающих также указывает на преимущественно степную экологию с редкой растительностью из лиственных деревьев. Максимальная плотность лесной растительности зарегистрирована в основании подразделения *V*, с постепенным повышением аридности по направлению к ее вершине. Останки крупных млекопитающих, напротив, свидетельствуют о смешении преимущественно лиственных лесов с незначительным компонентом из аридных и степных элементов; кроме того, обнаружены признаки большей аридности на вершине подразделения. Данные, полученные из фрагментов древесного угля, показывают, что растительность в окрестностях пещеры была представлена широколиственными формами – главным образом низкорослыми деревьями и кустарниками. Различия между экологическими сигналами от крупных млекопитающих и других источников информации объясняются тафономически; по общему мнению, пещера была расположена близко к границе лес/степь в течение всего рассмат-
риваемого периода, а сама граница поднималась вверх и опускалась вниз вместе с изменением климата.

Keywords Taphonomy • Armenia • Nagorno-Karabakh • Ordination • Fossil fauna • Fossil flora • Hominins

Introduction

The flora and fauna from Azokh 1 are investigated to reconstruct the paleoecology of the region during the middle to late Pleistocene. Sources of evidence for the reconstructions presented here draw on the following chapters in this volume: Chap. 6, large mammals by Van der Made et al.; Chap. 7, small mammals by Parfitt; Chap. 8, bats by Sevilla; Chap. 9, amphibians and reptiles by Blain; Chap. 13, phytoliths by Scott et al.; Chap. 14, charcoal by Allué. In addition, Chap. 10 on large mammal taphonomy (Marin-Monfort et al. 2016) is complemented in the present chapter with observations on small mammal taphonomy, both prerequisites for interpreting paleoecology.

Azokh Cave is situated in Nagorno-Karabakh, at 850 m asl, and about 200 m above the nearby village of Azokh. It is situated is on the edge of the mountains, opening into a broad river valley (Ishxanaget River) sheltered by the mountains of the Lesser Caucasus to the north and west. Drainage at the present time is to the south and east, and evidence of the cave formation indicates this was the case in the past (see Fig. 3 in Fernández-Jalvo et al. 2004, 2010). It is close to the transition from broadleaved forest on the mountain slopes (to the west) to arid steppe on the low-lying land to the east.

The biota is analyzed by stratigraphic unit (Murray et al. 2016; Domínguez-Alonso 2016), and the five sedimentary units are briefly summarized here. All units have produced mammal fossils and almost all also have evidence of human occupation. The most abundant mammals are *Ursus spelaeus* and up to 13 species of bats. Cervids and bovids are also relatively abundant, with several species of carnivore, including large felids and canids. There are at least 20 species of rodent and four lagomorph species, and the reptile and amphibian fauna includes three anurans, at least four lizards and seven snakes. Some species are present in all units, such as the cave bear, and many are present in several units, while others occur in only one, such as bison in Unit II; rhinoceros (*Stephanorhinus*) and badger in Unit Vu; and wolf, jackal, hyaena, *Megaloceros* and roe deer in Unit Vm. The taxonomy of the fauna and flora is described in other chapters of this volume, and the species lists from these chapters are summarized at the end of this chapter.

The stratigraphic sequence at Azokh 1 is as follows: (Murray et al. 2010, 2016):

- Unit Vm is the lowest part of the fossiliferous section excavated so far. It is a reddish-brown clay loam unit in which the partial mandible of Middle Pleistocene hominin was found (Kasimova 2001). *Ursus spelaeus* is common in this unit as is *Cervus elaphus*. Stone tools are present (Asryan et al. 2016).
- Unit Vu rests conformably on Unit Vm; it is a friable medium greyish-brown calcareous clay. Fossil remains include *Ursus spelaeus* and herbivore fossils (Van der Made et al. 2016) bearing cut marks related to human butchery (Marin-Monfort et al. 2016). The small mammal fauna is by far the largest in the Azokh 1 sequence.
- Unit IV has not yet been excavated, but it appears to contain lithics and mammal fossils, including cave bears.
- Unit III is a medium tan-brown clay. Fossil remains of mainly cave bears are abundant together with Mousterian stone tools.
- Unit II is a reddish-brown sandy loam, but it has been strongly diagenetically altered in the center of the passageway by accumulations of bat guano, and this has affected preservation of fossil bones. Next to the cave walls, neither the sediment nor the fossils have been altered and both have characteristic dark red-brown color. Fossils include mainly cave bears, some with cut marks. Stone tools of Levallois technology (Asryan et al. 2016) are present.
- The top of Unit II has an erosional disconformity obscuring the transition to Unit I, which is a 1.35–1.5 m thick, reddish-brown friable to loose clay.

Almost all units show evidence of human activity: hearths in the upper level, stone tools and cut marked bones in all levels. Faunal remains associated with human activity consist mainly of low meat- and marrow-bearing elements, including numerous fibulae, hand and foot bones, mostly complete. This pattern suggests that those bones that were not worth

transporting due to low nutritional content were abandoned in the cave (Marin-Monfort et al. 2016). In Unit II this pattern slightly changes. This unit yields complete large limb bones of bears usually found close to the cave walls; these bones would have been highly rich in marrow, and they are found together with highly broken bones and stone tools. This pattern suggests that some of the bones may derive from hibernation deaths and were not eaten, perhaps because of advanced decay. In contrast, Unit Vm shows bear and herbivores bones, as well as stone tools, scattered and dispersed, suggesting no clear pattern of occupation.

Materials and Methods

The fossil material is housed in the Stepanakert Museum. All identifications have been accepted without change from the other chapters in this volume, and the method of analysis adopted here is based on their taxonomic identifications. In some cases, the species present in the faunas and floras are extant, and direct comparison can be made with the environments where these taxa occur today. In the case of the mammals, some are extant and some extinct, and the faunal analysis of the fossil faunas uses the Taxonomic Habitat Index (THI) derived from weighted averages ordination of living species (Gauch 1989; Andrews 1990). The Taxonomic Habitat Index, as its name implies, is based on data that are primarily taxonomic, for the fossil material is not complete enough to employ methods such as ecomorphology (Kappelman 1988). Bats, amphibians and reptiles were not available for taphonomic analysis, and these also are not included in these analyses.

Habitat Weightings

Taxonomic lists of species are ordinated by weighted averages, a simple ordination technique (Whittaker 1948; Rowe 1956; Gauch 1989). It is designed to produce additive ordination scores based on previous knowledge of species from known habitats. The ordination scores for each habitat type investigated are based on the sums of the habitat weightings of the constituent species for each habitat (Gauch 1989) using an ecological scale based on the range of habitat preferences of each species. A seven habitat system is used here based in part on climate, in part on degree and type of vegetation cover and in part on altitude. There is some redundancy in this system, and for the purposes of the Azokh 1 paleoecological analysis some comparisons will be limited to three or four of the categories. The seven habitat types are as follows:

- Tundra – Characteristics of tundra include: extremely cold climate, low biotic diversity, simple vegetation structure, poor drainage, short season of growth, large population oscillations. Trees are absent or are low growing in protected areas.
- Boreal forest – Characteristics of boreal forest include very low temperatures, precipitation is primarily in the form of snow, cold dry winters and moist warm summers, the soil is thin, nutrient-poor, and acidic, trees mainly conifers, tree canopies may be dense so that ground cover is limited, and the flora consists mostly of cold-tolerant evergreen conifers with needle-like leaves, such as pine, fir, and spruce.
- Deciduous forest – Characteristics of temperate deciduous forest include moderate but variable temperature varying from –30 to 30 °C, precipitation is distributed evenly throughout the year, the soil is fertile, enriched with decaying litter, the tree canopy is moderately dense and allows light to penetrate, resulting in well-developed and richly diversified understory vegetation and stratification of animals, and the flora is characterized by 3–4 tree species per km^2. Trees are distinguished by broad leaves that are lost annually and include such species as oak, hornbeam, beech, hemlock, maple, basswood, cottonwood, elm, willow, and spring-flowering herbs.
- Mediterranean forest – Characteristics include hot dry summers and cool wet winters, the soil is less fertile as leaf litter is limited, and many of the tree and shrub species have sclerophyllous adaptations in which the leaves of the trees and shrubs are hard, thick, leathery, evergreen and usually small. These adaptations allow the plants to survive the pronounced hot, dry season.
- Steppe – Characteristics include dry areas of grassland with hot summers and cold winters, plants are usually greater than 30 cm tall, the soil is deep and dark, with fertile upper layers. It is nutrient-rich from the growth and decay of deep, many-branched grass roots. The rotted roots hold the soil together and provide a food source for living plants.
- Arid or semi-arid – Characteristics include low rainfall and extreme variations in temperature, soil ranges from sandy and fine-textured to loose rock fragments, gravel or sand, may develop caliche hardpans, vegetation with limited diversity of trees and shrubs, deciduous and often protected by thorns, ground vegetation sparse and dominated by annuals.

The full geographical range of each of the mammal species, taking into account seasonal variations, is assessed and is weighted according to the estimated importance of the above habitats to individual species across its species range and taking account of seasonal variation. For example, a species

living mainly in boreal forest but ranging into tundra during the summer and into deciduous forest during winter, would be weighted as follows: boreal 0.6, tundra 0.3, deciduous forest 0.1. The weighting is both the most important aspect of this method, and it's most controversial, for there is limited information on habitat ranges for many mammal species. After each species is given its weighting, the habitat scores for all species present in a unit can then be added together, and when divided by the number of species it gives an average weighted score for each habitat for that faunal unit.

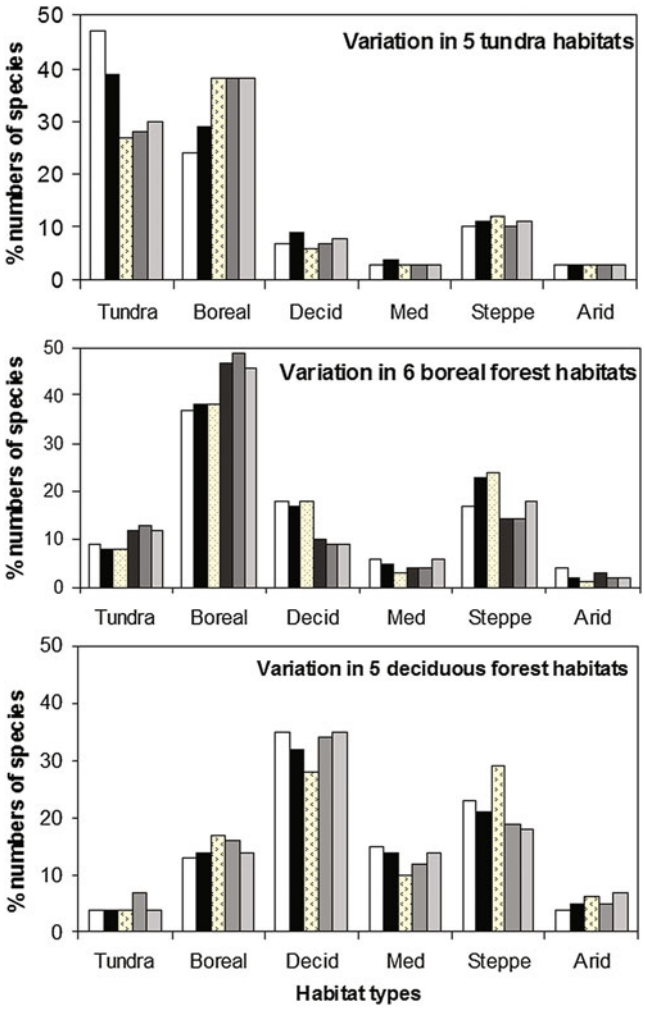

Fig. 15.1 Weighted average scores for modern temperate faunas (excluding bats). Top, average scores for five tundra faunas are shown as differently shaded bars for each locality. The five faunas are clustered as tundra and boreal forest, the two habitats which share many mammal species and between which there is considerable movement seasonally; middle, average scores for six boreal forest faunas, which show that large parts of the boreal faunas are restricted to this biome; and where there is movement across biomes it is into deciduous forest and steppe rather than tundra; bottom, average scores for five deciduous woodland faunas, which show highest numbers in deciduous woodland (Decid) and overlap in mammal distributions with Mediterranean woodlands (Med) and steppe and to a lesser extent with boreal forest. The locations of all 16 recent faunas are given in Andrews (2006)

To illustrate the degree of variation of the ordination scores for modern faunas of known habitat, Fig. 15.1 shows results from the analysis of 16 recent faunas from three ecological zones, the tundra biome, boreal forest biome and the temperate deciduous woodland biome (Andrews 2006). These 16 faunas show variations in habitat within each of the three biozones, and they were based on well documented habitats compiled from the literature (references in Andrews 2006). The tundra biome index (converted here into percentages) has high values for both tundra and boreal forest, for few mammals can subsist exclusively in tundra habitats. By contrast, the boreal forest faunas are dominated by boreal forest ordination values, with lower values for tundra, deciduous woodland and steppe environments. Similarly, the deciduous woodland faunas are dominated by deciduous woodland ordination values but with some boreal forest and steppe representation.

Calculation of Taxonomic Habitat Index (THI)

Extant species present in a fossil fauna can be assigned the habitat weighting of their living counterparts and their habitat ranges ordinated as described above. Where fossil species are extinct, however, their habitat preferences are unknown. If we can attribute the fossil species to an extant genus, the habitat weighting for all living species in that genus can be averaged to produce a genus score which can then be applied to any extinct species of that genus. This is the basis for calculation of THI scores (Evans et al. 1981), and this is what is done intuitively when habitats are assigned to extinct "indicator species", but in the present analysis the assignment is quantified by calculating average scores for all extant species in particular genera. It will obviously be less precise than the species scores, but since species in the same genus tend to occupy similar ranges of habitats, there is still useful information in the genus scores.

This principle can be extended to higher taxonomic levels, for example by averaging species scores in tribes or subfamilies, while still retaining some useful ecological information for some habitats. Calculation of the THI thus entails the taxonomic averaging of habitat scores based on the nearest identified taxonomic level for fossil species.

Faunal Bias

In addition to the fact that fossil faunas are largely composed of animals with unknown habitat preferences, most if not all fossil faunas have been subjected to processes which alter

their taxonomic composition. These may reduce the numbers of species from those present in the source areas, usually as a result of taphonomic bias, or species numbers may be augmented if the faunas are derived from different or complex habitats or again as a result of taphonomic bias (Brain 1981; Andrews 1990; Lyman 1994, and references therein).

Results

Taxonomic Composition of the Azokh Faunas

The bat faunas from Azokh 1 are described by Sevilla (2016). Numbers of species for the five units in the cave range from 2 to 11 species, but the numbers of species are only weakly correlated with numbers of specimens. Unit Vu is the richest level, with the highest number of specimens (N = 2314) and the highest number of species (N = 11), but the Unit Vm fauna with 10 species has greater relative species richness for the sample size is only 133 specimens (Sevilla 2016). Similarly, species numbers in Units I and II do not relate closely with numbers of specimens. Unit III has only three bat specimens and is essentially sterile as far as bats are concerned. The two levels with the highest species richness relative to sample size are Units II and Vm, while Units I and Vu have relatively low species richness.

The Unit Vm bat fauna is dominated by *Miniopterus schreibersii*, a species common today in the Karabakh uplands (Sevilla 2016). *Myotus blythii* and *Rhinolophus* species are the other bat species common at this level. This situation is reversed in Unit Vu, with the latter species becoming much more common, and *M. schreibersii* declining in importance. Units II and I also have *Myotis blythii* as the most common species, together with varying numbers of *Rhinolophus* species, and the bat fauna in Unit I is said to represent a 'modern' sample of bats living today in the cave (Sevilla 2016).

The small mammal faunas from Azokh 1 range from 11 to 24 species in the five units studied here. The number of species per stratigraphic unit is directly related to sample size recovered from each unit (Fig. 15.2). Those units with least numbers of specimens have the lowest species numbers, and the unit with the biggest sample (Unit Vu) has by far the highest number of species. As a result, species richness does not of itself provide any indication of environment.

The list of small mammal species identified by Parfitt (2016) is placed here in Species List (S.L.) Table 15.2. The data provided by Parfitt show that small mammal assemblages are dominated by arvicolid rodents, especially members of the *Microtus arvalis* and *M. socialis* groups that are said to indicate woodland/meadows and steppic vegetation respectively. Hamsters (*Mesocricetus* sp., *Cricetulus migratorius*), jirds (*Meriones* spp.) and mole voles (*Ellobius* sp.) are also well represented throughout the sequence (Parfitt 2016). Many of the small mammals are related to or are extant dwellers of steppe and arid environments today.

Large mammal taxonomic data for the Azokh sequence have been provided by Van der Made et al. (2016) and included here as S.L. Table 15.3. In the whole sequence 29 species are represented. Some, such as *Cervus elaphus* (red deer) are present at all levels, and some are present in only one unit. Domestic horse and pig are present in Unit I, but they have been omitted from further analysis since they represent selection by the human population during historic times and do not reflect the local ecology. *Ursus spelaeus* is common in Units II to V (those that have been found in Unit I were almost certainly introduced by recent burrowing activities of animals living in the cave in recent times, see Marin-Monfort et al. 2016). The unit with greatest species richness is Unit Vm, with 21 species including 8 carnivores, two equids, two rhinoceros and nine artiodactyls. By contrast, Unit Vu has only seven large mammal species, and the other levels are intermediate (see S.L. Table 15.3). The fauna has a strong central Asian aspect.

There is no relationship between species numbers of large mammals compared with small mammals, for the largest species number for small mammals in Unit Vu is set alongside almost the lowest number for large mammals: see S.L. Tables 15.2 and 15.3. Similarly, the low number of small mammal species in Unit Vm contrasts with the highest number of large mammal species in the Azokh sequence. This suggests that the factors underlying the accumulation and preservation of large mammals are distinct from those for small mammals, and it might be expected, therefore, that the ecological signals of the two sets of data may also be different.

The herpetofauna of Azokh 1 is composed exclusively of extant genera and species. The list of amphibian and reptile species identified by Blain (2016) is taken from their chapter and placed here in S.L. Table 15.4. Sample sizes are not

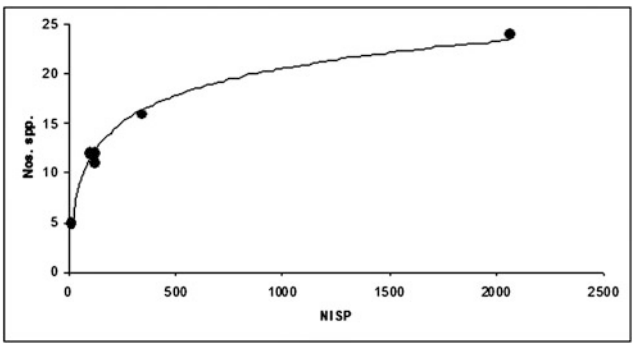

Fig. 15.2 Relationship between numbers of mammal species excluding bats in the six units of Azokh 1 (see Species List Tables) with numbers of specimens (NISP) recovered (least squares line)

available for the amphibians and reptiles, but species presence/absences are described by Blain (2016). The lowest unit, Unit Vm, has one lizard, *Lacerta* sp. and one snake, *Eryx jaculus*. Unit Vu has two each of amphibian and lizard species, and five snakes. They include the lizard *Pseudopus apodus* and the snakes *Elaphe sauromates* and *Malpolon insignatus*, while the exclusive presence of the snake *Pelophylax ridibundus*, which is associated with aquatic environments, suggests the nearby presence of water. Unit III has a single lizard species and three snakes, similar to those in Unit Vu, with the presence of *Vipera* (*Pelias*) sp. indicating high altitude environments. Unit II is similar to Unit Vu in having two amphibian species, two lizards and four snakes. Unit I has the highest species richness of lizards and snakes and includes one amphibian, four species of lizard and six snakes, higher even than Unit Vu.

Taphonomy

In an investigation of the taphonomy of large mammals (Marin-Monfort 2016) state that some of the cave bear remains are relatively complete, with some associations between elements, and that the lack of any evidence of transport suggests that the bears were living in the cave, using it as a den. Remains of other mammals are rare in most units, and they are extremely fragmentary, consisting mainly of teeth, horn/antler cores, and foot bones. All are highly fragmentary, including most of the cave bears, and this was probably due to post-depositional breakage within the cave. Carnivore chewing marks are present on some fossil bones, both cave bear and other species, but most of the breakage so common at the site does not appear to be due to carnivore activity. Cut marks and percussion marks are present, again on all species, including cave bears, and a small number of burnt bones are also present. Signs of trampling are common, and it is considered likely that the trampling agent was the cave bears living in the cave. Many bone fragments are rounded, some heavily, but their taxonomic assignment is not known. Both trampling and carnivore activity are likely causes of the rounding, not transport.

Little is known on the taphonomy of the bats. Evidence of digestion is seen on the teeth and bones of *Pipistrellus pipistrellus*, *Miniopterus schreibersii* and *Myotus blythii*, but no data are available on numbers of specimens affected. The latter two species are the most common at all levels (excluding Unit III which has almost no bats), so that there is some degree of predator action, but the absence of digestion on other species of bat does not by itself exclude the possibility of predator action since sample sizes are so small (Sevilla 2016). On the other hand, all of the bat species present at Azokh 1 are known to roost in caves or rock fissures, and it is likely that much of the bat fauna present in the cave came from natural deaths inside the cave. The collections of small mammals are strongly biased towards cranial and dental remains, with no postcrania available for study, and analysis of the small mammals has therefore been restricted exclusively to their teeth.

Many of the small mammal molars show evidence of digestion by predators. Digestion levels vary from around 20% of arvicolid molars in Units I and Vm up to 55% in Unit Vu. Degrees of digestion according to Andrews (1990) are light to moderate at all levels, and only Unit Vu has a small number of arvicolid molars that are heavily digested (Fig. 15.3). The high frequency of digested teeth is also shown in Fig. 15.4, which compares frequency of digestion of arvicolid teeth with that of murids and soricids. In nearly all cases, levels of digestion are lower for the two latter groups, and this appears to be the case because their teeth are lower crowned and thus less vulnerable to digestion. We are currently investigating this to try to measure the different degrees of digestion, and first indications are that small mammals with lower crowned teeth show evidence of digestion at least one category less than that seen in arvicolids when digested by the same predator (Fig. 15.4).

Rodent incisors have less morphological variation than do the molars, and in terms of the profile they present to digestive juices of predators, their main variation is that of size. Some rodent incisors are grooved, but this appears to have little effect on their susceptibility to digestion. It has been claimed, therefore, that rodent incisors are the single most useful body part for distinguishing digestion (Andrews

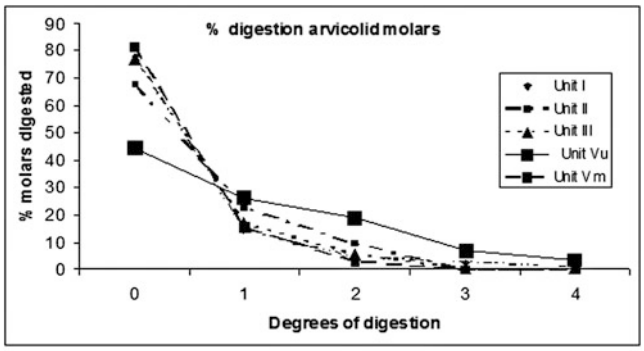

Percentage numbers of molars

Degrees of digestion	Unit I	Unit II	Unit III	Unit Vu	Unit Vm
0	78.0	67.9	77.4	44.5	81.6
1	14.3	22.6	17.0	26.3	15.5
2	4.5	9.5	5.7	19.2	2.9
3	2.2	0	0	6.7	0
4	0.9	0	0	3.4	0
N	223	84	106	1389	103

Fig. 15.3 Percentage digestion of arvicolid molars from five units of Azokh 1. Five digestion categories are shown on the horizontal axis (Andrews 1990), with the figure 0 signifying absence of digestion and 4 indicating heavy digestion, and the percentage number of teeth digested is shown on the vertical scale

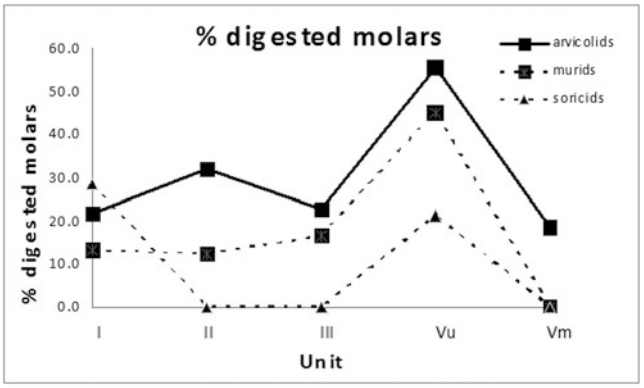

Fig. 15.4 Differences in percentage numbers of molars digested for arvicolids, murids and soricids, showing that within each of the Azokh 1 units there are consistent differences in degrees of digestion between the three mammal groups. The five Azokh units are shown on the horizontal scale and percentage numbers of teeth digested on the vertical scale

1990; Mathews and Parkington 2006). The pattern of digestion of all rodent incisors does not vary greatly, but numbers of digested teeth are greater than in arvicolid rodents, with three stratigraphic units having 40–50% of teeth showing evidence of digestion (Units I, II and Vm) and Unit Vu having 74% of teeth with digestion (Fig. 15.5). Unit III also appears to have a similar level of digestion to that of Unit Vu, but since the sample size is only ten it is likely that this result is anomalous, especially since the molars from Unit III also show no evidence of high digestion.

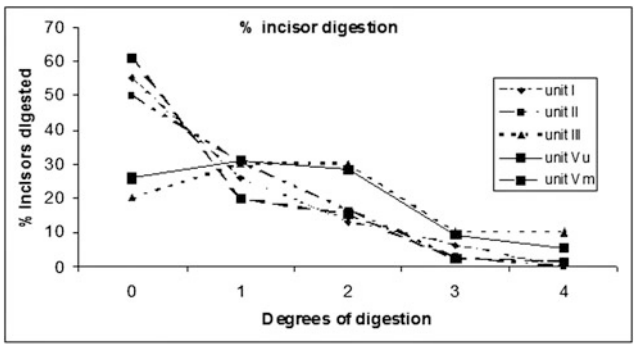

Percentage numbers of incisors

Degrees of digestion	Unit I	Unit II	Unit III	Unit Vu	Unit Vm
0	55.0	50.0	20.0	26.0	61.1
1	26.0	30.6	30.0	30.9	19.8
2	13.0	16.7	30.0	28.3	15.3
3	6.1	2.8	10.0	9.4	2.3
4	0.0	0.0	10.0	5.3	1.5
N	131	36	10	434	131

Fig. 15.5 Percentage digestion of rodent incisors from five units of Azokh 1. Five digestion categories are shown on the horizontal axis (Andrews 1990), with the figure 0 signifying absence of digestion and 4 indicating heavy digestion, and the percentage number of teeth digested is shown on the vertical scale

The conclusion from both molars and incisors is that Units I, II and Vm have similar distributions and degrees of digestion, and these show that the small mammal faunas were accumulated by a category 1 predator, following the Andrews (1990) classification. The Unit Vu small mammal sample has a different pattern of digestion, higher both in degree and in number, and this indicates that it was accumulated by a category 3 predator (Andrews 1990). The sample size of Unit III is too small for any conclusion to be drawn other than the fact that it was also evidently a predator accumulation. The most likely category 1 predator is the barn owl (*Tyto alba*), which is a vole specialist over much of its range across Europe and central Asia and which is also known to inhabit caves. It is by far the most common owl found in cave habitats, and it produces the least effect on its prey, with low degrees of digestion except at its nest site. The most likely category 3 predator is the European eagle owl (*Bubo bubo*), as the digestion levels of this species is less than that of the tawny owl, the only other category 3 predator known so far (Andrews 1990). This species does not inhabit caves, but it often nests on rocky cliffs or in small holes in cliffs, and the entrance to Azokh cave at the base of a cliff would be a suitable habitat for an eagle owl. It also feeds on a wider variety of prey than most other owls, and the high small mammal diversity in Unit Vu (S.L. Table 15.2) is probably a reflection of this.

Paleoecology

Weighted averages ordination has been described above for three temperate habitats (Fig. 15.1). In all three cases, the distribution of species ranges through six habitat types is shown, and it should be noted that these analyses exclude bats, since they are rarely preserved as fossils (Andrews 1990). These three analyses form the basis for comparison with the reconstructed ordination scores for the Azokh fossil faunas. The scores for fossil taxa have been estimated based on the Taxonomic Habitat Index, which assigns habitat distributions based on species scores, if the species is still extant, or on genus scores if the species is extinct. As explained above, this method seeks to reduce the bias inherent in assigning arbitrary habitats based only on closest living relatives. THI analyses have been performed separately on the large and small mammal as well as on the combined mammal fauna (Table 15.1, Fig. 15.6).

The large mammal fauna in Units II to V have the highest index values for deciduous woodland but also high values for Mediterranean evergreen woodland and, in the case of Unit Vm, high levels for steppe and arid environments. Unit I is the most distinct, with steppe and arid index values equal to or greater than deciduous woodland. From Unit Vm to Unit III

there is a gradual increase in deciduous woodland indicated by the THI index, with slight reduction in arid environments and steppe, and while the small sample size in Unit Vu makes its value suspect, the trend is continued into Unit III with a slightly larger sample size. Overall, there is consistency in the proportions between different levels, suggesting the environment over most of the period represented by Units V to II consisted of areas of woodland mixed with steppe and arid environments, with slight increases in areas of woodland up to Unit III. Such a mixture could be the outcome of increasing woodland on mountain slopes and river valleys, with the low ground ranging from steppe to semi-desert and expanding in area in Units II and I (see below).

Calculation of the THI scores for the small mammal faunas for the five units from Azokh 1 (middle bar chart in Fig. 15.6) show that all five stratigraphic units are dominated by animals living today in steppe and semi-desert. Index values for deciduous woodland are lower than those for steppe and semi-desert in all samples except Unit Vm, which is the only unit to have a relatively high value for deciduous woodland, although even here the highest THI value is for steppe. The proportion of steppe/arid species increases from Unit V to Unit II, while at the same time the THI index values for deciduous woodland decreases. There is a minor reversal of this trend in Unit I at the top of the sequence. Again there is a high degree of consistency in the results from the small mammals, showing a mixture of woodland and steppe/semi-desert environments, with the arid environments greater in extent and increasing up the section and woodland decreasing.

One explanation for the differences in paleoecological reconstruction between large and small mammal accumulations at Azokh Cave is that they had different taphonomic trajectories. The two predators identified for the small mammal assemblages, barn owls and eagle owls, are both generalists and open country hunters, whether quartering the ground (barn owl) or perch and pounce (eagle owl), they habitually seek open spaces to hunt. This could well explain the greater prominence of small mammals with steppe and arid country affinities. By contrast, many of the large mammals, such as the cervids, suids and felids, are woodland dwellers and may have been living closer to the fossil site, which is half way up a mountain and like today's habitats probably had woodland vegetation. It is evident from this that some knowledge of the taphonomy of an assemblage is necessary in order to clarify an otherwise confusing contrast in data.

When the large and small mammals are combined into a single THI analysis, the results become less clear. This could be predicted from the separate analyses, for the two samples provide evidence of different proportions of habitat resulting from different taphonomic histories. The bottom bar chart in Fig. 15.6 reflects this contrast and does not indicate any clear trend or pattern in Units V to II other than the fact that woodland and steppe were more or less equally represented. Only in Unit I does the value for deciduous woodland

Table 15.1 Taxonomic Habitat scores for the faunas from the five stratigraphic units at Azokh 1. THI scores are shown for six modern habitat types for each fossil fauna, and the analyses have been shown for small and large mammals separately and for the two combined. N = numbers of species

		Unit Vm	Unit Vu	Unit III	Unit II	Unit I
Small mammal fauna	Tundra	0.021	0.019	0.006	0.008	0.021
	Boreal forest	0.065	0.048	0.046	0.038	0.057
	Deciduous forest	0.182	0.132	0.155	0.089	0.116
	Mediterranean	0.149	0.126	0.118	0.071	0.100
	Steppe	0.279	0.318	0.312	0.381	0.313
	Arid	0.177	0.254	0.275	0.336	0.270
	N	12	24	14	14	16
Large mammal fauna	Tundra	0.007	0.000	0.000	0.014	0.000
	Boreal forest	0.076	0.100	0.055	0.111	0.083
	Deciduous forest	0.247	0.314	0.336	0.300	0.217
	Mediterranean	0.190	0.257	0.236	0.209	0.167
	Steppe	0.209	0.157	0.173	0.136	0.217
	Arid	0.212	0.129	0.164	0.118	0.250
	N	21	7	6	11	6
All mammals	Tundra	0.012	0.015	0.004	0.010	0.015
	Boreal forest	0.072	0.059	0.056	0.070	0.064
	Deciduous forest	0.223	0.172	0.270	0.182	0.145
	Mediterranean	0.175	0.155	0.195	0.132	0.119
	Steppe	0.234	0.283	0.267	0.273	0.285
	Arid	0.199	0.227	0.241	0.240	0.264
	N	33	31	20	25	22

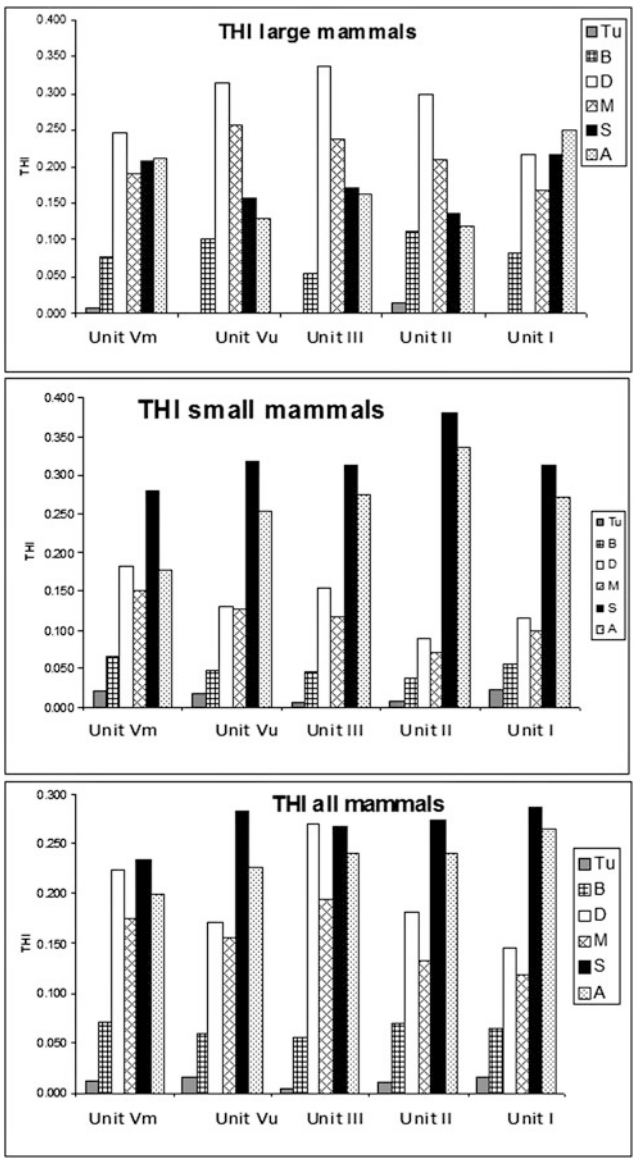

Fig. 15.6 THI analyses for large mammals (top), small mammals (middle) and the two combined (bottom). The five stratigraphic units are shown on the horizontal axis and THI values on the vertical axis

decrease significantly and the values for steppe and semi-desert increase.

The bat fauna from Azokh 1 is made up of extant genera and species, and their species richness is strongly linked with distribution of vegetation (Sevilla 2016). "The richest habitats in bat species are the mountain steppes, closely followed by mountain forest habitats. The lowest values are observed in mountain grasslands" (Sevilla 2016). These of course are the habitats the insectivorous bats are adapted to hunt over, and it shows the presence of these habitats within the hunting ranges of the bats and not necessarily what the habitat was like in the immediate vicinity of the cave. The level with the greatest relative species richness, Unit V, is dominated by species with Mediterranean or humid affinities, so the evidence from the bats indicates woodland conditions at this level. Unit Vu has 11 bat species compared with the 10 species in Unit Vm, but bats are 20 times more abundant based mainly on the large number of specimens of *Myotis blythii* and *Rhinolophus* species. These indicate a change to open steppe environments, with a warmer and more arid climate (but see below). Unit III has almost no bats, but the Unit II bat fauna suggests a change to cooler conditions. The Unit I bats are similar to those from Unit II, but with a minor change suggesting a slight increase in aridity (Sevilla 2016).

The majority of snakes and amphibians belong to thermophilous and xeric-adapted forms (e.g., *Pelobates syriacus*, Agamidae, *Pseudopus apodus*, *Eryx jaculus*, *Elaphe sauromates*, *Malpolon insignatus* etc.). Sample sizes are not available for the amphibians and reptiles, but species presence/absences are described by Blain (2016). The lowest unit, Unit Vm, has *Lacerta* sp. and *Eryx jaculus*, both associated today with warm xeric conditions (Blain 2016). Unit Vu has *Pseudopus apodus* and the snakes *Elaphe sauromates* and *Malpolon insignatus* that are also associated today with warm xeric conditions (Blain 2016), while the exclusive presence of the snake *Pelophylax ridibundus*, which is associated with aquatic environments, suggests the nearby presence of water. All these species in Unit Vu, with one exception, frequent woody environments. Unit III is similar to Unit Vu, with the presence of *Vipera* (*Pelias*) sp. indicating high altitude environments (Blain 2016). Unit II is also similar to Unit Vu in having eight species indicating warm xeric conditions with an element of high altitude environments. Unit I has the highest species richness of lizards and snakes and with 11 taxa, and the presence of an agamid lizard suggests more arid conditions than present at lower levels (Blain 2016). In general, however, most of the taxa present in the Azokh sequence frequent wooded or bushy areas, and while there is some indication of a trend towards more arid conditions from Units V to I, the evidence is based to some extent on the presence of agamids in the uppermost unit. On the other hand, the slight increase in species richness from Unit V to Unit I suggests that if conditions were more arid, there was also greater habitat variability in the upper units.

Wood is present in two units at Azokh, in both cases preserved as charcoal. The wood may have been carried into the cave by the hominin populations and so may reflect their choice as the most suitable firewood, but it may also have been carried in by animals or even fallen in through avens in the cave roof after natural surface fires. The list of plant species identified by Allué (2016) is taken from their chapter and placed here in S.L. Table 15.5. Just over 80% of the wood identified in Unit II is attributed to *Prunus* species (N = 709 out of a total of 886 specimens). This is a genus of small trees

and shrubs with a broad distribution in temperate and tropical (montane) regions of the world. Also present are remains of maples (*Acer*), deciduous oak species (*Quercus*), and species of the apple family (Maloideae), a combination of large woodland trees and small trees and shrubs. Allué (2016) makes the point that this plant association has no equivalent in the area today, but it shows the presence of broadleaved forests with understorey trees and shrubs in the vicinity of the cave. Pollen evidence cited by Allué (2016) from areas near the site also shows the presence of broad leaved woodland although without the curious dominance of *Prunus* species. The Unit Vu flora, although much smaller than that from Unit II, has the same species represented and in similar proportions (N = 21), and it is also dominated by *Prunus* and Maloideae species, both of which include many species with edible fruits.

Searches for pollen were for the most part unsuccessful, both in the cave sediment and in fossil coprolites (Scott et al. 2016), and the few pollen grains found were not diagnostic. Greater success came with the discovery of abundant phytolith assemblages, and nine different types of grass silica short cell phytoliths were identified, indicating a temperate C_3-grass steppe mosaic (Scott et al. 2016). There is clearly greater potential for further phytolith studies at Azokh, and a key issue here will be identifying how the phytoliths entered the cave system.

Present Day Vegetation in the Azokh Region

Indications from the fossil faunas and floras from Azokh 1 of the past environmental trends call into question what is the nature of the present vegetation in the vicinity of the cave. Both woodland and steppe conditions have been indicated, but the area today is heavily wooded with the nearest steppe environments 4–6 km east of the cave.

A number of vegetation transects and sample plots have been measured, but the one in the immediate vicinity of the cave is suspect because the area has been largely cleared of trees by fire and grazing by livestock. The few remnants of woodland indicate an association of (*Zelkova-Quercus*), with an understory of field maple (*Acer campestre*), *Prunus* species, dogwood (*Cornus sanguinea*), hazel (*Corylus*) and hawthorn (*Cretaegus*). The mountain slopes below Azokh 1 are covered by a dense association of Jerusalem thorn (*Paliurus spina-christi*), which would have been present as an under-story bush but which has spread over the whole hillside after clearing. Hackberry trees (*Celtis*), *Zelkova* and figs occur in patches (see Table 15.6) for botanical names of plants. This is similar to the tree associations that are widespread on the mountains surrounding the site, where *Zelkova*, hornbeam and ash (*Fraxinus*) are the dominant species on north sloping faces and oak (*Quercus macranthera*) and *Zelkova* on the south facing faces, with less *Prunus* and dogwood and the addition of elm, beech and second species each of ash and oak. It is also the association found in the river valley below the site, with greater frequencies of ash and hackberry and the addition of plane trees, more lime, and willow actually by the water's edge. However, it should be noted that all woodlands seen were secondary, with evidence of extensive felling and secondary regrowth. The majority of hornbeam and ash had evidently regrown from cut stumps, for the rotting stumps could still be seen, and based on two 900 m^2 sample plots the secondary growth of hornbeam and ash is estimated to be about 60–70 years old. Information from local people is that the forests were extensively cut during Soviet times, but they are still being cut for firewood and used for grazing stock by local communities.

The river valleys are highly altered by human activity, but two 100 m transects along the valley adjacent to the site demonstrated the importance of variations in soil and geology. One association where the valley cut through limestone differed little from the upper slopes of the valley except in the dominance of *Zelkova*. There were few oaks and there was a lower canopy of hazel in places. This association may have been altered by human activity, with some species like oak being selectively removed, but the other association, however, was dominated by oak and ash, with hornbeam and field maple and with willows by the water's edge. This association was growing on volcanic tuffs, which outcropped on one side of the valley (the trend of the valley was 340°), almost north-south, and the tuffs outcropped on the south facing side of the valley, and this may also have affected the change in vegetation. The lower canopy in all cases is dominated by hazel, dogwood and some field maple. The vegetation of the permanent Ishkhanaget River, which drains the Azokh region, has been greatly altered by human action, and the trees observed along one short section of the river were mainly willows and one large plane tree.

For comparison with Azokh Cave, three vegetation sample plots were examined in the region of Karintak. Two 30 m diameter sample plots had 90–94% hornbeam, with oak and field maple the only other tree species. One sample plot had an understory of hazel, but the other had almost no hazel. This area again had clearly been felled, an estimated 100 years ago, and the hornbeam had regrown alongside the rotting stumps. For comparison with this relatively undisturbed forest, A 30 m square sample plot was placed immediately outside the entrance of a large cave in the Karintak forest, on the steep slope down from the cave. The woodland was nearly half ash and field maple, and hornbeam and *Prunus* species were also common, the latter mainly by the cave entrance, with Maloideae, *Zelkova*, elder and dogwood also present. Here too there was evidence that the area had been cleared, and the trees were approximately 40–

60 years in age, but there were also some much larger trees of lime and maple which apparently survived the felling.

The concentration close to cave entrances of *Prunus*, Maloideae and *Sambucus*, and their rarity in woodlands removed from caves, is strongly suggestive. All of them are fruit-bearing small trees with fruits both accessible and edible for humans and bears, and we may speculate that their presence close to cave entrances may be the result of self-seeding from seeds discarded by humans or bears living in the cave. It is probable that the self-seeding was unintentional, but it is interesting to compare this with the high proportions of *Prunus* species identified by charcoal remains in Units II and V. It is possible that there was a self-seeded concentration of *Prunus* species (and pomes) in the vicinity of Azokh 1 during the Pleistocene, unintentionally brought there by the human population, and this then provided an easily accessible firewood source.

A second cave was also investigated towards one end of the Shushi Gorge. This is a precipitous gorge over 350 m deep with near vertical cliffs. The cave had a narrow shelf running approximately north-south along the side of the gorge with a thin strip of woodland extending along it. Because of limitations of space, a 300 m transect was run along this strip, and plants recorded both by abundance and by their proximity to the cave. Elder was abundant at the cave entrance but rare elsewhere; *Prunus* species and figs were common immediately outside the cave entrance (see above), but less common elsewhere; *Zelkova* was the most common species away from the cave, with ash, dogwood and hawthorn next most common along the cliff shelf; hazel, *hackberry* and field maple were also present. The ground vegetation was brambles, grasses, nettles in open areas and dogs mercury and celandines under woodland canopy.

Two of the higher mountains in Nagorno-Karabakh (Mets Kir and Dizapayt) are visible from the upper slopes above Azokh Cave, but we were not able to visit them. Above the tree line they probably had mountain steppe vegetation or alpine meadow, and one at least would have been within the range of larger birds of prey and large mammals (18 km by line of sight). The more extensive areas of upland alpine meadow in Nagorno-Karabakh, however, are far to the north of the country at the present time, and we were not able to visit them.

The vegetation map of Nagorno-Karabakh shows the presence of a broad belt of semi-xerophyll woodland on the lowlands 4–6 km to the east of Azokh (Manuk 2010). The areas we saw are either under cultivation or are remnant patches of juniper and evergreen oaks, together with Jerusalem Thorn, *Pistacia* and almond, that seem to have taken over areas cleared of broadleaved forest. Further to the east are belts of sagebrush steppe and sagebrush desert, and both would have been within the ranges of larger mammals and birds of prey. Unfortunately we were not able to visit any of these areas, and some at least are now greatly degraded. Given the location of Azokh on the eastern edge of the mountainous region of the country, it can be concluded that climatic variations would have brought about movements of vegetation zones between steppe and forest associations towards and away from the mountainous regions. Drier conditions would have led to the spread of the xerophyl/sagebrush steppe closer to Azokh, and retreat of broadleaved forest up the mountain slopes; and wetter conditions would have led to the reverse trend. This is entirely consistent with the palaeontological and palaeobotanical evidence from Azokh 1, and it suggests that the range of palaeoenvironments present for the past 200 kyr was little different from that existing today.

Discussion

A number of sites in the Caucasus have provided evidence of the palaeoenvironment during the second half of the Pleistocene. The site of Akhalkalaki at 1600 m altitude had a fauna for which it is said that 23 species are inhabitants of open habitats and seven are forest dwellers (Vekua 1962). The paleobotanical data supports the development of xerophitic landscapes (Vekua 1962, 1987). On the other hand, the palynological data and faunal remains from Kudaro suggest that the Lower Paleolithic layers accumulated under warm and humid conditions (Zelikson and Gubonina 1985; Mamatsashvili 1987). During the late Pleistocene, several cave sites found near Kutaisi (Bronze cave, Double Cave, Bizon, Bears Cave and the Upper Cave) yielded rich Mousterian assemblages that were dominated by cave bears, with bison and *Capra* also well represented (Vekua 1987). The palynological data shows that forests were widespread near the cave during the accumulation of the Mousterian levels (Mamatsashvili 1978). Later on during the last glaciation (Ollivier et al. 2010), the site of Dzudzuana showed a transition from a mixed coniferous-deciduous forest to more open pine-spruce forests combined with open steppe occupied by Chenopodiaceae, Poaceae and Asteraceae. Floral remains from the upper portion of the section then show the expansion of deciduous forests. The structure of the recovered faunal remains is in agreement with the evidence from floral data (Vekua and Lordkipanidze 1998). The evidence from these sites indicates the alternation of forests and steppe conditions through the Pleistocene, which is what is seen in the Azokh sequence.

A feature of the Azokh sequence is that there is an apparent conflict of evidence between the botanical and large mammal evidence on the one hand and the small mammal and herpetofaunal evidence on the other. The first indicates woodland in the vicinity of Azokh Cave during the time of accumulation of the sediment and faunas, and the second indicates steppe/arid environments. How do we interpret this?

Evidence for Woodland

It has been shown that the evidence from charcoal is available from two levels only, Units II and Vu, both of which share a similar profile (Allué 2016). Both are also said to be the result of human action, collecting fire wood and carrying it to the cave, although there is no direct evidence for this, and for both units the charcoal is derived from the wood of *Prunus* species, and it is interesting to speculate that the preponderance of small trees with edible fruits may have entered the cave through human or animal action, the fruits having been collected for consumption in the cave, and the nuts/seeds discarded in the vicinity of the cave so that they then grow naturally around the cave. Be that as it may, the combination of these trees with other broad leaved tree species identified from the charcoal indicates deciduous woodland in the vicinity of the cave.

A similar conclusion is reached from the analysis of large mammals (Van der Made et al. 2016). The largest sample is available from Unit Vm (N = 21 species), which has an estimated age of 2–300 ka (see Appendix, ESR and racemization). The fauna has elements indicating deciduous woodland, evergreen (Mediterranean) woodland, steppe and semi-desert in almost equal proportions (Fig. 15.6), so that while deciduous woodland was present in the area, there was clearly considerable habitat heterogeneity. Figure 15.1 showed the variability in five deciduous woodland habitats, but the Unit Vm ecological spectrum does not match any of these (compare Fig. 15.6 with Fig. 15.1). We therefore investigated the effects of mixing faunas from different habitats, following the procedure in Andrews (2006). Equal mixtures of woodland with steppe faunas was weighted towards the steppe faunal elements, but when the faunas were mixed in a 2:1 ratio, i.e. with an entire woodland fauna mixed with half a steppe fauna, there was a close match with the Azokh faunas. The results for four such mixtures are shown in Fig. 15.7, which is shown here compared with the large mammal analysis of the Azokh faunas from Units Vu and I. These two fossil faunas were selected as representing the extremes of the stratigraphic section, but in fact they vary little from each other and little also from most of the modern mixes of deciduous forest with a minor steppe element. It should also be noted that Unit III has an even higher representation of woodland elements than Units I and Vm (Fig. 15.6), and they are closest to the index values for pure woodland, with only a minor steppe element. The large mammals therefore indicate a preponderance of woodland habitats throughout the section, increasing from Unit Vm through Unit III, and then dropping again to Unit I, with increase in steppe elements at the top of the section.

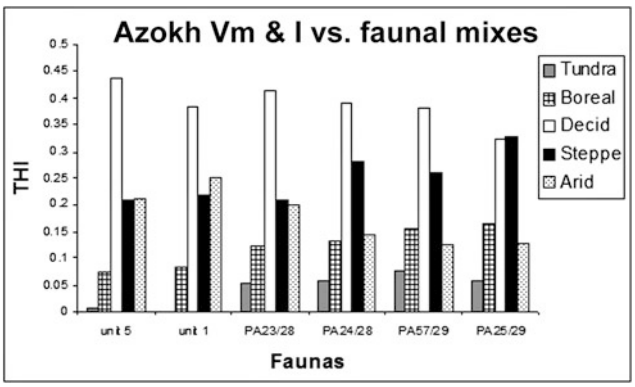

Fig. 15.7 The large mammal faunas from Unit Vm at the bottom of the Azokh 1 stratigraphic sequence and Unit I at the top are compared with four modern faunas derived from mixtures of deciduous woodland faunas and steppe faunas. The mixtures are in the ratio 2:1 woodland: steppe. The four recent faunas details as follows: PA23 woodland, 50° N 10° E, N = 43; PA24 woodland, 50° N 20° E, N = 46; PA25 woodland, 50° N 30° E, N = 51; PA28 steppe, 50° N 60° E, N = 39; PA29 steppe, 50° N 70° E; PA57 woodland, N = 22. The habitats that the modern faunas represent are Tu, tundra, B, boreal forest, D, deciduous forest, Mediterranean forest, S, steppe, A, arid environments

Evidence for Steppe

The richest level for small mammals is Unit Vu (Parfitt 2016) (S.L. Table 15.2). Despite differences in sample size the THI patterns for the small mammals from all units are similar, with steppe and arid environments predominant (Fig. 15.6). There is, however, a trend of increasing steppe elements from Unit V to Unit II and decreasing proportions of deciduous woodland elements, suggesting this pattern is changing through time (Fig. 15.6). These trends are reversed in Unit I, but given small sample sizes this may not be significant.

None of the small mammal faunas have an exact match with any of the modern faunas we have investigated. Steppe faunas tend to be dominated by steppe and arid elements, almost to the exclusion of all else, whereas the Azokh faunas also have significant elements of woodland. We therefore compared them with a mixture of habitats (Andrews 2006), mixing steppe with woodland. In this case, however, the steppe and woodland faunas were mixed in the ratio of 2:1; that is complete steppe faunas combined with half woodland faunas. As would be expected, this has had the effect of increasing the woodland component similar to that seen in the Azokh faunas, indicating that these faunas were derived from an area of steppe with minor amounts of woodland.

The amphibians and reptiles in the Azokh faunas are mostly small, equivalent in body size to the small mammals, and they also indicate the presence of steppe and arid conditions throughout the sequence and increasing up the section (Blain 2016). It is most likely that the differences between them may be accounted for by the fact that they

were derived from different parts of the environment. This is all the more likely to be true if some part of the Azokh fauna and flora has been transported to the site, and it has been shown that the small mammals were brought to the site by predators, interpreted as barn owls and eagle owls, which are predators that habitually hunt over open steppe and semi-desert. Predators hunt by size and availability rather than by taxonomic group (Andrews 1990), and it is common to find reptiles and mammal together in the prey remains of some predators. The taphonomy of the former group has not yet been investigated, but it can be predicted that the reptiles and amphibians will also be shown to have been predated, probably by the same predators as the small mammals.

Combining all lines of evidence, the evidence at Azokh from the middle to late Pleistocene deposits is that the cave was situated close to both woodland and steppe environments. The most likely explanation for this is to be seen in its location part way up a mountain slope, with woodland immediately adjacent to the cave, covering the mountain slopes as it does today, and steppe environments on the lower lands to the south and east of the mountains but within a few kilometres of the cave. The steppe would have been within the hunting range of the predators accumulating the small mammal faunas, and there may also have been alpine steppe on the tops of nearby mountains also within the predators' hunting ranges.

Conclusions

1. Present day vegetation in the mountainous region around Azokh is exclusively deciduous woodland, with variations of hornbeam, *Zelkova*, oak, ash, field maple, lime and many smaller species, including *Prunus* and Maloideae species. The area around the cave entrances has been degraded by fire and grazing and is not typical of the area, having pomegranates (*Punica granatum*) mulberry and figs. The nearest steppe vegetation at present is 4–6 km to the east of the cave.
2. The large mammal fauna indicates woodland close to Azokh Cave with some evidence of steppe conditions in an approximate ratio of 2:1 (woodland:steppe). This ratio increased from Unit Vm to Unit III, with greater proportions of woodland, and then it decreased from Unit II to Unit I, with increasing steppe.
3. The small mammal fauna indicates steppe conditions and less woodland in the approximate ratio of 1:2 (woodland: steppe). Taphonomic evidence showed that the faunas were brought to the cave by barn owls and eagle owls that habitually hunt over open areas, and it is inferred that steppe conditions may have been some distance from the cave. Steppe conditions expanded slightly in the upper levels. There is slight evidence of increasing aridity in the upper units of the Azokh 1 sequence.
4. The bat fauna indicates Mediterranean woodland conditions at the bottom of the cave sequence changing first to warmer, more arid steppe environments and then to cooler steppe environments at the top of the sequence.
5. The amphibian and reptile fauna indicates steppe conditions in the vicinity of the cave and less woodland, similar to the evidence from the small mammals, but taphonomic analyses have not yet been done to see if it was accumulated in the same way as the small mammals.
6. The botanical evidence indicates woodland, with some of the wood possibly entering the cave through human or animal action and some possibly blown in from natural fires. In either event, it suggests woodland in the vicinity of the cave, dominated by fruit-bearing *Prunus* species that may have been self-seeded near the cave as a result of human or animal (cave bear) activity.
7. Phytoliths collected from the sediments and from coprolites show the presence of numerous types of grasses, indicating temperate steppe grasslands.

Acknowledgments We are grateful to Ethel Allué, Marion Bamford, Levon Yepiskoposyan and three anonymous referees for discussion and help with this chapter.

Species List Tables

Table 15.2 Presence/absence of small mammals at Azokh 1. Data from Parfitt (2016)

Unit number	Vm	Vu	III	II	I
Insectivora					
Soricidae					
Sorex minutus group		+			
Sorex araneus group	+	+			+
Crocidura spp.	+	+	+		+
Talpidae					
Talpa sp.	+				
Carnivora					
Mustelidae					
Mustela nivalis		+			
Lagomorpha					
Ochotonidae					
Ochotona sp.		+	+	+	+
Ochotona cf. rufescens					
Ochotona sp. large					
Leporidae					
Lepus sp.		+			+
Rodentia					
Sciuridae					
Marmota sp.				+	
Spermophilus sp.				+	

(continued)

Table 15.2 (continued)

Unit number	Vm	Vu	III	II	I
Muridae					
Cricetulus migratorius	+	+		+	+
Mesocricetus sp.		+	+	+	+
Allocricetulus sp.	+	+		+	
Myodes glareolus	+	+	+		
Microtus arvalis/socialis	+	+	+	+	+
Microtus (*Terricola*) spp.	+	+	+	+	+
Chionomys nivalis	+	+		+	+
Chionomys gud	+	+			+
Ellobius sp.	+	+	+	+	+
Meriones small		+	+		+
Meriones medium		+		+	
Meriones large sp		+	+		+
Apodemus spp.	+	+	+	+	+
Rattus sp.		+			
Mus cf. *macedonicus*		+	+		+
Gliridae					
Dryomys nitedula		+			
Dipodidae					
Allactaga large		+			+
Allactaga small		+			
NISP	120	2065	121	101	346
Number of species	12	24	11	12	16

Table 15.3 Presence/absence of large mammals at Azokh 1. Data from Van der Made et al. (2016)

	Units				
	Vm	Vu	III	II	I
Canis lupus	cf	x		x	
Canis aureus	x				
Vulpes vulpes				x	
Meles meles	x	x			
Martes cf. *foina*	x				
Crocuta crocuta	x	x			
Felis chaus	x				
Panthera pardus	x		x	x	
Ursus spelaeus	x	x	x	x	
Ursus sp (aff. *arctos/thibetanus*)				x	
Equus hydruntinus	x		x		
Equus asinus					cf
Equus ferus	x				
Equus caballus					cf
Stephanorhinus hemitoechus	x	?	x		
Stephanorhinus kirchbergensis	x	?	x		
Sus scrofa	x		x	x	
Sus scrofa – domestic					x
Capreolus pygargus	x		x	x	
Dama aff. *peloponesiaca*	x	?			
Dama sp.			x	x	x
Megaloceros solilhacus	x				

(continued)

Table 15.3 (continued)

	Units				
	Vm	Vu	III	II	I
Cervus elaphus	x	x	x	x	x
Bison schoetensacki/Bison-Bos	x		cf	x	
Ovis ammon	x		x		x
Capra aegagrus	x	x	x	x	
Capra hircus					cf
Saiga tatarica	x			x	
Bovidae indet.	x				

Table 15.4 Presence/absence of amphibians and reptiles at Azokh 1. Data from Hugues-Alexandre Blain (2016)

Unit number	Vm	Vu	III	II	I
Pelobates cf. *syriacus*				+	
Bufo viridis		+		+	+
cf. *Pelophylax ridibundus*		+			
Agamidae indet.					+
Pseudopus apodus		+		+	+
Lacerta sp.	+	+	+	+	+
Lacertidae indet.					+
Eryx jaculus	+	+	+	+	+
cf. *Coronella austriaca*		+		+	+
cf. *Elaphe* sp. 1 (*sauromates*)		+		+	+
cf. *Elaphe* sp. 2		+	+	+	+
cf. *Malpolon* sp. (*insignitus*)		+			
Vipera (*Pelias*) sp. (‘*ursinii*’ complex)			+		+
Viperidae indet. (‘Oriental’ vipers)					+

Table 15.5 Charcoal analysis from Units II and Vu from Azokh 1 cave. Data from Allué (2016)

Taxa	Unit II		Unit Vu
	Num. frags	%	Num. frags
Acer	34	3.84	
Carpinus	1	0.11	
Celtis/Zelkova	4	0.45	
Euonymus	2	0.23	
Lonicera	9	1.02	
Maloideae	23	2.60	3
Prunus	709	80.02	15
Quercus sp. decidous	28	3.16	2
Quercus/Castanea	2	0.23	
Paliurus/Ziziphus	3	0.34	
Ulmaceae	4	0.45	
cf. *Acer*	3	0.34	
cf. Maloideae	1	0.11	
cf. *Prunus*	13	1.47	
cf. *Quercus*			1
cf. Ulmaceae	1	0.11	
Undetermined angiosperm	48	5.42	
Undetermined	1	0.11	
Total number of fragments	886		21

Table 15.6 List of recent tree species in the Azokh region

Hornbeam	*Carpinus caucasica*
Zelkova	*Zelkova carpinifolia*
Oak, deciduous	*Quercus iberica*
Mountain oak	*Quercus macranthera*
Oak, evergreen	*Quercus* sp.
Ash	*Fraxinus excelsior*
Field maple	*Acer campestre*
Hazel	*Corylus avellana*
Prunus*	*Prunus* spp. (*Amygdalus* sp.)
Fig*	*Ficus* sp.
Beech	*Fagus orientalis*
Celtis	*Celtis caucasica*
Maple	*Acer platanoides*
Apple*	Maloidea, cf. *Malus orientalis*
Willow	*Salix* sp.
Plane	*Platanus orientalis*
Pine	*Pinus kochiana*
Lime (small leaf)	*Tilia cordata*
Lime (large leaf)	*Tilia platyphylous*
Jerusalem thorn	*Paliurus spina-christi*
Rose	*Rosa* sp.
Dogwood	*Cornus sanguinea*
Service tree	*Sorbus torminalis*
Hawthorn	*Crataegus monogyna*
Privet	*Ligustrum vulgare*
Elder	*Sambucus nigra*
Juniper	*Juniperus* sp.
Spindle	*Euonomys europaeus*
Buckthorn	*Hippophae rhamnoides*
Nettles	*Urtica* sp.
Brambles	*Rubus* sp.

*Usually found associated with human habitation, past or present

References

Allué, E. (2016). Charcoal remains from Azokh 1 Cave: Preliminary results. In Y. Fernández-Jalvo, T. King, L. Yepiskoposyan & P. Andrews (Eds.), *Azokh Cave and the Transcaucasian Corridor* (pp. 297–304). Dordrecht: Springer.

Andrews. P. (1990). *Owls, caves and fossils*. Natural History Museum, London.

Andrews, P. (2006). Taphonomic effects of faunal impoverishment and faunal mixing. *Palaeogeography, Palaeoclimatology, Palaeoecology, 241*, 572–589.

Appendix: Fernández-Jalvo, Y., Ditchfield, P., Grün, R., Lees, W., Aubert, M., Torres, T., et al. (2016). Dating methods applied to Azokh Cave sites. In Y. Fernández-Jalvo, T. King, L. Yepiskoposyan & P. Andrews (Eds.), *Azokh Cave and the Transcaucasian Corridor* (pp. 321–339). Dordrecht: Springer.

Asryan, L., Moloney, N., & Ollé, M. (2016). Lithic assemblages recovered from Azokh 1. In Y. Fernández-Jalvo, T. King, L. Yepiskoposyan & P. Andrews (Eds.), *Azokh Cave and the Transcaucasian Corridor* (pp. 85–101). Dordrecht: Springer.

Blain, H.-A. (2016). Amphibians and squamate reptiles from Azokh 1. In Y. Fernández-Jalvo, T. King, L. Yepiskoposyan & P. Andrews (Eds.), *Azokh Cave and the Transcaucasian Corridor* (pp. 211–249). Dordrecht: Springer.

Brain, R. (1981). *The hunters or the hunted*. Chicago: Chicago University Press.

Domínguez-Alonso, P., Aracil, E., Porres, J. A., Andrews, P., & Lynch, E. P. (2016). *Geology and geomorphology of Azokh Caves* (pp. 55–84). Dordrecht: Springer.

Evans, E. M., Van Couvering, J. A. H., & Andrews, P. (1981). Palaeoecology of Miocene sites in Western Kenya. *Journal of Human Evolution, 10*, 99–116.

Fernández-Jalvo, Y., King, T., Andrews, P., Moloney, N., Ditchfield, P., Yepiskoposyan, L., et al. (2004). Azokh Cave and Northern Armenia. In E. Baquedano & S. Rubio Jara (Eds.), *Miscelanea en Homenaje a Emiliano Aguirre* (Vol. IV, pp. 158–168). Museo Arqueologico Regional series, Arqueologıa. Alcala de Henares.

Fernández-Jalvo, Y., King, T., Andrews, P., Yepiskoposyan, L., Moloney, N., Murray, J., et al. (2010). The Azokh Cave complex: Middle Pleistocene to Holocene human occupation in the Caucasus. *Journal of Human Evolution, 58*, 103–109.

Gauch, H. G. (1989). *Mulltivariate analysis in community ecology*. Cambridge: University of Cambridge Press.

Kappelman, J. (1988). Morphology and locomotor adaptations of the bovid femur in relation to habitats. *Journal of Morphology, 198*, 119–130.

Kasimova, R. M. (2001). Anthropological research of Azykh Man osseous remains. *Human Evolution, 16*, 37–44.

Lyman, R. L. (1994). *Vertebrate Taphonomy*. Cambridge: Cambridge University Press.

Mamatsashvili, N. (1978) Palynologycheskoe izuchenie peshchernickh otlojenii In (Maruashvili LI.Ed) *Izuchenie Pescher Kolkhidi*. Tbilisi, Metsmereba. 94–127.

Mamatsashvili, N. (1987). *Paleolithic Verterbrata Fauna of the cave Tsona. Georgian Caves*. Tbilisi, V.ll. 92–100.

Manuk, V. (2010). Atlas of the Ngorno-Karabagh Republic. Stepanakert 2010.

Marin-Monfort, M. D., Cáceres, I., Andrews, P., Pinto A. C., & Fernández-Jalvo, Y. (2016). Taphonomy and site formation of Azokh 1. In Y. Fernández-Jalvo, T. King, L. Yepiskoposyan & P. Andrews (Eds.), *Azokh Cave and the Transcaucasian Corridor* (pp. 211–249). Dordrecht: Springer.

Mathews, T., & Parkington, J. (2006). The Taphonomy of the Micromammals from the Late Middle Pleistocene Site of Hoedjiespunt 1 (Cape Province, South Africa). *Journal of Taphonomy, 4*, 1–16.

Murray, J., Dominguez-Alonso, P., Fernández-Jalvo, Y., King, T., Lynch, E. P., Andrews, P., et al. (2010). Pleistocene to Holocene stratigraphy of Azokh 1 Cave, Lesser Caucasus. *Irish Journal of Earth Sciences, 28*, 75–91.

Murray, J., Lynch, E. P., Dominguez-Alonso, P., & Berham, M. (2016). Stratigraphy and sedimentology of Azokh Caves, South Caucasus. In Y. Fernández-Jalvo, T. King, L. Yepiskoposyan & P. Andrews (Eds.), *Azokh Cave and the Transcaucasian Corridor* (pp. 27–54). Dordrecht: Springer.

Ollivier, V., Nahapetyan, S., Roiron, P., Gabrielyan, I., Gasparyan, B., Chataigner, C., et al. (2010). Quaternary volcano-lacustrine patterns and palaeobotanical data in southern Armenia. *Quaternary International, 223–224*, 312–326.

Parfitt, S. (2016). Rodents, lagomorphs and insectivores from Azokh Cave. In Y. Fernández-Jalvo, T. King, L. Yepiskoposyan & P. Andrews (Eds.), *Azokh Cave and the Transcaucasian Corridor* (pp. 161–175). Dordrecht: Springer.

Rowe, J. S. (1956). Uses of undergrowth plant species in forestry. *Ecology, 37*, 463–473.

Scott, L., Rossouw, L., Cordova, C., & Risberg, J. (2016). Palaeoenvironmental context of coprolites and plant microfossils from

Unit II. Azokh 1. In Y. Fernández-Jalvo, T. King, L. Yepiskoposyan & P. Andrews (Eds.), *Azokh Cave and the Transcaucasian Corridor* (pp. 287–295). Dordrecht: Springer.

Sevilla, P. (2016). Bats from Azokh Caves. In Y. Fernández-Jalvo, T. King, L. Yepiskoposyan & P. Andrews (Eds.), *Azokh Cave and the Transcaucasian Corridor* (pp. 177–189). Dordrecht: Springer.

Van der Made, J., Torres, T., King, T., & Fernández-Jalvo, Y. (2016). The new material of large mammals from Azokh and comments on the older collections. In Y. Fernández-Jalvo, T. King, L. Yepiskoposyan & P. Andrews (Eds.), *Azokh Cave and the Transcaucasian Corridor* (pp. 117–159). Dordrecht: Springer.

Vekua, A. (1962). *Akhalkalakskaia nijnepleistotsenovaia fauna Mlekopitaiushikh*. Metsmereba: Tbilisi.

Vekua, A. (1987). The Lower Pleistocene Mammalian Fauna of Akhalkalaki. *Palaeontographia Italica, 74*, 63–96.

Vekua, A., & Lordkipanidze, D. (1998). The Pleistocene palaeoenvironment of the Transcaucasus. *Quaternaire, 9*, 261–266.

Whittaker, R. H. (1948). *A vegetation analysis of the Great Smokey Mountains.* PhD dissertation, University of Illinois, Urbana.

Zelikson, E., & Gubonina, Z. (1985). Cmeshenie Visotnoio Poiastnosti kak Osnova Pekonstuktsii Klimaticheskikh Izmenenii (vE dG)o.r Mniketho dSit rPaenkaoknhs.t rIunk Vtsenli cpkaole oAk. *liSmeraetborvi.a nMnoi skLv.,a .G uNratuokvaa*.i a 2E9-.38.

Chapter 16
Appendix: Dating Methods Applied to Azokh Cave Sites

Yolanda Fernández-Jalvo, Peter Ditchfield, Rainer Grün, Wendy Lees, Maxime Aubert, Trinidad Torres, José Eugenio Ortiz, Arantxa Díaz Bautista, and Robyn Pickering

Abstract Dating is basic for archaeological and paleontological investigations and results of different dating methods used in Azokh caves are described in this chapter. Fossils from Azokh were not dated by any method previously. Lithic technology and taxonomy suggested a middle Pleistocene age for Unit V (from where Acheulian industries and a human mandible fragment were recovered) while Units III and II yielded Mousterian industries indicating middle Paleolithic ages. Dates from Azokh by Electron Spin Resonance (ESR) previously published elsewhere were given before final calculations and they slightly differ from those given in this Appendix, which are the definitive dating results.

Y. Fernández-Jalvo (✉)
Museo Nacional de Ciencias Naturales (CSIC), José Gutiérrez Abascal, 2, 28006Madrid ES, Spain
e-mail: yfj@mncn.csic.es

P. Ditchfield
Research Laboratory for Archaeology and the History of Art, University of Oxford, Dyson Perrins Building, South Parks Road, Oxford, OX1 3QY, UK
e-mail: peter.ditchfield@rlaha.ox.ac.uk

R. Grün · W. Lees · M. Aubert
Research School of Earth Sciences, The Australian National University, Canberra, ACT 2601, Australia
e-mail: Rainer.Grun@anu.edu.au

T. Torres · J.E. Ortiz · A.D. Bautista
Biomolecular Stratigraphy Laboratory (BSL), E.T.S.I. Minas, Polytechnical University of Madrid, Rios Rosas 21, 28003 Madrid, Spain
e-mail: trinidad.torres@upm.es

J.E. Ortiz
e-mail: joseeugenio.ortiz@upm.es

A.D. Bautista
e-mail: arantxa.diaz@gcpv.com

R. Pickering
School of Earth Sciences, University of Melbourne, Parkville, Melbourne, VIC 3010, Australia
e-mail: r.pickering@unimelb.edu.au

Резюме Датировка является важнейшим этапом археологических и палеонтологических исследований, и в данном разделе описаны результаты различных техник датировки, использованных для Азохской пещеры. Находки из Азоха ранее не были датированы каким-либо методом. Технология получения каменных орудий и таксономия фауны указывают на среднеплейстоценовый возраст подразделения *V* (где были найдены ашельские орудия и фрагмент нижней челюсти человека), в то время как подразделения *III* и *II* с мустерианской индустрией имеют среднепалеолитический возраст. Датировки Азоха методом электронного спинового резонанса (ЭСР), ранее опубликованные в литературе, были получены до проведения завершающих вычислений и потому они немного отличаются от представленных в этом приложении, являющихся окончательными оценками. Результаты ЭСР и метода рацемизации указывают на возраст около 300 тыс. лет для находок из подразделения *V*, в то время как техника ЭСР для поверхностных горизонтов плейстоценовых седиментов в *Азох 1* дает оценку около 100 тыс. лет.

Серия изотопов урана была использована для датировки спелеотема из маленьких цельных камер во фронтальной и самой нижней секциях *Азох 1*. Возраст спелеотема оказался в пределах 1,19 ± 0,08 млн. лет. Это является минимальной оценкой времени зарождения самой пещеры, подтверждая древность отложений и указывая на возможность существования более ранних слоев со следами заселения.

Датировка методом ^{14}C была использована для наиболее молодых отложений. Современные останки, найденные в подразделении *2* пещеры *Азох 2*, имели надежную датировку между 670 и 805 гг. н.э. Радиоуглеродная датировка древесного угля, обнаруженного рядом с современным зубом в подразделении *A* пещеры *Азох 5*, старше и имеет возраст от 722 до 384 гг. до н.э., в то время как верхняя поверхность седиментов в *Азох 5* имеет возраст между 126 и 178 гг. н.э.

Yolanda Fernández-Jalvo et al. (eds.), *Azokh Cave and the Transcaucasian Corridor*, Vertebrate Paleobiology and Paleoanthropology, DOI 10.1007/978-3-319-24924-7_16

Keywords Dating methods • Radiocarbon • Electron Spin Resonance (ESR) • Racemization • Uranium-Lead (U-Pb) dating

Introduction and Summary (Yolanda Fernández-Jalvo)

Dating is basic for archaeological and paleontological investigations, and results of the different dating methods used in Azokh caves are especially relevant. Fossils from Azokh have not been previously chronometrically dated by any method. Lithic technology and taxonomy suggested a Middle Pleistocene age for Unit V (from where Acheulian industries and a human mandible fragment were recovered) while Units III and II yielded Mousterian industries, indicating Middle Paleolithic ages (Lioubine 2002). Dates from Azokh by Electron Spin Resonance (ESR), previously referred to by Fernández-Jalvo et al. (2010), were published before final calculations, and revised dates are given in this Appendix, in Table 16.1.

Previous archaeological work conducted before the 1980s in the cave removed most sediments from the Azokh 1 site. Excavations performed since 2002 have focused on the undisturbed sediments located at the back of the cave, about 40 m from the open air connection. Most sediment infill of this cave system has been deposited from the interior towards the exterior (Murray et al. 2016). The location of the excavation area and the internal origin of sediments restrict the application of some methods based on cosmic radiation to obtain dates for fossils contained in these sediments. Two of these methods are optically stimulated luminescence (OSL) and thermoluminiscence (TL). These are dating methods determining the time elapsed since the crystalline mineral contents in sediments (e.g., quartz, feldspars) were last exposed to sunlight ('zeroing' event). In the case of TL, clock resetting also occurs when materials are exposed to heating (e.g., burnt flint, ceramics or lava). The age is determined by measuring the amount of radiation per unit time (dose) that the sample was exposed to sunlight (and/or fire in the case of TL). Samples from Azokh 1 could not be dated by OSL or TL due to the distance from the open air and lack of exposure to the sun or fire.

Radiocarbon

Radiocarbon dating has been applied to the youngest sediments recorded in the Azokh sites (see Sect. 16.2 below). This method is based on radioactive decay of the isotope ^{14}C, which provides highly reliable dates (Weiner 2010). The use

Table 16.1 Total samples submitted for dating from Azokh cave sites (* dismissed dating)

	Lab no.	Site-unit	Depth (cm)	Fossil label	Type of sample	Dating	
^{14}C dating (yr)	P20071	Azokh1-I	110	E51 #60	Bone	Failed	
	P23186/OxA19424	Azokh1-I	141	D51 #3	Charcoal		157 ± 26*
	P21735	Azokh1-I	213	D52 #26	Bone	Failed	
	P23187	Azokh1-I	219	D51 #4	Bone	Failed	
	P16418/OxA14316	Azokh1-III	435	D46 #159	Charcoal		>62,600*
	P16419/OxA14317	Azokh1-III	441	D45 #31	Charcoal		>62,100*
	P27704	Azokh2-1	29	N11 #18	Charcoal	Failed	
	P27705/OxA22888	Azokh2-1	31	N11 #11	Charcoal		268 ± 22*
	P28298/OxA23540	Azokh2-1	31	N11 #13	Bone		167 ± 24*
	P28298B/OxA23541	Azokh2-1	31	N11 #13	Bone		165 ± 23*
	P28299/OxA23542	Azokh2-1	31	N11 #14	Bone		122 ± 23*
	P27706	Azokh2-1	32	N11 #16	Charcoal	Failed	
	P21734/OxA18875	Azokh2-1base	100	O11 #1	Bone		1265 ± 23
	P28300B/OxA23544	Azokh5-A	645	M48 #154	Bone		1896 ± 26
	P28300/OxA23543	Azokh5-A	649	M48 #153	Bone		1941 ± 26
	P28297/OxA23364	Azokh5-A	650	M48 #121	Charcoal		1214 ± 23
	P20070/OxA17589	Azokh5-A	1071	M19 #14	Charcoal		2366 ± 35
	P21264	Azokh5-A	1122	M19 #31	Bone	Failed	
ESR dating (kyr)	2668A	Azokh1-II	247	I49 #19	M1 from bear mandible		100 ± 7
	2668B	Azokh1-II					110 ± 6
	2387	Azokh1-II	296	E48 #120	Bear canine	Failed	
	2689A	Azokh1-II	323	D46 #7	Bear molar		130 ± 13
	2689B	Azokh1-II					138 ± 11
	2690	Azokh1-II	335	C46 #376	Bear canine	Failed	

(continued)

Table 16.1 (continued)

	Lab no.	Site-unit	Depth (cm)	Fossil label	Type of sample	Dating	
	2692A	Azokh1-II	345	C46 #360	Bear molar		162 ± 16
	2692B	Azokh1-II					165 ± 32
	2386	Azokh1-II	348	D45 #19	Suid canine	Failed	
	2383	Azokh1-II	333–365	Non-coord.	Bear molar		184 ± 13
	2691A	Azokh1-IV	555	D45 #54	Bear molar		205 ± 16
	2691B	Azokh1-IV					216 ± 18
	2384	Azokh1-Vm	830	E41 #2	Deer premolar		195 ± 13
	2388	Azokh1-Vm	833	E41 #1	Bear premolar		No ESR analysis
	2382a	Azokh1-Vm	846	E42 #11	Deer premolar		271 ± 22
	2382b	Azokh1-Vm					258 ± 27
	2380	Azokh1-Vm	848	E39 #6	Bear molar		293 ± 23
	2381	Azokh1-Vm	850	E39 #7	Bear premolar		No ESR analysis
	2385	Azokh5/ B	Taken from the section		Mandible of sheep	Failed	
Racemization dating (kyr)	8005	Azokh1-II	240	F51 #26	Bear molar		97*
	8293	Azokh1-II	292	C46 #88	Bear lower canine		175
	8294	Azokh1-II	319	C46 #294	Bear lower molar M2		242
	8006	Azokh1-II	323–388	Rescue	Bear incisor		166
	8004	Azokh1-II	323–388	Rescue	Bear incisor		134
	8295	Azokh1-II	335	C46 #376	Bear tooth fragment		189
	4687	Azokh1-II	343	D46 #84	Bear upper canine,		228
	4684	Azokh1-II	347	D45 #30	Bear lower canine		165
	4686	Azokh1-II	353	D46 #70	Bear upper incisor I3	Failed	
	4685	Azokh1-II–III	394	D45 #17	Bear lower incisor I2	Failed	
	4490	Azokh1-II	Rescue	RC45 #7	Bear upper incisor I3	Failed	
	4491	Azokh1-II	Fallen	E42 #2	Bear lower incisor I2	Failed	
	4689	Azokh1-II	Rescue	RD45 #20	Bear lower incisor I3	Failed	
	4688	Azokh1-III	435	D46 #154	Bear upper incisor I3		356*
	8292	Azokh1-IV	549	D45 #33	Bear tooth fragment		138
	4416	Azokh1-IV	534–555	Gen.finds	Bear upper incisor I3		272*
	4683	Azokh1-Vm	816	D42 #8	Bear upper molar		202
	4414	Azokh1-Vm	822	F42 #1	Bear canine		266
	4415	Azokh1-Vm	822	F42 #1b	Bear upper incisor I3		504*
	Lab no.	Site-unit	Depth (cm)	Fossil label	Type of sample	Dating	
U-Pb dating (Ma)	UniMelb_A1	Near V1	N/a	N/a	Speleothem	Failed	
	UniMelb_A2	~2.2 m into the cave	N/a	N/a	Speleothem		1.19 ± 0.08 Ma

of accelerator mass spectrometry (AMS) has greatly reduced the amount of sample needed, has increased the precision of radiocarbon dating and extended the limit of this method up to 60 ka. Dates obtained through radiocarbon methods are expressed as years ^{14}C BP (uncalibrated radiocarbon years before present, considering 'present' as 1950). This is based on the assumption that the atmospheric carbon concentration has always been the same since 1950. Radiocarbon dates can be calibrated by dendrochronology, together with the Intcal 09 calibration data set (Reimer 2009). Plots obtained from calibration confirm the validity of the results obtained and provide an accurate crosscheck (Fig. 16.1). These plots show a double set of curves. The left hand axis (Y-axis) shows the radiocarbon concentration curve with a precision of ±30 to 20 years error (see Table 16.1, ^{14}C dating) expressed in years BP (before present). The bottom axis (X-axis) shows the calibration curves given as an age range of possible dates expressed in cal [k]BP, calAD or calBC (calibrated or calendar years). The results of calibration in these plots are expressed as a percentage of confidence.

The material to be dated by radiocarbon includes all organic matter, burnt or not, such as vegetal remains (charcoal or seeds) as well as fossil bone. However, the carbon-oxygen bond is relatively fragile, and re-crystallization and incorporation of exogenous ions into the mineral phase of the originally calcified tissues can occur during fossilization (Lee-Thorp 2002).

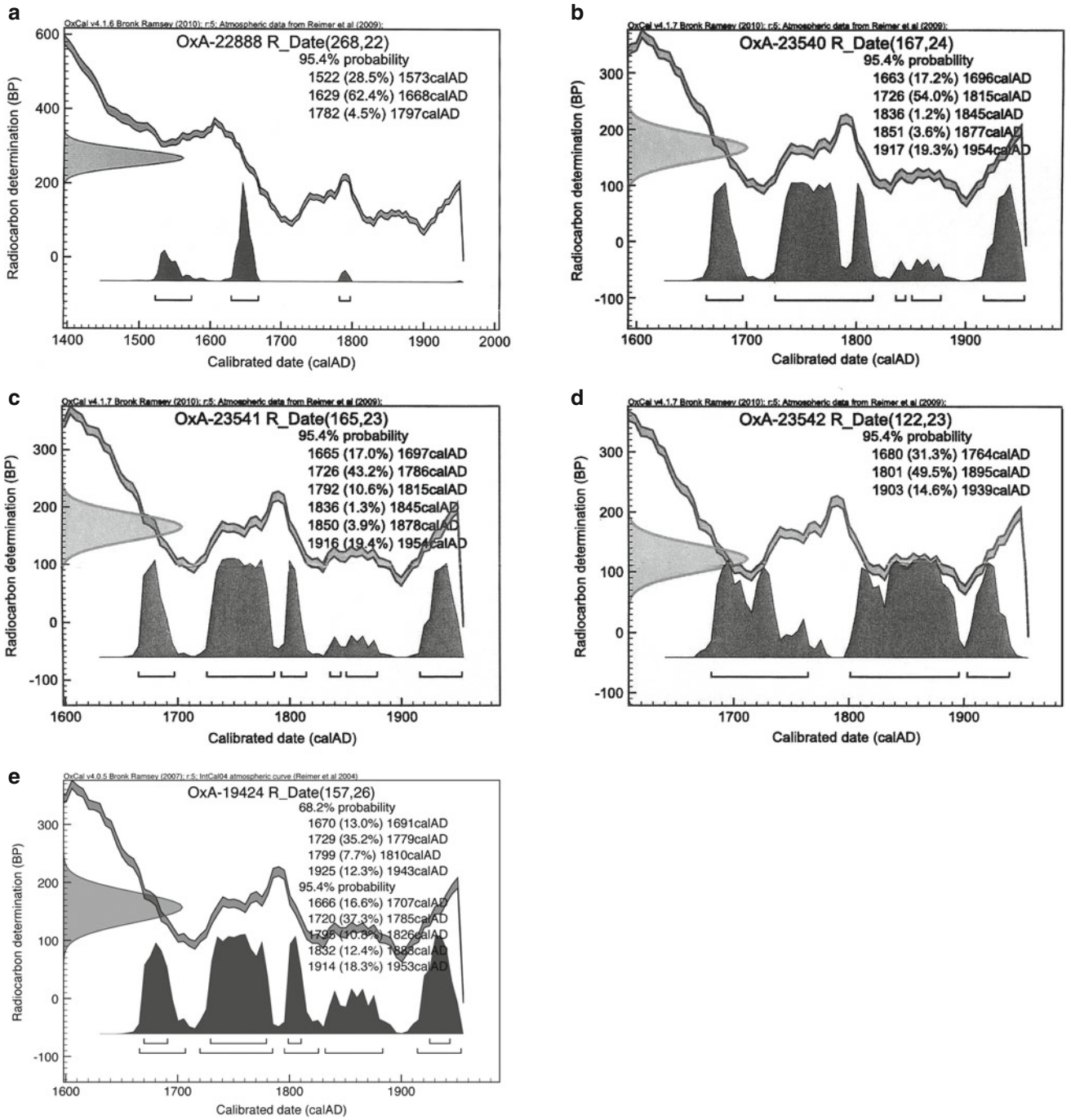

Fig. 16.1 Radiocarbon calibrated plots of different dated samples from Azokh sites for which ages are too young for radiocarbon methods to provide a valid dating. In these cases, calibrated dates become older than the radiocarbon age obtained

As a result, carbon-containing minerals are rarely dated (Weiner 2010), but carbon from collagen in bones is frequently dated by radiocarbon. In the case of Azokh 1, the bone materials did not contain enough carbon to be dated by radiocarbon, probably due to the action of bat guano (see Smith et al. 2016). Charcoal was the only possible material that did not fail from Azokh 1. However, results from Unit I are too young and those from Unit III are too old for radiocarbon dating (Table 16.1).

Valid results were obtained from Azokh 2 (Unit 2) that gave an age between 670 and 805 years calAD. This site is close to the cave entrance (Murray et al. 2016), so that bat guano has not affected the results. Both vegetal and bone material from Unit 1 are too young to date (as was the case with those of Unit I from Azokh 1).

The Azokh 5 site has provided good radiocarbon dating results both for bone and charcoal. AZK14 (OxA 17589) is a

charcoal fragment sampled from a small 1 × 2 m test trench made from Unit A up to Unit E in the cave wall sedimentary section. AZK14 charcoal was found at the same height as and next to modern human teeth found in Unit A Azokh 5 (King et al. 2016). Charcoal AZK14 (OxA 17589) yielded an age between 722 and 384 years calBC. The bone was not affected by guano. These excavations, and especially the section located near the cave wall, are protected from bat guano deposition. Results obtained from bone (OxA 23543 and OxA 23544) recovered from the excavation on top of the sequence have a likely age between 126 calAD and 178 calAD (see Fig. 16.2). Charcoal (OxA 23364) gave an age between 715 and 888 years calAD, which may suggest possible contamination.

Uranium Series

Uranium series dating has also been applied to fossils from Azokh. The effective dating range of this method is between 1,000 to 350,000 years, but it can be extended (if the range of error is acceptable) to ~400–500 ka. This method is based on radioactive decay of uranium series isotopes ($^{230}Th/^{234}U$, $^{234}U/^{238}U$). Uranium, relatively soluble, is originally incorporated into the sample when the material (bone or stone) is formed, and thorium is incorporated into the sample with time. The ratio of uranium/thorium is then a direct measurement of the time elapsed since the sample formed. The most reliable material to date is cave speleothem, but so far the only one found developed in Azokh 1 is in a small chamber located at the front of the Azokh 1 cavity which was discovered in 2009 (see Sect. 16.5 below). Fossils (bones or teeth) have traditionally been considered to be unreliable due to their facility to uptake exogenous uranium after burial (Pike et al. 2002). In addition, uranium can be leached out of a bone, but not thorium, leaving a thorium excess leading to overestimated U-series dates. This, however, can be corrected using a diffusion-adsorption model (Millard and Hedges 1996) based on the geochemical context of bone-uranium-burial environment interactions (Pike et al. 2002). Initial dating by this method on fossil bones on the surface of Unit Vm in Azokh 1 gave ages between 191 +68/–36 ka and 186 +91/–48 ka. Simultaneously, results obtained by electron-spin resonance (ESR) as well as by racemization methods indicated an age ca. 300 ka for contemporaneous fossils. Although it is our intention to continue dating by this method, we need to come to a better understanding of the diagenetic and microgeomorphological processes operating in the cave to better understand the burial environment of the site. This is especially relevant as results from ESR methods indicate anomalies that could be explained by some U-leaching influenced by guano or fossil reworking (see Sects. 16.3 and 16.4 below). Reworking, however, has been shown by taphonomic analyses not to have altered these fossil bones (Marin-Monfort et al. 2016).

As well as U-Th dating, Uranium-Lead (U-Pb) dating was used to attempt to determine the age of the speleothem deposits, in this case, stalagmites, in the cave. As outlined above, U-Th dating is useful for ages up to about 400 ka, beyond which the Th isotopes themselves have decayed away. U-Pb dating uses stable Pb istopes at the end of the U-series decay chain and has recently been successfully applied to speleothem (cave) carbonates from a few hundred thousand years (Richards et al. 1998) to material of several million years (Woodhead et al. 2006). Speleothem samples for U-Pb dating were collected from a large stalagmite boss near the entrance of the cave and from a number of small stalagmites situated at the very back of the cave. Initial attempts at dating Azokh cave speleothem were unsuccessful given the high Pb content of the material. A second attempt using cleaner, clearer calcite provided an age of 1.19 ± 0.08 Ma (see Sect. 16.5 below). This is currently the oldest age for any material from the Azokh Cave Complex and gives a minimum age for the formation of the cave itself. This opens up the possibility for the presence of older occupation layers.

ESR

Electron-spin resonance (ESR) dating was applied to several samples from Azokh 1 (see Sect. 16.3 below). This method is based on determining the natural radiation dose to which a sample has been exposed during its burial period. The sources of radiation are mainly from uranium and thorium in the sample itself, and from the radioactive isotopes of uranium, thorium and potassium in the surrounding sediment (Grün 2006). The most reliable material is tooth enamel because hydroxyapatite crystals are larger and more stable and closely packed than in bone. Modern enamel does not contain uranium, which is incorporated in the enamel crystals after burial, and uptake depends on the manner by which uranium enters into the enamel. Natural radiation generates new free radicals, trapped electrons and holes. The signal of the sample is called the natural intensity, which is dependent on the number of traps, the strength of the radioactivity (dose rate, D) and time (Grün 2006). To obtain a date, the fossil tooth is processed together with sediment underneath it. Dating of tooth enamel has been recognized as a useful tool for chronometric dating in the time range beyond the limit of radiocarbon and up to at least 2 Ma (Schwarcz et al. 1994).

Pleistocene fossils from Azokh 1 were dated by ESR (see Sect. 16.4 below). Six of these samples failed because the enamel was not thick enough. This happened for all bear canines and two bear premolars. Sample 2691 has been recovered from the base of Unit IV, close to the contact with

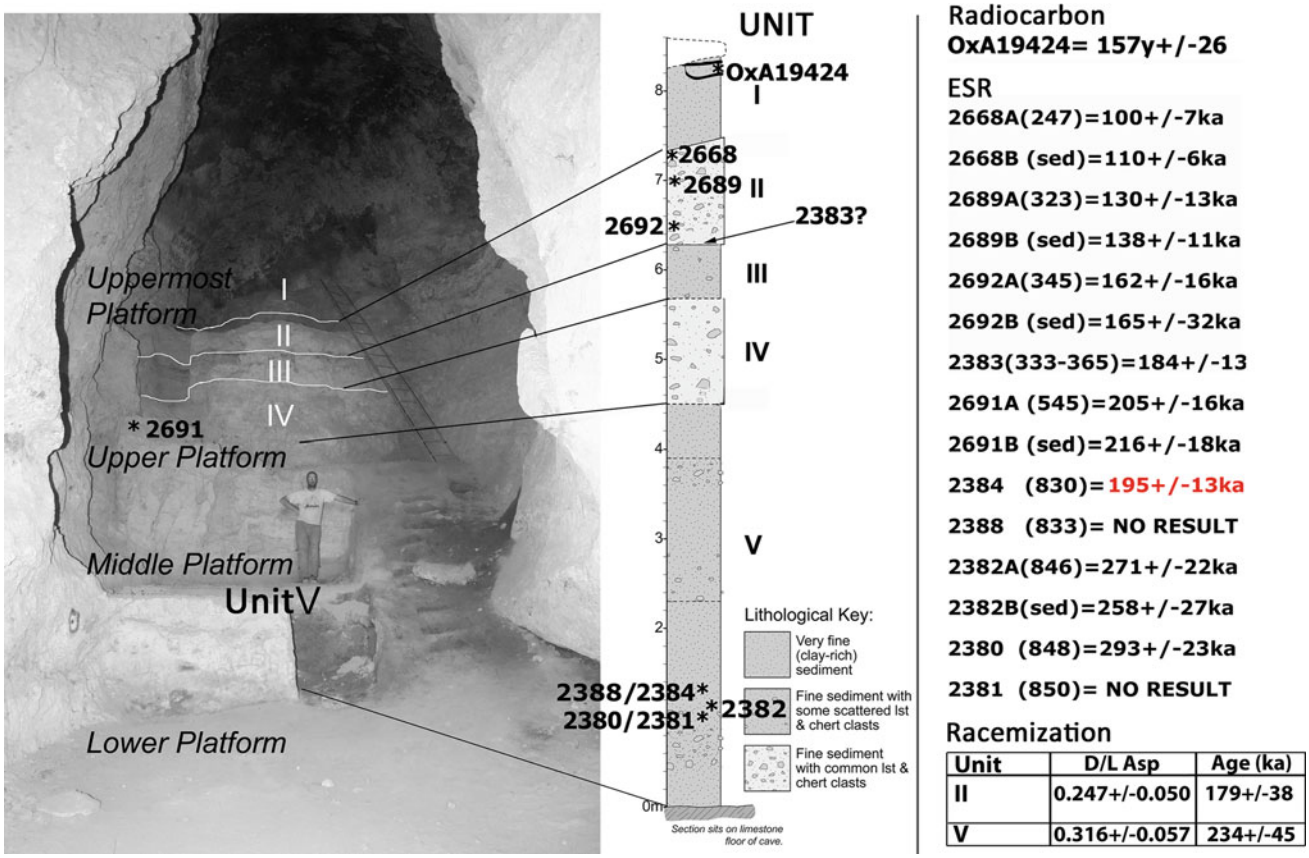

Unit	D/L Asp	Age (ka)
II	0.247+/-0.050	179+/-38
V	0.316+/-0.057	234+/-45

Fig. 16.2 Summary figure of dates obtained in Azokh 1 site by radiocarbon, ESR and racemization methods in stratigraphic position and referred to platforms (uncoventional field names applied to sampling/excavation areas before geological work established definitive stratigraphical units). An ESR date (2691) of 205 ± 16 ka has been calculated for the general area of the contact between the top of Unit V and the base of Unit IV (close to the contact with Unit Va described by Murray et al. 2016). Radiocarbon dating (OxA19424) of Unit I is not methodologically reliable dating, because the radiocarbon age is too recent. Ceramics and domestic animals recovered from Unit I indicate recent age for this unit

Unit V (equivalent to the top of Vu). Unit III has not yielded teeth with sufficient enamel thickness to be dated. A mandible of sheep from the section of Azokh 5, Unit B, was also processed, but dating failed. Results obtained by ESR have provided dates that are congruent with depth (Fig. 16.2). There is, however, an exception for sample 2384 (Table 16.1), which has given a younger age than the preceding and subsequent stratigraphically ordered samples. Once the depths of partial excavation Z coordinates have been referred to the datum, consecutive age results obtained by ESR according to depth support the lack of reworking processes involved in the site formation of Azokh 1.

Amino-acid Racemization

Racemization dating (see Sect. 16.4 below) measures the decay rate of protein amino acids in past living organisms. These amino acids can have two different chiral forms (mirror images of each other), of which left-handed (levo, or L) is the condition when the organism was living. Once the organism dies the amino acids slowly turn into right-handed (dextro or D) amino acids until equilibrium is reached. This process is called amino acid racemization. The D/L ratio can be used for dating up to the time of equilibrium (D/L ∼1) (Fernández et al. 2009). Racemization is a chemical process that is highly temperature dependent and occurs faster under warmer conditions. These effects restrict the application of racemization and usually requires comparison with other dating methods. Diagenetic studies by Smith et al. (2016) indicate that collagen is generally absent from the Azokh fossil bones. However, racemization dating has provided ages that overlap the ESR dates (Fig. 16.3). This may result from sampling for racemization which uses dentine covered by enamel, and this may protect collagen at these particular areas from the destructive diagenetic effects observed in Azokh 1 due to bat guano (Marin-Monfort 2016). This explanation, however, needs further investigation.

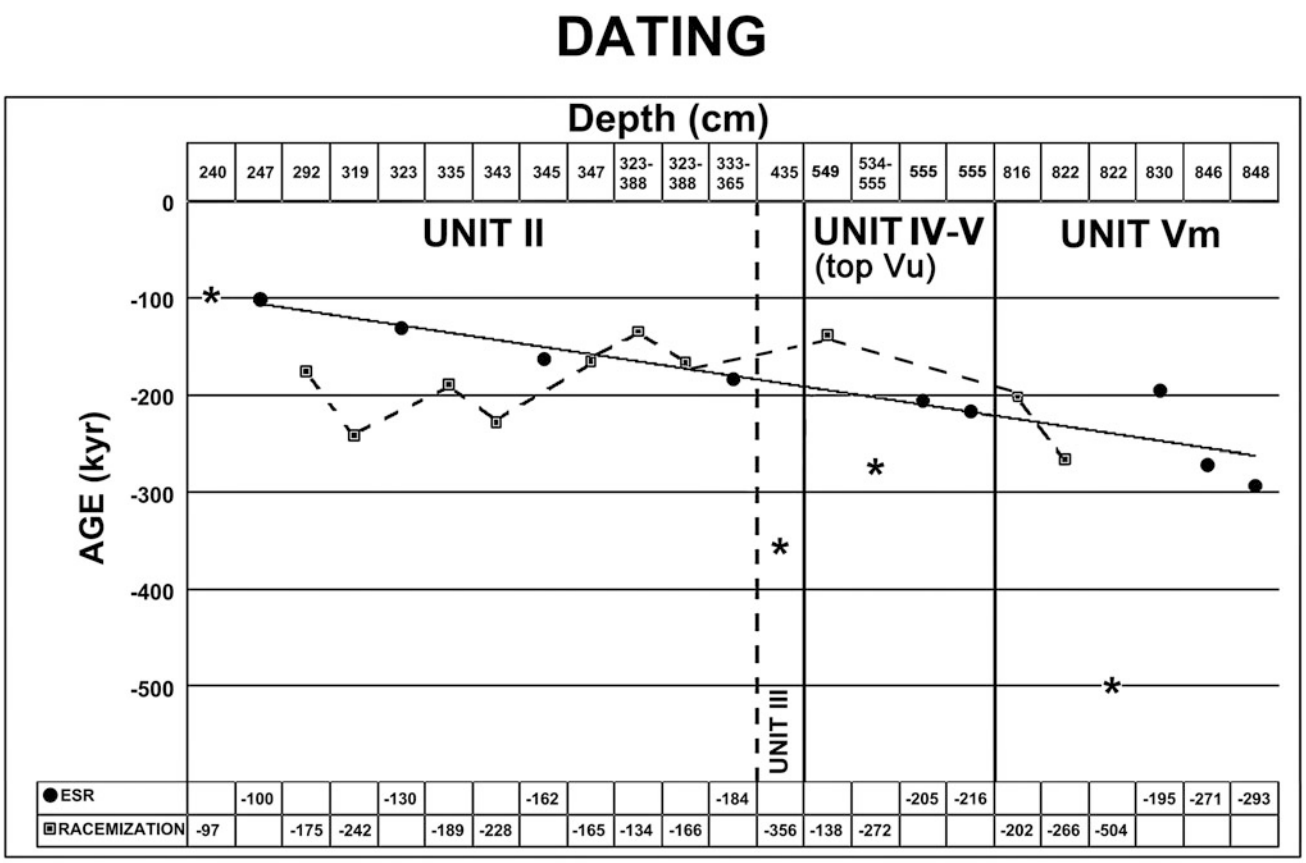

Fig. 16.3 Comparison of ESR dates and racemization results (bottom charts) according to depth (top chart in cms) from Azokh1 site. Samples marked with an asterisk (*) were not considered for the age calculation because of their high deviation from mean values

Radiocarbon Dating of Samples from the Azokh Cave Complex (Peter Ditchfield)

A total of 18 samples from the Azokh Cave Complex have been submitted for radiocarbon dating by AMS at Oxford Radiocarbon Accelerator Unit (ORAU), the details of which are listed in Table 16.1. These consisted of nine charcoal samples and nine bone samples from Azokh 2. Six of the twelve samples (four bones and two charcoal samples) failed during pre treatment and yielded no datable material. Ten of the samples yielded finite ages ranging from 2366 ± 35 to 122 ± 23 ^{14}C BP (Before Present – AD 1950). Two charcoal samples yielded dates greater than 62,000 ^{14}C BP.

Pretreatment and Measurement

Chemical pretreatment, target preparation and AMS measurement of the samples were carried out by standard methods employed at ORAU. Details of the current pretreatment methods used at ORAU can be found in Brock et al. (2010) and are briefly summarized below.

Collagen was extracted from bone samples using a sequential acid-base-acid wash at room temperature consisting of 0.5 M hydrochloric acid (3 washes over approx. 18 h), 0.1 M sodium hydroxide (30 mins) and 0.5 M hydrochloric acid (15 mins), with thorough rinsing with ultrapure (Milli-Q) water after each step. The crude collagen was gelatinized at 75 °C and pH3 for 20 h. The gelatin solution was filtered using a 45–90 micron Eezi-filter™ and then ultrafiltered using a Vivaspin™ 15–30 kD MWCP ultrafilter.

Charcoal samples underwent a similar acid-base-acid pre-treatment of 1 M hydrochloric acid (~20 mins or until effervescence has finished), 0.2 M sodium hydroxide (20 mins) and 1 M hydrochloric acid (1 h) at 80 °C.

The samples were then freeze-dried before being combusted and the resulting carbon dioxide collected cryogenically and graphitized prior to AMS dating, as described by Brock et al. (2010). For details of the target preparation and AMS measurement see Bronk Ramsey et al. (2004a, b, c).

Calibration

Of the twelve samples that yielded radiocarbon dates, two were "greater than" ages, and five were relatively recent. Thus there are only five dates where calibration is either possible or appropriate. These are samples AZK14 (**OxA 17589**), No. 121 (**OxA 23364**), No. 153 (**OxA 23543**, **OxA23544**) and Sample 1 (**OxA 18875**). The latest is a bone fragment from Azokh 2, the rest are from Azokh 5 (top of the series, i.e. Unit A). These were calibrated using the OxCal calibration program version 4.1.6 (Bronk Ramsey 2010) and the Intcal 09 calibration data set. The calibration plots of these samples are shown in Figs. 16.4 and 16.5.

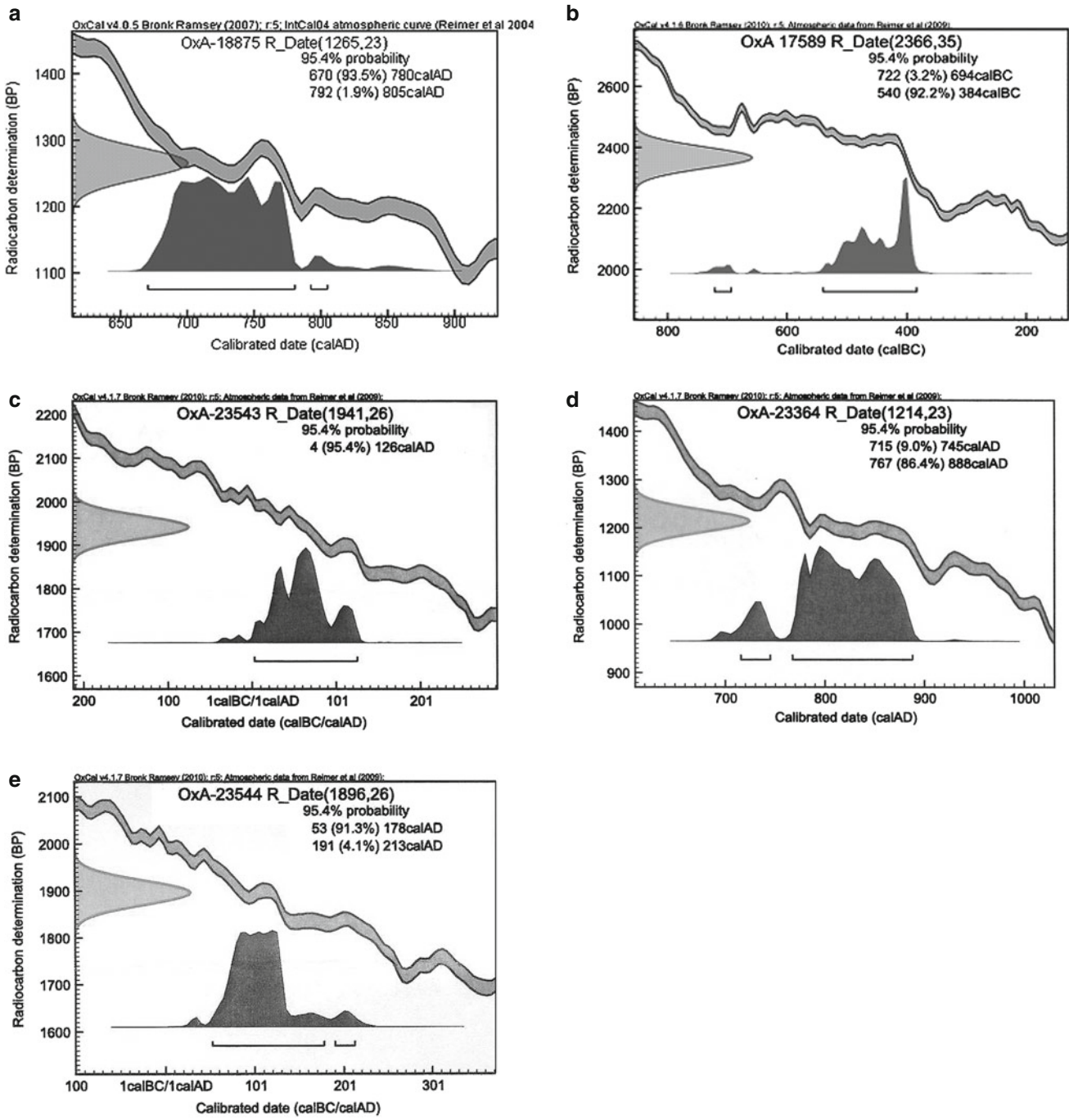

Fig. 16.4 Radiocarbon calibrated plots of different dated samples from Azokh sites where calibration is either possible or appropriate. The number of possible ages provide 95% confidence

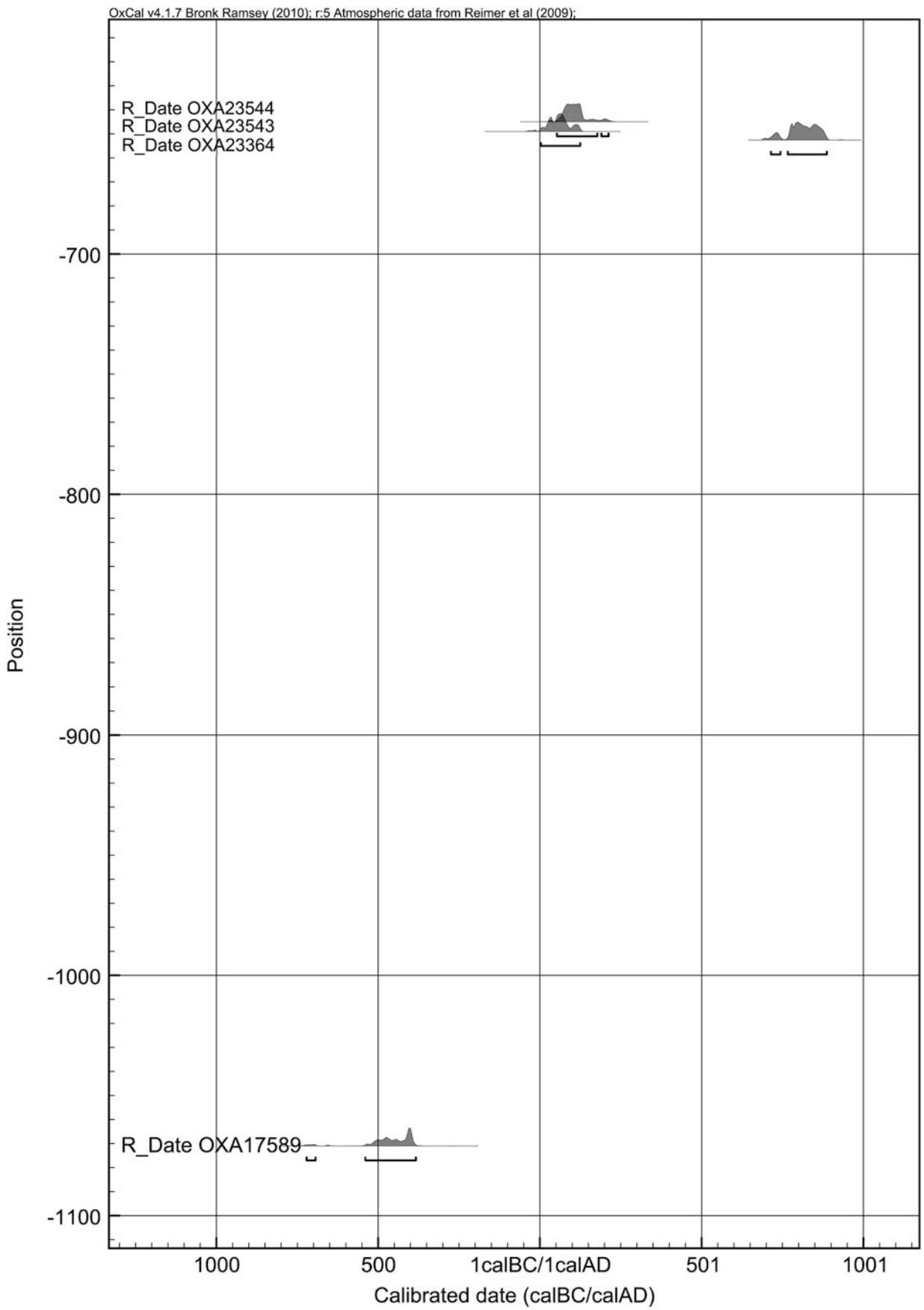

Fig. 16.5 Azokh 5 radiocarbon calibrated plots arranged by depth. This plot makes the point that sample OxA 23364 (charcoal) is well out of the dating sequence. The two bones (OxA 23544 and OxA 23543), recovered from similar depth as the OxA 23364 charcoal, provide a more consistent age. The deepest specimen (charcoal OxA 17589) gives the oldest age 540 cal BC for the base of unit A

Electron Spin Resonance (ESR) Dating (Rainer Grün, Wendy Lees, Maxime Aubert)

All samples were collected *in situ* and submitted by the excavators along with sediment directly attached to the samples. The dating procedures followed those routinely applied in the ANU ESR dating laboratory. From each tooth, an enamel fragment with attached dentine was removed and analysed for uranium and thorium using laser ablation ICP-MS (Eggins et al. 2003, 2005). The sediments were analysed for U, Th, and K by solution ICP-MS (Genalysis, Perth). For ESR dose analysis, the enamel was powdered and successively irradiated in 24 steps to 3188 Gy (samples 2380, 2382, 2383, 2384, in 2007) and 16 steps to 1839 Gy (2668, 2689, 2691 and 2692, in 2009). Radiation doses were monitored with alanine dosimeters and evaluated against a calibrated dosimeter set (A. Wieser, Messtechnik, München). Dose values were obtained fitting the natural spectrum back into the irradiated ones (Grün 2002).

For the calculation of the internal dose rate values, the beta attenuation values of Marsh (1999) and an alpha efficiency of 0.13 ± 0.02 (Grün and Katzenberger-Apel 1994) were used. No in-situ gamma spectrometric measurements were carried out. Considering that about 50% of the gamma dose rate is generated by the 5 cm surrounding of the sample (Aitken et al. 1985), the gamma dose rate was calculated to 50% from the sediment attached to the sample and to 50% from the average of all sediment samples from that particular bed. A time averaged water content of 15 ± 5 was assumed for the sediments. Age calculations were carried out with the ESR-DATA program (Grün 2009a). The ESR results are presented for early U-uptake (EU) as well as combined U-series/ESR. In most cases it was not possible to use the p-value system for combining the U-series and ESR data sets (Grün et al. 1988). Instead, ages were calculated according to the closed system U-series (CSUS) ESR system (Grün 2000), which is more robust and allows solutions when U-leaching occurs. Because most EU-ESR and closed system U-series ages were quite close, the choice of the U-uptake model was not critical (Grün 2000). At most archaeological sites, faunal samples experience delayed U-uptake (Grün 2009b). Here, the EU-ESR age presents the minimum age estimate, and the CSUS-ESR result the maximum possible. However, when U-leaching may have occurred (see below), the EU-ESR age is a maximum age estimate and the CSUS-ESR result gives an indication of the age overestimate.

Results and Discussion

All analytical data are listed in Table 16.2, sorted according to the depth in the profile. The only non-provenanced sample is 2383. The four digit sample numbers indicate an individual tooth, A and B repeat analyses on the same tooth, but on different enamel pieces.

Surprisingly, the EU ESR results of all provenance samples are in stratigraphical order because at most cave sites reworking of teeth leads to a large scatter in the ESR results. However, there are some problems. Some of the U-series results, particularly from Unit II are older than the EU ESR results. This is only possible, if either some U-leaching has occurred in the samples, or if they were reworked from other layers with a lower environmental dose rate. If leaching has occurred (perhaps influenced by guano), the CSUS calculation gives an indication of how strongly the age results were affected by this process. If the samples were reworked any assumption of when they were incorporated into Unit II, i.e. when Unit II was formed, is pure conjecture. The base of Unit II seems to have been deposited during MIS 6. If the teeth below Unit II were deposited in-situ, the contact between Units IV and V has an age of around 200 ka, and Unit Vm was deposited between ~200 and ~300 ka.

Amino Acid Racemization Dating of Fossil Bears from Azokh 1 (Trinidad Torres, José Eugenio Ortiz, Arantxa Díaz Bautista)

Introduction

The amino acid racemization dating method is based on a chemical reaction (racemization) which allows the establishing of aminozones that reasonably have the same age (isochronous). If independent (radiometric) datings are available, it is possible to calibrate amino acid racemization analysis results and to use the method as a numerical dating system.

In general terms, cave bear localities are the best sites for sampling because they are clean, and the cavern's thermal history did not show strong variations, with average temperatures moderately low (Torres et al. 2003). In a recent experiment the winter-summer temperature variation within the cave sediment at 30 cm deep was 0.5 °C. Outstanding amounts of amino acids were found in bear dentine samples with ages ranging from 10,000 to more than 300,000 years (Torres et al. 1999).

Table 16.2 ESR (part 1)

ESR (part 1)

Lab no.	Unit	Depth (cm)	De (Gy)	De-error (Gy)	U-Enamel (ppm)	Error	U-Dentine (ppm)	Error	R48	Error	R04	Error	App U-series (ka)
2668A	Unit II	247	192	7	0.38	0.08	4.2	0.3	1.2015	0.0194	0.7664	0.0332	148
2668B			207	4									
2689A	Unit II	323	300	18	0.18	0.05	17.1	1.3	1.328	0.0081	0.9152	0.0116	215
2689B			307	13									
2692A	Unit II	345	355	23	0.47	0.11	16.2	0.9	1.2943	0.0141	0.8209	0.0172	167
2692B			350	50									
2383	Unit II	333–365/ non-coordinated	315	11	0.07	0.003	7.1	0.3	1.1657	0.0320	0.8024	0.0452	165
2691A	Unit IV	545	337	18	0.3	0.07	6.9	0.4	1.2119	0.0199	0.848	0.0299	184
2691B			354	20									
2384	Unit Vm	830	482	14	0.25	0.005	12.3	1.9	1.2179	0.0197	0.9465	0.0242	252
2388	Unit Vm	833	No ESR analysis				55.7	0.2	1.1513	0.0042	0.7048	0.0058	127
2382a	Unit Vm	846	566	16	1.11	0.01	6.1	3.5	1.1736	0.0393	0.8256	0.0459	175
2382b	Unit Vm		544	33									
2380	Unit Vm	848	510	24	0.19	0.18	6	0.9	1.1805	0.0227	0.7648	0.0343	148
2381	Unit Vm	850	No ESR analysis						1.1744	0.0170	0.7656	0.0222	149

ESR (part 2)

Lab No.	Unit	Depth (cm)	+Error	–Error	Thickness (μm)	Thickness error (μm)	S1/S2	Sediment						
								U-Sediment (ppm)	Th-Sediment (ppm)	K-Sediment (%)	Gamma dose rate (μGy/a)	Gamma error (μGy/a)	Beta dose rate (μGy/a)	Beta error (μGy/a)
2668A	Unit II	247	14	13	730	30	20	5.01	8.69	2.264	1246	81	382	31
2668B					780	30	20	5.01	8.69	2.264	1246	81	363	30
2689A	Unit II	323	8	8	840	30	20	5.38	7.27	2.484	1258	82	365	30
2689B					900	30	20	5.38	7.27	2.484	1258	82	344	28
2692A	Unit II	345	8	8	580	20	20	4.68	7.02	2.279	1199	78	441	35
2692B					660	40	20	4.68	7.02	2.279	1199	78	401	35
2383	Unit II	333–365/ non-coordinated	23	20	700	100	50	4.57	7.35	2.302	1203	79	371	52
2691A	Unit IV	545	18	16	790	50	20	3.84	6.75	2.297	1095	72	333	30
2691B					770	90	20	3.84	6.75	2.297	1095	72	340	39

(continued)

Table 16.2 (continued)

ESR (part 2)														
Lab No.	Unit	Depth (cm)	+Error	–Error	Thickness (μm)	Thickness error (μm)	S1/S2	Sediment						
								U-Sediment (ppm)	Th-Sediment (ppm)	K-Sediment (%)	Gamma dose rate (μGy/a)	Gamma error (μGy/a)	Beta dose rate (μGy/a)	Beta error (μGy/a)
2384	Unit Vm	830	27	23	1000	100	50	15	4.36	1.656	1693	111	382	47
2388	Unit Vm	833	13	12										
2382a	Unit Vm	846	27	22	800	100	50	10.4	4.16	1.471	1452	95	351	62
2382b	Unit Vm				800	100	50	10.4	4.16	1.471	1452	95	351	62
2380	Unit Vm	848	15	13	800	100	50	7.49	4.19	1.692	1341	87	319	56
2381	Unit Vm	850	12	11										

ESR (part 3)										
Lab no.	Unit	Depth (cm)	Early U-Uptake						US-ESR	
			enamel+dentine DR (μGy/a)	int.+Dentine error (μGy/a)	Total dose rate (μGy/a)	Total error (μGy/a)	Age (ka)	Age error (ka)	Age (ka)	Age error (ka)
2668A	Unit II	247	173	16	1801	88	106	6	100	7
2668B			178	16	1787	88	115	6	110	6
2689A	Unit II	323	370	36	1993	94	150	11	130	13
2689B			359	35	1961	94	156	9	138	11
2692A	Unit II	345	529	52	2169	100	163	12	162	16
2692B			504	52	2104	100	166	24	165	32
2383	Unit II	333–365/ non-coordinated	154	16	1728	96	182	11	184	13
2691A	Unit IV	545	239	31	1667	84	202	14	205	16
2691B			243	32	1678	88	210	16	216	18
2384	Unit Vm	830	288	38	2363	126	203	12	195	13
2388	Unit Vm	833								
2382a	Unit Vm	846	498	75	2301	136	246	16	271	22
2382b	Unit Vm		493	75	2296	136	236	20	258	27
2380	Unit Vm	848	185	72	1845	126	276	22	293	23
2381	Unit Vm	850								

Material and Methods

Twenty bear teeth from different levels of the Azokh 1 cave were analyzed by amino acid racemization. The Biomolecular Stratigraphy Laboratory (BSL) uses dentine for amino acid racemization dating of vertebrates. Bones are rejected because they are more prone to diagenetic interference (Masters 1986, 1987). Dentine collagen samples were obtained by drilling the root of the teeth with a dental diamond drill. A hole 2–3 mm in diameter was drilled near the tooth neck to reach the dentine, which is protected by the crown. Between 5 and 46 mg of dentine were obtained. The outermost part of the root (mostly cementum) was discarded. For the establishment of the chronology of Azokh Cave, we used only the aspartic acid content of the samples, because that racemizes fastest. Goodfriend (1991) noted that the analysis of more than one amino acid provides largely redundant information on sample age (Torres et al. 2002).

For details on sample pretreatment and amino acid extraction, see Kaufman and Manley (1998) and Kaufman (2000). The samples were pretreated with 2 N HCl at room temperature and a posterior dialysis step (Spectra/Por mnco 3500 D membrane) to eliminate dissolved mineral fraction and free amino acids (Marzin 1990; Torres et al. 1999, 2000). Subsequently, hydrolysis was performed under N_2 atmosphere in 7 µl of 6 M HCl for 20 h at 100 °C. The hydrolysates were evaporated to dryness in *vacuo*, and then rehydrated in 7 µl 0.01 M HCl with 1.5 mM sodium azide and 0.03 mM L-*homo*-arginine (internal standard). For derivatization, the samples were mixed (2 µl) with the pre-column derivatization reagent (2.2 µl), which comprised 260 mM isobutyryl-L-cysteine (chiral thiol) and 170 mM o-phtaldialdehyde, dissolved in 1.0 M potassium borate buffer solution at pH 10.4. Eluent A consisted of 23 mM sodium acetate with 1.5 mM sodium azide and 1.3 mM EDTA, adjusted to pH 6.00 with 10 M sodium hydroxide and 10% acetic acid. Eluent B was HPLC-grade methanol, and eluent C consisted of HPLC-grade acetonitrile.

The amino acid concentrations and ratios were measured with an Agilent HPLC-1100, equipped with a fluorescence detector. Excitation and emission wavelengths were programmed at 335 nm and 445, respectively. A Hypersil BDS C18 reverse-phase column (5 µm; 250 × 4 mm i.d.) was used for the analysis. A linear gradient was obtained at 1.0 ml/min and 25 °C, from 95% eluent A and 5% eluent B upon injection to 76.6% eluent A, 23% eluent B, and 0.4% eluent C at min 31.

Results

The results of the individual analyses of the Azokh samples are shown in Table 16.3. The aspartic acid content can be used as an indicator of collagen integrity for further DNA analysis: low aspartic acid concentrations indicate deep degradation of the organic matrix of the dentine and, therefore, low DNA amount. The D/L ratios of other amino acids are not provided because in many cases the D enantiomers could not be identified in the chromatograms. The mean aspartic acid racemization ratios of the different levels are shown in Table 16.3.

Samples LEB-4685, 4686, 4490 and 4491 (Table 16.3) did not provide enough collagen to determine their amino acid content. Samples marked with an asterisk were not considered for the age calculation because of their high deviation from mean values, although we cannot rule out that they were affected by re-working processes. According to our own experience in the Amutxate cave in Spain (Torres et al. 2007), reworking of sediments and bones in ancient deposits constitutes the norm and not the exception.

The aspartic acid D/L ratios of dentine collagen samples were introduced in the age calculation algorithm (Table 16.3). For the age-calculation algorithm (Fig. 16.6), we used the racemization values from eight cave-localities dated through different radiometrical methods: ^{14}C in bones (Eirós, Galicia; Grandal d'Anglade and Vidal Romaní 1997), Th/U in speleothems (La Lucia, Cantabria; Torres et al. 2001), electron spin resonance (ESR) and uranium series in bear teeth (Sima de los Huesos, Burgos; Bischoff et al. 1997), ESR results on bear teeth from Amutxate (Torres et al. 2007) and unpublished ESR data obtained from bear teeth (Navarra; Troskaeta and Santa Isabel, Vizcaya; La Lucia and La Pasada, Cantabria). We have calculated the mean age from the individual values obtained from each sample, and the age uncertainty is the standard deviation (Table 16.4, Fig. 16.6). In this sense, the use of monogeneric samples reduces taxonomically controlled variability in D/L ratios (Murray-Wallace 1995; Murray-Wallace and Goede 1995).

Table 16.3 Amino acid racemization dating details. Sample weight, relative abundance of D and L aspartic acid, D/L Asp ratio and corresponding age of the U. spelaeus teeth from the Azokh cave. *Samples marked with an asterisk were not considered for the age calculation here because of their high deviation from mean values

Sample	LEB 4414	*LEB 4415	LEB 4683	*LEB 4416	LEB 8292	LEB 4684	LEB 4685	LEB 4686	LEB 4687	*LEB 4688	LEB 4689	LEB 4490	LEB 4491	LEB 8004	*LEB 8005	LEB 8006	LEB 8293	LEB 8294	LEB 8295
Unit	Vm	Vm	Vm	Vu	IV	II	II	II	II	III	II	II	II	II	II	II	II	II	II
Weight (mg)	41.8	44.8	42	45.7	40	43.1	11.2	36.7	42.6	40.6	5.4	11.7	8.8	5	4.6	10	30.2	27.8	27.5
D Asp	4544	15736	532	5268	74.8	321	–	–	3824	4872	–	–	–	67.8	22.4	40.7	177.7	91.7	69.4
L Asp	12761	26092	1926	14514	386.6	1402	–	–	12363	10618	2164	–	–	359.3	160.3	176.6	735.5	280.6	266.5
D/L Asp	0.356	0.603	0.276	0.363	0.193	0.229	–	–	0.309	0.459	–	–	–	0.189	0.140	0.230	0.242	0.327	0.260
Age (ka)	266	504	202	272	138	165	–	–	228	356	–	–	–	134	97	166	175	242	189

Table 16.4 Mean amino acid racemization aspartic acid D/L values obtained in the dentine of bear teeth from Units II and V together with their correspondent mean numerical age

Unit	D/L Asp	Age (ka)
II	0.247 ± 0.050	179 ± 38
V	0.316 ± 0.057	234 ± 45

Conclusions

Possible diagenetic processes linked to acid leaching and to guano accumulation could be responsible for the individual age scattering. The time-average of Units II and V of Azokh cave has been calculated and we can provisionally conclude that both correspond to the later part of the Middle Pleistocene.

Uranium-Lead (U-Pb) Dating of Stalagmites from the Azokh Cave Complex (Robyn Pickering)

Introduction

Two stalagmite samples from the Azokh Cave Complex were selected for U-Pb dating (Table 16.1). The first attempt (sample 1) was focused on the large stalagmite boss near the entrance of the cave, but this material contained too much common ^{206}Pb for an age determination to be made. During a second field season, a number of small stalagmites at the very back of the cave were considered, and the best preserved one selected for dating (sample 2). This second

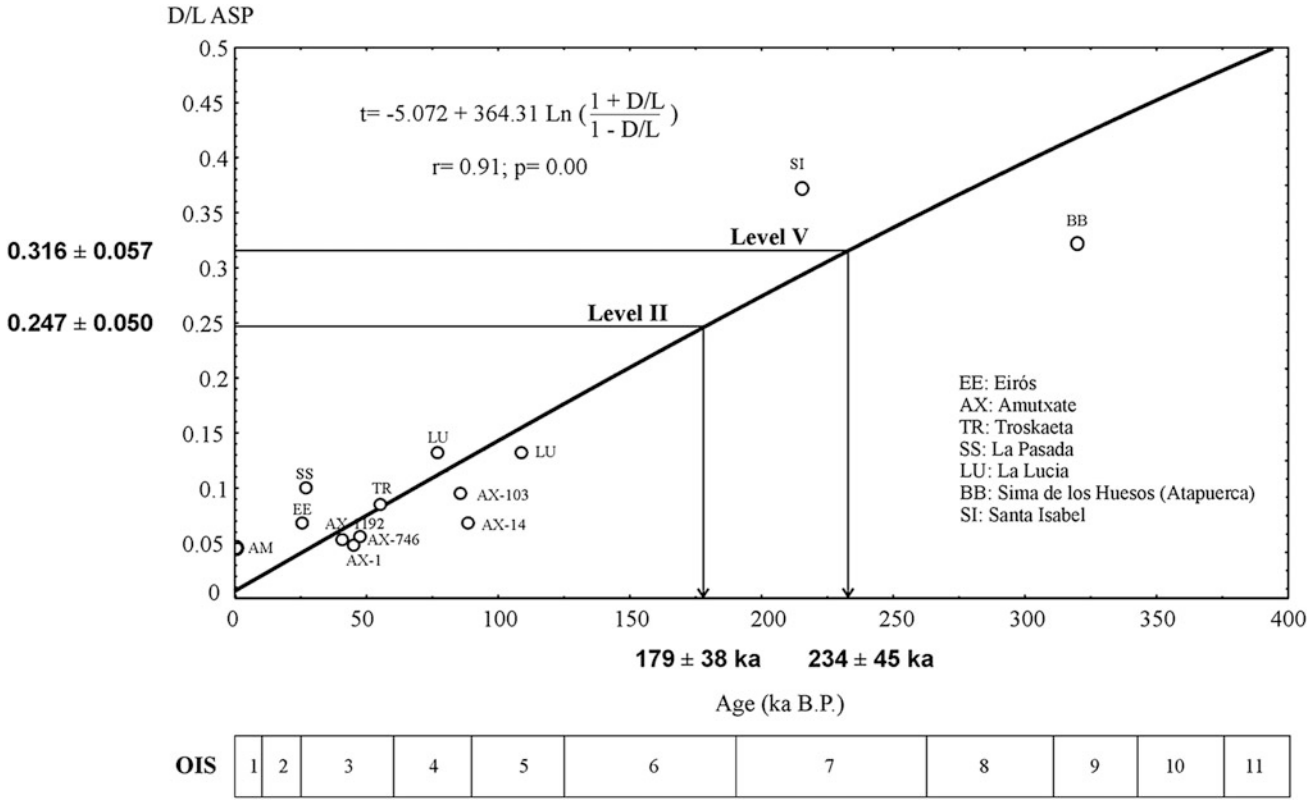

Fig. 16.6 Age calculation of levels (Units) II and V from Azokh cave by introducing the aspartic acid D/L ratios of the dentine collagen of *U. spelaeus* teeth into the dating algorithm (modified from Torres et al. 2001, 2002). Circles represent the bear localities dated by different dating methods: ^{14}C in bones (Eirós Cave, Galicia; Grandal d´Anglade and Vidal Romaní 1997), Th/U in speleothems (La Lucia Cave, Cantabria; Torres et al. 2001), electron spin resonance (ESR) and uranium series in bear teeth (Sima de los Huesos, Burgos; Bischoff et al. 1997) and unpublished ESR data obtained from bear teeth (Amutxate Cave, Navarra; Troskaeta and Santa Isabel Caves, Vizcaya; La Lucia and La Pasada Caves, Cantabria)

sample consisted of clear to creamy coloured calcite and produced an age of 1.19 ± 0.08 Ma. All sample preparation and dating was undertaken at the School of Earth Sciences at the University of Melbourne, Australia.

Laser-ablation Pre-screening

Successful U-Pb dating depends on the concentration of U present in the sample, as well as the amount of Pb. Too much common ^{206}Pb can mask the radiogenic daughter ^{206}Pb, making it impossible to date the material in question. Laser ablation ICP-MS is used to map out the U and Pb concentrations in samples prior U-Pb analysis so that layers with high U and low Pb can be identified and selected for dating. Speleothem samples are cut, set in resin and polished into 10 × 5 × 1 cm blocks to fit into the laser cell. The laser ablation results of samples 1 and 2 are shown in Fig. 16.7. From the laser scans it is clear that sample 1 (Fig. 16.7a) is not suitable for U-Pb dating, given the dominance of the Pb signal and the low U content. Sample 2 (Fig. 16.7b), however, is highly suitable for dating, with several layers with U concentrations of close to 10 ppm, and very low Pb. Based on these results, dating was focused on sample 2.

Sample Preparation and Measurement

Once a U-rich layer has been identified from the laser ablation tracks, small (~3 mm^3) blocks of speleothem material are cut using a hand operated dentist drill. These small blocks are then etched in a mild HCl solution to remove the outer layer and decrease the risk of Pb contamination from the drilling and subsequent handling of the samples. Samples are spiked with a mixed ^{235}U–^{205}Pb spike and dissolved in 6 M HCl and left to equilibrate on a hot plate overnight. Uranium and lead are extracted and concentrated using a standard ion-exchange resin column separation, following the protocol outlines in Woodhead et al. (2006).

Uranium and lead from each of the multiple aliquots from the single U-rich layer are then measured on a Nu-Instruments MC-ICP-MS, again following Woodhead et al. (2006).

Results

Element concentrations and isotope ratios are obtained for sample 2 and are summarized in Table 16.5. The average U concentration for the layers analysed is 5.7 ppm, while the Pb is much lower at 0.03 ppm. ^{238}U/^{206}Pb ratios vary between 389 and 849, giving enough spread to produce a range of ^{207}Pb/^{206}Pb ratios from 0.711 to 0.772. An age for sample 2 was calculated using the ^{238}U/^{206}Pb and ^{207}Pb/^{206}Pb ratios to construct a Tera-Wasserberg isochron (Fig. 16.8). Ideally the individual analyses should plot along a straight line, the slope of which is a function of the age of

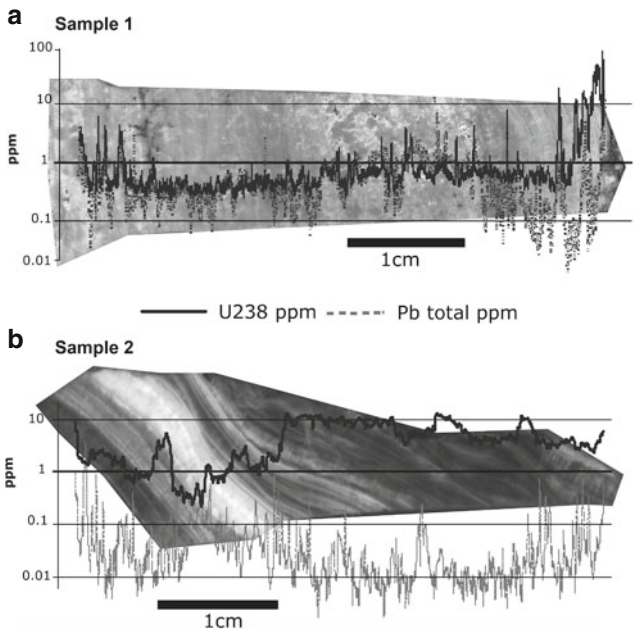

Fig. 16.7 Laser ablation uranium and lead scans for Azokh Cave speleothem **a** sample 1 and **b** sample 2, plotted against a photograph of the sample for comparison and on a log scale. Sample 1 has U concentrations of generally below 1 ppm, with similar Pb concentrations, with no obvious layers suitable for dating. Sample 2 has much higher U concentrations, up to 10 ppm and a clear series of layers with high U and low Pb, perfect for dating

Table 16.5 Uranium and lead concentrations and isotope ratios used to calculate ages for a small stalagmite at the very back of the Azokh Cave Complex (sample A2)

Compositional Parameters			Sample (Radiogenic + Initial Pb) Isotope Ratios																
Sample	U	Pb	^{238}U		^{207}Pb		corr. coef.	^{238}U		^{206}Pb		corr. coef.	Present		**U-Pb (T-W)**		%	Initial	
	ppm	ppm	^{206}Pb	% err	^{206}Pb	% err	8/6–7/6	^{204}Pb	% err	^{204}Pb	% err	8/4–6/4	$^{234}U/^{238}U$	±	Age **(Ma)**	**2SE**	% Error	$^{234}U/^{238}U$	±
A2-5	3.6	0.02	512.5	9.3	0.750	0.1	–0.0649	10700	9.4	20.88	0.2	0.0716	1.0077	0.0001	**1.19**	**0.080**	6.6	1.223	0.049
A2-6	6.9	0.04	561.0	0.4	0.753	0.1	–0.9932	11500	0.5	20.50	0.1	0.8009							
A2-8	6.0	0.02	850.0	1.0	0.714	0.3	–0.9956	18841	1.4	22.17	0.4	0.9095							
A2-9	5.3	0.02	806.6	1.5	0.715	0.4	–0.9881	17529	2.0	21.73	0.6	0.8487							
A2-10	6.2	0.03	620.3	1.0	0.744	0.2	–0.9990	13136	1.2	21.18	0.3	0.8570							
A2-11	5.2	0.04	466.3	1.0	0.764	0.2	–0.9838	9571	1.2	20.52	0.3	0.7997							
A2-12	4.8	0.02	835.9	1.8	0.711	0.5	–0.9915	18666	2.4	22.33	0.8	0.8675							
A2-13	7.4	0.06	389.4	1.0	0.772	0.2	–0.9793	7874	1.3	20.22	0.4	0.6935							

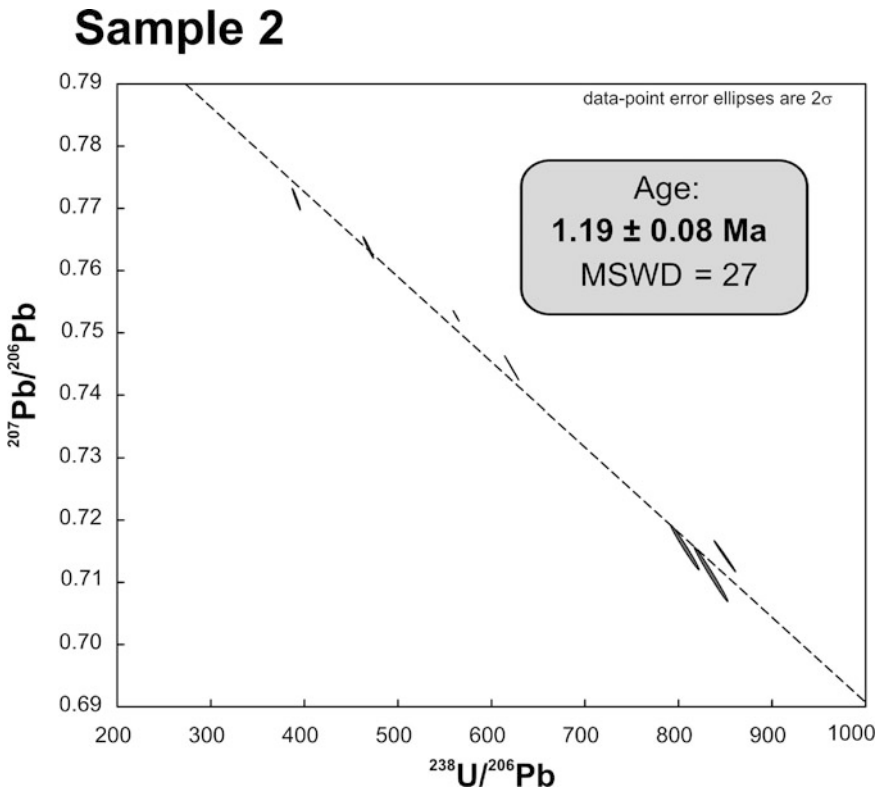

Fig. 16.8 Isochron age plot for Azokh speleothem sample 2, giving an age of 1.19 ± 0.08 million years for a small stalagmite at the very back of the cave. This gives a minimum age for the cave itself and hints at the possibility of older occupation deposits

the sample. In this case, all seven analyses do fall on or close to the line. The slope of this line and the measured $^{234}U/^{238}U$ ratio are then used to calculate an age of 1.19 ± 0.08 Ma. In samples such as this one, the initial $^{234}U/^{238}U$ may well have been >1 and must therefore be taken into account when calculating the age. If not, ages tend to be over-estimated. The residual $^{234}U/^{238}U$ excess was still measurable in the sample 2, and a $^{234}U/^{238}U$ ratio of 1.0077 ± 0.001 was obtained, following the protocol outlined in Pickering et al. (2011).

Conclusions

Speleothem material from two stalagmites within the Azokh Cave Complex were considered for U-Pb dating. The first of these, sample 1, from the large stalagmite boss near the entrance of the cave proved to be unsuitable for U-Pb dating given the low U content and dominance of common Pb. Sample 2, from a small stalagmite towards the very back of the main cave, on the other hand was highly suitable for U-Pb dating, with U concentrations of close to 10 ppm, and very low Pb. This sample yielded an age of 1.19 ± 0.08 Ma which provides a minimum age for the cave itself, confirms the antiquity of the deposits, and hints at the possibility of even older occupation layers.

References

Aitken, M. J., Clark, P. A., Gaffney, C. F., & Lovborg, L. (1985). Beta and gamma gradients. *Nuclear Tracks,10*, 647–653.

Bischoff, J. L., Fitzpatrick, J. A., Falgueres, C., Bahain, J. J., & Bullen, T. T. (1997). Geology and preliminary dating of the hominid-bearing sedimentary fill of the Sima de los Huesos Chamber, Cueva Mayor of the Sierra de Atapuerca, Burgos, Spain. *Journal of Human Evolution,33*, 129–154.

Brock, F., Higham, T., Ditchfield, P., & Bronk-Ramsey, C. (2010). Current pretreatment methods for AMS radiocarbon dating at the oxford Radiocarbon Accelerator unit (ORAU). *Radiocarbon,52*(1), 103–112.

Bronk Ramsey, C., Higham, T., & Leach, P. (2004a). Towards high precision AMS: Progress and limitations. *Radiocarbon,46*(1), 17–24.

Bronk Ramsey, C., Higham, T., Bowles, A., & Hedges R. (2004b). Improvements to the pretreatment of bone at Oxford. *Radiocarbon46*(1), 155–163.

Bronk Ramsey, C., Higham, T., Owen, D. C, Pike, A., & Hedges, R. (2004c). Radiocarbon Dates from the Oxford Ams System: *Archaeometry* Datelist 31. *Archaeometry 44* (3 Supplement 1), 1–149.

de Torres, T., García-Alonso, P., Canoira, L., & Llamas, J. F. (2000). Aspartic acid racemization and protein preservation in the dentine of European bear teeth. In M. J. C. G. A. Goodfriend, M. L. Fogel, S. A. Macko, & J. F. Wehmiller (Eds.), *Perspectives in amino acids and protein geochemistry* (pp. 349–355). Oxford: Oxford University Press.

Eggins, S., Grün, R., Pike, A., Shelley, A., & Taylor, L. (2003). ^{238}U, ^{232}Th profiling and U-series isotope analysis of fossil teeth by laser ablation ICPMS. *Quaternary Science Reviews,22*, 1373–1382.

Eggins, S. M., Grün, R., McCulloch, M., Pike, A., Chappell, J., Kinsley, L., et al. (2005). *In situ* U-series dating by laser-ablation multi-collector ICPMS: New prospects for *Quaternary geochronology*. *Quaternary Science Reviews,24*, 2523–2538.

Fernández, E., Ortiz, J. E., Pérez-Pérez, A., Pratts, E., Turbón, D., Torres, T., et al. (2009). Aspartic acid racemization variability in ancient human remains: Implications in the prediction of ancient DNA recovery. *Journal of Archaeological Science,36*, 965–972.

Fernández-Jalvo, Y., King, T., Andrews, P., Yepiskoposyan, L., Moloney, N., Murray, J., et al. (2010). The Azokh Caves complex: Middle Pleistocene to Holocene human occupation in the Caucasus. *Journal of Human Evolution,58*, 103–109.

Goodfriend, G. A. (1991). Patterns of racemization and epimerisation of aminoacids in land snails shells over the course of the Holocene. *Geochimica et Cosmochimica Acta,55*, 293–302.

Grandal d´Anglade, A., & Vidal Romaní, J. R. (1997). A population study on the cave bear (*Ursus spelaeus* Ros.Hein.) from Cova Eirós (Triacastela, Galicia, Spain). *Geobios,30*(5), 723–731.

Grün, R. (2000). An alternative for model for open system U-series/ESR age calculations: (closed system U-series)-ESR, CSUS-ESR. *Ancient TL,18*, 1–4.

Grün, R. (2002). ESR dose estimation on fossil tooth enamel by fitting the natural spectrum into the irradiated spectrum. *Radiation Measurements,35*, 87–93.

Grün, R. (2006). Direct dating of human fossils. *Yearbook of Physical Anthropology,49*, 2–48.

Grün, R. (2009a). The DATA program for the calculation of ESR age estimates on tooth enamel. *Quaternary Geochronology,4*, 231–232.

Grün, R. (2009b). The relevance of parametric U-uptake models in ESR age calculations. *Radiation Measurements,44*, 472–476.

Grün, R., & Katzenberger-Apel, O. (1994). An alpha irradiator for ESR dating. *Ancient TL,12*, 35–38.

Grün, R., Schwarcz, H. P., & Chadam, J. M. (1988). ESR dating of tooth enamel: Coupled correction for U-uptake and U-series disequilibrium. *Nuclear Tracks and Radiation Measurements,14*, 237–241.

Kaufman, D. S. (2000). Amino acid racemization in ostracodes. In G. Goodfriend, M. Collins, M. Fogel, S. Macko & J. Wehmiller (Eds.), *Perspectives in amino acid and protein geochemistry* (pp. 145–160). Oxford: Oxford University Press.

Kaufman, D. S., & Manley, W. F. (1998). A new procedure for determining DL amino acid ratios in fossils using reverse phase liquid chromatography. *Quaternary Geochronology,17*, 987–1000.

King, T., Compton, T., Rosas, A., Andrews, P., Yepiskoyan, L., & Asryan, L. (2016). Azokh cave hominin remains. In Y. Fernández-Jalvo, T. King, L. Yepiskoposyan & P. Andrews (Eds.), *Azokh Cave and the Transcaucasian Corridor* (pp. 103–116). Dordrecht: Springer.

Lee-Thorp, J. (2002). Two decades of progress towards understanding fossilization processes and isotopic signals in calcified tissue minerals. *Archaeometry,44*, 435–446.

Lioubine, V. P. (2002). *L'Acheuléen du Caucuase*. Liège: Études et Recherches Archéologiques de l'Université de Liège, ERAUL 93.

Marin-Monfort, M. D., Cáceres, I., Andrews, P., Pinto, A. C., & Fernández-Jalvo, Y. (2016). Taphonomy and site formation of Azokh 1. In Y. Fernández-Jalvo, T. King, L. Yepiskoposyan & P. Andrews (Eds.), *Azokh Cave and the Transcaucasian Corridor* (pp. 211–249). Dordrecht: Springer.

Marsh, R. E. (1999). Beta-gradient isochrons using electron paramagnetic resonance: Towards a new dating method in archaeology. MSc thesis, McMaster University, Hamilton.

Marzin, E. (1990). *Essai de normalisation du protocole d'analyse des taux de racémisation des acides aminés: Applications a la datation d'ossements fossiles* (pp. 167–178). VIII: Travaux du LAPMO.

Masters, P. M. (1986). Amino acid racemisation dating. In M. R. Zimmerman & J. L. Angel (Eds.), *Dating and age determination of biological materials* (pp. 39–58). London: Croom Helm.

Masters, P. M. (1987). Preferential preservation of non-collagenous protein during bone diagenesis: Implications for chronometric and stable isotopic measurements. *Geochimica et Cosmochimica Acta,51*, 3209–3214.

Millard, A. R., & Hedges, R. E. M. (1996). A diffusion-adsorption model of uranium uptake by archaeological bone. *Geochimica et Cosmochimica Acta,60*, 2139–2152.

Murray, J., Lynch, E. P., Domínguez-Alonso, P., & Barham, M. (2016). Stratigraphy and sedimentology of Azokh caves, South Caucasus. In Y. Fernández-Jalvo, T. King, L. Yepiskoposyan & P. Andrews (Eds.), *Azokh Cave and the Transcaucasian Corridor* (pp. 27–54). Dordrecht: Springer.

Murray-Wallace, C. V., & Goede, A. (1995). Aminostratigraphy and electron spin resonance dating of Quaternary coastal neotectonism in Tasmania and the Bass Strait islands. *Australian Journal of Earth Sciences,42*, 51–67.

Pickering, R., Dirks, P. H. G. M., Jinnah, Z., de Ruiter, D. J., Churchill, S. E., Herrires, A. I. R., et al. (2011). *Australopithecus sediba* at 1.977 Ma and implications for the origins of Genus Homo. *Science,333*, 1421–1423.

Pike, A. W. G., Hedges, R. E. M., & Van Calsteren, P. (2002). U-series dating of bone using the diffusion-adsorption model. *Geochimica et Cosmochimica Acta,66*, 4273–4286.

Reimer P. J. (2009) (Guest Editor) *IntCal 09 Calibration Issue*. Radiocarbon 51, 1111–1187.

Richards, D. A., Bottrell, S. H., Cliff, R. A., Strohle, K., & Rowe, P. J. (1998). U-Pb dating of a speleothem of Quaternary age. *Geochimica et Cosmochimica Acta,62*, 3683–3688.

Schwarcz, H. P., GriJn, R., & Tobias, P. V. (1994). ESR dating of the australopithecine site of Sterkfontein, Transvaal, South Africa. *Journal of Human Evolution,26*, 175–181.

Smith, C. I., Faraldos, M., & Fernández-Jalvo Y. (2016). Bone diagenesis at Azokh cave, Nagorno-Karabakh. In Y. Fernández--Jalvo, T. King, L. Yepiskoposyan & P. Andrews (Eds.), *Azokh Cave and the Transcaucasian Corridor* (pp. 251–269). Dordrecht: Springer.

Torres, T., Llamas, J. F., Canoira, L., & García-Alonso, P. (1999). Aspartic acid racemization in the dentine of bears (*Ursus etruscus* G. Cuvier, *Ursus prearctos* Boule, *Ursus deningeri* von Reichenau and *Ursus spelaeus* Rosenmüller-Heinroth). Tooth dentine amino acids versus Mollusca amino acids. In G. Palyi, C. Zucchi & L. Caglioti (Eds.), *Advances in biochirality* (pp. 247–256). Amsterdam: Elsevier.

Torres, T., Ortiz, J. E., García, M. J., Llamas, F. J., Canoira, L., García de la Morena, M. A., et al. (2001). Geochemical evolution of amino acids in Pleistocene bears. *Chirality,13*(8), 517–521.

Torres, T., Ortiz, J. E., Llamas, F. J., Canoira, L., Juliá, R., & García-Martínez, M. J. (2002). Bear dentine aspartic acid racemization analysis, proxy for pleistocene cave infills dating. *Archeometry,44*(3), 417–426.

Torres, T., Ortiz, J. E., & Cobo, R. (2003). Deep cave sediments characteristics: Their influence in fossil preservation. *Estudios Geológicos,59*(1–4), 195–204.

Torres, T., Ortiz, J. E., Cobo, R., de Hoz, P., García-Redondo, A., & Grün, R. (2007). Hominid exploitation of the environment and cave bear populations. The case of Ursus spelaeus Rosenmüller-Heinroth in Amutxate cave (Aralar, Navarra-Spain). *Journal of Human Evolution,52*, 1–15.

Weiner, S. (2010). *Microarchaeology: Beyond the visible archaeological record*. Cambridge: Cambridge University Press.

Woodhead, J., Hellstrom, J., Maas, R., Drysdale, R., Zanchetta, G., Devine, P., et al. (2006). U-Pb geochronology of speleothems by MC-ICPMS. *Quaternary Geochronology,1*, 208–221.

Index

Note: Page numbers followed by *f* and *t* refer to figures and tables, respectively

Yolanda Fernández-Jalvo et al. (eds.), *Azokh Cave and the Transcaucasian Corridor*,
Vertebrate Paleobiology and Paleoanthropology, DOI 10.1007/978-3-319-24924-7

M

N

O

S